Synthesis, Characterisation and Biological Activity of Selected Pyrazoles and Naphthyridines

Thesis submitted to the Durban University of Technology in fulfillment of the requirements for the award of the degree of

DOCTOR OF PHILOSOPHY

IN

CHEMISTRY

By

TALENT RAYMOND MAKHANYA

Under the guidance of

Prof. R. M. GENGAN

Department of Chemistry
Durban University of Technology
Faculty of Applied Sciences
Durban-4001
South Africa.

April, 2019

DECLARATION

This dissertation is being submitted to the Durban University of Technology for the degree of Doctor of Philosophy in Chemistry. I declare that this work is my own and has not been submitted before for any degree or examination to this or any other university or institution for this or any other degree or award.

Student Number: **20427519**

Student: [redacted] Date: 11/04/19

Mr Talent Raymond Makhanya

Supervisor: [redacted] Date: 11/04/2019

Prof. Robert Moonsamy Gengan

ACKNOWLEDGEMENT

First and foremost, I wish to convey my deepest gratitude to God for all the spirit and dedication that I as a person developed over time, despite obstacles and unfortunate situations that befell me in the course of my studies.

My sincere appreciation, deep sense of gratitude and indebtedness to my supervisor and mentor Professor **Robert M. Gengan** *Department of Chemistry, Durban University of Technology, Durban,* for his guidance, constant encouragement, remarkable patience, perusal of the manuscript and motivation throughout my course of study. You are a motivating factor, great source of inspiration and academician par excellence.

Further, I also take this opportunity to thank Dr. **Daniel Hugo Pienaar** and Dr. **Charlette Tiloke** for perusal of the manuscript and motivation throughout my course of study. I also thank all the chemistry staff for their encouragement and support throughout the course of this study.

My sincere gratitude goes to Professor **Suren Singh,** Executive Dean, **Ms Gill Shackleford,** Faculty of Applied Sciences at DUT for their kind assistance with logistics pertaining to research.

My special thanks also goes to Professor **Ata Athar** from the University of Winnipeg, in Canada, for granting me a golden opportunity to visit his research laboratory. This opportunity nurtured and enlightened me in organic synthesis and hence accelerated my studies. His dedication, diligence, hard work, creativity and wealthy of knowledge has inspired me.

My sincere gratitude to Mr **Laurel Kabange Kasumbwe** for his support and assistince with the biological study.

My sincere appreciation goes to all the members of the Organic Research Group, Chemistry Department, Faculty of Applied Sciences, Durban University of Technology especially to Thangaraj Muthu, Arul Murugesan, Vasantha Kumar Arumugam, Sureshkumar Mahalingam, S'busiso Nkosi and Nosipho Ndamane for their constant words of encouragement and willingness to offer a helping hand at all times.

Sincere thanks also goes to Mr. **Dilip Jagjiven** from UKZN, Westville Campus, for providing training in NMR spectral data analysis.

My sincere gratitude goes to the National Research Foundation (South Africa) and Canadian Common Wealth Scholarship Plain-Canada for funding my study.

Finally, my biggest thanks and gratitude goes to my family, extended family and friends for their blessings, support and encouragement during my study especially my mother Mrs **Thuleleni Doreen Makhanya** for her invaluable support and words of wisdom during difficult situations. Of course none of this work would have been possible without the love, care, understanding and support of my adorable fiancé Ms **Thembeka Ngwazi**: the wind beneath my wings and source of quiet strength.

DEDICATED TO MY FAMILY AND FRIENDS

ABBREVIATIONS

ATP	- adenosine triphosphate
DNA	- deoxyribonucleic acid
RNA	- ribonucleic acid
pH	- potential of hydrogen
MCRs	- multi-component reactions
MS	- Mass Spectrometry
Calcd	- Calculated
m.p.	- melting point
CDKs	- cyclin-dependent kinase
mL	- milliliter
mmol	- millimole
µL	- microliter
nm	- nanometer
h	- hour (s)
min	- minutes
mg	- milligram
µg	- microgram
µM	- micromolar
%	- percent
α	- alpha
β	- beta
g	- gram
^{0}C	- degree Celsius
m	- meter
cm	- centimeter
MHz	- megahertz
ppm	- parts per million
TLC	- thin-layer chromatography
NaOH	- sodium hydroxide
NaOAc	- sodium acetate

KBr	- potassium bromide
$CDCl_3$	- deuterated-chloroform
DMSO-d_6	- deuterated-dimethyl sulfoxide
MTT	- 3(4,5-dimethylthiazol-2-yl)-2,5-diphenyl tetrazolium bromide
PBS	- phosphate buffered saline
CCM	- cell culture medium
TFOH	- triflic acid
$BF_3.OEt_2$	- boron triflouride diethyl etherate
$InCl_3$	- indium chloride
TFA	- triflouro acetic acid
$POCl_3$	- phosphorus oxy trichloride
VHR	- Vilsmeier-Haack reaction
rt	- room temperature
PPh_3	- triphenyl phosphine
$PtCl_4$	- platinum tetrachloride
$PhCH_3$	- toluene
NaH	- sodium hydride
Ac_2O	- acetic anhydride
Et_3N	- tri ethyl amine
ZnO	- zinc oxide
NH_3	- ammonia
HCl	- hydrochloric acid
$SOCl_2$	- thionyl chloride
LDA	- lithium di-isopropyl amine
CO_2	- carbon dioxide
Na	- sodium
SA	- South Africa
TB	- mycobacterium tuberculosis
$CHCl_3$	- chloroform
CH_2Cl_2	- dichloromethane
DMF	- dimethylformamide
MeOH	- methanol
EtOH	- ethanol

CH_3CN	- acetonitrile
H_2O	- water
H_2SO_4	- sulphuric acid
HOA_C	- acetic acid
$H_3PW_{12}O_{40}$	- phosphotungstic acid
$H_3SiW_{12}O_{40}$	- silicotungstic acid
THF	- tetrahydrofuran
DMSO	- dimethyl sulfoxide
p-TSA	- para toluene sulphonic acid
HCN	- hydrogen cyanide
BFE	- bond forming efficiency
HIV	- human immune deficiency virus
LPS	- lipopolysaccharide
AgNPs	- silver nano particles
ROS	- reactive oxygen species
CD4	- cluster of differentiation 4
IC_{50}	- half maximal inhibitory concentration
MIC	- minimium inhibitory concentration
SAR	- structural activity relationships
FT-IR	- fourier transform infrared spectrometry
^{1}H NMR	- proton nuclear magnetic resonance
^{13}C NMR	- carbon 13 nuclear magnetic resonance
GC-MS	- gas chromatography mass spectrometry
EI-MS	- electron ionisation mass spectrometry
TOF-MS	- time of flight mass spectrometry
COSY	- homonuclear correlation spectrometry
HSQC	- heteronuclear single quantum correlation
HMBC	- heteronuclear multiple bond correlation
DEPT	- distortion-less enhancement polarisation transfer
2D-NMR	- two dimensional nuclear magnetic resonance
NMR	- Nuclear magnetic resonance
SD	- standard deviation

GENERAL REMARKS

The numbering representing the structures, figures, schemes and tables are meant for the particular chapter only. All the figures pertinent to a chapter are placed after the relevant discussion in the following sequence, FT-IR, NMR and GC-MS spectra. Each chapter contains a separate experimental section.

Chemicals were purchased from Merck and Sigma Aldrich. The reaction and purity of the product were monitored by TLC. FT-IR spectra were recorded in the range of 4000-400 cm^{-1} on a JASCO FT/IR-460 spectrophotometer using KBr pellets. A TOF-MS analyser for accurate mass was used. The melting point (m.p) was recorded on a Buchi B-545 apparatus using open capillary tubes. The elemental analyses (C, H and N) were obtained from a Perkin Elmer precisely 2400 analyser. The NMR spectra were recorded using Bruker Advance 400 MHz or 600 MHz instrument. The chemical shifts (δ) were expressed in ppm. The following abbreviations are used in the NMR spectral data.

s	- singlet
d	- doublet
t	- triplet
q	- quartet
m	- multiplet
dd	- doublet of doublet
brs	- broad singlet
J	- coupling constant.

TABLE OF CONTENTS

ABSTRACT

The world continue to be threaten by various diseases from viruses, fungi and bacteria that cannot be cured. This arises due to the emergency of multidrug resistance in microorganisms hence current available drugs are becoming less potent. The solution to overcome this predicament is to further synthesize novel heterocyclic compounds which can display good therapeutic properties. Hence, this study focuses on the synthesis, characterization and biological evaluation of selected novel naphthyridinones, naphthyridines and pyrazoles. A total of 53 novel compounds were prepared by using multi-component reactions (MCRs), Povarov's [4+2] and Povarov's [3+2] reactions. The MCR was used for a solvent free synthesis of eight novel [1, 8] naphthyridinones from a mixture of 2-aminopicoline, various benzaldehyde derivatives and dimedone. A conventional heating protocol was used whilst the reaction was catalysed by phosphotungstic acid. The compounds were identified as 4, 8, 8-trimethyl-5-phenyl-5, 5a, 8, 9-tetrahydrobenzo[*b*] [1, 8] naphthyridin-6(7H)-ones with the aid of spectroscopic techniques, viz., FT-IR, NMR, EI- MS and elemental analysis. These eight compounds were screened for their anticancer activity against A549 lung cancer cells. Cell viability assays showed these compounds have a biological effect at various concentrations. Two compounds showed that good potential as an anti-proliferative agent and exhibited a dose-dependent decline in cell viability which was seen. The Povarov's [4+2] cycloaddition reaction was used to synthesize nine novel fused indolo [1, 8] naphthyridines. Indole was used as the dienophile whilst N-aryl aldimines were selected as the diene which were produced by reacting 2-amino-4-picoline and benzaldehyde**.** The reaction was catalysed by indium chloride to produce 1-methyl-6-phenyl-6,6a,7,11b-tetrahydro-5H-indolo[3,2-*c*][1,8]naphthyridine which was characterized by FT-IR, NMR, TOF-MS and elemental analysis. Furthermore, all synthesized compounds were screened for their antimicrobial activity. The results of the bioassay demonstrated that some fused indolo [1, 8] naphthyridines exhibited good inhibitory effect with an MIC value ranging from 0.04687 to 0.09375 µM against *Bacillus cereus* and *Staphylococcus aureus*. The toxicity of the synthesized compounds were evaluated through mutagenicity test against *Salmonella typhimurium* TA 98 and TA100 strains. All compounds showed no mutagenic effects against *Salmonella tyhphimurium* TA 98 and TA 100 strains. The Povarov's [3+2] cycloaddition was used to synthesize twenty six novel fused indolo pyrazole in the presence of a catalytic amount of indium chloride. The compounds were identified as 3-phenyl-2, 3-dihydropyrazolo [3, 4-*b*] indole-1(4H)-carbothioamides with the aid of

spectroscopic techniques such as FT-IR, NMR and TOF-MS. All compounds were screened for their antimicrobial activity against various strains of pathogenic bacteria and fungi. These compounds showed good activity against *Candida albicans*, *Candida utilis*, and *Saccharomyces cerevisiae* with MIC of 1.5; 1.1 and 0.375 µM respectively. In addition, all the compounds showed no mutagenic activity against *Salmonella tyhphimurium* TA 98 and TA100 strains. The scope of the Povarov's [3+2] reaction was further investigated using isoniazid to synthesise ten novel nicotinyl fused indolo pyrazoles in the presence of a catalytic amount of indium chloride. These compounds were identified as (3-phenyl-2,3-dihydropyrazolo[3,4-*b*]indol-1(4H)-yl)(pyridin-4-yl)methanone with the aid of spectroscopic techniques such as FT-IR, NMR and TOF-MS. All compounds were screened for their antimicrobial activity against various strains of pathogenic bacteria and fungi. The synthesized compounds showed weak activity against *Streptococcus faecalis*, *Micrococcus luteus* and *Bacillus coagullans* with a zone inhibition diameter of 9 mm and MIC of 0.75 µM. Furthermore, all synthesized compounds were tested for their toxicity against *Salmonella tyhphimurium* TA 98 and TA100 strains: none showed mutagenic activity.

Chapter One: Introduction, Aim and Objectives

1.1 Heterocyclic Compounds

Heterocyclic compounds have beeb know to play a huge role in biological processes in the human body: vitamins, enzymes, coenzymes, ATP, DNA, RNA and serotonin are involved in fundamental processes and mechanisms of life as the provider of sight, energy, transmission of nerve impulse and metabolism (Dua *et al*. 2011:120). Haemoglobin and chlorophyll are also important pigment that contain heterocycles as they are involved in the respiration mechanism. The question arises as to why nature utilizes so many heterocycles? This question could be answered by considering the fact that heterocycles are involved in an extraordinarily wide range of chemical reactions and have properties such as:

i. pH dependence and therefore may behave as acids or bases
ii. reactivity with electrophilic or nucleophiles reagents
iii. oxidation or reduction capability
iv. complexing with metal ions

The wide biological application of heterocyclic compounds has attracted the attention of synthetic organic chemists who have developed heterocyclic chemistry into a major category of organic chemistry (Arora *et al*. 2012:2947). Their contribution has led to:

a) regio, stereo, and chemo-selective functionalization of organic molecules
b) optimization of reaction conditions to permit increased tolerance of assorted functional groups
c) avoidance of utilizing the protecting groups, whilst enabling late stage modification of complex intermediates
d) rationalization synthesis by eliminating steps or joining steps into single step protocol
e) exclusion of toxic or highly cost reagents, rigorous conditions and tedious product separation

In spite of these developments, the majority of frequently used reactions for the synthesis of heterocyclic systems tend to be linear and require harsh reaction conditions. Therefore, there has been a sharp interest in multi-component reactions (MCRs) for the synthesis of heterocyclic systems (Taylor *et al*. 2016:6611). These reactions involve a chemical transformation amongst three or more substrates which are allowed to react together in one-pot to generate a particular

target molecule (Fu *et al*. 2014:238). In addition MCRs give better atom efficiency whereas circumventing time-consuming isolation and continuous purification of intermediates thereby decreasing the cost of materials, reducing waste production and cost of sequential construction of complex heterocycles systems (Fan *et al*. 2013: 1282). Some popular MCRs reported over the years include the Strecker amino acid synthesis, the Hantzsh dihydropyridine synthesis, the Biginelli reaction, Manning reaction, Ugi-4-component condensation, Passerini-3-component and Prins reaction (Khan *et al*. 2016:42045). These protocols are rapidly accelerating drug discovery through synthesis and exhibit tremendous superiority in contrast with the traditional synthetic methods. Furthermore, MCRs have revolutionized heterocyclic synthesis and offered an efficient protocol in combinational chemistry which plays a huge role in drug development to access new bioactive heterocyclic compounds.

1.2 Research Aim and Objectives

The research aim was to synthesize [1, 8] naphthyridines, fused indolo [1, 8] naphthyridines and fused indolo-pyrazoles with evaluation of their biological activity studies.

The objectives of the study were to synthesize and characterize:

1. Phenyl [1,8] naphthyridinone derivatives and determine their anticancer activity
2. Fused indolo [1,8] naphthyridine derivatives and determine their antimicrobial activity
3. Fused indolo-pyrazole derivatives and determine their antimicrobial activity

Various diseases from viruses, fungi and bacteria continue to threaten our society due to emerging of multidrug resistance in microorganisms. Hence, current available drugs are becoming less potent. To overcome this predicament synthesis of nitrogen based heterocyclic compounds has to be further explore to fight the multidrug resistance microorganisms. The synthesis of naphthyridines and pyrazoles were choosen because such heterocyclic compounds have exhibited good therapeutic properties against various diseases such as TB, HIV, Cancer and microbial infections. Hence, the study focuses on utilizing new efficient protocol to develop novel nitrogen based heterocyclic compounds. The research scope is presented in Scheme 1.

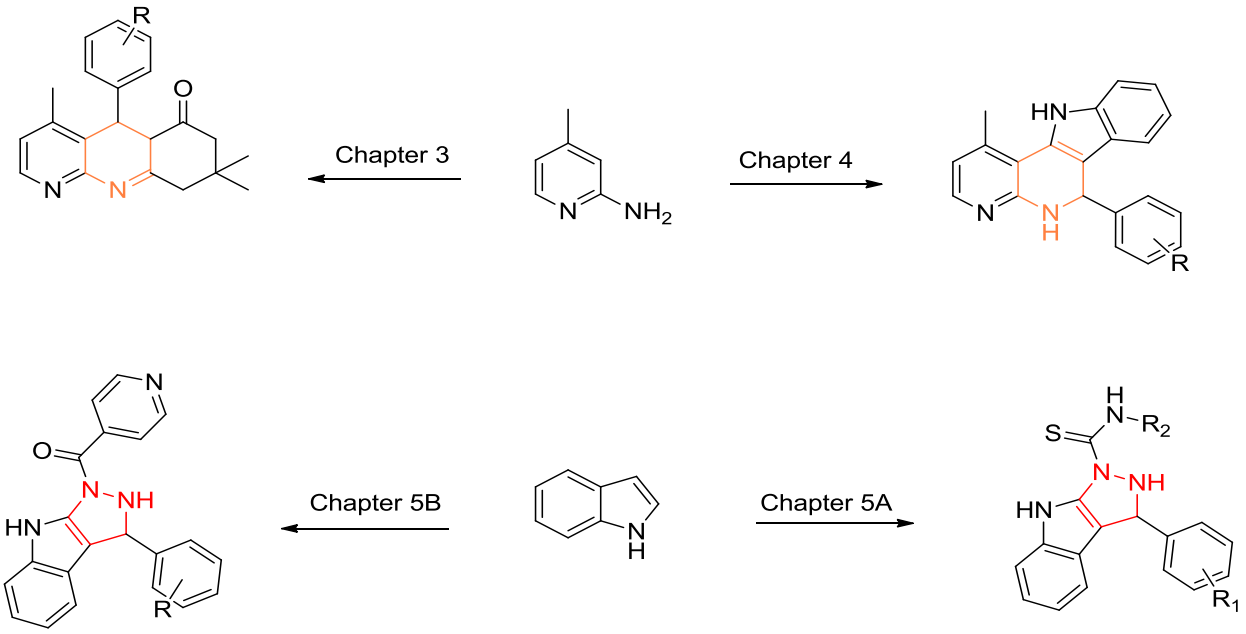

Scheme 1: Synthetic route for this study

The outcome of this research investigation is outlined in five chapters as presented below:

Chapter 1 gives a brief introduction to the importance of organic compounds, their methodology and finally outlined the aim and objectives of the study

Chapter 2 describes the historical background of heterocyclic compounds and biological relevance of five and six membered heterocyclic compounds, historical background of multi-component reactions, advancement of multi-component reactions in the synthesis of heterocyclic compounds.

Chapter 3 describes the brief synthetic procedure of [1, 8] naphthyridines, the synthesis and characterization of phenyl [1, 8] naphthyridinone derivatives with evaluation of their anticancer activity.

Chapter 4 discusses the importance of Povarov's reaction, synthesis and characterization of novel fused indolo [1, 8] naphthyridine derivatives with investigation of their antimicrobial activity.

Chapter 5: discusses the synthetic procedure of pyrazoles, the synthesis and characterization of fused indolo pyrazole derivatives with evaluation of their antimicrobial activity.

1.3 References

1. Dua R., Shrivastava S., Sonwane S.K. and Srivastava S.K. 2011. Pharmacological significance of synthetic heterocycles scaffold. *Advances in Biological Research,* 5(3): 120-144.
2. Arora P., Arora V., Lamba H.S. and Wadhwa D. 2012. Importance of heteroclyclic chemistry. *International Journal of Pharmaceutical Sciences and Research,* 3(9):2947-2954.
3. Taylor A.P., Robinson, R.P., Fobian, Y.M., Blakemore D.C., Jones L.H. and Fadeyi O. 2016. Modern advances in heterocyclic chemistry in drug discovery. *Organic and Biomolecular Chemistry,* 14: 6611-6637.
4. Fu L., Lin W., Hu M.H., Liu X.C., Huang Z.B. and Shi D.Q.2014. Efficient synthesis of functionalized benzo[*b*][1,8]naphthyridine derivatives via three-component reaction catalyzed by L-Proline, *American Chemical Society,* 16:238-243.
5. Fan W., Ye Q., Xu H.W., Wang S.L. and Tu S.J. 2013. Novel double [3+2+1] heteroannulation for forming unprecedented dipyrazolo-fused 2, 6-naphthyridines, *Organic Letters*, 25: 1282-1286.
6. Khan M.M., Khan S., Saigal and Iqbal S. 2016. Recent developments in multicomponent synthesis of structurally diversified tetrahydropyridines, *The Royal Society of Chemistry*, 6:42045-420

Chapter Two: Literature Review

2.1 Nitrogen Containing Heterocyclic Compounds

A heterocyclic compound is one in which one or more carbon atoms in ring formation is replaced by another element such as sulfur, nitrogen or oxygen. The non-carbon atom is called hetero-atom and this atom contains lone pairs of electrons (Sharma *et al.* 2010:491) thereby providing new chemical and biological properties compared to their hydrocarbon counter-part. Typical examples of some simple heterocyclic molecules are presented in Figure 1.

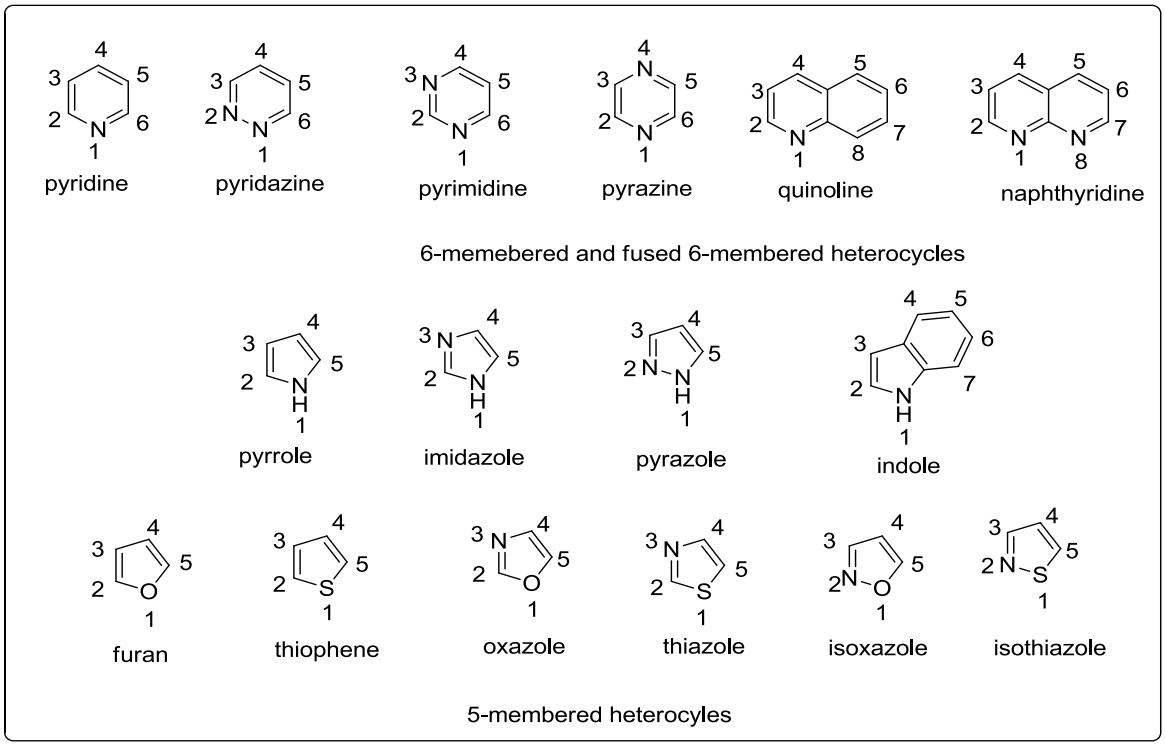

Figure 1: Some simple heterocyclic compounds

2.2 Biological Activity of Five and Six Membered Heterocyclic Compounds

The five and six membered nitrogen heterocycles are present in abundance in natural products and play a vital role in biological processes. It is estimated that more than 90 % of new drugs contain one or more nitrogen atoms thereby indicating their importance compared to other heteroatoms (Saini *et al.* 2013:66). The orientation of the nitrogen atom in the ring structure can vary in position leading to various classes and sub-classes of heterocycles. However, for this study the pyrazole and naphthyridine were selected because several of their derivatives display good potential as chemotherapeutic and pharmacotherapeutic agents.

2.2.1 The Pyrazoles as Modern Drugs

The pyrazole-scaffold (Figure 2**)** is an unsaturated five membered ring with two adjacent nitrogen atoms within the ring system.

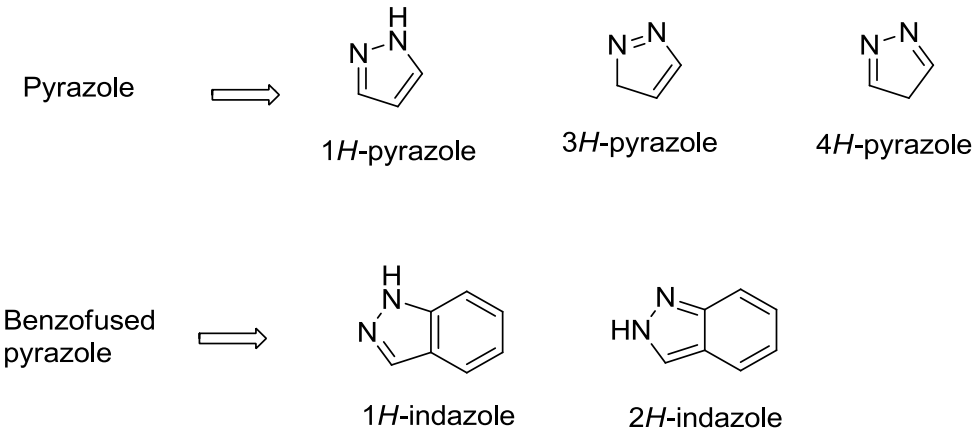

Figure 2: Typical structures of Pyrazole Type Compounds (Kumar *et al.* 2013:248)

When it is fused to an aromatic ring, it is called indazole (Pal *et al.* 2012:98). Phenazon (Figure 3) was the first pyrazole compound that was discovered and used to alleviate pain, reduce inflammation and manage fever (Kucukguzel *et al.* 2015:786).

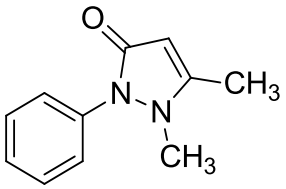

Figure 3: Phenazon

This discovery sparked and increased interest in developing better derivatives with improved biological activity. Consequently, a vast number of pyrazoles were synthesized which possess important pharmacological activity (Abrigach *et al.* 2016:292).

Studies on the biochemical activity of pyrazoles revealed interesting inhibitory activity against BRAFV600E, Epidermal Growth Factor Receptor (EGFR), ROS Receptor Tyrosine Kinase and Aurora-A kinase (Kucukguzel *et al.* 2015:786). Some important drugs are presented in Figure 4.

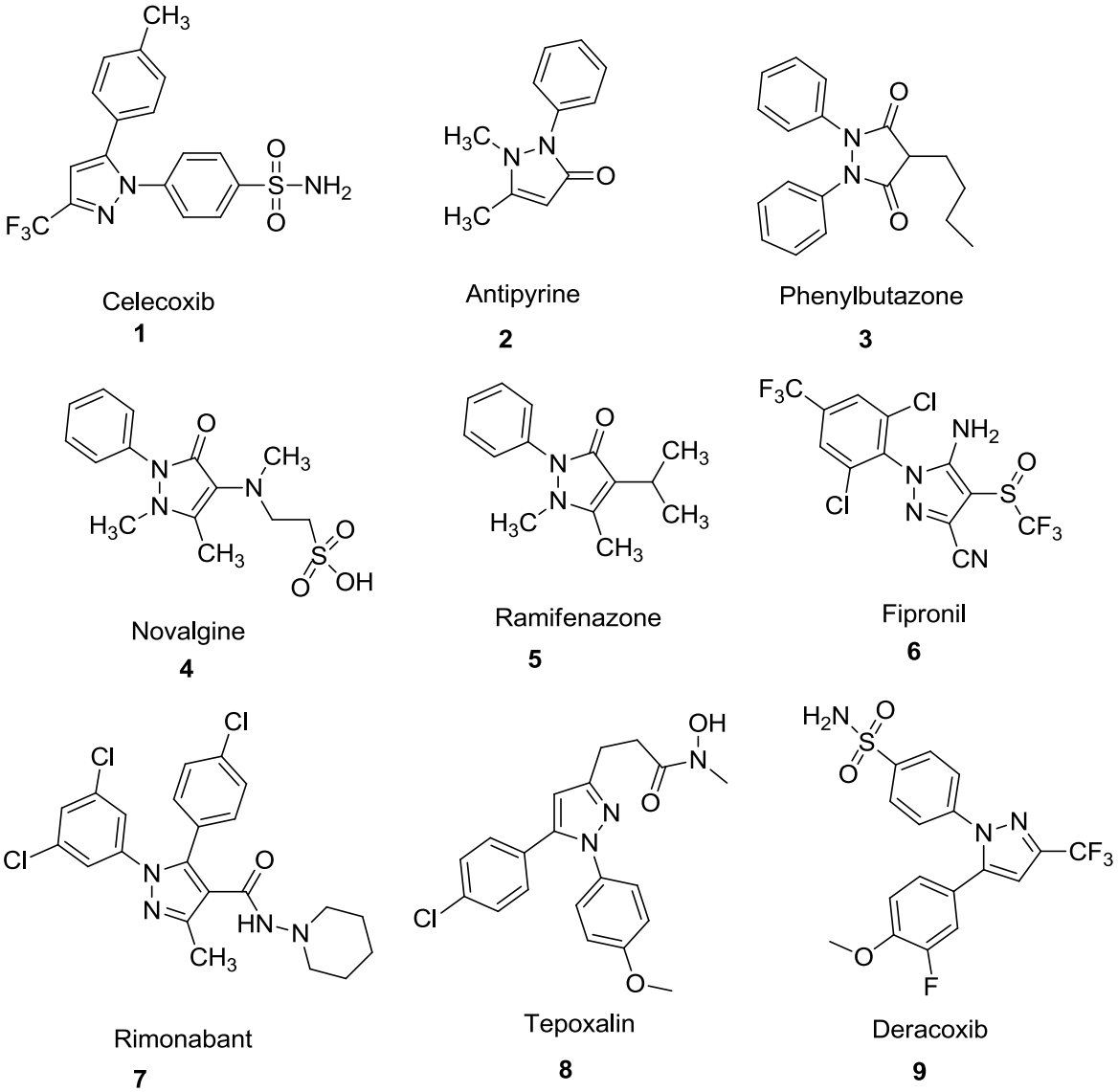

Figure 4: Some important drugs containing the pyrazole scaffold (Kucukguzel *et al*. 2015:786)

2.2.1.1 Pyrazole as Anticancer Drugs

There is currently a more vigorous search for anticancer drugs because of the increased incidence in cancer and its high mortality rate. Also, the current regiment of drugs cause side effects to patients. This problem has not been resolved. In the last decade, thousands of pyrazole derivatives were synthesized and evaluated against cancer. A majority of these drugs exhibits potent activity against cyclin-dependent kinase (CDKs) which are responsible for eukaryotic cell cycle regulation (Balbi *et al.* 2011:5293). Some typical examples of pyrazole molecules that inhibit various enzymatic systems are presented in Figure 5.

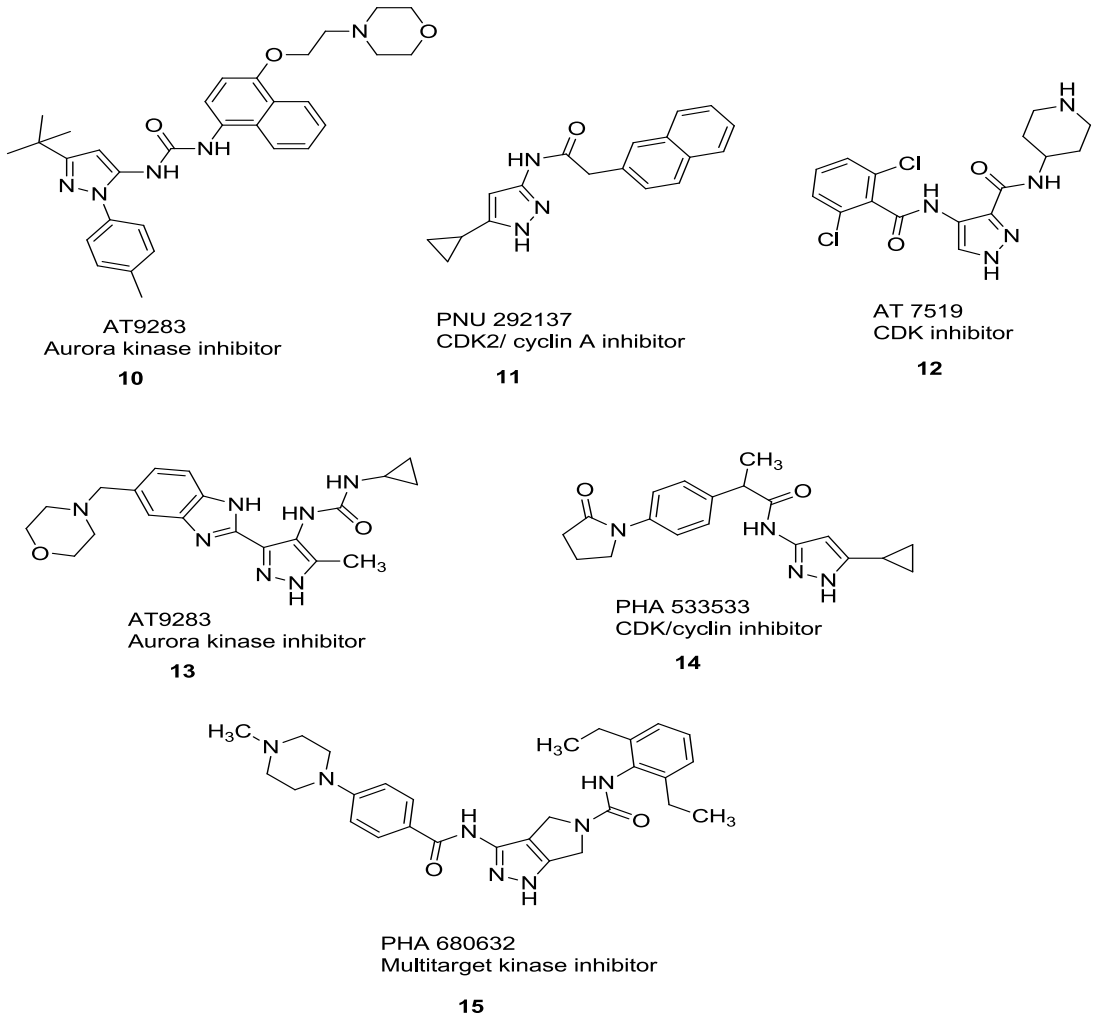

Figure 5: Some selected anticancer pyrazole based drugs (Nitulescu *et al* 2013:21805 and Nitulescu *et al.* 2010: 4914)

Pyrazole-scaffolds which contain a urea moiety also exhibit promising anti-proliferative effects by inhibiting Aurora kinase activity. Most protein kinases are targets of pyrazoles which

inhibits the transmuting of growth factor-beta type I receptor kinase sphere. Other interesting protein kinase inhibitors are the amino-pyrazoles which can inhibit Aurora kinases and thus induce apoptosis in tumor cells. In-spite of these good reports, there is a scope for exploring new pyrazoles as anticancer agents (Nitulescu *et al.* 2013:21805, Raffa *et al.* 2015:732, Saleh *et al.* 2016:199 & Kasiotis *et al.* 2014:1).

2.1.1.2 Pyrazole as Antibacterial Agents

In the past decades microbial diseases have been the main source of morbidity, responsible for several toxicity syndromes and even the recurrence of disease. [B'Bhatt *et al*. 2017: S1590]

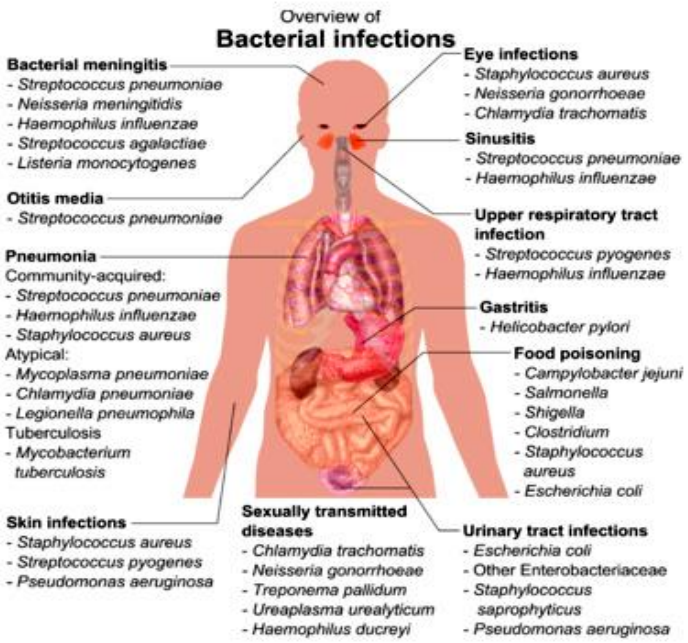

Figure 6: Overview of bacterial infections [Whitman. 1998: 6578]

Compounds containing the pyrazole scaffold possess remarkable antibacterial activity and diverse bio-activities (Malladi *et al*. 2012: 43; Amir *et al*. 2012: 1261; Jamwal *et al*. 2013: 114; Kumar *et al*. 2016: 614; B'Bhatt *et al*. 2017: S1590;). Some effective pyrazoles are presented in Figure 7.

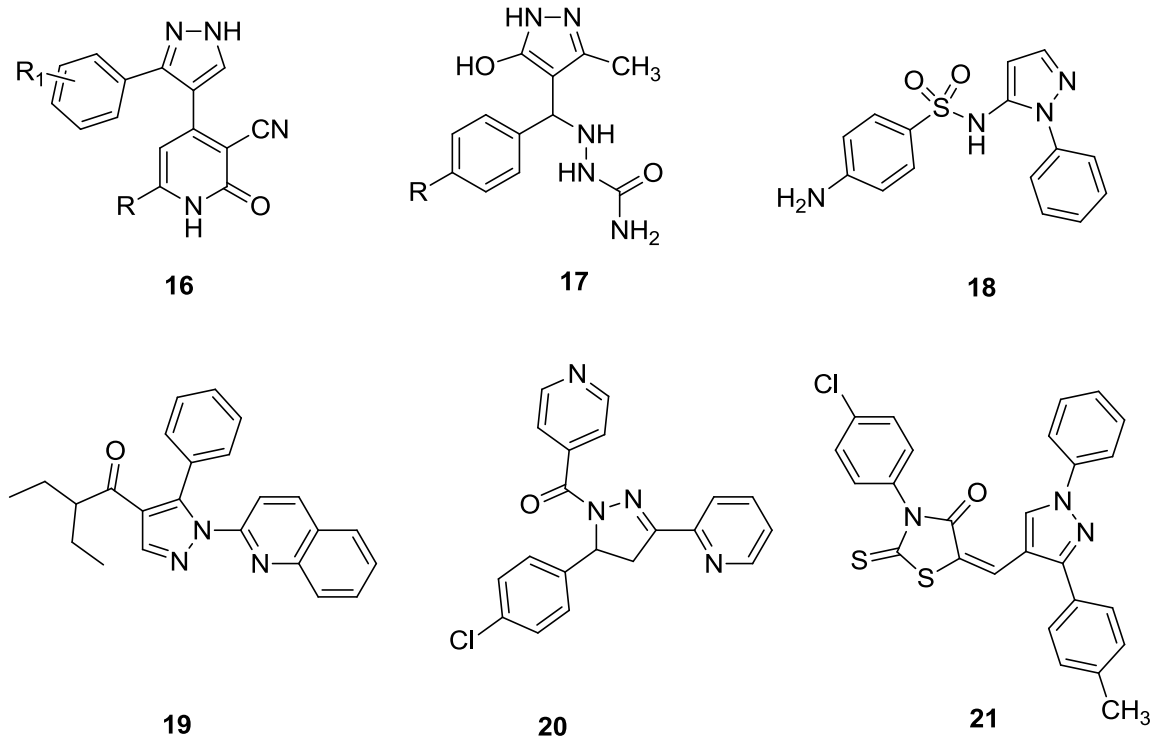

Figure 7: Some antibacterial drugs bearing the pyrazole moiety.

2.3.2 The Naphthyridines as Modern Drugs

Naphthyridine is a 6-membered heterocyclic system containing two fused pyridine rings with nitrogen atom in both rings (Saeed *et al.* 2011:66). The location of the nitrogen atom can vary resulting in the formation of six possible isomers (Figure 8). Various naphthyridines containing nitrogen atom at positions 1, 6; 1, 7; 2, 6; 2, 7 were reported (Litvnov *et al.* 2006:189 and Madaan *et al*. 2015:837)

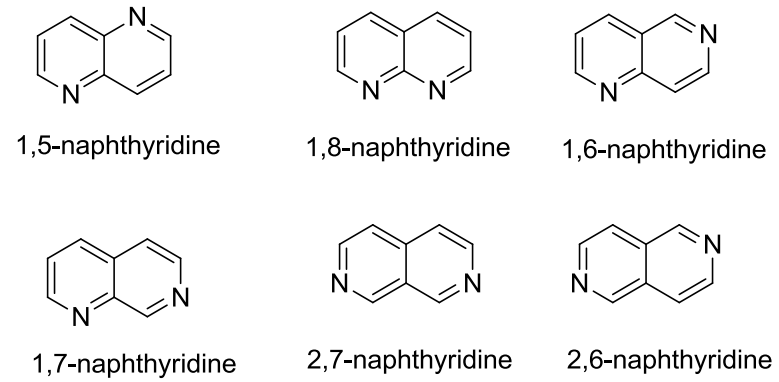

Figure 8: Naphthyridines scaffolds (Litvnov *et al.* 2006:189 & Madaan *et al*. 2015:837)

From all the isomers, the 1, 8-naphthyridines is the most studied because they display the best antibacterial property as illustrated by nalidixic acid **24**. (Wiik 2012: 14) In addition, they are used as an inhibitor of farnesyl transferase protein and as antimalarial agents at sub-micro-molar levels (Olepu *et al.* 2008:494). They can be used as an HIV integrase inhibitor since they significantly decrease the viral load and increase CD4 cell count in patients infected with HIV (Melamed *et al.* 2008:5307 & Nagasawa *et al.* 2011:760). Typical examples of naphthyridines which serve as HIV integrase inhibitors are **22, 26** and **28** (Figure 9).

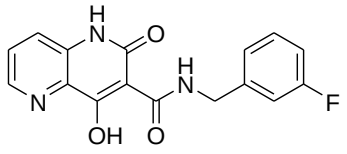

Inhibits HIV integrase and HIV replicant

22

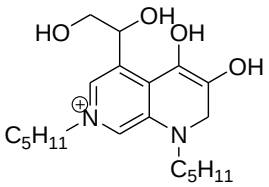

Antidiabetic drug

23

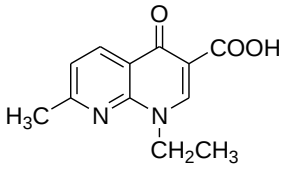

Strong antibacterial

24

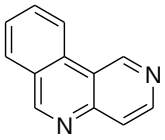

Derivatives for male impotence and female sexual dysfunction

25

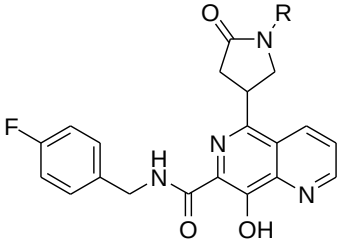

HIV-integrase inhibitor

26

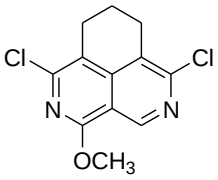

Treatment of asthma and lowering blood pressure

27

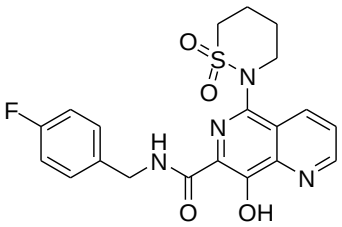

HIV-integrase inhibitor

28

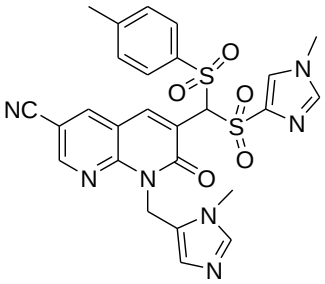

Malaria inhibitor

29

Figure 9: Some selected naphthyridines derivative which are used as drugs (Egbertson *et al.* 2007:1392, Srivastava *et al.* 2007:685 and Wiik 2012:14)

2.3.2.1 Naphthyridines as AntiCancer Drugs

The naphthyridines are currently investigated because of their ability to either intercalate amongst the base pairs of DNA or interfere with the activeness of the enzyme topoisomerase II that leads to the breaking and emancipating of DNA strands (You *et al.* 2009:5649, Shaabani *et al.* 2009:6355; Awasthi *et al.* 2014:710 and Alonso *et al.* 2016:179). The [1, 8] naphthyridines block microtubule networks which impairs mitotic spindle formation thereby leading to mitotic catastrophy (Capozzi *et al* 2012:653). Some synthesized [1.8] naphthyridines such as **30**, SNS-595 **31** and AT-3639 **32** (Figure 10) exhibit promising anticancer activity (Tomita *et al.* 2002:5564; Srivasta *et al.* 2007:6660 and Wu *et al.* 2015:3251). Furthermore, the [1, 8] naphthyridine SNS-595 **31** (Figure 10) are currently in the second phase of clinical trials for cancer chemotherapy: these derivatives can be further modified to improve their activity against cancer (Kumar *et al.* 2009:3356).

Studies on the structural activity relationships (SAR) of naphthyridines indicated that correct structure modification can enhance their anticancer activity: e.g. the 2-thiazolyl group when attached at the N-1 position becomes the main moiety displaying antitumor activity. It was reported (Tomita *et al*. 2002: 5564-5575) that the aminopyrrolidine functionality at position C-7, was more effective when compared with amine or thio-ether derivatives. These results prompted us to synthesize new compounds and evaluate them in commonly used biological systems.

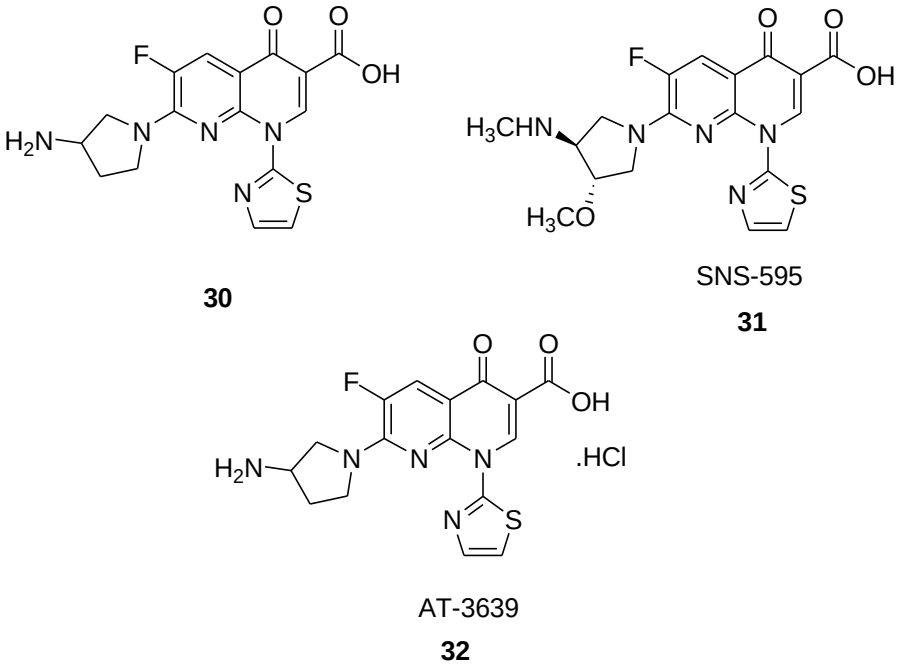

30

SNS-595

31

AT-3639

32

Figure 10: Some selected naphthyridines possessing anticancer activity (Tomita *et al.* 2002: 5564 and Srivasta *et al*. 2007: 6660).

2.3.2.2 Naphthyridines as Antibacterial Drugs

In 1962, during distillation of chloroquine, Lesher and co-workers [Lesher *et al*. 1962: 1063] discovered nalidixic acid **24** (Figure 9) as an antimalarial agent. This was the first [1, 8] naphthyridine that was used as an antibacterial agent to cure gram-negative urinary tract infections. This discovery catalyzed further discovery of other antibacterial [1, 8] naphthyridine compounds through synthesis. Some synthetic [1.8] naphthyridines which display antibacterial activities are presented in Figure 11 (Saundane *et al*. 2012: 1593 and Madaan *et al*. 2015:837).

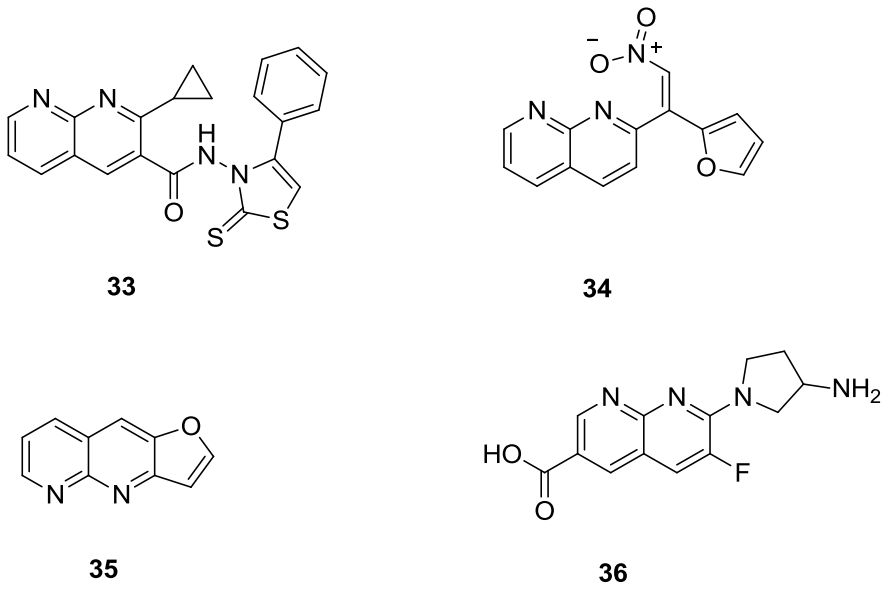

Figure 11: Other synthesized antibacterial [1.8] naphthyridine compounds

(Madaan *et al*. 2015: 837)

2.4 The Synthesis of Heterocycles

2.4.1 The Multi-Component Reaction

Multi-component reactions (MCRs) (Figure12) are used in accelerating drug discovery and exhibit tremendous superiority in contrast with the traditional synthetic methods. The reaction times are short, yields of products are high and regio-specific and stereo-specificity are evident (Khan *et al*. 2016: 42045). These reactions have also reduced the production of waste because of a decrease in the number of purification steps. All of these advantages offered by MCRs are due to the formation of numerous bonds in a one pot reaction. Hence, the desired product comprise all the substrates used as starting materials. MCR provides:

a) sequential formation of a number of bonds in a single step reaction
b) an increase in structural complexity of the product through systematic variation of the starting materials
c) flexibility in providing a wealth of novel products.

Today most MCRs meet the desire for effectual high-throughput synthesis of compounds in a cost and time-effective method. Furthermore, the carbon-carbon, carbon-nitrogen and other carbon-heteroatom bonds are rapidly formed to produce new organic molecules (Shodhganga

2009: 1). Therefore, MCRs have revolutionized heterocyclic synthesis and offered an efficient protocol in combinational chemistry which play a huge role in drug development to access new bioactive compounds.

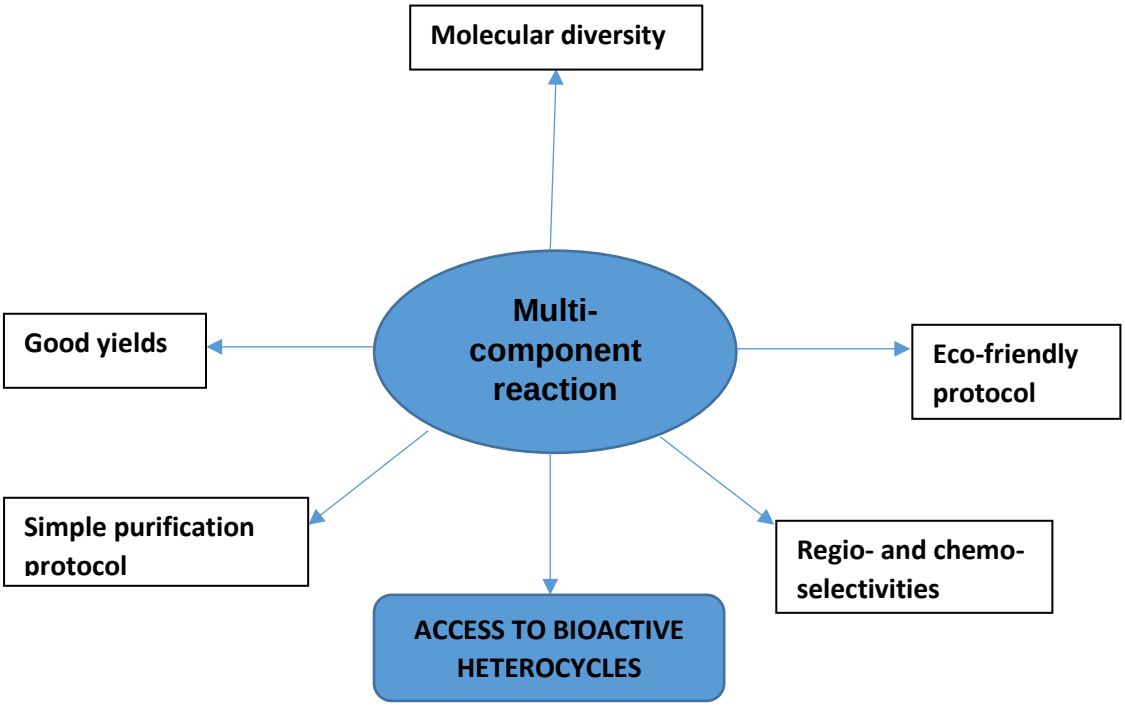

Figure 12: MCRs an efficient protocol for development of new bioactive molecules

The evolution of MCRs was dated to the pre-biotical formation of adenine through the condensation of five molecules of HCN. This reaction is catalyzed by ammonia (Scheme 1) (Katritzky 2004: 2125-2126). However, it was only in 1850 that MCRs was introduced in synthesis: Strecker in 1850 reported the formation of alpha-amino nitriles from aldehydes, HCN and amine using a one pot reaction (Scheme 2). Subsequent hydrolysis generated amino acids.

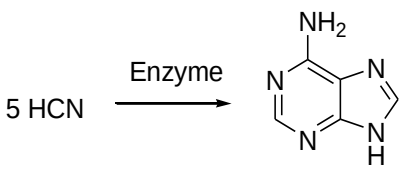

37

Scheme 1: Prebiotic synthesis of adenine **37** (Duque *et al.* 2010: 2318)

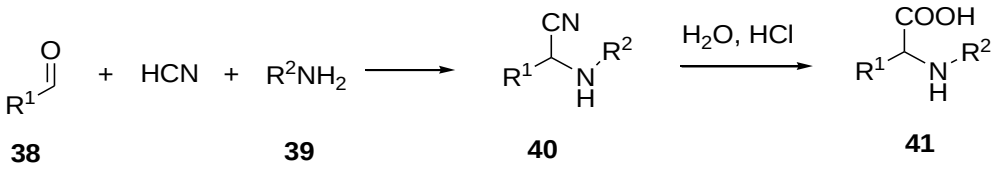

Scheme 2: The Strecker Synthesis of Alpha-amino Acids **41**

(Duque *et al.* 2010: 2318)

In 1882, Hantzsh used MCRs to synthesize symmetrically substituted dihydropyridines **45** from aldehydes **42,** two equivalents of beta-ketoesters **43** and ammonium acetate **44** (Katritzky 2004:2125) and Duque *et al.* 2010: 2318).

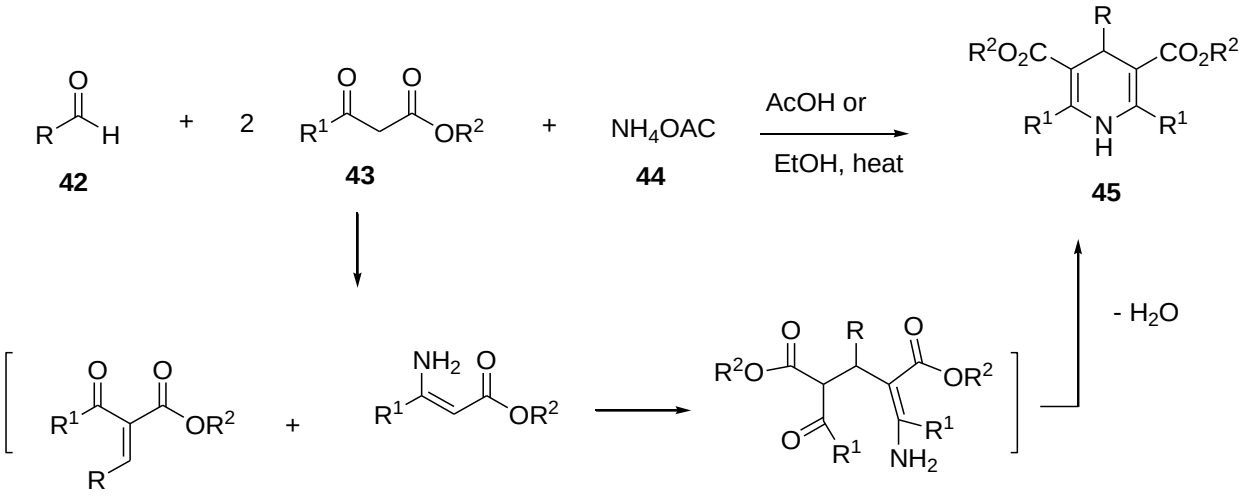

Scheme 3: General reaction of the Hantzsch's 1,4-DHPs synthesis **45**

In 1893, Biginelli synthesized multi-functionalized dihydropyrimidines **49** through acid-catalyzed cyclo-condensation of beta-keto-esters **46**, benzaldehyde **47** and urea **48 (**Duque *et al.* 2010: 2318 and Nefzi *et al.* 1997:449).

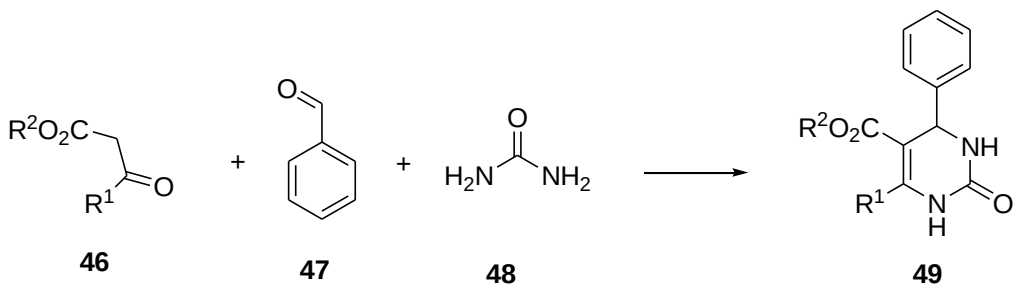

Scheme 4: The Biginelli Synthesis of Dihydropyrimidines **49**

Another important application of MCRs was through Robinson annulation synthesis of the alkaloid tropinone **53** (Scheme 5). This synthesis was a one pot reaction of succinic dialdehyde **50**, methyl amine **51** and the calcium salt of acetonedicarbocylic acid **52** (Ambhaikar 2004: 6109). This reaction encouraged synthetic organic chemists to use MCRs to mimic the proficiency displayed in nature's biosynthetic processes. MCRs was recognized as a powerful protocol for rapid discovery of diverse and complex molecules. Hence this approach has an enormous impact on improving the capacity and re-shaping retrosynthetic analysis by providing new innovative transformations in short sequences (Isambert *et al*. 2008: 8444).

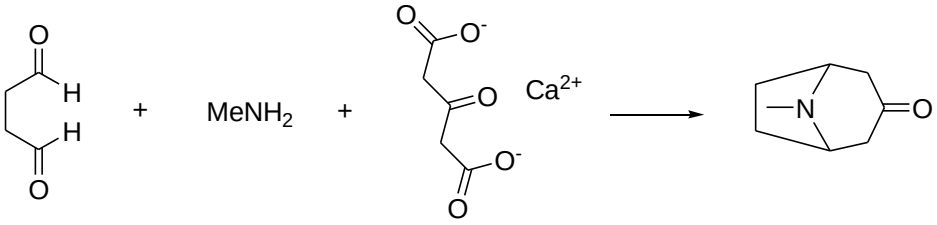

50 **51** **52** **53**

Scheme 5: The Robinson Synthesis of Tropinone **53**

2.4.2 Synthesis of Five Membered Nitrogen Based Heterocycles

The synthesis of 2,3-dioxopyrrolidine derivatives **55** (Scheme 6) was carried out by MCR. Herein an equivalent amount of ethyl oxaloacetate **54,** either ammonia or primary amine **51** and benzaldehyde **47**, in presence of ethanol or acetic acid, was used. This methodology permits the synthesis of other small functionalized molecules which may have potential biological activity.

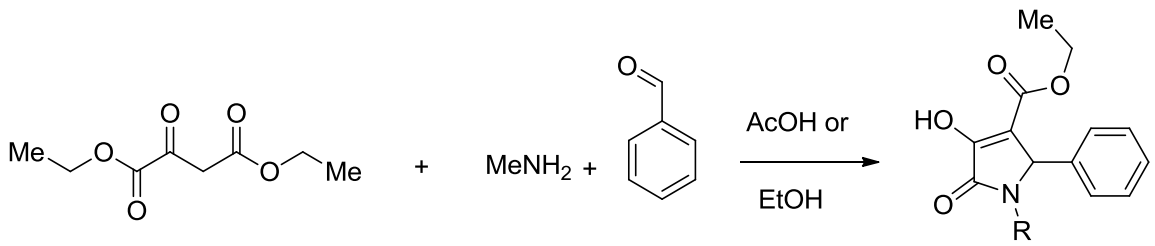

54 **51** **47** **55**

Scheme 6: Three component synthesis of 2, 3-dioxopyrrolidine derivatives **55**

Among the various synthetic methods reported for accessing functionalized pyrazole, the most well-known method is the Knorr synthesis (discussed in Chapter Five). The disadvantage of this methodology is poor regio-selectivity when unsymmetrical β-keto ester are used. However, the use of MCRs with an aldehyde **56**, phenylhydrazine **57** and β-keto ester **58**, using ytterbium perfluorooctanoate as heterogenous catalyst enabling solvent-free conditions, yielded pyrazole derivatives **59** & **60** in high yield (Scheme 7).

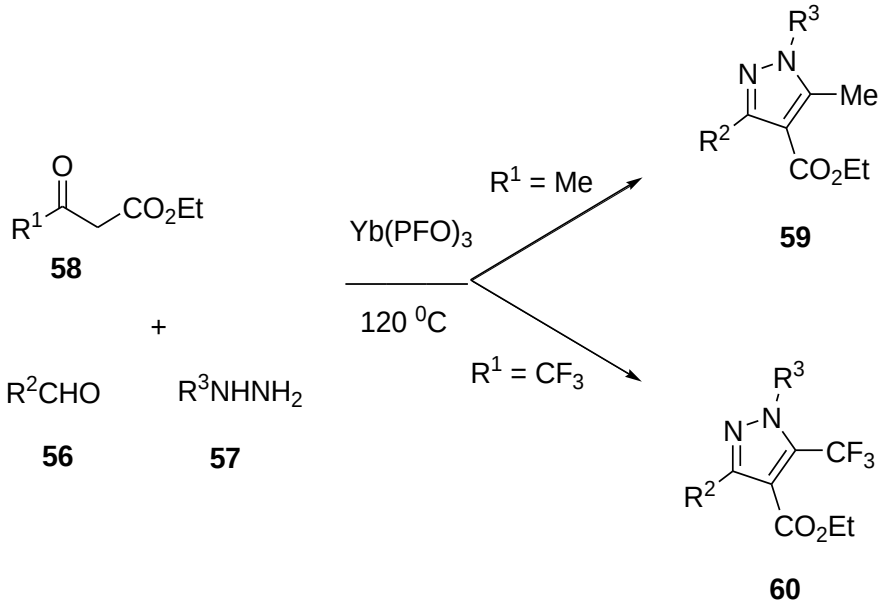

Scheme 7: [$Yb(PFO)_3$]-catalyzed three component synthesis of substituted pyrazoles (Duque *et al.* 2010: 2318)

The scope to develop new and simpler methods for accessing diverse substituted pyrazoles from readily available starting materials is unlimited use with deserves future investigation. In addition, compounds containing the pyrazole scaffold display important pharmacological activity. Therefore, the synthesis of novel pyrazole derivatives by MCRs is important (Duque *et al.* 2010: 2318; Ivantsova *et al.* 2012:626 and Driowya *et al.* 2016:1).

2.4.3 Synthesis of Six Membered Nitrogen Based Heterocycles

Dondoni and co-workers, 2010 reported organo-catalyzed type of Hantzsch reaction using C-glycosyl aldehydes **62**. This reaction was promoted by L-proline and continues through the condensation of an *in situ* produced alkylidene malonate with enaminoester derivatives **63**, subsequently cyclo-dehydration to produce symmetrically and unsymmetrically substituted 1,4-dihydropyridine **64**.

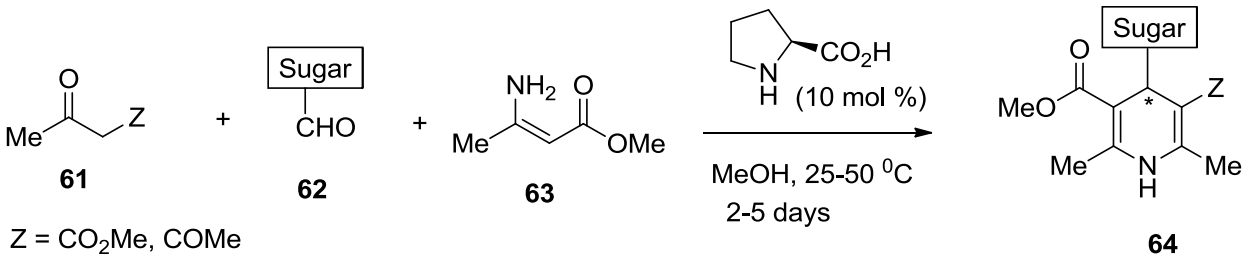

Scheme 8: Organo-catalyzed asymmetric three-component Hantzsch-like reaction (Duque *et al.* 2010: 22318)

Further development to MCRs was made by generating a six membered heterocyclic acridine derivative **67** from two equivalents of 1,3-cyclohexanedione instead of beta-keto-esters (Scheme 9). However when only one equivalent of each cyclic 1, 3-dicarbonyl **65** and beta-ketoester **68** was used, an unsymmetrical product **69** was formed (Duque *et al.* 2010: 2318).

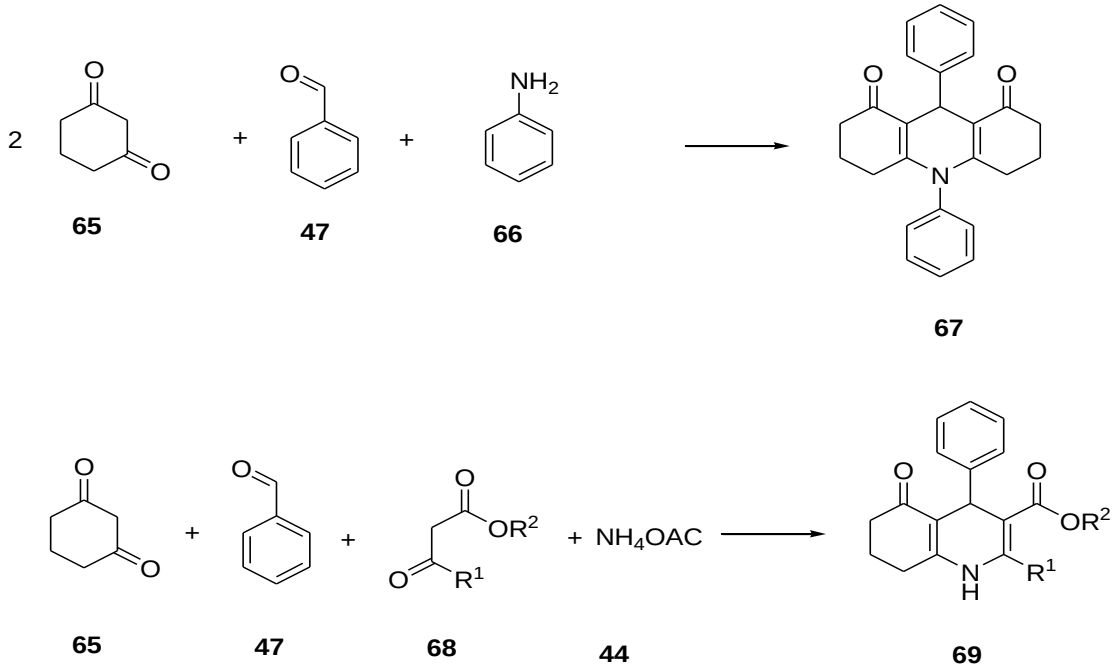

Scheme 9: Synthesis of acridines **67** via Hantzsch reaction (Duque *et al.* 2010: 2318)

The Hantzsch approach was further explored during the synthesis of pyrazoloiquinolones derivatives **72**. It was observed that regio and chemo-selectivity of fused heterocyclic skeletons depended on base catalysis: the alkalinity and nucleophilicity of the selected base were vital for MCR. In the presence of triethyl amine, the reaction proceeds through the Knoevenagel, Michael addition and cyclodehydration sequence. In the presence of a strong bulky base such as potassium tert-butoxide, the reaction occurs through ring opening followed by intramolecular trans-amidation to produce angular fused systems (Duque *et al.* 2010: 2318). These reactions indicated that a small amount of catalyst was required.

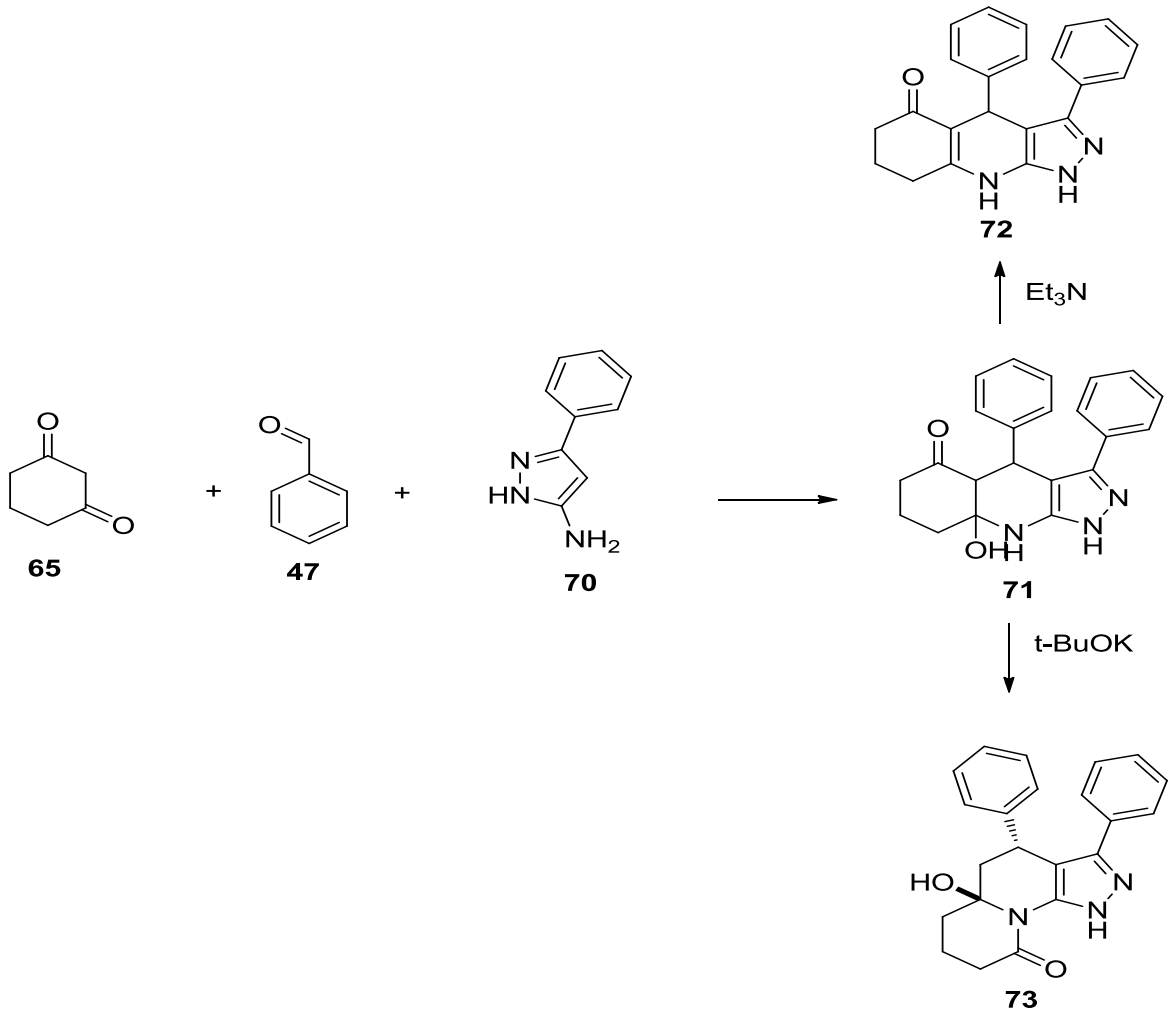

Scheme 10: Regio and chemoselective access to tricyclic heterocycles (Duque *et al.* 2010: 2318)

Generally, the introduction of MCRs has revolutionized and catalysed the development of heterocyclic chemistry. Diverse types of functionalized molecules such as quinoline systems were available and can be further modified by MCRs. Conventional approaches of constructing quinoline systems were based on Skraup and Doebner-Miller methods (Yamashkin *et al* 2006:701). However, MCRs allows access of many strategies to synthesize highly functionalized quinoline derivatives such as those presented in Schemes 11 & 12.

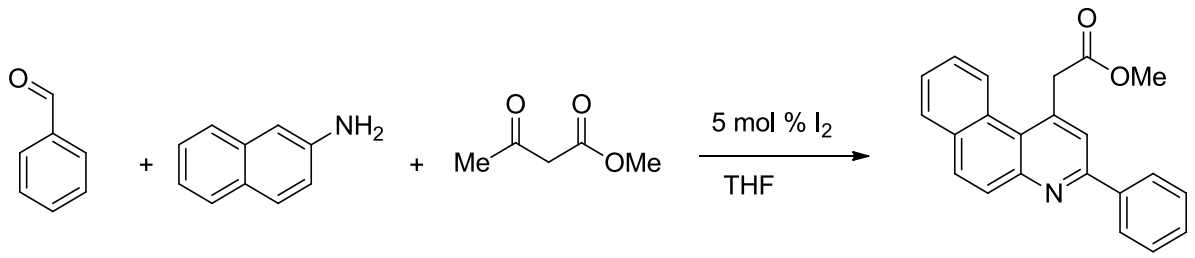

47 **73** **75** **76**

Scheme 11: Iodine catalyzed three component synthesis of benzo[*f*]quinolone derivatives **76**

(Yamashkin *et al* 2006:701)

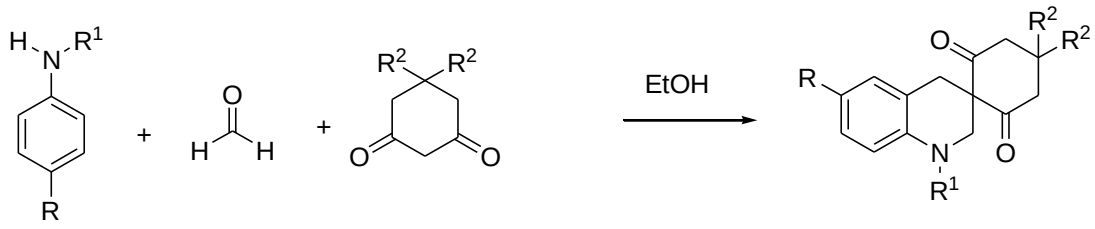

77 **78** **79** **80**

Scheme 12: Multi-component synthesis of 3-spirosubstituted tetrahydroquinolines **80**

(Yamashkin *et al* 2006:701)

2.5 Some Important Named Multi-Component Reaction used in This Study

Named reaction such as the domino Knoevenagel condensation - Michael addition, Povarov's reaction [4+2] & [3+2] are particularly important for the synthesis of novel heterocyclic systems.

2.5.1 Domino Knoevenagel Condensation-Michael Addition

The domino reaction is a series of consecutive reactions where the subsequent transformation occurs only if the correct functional group is present in the product of the previous reaction (Tietze 1996: 115). The Knoevenagel condensation involves the condensation of either an aldehyde or ketone with an active methylene compound: organic and inorganic bases are used. This reaction is the most effective method for synthesizing α, β-unsaturated di-carbonyl compounds or related compounds. Scheme 13 illustrates the mechanism of the domino Knoevenagel condensation-Michael addition reaction in the synthesis of pyrrolidines **85**.

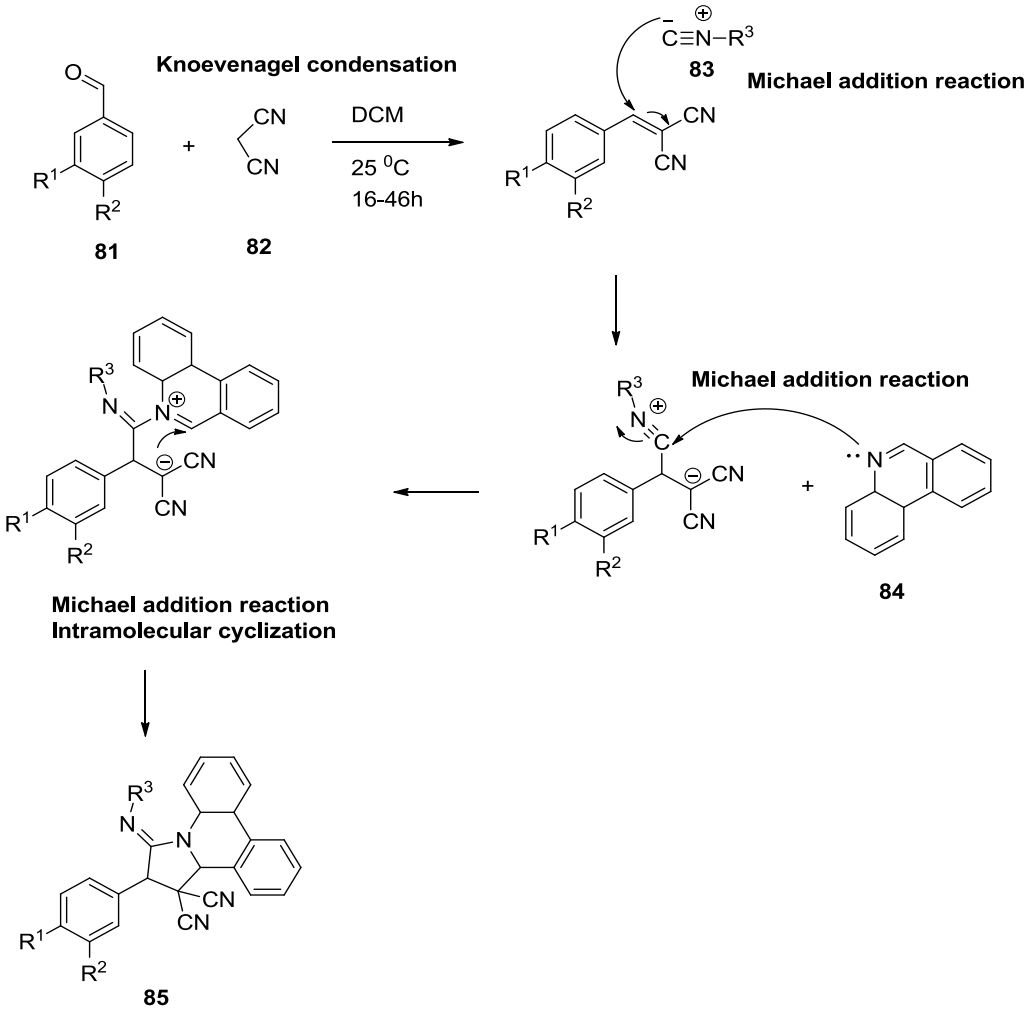

Scheme 13: Knoevenagel condensation-Michael addition synthesis of nitrogen poly substituted pyrrolidines **85** (Tietze 1996: 115).

Nowadays the Knoevenagel condensation is very popular and is widely applied in modern organic synthesis because it promotes the domino process by generating the reactive α, β-unsaturated di-carbonyl moieties which can trigger the consecutive reaction. This efficacy is due to the high reactivity of α, β-unsaturated di-carbonyl compounds. The Knoevenagel condensation is frequently coupled with Michael addition reaction. A Michael addition reaction occurs when the enol or nucleophile is added onto α, β-unsaturated di-carbonyl to produce a new covalent bond through beta carbon because of its electrophilicity. In the above scheme, the Knoevenagel condensation triggers the domino reaction and allows for the efficient synthesis of complex heterocyclic compounds. Further interesting developments for the synthesis of heterocyclic systems were reported: recently Kommidi and co-workers, 2016

reported the synthesis of thiazolidine 2, 4-dione azepine **89** derivatives through a one pot reaction through Domino Knoevenagel condensation-Michael addition (Scheme 14) (Kommidi *et al.* 2016: 1071).

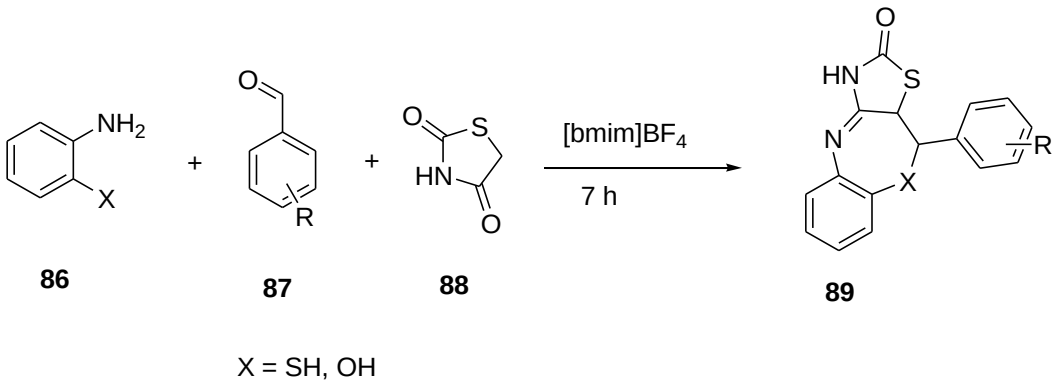

86 **87** **88** **89**

X = SH, OH

Scheme 14: Synthesis of thiazolidine 2, 4-dione azepine derivatives **89**

(Kommidi *et al.* 2016: 1071).

2.5.2 The Povarov's Reaction

Povarov's reaction is a tool for the creation of nitrogen heterocycles with high molecular diversity that can provide broader industrial application (Alonso *et al* 2017: 6379). This reaction involves an imine and alkene and can be described as conforming to the general π 4s + 2s π cycloaddition reaction. In the Povarov's reaction, the [4+2] cyclo-addition reaction occurs between the N-aryl imines (Schiff's bases, diene) and activated alkenes (electron rich dienophiles) such as vinyl enol ethers, vinyl enamides, vinyl sulfide, cyclopentadiene, indene, alkynes and enamines. N-aryl imines are readily prepared by reacting an aldehyde or ketone with amine and therefore a variety of N-aryl imines can be prepared. However, the reaction is more convenient when using an N-aryl imine as the diene in conjunction with activated alkenes as the dienophiles (Figure 13) (Buonora *et al.* 2001: 6099 and Kouznetsov *et al*. 2009: 2721).

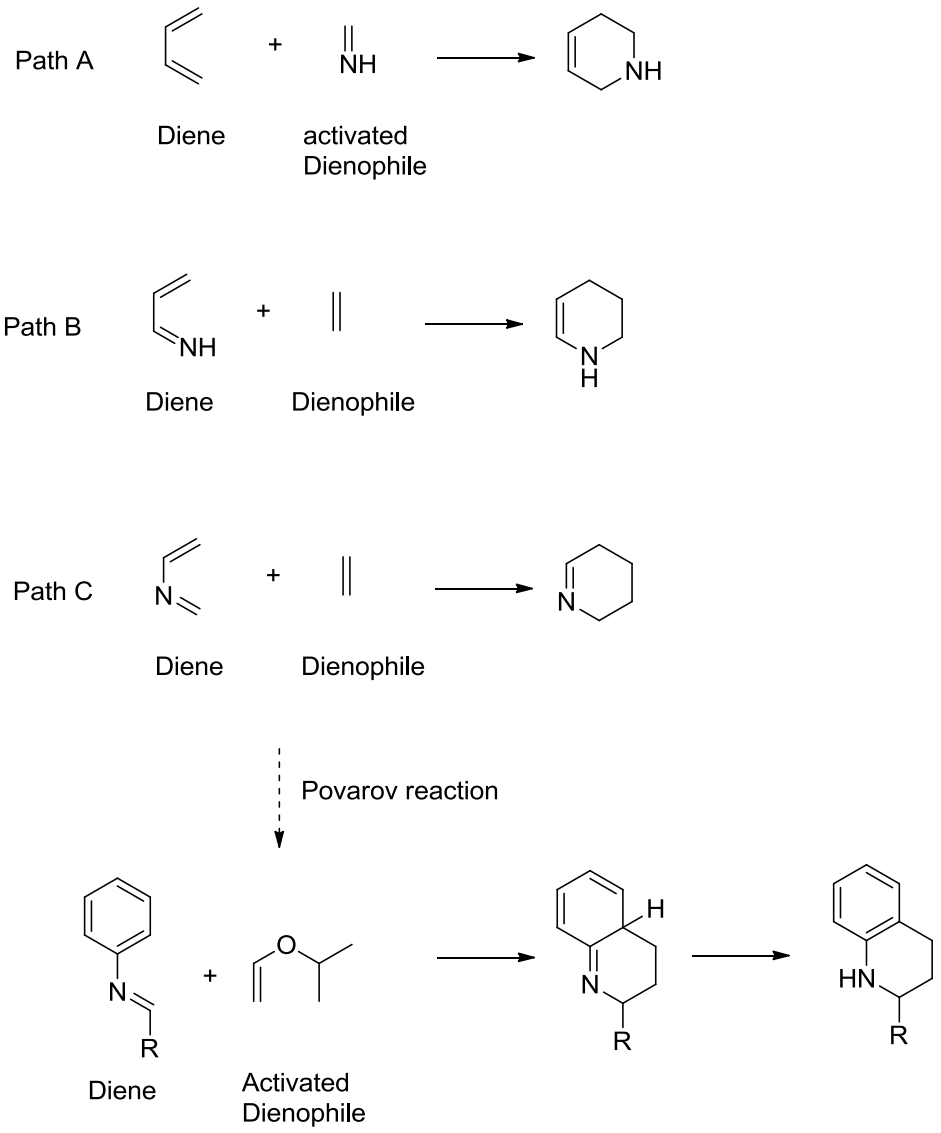

Figure 13: Povarov's reaction pathways (Buonora *et al* .2001: 6099 and Kouznetsov *et al* .2009: 2721).

A more in-depth literature survey on the domino Knoevenagel condensation-Michael addition and Povarov reactions are presented in Chapters 3 and 5, respectively.

2.6 References

1. Sharma V., Kumar P. and Pathak D. 2010. Biological importance of the indole nucleus in recent years. *Journal of Heterocyclic Chemistry*, 47: 491-502.
2. Clark J.S. 2011. Heterocyclic chemistry. http://www.chem.gla.ac.uk/staff/stephenc/UndergraduateTeaching.html
3. Suvarana A.S. 2015. A review on synthetic heterocyclic compounds in agricultural and other applications. *International Journal of Pharmaceutical Technology Research*, 8(8): 170-179.
4. Butkovic K., Marinic Z., Molcanov K., Kojic-Prodic B. and Sindler-Kulyk M. 2011. Photochemical and thermal intramolecular 1, 3-dipolar cycloaddtion reactions of new *o*-stilbenemethylene-3-sydnones and their synthesis. *Beilstein Journal of Organic Chemistry*, 7: 1663-1670.
5. Campaigne E.1986. Adrien Albert and the rationalization of heterocyclic Chemistry. *Journal of Chemical Education*, 63(10): 860-863.
6. Arora P., Arora V., Lamba H.S. and Wadhwa D. 21012. Importance of heterocyclic chemistry. *International Journal of Pharmaceutical Sciences and Research*, 3(9): 2974-2954.
7. Martins P., Jesus J., Santos S., Raposo L.R., Roma-Rodriques C., Baptista P.V. and Fernades A.R. 2015. Heterocyclic anticancer compounds: Recent advances and the paradigm shift towards the use of nanomedicine's tool box. *Molecules*, 20: 16852-16891.
8. Cabrele C. and Reiser O. 2016. The modern face of synthetic heterocyclic chemistry. *Journal of Organic Chemistry*, 81: 10109-10125.
9. Saini M.S., Kumar A., Dwivedi J. and Singh R. 2013. A review: Biological significances of heterocyclic compounds. *International Journal of Pharma Sciences and Research*, 4(3): 66-77.
10. Pal D., Saha S., and Singh S. 2012. Importance of pyarzole moiety in the field of cancer. *International Journal of Pharmacy and Pharmaceutical Sciences*, 4(2): 98-104.
11. Kumar H., Saini D., Jain S. and Jain N. 2013. Pyrazole scaffold: A remarkable tool in the development of anticancer agents. *European Journal of Medicinal Chemistry*, 70: 248-258.
12. Abrigach F. and Touzani R. 2016. Pyrazole derivatives with NCN junction and their biological activity. *Medicinal chemistry*, 6(5): 292-298.

13. Kucukguzel S.G. and Senkardes S. 2015. Recent advances in bioactive pyrazole. *European Journal of Medicinal Chemistry*, 97: 786-815.
14. Balbi A., Anzaldi M., Maccio C., Aiello C., Mazzei M., Gangemi R., Castagnola P., Miele M., Rosano C. and Viale M. 2011. Synthesis and biological evaluation of novel pyrazole derivatives with anticancer activity. *European Journal of Medicinal Chemistry*, 46: 5293-5309.
15. Nitulescu G.M., Draghici C. and Olaru O.T. 2013. New potential antitumor pyrazole derivatives: Synthesis and cytotoxic evaluation. *International Journal of Molecular Sciences*, 14: 21805-21818.
16. Nitulescu G.M., Draghici C. and Missir A.V. 2010. Synthesis of new pyrazole derivatives and their anticancer evaluation. *European Journal of Medicinal Chemistry*, 45: 4914-4919.
17. Raffa D., Maggio B., Raimondi M.V., Cascioferro S., Plescia F., Cancemi G. and Daidone Giuseppe. 2015. Recent advanced in bioactive systems containing pyrazole fused with a five membered heterocycle. *European Journal of Medicinal Chemistr*y, 97: 732-746.
18. Saleh A.M, Taha M.O., Aziz M.A., Al-Qudah M.A., AbuTayeh R.F. and Rizvi S.A. 2016. Novel anticancer compound [trifluoromethyl-substituted pyrazole N-nucleoside] inhibits FLT3 activity to induce differentiation in acute myeloid leukemia cells. *Cancer Letters*, 373: 199-208.
19. Kasiotis K.M., Tzanetou E.N. and Haroutounian S.A. 2014. Pyrazole as potential anti-angiogenesis agents: a contemporary overview. *Frontiers in chemistry*, 2(78): 1-7.
20. B'Bhatt H.and Sharma S. 2017. Synthesis and antimicrobial activity of pyrazole nucleus containing 2-thioxothiazolidin-4-one derivatives. *Arabian Journal of Chemistry*, 10: S1590-S1596.
21. Jamwal A., Javed A. and Bhardwaj V. 2013. A review on pyrazole derivatives of pharmacological potential. *Journal of Pharmaceutical and Biosciences*, 3: 114-123.
22. Amir M., Javed S.S. and Hassan M.Z. 2012. Synthesis and antimicrobial activity of pyrazolinones and pyrazoles having benzothiazole moiety. *Medicinal Chemistry Research*, 21: 1261-1270.
23. Kumar R.S., Arif I.A., Ahmed A. and Idhayadhulla A. 2016. Anti-inflammatory and antimicrobial activities of novel pyrazole analogues. *Saudi Journal of Biological Sciences*, 23: 614-620.

24. Shridhar M., Arun M.I., Peethambar S.K., Ganesh B.M. and Palusa S.G., 2012. Synthesis and anti-microbial activity of some new pyrazole containing cyanopyridone derivatives. *Der Pharma Chemica*, 4(1): 43-52.
25. Saeed M.S., Elerafi M.G. and Mohamed R. 2011. Synthesis of Benzo-fused six membered aromatic heterocycles. *Pelagia Research Library*, 2(1): 66-69.
26. Litvinov V.P. 2006. Advances in the chemistry of naphthyridines. Advances in *Heterocyclic Chemistry*, 91: 189-197.
27. Wiik J.2012. Naphthyridine based molecular switches: 12-14.
28. Olepu S., Suryadevara P.K., Rivas K., Yokoyama K., Verlinde C.L.M.J., Chakrabarti D., Van Voorhis W.C. and Gelb M.H. 2008. 2-Oxo-tetrahydro-1, 8-naphthyridines as selective inhibitors of malarial protein farnesyltransferase and as anti-malarials. *Bioorganic and Medicinal Chemistry Letters*, 18: 494-497.
29. Melamed J.Y., Egbertson M.S., Varga S., Vacca J.P., Moyer G., Gabryelski L., Felock P.J., Stillmock K.A., Witmer M.V., Schleif W., Hazuda D.J., Leonard Y., Jin L., Ellis J.D. and Young S.D. 2008. Synthesis of 5-(1-H or 1-alky-5-oxopyrrolidini-3-yl)-8hydroxy-[1, 6]-naphthyridine-7-carboxamide inhibitors of HIV-1 integrase. *Bioorganic and Medical Chemistry Letters*, 18: 5307-5310.
30. Nagasawa J.Y., Song J., Chen H., Kim H.W., Blazel J., Ouk S., Groschel B., Borges V., Ong V., Yeh L.T., Girardet J.L, Vernier J.M., Raney A.K. and Pinkerton A.B. 2011. 6-Benzylamino 4-oxo-1, 4-dihydro-1,8-naphthyridines and 4-oxo-1,4-dihydroquinolines as HIV integrase inhibitors. *Bioorganic and Medicinal Chemistry Letters*, 21: 760-763.
31. Capozzi A., Mantuano E., Matarrese P., Saccomanni G., Manera C., Mattei V., Gambardella L., Malorni W., Sorice M. and Misasi R. 2012. A new 4-phenyl-1, 8-naphthyridine derivatives affects carcinoma cell proliferation by impairing cell cycle progression and inducing apoptosis. *Anti-cancer agents in Medicinal Chemistry*, 12: 653-662.
32. Kumar V., Jaggi M., Singh A.T., Madaan A., Sanna V., Singh P., Sharma P.K., Irchhaiya R., Burman A.C. 2009. 1, 8-Naphthyridine-3-carboxamide derivatives with anticancer and anti-inflammatory activity. *European Journal of Medicinal Chemistry*, 44: 3356-3362.
33. Egbertson M.S., Moritz H.M., Melamed J.Y., Han W., Perlow D.S., Kuo M.S., Embrey M., Vacca J.P., Zrada M.M., Cortes A.R., Wallace A., Leonard Y., Hazuda D.J., Miller M.D., Felock P.J., Stillmock K.A., Witmer M.V., Schleif W., Gabryelskis L.J., Moyer

G., Ellis J.D., Jin L., Xu W., Braun M.P., Kassahun K., Tsou N.N. and Young S.D. 2007. A potent and orally active HIV-1 integrase inhibitor. *Bioorganic and Medicinal Chemistry Letters*, 17: 1392-1398.

34. Srivastava S.K., Jha A., Agarwal S.K., Mukherjee R. and Burman A.C. 2007. Synthesis and structure-activity relationships of potent antitumor active quinoline and naphthyridine derivatives. *Anti-Cancer agents in Medicinal Chemistry*, 7: 685-709.
35. Alonso C., Fuertes M., Gonzalez M., Rubiales G., Tesauro C., Knudsen B.R. and Palacios F. 2016. Synthesis and biological evaluation of indeno[1,5]naphthyridines as topoisomerase I (TopI) inhibitors with antiproliferative activity. *European Journal of Medicinal Chemistry*, 115: 179-190.
36. You Q.D., Li Z.Y., Huang C.H., Yang Q., Wang X.J., Guo Q.L., Chen X.G., He X.G., Li T.K. and Chern J.W. 2009. Discovery of a novel series of quinolone and naphthyridine derivatives as potential Topoisomerase I Inhibitors by scaffolds modification. *Journal of Medicinal Chemistry*, 52: 5649-5661.
37. Shaabani A., Seyyedhamzeh M., Maleki A. and Behnam Maryam. 2009. A four-component, one-pot synthesis of highly substituted 1, 4-dihydro-1, 8-naphthyridine-3-carboxamides. *Tetrahedron Letters*, 50: 6355-6357.
38. Awasthi A., Lohani M., Singh M.K., Singh A.T. and Jaggi M. 2014. Pharmacokinetic evaluation of C-3 modified 1, 8-naphthyridine-3-carboxamide derivatives with potent anticancer activity: leading finding. *Journal of Enzyme Inhibition and Medicinal Chemistry*, 29(5): 710-721.
39. Srivastava S.K., Jaggi M., Singh A.T., Madan A., Rani N., Vishnoi M., Agarwal S.K., Mukherjee R. and Burman A.C. 2007. Anticancer and anti-inflammatory activities of 1, 8-naphthyridine-3-carboxamide derivatives. *Bioorganic and Medicinal Chemistry Letters*, 17: 6660-6664.
40. Tomita K., Tsuzuki Y., Shibamori K., Tashima M., Kajikawa F., Sato Y., Kashimoto S., Chiba K. and Hino K. 2002. Synthesis and structure-activity relationships of novel 7-substituted 1, 4-dihydro-4-oxo-1-(2-thiazolyl)-1,8-naphthyridine-3-carboxylic acids as antitumor agents. Part 1. *Journal of Medicinal Chemistry*, 45(25): 5564-5575.
41. Madaan A., Verma R., Kumar V., Singh A.T., Jain S.K. and Jaggi M. 2015. 1,8-Naphthyridine derivatives: A review of multiple biological activities. *Arch. Pharm. Life Sci*, 348: 837-860.

42. Saundane A.R. and Prabhaker W. 2012. Synthesis, antimicrobial and antioxidant activities of some indole analogues containing naphthyridine and pyrimidonaphthyridine systems. *Indian Journal of Chemistry*, 51B: 1593-1606.
43. Wu J.F., Liu M.M, Huang S.X. and Wang Y. 2015. Design and synthesis of novel substituted naphthyridines as potential c-Met kinase inhibitors based on MK-2461. *Bioorganic and Medicinal Chemistry Letters,* 25: 3251-3255.
44. Katritzky A.R. 2004. Introduction: Heterocycles. *Chemical Review*, 104 (5): 2125-2126.
45. Duque M.M.S., Allais C., Isambert N., Constantieux T. and Rodriguez J. 2010. Beta-diketo building blocks for MCRs-based syntheses of heterocycles. *Top Heterocycl Chem*: 2318-2335.
46. Nefzi A., Ostresh J.M. and Houghten R.A. 1997. The current status of heterocyclic combinatorial libraries. *Chemical Review*, 97: 449-472.
47. Ambhaikar N. 2004. Multi-component meeting: 6109-6111. www.scripps.edu/baran/images/grpmtgpdf/Ambhaikar_July_04.pdf.
48. Isambert N. and Lavilla R. 2008. Heterocycles as key substrates in multicomponent reactions: The fast lane towards molecular complexity. *Chemistry A European Journal*, 14: 8444-8454.
49. Khan M.M., Khan S. and Iqbal S.S. 2016. Recent developments in multi-component synthesis of structurally diversified tetrahydropyridines. *Royal Society of Chemistry*, 6: 42045-42061.
50. Shodganga 2009. Multi-componet reactions for the synthesis of diverse heterocyclic scaffolds:1-5. http://shodhganga.inflibnet.ac.in/bitstream/10603/13532/5/05_chapter%201.pdf
51. Yamashkin S.A. and Oreshkina E.A. 2006. Traditional and morden approaches to the synthesis of quinoline system by the Skraup and Doebner-Miller methods. *Chemistry of Heterocyclic Compounds*, 42(6): 701-718.
52. Tietze L.F. 1996. Domino reactions in organic synthesis. *American Chemical Society*, 96 (1): 115-136.
53. Ivantsova M.N., Tokareva M.I. and Mironov M.A. 2012. Multicomponent interphase synthesis of heterocyclic compounds. *Chemistry of Heterocyclic Compounds*, 48 (4): 584-600.

54. Driowya M., Saber A., Marzag H., Demange L., Benhida R. and Bougrin K. 2016. Microwave-assisted synthesis of bioactive six-membered heterocycles and their fused analogues. *Molecules*, 21(492): 1-55.
55. Kommidi D.R., Pagadala R., Varkolu M., Koorbanally N.A. and Moodle B. 2016. New route for the synthesis of thiazolidine 2,4-dione azepine derivatives. *Journal of Heterocyclic Chemistry,* 54: 1071-1076.
56. Buonora P., Olsen J.C. and Oh T. 2001. Recent developments in imino Diels-Alder reactions. *Tetrahedron*, 57: 6099-6138.
57. Kouznetsov V.V. 2009. Recent synthetic developments in a powerful imino Diels-Alder reaction (Povarov reaction): application to the synthesis of *N*-polyheterocycles and related alkaloids. *Tetrahedron*, 65: 2721-2750.
58. Duarte Y., Gutierrez M., Astudillo L., Morales J.A. and Valdes N. 2013. Synthesis of Bistetrahydroquinolines as potential anticholinesterasic agents by double Diels-Alder reactions. *Molecules,* 18: 12951-12965.
59. Parvatkar P.T., Kadam H.K. and Tilve S.G. 2014. Intramolecular Diels-Alder reaction as a key step in tandem or sequential processes: a versatile tool for the synthesis of fused and bridged bicyclic or polycyclic compounds. *Tetrahedron,* 70: 2857-2888.

Chapter Three

Multi-Component Synthesis of 4, 8, 8-Trimethyl-5-Phenyl-5, 5a, 8, 9-Tetrahydrobenzo[*b*] [1, 8] Naphthyridin-6(7H)-One Derivatives and their Biological Activity against A549 Lung Cancer Cells

3.1 Abstract

Cancer is one of the leading causes of mortality and existing drugs such as camptothecin and its derivatives are used in therapy. However, there are various side-effects and limitations and therefore alternative drugs are being investigated. A facile one-pot multi-component synthesis of novel [1, 8] naphthyridinones was achieved by using 2-aminopicoline, various benzaldehyde derivatives and dimedone by conventional heating under solvent-free conditions. Phosphotungstic acid was used as a catalyst. The compounds were identified as 4, 8, 8-trimethyl-5-phenyl-5, 5a, 8, 9-tetrahydrobenzo[*b*] [1, 8] naphthyridin-6(7H)-ones (TPDHBNS) by using spectroscopic techniques FT-IR, NMR, MS and elemental analysis.

TPDHBNS were screened for their anticancer activity against A549 lung cancer cells. Compounds **38c** and **38e** increased cell viability at 24 hours which exhibiting 94 % viable cells at 1000 µM. Both **38h** and **38f** initially caused A549 cell proliferation and thereafter resulted in a dose-dependent decrease with their IC_{50} calculated as 724.7 and 541.8 µM, respectively. The IC_{50} was determined for all the remaining compounds.

3.2 Background on Synthesis of Naphthyridines

Naphthyridines are important nitrogen-containing poly-heterocyclic compounds which occur either as natural products or are synthesized in the laboratory (Mogilaiah *et al.*, 2003: 636 and Hwang *et al.*, 2013: 517). They are planar molecules and are potentially good DNA intercalators against HIV/AIDS. They also possess a wide spectrum of biological activities against cancer, malaria and tuberculosis (Badawneh *et al.*, 2002: 631;Yamuna *et al.*, 2012: 1514; Bernardino *et al.*, 2012:1; Pitchai *et al.*, 2013: 776 and Srivastava *et al.*, 2014: 18). These molecules show manifold application in pharmaceutical industries (Li *et al.*, 2010: 9298; Plodek *et al.*, 2012: 4693 and Xu *et al.*, 2014: 2590) due to their significant medicinal properties.

The synthesis of [1, 8] naphthyridines dates back to the 1930's when Koller and Albert (Paudler *et al.*, 1966: 832) used a five-step sequence with 2-aminonicotinate as a starting substrate (Leshner *et al.*, 1962: 1063) to synthesize 4-hydroxy[1,8] naphthyridine-3-carboxylic acid **5** from 2-amino-pyridine **1** and diethyl ethoxymethylenemalonate **2.**

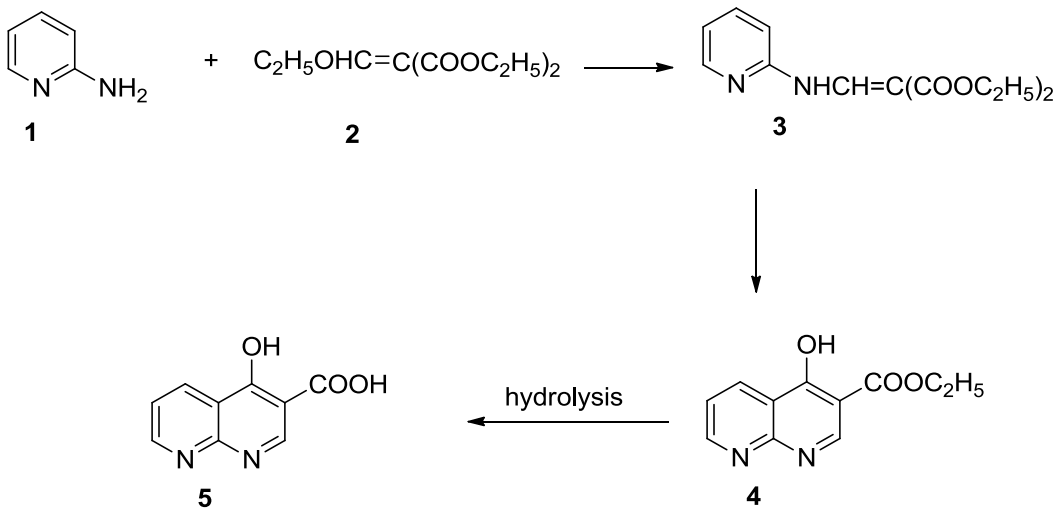

Scheme 1: Synthesis of 4-hydroxy-1, 8 naphthyridine-3-carboxylic acid **5**

(Leshner *et al.*, 1962: 1063)

Thereafter the synthesis of 1, 8-naphthyridines focused on the substrate **1** and active methylene dicarbonyl compounds such as malonic acid, malonic ester **6** and acetyl acetone. Various cyclization reaction such as the Doebner, Skraup and Knorr's reactions became prominent. The Knorr synthesis is presented in Scheme 2 (Allen 1950: 275).

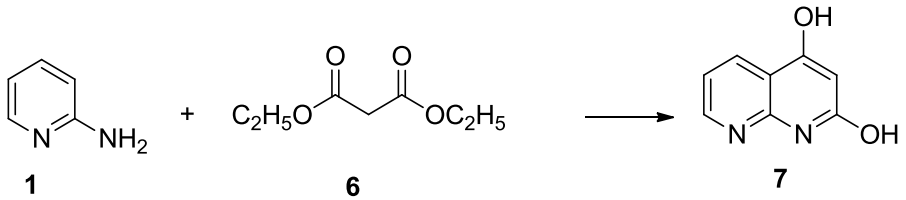

Scheme 2: Synthesis of 2, 4-dihydroxy-1, 8-naphthyridine **7** (Allen, 1950: 275;

Badawneh *et al.*, 2002:631)

Later, many other synthetic procedures were developed. The condensation of ethyl 2-chloronicotinoyl acetate **8** with acetic anhydride and dimethyl acetal produced **9** which eventually led to [1, 8] naphthyridone **11** by a sequence of reactions **(**Scheme 3) (Mekheimer *et al.*, 2007: 269).

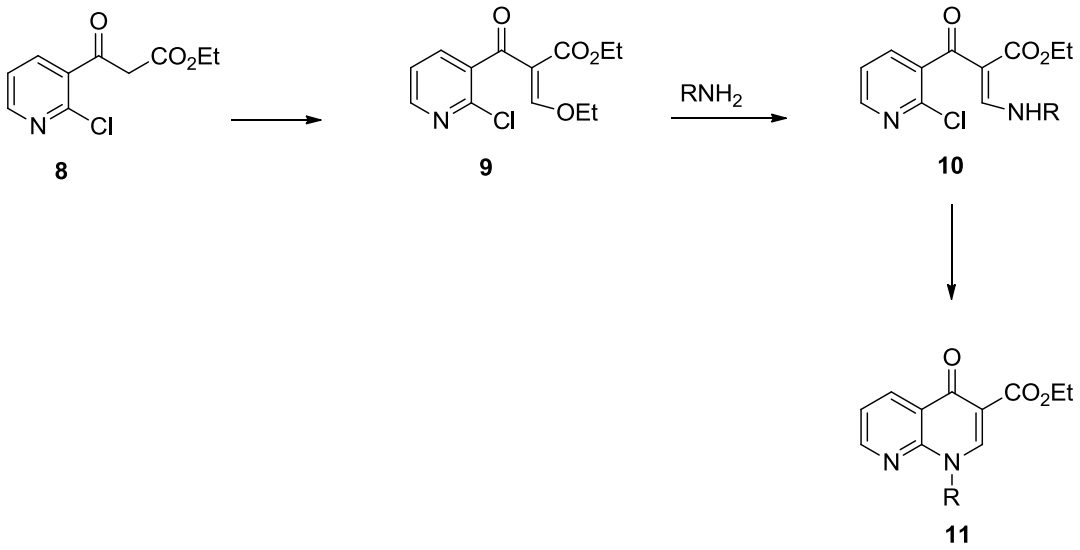

Scheme 3: Synthesis of ethyl 4-oxo-1, 4-dihydro-1, 8-naphthyridine-3-carboxylate **11**

(Mekheimer *et al*, 2007: 269)

Naik and co-worker, 2006 reported a multi-step synthesis of a thieno-[2, 3-b] benzo [1, 8] naphthyridine-2-carboxylic acids **17** (Scheme 4) through the Vilsmeier-Haack reaction (Naik *et al.*, 2006: 84).

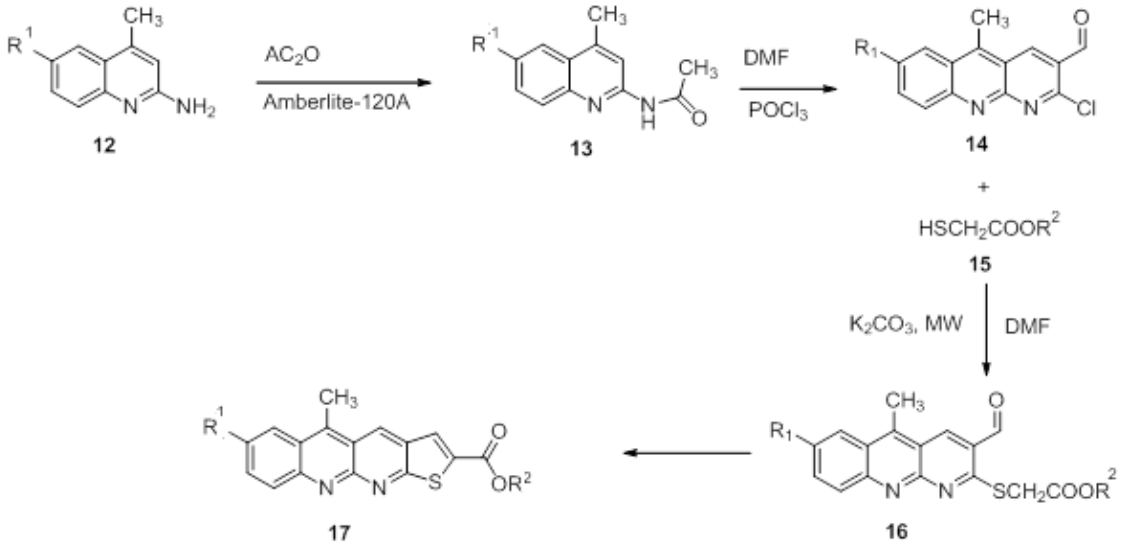

Scheme 4: Synthesis of a thieno [2, 3-b] benzo [1, 8] naphthyridine-2-carboxylic acid

(Naik *et al.*, 2006: 84)

Another interesting procedure was reported, in 2011, by Kanaouni *et al*. for the synthesis of a [1,8]-naphthyridine-2, 5-dione through the multi-step Gould-Jacobs reaction (Scheme 5) (Kanouni *et al.*, 2011: 477).

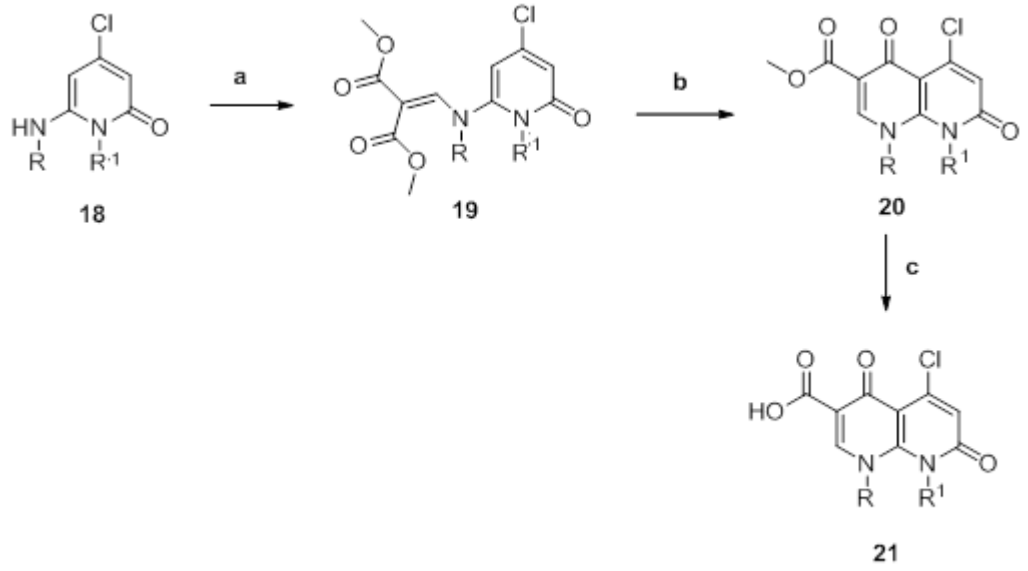

Scheme 5: Synthesis of a naphthyridinedione ring system. Reagents and conditions: (a) dimethyl methoxy-methylene-malonate, o-dichloro-benzene or bromo-benzene, 150-170 ^{0}C; (b) polyphosphoric acid, 110 ^{0}C; (c) H_2SO_4, H_2O / HOAc. (Kanouni *et al.*, 2011: 477)

Recently, organic chemists have focused on implementing of simple and highly effective methods to construct complex [1, 8] naphthyridine molecules from readily obtainable starting substrates. The multi-component reaction is currently the effective approach for enhancing synthetic efficiency, reduction of reaction time and improving the percentage yield.

To illustrate the immense contribution made to synthesis, Feng *et al.,* 2014 reported an interesting synthesis of a functionalized [1, 8] naphthyridone **25** using glutaraldehyde **22**, malononitrile **23**, 3-oxo-3-phenyl-N-(*p*-tolyl) propanamide **24** in a one-pot (Scheme 6) (Feng *et al*., 2014: 973 and Wen *et al*., 2011: 293).

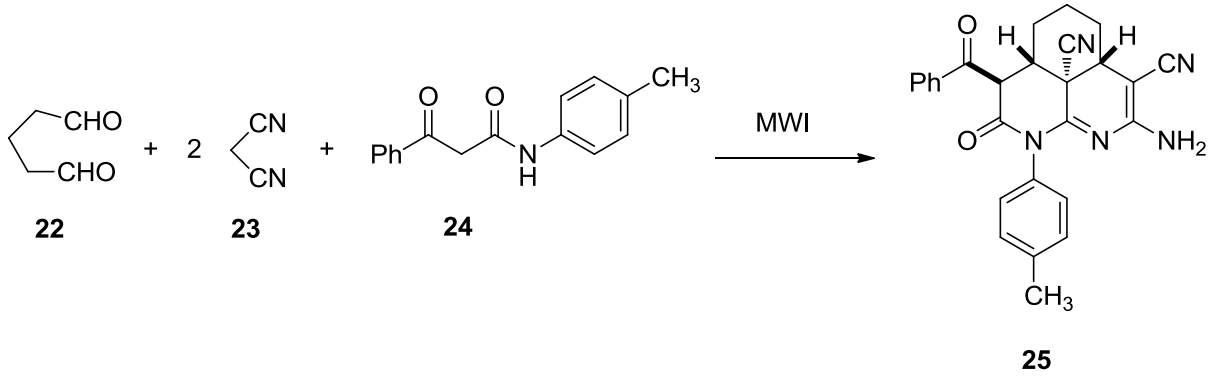

22 **23** **24** **25**

Scheme 6: Synthesis of a functionalized [1, 8]-naphthyridone **25** (Feng *et al.*, 2014: 973-981)

The Cascade-Domino reaction thereafter gained popularity. To illustrate the reaction, 2-amino-4-methylquinolines **26** were treated with malononitrile **23** and aromatic aldehydes **27** to produce benzo[b] [1, 8] naphthyridines **28** (Scheme 7) (Naik *et al.,* 2008: 1; Shelar *et al.,* 2011: 1033 and Ghorbani-Vaghei *et al.,* 2016: A). This multi-component reaction is simple and feasible for synthesizing various other substituted naphthyridines.

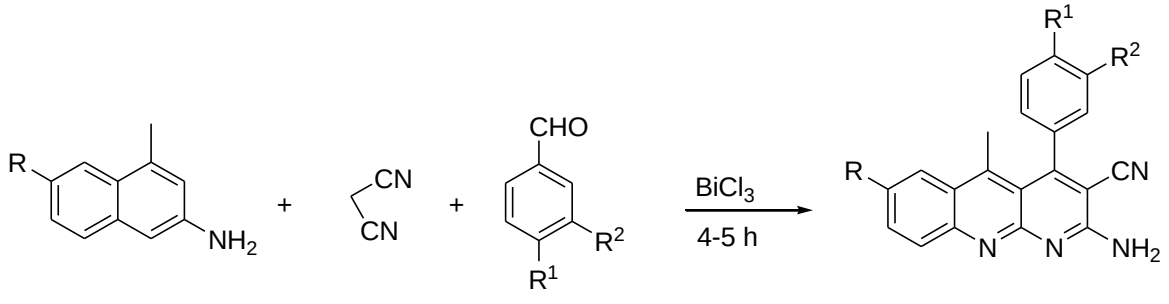

26 **23** **27** **28**

Scheme 7: Synthesis of a substituted 2-amino-5-methyl-4-phenylbenzo[*b*] [1, 8]

naphthyridine-3-carbonitrile **28** (Naik *et al.*, 2008: 1)

Recently, an advanced Friedlander annulation reaction was used to synthesize pyrazolo [3, 4-b] [1, 8] naphthyridin-5-amine **31** from 6-amino-3-methyl-1, 4-diphenyl-1H-pyrazolo [3, 4-b] pyridine-5-carbonitrile **29** and cyclo-hexanone **30** with the aid of catalytic amounts of a Lewis acid (Scheme 8) (Acosta *et al.,* 2015: 8499).

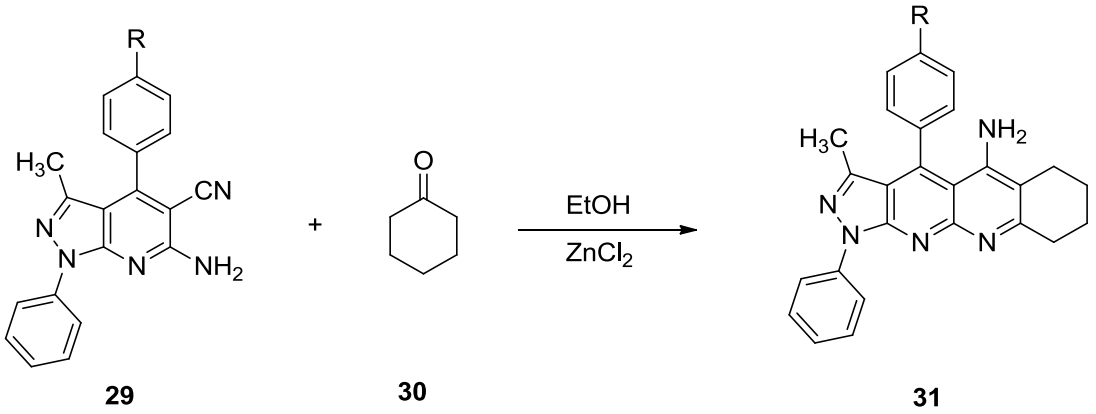

29 **30** **31**

Scheme 8: Synthesis of pyrazolo [3, 4-*b*] [1, 8] naphthyridin-5-amine **31**

(Acosta *et al.,* 2015: 8499).

In addition, a synthesis of novel functionalized 1, 8-naphthyridine **34** was developed via a cascade reaction of 2-chloroquinoline-2-carbaldehyde **32** and enaminones **33** (Scheme 9) (Fu *et al*., 2014: 1).

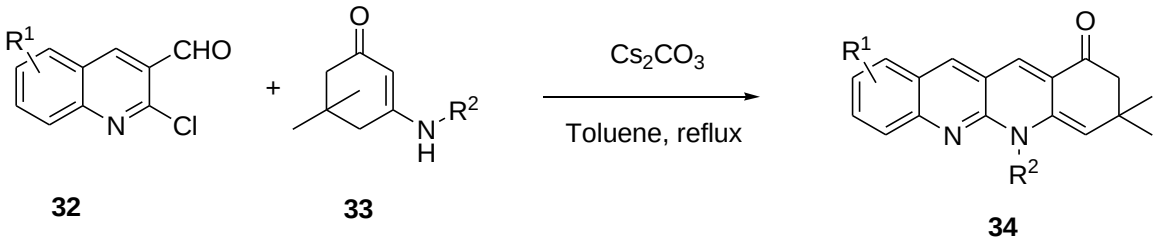

32 **33** **34**

Scheme 9: Cascade synthesis of novel functionalized 1, 8-naphthyridine derivatives

Alonso *et al.,* 2016 synthesized naphthyridine derivatives and assessed their effect on topoisomerase I activity and their cytotoxic activity in cancer cells (A549 lung, BT20 breast and SKOV3 ovarian cancer cells) (Alonso *et al.,* 2016:179). The synthesized compounds were able to inhibit topoisomerase I activity. They also determined that the fluorinated indeno [1, 5] naphthyridine derivative was cytotoxic to A549 and SKOV3 cells. In addition, the nitrogen derivatives were cytotoxic to the A549 cell line.

Since there is limited reports on the synthesis of new bioactive 1, 8-naphthyridinones, this study investigated a multi-component reaction using 2-aminopicoline as one of the starting substrates. To catalyze the reaction, phosphotungstic acid was chosen because there is limited reports on it. Furthermore, anticancer studies were undertaken with A549 lung cancer cell lines.

3.3 Results and Discussion

3.3.1 Synthesis and Characterization of A Novel 4, 8, 8-Trimethyl-5-Phenyl-5, 5a, 8, 9-Tetrahydrobenzo[*b*] [1, 8] Naphthyridin-6(7H)-One (38a)

As a model reaction, a one-pot synthesis of 4, 8, 8-trimethyl-5-phenyl-5, 5a, 8, 9-tetrahydrobenzo [*b*] [1, 8] naphthyridin-6(7H)-one (**38a**) was undertaken with an equimolar (1 mmol) quantity of 2-aminopicoline **35**, dimedone **36** and benzaldehyde **37a**. Briefly, the three components were mixed with phosphotungstic acid and heated under solvent-free conditions at 80 ^{0}C (Scheme 10). The progress of the reaction was monitored by TLC. After 8 hours, **38a** formed: it was extracted with ethyl acetate, filtered and the filtrate was evaporated *in vacuo*. The solid from the filtration process was collected for a recycling investigation. **38a** was identified as 4, 8, 8-trimethyl-5-phenyl-5, 5a, 8, 9-tetrahydrobenzo[*b*] [1, 8] naphthyridin-6(7H)-one by FT-IR, NMR, EI-MS and elemental analysis.

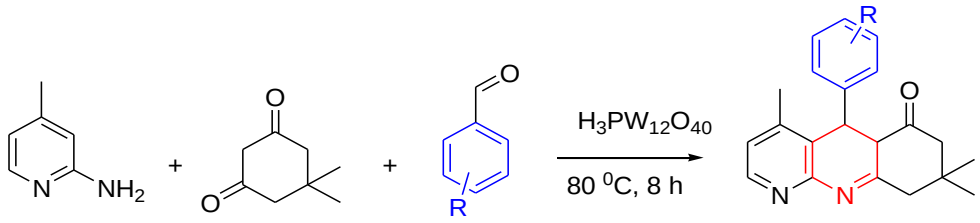

35 **36** **37a-h** **38a-h**

Key: R = H(**38a**), *p*-CH_3 (**38b**), *p*-Cl (**38c**), *p*-F (**38d**), *p*-CF_3 (**38e**), *p*-NO_2 (**38f**), *p*-OCH_3 (**38g**), *m*(OCH_3)-*p*(OH) (**38h**)

Scheme 10: Synthesis of 4, 8, 8-trimethyl-5-phenyl-5, 5a, 8, 9-tetrahydrobenzo[*b*] [1, 8] naphthyridin-6(7H)-ones

Compound **38a** was selected as a template to discuss unambiguous the characterization of different results of which could be easily extrapolated to other derivatives because of similarity of the structures.

The FT-IR spectrum (Appendix 3.1) showed stretching absorptions (cm^{-1}) at 2854, 1675, 1618 and 1561 cm^{-1}which was assigned to C-H (sp^3), C=O, aromatic (C=C) and imine (aromatic C=N), respectively. The numbers for peripheral atoms depicted in Figure 1 were used to facilitate the assigning of proton and carbon for NMR spectral interpretation.

The ^1H NMR spectrum (Appendix 3.2) showed a sharp singlet at δ 2.5 ppm for CH_3 (C-5a) of the picoline moiety. The doublets at δ 4.8 was assigned to C4-CH and another doublets at 2.5 which mingles with CH_3 (C-5a) was assigned to C3-CH. The aromatic protons C6-H and C7-H appeared at 7.1 (1H, d, J = 7.2 Hz, Ar) and δ 7.3 (1H, d, J = 7.2 Hz, Ar), respectively. Whereas, phenyl protons C2'-H, C6'-H appeared at δ 7.3 (1H, d, J = 7.2 Hz, Ar), respectively; C3'-H, C5'-H appeared at δ 7.3 (1H, d, J = 7.2 Hz, Ar), respectively and C4'-H appeared at δ 7.2 (1H, t, J = 7.6 Hz, Ar). The C9-CH_2 and C11-CH_2 appeared at δ 2.1 and 2.2, respectively. The C13-CH_3 and C14-CH_3 were indistinguishable at δ 1.1.

The ^{13}C NMR spectrum (Appendix 3.3) showed the presence of one C=O group at δ 196.4 whilst the C2, C3, C4, C4a and C5 were assigned to δ 162.3, 31.9, 31.8, 115.7 and 144.1, respectively. Appendix 3.4 and Appendix 3.5 present the 90^0 DEPT and 135^0 DEPT, respectively, which confirms the three methyl groups resonated at δ 31.9 (C5a), 29.2 (C13) and 27.3 (C14). Also, showed the two methylene groups resonated at δ 50.7 (C11) and 40.9 (C9), respectively. The complete proton and carbon assignments were deduced using ^1H, ^{13}C NMR, DEPT and HSQC spectra (Appendix 3.7**)**, these presented in Figure 1.

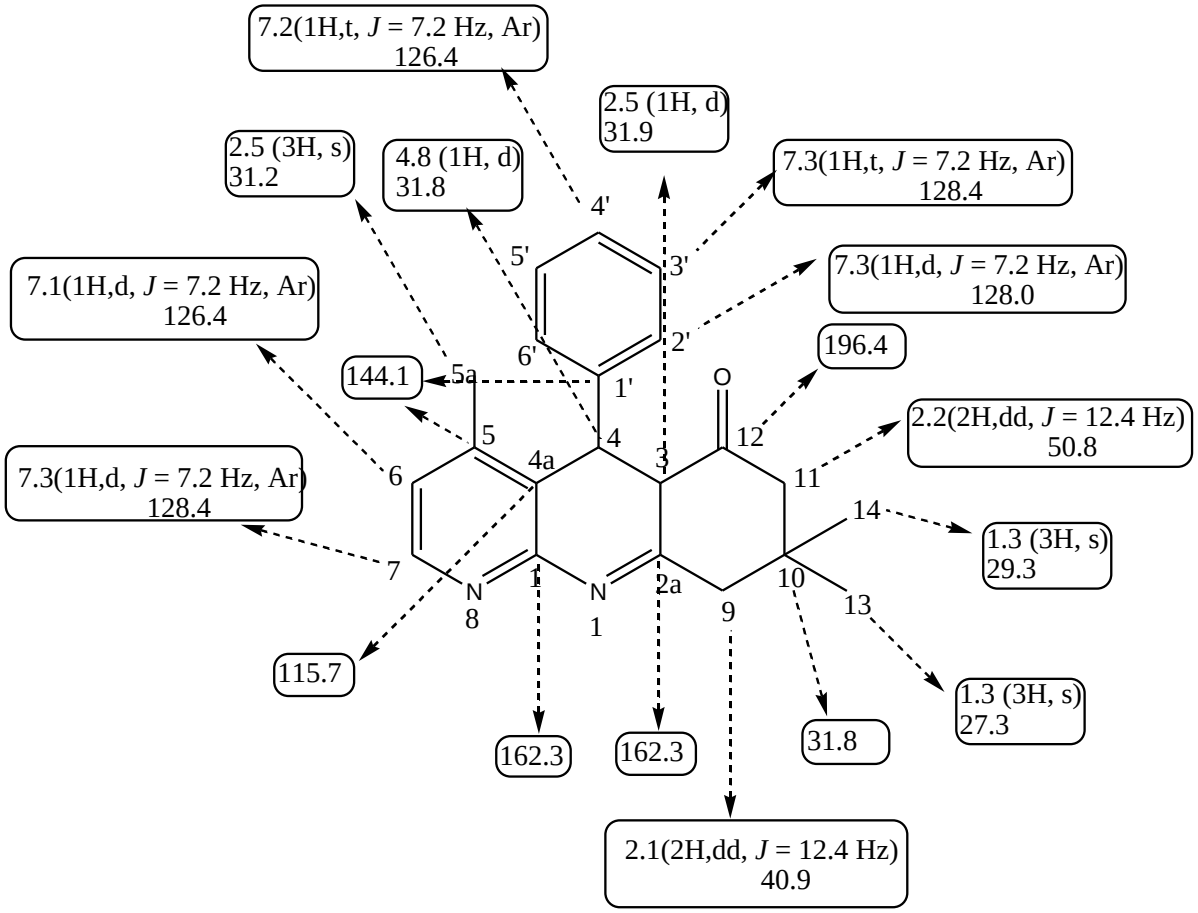

Figure 1: ^{1}H and ^{13}C NMR chemical shifts of **38a.**

The 2-D NMR analysis of COSY and HMBC were used to confirm the identity of compound **38a** through correlation between proton and carbon as presented in Figure 2.

The ^{1}H, ^{1}H-COSY spectrum (Appendix 3.6**)** showed strong coupling between H-4 (δ 4.8) and H-3 (δ 2.5). Another weak coupling occurred between H-4 (δ 4.8) and H-2' (δ 7.2); H-4 (δ 4.8) and H-6' (δ 7.2).

The HMBC spectrum (Appendix 3.8**)** showed the proton and quaternary carbon coupling: H-3 (δ 2.5) coupled with C-4a (δ 115.7); H-4 (δ 4.8) coupled with C-4a (δ 115.7) and C-5 (δ 144.1**)**; H-5a (δ 2.5) coupled with C-4a (δ 115.7) and C-5 (δ 144.1); H-6 (δ 7.27) coupled with C-5 (δ 144.1); the H-2',H-6' (δ 7.29) coupled with C-1' (δ 144.1); H-13 (δ 1.11) and H-14 (δ 1.10) coupled with C-10 (δ 31.8); H-9 (δ 2.19) and H-11 (δ 2.22) coupled with C-10 δ 31.8).

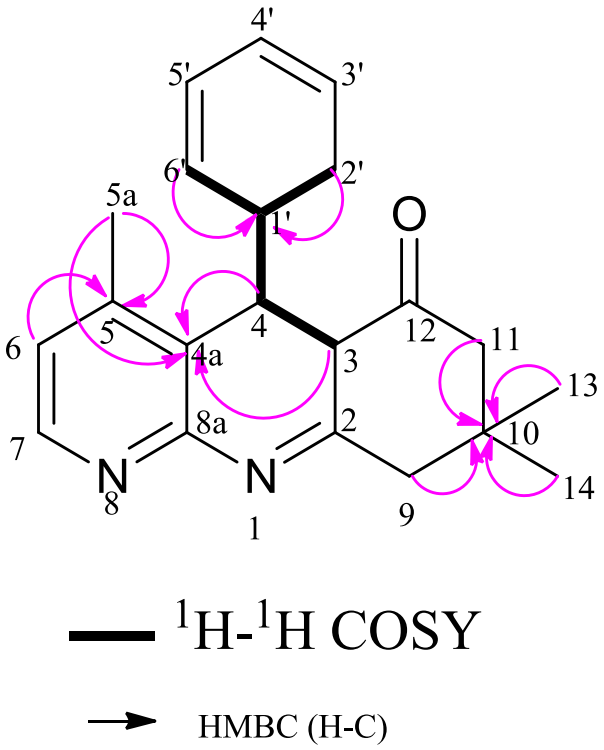

Figure 2. COSY and HMBC correlations for compound **38a**

Finally the mass spectrum (Appendix 3.9) EI-MS showed 318 [M^+] for the molecular ion. Scheme 11 depicts a fragment pattern after the loss of phenyl group. Aliphatic fragmentation was also observed in the mass spectra for other derivatives which might be caused by sample contamination during preparation or source contamination of the instrument.

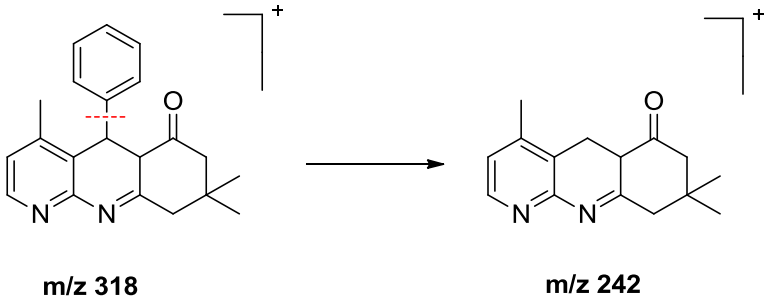

Scheme 11: Fragmentation of compound **38a**

CHN analysis (%) for $C_{21}H_{22}N_2O$ calculated: C, 79.21; H, 6.96; N, 8.80; found: C, 79.23; H, 6.99; N, 8.81 confirmed the compound **38a** as 4, 8, 8-trimethyl-5-phenyl-5, 5a, 8, 9-tetrahydrobenzo[b] [1, 8] naphthyridin-6(7H)-one.

3.3.2 Catalysis

Various hetero-polyacids such as silicotungstic, p-toulenesulfonic acid and silica sulphuric acid were separately investigated to synthesize **38a**. The results (Table 1) showed that the best yield of **38a** was 98% when 0.25 mol % $H_3PW_{12}O_{40}$ was used. Either increasing or decreasing the amount of catalyst caused a decrease in yield. The other three catalysts tested for the reaction showed low yield thereby suggesting their low selectivity for the substrates used. The re-usability potential of $H_3PW_{12}O_{40}$ was studied in the model reaction to synthesize **38a**: briefly, the solid was rinsed with ethyl acetate, washed with ethanol then dried in the oven at 105 ^{0}C then reused in another reaction. It was found that $H_3PW_{12}O_{40}$ can be re-utilized five times with only 4% loss of catalytic activity (Table 2).

Table 1. Effect of hetero-polyacids as a catalyst for the synthesis of **38a**

Entry	Catalyst (mol %)	Time (hours)	Yield (%)[a]
1	$H_3PW_{12}O_{40}$ (0.1)	8	45
2	$H_3PW_{12}O_{40}$ (0.25)	8	98
3	$H_3PW_{12}O_{40}$ (0.5)	8	94
4	$H_4SiW_{12}O_{40}$ (0.1)	8	20
5	$H_4SiW_{12}O_{40}$ (0.25)	8	43
6	$H_4SiW_{12}O_{40}$ (0.5)	8	68
7	p-TSA (0.1)	8	16
8	p-TSA (0.25)	8	28
9	p-TSA (0.5)	8	39
10	Silica Sulphuric (0.1)	8	35
11	Silica Sulphuric (0.25)	8	50
12	Silica Sulphuric (0.50)	8	58

[a] Isolated yields

Table 2. Reusability of $H_3PW_{12}O_{40}$ in the solvent-free synthesis of **38a**.

Run no.	Yield (%)[b]	Time (h)
1	98	8
2	98	8
3	97	8
4	96	8
5	94	8

[b] Isolated yield

3.3.3 A Proposed Reaction Mechanism

Since this is a new reaction, a proposed mechanism in Scheme 12 is presented to support the formation of **38a** which was the model reaction for the new reaction scheme. Firstly, the catalyst protonates the carbonyl group of both substrates. This caused the methylene carbon to be more acidic and be easily removed by the Bronsted base **35** to form **39** which subsequently attacked the aromatic aldehyde **37** to produce α, β unsaturated ketone intermediate **40,** through Knoevenagel condensation, with loss of H_2O. Thereafter, an intramolecular rearrangement occurred in **35** which caused the pyridine ring to be nucleophilic and leads to Michael addition to produce the intermediate product **41** which subsequently undergone Schiff base condensation to generate the desired target compound **38a**.

.

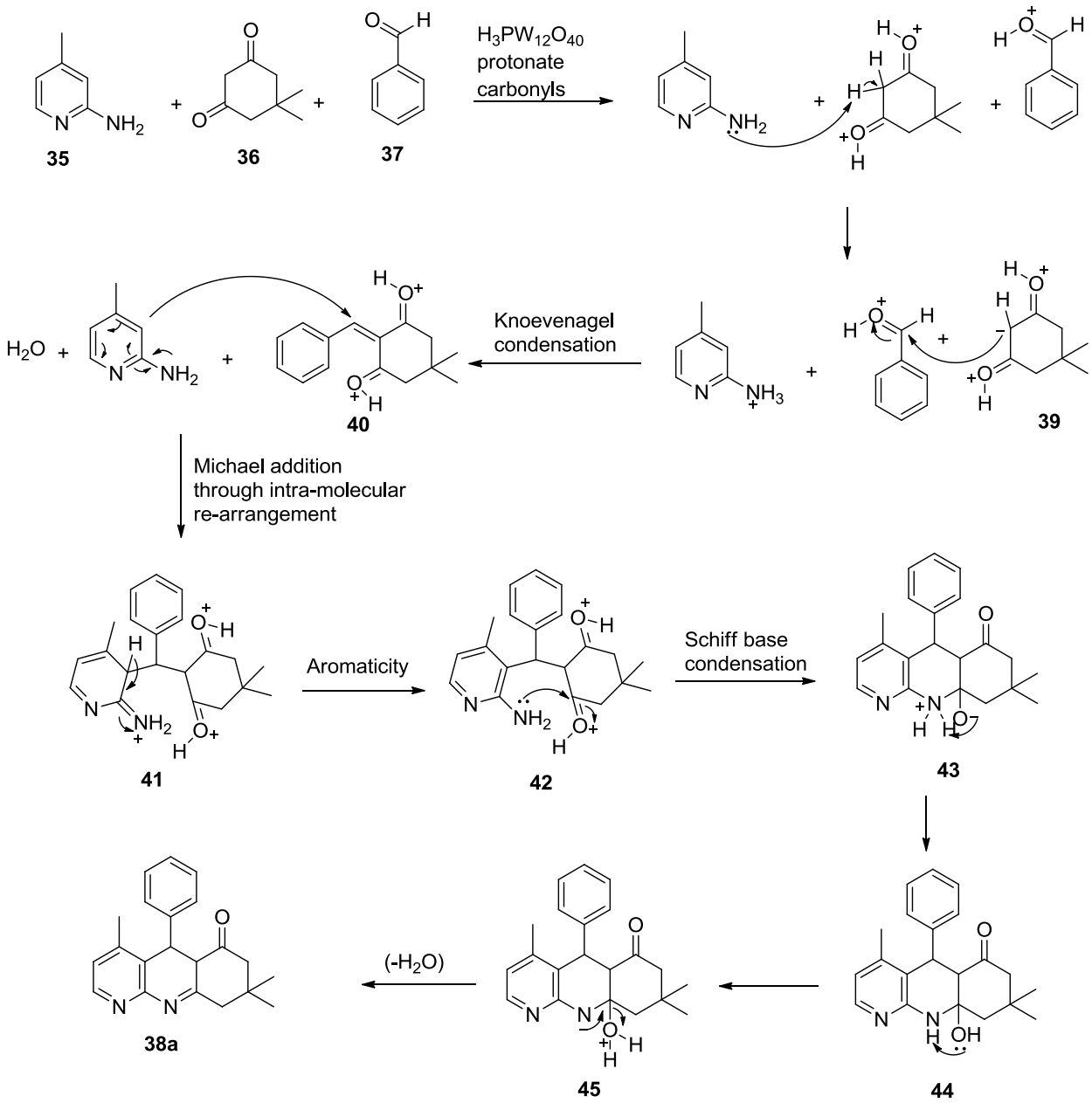

Scheme 12: The proposed mechanism for synthesis of 4, 8, 8-trimethyl-5-phenyl-5, 5a, 8, 9-tetrahydrobenzo[b] [1, 8] naphthyridin-6(7H)-ones

3.3.4 The Synthesis and Characterization of Novel 4, 8, 8-Trimethyl-5-Phenyl-5, 5a, 8, 9-Tetrahydrobenzo[*b*] [1, 8] Naphthyridin-6(7H)-Ones (38b-H) Derivatives

After successful synthesis of **38a** by a solvent-free one-pot reaction and its characterization, the other 7 derivatives were synthesized. In each reaction, only the benzaldehyde substrates were varied. The *para* substituted benzaldehyde bearing activating groups at R gave good yields (Table 3**,** entry 1, 2, 3, 4, 7) whilst the benzaldehyde derivatives bearing electron withdrawing groups at R (entry 5, 6) and the functionalized aldehyde vanillin (entry 8) gave marginally lower yield.

Table 3. The synthesis of novel phenyl-8, 9-dihydrobenzo[*b*] [1, 8] naphthyridin-6(7H)-ones under solvent-free conditions in the presence of $H_3PW_{12}O_{40}$.

Entry	Benzaldehydes	Product (38a-38h)	Time (h)	Isolated yield (%)
1	C_7H_6O	38a	8	98
2	C_8H_8O (*p*)	38b	8	98
3	C_7H_5ClO (*p*)	38c	8	97
4	C_7H_5FO (*p*)	38d	8	96
5	$C_8H_5F_3O$ (*p*)	38e	8	94
6	$C_7H_5NO_3$ (*p*)	38f	8	89
7	$C_8H_8O_2$ (*p*)	38g	8	92
8	$C_8H_8O_3$ (*m* & *p*)	38h	8	90

3.3.5 A549 Lung Cancer Cell's Lines Studies

The effect of the synthesized 4, 8, 8-trimethyl-5-phenyl-5, 5a, 8, 9-tetrahydrobenzo[*b*] [1, 8] naphthyridin-6(7H)-ones on A549 lung cancer cell viability was assessed and the data are presented in Table 4 and Table 5. The results from the cell viability assay showed that the synthesized compounds exhibit remarkable biological effect at various concentrations in the A549 lung cancer cells. **38g-p-OCH_3** and **38c-p-Cl** increased cell viability at 24 h however **38g-p-OCH_3** at 1000 µM had 94 % viable cells. Interestingly, **38h-VAN** initially caused A549 cell proliferation and thereafter resulted in a dose-dependent decrease with an IC_{50} of 724.7 µM. A similar trend was seen for **38e-p-CF_3** and an IC_{50} of 541.8 µM was determined. The IC_{50} was determined for compounds **38a-p-H**, **38b-p-CH_3**, **38f-p-NO_2** and **38d-p-F** which was extrapolated from the concentration-response inhibition curve (562.4, 325.2, 413.8 and 498.9 µM respectively). Similarly in this study, the novel synthesized compounds **38h-VAN** and **38e-p-CF_3** showed potential as an antiproliferative agent against lung cancer as a dose-dependent decline in A549 lung cancer cell viability was observed.

Table 4: Viability of cancerous A549 lung cells after treatment with **38a, 38b, 38c, 38e** and **38h**.

Conc. (μM)	Camptothecin	Conc (μM)	38a-*p*-H	38b-*p*-CH_3	38c-*p*-Cl	38e-*p*-OCH_3	38h-VAN
Control	0.278 ± 0.041 (100%)	Control	0.173 ± 0.022 (100%)	0.256 ± 0.015 (100%)	0.121 ± 0.003 (100%)	0.157 ± 0.004 (100%)	0.221 ± 0.021 (100%)
1	0.394 ± 0.039 (142%)***	10	0.365 ± 0.083 (211%) **	0.417 ± 0.022 (163%) ***	0.247 ± 0.031 (204%) ***	0.279 ± 0.066 (178%) ***	0.464 ± 0.067 (210%) ***
5	0.392 ± 0.027 (141%)***	50	0.361 ± 0.073 (209%) **	0.431 ± 0.004 (169%) ***	0.179 ± 0.031 (148%) *	0.299 ± 0.041 (191%) ***	0.431 ± 0.057 (196%) ***
10	0.386 ± 0.023 (139%)***	100	0.351 ± 0.082 (203%) **	0.431 ± 0.009 (168%) ***	0.223 ± 0.017 (184%) ***	0.298 ± 0.043 (190%) ***	0.327 ± 0.038 (148%) **
20	0.326 ± 0.016 (117%)	200	0.272 ± 0.046 (157%)	0.381 ± 0.025 (149%) ***	0.200 ± 0.036 (166%) **	0.256 ± 0.010 (164%) **	0.304 ± 0.006 (138%) *
30	0.319 ± 0.004 (115%)	400	0.272 ± 0.046 (157%)	0.273 ± 0.024 (107%)	0.169 ± 0.006 (139%)	0.278 ± 0.001 (178%) **	0.175 ± 0.007 (80%)
40	0.319 ± 0.012 (115%)	600	0.222 ± 0.015 (128%)	0.271 ± 0.007 (106%)	0.140 ± 0.007 (156%)	0.227 ± 0.010 (145%)	0.133 ± 0.026 (60%) *
50	0.313 ± 0.022 (113%)	800	0.186 ± 0.019 (108%)	0.260 ± 0.013 (102%)	0.210 ± 0.004 (173%) ***	0.208 ± 0.015 (133%)	0.109 ± 0.006 (49%) **
60	0.253 ± 0.011 (91%)	1000	0.183 ± 0.007 (106%)	0.193 ± 0.023 (75%) **	0.245 ± 0.013 (203%) ***	0.147 ± 0.007 (94%)	0.052 ± 0.010 (24%) ***
70	0.223 ± 0.021 (80%)						
80	0.206 ± 0.011 (74%)**						
90	0.234 ± 0.015 (84%)						
100	0.175 ± 0.011 (63%)***						
IC_{50}	114.0		562.4	325.2	-	-	724.7

*$p < 0.05$, **$p < 0.001$, *** $p < 0.0001$ significantly different compared to the controls using a one way analysis of variance with the Dunnets Multiple Comparisons Test.

Table 5: Viability of cancerous A549 lung cells after treatment with **38d, 38f** and **38g**.

Concentration (μM)	**38d-*p*-NO_2**	**38f-*p*-CF_3**	**38g-*p*-F**
Control	0.212 ± 0.019 (100%)	0.153 ± 0.037 (100%)	0.179 ± 0.012 (100%)
10	0.345 ± 0.031 (162%)	0.313 ± 0.026 (205%)	0.431 ± 0.038 (241%)
	***	***	***
50	0.319 ± 0.019 (150%)	0.351 ± 0.007 (229%)	0.489 ± 0.045 (274%)
	***	***	***
100	0.267 ± 0.031 (126%)	0.349 ± 0.022 (228%)	0.474 ± 0.059 (266%)
	*	***	***
200	0.260 ± 0.021 (122%)	0.323 ± 0.043 (211%)	0.465 ± 0.028 (260%)
		***	***
400	0.227 ± 0.020 (107%)	0.198 ± 0.028 (129%)	0.448 ± 0.017 (251%)
			***
600	0.184 ± 0.024 (87%)	0.193 ± 0.016 (126%)	0.245 ± 0.020 (137%)
800	0.164 ± 0.022 (77%)	0.131 ± 0.022 (86%)	0.252 ± 0.006 (141%)
1000	0.149 ± 0.008 (70%)		0.192 ± 0.027 (108%)
IC_{50}	**413.8**	**541.8**	**498.9**

3.4 Conclusion

Phosphotungstic acid was used as a catalyst for the synthesis of novel 4, 8, 8-trimethyl-5-phenyl-5, 5a, 8, 9-tetrahydrobenzo[*b*] [1, 8] naphthyridin-6(7H)-ones under solvent-free conditions. The catalyst was easily recovered and displayed high activity for the multi-component reaction. Furthermore, this one-pot reaction created new types of [1, 8] naphthyridin-6(7H)-one derivatives which have suitable functionality for a host of possible biochemical applications. The cell viability assay results showed that the synthesized compounds exhibit remarkable biological effect at various concentrations in the A549 lung cancer cell. Compounds **38f** and **38h** showed potential as an anti-proliferative agent against A549 lung cancer cell lines and a dose-dependent decline in cell viability.

3.5 Experimental

3.5.1 Typical Procedure for the Multi-Component Synthesis of Novel 4, 8, 8-Trimethyl-5-Phenyl-5, 5a, 8, 9-Tetrahydrobenzo[*b*] [1, 8] Naphthyridin-6(7H)-One Derivatives

A mixture of 2-aminopicoline **35** (1 mmol), dimedone **36** (1 mmol), benzaldehyde derivatives **37** (1 mmol) and phosphotungstic acid (0.025 mmol) was mixed thoroughly and heated under solvent-free conditions at 80 ^{0}C. After completion of the reaction, as monitored by TLC (eluent: 3:1 n-hexane/ ethyl acetate), the reaction mixture was poured into 30 mL ethyl acetate to extract the desired product. After simple filtration, the filtrate was collected and evaporated *in vacuo* to produce the solid as pure compounds **38a-38h** in good yield. The solid, collected after filtration, was rinsed with ethanol and then dried in the oven at 105 ^{0}C. This solid material was re-used to test its recyclability potential. The spectroscopic data for all derivatives is presented below:

3.5.1.1 The Spectroscopic Analysis of 38a-h

4,8,8-trimethyl-5-phenyl-5,5a,8,9-tetrahydrobenzo[*b*][1,8]naphthyridin-6(7H)-one (38a)

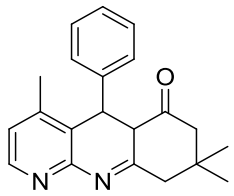

38a

Yield 96%, white solid, m.p. 197-199 ^{0}C. **IR (KBr)**: ν 2854, 1675, 1618, 1561, 1479, 1383, 1123, 767 and 464 cm^{-1}. **^{1}H NMR (400 MHz, CDCl$_3$)** δ: 7.3 (5H, d, *J* = 7.2 Hz, Ar), 7.1 (1H, d, *J* = 7.2 Hz, Ar), 4.8 (s, 1H, CH pyridine ring), 2.5 (s, 4H, Ar-CH$_3$ & CH pyridine ring), 2.2(dd, *J* = 9.6 &12.4 Hz, 2H, CH$_2$ aliphatic), 2.1 (dd, *J* = 9.8 &12.4 Hz, 2H, CH$_2$ aliphatic), 1.1 (s, 6H, CH$_3$ aliphatic) ppm. **^{13}C NMR (400 MHz, CDCl$_3$)** δ: 27.3, 29.2, 31.4, 32.7, 40.9, 50.8, 115.7, 126.3, 128.0-128.4, 144.1, 162.3 and 196.4 ppm. **EI-MS** found: 318.1 [M$^+$], **EI-MS** calculated: 318.4 [M$^+$]. **CHN analysis** (%) for $C_{21}H_{22}N_2O$ calcd: C, 79.21; H, 6.96; N, 8.80; found: C, 79.23; H, 6.99; N, 8.81.

4,8,8-trimethyl-5-(*p*-tolyl)-5,5a,8,9-tetrahydrobenzo[*b*][1,8]naphthyridin-6(7H)-one (38b)

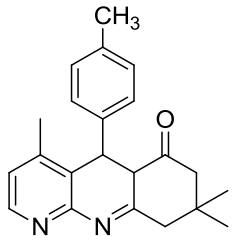

38b

Yield 95%, white solid, m.p. 217-219 ^{0}C. **IR (KBr)**: ν 2959, 1668, 1618, 1511, 1467, 1360, 1136, 773 and 519 cm $^{-1}$. **^{1}H NMR (400 MHz,CDCl$_3$)**: δ 7.2 (1H, d, *J* = 8.0 Hz, H-7), 7.2 (2H, d, *J* = 8.0 Hz, H-3'& H-5'), 7.0 (1H, d, *J* = 8.0 Hz, H-6), 7.0 (2H, d, *J* = 8.0 Hz, H-2' & H-6'), 4.7 (1H, s, H-4), 2.5 (3H, s, H-5a), 2.3 (3H, s, H-4a'), 2.2 (2H, dd, *J* = 9.6 & 12.4 Hz, H-9), 2.1 (2H, dd, *J* = 9.7 & 12.4 Hz,H-11), 1.7 (1H,s, H-3), 1.1 (6H s, H-13 & H-14) ppm. **^{13}C NMR (400 MHz, CDCl$_3$)**: δ 21. 0, 27.3, 29.2, 31.4, 32.7, 40.9, 50.8, 115.7, 128.0, 128.4, 135. 8, 141.1, 162.3 and 196.4ppm. **EI-MS** found: 332.2 [M^{+}], **EI-MS** calculated: 332.4 [M^{+}]. **CHN analysis** (%) for $C_{22}H_{24}N_2O$ calcd: C, 79.48; H, 7.28; N, 8.43; found: C, 79.51; H, 7.32; N, 8.47.

5-(4-chlorophenyl)-4, 8, 8-trimethyl-5, 5a, 8, 9-tetrahydrobenzo[*b*] [1, 8] naphthyridin-6(7H)-one (38c)

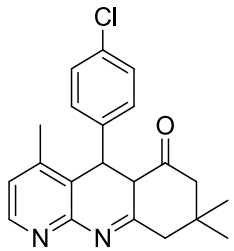

38c

Yield 94%, white solid, m.p. 234-236 ^{0}C **IR (KBr)**: ν 2961, 1660, 1625, 1561, 1469, 1361, 1198, 850 and 528 cm $^{-1}$. **^{1}H NMR (400 MHz,CDCl$_3$)**: δ 7.2 (1H, d, *J* = 8.8 Hz, H-7), 7.2 (2H, d, *J* = 8.0 Hz, H-3'& H-5'), 7.1 (1H, d, *J* = 8.0 Hz, H-6), 7.1 (2H, d, *J* = 8.0 Hz, H-2' & H-6'), 4.6 (1H, s, H-4), 2.4 (3H, s, H-5a), 2.1 (4H, dd, *J* = 12.4 Hz, H-9 & H-11), 1.5 (1H,s, H-3),

1.0 (6H s, H-13 & H-14) ppm. **^{13}C NMR (400 MHz, $CDCl_3$)**: δ 27.3, 29.2, 31.4, 32.7, 40.9, 50.8, 114.5, 123.0-129.3, 146.5, 151.5, 162.9 and 196.3 ppm. **EI-MS** found: 352.1 [M^+], **EI-MS** calculated: 352.8 [M^+]. **CHN analysis** (%) for $C_{21}H_{21}ClN_2O$ calcd: C, 71.48; H, 6.00; N, 7.94; found: C, 71.51; H, 6.02; N, 7.96.

5-(4-fluorophenyl)-4, 8, 8-trimethyl-5, 5a, 8, 9-tetrahydrobenzo[*b*] [1, 8] naphthyridin-6(7H)-one (38d)

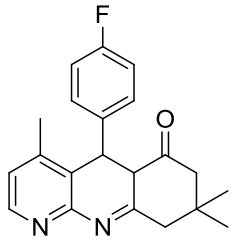

38e

Yield 94%, white solid, m.p. 227-229 ^{0}C **IR (KBr)**: 2955, 1667, 1625, 1507, 1467, 1362, 1163, 850 and 536 cm $^{-1}$. **^{1}H NMR (400 MHz,$CDCl_3$)**: δ 7.2 (1H, d, *J* = 8.8 Hz, H-7), 7.2 (2H, d, *J*= 8.0 Hz, H-3'& H-5'), 6.9 (1H, d, *J*= 8.0 Hz, H-6), 6.9 (2H, d, *J*= 8.0 Hz, H-2' & H-6'), 4.7 (1H, s, H-4), 2.4 (3H, s, H-5a), 2.1 (4H, dd, *J* = 12.4 Hz, H-9 & H-11), 1.6 (1H, s, H-3), 1.0 (6H s, H-13 & H-14) ppm. **^{19}F NMR (400 MHz, $CDCl_3$)**: δ -116.8 ppm (Ar-F). **^{13}C NMR (400 MHz, $CDCl_3$)**: δ 27.3, 29.2, 31.2, 32.2, 40.9, 50.7, 114.8, 115.5, 129.8, 129.9, 139.9, 162.9 and 196.4 ppm. **EI-MS** found: 336.2 [M^+], **EI-MS** calculated: 336.4 [M^+]. **CHN analysis** (%) for $C_{21}H_{21}FN_2O$ calcd: C, 74.98; H, 6.29; N, 8.33; found: C, 74.99; H, 6.31; N, 8.34.

4, 8, 8-trimethyl-5-(4-(trifluoromethyl) phenyl)-5, 5a, 8, 9-tetrahydrobenzo [*b*] [1, 8] naphthyridin-6(7H)-one (38e)

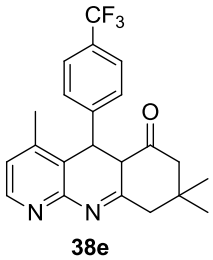

38e

Yield 92%, white solid, m.p. 246-248 ^{0}C **IR (KBr)**: ν 2962, 1665, 1625, 1561, 1468, 1363, 1117, 859 and 609 cm $^{-1}$. **^{1}H NMR (400 MHz,CDCl$_3$)**: δ 7.3 (1H, d, *J* = 8.0 Hz, H-7), 7.2 (2H, d, *J*= 8.4 Hz, H-3'& H-5'), 7.2 (1H, d, *J*= 8.4 Hz, H-6), 7.2 (2H, d, *J* = 8.4 Hz, H-2' & H-6'), 4.6 (1H, s, H-4), 2.3 (3H, s, H-5a), 2.0 (4H, dd, *J* = 12.4 Hz, H-9 & H-11), 1.4 (1H, s, H-3), 0.9 (6H s, H-13 & H-14) ppm. **^{19}F NMR (400 MHz, CDCl$_3$)**: δ -62.4 ppm (Ar-CF_3). **^{13}C NMR (400 MHz, CDCl$_3$)**: δ 27.3, 29.2, 32.0, 32.2, 40.9, 50.7, 115.0, 122.9, 128.8, 148.0, 162.7 and 196.3 ppm. **EI-MS** found: 386.2 [M^+], **EI-MS** calculated: 386.4 [M^+]. **CHN analysis** (%) for $C_{22}H_{21}F_3N_2O$ calcd: C, 68.38; H, 5.48; N, 7.25; found: C, 68.40; H, 5.49; N, 7.26.

4, 8, 8-trimethyl-5-(4-nitrophenyl)-5, 5a, 8, 9-tetrahydrobenzo [*b*] [1, 8] naphthyridin-6(7H)-one (**38f)**

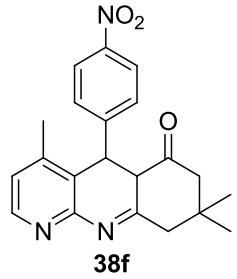

38f

Yield 89%, white solid, m.p. 229-231 ^{0}C. **IR (KBr)**: ν 2960, 1660, 1625, 1513, 1468, 1362, 1137, 865 and 563 cm $^{-1}$. **^{1}H NMR (400 MHz, CDCl$_3$)**: δ 8.1 (1H, d, *J* = 8.0 Hz, H-7), 8.1 (2H, d, *J*= 8.4 Hz, H-3'& H-5'), 7.3 (1H, d, *J*= 8.4 Hz, H-6), 7.5 (2H, d, *J* = 8.4 Hz, H-2' & H-6'), 4.8 (1H, s, H-4), 2.5 (3H, s, H-5a), 2.2 (4H, dd, *J* = 12.4 Hz, H-9 & H-11), 1.6 (1H, s, H-3), 1.1(6H s, H-13 & H-14) ppm. **^{13}C NMR (400 MHz, CDCl$_3$)**: δ 27.3, 29.2, 31.4, 32.7, 40.9, 50.8, 114.5, 123.0-129.3, 146.5, 151.5, 162.9 and 196.3 ppm. **EI-MS** found: 363.2 [M^+], **EI-MS** calculated: 363.4 [M^+]. **CHN analysis** (%) for $C_{21}H_{21}N_3O_3$ calcd: C, 69.41; H, 5.82; N, 11.56; found: C, 69.44; H, 5.85; N, 11.58.

5-(4-methoxyphenyl)-4, 8, 8-trimethyl-5, 5a, 8, 9-tetrahydrobenzo [*b*] [1, 8] naphthyridin-6(7H)-one (**38g)**

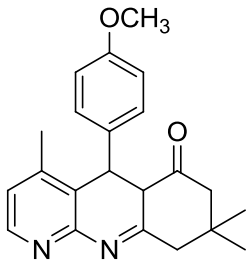

38g

Yield 90%, white solid, m.p. 239-241 ^{0}C. **IR (KBr)**: v 2958, 1666, 1625, 1511, 1461, 1357, 1137, 1033, 841 and 570 cm $^{-1}$. **^{1}H NMR (400 MHz, CDCl$_3$)**: δ 7.2 (1H, d, *J* = 8.8 Hz, H-7), 7.2 (2H, d, *J*= 8.8 Hz, H-3'& H-5'), 6.8 (1H, d, *J*= 8.8 Hz, H-6), 6.8 (2H, d, *J* = 8.8 Hz, H-2' & H-6'), 4.7 (1H, s, H-4), 3.7 (3H, s, OCH_3), 2.5 (3H, s, H-5a), 2.5 (1H, s, H-3), 2.2 (4H, dd, *J* = 12.4 Hz, H-9 & H-11), 1.1 (6H s, H-13 & H-14) ppm. **^{13}C NMR (400 MHz, CDCl$_3$)**: δ 21.0, 27.3, 29.2, 31.4, 32.7, 40.9, 50.8, 115.7, 128.0, 128.4, 135. 8, 141.1, 162.3 and 196.4 ppm. **EI-MS** found: 348.1 [M^+], **EI-MS** calculated: 348.4 [M^+]. **CHN analysis** (%) for $C_{22}H_{24}N_2O_2$ calcd: C, 75.83; H, 6.94; N, 8.04; found: C, 77.86; H, 6.98; N, 8.05.

5-(4-hydroxy-3-methoxyphenyl)-4, 8, 8-trimethyl-5, 5a, 8, 9-tetrahydrobenzo [*b*] [1, 8] naphthyridin-6(7H)-one (**38h)**

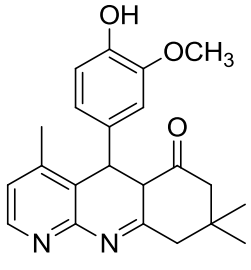

38h

Yield 90%, white solid, m.p. 230-232 ^{0}C. **IR (KBr)**: 3410, 2963, 1668, 1623, 1514, 1465, 1359, 1135, 1029, 624 and 462 cm $^{-1}$. **^{1}H NMR (400 MHz, CDCl$_3$)**: δ 7.3 (1H, s, OH), 7.0 (1H, d, *J* = 8.8 Hz, H-7), 7.0 (1H, d, *J* = 8.8 Hz, H-5'), 6.8 (1H, d, *J* = 8.4 Hz, H-6), 6.6 (1H, d, *J* = 8.4 Hz,H-6'), 6.6 (1H, s, H-2'), 4.7 (1H, s, H-4), 3.9 (3H, s, OCH_3), 2.5 (3H, s, H-5a), 2.5 (1H, s, H-3), 2.2 (4H, dd, *J* = 12.4 Hz, H-9 & H-11), 1.1 (6H s, H-13 & H-14) ppm. **^{13}C**

NMR (400 MHz, $CDCl_3$): δ 27.3, 29.3, 31.3, 32.2, 40.9, 50.7, 55.9, 112.3, 113.9, 115.8, 120.0, 136.5, 144.0, 145.9, 162.1 and 196.6 ppm. **EI-MS** found: 364.1 [M^+], **EI-MS** calculated: 364.4 [M^+]. **CHN analysis** (%) for $C_{22}H_{24}N_2O_3$ calcd: C, 72.50; H, 6.64; N, 7.69; found: C, 72.52; H, 6.65; N, 7.71.

3.6 Anticancer Studies

3.6.1 A549 Cell Viability Studies

A549 cell viability was determined using the 3-(4, 5-dimethyl-2-thiazolyl)-2, 5-diphenyl-2H-tetrazolium bromide (MTT) assay (Mossman, 1983). A549 cells (15,000 cells/well) were seeded into a 96-well microtitre plate. The synthesized compounds were dissolved in 10 % dimethyl sulphoxide (DMSO). A549 cells were then exposed to various compound dilutions (0-1000 µM) and a positive control camptothecin (0-100 µM) in three replicates (300 µl/well) and incubated (37 ºC, 5 % CO_2) for 24 hours. A vehicle control of A549 cells incubated with 10 % DMSO was used. Following incubation, cells were washed in 0.1 M PBS. A CCM / MTT salt solution (5 mg/ml) was then added (120 µl/well) and the plate was incubated (37 ºC, 4 hours). Thereafter, supernatants were removed; DMSO 100 µl/well was added and incubated for 1 hour. The optical density of the formazan product was measured (570/690 nm) using a spectrophotometer (Bio Tek µQuant). The results were expressed as percentage cell viability relative to the control. The concentration of half the maximum inhibition (IC_{50}) of the various compounds and camptothecin for the A549 cells was subsequently determined (Mossman *et al.*, 1983).

3.7 References

1. Mogilaiah K. and Sudhakar G.R. 2003. Synthesis of pyrazoline, pyrimidine and 1, 5-benzodiazepine derivatives of 1, 8-naphthyridine and evaluation of antibacterial activity. *Indian Journal of Chemistry*, 42B: 636-640.
2. Hwang Y.J., Chung M.L., Sohn U.D. and Im C. 2013. Cytotoxicity and structure-activity relationships of naphthyridine derivatives in Human cervical cancer, Leukemia and Prostate cancer. *Korea Journal of Physiol Pharmacol*, 17: 517-523.
3. Yamuna E., Zeller M. and Prasad K.J.R. 2012. Microwave assisted synthesis of indolo[2,3-b]dibenzo[b,g][1,8]naphthyridines. *Tetrahedron Letters*, 53: 1514-1517.
4. Bernardino A. M.R., Azevedo A.R., Pinheiro L.C.S., Borges J.C., Paixao I. C. P., Mesquita M., Souza T.M.L. and Santos M.S. 2012. Synthesis and anti-HSV-1 evaluation of new 3H-benzo[b]pyrazolo[3,4-h]-1,6-naphthyridines and 3H-pyrido[2,3-b]pyrazolo[3,4-h]-1,6-naphthyridines. *Organic and Medicinal Chemistry Letters*, 2(3): 1-7.
5. Pitchai P., Uvarani C., Gengan R.M. and Mohan P.S. 2013. A one pot microwave assisted synthesis of 3-acyl-2, 4-dihydroxyquinoline followed by synthesis of 7-methyldibenzo[c,f][2,7]naphthyridin-6(5H)-ones via three routes. *Indian Journal of Chemistry*, 52B: 776-786.
6. Srivastava K.P., Singh I. and Kumari A. 2014. Environmentally benign green synthesis and characterization of 4-methyl-2, 6-naphthyridines under microwave irradiation. Research and Reviews: *Journal of Chemistry*, 3(4): 18-26.
7. Badawneh M., Manera C., Mori C., Saccomanni G. and Ferrarini P.L. 2002. Synthesis of variously substituted 1,8-naphthyridine derivatives and evaluation of their antimycobacterial activity. *IL Farmaco*, 57: 631-639.
8. Plodek A., Raeder S. and Bracher F. 2012. Regioselective hemolytic substitution of benzo[*c*][2,7]naphthyridines. *Tetrahedron*, 68: 4693 – 4700.
9. Li X.L., Xu M.J., Zhao Y.L. and Xu J. 2010. A novel benzo[*f*][1,7]naphthyridine produced by streptomyces albogriseoulus from mangrove sediments. *Molecules*, 15: 9298-9307.
10. Xu D.B., Ye W.W., Han Y., Deng Z.X. and Hong K. 2014. Natural products from mangrove actinomycetes. *Marine drugs*, 12: 2590-2613.
11. Paulder W.W. and Kress T.J. 1966. A one-step synthesis of 1,8-naphthyridines. 32: 832-833.

12. Allen C.F.H. 1950. The naphthyridines. *Communication*, 1319: 275-305.
13. Leshner G.Y., Froelich E.J., Gruett M.D., Bailey J.H. and Brundage R.P. 1962. 1,8-Naphthyridine derivatives, a new class of chemotherapeutic agents. *Communication*: 1063-1065.
14. Mekheimer R.A., Hameed A.M.A. and Sadek K.U. 2007. 1,8-Naphthyridine II: synthesis of novel polyfunctionally substituted 1,8-naphthyridinones and their degradation to 6-aminopyridones. *Arkivoc:* 269-281.
15. Naik T.R.R., Naik H.S.B., Raghavendra M. and Naik S.G.K. 2006. Synthesis of thieno [2,3-*b*][benzo][1,8]naphthyridine-2-carboxylic acids under microwave irradiation and interaction with DNA studies. *Arkivoc*: 84-94.
16. Kanouni T. Dong Q., Abelovski B. and Wallace M.B. 2011. Synthetic approaches to 1,8-naphthyridine-2,5-dione compounds. *Tetrahedron Letters*, 52: 477-479.
17. Feng X., Wang J.J., Zhang J.J., Cao C.P., Huang Z.B. and Shi D.Q. 2014. Regioslective synthesis of functionalized [1,8]-naphthyridine derivatives via three-component domino reaction under catalyst-free conditions. *Royal Society of Chemistr*y, 17: 973-981.
18. Wen L.R., Jiang C.Y., Li M. and Wang L.J. 2011. Application of 2-(2-chloroaroyl)methyleneimidazolidines in domino and multicomponent reaction: new entries to imidazo [1,2-*a*]pyridines and benzo[*b*]imidazo[1,2,3-*ij*][1,8]naphthyridines. *Tetrahedron*, 67: 293-302.
19. Naik T.R.R., Naik H.S.B., Naik H.R.P. and Bindu P.J. 2008. Three-component one-pot synthesis of novel benzo[*b*]1,8-naphthyridines catalyzed by bismuth (III) chloride. *Research letter in Organic Chemistry*: 1-4.
20. Ghorbani-Vaghei R. and Malaekehpoor S.M. 2016. Multicomponent approach for the synthesis of substituted 1,8-naphthyridine derivatives catalyzed by N-bromosulfonamides. *Synthesi*s, 48: A-G.
21. Shelar D.P., Patil S.R., Rote R.V., Toche R.B. and Jachak M.N. 2011. Synthesis and flruorescence investigation of differently substituted benzo[*b*][1,8]naphthyridines: interaction with different solvents and bovine serum albumin. *Journal of Fluorescen*t, 21: 1033-1047.
22. Acosta P., Butassi E., Insuasty B., Ortiz A., Abonia R., Zacchino S.A. and Quiroga J. 2015. Microwave-assisted synthesis of novel pyrazolo[3,4-*g*][1,8]naphthyridin-5-amine with potential antifungal and antitumor activity. *Molecules*, 20: 8499-8520.

23. Fu L., Feng X., Wang J., Xun Z., Hu J., Zhang J., Zhao Y., Huang Z. and Shi D. 2014. Efficient synthesis and evaluation of antitumor activities of novel functionalized 1,8-naphthyridine derivatives. *American Combinatorial Science*: 1-18.
24. Mossman T. 1983. Rapid colorimetric assay for cellular growth and survival: application to proliferation and cytotoxicity assays. *Journal of Immunological Methods*, 65:55.
25. Alonso C., Fuertes M., Gonzalez M., Rubiales G., Tesauro C., Knudsen B.R, Palacios F. 2016. Synthesis and biological evaluation of indeno [1,5]naphthyridines as topoisomerase I (TopI) inhibitors with antiproliferative activity. *European Journal of Medicinal Chemistry*, 115:179-190.

Appendix - III

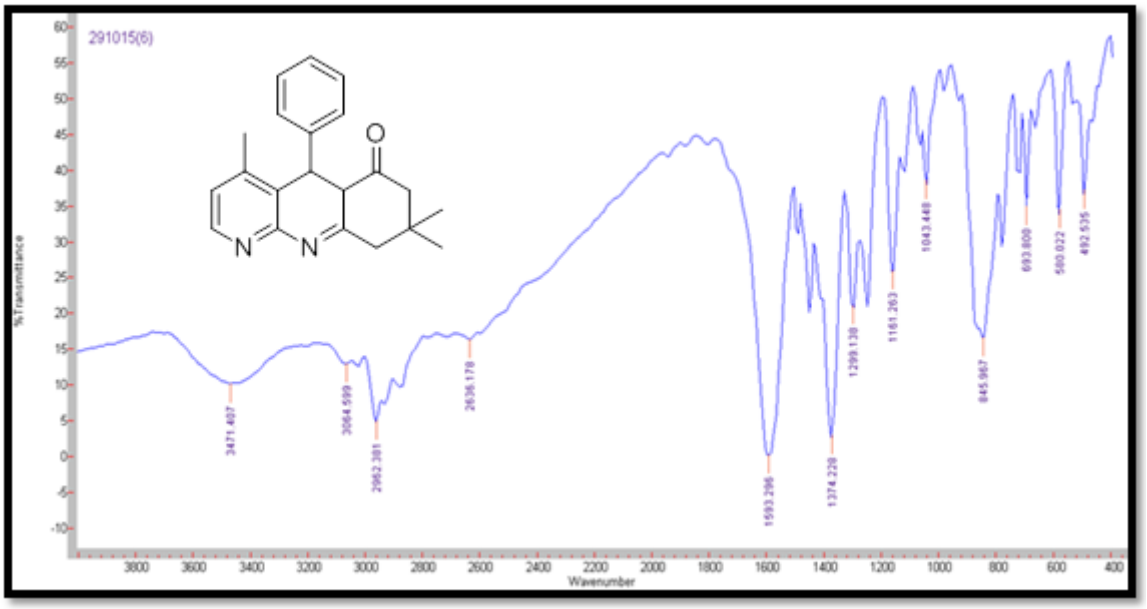

Appendix 3.1: IR spectrum for compound **38a**

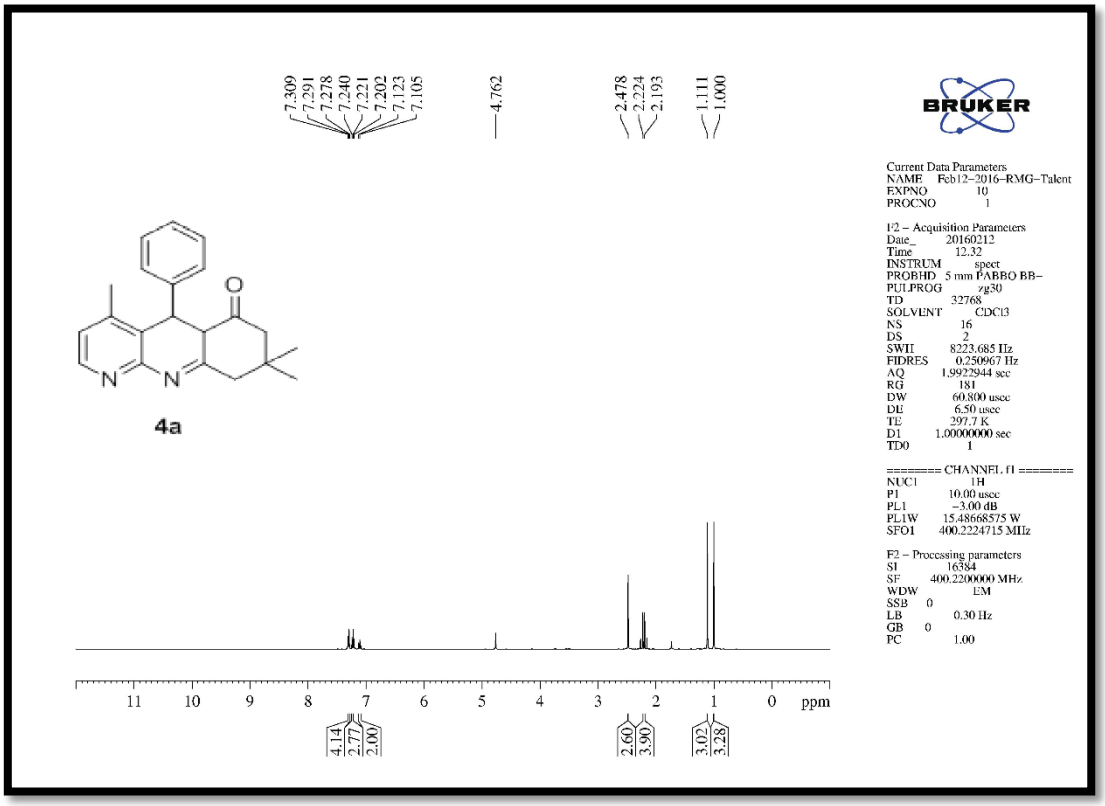

Appendix 3.2: ^{1}H-NMR spectrum for compound **38a**

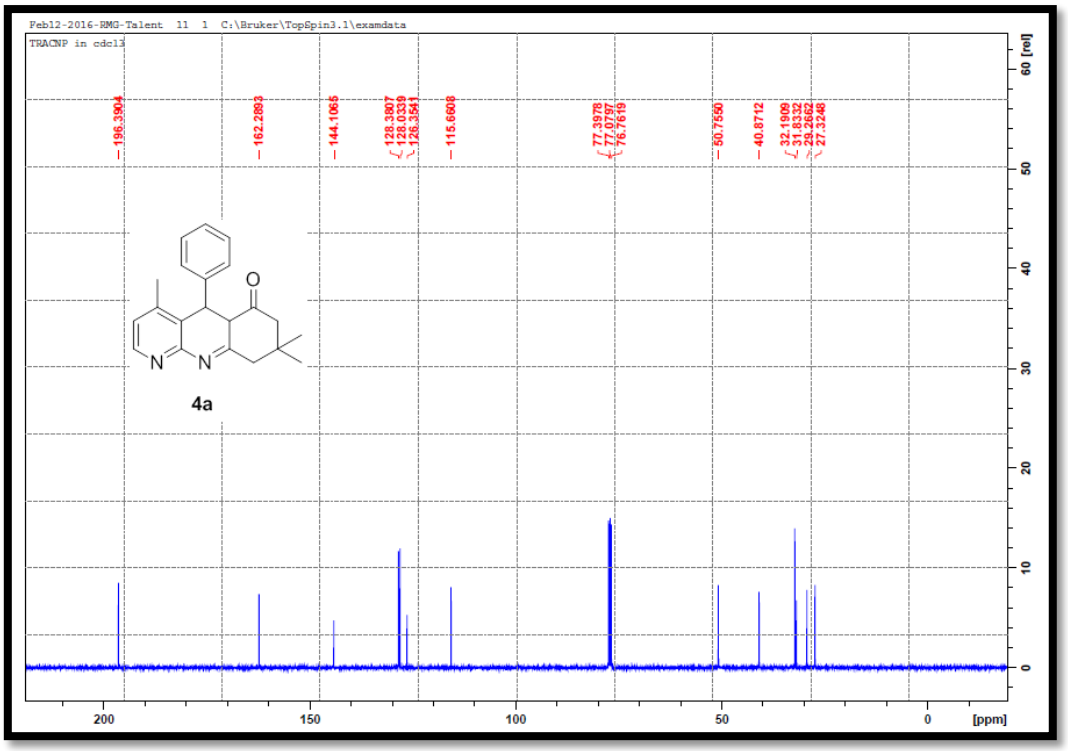

Appendix 3.3: ^{13}C NMR spectrum for compound **38a**

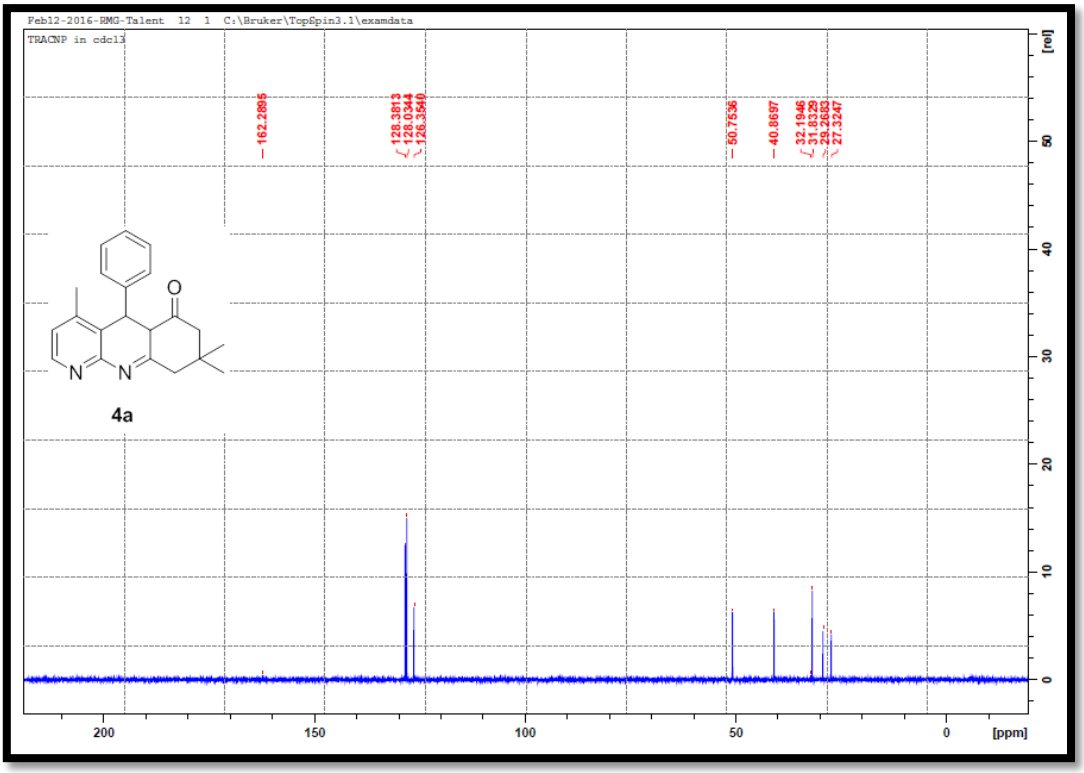

Appendix 3.4: 90^0 DEPT NMR spectrum for compound **38a**

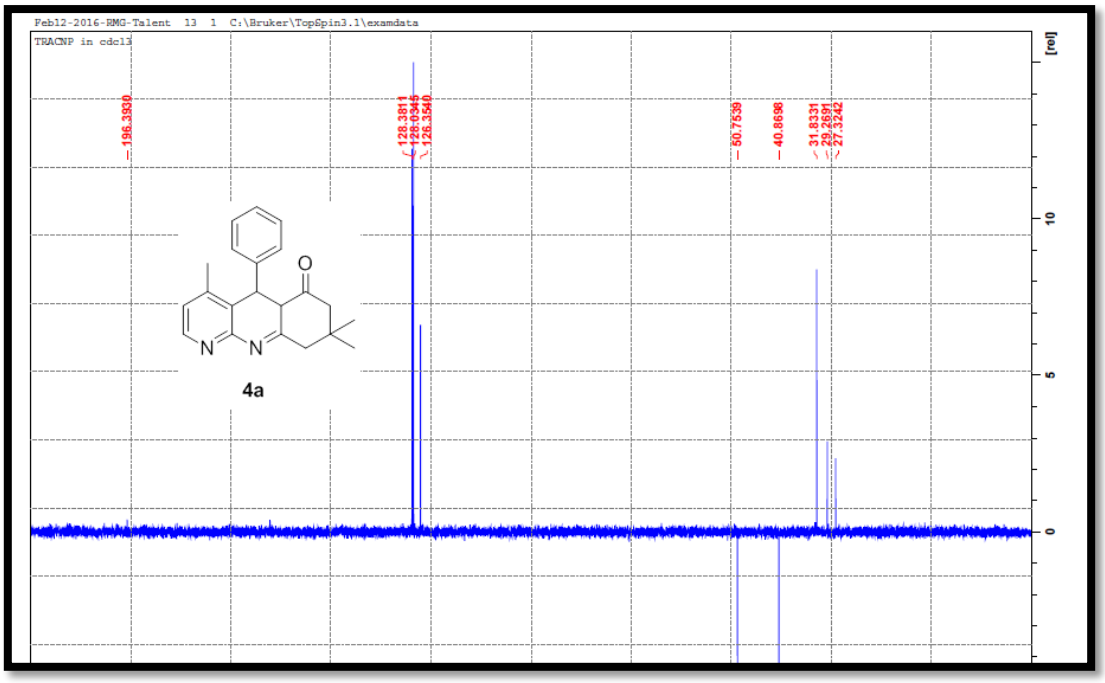

Appendix 3.5: 135^0 DEPT NMR spectrum for compound **38a**

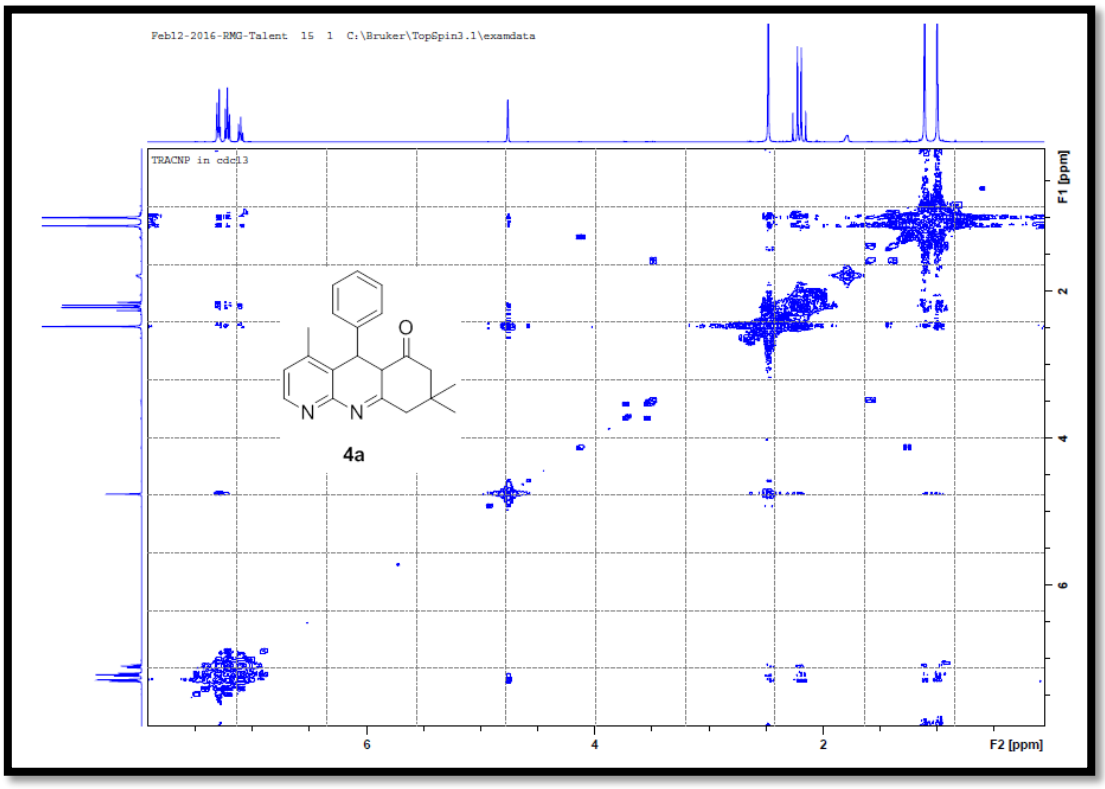

Appendix 3.6: COSY NMR spectrum for compound **38a**

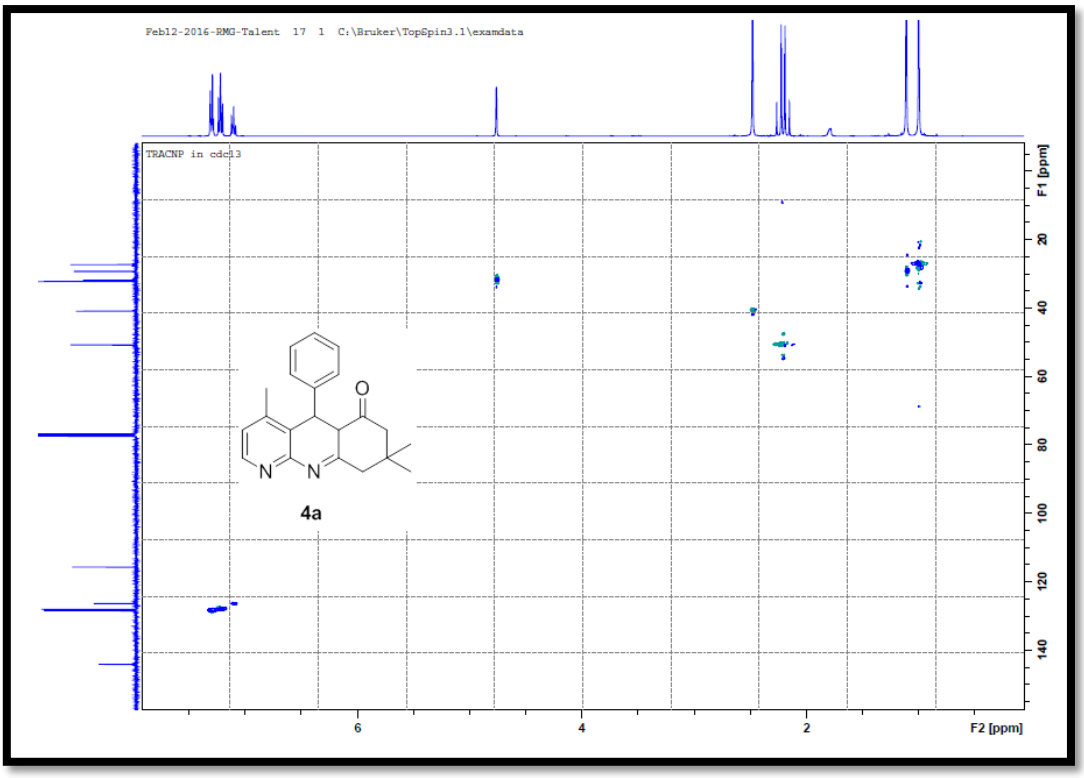

Appendix 3.7: HSQC NMR spectrum for compound **38a**

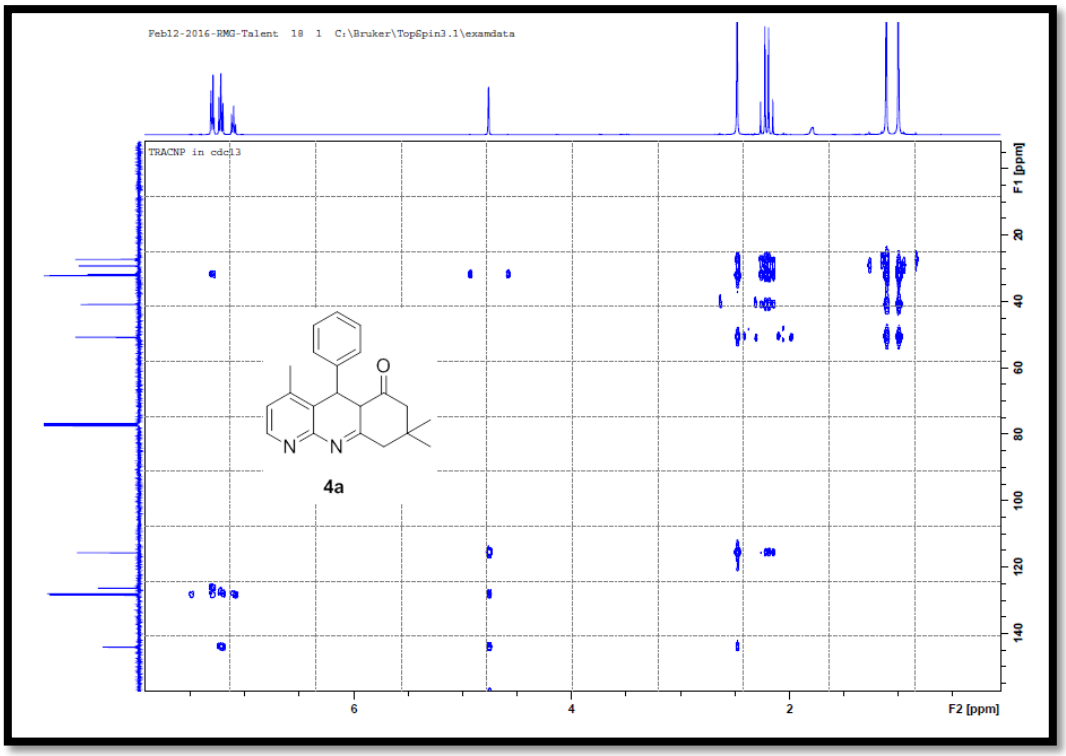

Appendix 3.8: HMBC NMR spectrum for compound **38a**

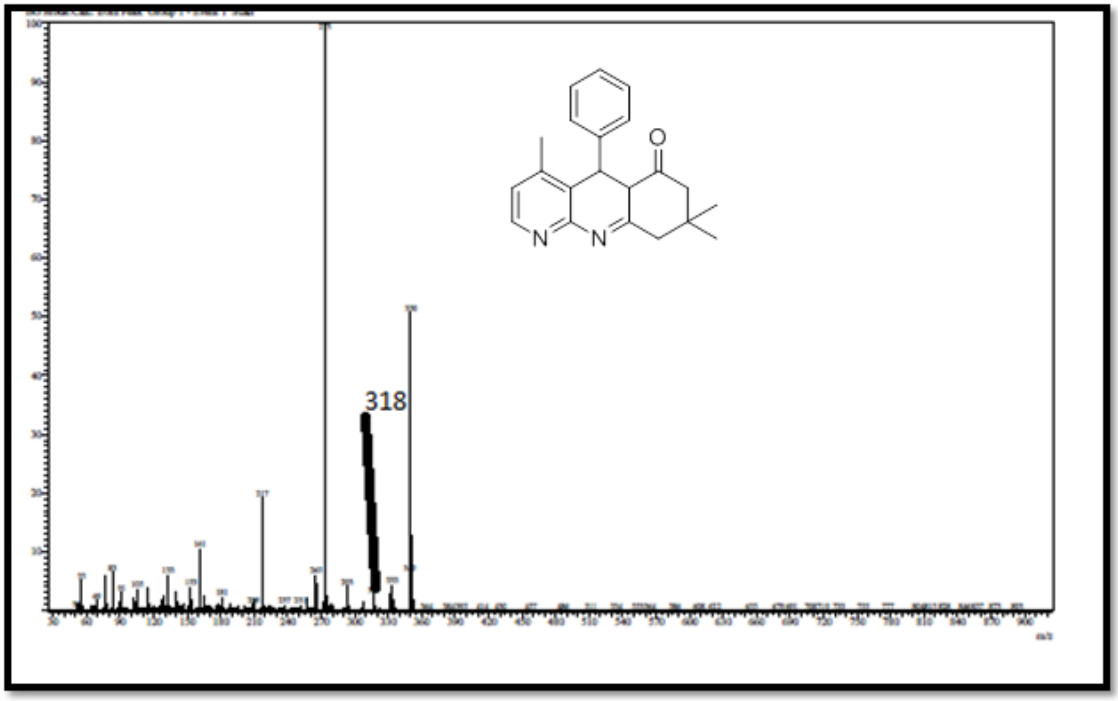

Appendix 3.9: EI-MS spectrum for compound **38a**

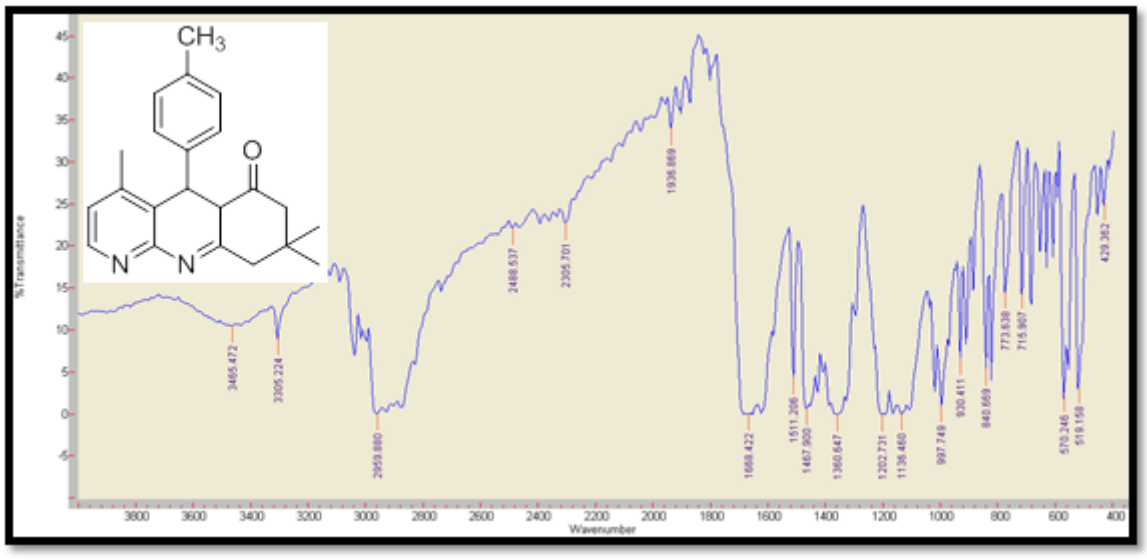

Appendix 3.10: IR spectrum for compound **38b**

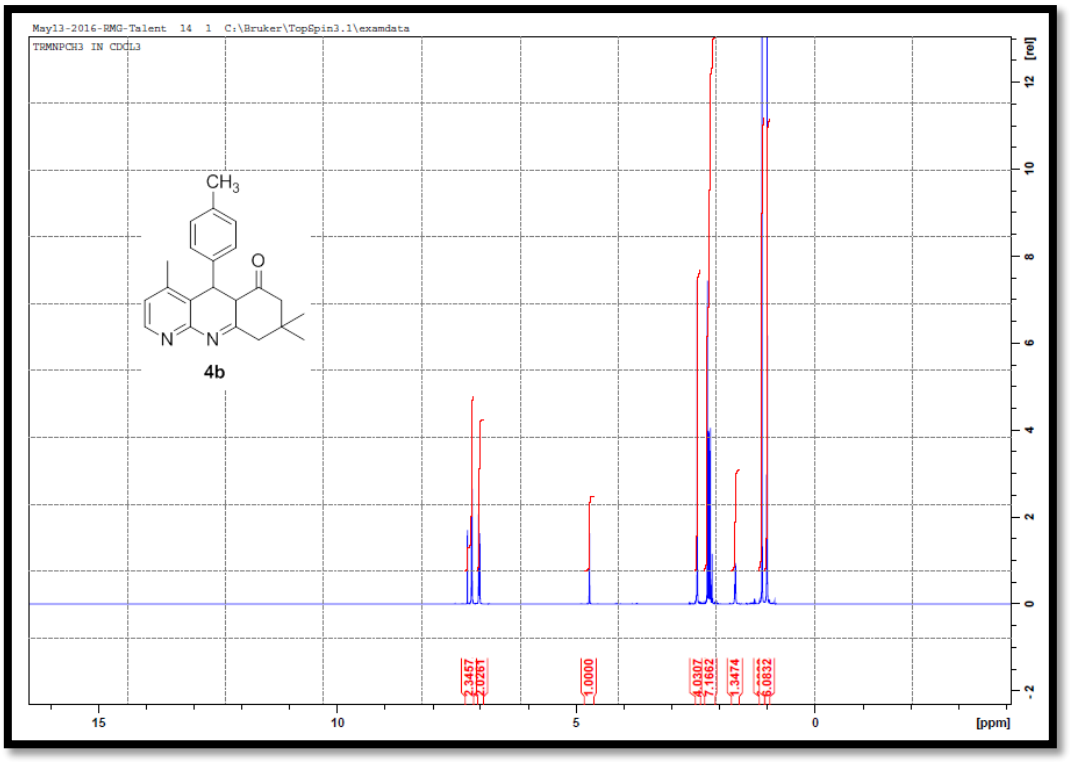

Appendix 3.11: ^{1}H-NMR spectrum for compound **38b**

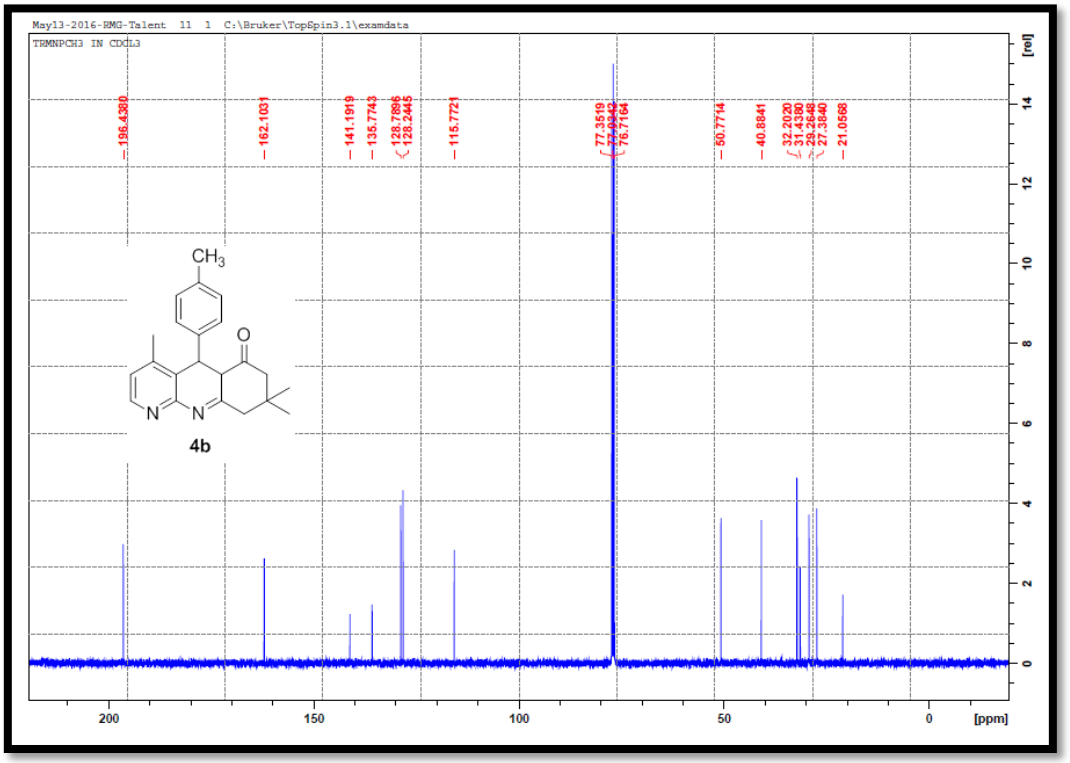

Appendix 3.12: ^{13}C-NMR spectrum for compound **38b**

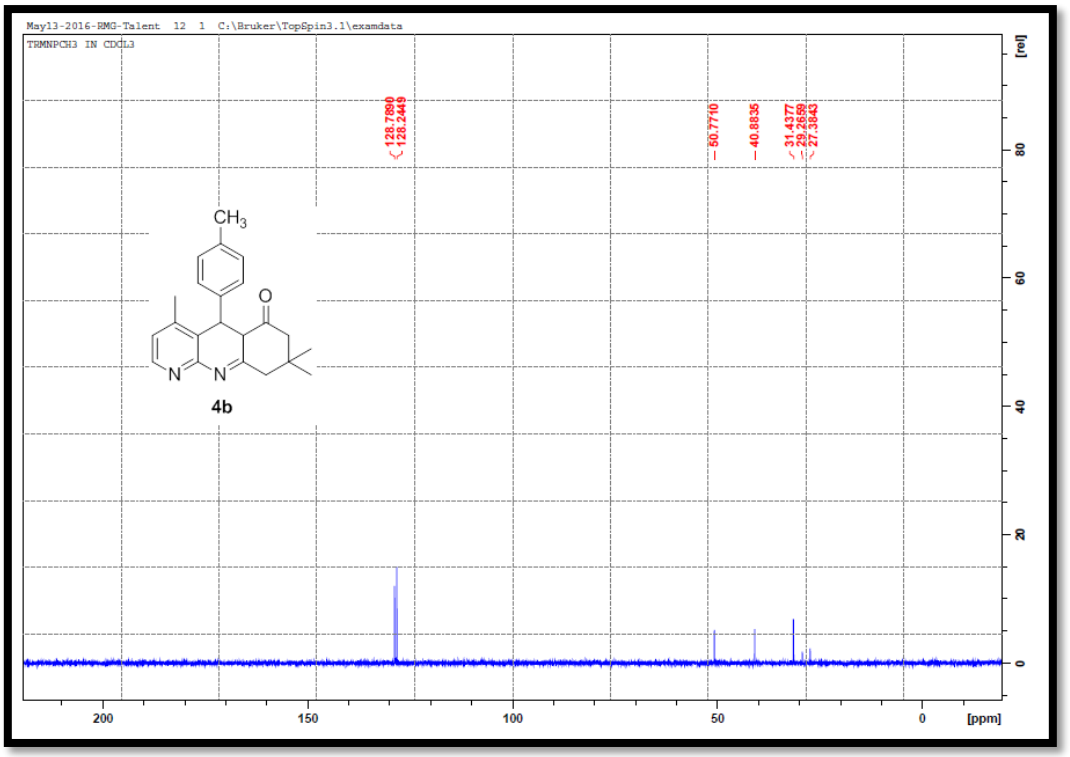

Appendix 3.13: 90^0 DEPT NMR spectrum for compound **38b**

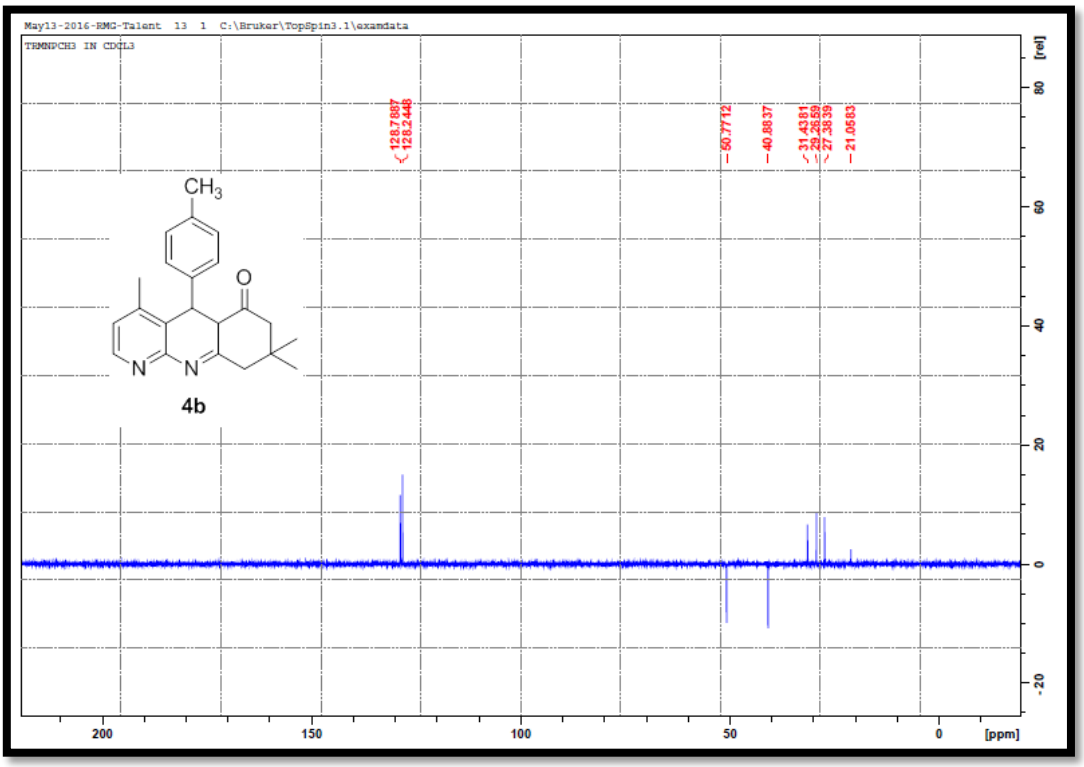

Appendix 3.14: 135^0 DEPT NMR spectrum for compound **38b**

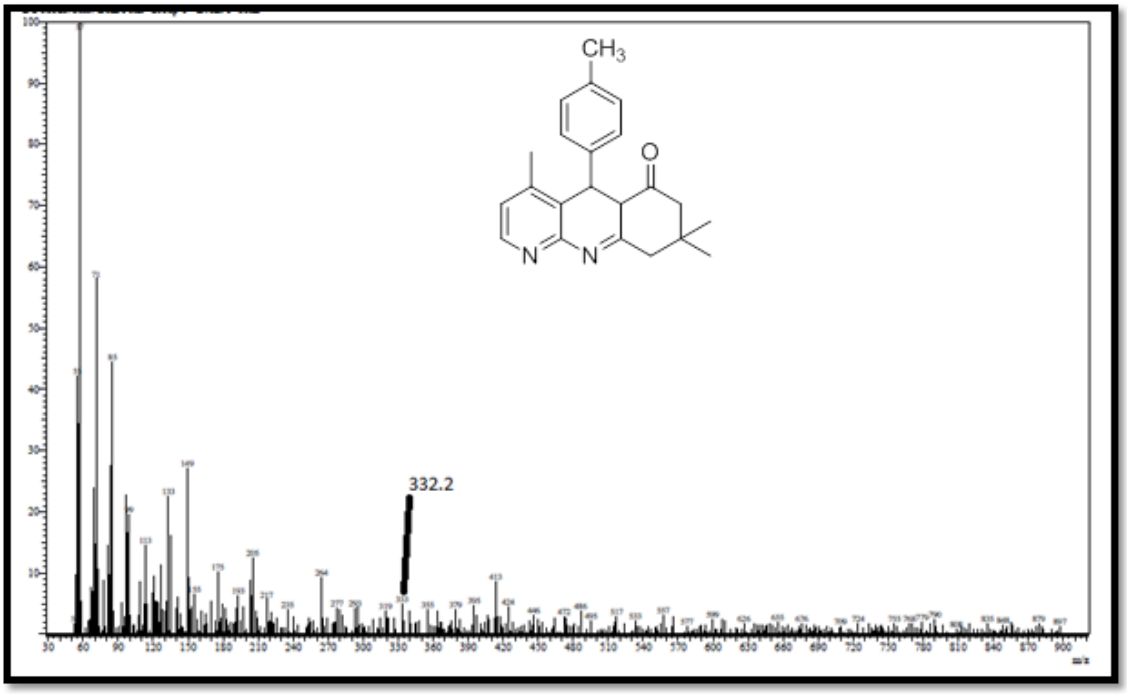

Appendix 3.15: EI-MS spectrum for compound **38b**

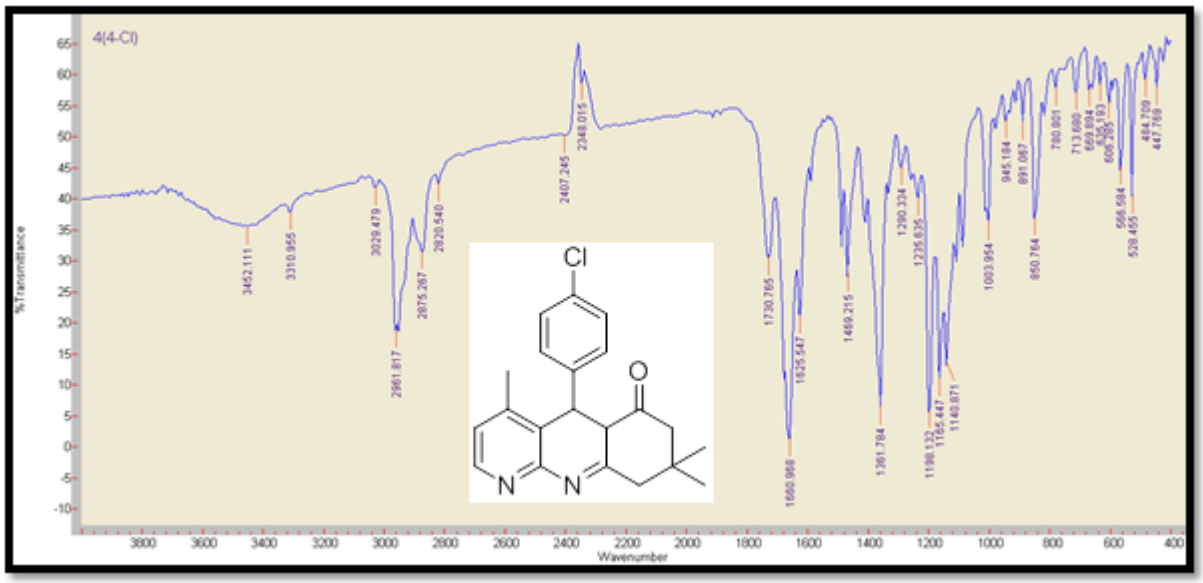

Appendix 3.16: IR spectrum for compound **38c**

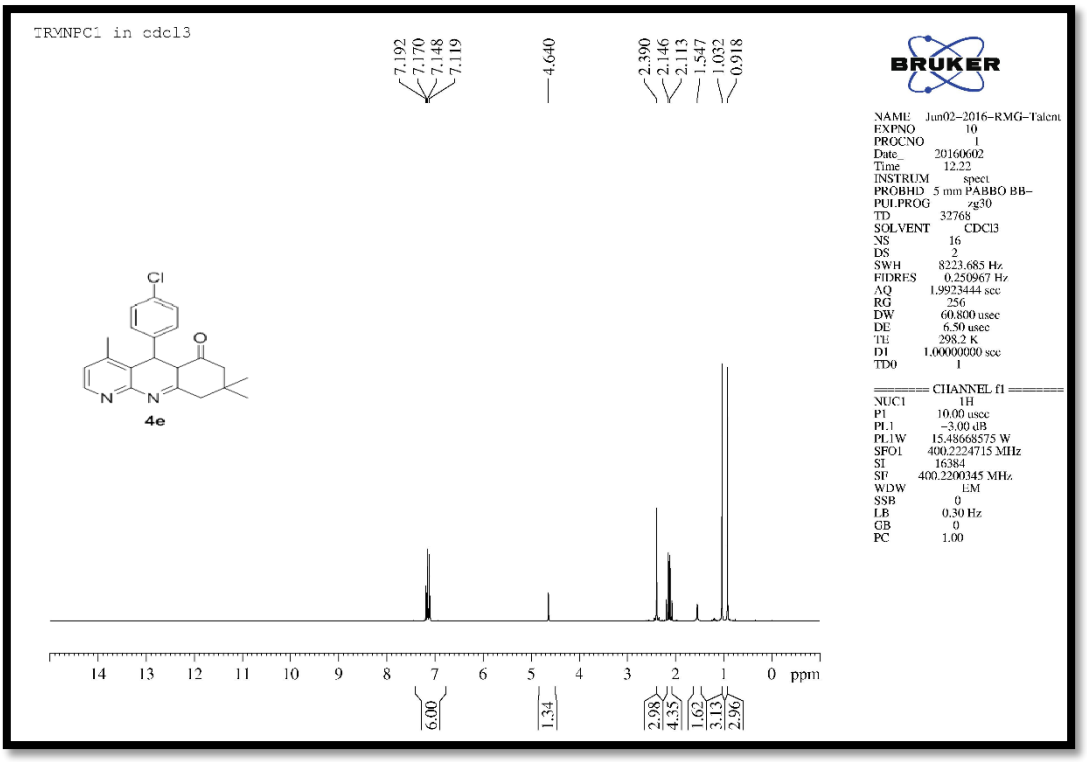

Appendix 3.17: ^{1}H-NMR spectrum for compound **38c**

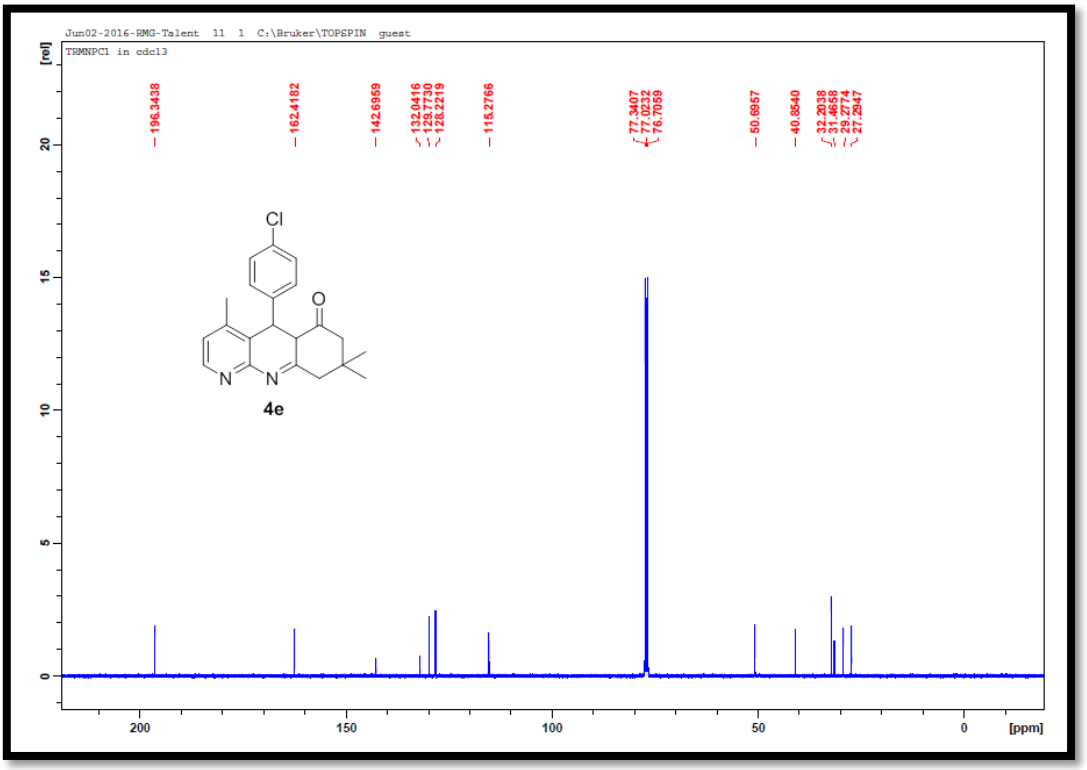

Appendix 3.18: ^{13}C-NMR spectrum for compound **38c**

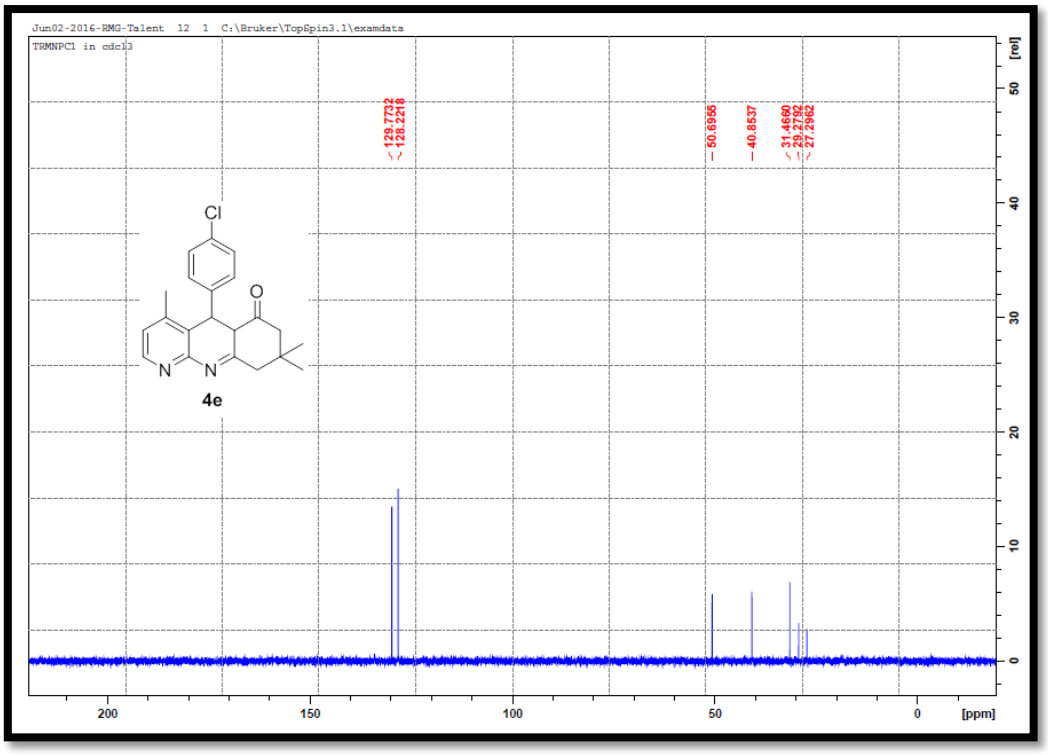

Appendix 3.19: 90^0 DEPT NMR spectrum for compound **38c**

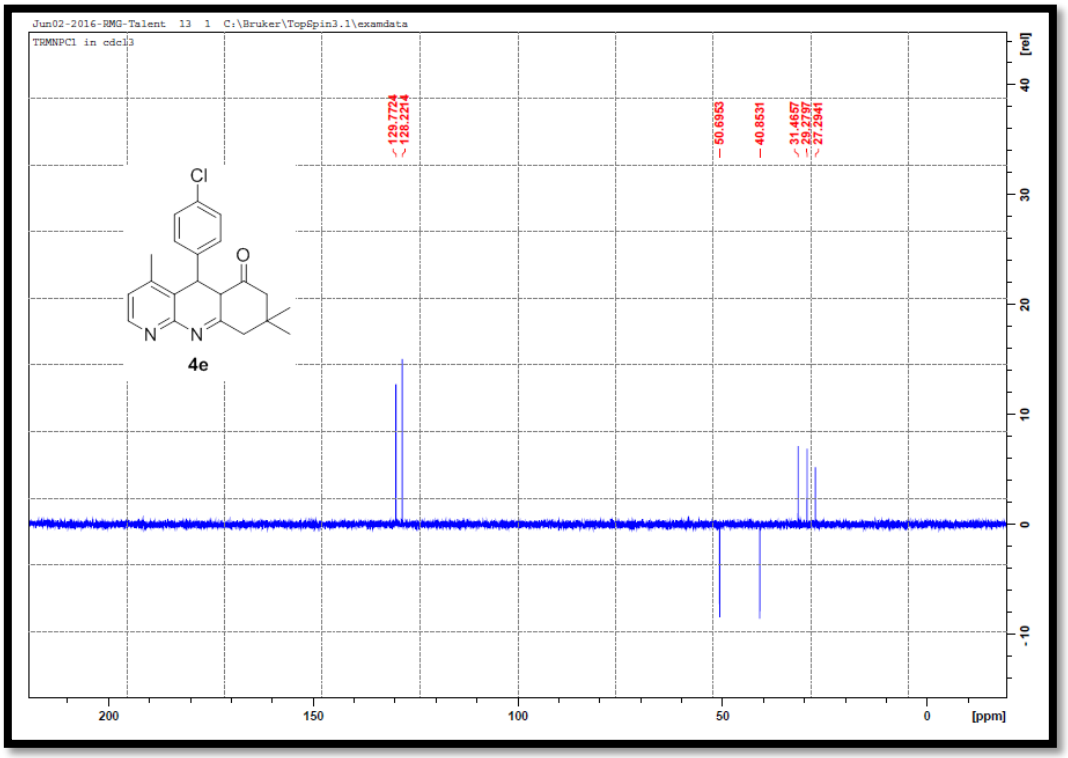

Appendix 3.20: 135^0 DEPT NMR spectrum for compound **38c**

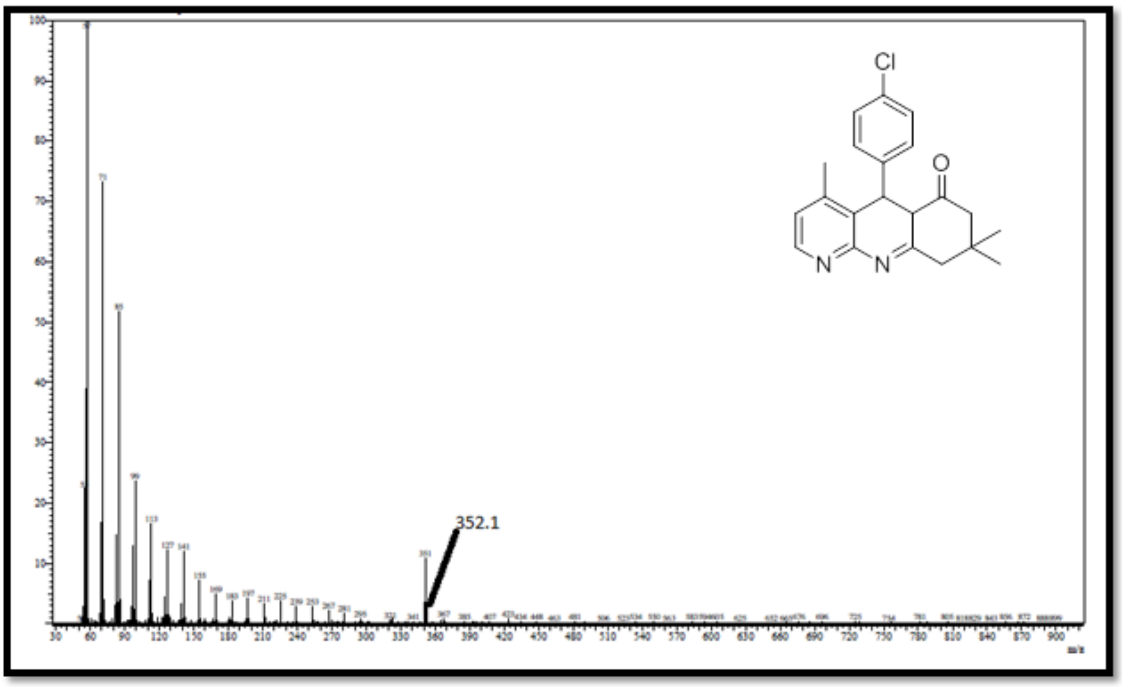

Appendix 3.21: EI-MS spectrum for compound **38c**

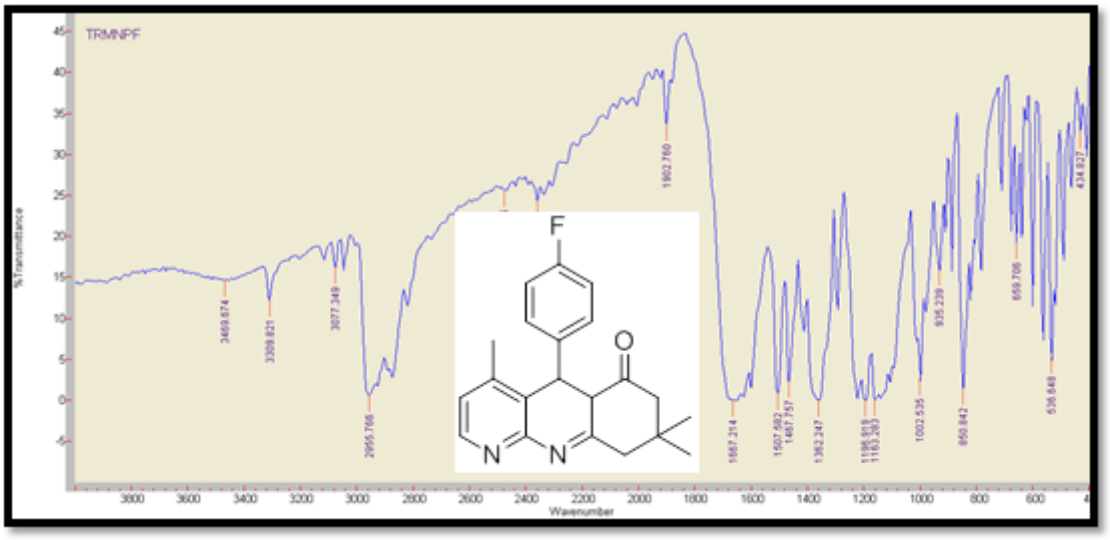

Appendix 3.22: IR spectrum for compound **38d**

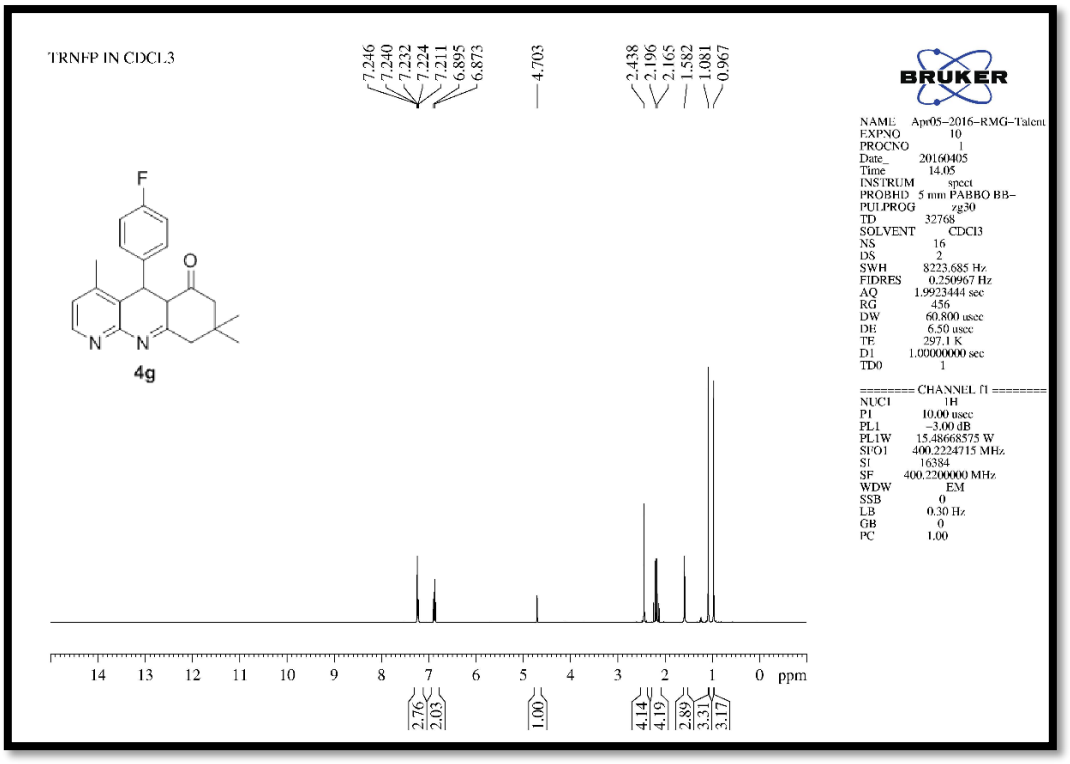

Appendix 3.23: ^{1}H-NMR spectrum for compound **38d**

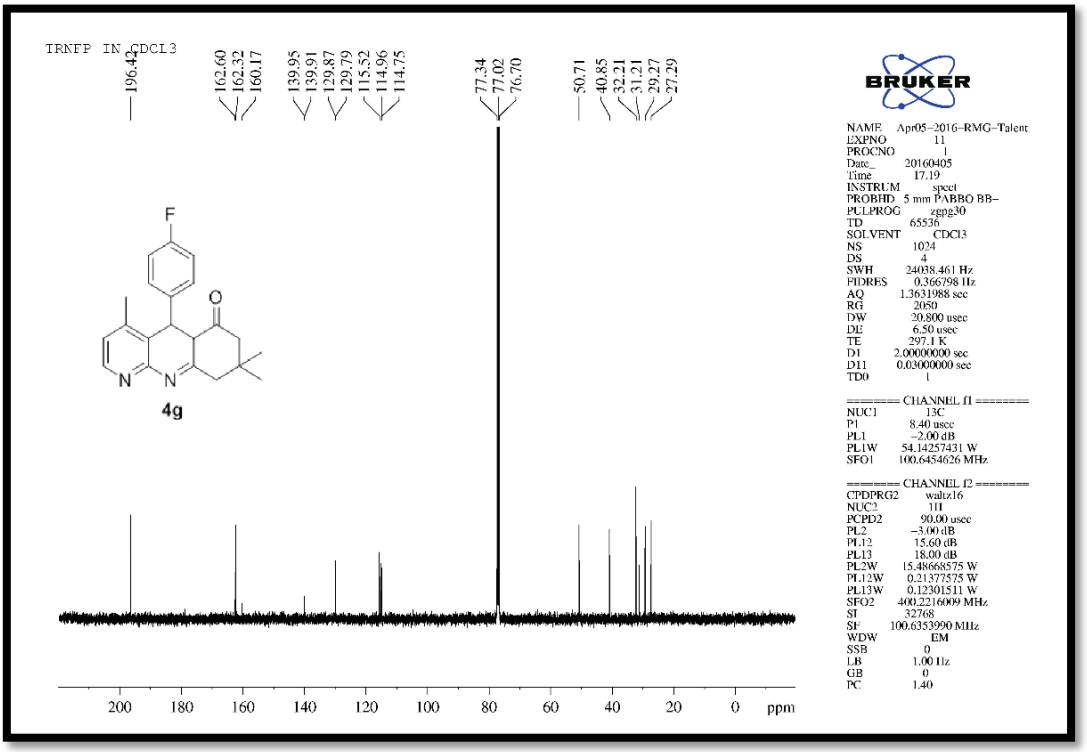

Appendix 3.24: ^{13}C-NMR spectrum for compound **38d**

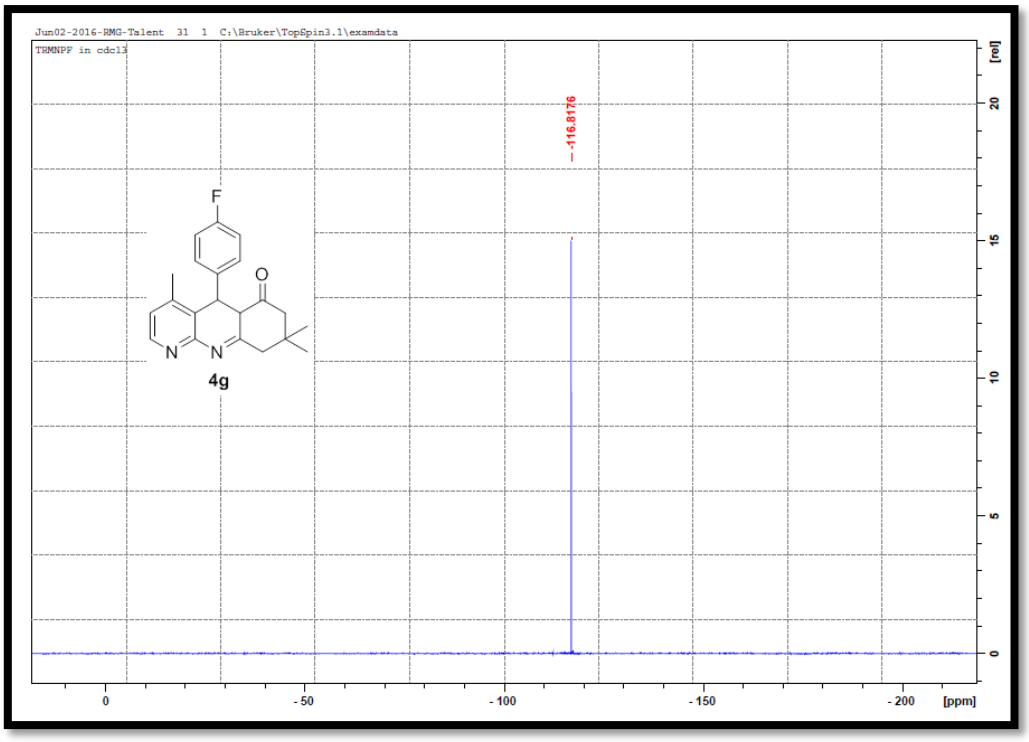

Appendix 3.25: ^{19}F NMR spectrum for compound **38d**

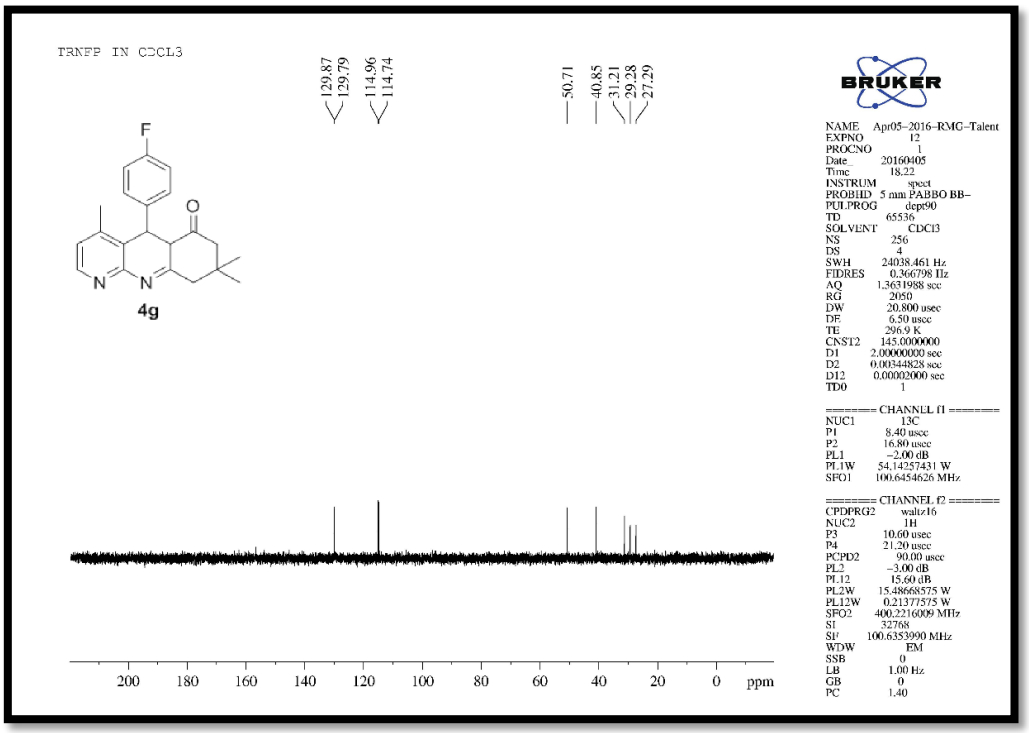

Appendix 3.26: 90^0 DEPT NMR spectrum for compound **38d**

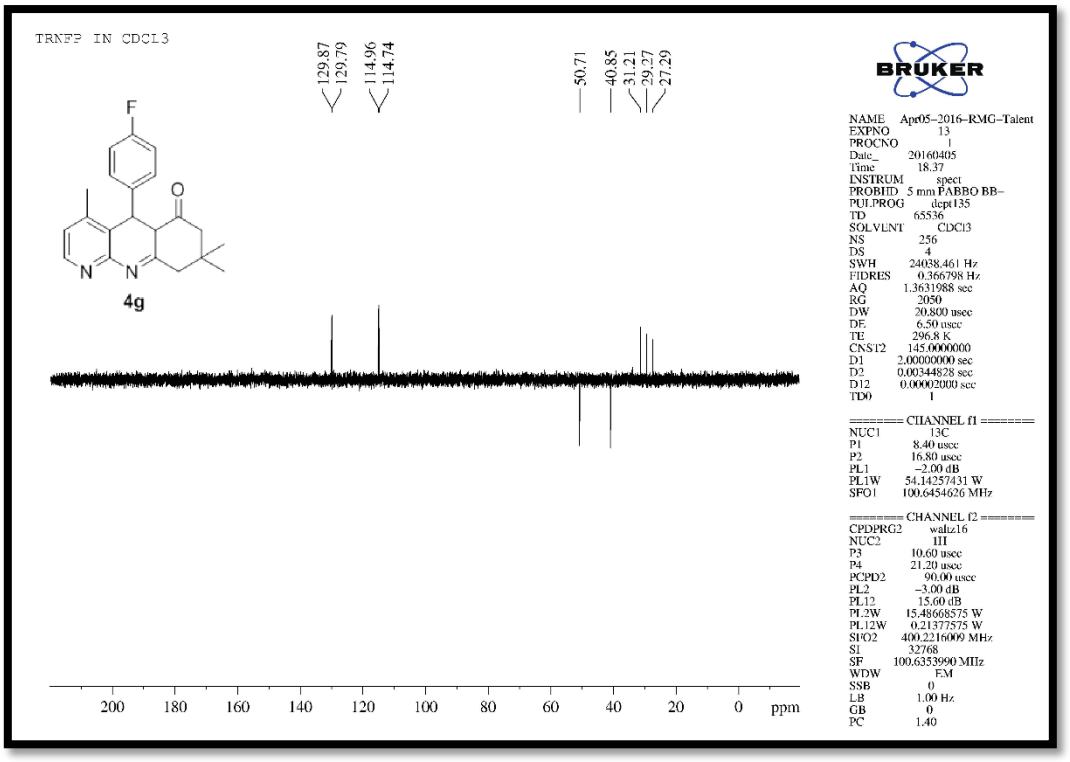

Appendix 3.27: 135^0 DEPT spectrum for compound **38d**

Appendix 3.28: EI-MS spectrum for compound **38d**

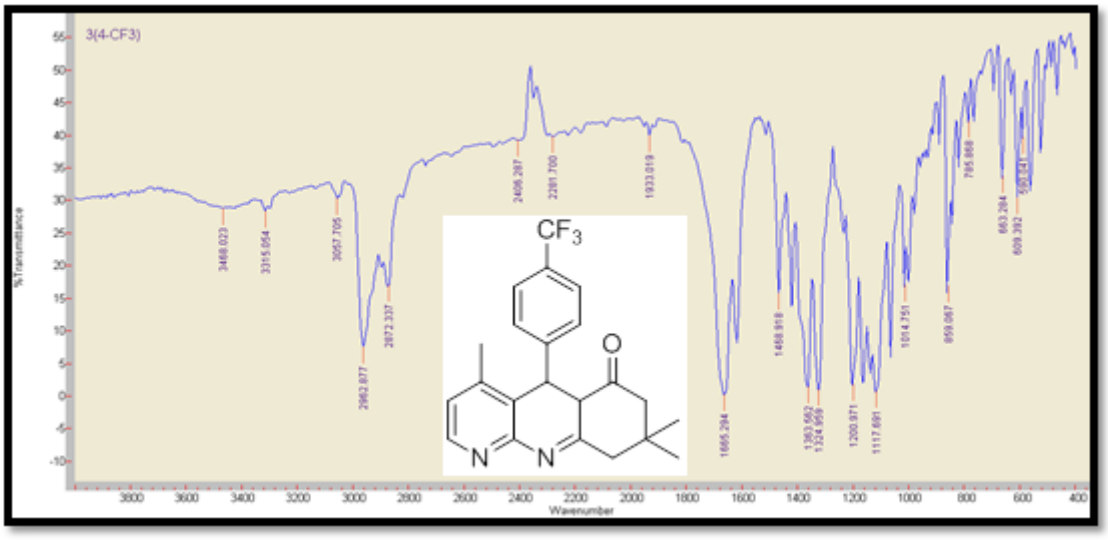

Appendix 3.29: IR spectrum for compound **38e**

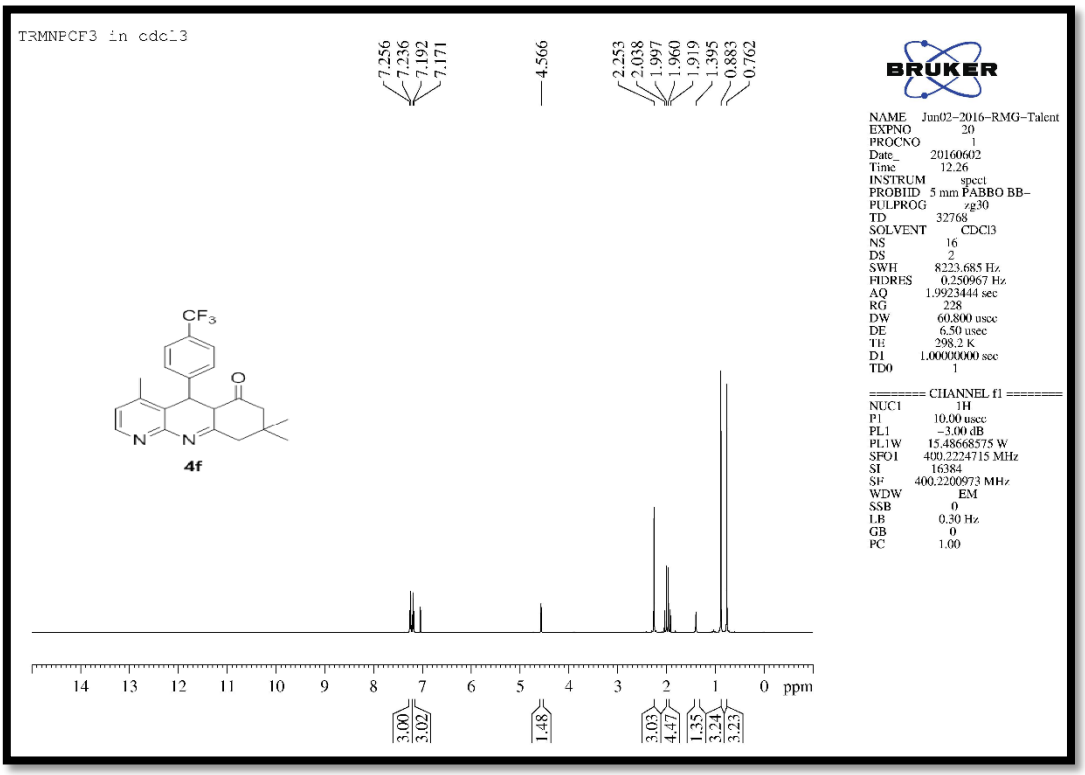

Appendix 3.30: ^{1}H-NMR spectrum for compound **38e**

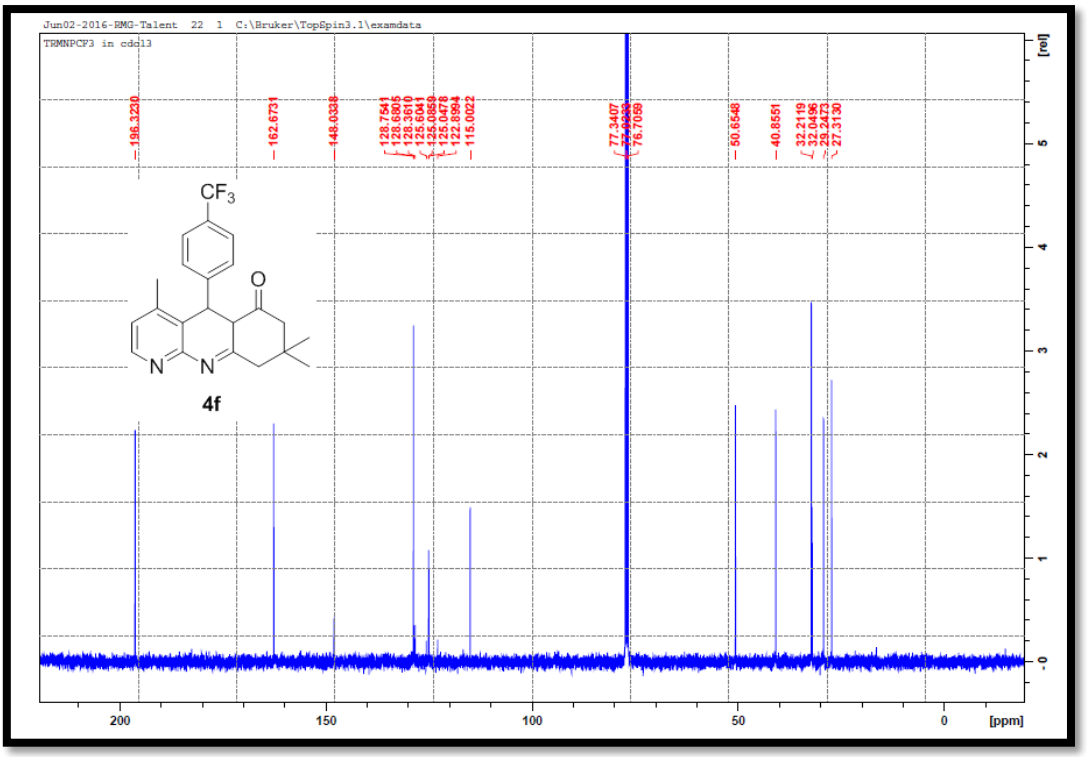

Appendix 3.31: ^{13}C-NMR spectrum for compound **38e**

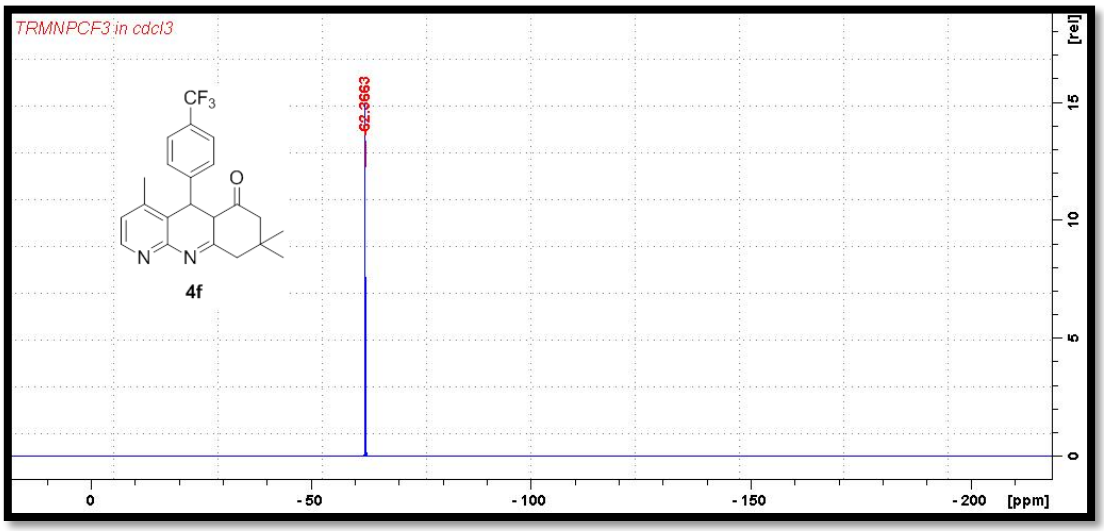

Appendix 3.32: ^{19}F-NMR spectrum for compound **38e**

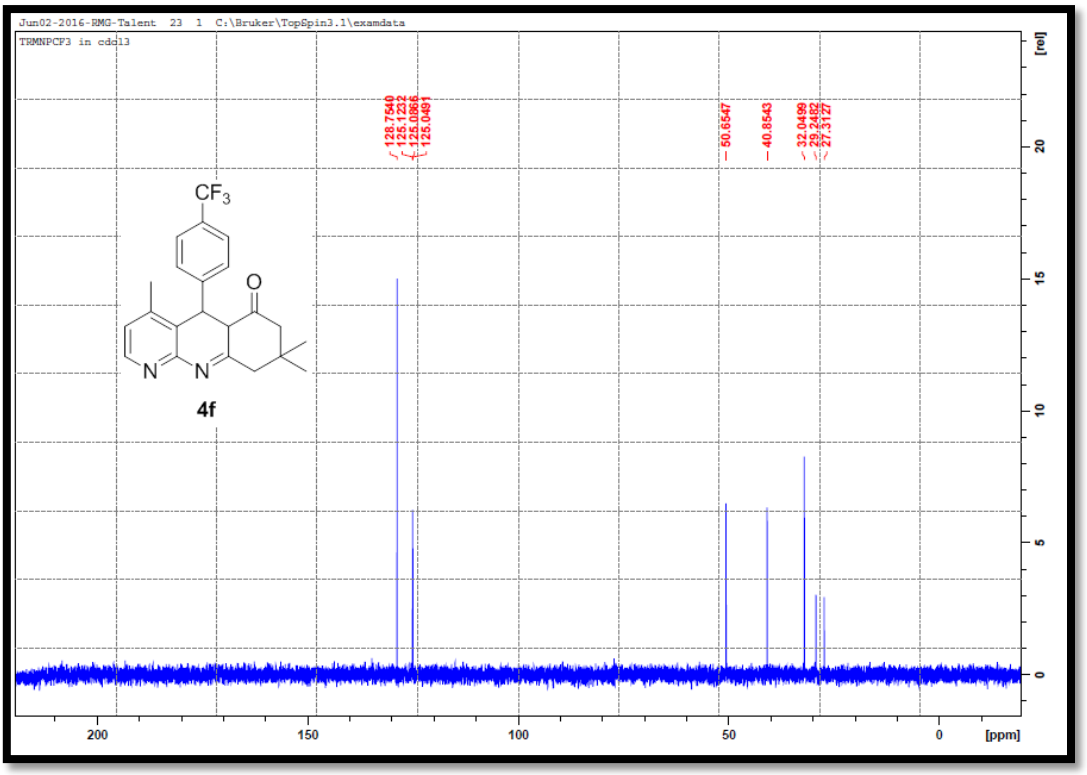

Appendix 3.33: 90^0 DEPT NMR spectrum for compound **38e**

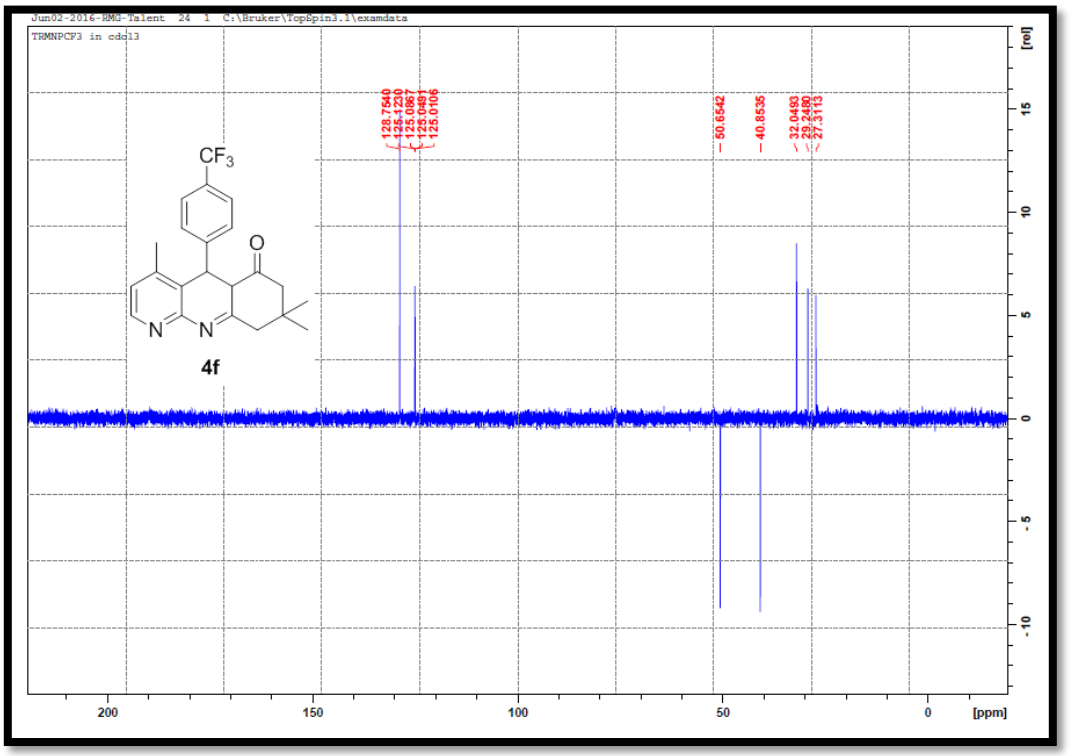

Appendix 3.34: 135^0 DEPT NMR spectrum for compound **38e**

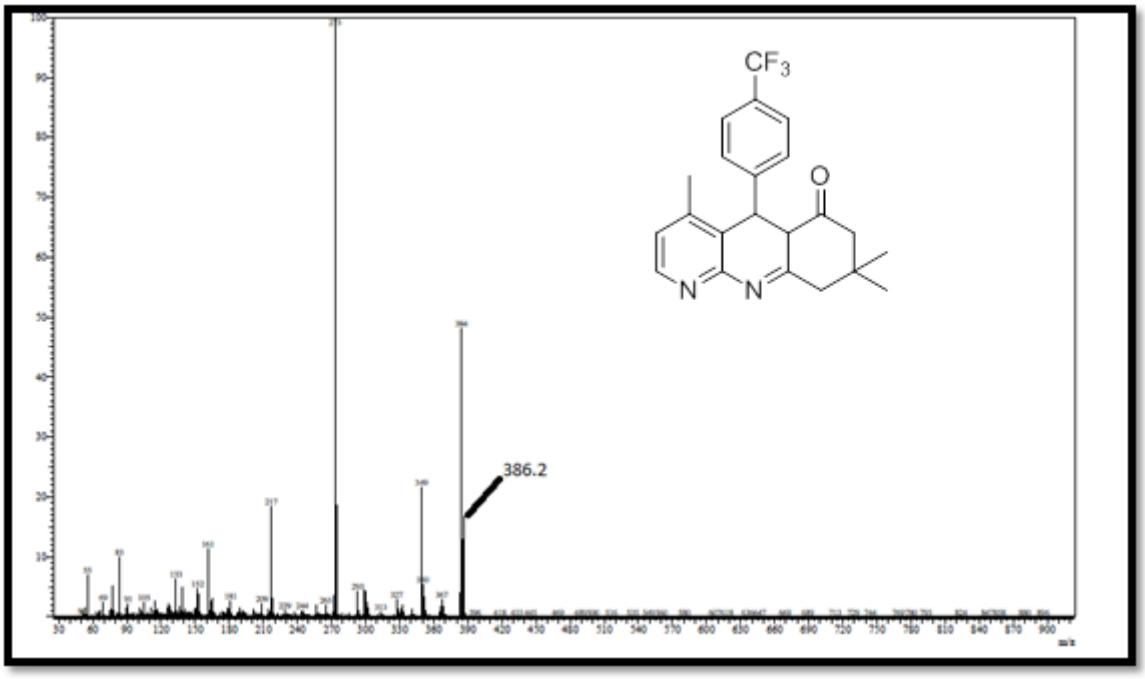

Appendix 3.35: EI-MS spectrum for compound **38e**

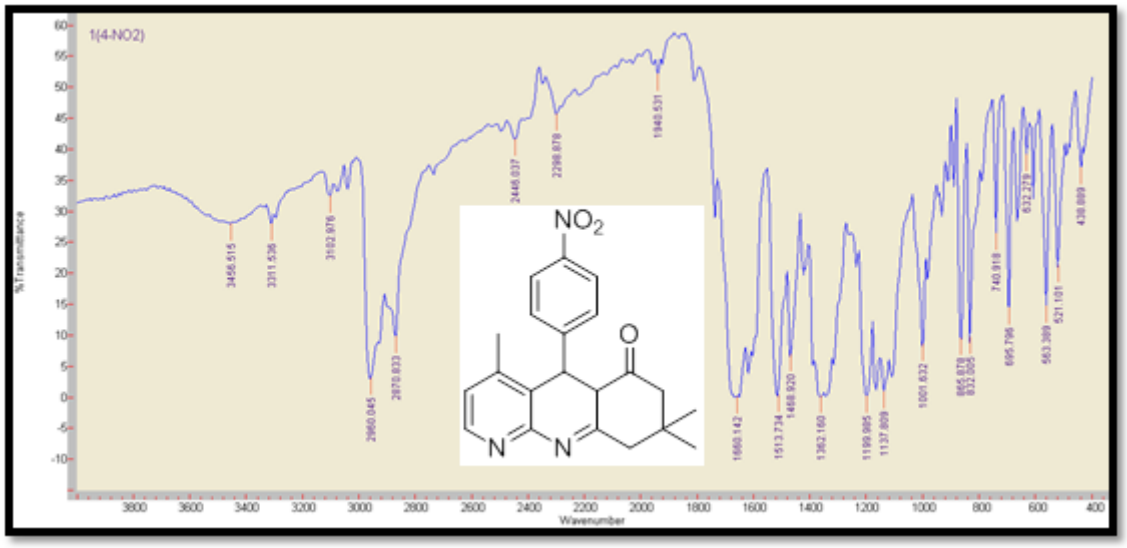

Appendix 3.36: IR spectrum for compound **38f**

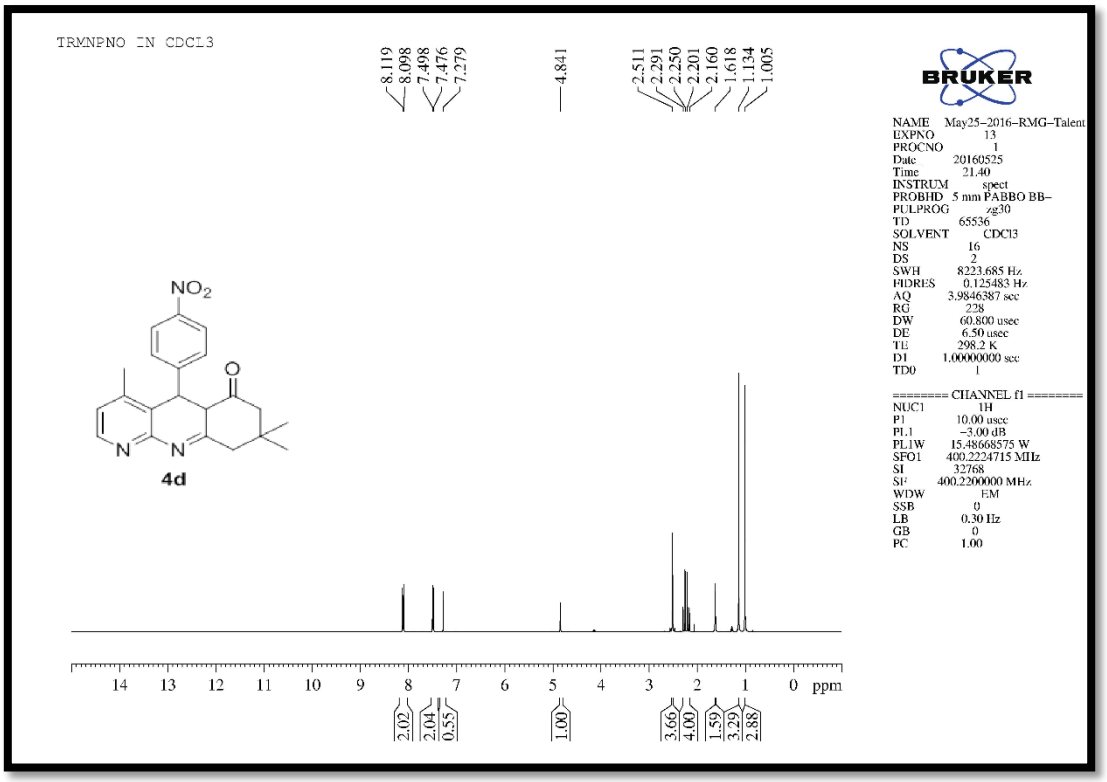

Appendix 3.37: ^{1}H-NMR spectrum for compound **38f**

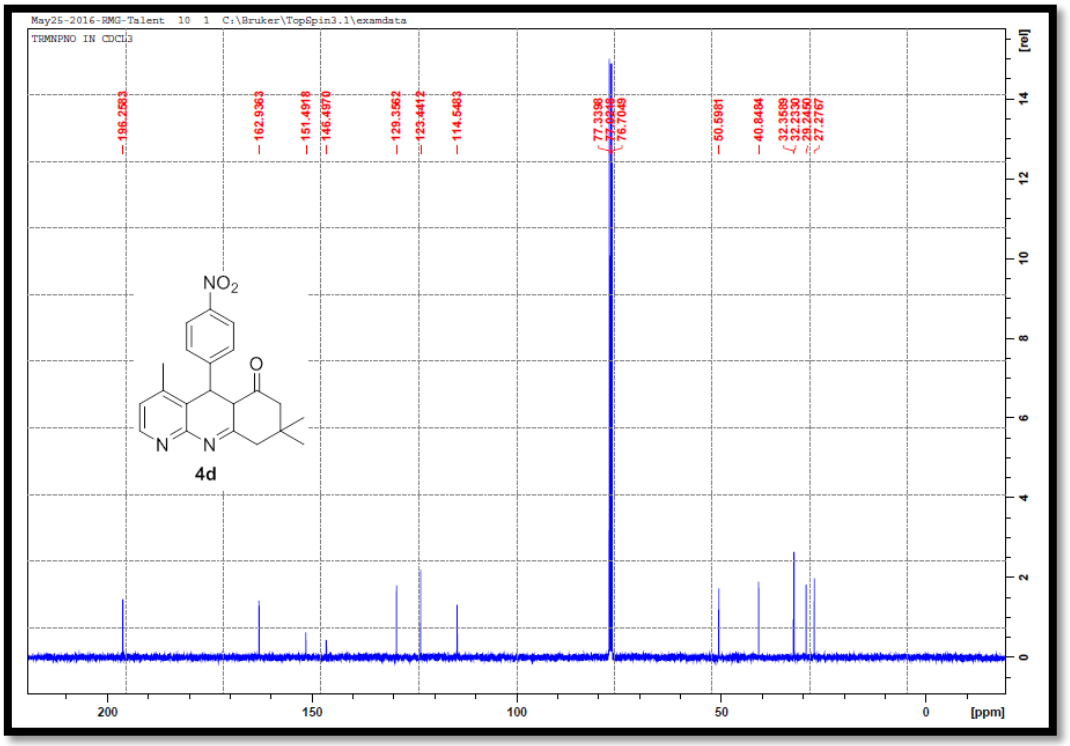

Appendix 3.38: ^{13}C-NMR spectrum for compound **38f**

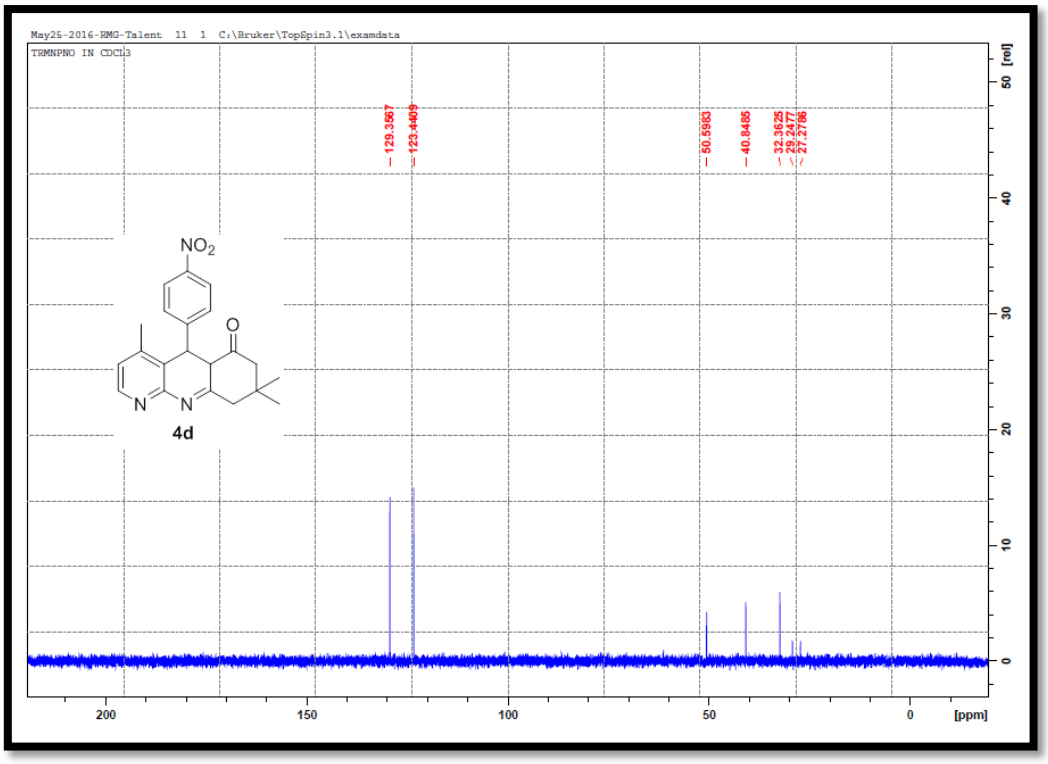

Appendix 3.39: 90^0 DEPT NMR spectrum for compound **38f**

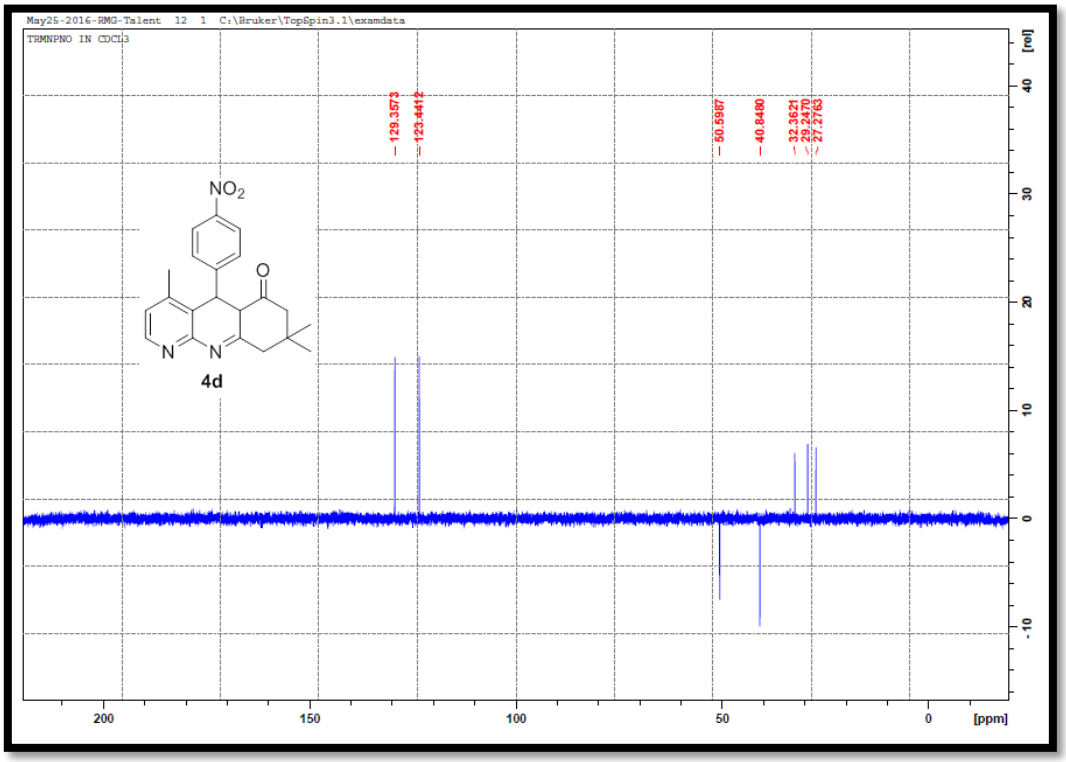

Appendix 3.40: 135^0 DEPT NMR spectrum for compound **38f**

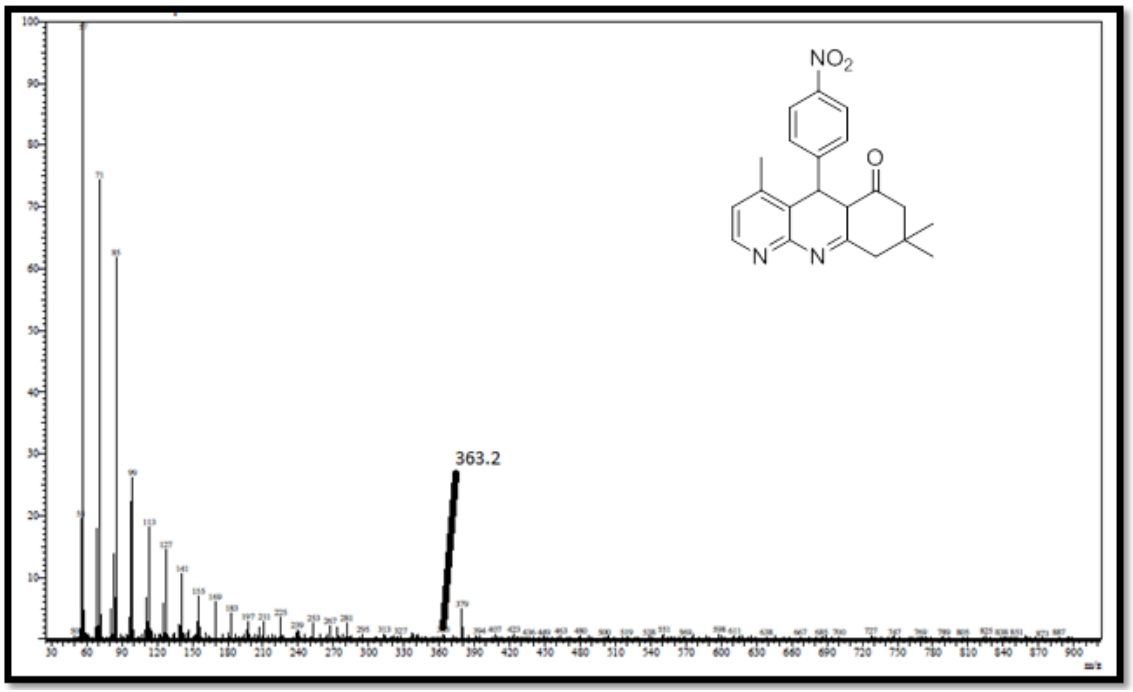

Appendix 3.41: EI-MS spectrum for compound **38f**

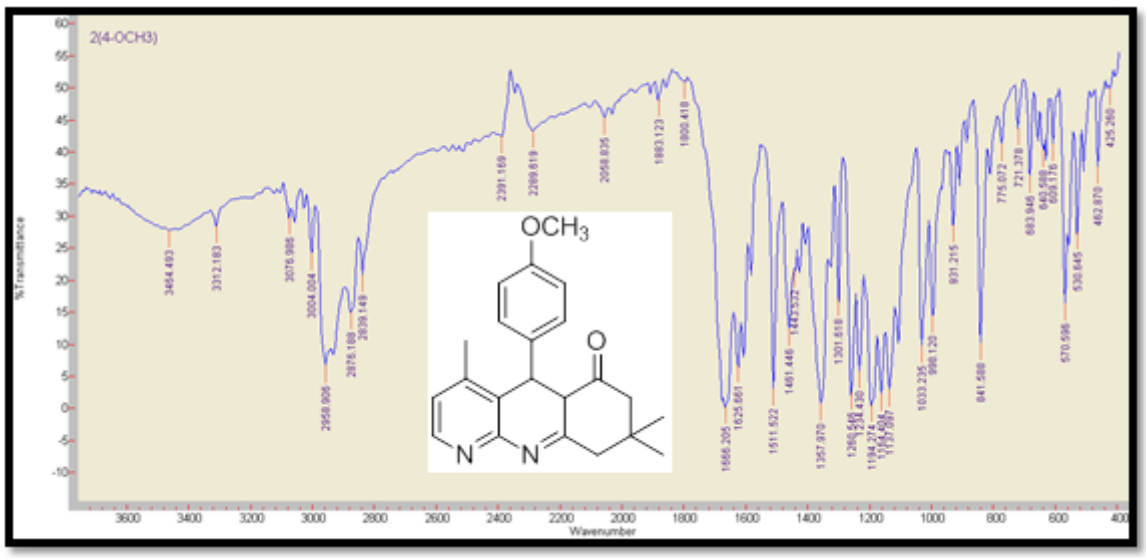

Appendix 3.42: IR spectrum for compound **38g**

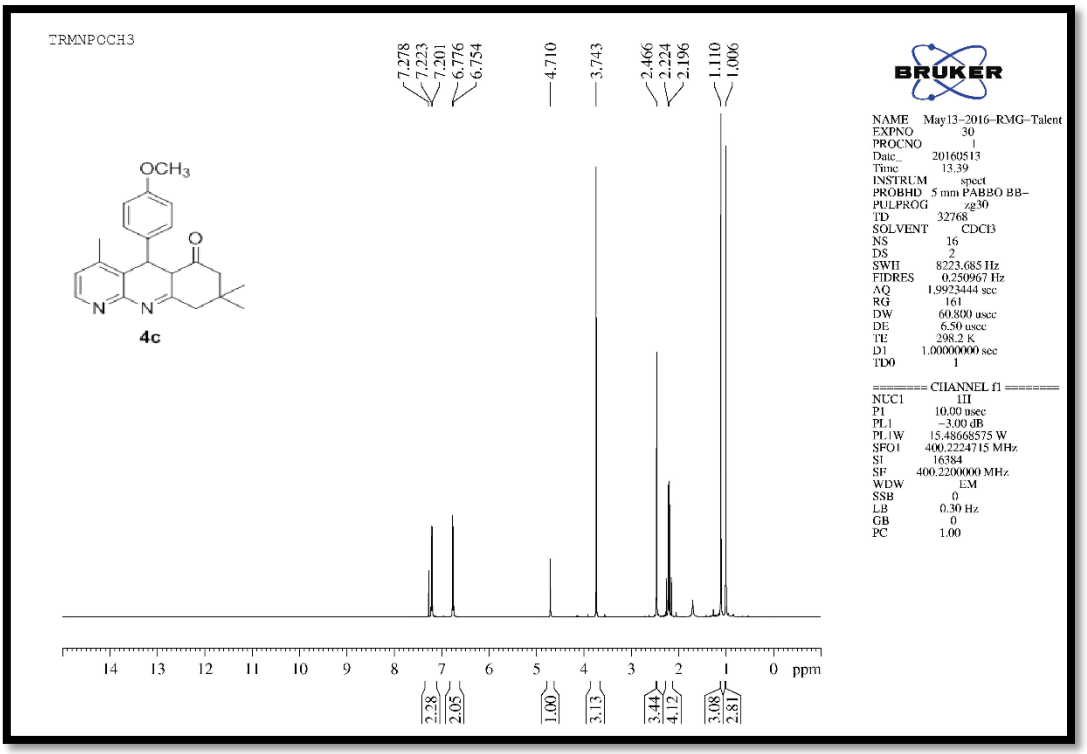

Appendix 3.43: ^{1}H-NMR spectrum for compound **38g**

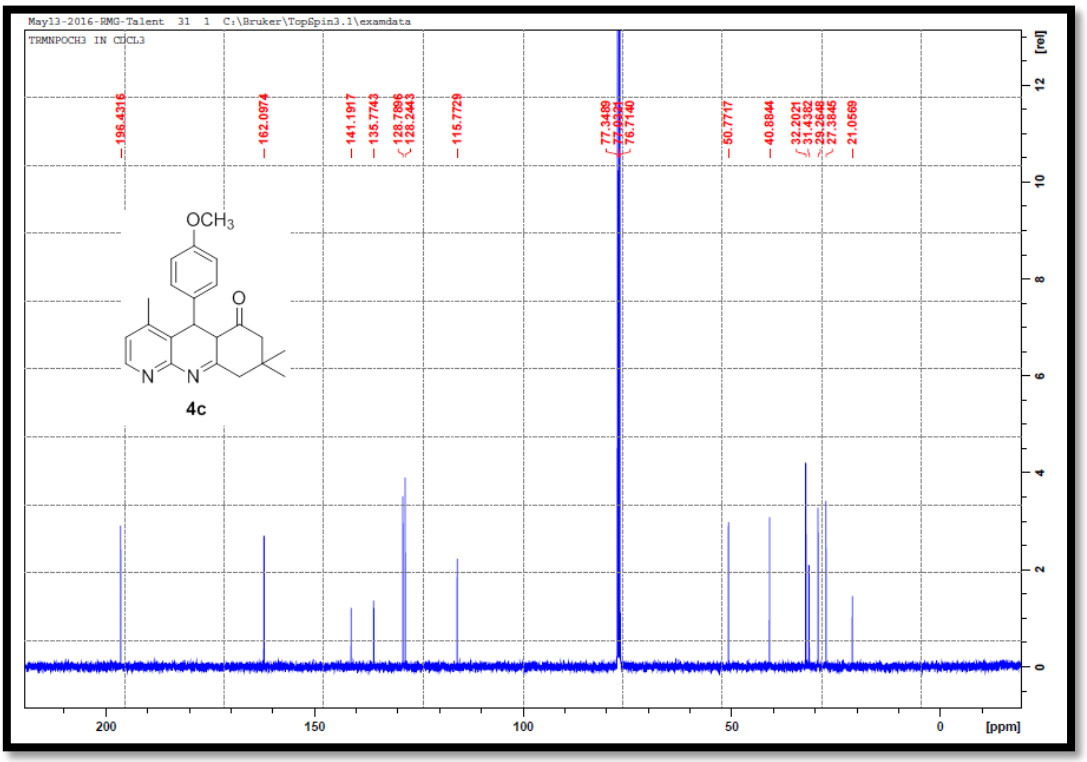

Appendix 3.44: ^{13}C-NMR spectrum for compound**38g**

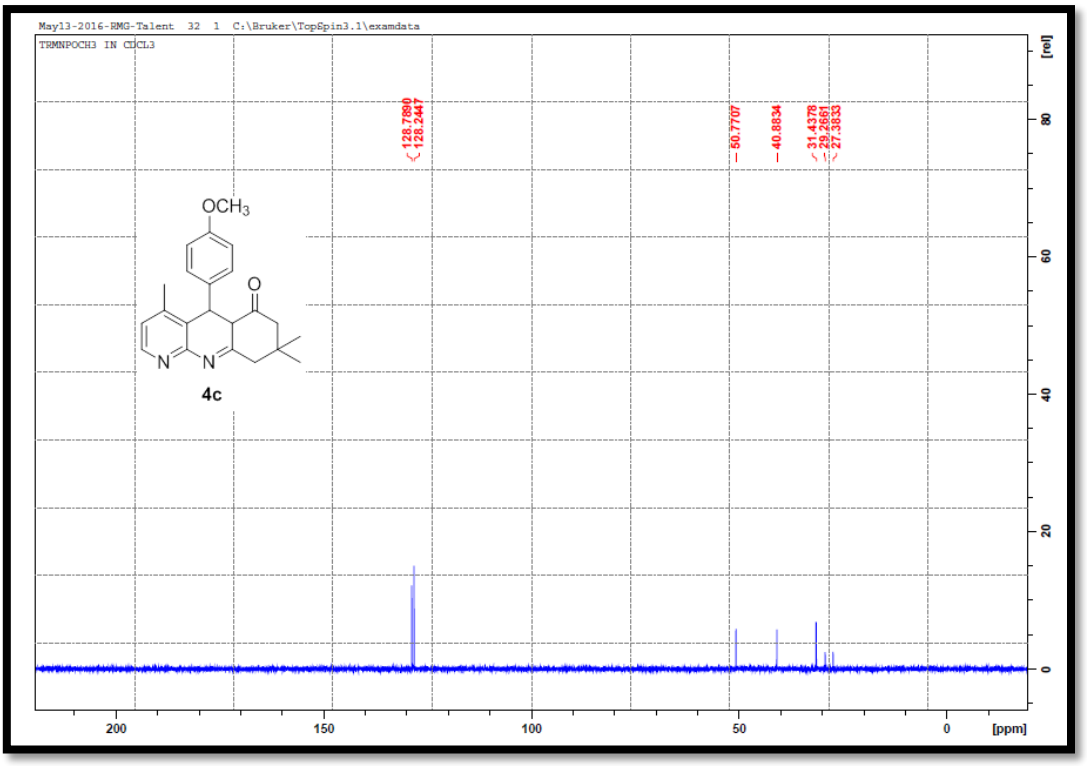

Appendix 3.45: 90^0 DEPT NMR spectrum for compound **38g**

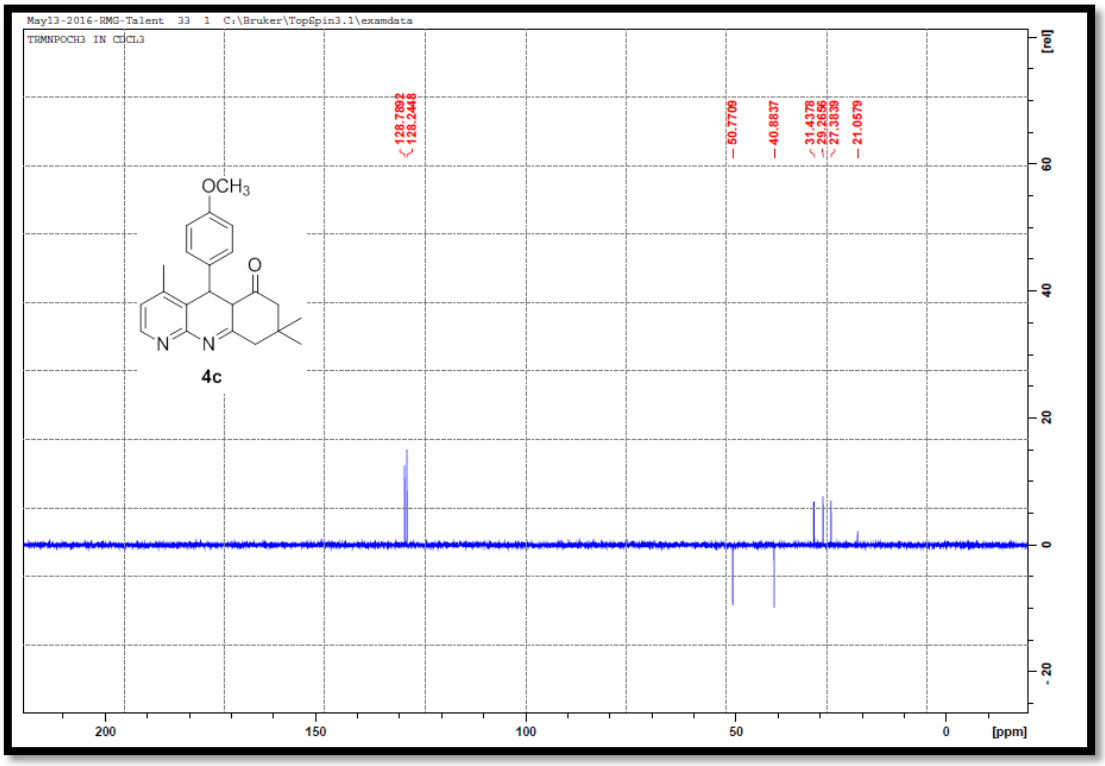

Appendix 3.46: 135^0 DEPT NMR spectrum for compound **38g**

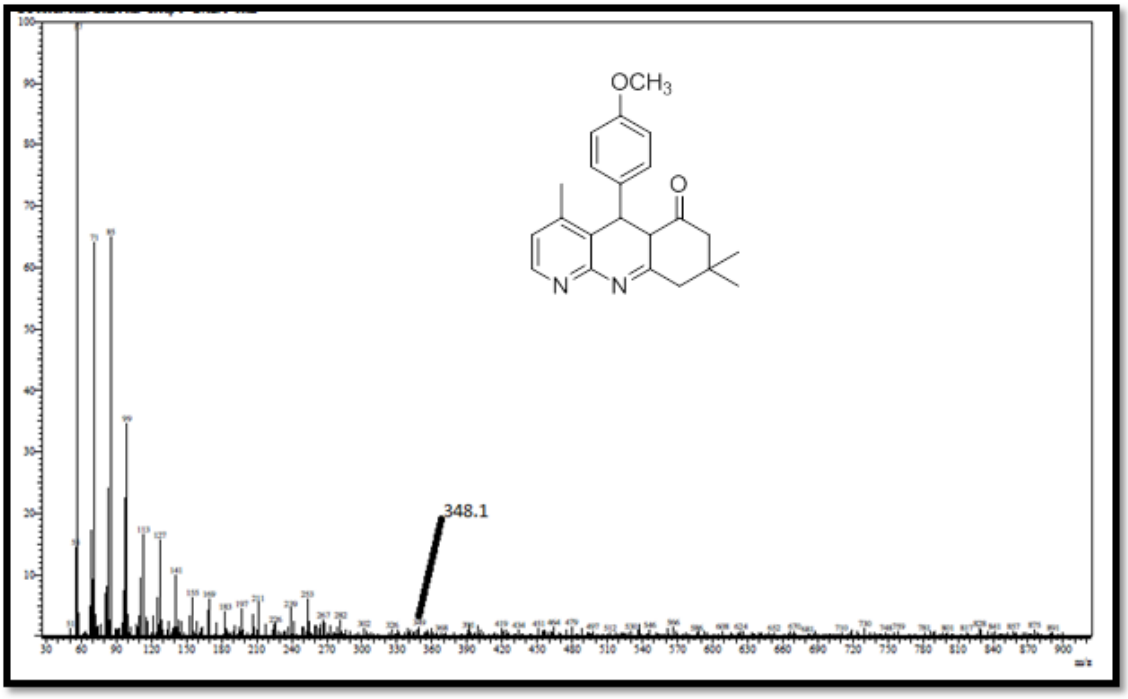

Appendix 3.47: EI-MS spectrum for compound **38g**

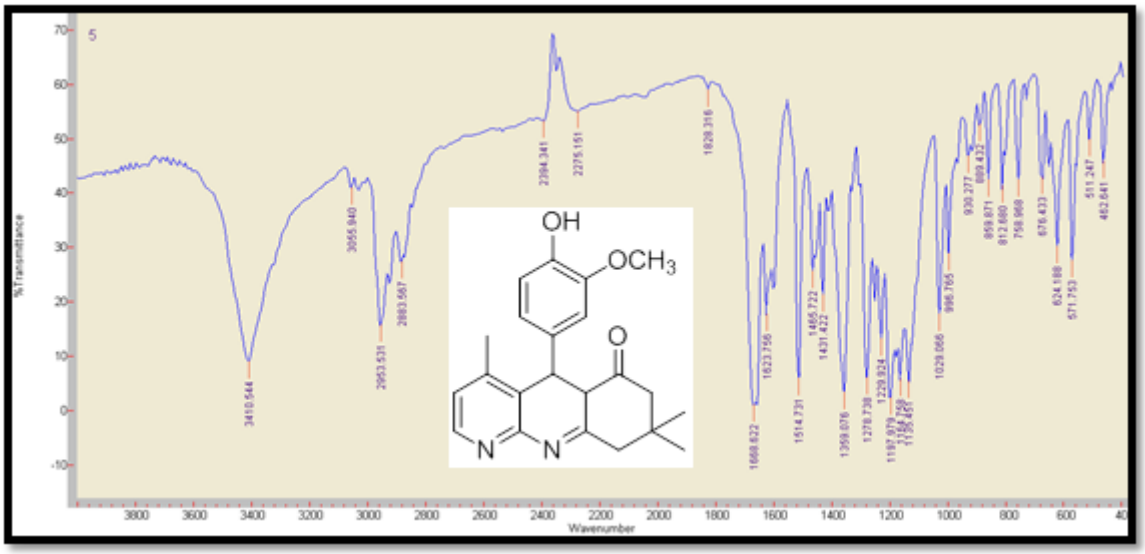

Appendix 3.48: IR spectrum for compound **38h**

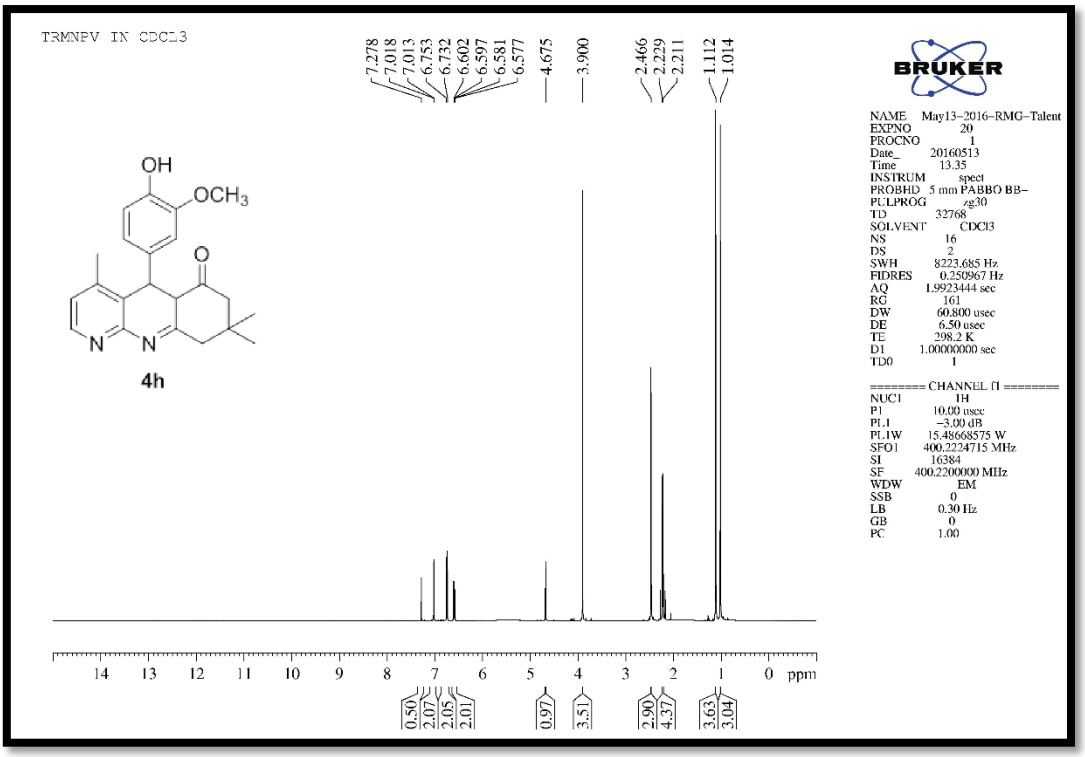

Appendix 3.49: ^{1}H-NMR spectrum for compound **38h**

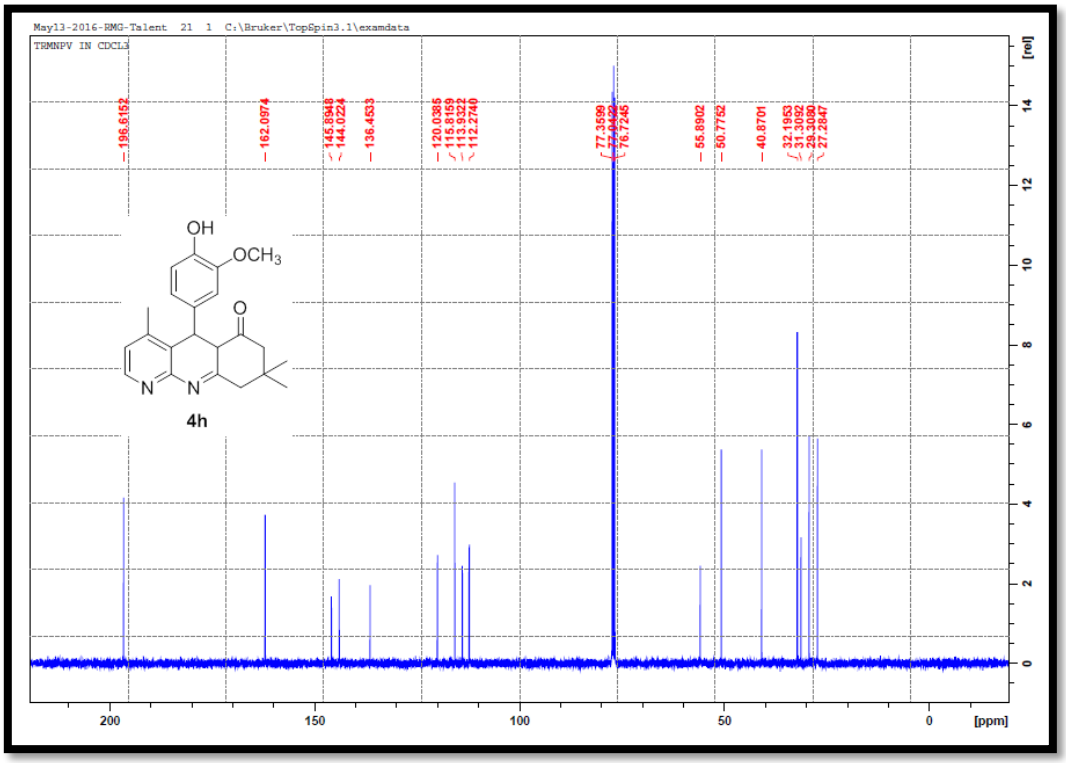

Appendix 3.50: ^{13}C-NMR spectrum for compound **38h**

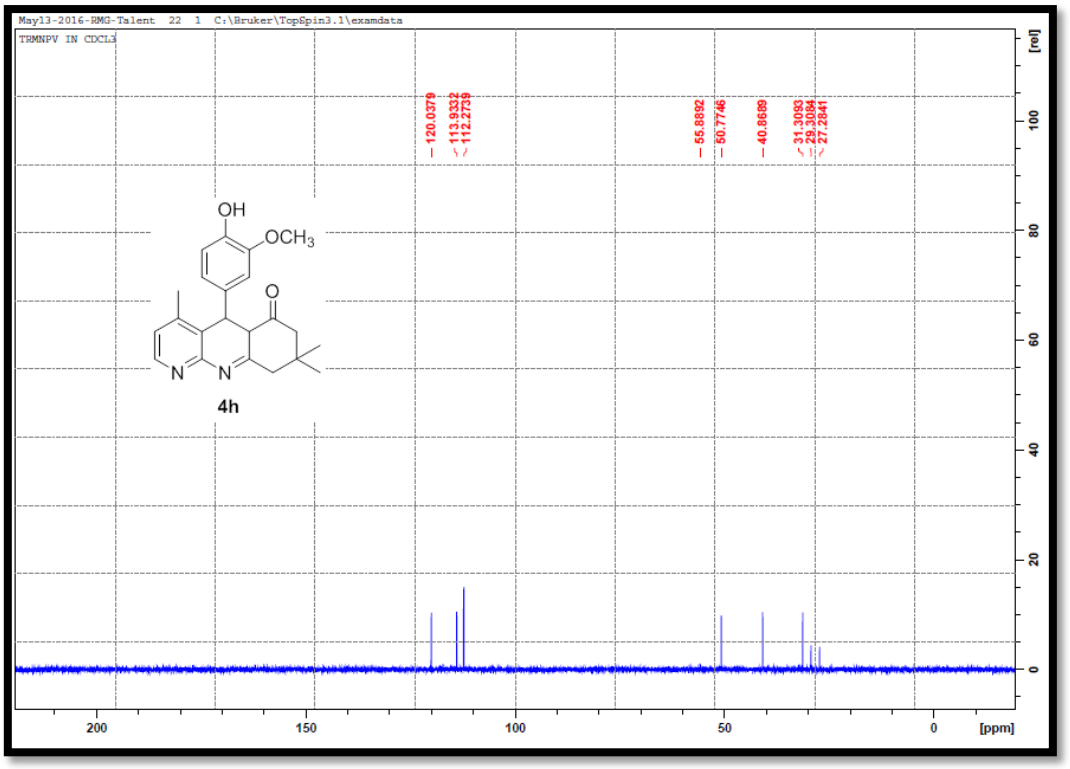

Appendix 3.51: 90^0 DEPT NMR spectrum for compound **38h**

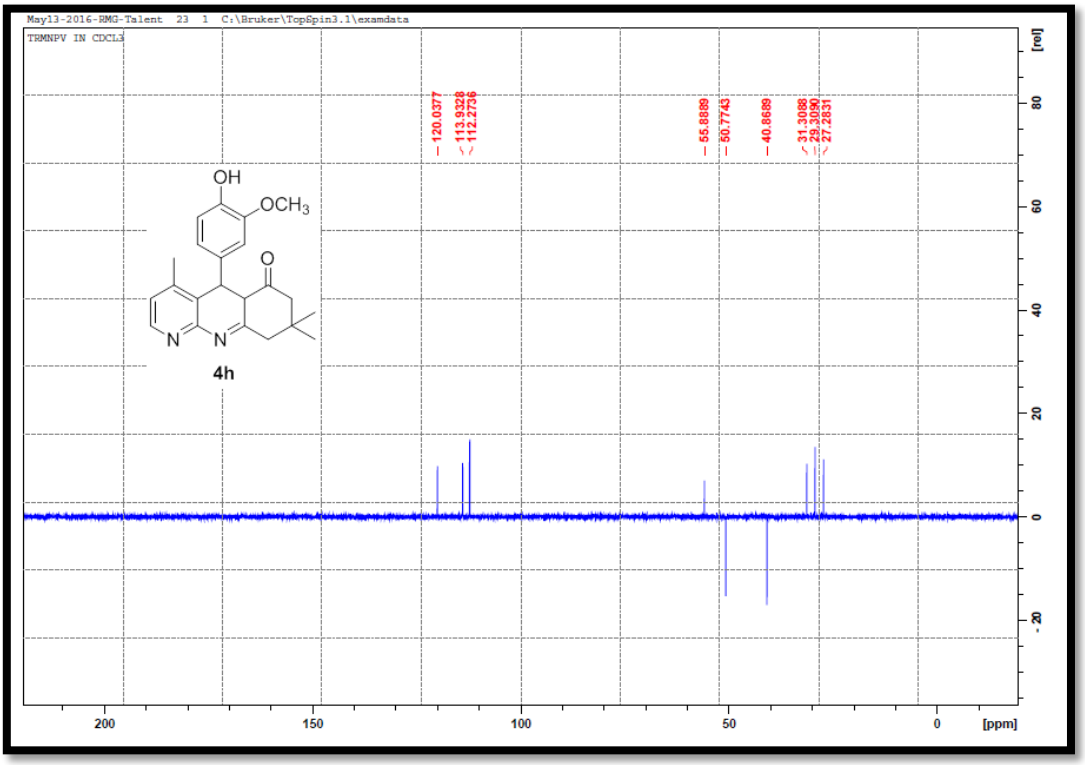

Appendix 3.52: 135^0 DEPT NMR spectrum for compound **38h**

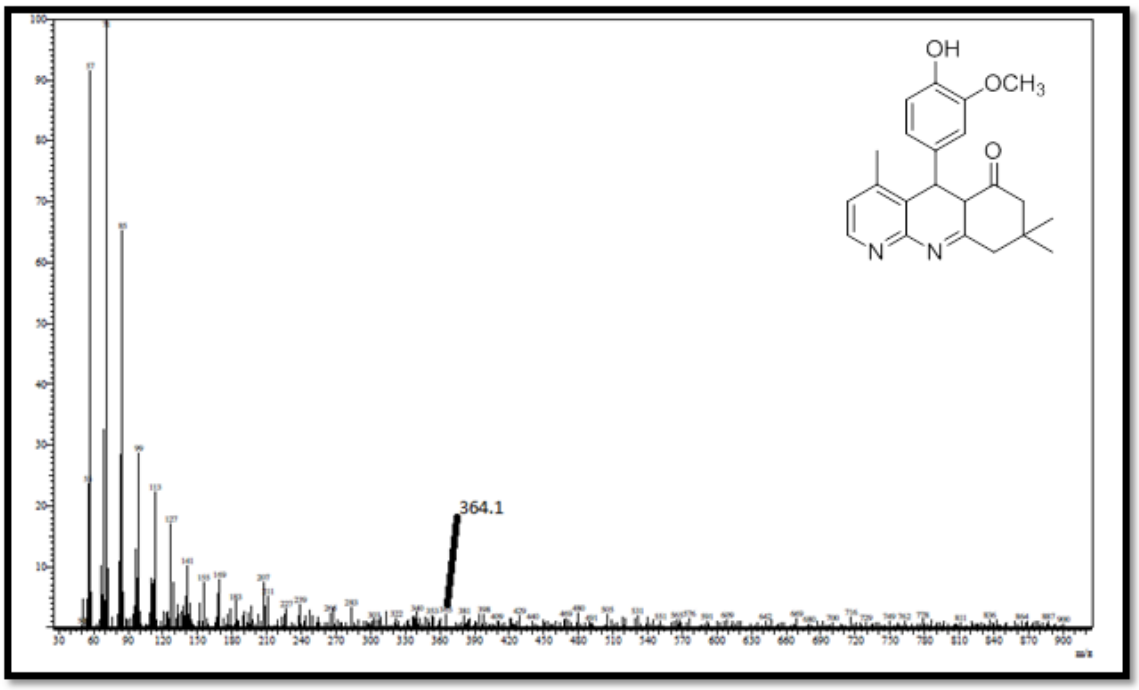

Appendix 3.53: EI-MS spectrum for compound **38h**

Chapter Four

Multi-Component Synthesis of Novel Fused Indolo [3, 2-*c*] [1, 8] Naphthyridines via Povarov Reaction and their Antimicrobial Activity

4.1 Abstract

Nine novel fused indolo [1, 8] naphthyridine derivatives were synthesized using the Povarov reaction, in a one-pot system. The compounds were fully characterized by spectroscopic techniques such as FT-IR, NMR, TOF-MS and elemental analysis. Furthermore, their antibacterial activity against six bacterial strains were investigated. The results of the bioassay demonstrated that compounds **36a, 36c** and **36i** showed good inhibitory effect with an MIC value ranging from 0.04687 to 0.09375 µM against *Bacillus cereus* and *Staphylococcus aureus*. The toxicity of **36a-i,** evaluated through mutagenicity test against *Salmonella typhimurium* TA 98 and TA100 strains, revealed that there was no significant proliferation in the number of revertant colonies in comparison with the control, sodium azide.

4.2 Historical Background of Povarov Reaction

In 1960, Povarov, Mikhailov and Grigos developed an impressive synthetic method which allowed for the formation of two new C-C bonds, one new ring and up to three new stereo-genic centers. It was a [4+2] cycloaddition reaction between a dienophile **2** and an aza-diene **1** which was promoted by boron trifluoride etherate, a Lewis acid catalyst (Scheme 1) (Kouznetsov 2009: 2721).

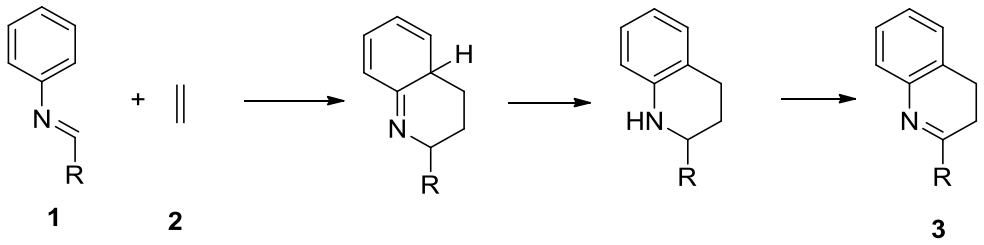

Scheme 1: Formal [4+2] cycloaddition synthesis of tetrahydroquinoline

(Kouznetsov, 2009: 2721)

Due to this development, the reaction was called the "Povarov reaction" but it is also commonly referred to as the aza-Diels-Alder reaction. The Povarov reaction initially received unsatisfactory attention however its use gained momentum and is now a major contributor in the synthesis of new organic compounds.

In the early 1990s, new catalysts were investigated as a potential promoter for the Povarov reaction. Various Lewis and Bronsted acid catalysts such as indium chloride, ytterbium (III) triflate, lanthanide triflate, triflic acid, trifluoroacetic acid and *p*-toluene sulphonic acid were tested (Buonora *et al*., 2001: 6099; Bharate *et al*., 2015:1 and Glushkov *et al*., 2008: 137). The Povarov reaction has made a major contribution to the efficient synthesis of novel organic compounds and is extensively used for the synthesis of highly substituted complex quinolines (Glushkov *et al*., 2008: 137). Currently, the Povarov reaction was used to produce medicinally active compounds that mimic natural products (Nino *et al*., 2016: 1117). Furthermore, this reaction was effectively applied in the total synthesis of Martinelline, Luotonin A and Camptothecin (Figure 1). (Powell *et al*., 2002:2913, Alonso *et al*., 2016: 179 and Tejeria *et al.*, 2016: 740).

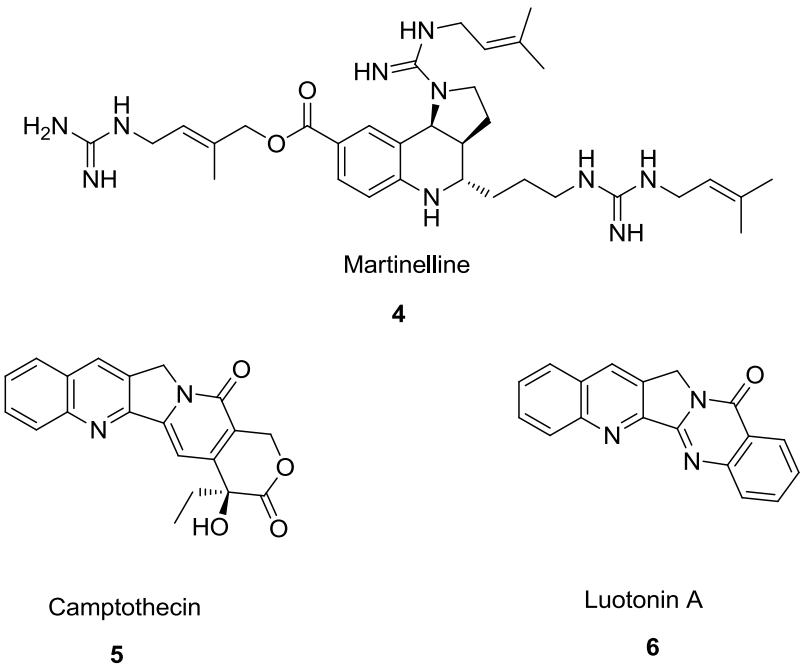

Figure 1: Natural products compounds synthesized via Povarov's reaction

(Twin *et al*., 2004: 4913)

4. 3 The Scope of the Povarov Reaction

In the past two decades, synthetic chemists have realized that the Povarov reaction is more efficient when an activated alkene **7,** dienophile reacts with N-aryl imine **1** to yield the desired product **8** (Scheme 2). An intermediate product formed which then undergoes a 1, 3-hydrogen shift in a formal [4+2] cyclo-adduct to yield a 1, 2, 3, 4-tetrahydroquinoline **8**.

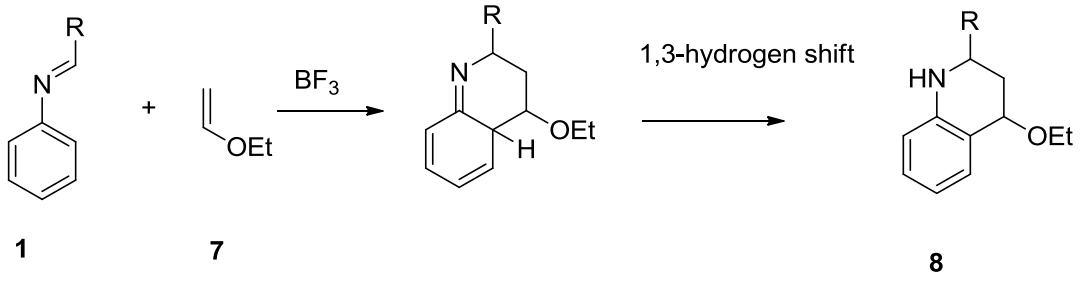

1 **7** **8**

Scheme 2: Formation of tetrahydroquinoline from the Povarov reaction

(Domingo *et al.*, 2014: 25268)

The Povarov reaction gained extensive recognition during the development of a three component reaction involving *in situ* generation of N-aryl imine from a reaction of carbonyl compounds with aromatic amines (Domingo *et al.*, 2014: 25268). Thereafter, the Povarov reaction was explored when a Schiff base **9** was treated with 1-ethoxycyclohexene **10** to produce ethoxyoctahydrophenanthridine **11** which was subsequently aromatized to produce 6-phenyltetrahydrophenanthridine **12** (Scheme 3) (Glushkov *et al.*, 2008: 137).

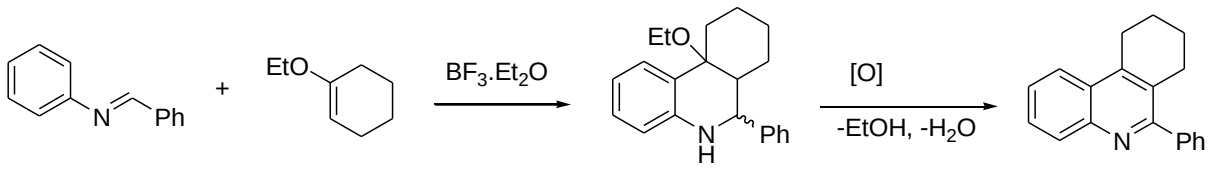

9 **10** **11** **12**

Scheme 3: Formation of 6-phenyltetrahydrophenanthridine **12** via the Povarov reaction

(Glushkov *et al.*, 2008: 137)

The N-aryl Schiff base **9** was also reacted with ethoxyacetylene **13** to produce 2-phenyl-4-ethoxy-quinoline **14** (Scheme 4).

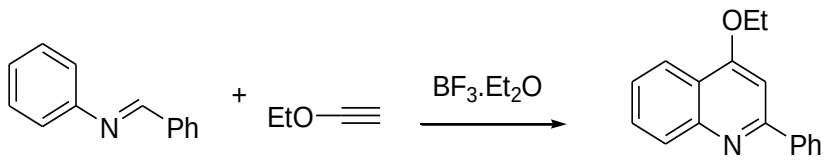

9 **13** **14**

Scheme 4: Formation of 2-phenyl-4-ethoxy-quinoline **14** via Povarov reaction

(Glushkov *et al.*, 2008: 137)

Most of the Povarov reactions are conducted in solvents such as benzene, diethyl ether, ethyl acetate and glacial acetic acid (Glushkov *et al.,* 2008: 137). Furthermore, the Povarov reaction progressed when researchers began to use polar solvents such as acetonitrile, dimethylformamide, tetrahydrofuran and dimethylsulfoxide. A vast number of functionalized polyheterocyclic compounds were synthesized successfully in the presence of acetonitrile. For example, Belal *et al*., 2015 reported the synthesis of pyrido [2, 3-*c*] coumarin derivatives **17** from 3-aminocoumarin **16** and *o*-propargylated salicyaldehydes **15** (Scheme 5).

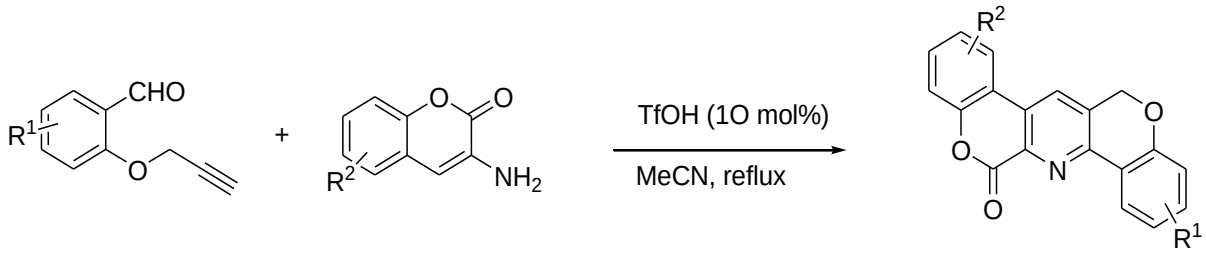

15 **16** **17**

Scheme 5: Synthesis of pyrido [2, 3-*c*] coumarin derivatives (Belal *et al*., 2015: A)

Nino *et al.,* 2016 reported the preparation of tetrahydro-1H-cyclopenta[c]quinolones **21** (Scheme 6).

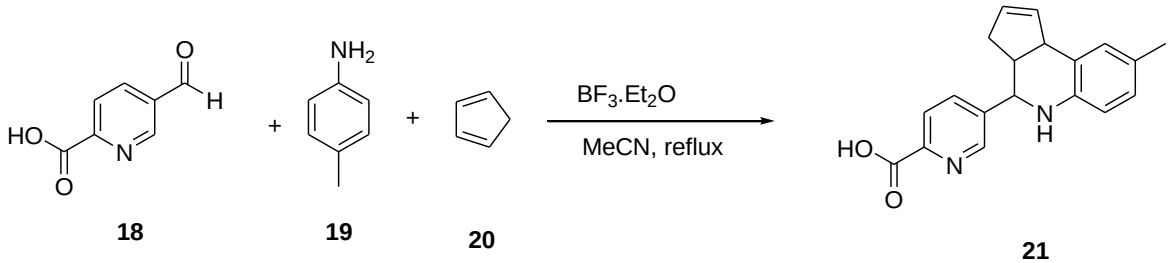

18 **19** **20** **21**

Scheme 6: Synthesis of tetrahydro-1H-cyclopenta[*c*]quinolines (Nino *et al.,* 2016: 1117)

Min *et al.*, 2014 reported an oxidative Povarov approach for the synthesis of polycyclic amines (Scheme 7). This method involved the functionalization of both a C (sp^3)-H and a C (sp^2)-H bond through oxidative reaction: the C (sp^2)-H was oxidized which triggered the cyclo-addition with various dienophiles.

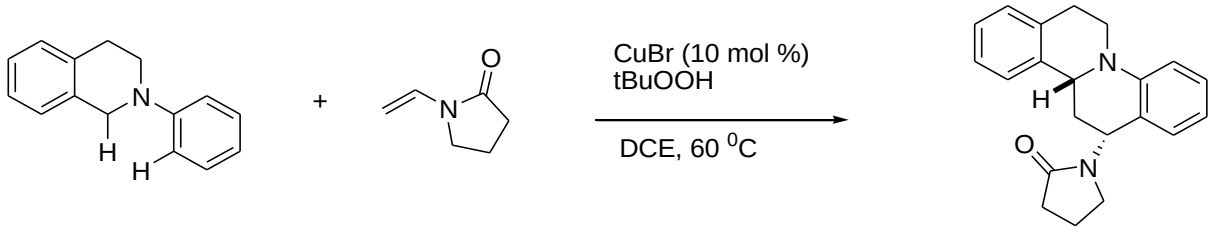

22 **23** **24**

Scheme 7: Synthesis of polycyclic amines via an oxidative Povarov approach

(Min *et al.*, 2014: A)

This study revealed that the Povarov reaction was not limited only to the synthesis of substituted tetrahydroquinolines but rather to a range of multi-functionalized compounds. Later, the Povarov reaction was used by Khan *et al. (*2011: 3455) to construct highly substituted naphthyridine derivatives **28** (Scheme 8).

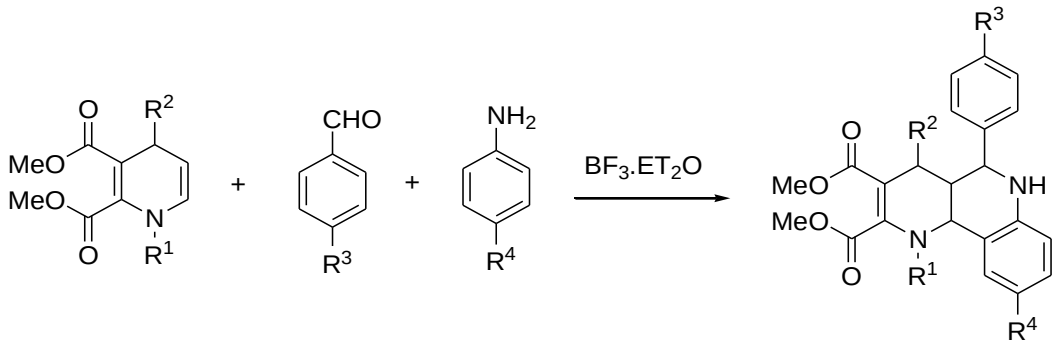

25 **26** **27** **28**

Scheme 8: Synthesis of substituted naphthyridine derivatives (Khan *et al.*, 2011: 3455)

Recently a new family of functionalized polycyclic 1, 5-naphthyridine derivatives **32** was reported by Alonso *et al*. (2016: 179) (Scheme 9).

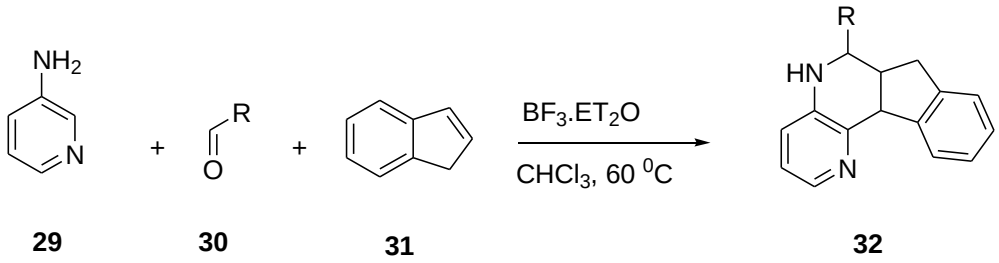

29 **30** **31** **32**

Scheme 9: Synthesis of indeno [1, 5] naphthyridines (Alonso *et al*., 2016: 179 and Tejeria *et al*., 2016: 740)

4.4 Fused Quinolines

Fused synthetic indole derivatives such as indolo-quinolines are abundantly available in natural products. Some of them were isolated from the root of the West African plant *Cryptolepis sanguinolent* (Hostyn *et al*., 2005: 1571). These isomeric indoloquinolines possess anti-plasmodial activity.

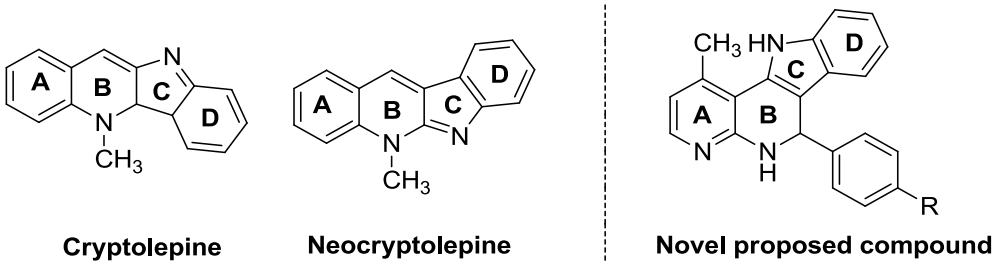

Figure 2: Novel proposed compound resembles isolated compounds from root of *Cryptolepis sanguinolenta* (Hostyn *et al*., 2005: 1571)

The indole alkaloids have developed great attention due to their broad spectrum of biological applications. The fused indolonaphthyridine comprises of an indole and a naphthyridine scaffold. They are important because they possess broad pharmaceutical applications such as anticancer, antimicrobial, antioxidant, anti-inflammatory and anti-HIV (Sharma *et al*., 2010: 491). This stimulated a need to discover alternative methodology to design novel bioactive heterocyclic compounds in a single step reaction. Thus, one of the primary goals of modern synthetic chemists is to develop an ideal one step procedure to access complex multi-functionalized organic compounds preferably from simple substrates.

To the best of our knowledge there little reports on the use of the Povarov reaction for the synthesis of fused indolo [1,8] naphthyridines. Hence, the aim of this study was to use the Povarov reaction to synthesize novel functionalized fused indolo [1,8] naphthyridine derivatives.

4.5 Results and Discussions

4.5.1 Synthesis and Characterization of a Novel Fused 1-Methyl-6-Phenyl-6, 6a, 7, 11b-Tetrahydro-5H-Indolo [3, 2-*c*] [1, 8] Naphthyridine

The synthesis of fused indolo [1, 8] naphthyridine derivatives **36a-36i** were successfully prepared through the Povarov reaction by [4+2] cycloaddition. In this reaction, an electron-rich dienophile **35** reacted with a diene (N-aryl aldimines) which was produced by a reaction between 2-amino-4-picoline **34** with benzaldehyde **33a.** The reaction was catalyzed by indium chloride to produce the target compound **36a** (Scheme 1): the product was identified as 1-methyl-6-phenyl-6,6a,7,11b-tetrahydro-5H-indolo[3,2-*c*][1,8]naphthyridine by FT-IR, NMR, TOF-MS and elemental analysis.

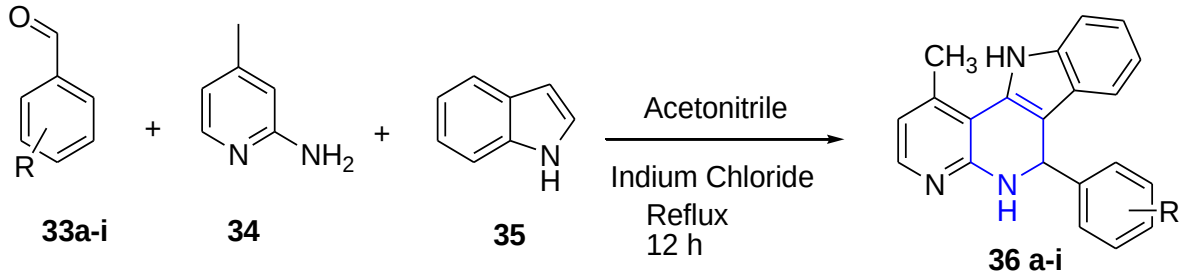

33a-i **34** **35** **36 a-i**

Key: R = H (**36a**), *p*-CH_3 (**36b**), *p*-Cl (**36c**), *p*-F (**36d**), *p*-CF_3 (**36e**), *p*-NO_2 (**36f**), *p*-OCH_3 (**36g**), *m* -OCH_3-*p*-OH (**36h)**, *m* -OCH_3-*p*-OH-*m*-Br (**36i**)

Scheme 10. Synthesis of 1-methyl-6-phenyl-6, 6a, 7, 11b-tetrahydro-5H-indolo[2,3-*c*][1,8]naphthyridines

Compound **36a** was selected as a template to discuss its unambiguous characterization and used to characterize the other 8 derivatives. The characteristic absorption band in the FT-IR spectrum (Appendix 4.1) showed stretching absorptions (cm $^{-1}$) at 3390-3271 due to the

secondary amine N-H stretch, 2854 due to C-H (sp^3) stretch, 1675- 1618 due to N-H bend and C=C stretch, 1479 due to C-N stretch and 744 cm^{-1} for N-H out of plane bend. The numbers for peripheral atoms depicted in Figure 3, were used to facilitate the assigning of proton and carbon for NMR spectral interpretation.

The ^1H NMR spectrum (Appendix 4.2 - 4.3) showed well distinct signal at δ 10.80 for overlapping NH-13 indole and NH-1 naphthyridine. The aromatic protons at δ 7.39 (1H, d, *J* = 8.1 Hz, H-15) and 6.85 (1H, d, *J* = 8.1 Hz, H-14) corresponded to naphthyridine –CH whilst a signal at δ 5.87 (s, H-2) exhibited the presence of –CH (sp^3) proton which confirmed the formation of a new ring. Two doublet at δ 7.37 (2H, d, *J* = 8.1 Hz, H-5 & H-8) were assigned to indole –CH. Two triplets at δ 7.07 (1H, t, *J* = 7.8 Hz, H-7) and 6.89 (1H, t, *J* = 7.8 Hz, H-6) were assigned to indole –CH. The phenyl ring exhibited five protons: one proton is triplets at δ 7.17 (1H, t, *J* = 8.2 Hz, H-4') and other four protons are doublets at δ 7.32 (2H, d, *J* = 8.1 Hz, H-2'& H-6') and δ 7.29 (2H, d, *J* = 7.4 Hz, H-3' & H-5'), see Figure 3.

The ^{13}C NMR (Appendix 4.4), DEPT (Appendix 5 & 6) and HSQC (Appendix 8) spectra showed the presence of twelve CH carbons at δ 39.7 (C2), 111.1 (C8), 118.0 (C14), 118.2 (C6), 120.9 (C7), 123.5 (C5), 125.8 (C4'), 127.9 (C2' & C6'), 128.4 (3' & C5') and 138.4 (C15). Whilst, eight quaternary carbons resonated at δ 111.4 (C3a), 119.1 (C12a), 128.2 (C4a), 131.0 (C11a), 136.6 (C9a), 138.4 (C1') and 144.9 (C13 & C16a), see Figure 3.

The 2-D NMR analyses of COSY and HMBC were used to confirm the identity of compound **36a** through correlation between proton and carbon as presented in Figure 4.

The ^1H, ^1H-COSY spectrum (Appendix 7) showed strong coupling between naphthyridines H-15 (δ 7.39) and H-14 (δ 6.85). Also, H-7 (δ 7.07) coupled with H-9 (δ 7.37). A strong coupling occurred between phenyl H-4' (δ 7.17) and H-3'/ H-5' (δ 7.29).

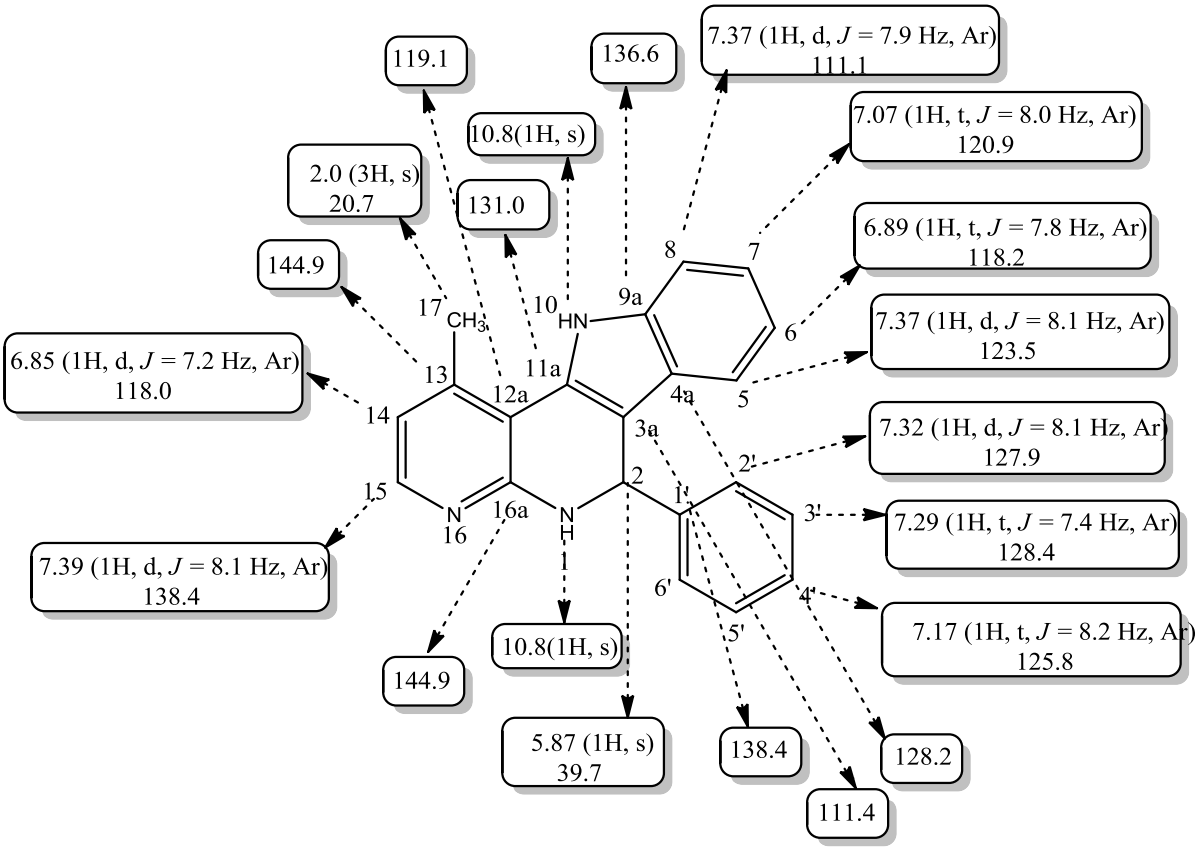

Figure 3: ^{1}H and ^{13}C NMR chemical shifts of **36a**.

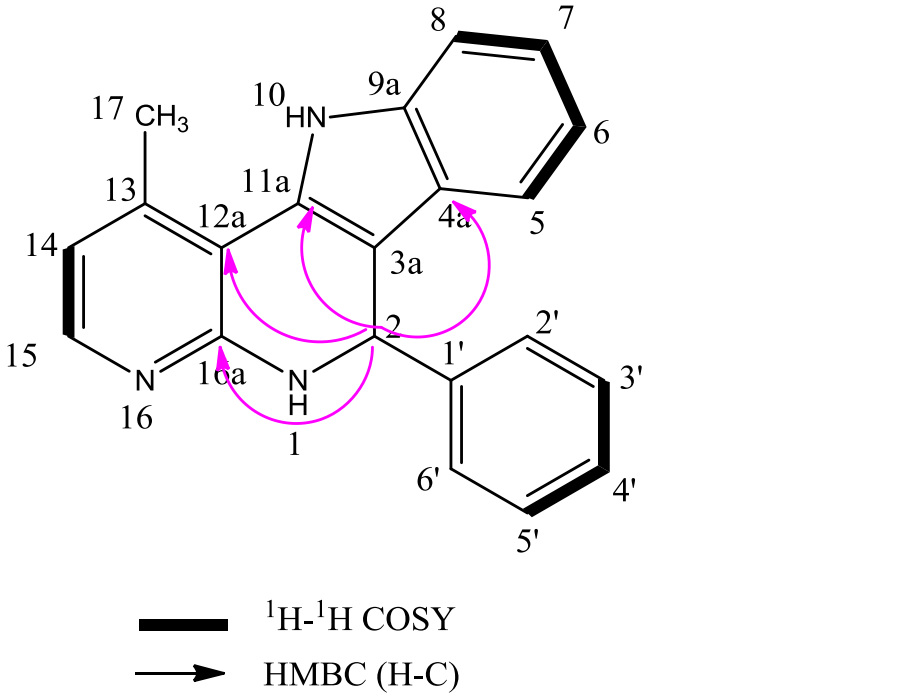

Figure 4: COSY and HMBC correlations of compound **36a.**

The HMBC spectrum (Appendix 4.9) showed the proton and quaternary carbon coupling: H-2 (δ 5.87) naphthyridine coupled with C16a (δ 144.9); C12a (δ 119.1); C4a (δ 128.2) and C11a (δ 131.0). The molecular ion peak at *m/z* 311.2 [M^+] in its mass spectrum (Appendix 4.10) corresponded to molecular formula $C_{21}H_{17}N_3$. Scheme 11 below depicts some other possible fragments. Finally elemental analysis also confirmed the structure of compound **36a** as 1-methyl-6-phenyl-6, 6a, 7, 11b-tetrahydro-5H-indolo [3, 2 - c] [1, 8] naphthyridine.

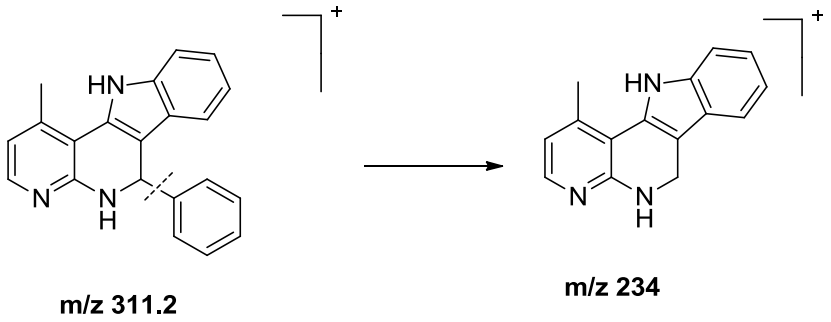

Scheme 11: Fragmentation of compound **36a**

4.5.2 Optimization of the Synthetic Method

The effect of solvent, catalyst and temperature was investigated for optimizing the reaction conditions. Initially the reaction was performed with a variety of solvents and catalysts such as indium chloride, boron trifluoride diethyl etherate, *p*-toluene sulphonic acid and trifluoro acetic acid (Table 2). It was observed that the combination of acetonitrile with indium chloride was the best amongst the tested mixtures for the yield and reaction time (Table 2, entry 17). To optimize the temperature, the reaction was conducted at 80, 100, 120 and 160 ^{0}C (Table 2, entries 18, 17, 19, 20). It was observed that the optimum temperature for the reaction was at 100 ^{0}C as there was not a significant change observed in yield at 120 and 160 ^{0}C (Table 2, entries 19, 20).

Table 1: Optimization of reaction conditions on the synthesis of fused Indolo [2, 3-c] [1, 8] naphthyridine **(36a)** [a]

Entry	Solvent	Catalyst	Temp. (^{0}C)	Time (h)[b]	Yield (%)[c]
1	Ethanol	PTSA	100	24	-
2	1.4 Dioxane	PTSA	100	24	26
3	Acetonitrile	PTSA	100	24	18
4	Benzene	PTSA	100	24	-
5	Water	PTSA	100	24	-
6	DMSO	PTSA	100	24	14
7	Ethanol	$BF_3.Et_2O$	100	24	15
8	1.4 Dioxane	$BF_3.Et_2O$	100	12	76
9	1.4 Dioxane	$BF_3.Et_2O$	100	24	74
10	Acetonitrile	$BF_3.Et_2O$	100	24	46
11	Benzene	$BF_3.Et_2O$	100	24	-
12	Water	$BF_3.Et_2O$	100	24	-
13	DMSO	$BF_3.Et_2O$	100	24	27
14	Ethanol	$InCl_3$	100	24	12
15	1.4 Dioxane	$InCl_3$	100	24	25
16	Acetonitrile	$InCl_3$	100	24	88
17	Acetonitrile	$InCl_3$	100	12	88
18	Acetonitrile	$InCl_3$	80	12	68
19	Acetonitrile	$InCl_3$	120	12	86
20	Acetonitrile	$InCl_3$	160	12	88
21	Benzene	$InCl_3$	100	24	-
22	Water	$InCl_3$	100	24	-
23	DMSO	$InCl_3$	100	24	34
24	Ethanol	TFA	100	24	-
25	1.4 Dioxane	TFA	100	24	24
26	Acetonitrile	TFA	100	24	23
27	Benzene	TFA	100	24	-
28	Water	TFA	100	24	-
29	DMSO	TFA	100	24	16

[a] Reactions were performed using equimolar of all reactants in solvent (20 mL).

[b] Reaction progress monitored by TLC

[c] Isolated yield.

4.5.3 Plausible Mechanism for the Formation of Fused Indolo [1, 8] Naphthyridine 36a

A plausible reaction pathway to rationalize the formation of fused indolo [1, 8] naphthyridine **36a-i** is depicted in Scheme 12.

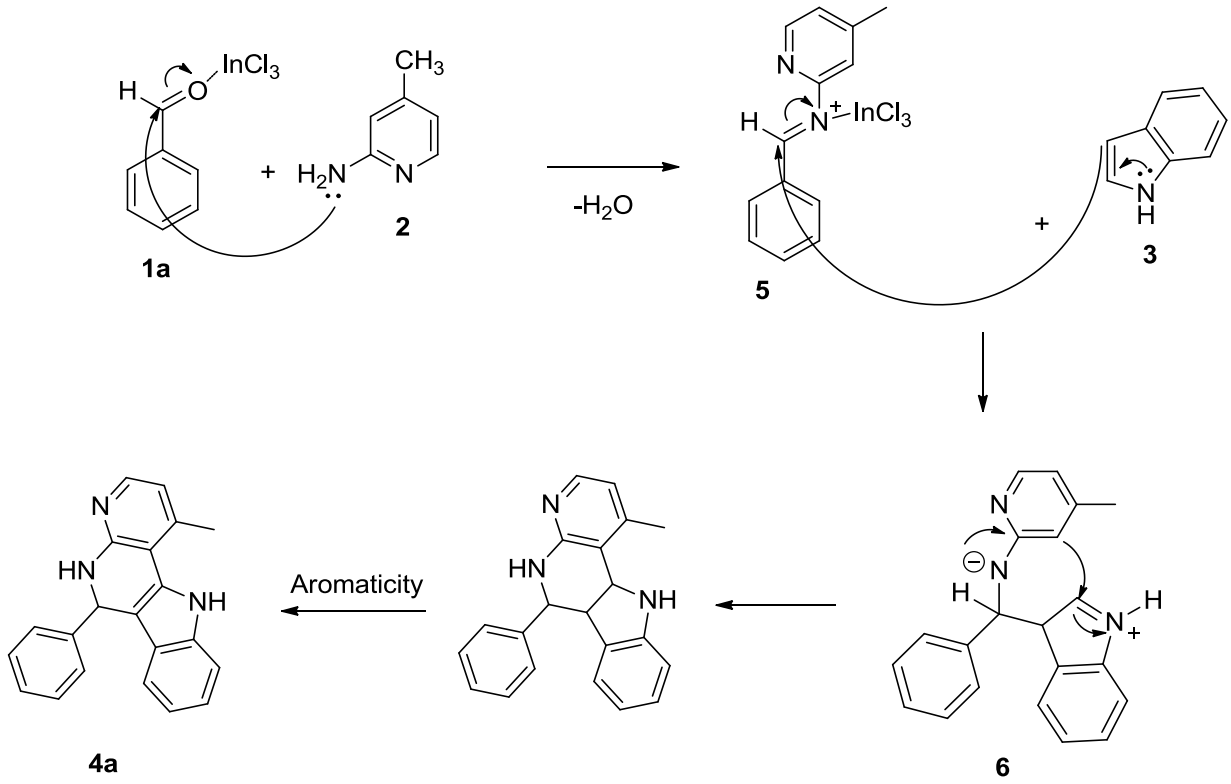

Scheme 12: Plausible mechanism for Povarov reaction for the synthesis of **36a**.

The above mechanism involves an interaction between a diene and dienophile. This reaction was triggered by the Schiff base reaction which occurred between benzalydehyde **33a** and 2-amino-4-picoline **34** to yield an imine product **37**. The latter is attacked by the lone pairs from indole nitrogen **35** due to nucleophilicity of enamines to yield an intermediate product **38**. At this stage, the compound **38** was unstable hence the delocalization of the lone pair from nitrogen caused a high electron density in the aromatic ring which eventually caused the aromatic ring to be nucleophilic. This instigated the attack of the electrophilic carbon from indole while compelling the hydrogen to depart. That hydrogen migrated and became attached to the nucleophilic nitrogen to stabilize it. Thereafter, aromaticity occurred to yield a stable desired compound **36a.**

4.5.4 The Synthesis and Characterization of Novel 1-Methyl-6-Phenyl-6, 6a, 7, 11b-Tetrahydro-5H-Indolo [3, 2- *c*] [1, 8] Naphthyridine (36b-36i)

To demonstrate the generality of this method, the synthesis of the other six derivatives were investigated under optimum condition, and the results are illustrated in Figure 5. It was observed that both electron-donating and electron-withdrawing groups, at the *para* position, gave the corresponding fused indolo-1, 8-naphthyridine in good yields. Also, functionalized aldehydes such as vanillin and 5-bromo vanillin gave good yields as depicted in Figure 5.

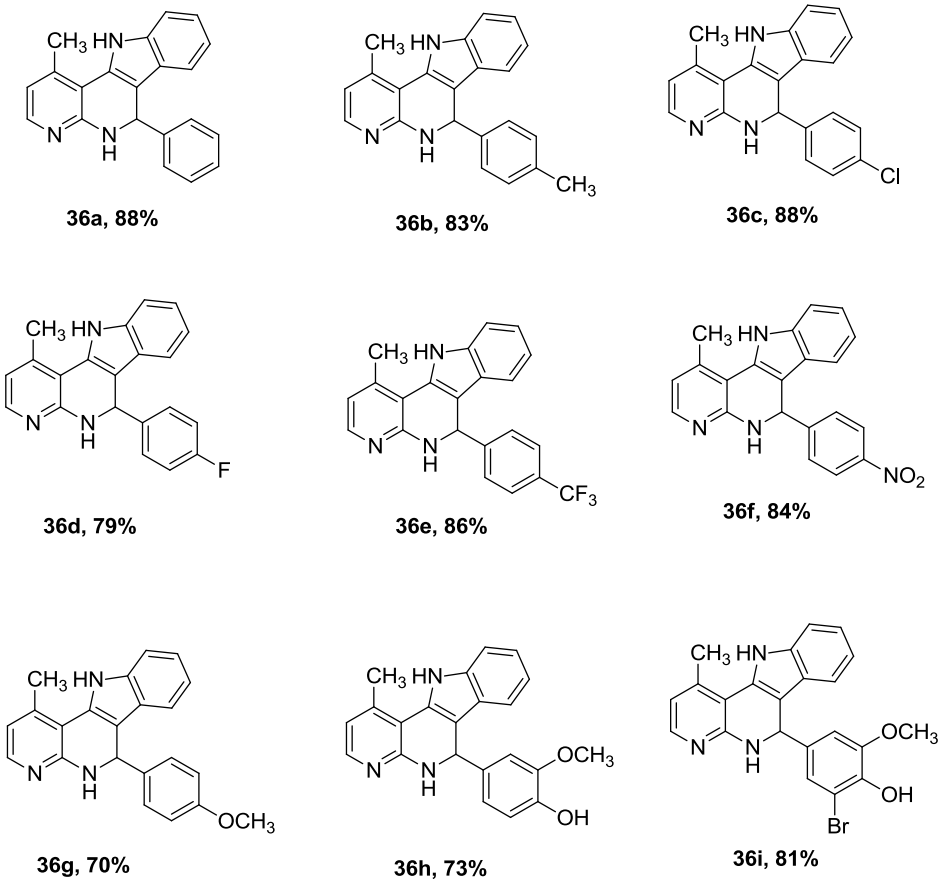

Figure 5: Synthesized novel fused 1-methyl-6-phenyl-6, 6a, 7, 11b-tetrahydro-5H-indolo-[3, 2- *c*] [1, 8] naphthyridine **(36a-36i)**

4.5.5 Antibacterial Activity

The antibacterial activity of compounds **36a-36i** was investigated against bacteria organisms *Staphylococcus aureus (S. aureus), Bacillus cereus (B. cereus), Citrobacter freundii (C. freundii), Serratia marcescens (S. marcescens), Klebsiella pneumonia (K. pneumonia)* and *Micrococcus luteus (M. luteus)* using Ciprofloxacin as positive and DMSO as negative control (Table 2). The activity was evaluated based on zone of inhibition in millimetre: compounds that showed zone of inhibition diameter greater than eight (>8mm) were considered as active compounds.

Table 2: Antibacterial activity of compounds 36a-36i.

	Bacteria organisms - zones of inhibition (mm)					
Compounds	***Staphylococcus aureus***	***Bacillus cereus***	***Citrobacter freundii***	***Serratia marcescens***	***Klebsiella pneumonia***	***Micrococcus luteus***
36 a	12 ± 0.3	10± 0.1	0	0	0	0
36 b	7 ± 0.1	7 ± 0.2	0	0	0	0
36 c	13 ± 0.5	12 ± 0.5	0	0	0	6±0.1
36 d	14 ± 0.2	11 ± 0.3	0	0	0	0
36 e	12 ± 0.5	7 ± 0.4	0	0	0	6±0.1
36 f	8.5 ± 0.4	8.5 ± 0.3	0	0	0	0
36 g	8.5 ± 0.2	0.0				
36 h	11 ± 0.4	9 ± 0.2	0	0	0	0
36 i	11 ± 0.1	10 ± 0.6	0	0	0	6±0.6
Ciprofloxacin	32± 0.2	30 ± 0.8	35±0.7	35±0.7	28±1.4	30±0.7
DMSO	-	-	-	-	-	-

Values are mean ±SD, number of samples (n=3)

The data in Table 2 showed that compounds **36a, 36c**, **36d**, **36e, 36h** and **36i** have promising zone of inhibition activity against *Staphylococcus aureus* with diameter of 12, 13, 14, 12, 11 and 11 mm, respectively (Figure 6). Whereas, compounds **36a, 36c**, **36d**, **36h** and **36i** also showed weak to moderate inhibitory activity against *Bacillus cereus* with diameter of 10, 12, 11, 9 and 10 mm, respectively. There was no inhibitory activity observed against *Citrobcter freundii*, *Serratia marcescens*, *Klebsiella pneuminiae* and *Micrococcus luteus*.

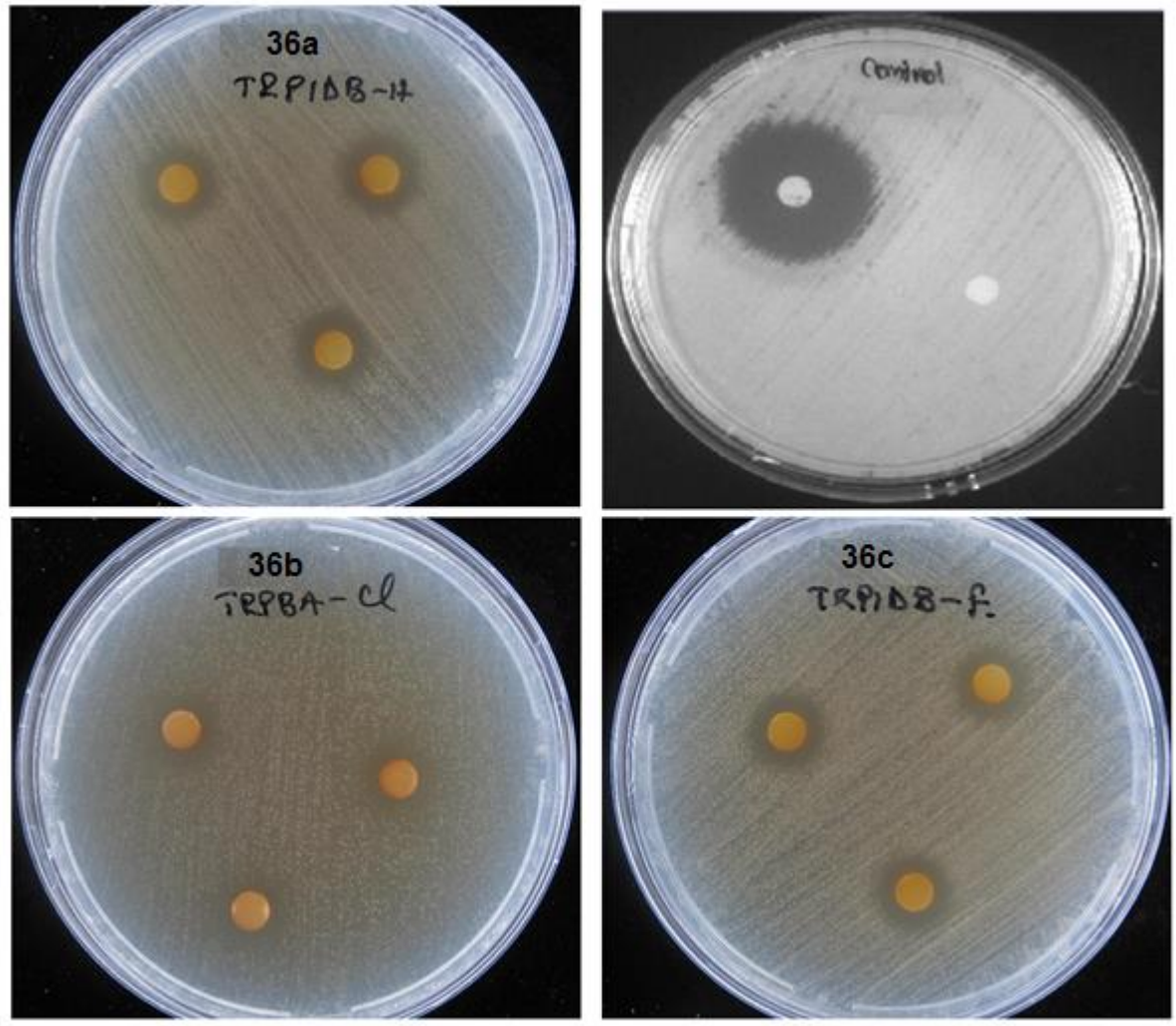

Figure 6: Zone of inhibition activity of compound **36a**, **36b** and **36c** against *Staphylococcus aureus*

Table 3: MIC for antibacterial activity of compound **36a, 36c, 36d, 36e, 36h and 36i**

Compound Code	Bacteria	MIC concentration (μM)
36a	*B. cereus, S. aureus*	0.09375, 0.046875
36c	*B. cereus, S. aureus*	0.09375, 0.046875
36d	*B. cereus, S. aureus*	0.09375, 0.046875
36e	*S. aureus*	0.375
36h	*B. cereus, S. aureus*	0.375
36i	*B. cereus*	0.1875

Furthermore, compounds **36a**, **36c** and **36i** in Table 3 above showed similar potent activity against *Bacillus cereus* with MIC value of 0.09375 µM, while a significant potent activity was also showed by compound **36a**, **36c and 36i** against *Staphylococcus aureus* with MIC value of 0.04687 µM.

4.5.6 Antifungal Activity

The antifungal activity of **36a-36i** was performed against fungal organisms *Candida albicans, Candida utilis, Saccharomyces cerevisiae, Aspergillus flavus* and *Aspergillus niger* using Ciprofloxacin as positive and DMSO as negative control. The synthesized compounds did not exhibit any antifungal activity.

4.5.7 Mutagenicity Studies

In genetics, mutagenicity refers to a chemical or physical agent's capacity to cause mutation (genetic alterations). Usually these agents damage the DNA of an organism causing lesions that result in cell death. This study was utilized to determine the toxicity of the newly synthesized compounds and their safety in biological application to living organisms. The mutant frequency was expressed as a fraction of the quotient of the number of revertant colonies over the number of colonies in the negative control sample. The formula as shown below (Maron and Ames, 1983:173)

$$\text{Mutant Frequency} = \frac{\text{Revertant number of colonies}}{\text{No.of colonies negative control}}$$

The above expression was used to determine the mutant frequency and should be less than two. The higher the number of revertant colonies, the greater mutant frequency was obtained. According to Maron and Ames (Maron and Ames, 1983:173) a mutagenic potential is presumed if the mutant frequency is higher than 2; a conceivable mutagenic potential is pressumed if the mutant frequency ranges between 1.7 and 1.9; and no mutagenic potential is pressumed if the mutant frequency is below 1.6.

When the mutant frequency is greater than two it is considered mutagenic indicating that the tested compounds can cause cell death. Hence, mutagenic active compounds are unsuitable for *in vivo* biological activity. Table 5 below shows that the synthesized compounds had no mutagenic activity against *Salmonella typhimurium* (*S. typhimurium)* TA 98 and TA100 strains. None of the tested compounds induced any significant proliferation in the number of revertant colonies in comparison with the control, sodium azide.

Table 5: Mutagenicity assay for synthesized compounds

Compounds	Mutant Frequency of revertant at different concentrations (µM)				
	5	10	20	100	1000
36c	na	0.62±0.6	na	0.9±1.3	1.2±1.2
	na	0.5±0.9	na	0.78±1.4	0.9±0.5
36d	na	0.23±0.2	na	0.41±1.2	0.65±1.5
	na	0.29±0.3	na	0.56±1	0.86±0.6
3a	na	0	na	0	0.1±0.2
	na	0.52±0.1	na	0.95±0.14	1.3±0.8
36h	na	0.45±0.6	na	0.89±1.1	1.1±1.6
	na	0.03±0.08	na	0.15±0.6	0.25±0.8
36f	na	0.08±0.3	na	0.18±0.9	0.24±0.65
	na	0.96±0.9	na	1.1±1.1	1.25±0.4
36e	na	0.13±0.12	na	0.49±0.3	0.75±0.52
	na	0.34±0.4	na	0.63±0.7	0.86±0.6
36b	na	0.12±0.23	na	0.28±0.65	0.42±0.07
	na	0.14±0.1	na	0.31±0.54	0.59±0.2
36i	na	0.22±0.1	na	0.47±0.3	0.68±1.0
	na	0.25±0.12	na	0.73±0.81	0.93±0.67
36g	na	0.4±0.6	na	0.9±0.52	1.3±0.2
	na	0.24±0.51	na	0.63±0.3	0.89±0.8
Sodium Azide	1.056±0.474	2.060±0.5	3.920±0.27	na	na
	1.065±0.26	2.173±0.3	4.50±0.6	na	na

Values are expressed as Mean ±SD, n=3, TA100: Black, TA98: Red, na: not applicable, 0=no activity

Sodium azide (NaN_3), was used to confirm the revertant colonies, if any, in the experiment. In this experiment, it was taken that a proliferation in the number of revertant colonies was in direct proportion to the concentration (Figure 7).

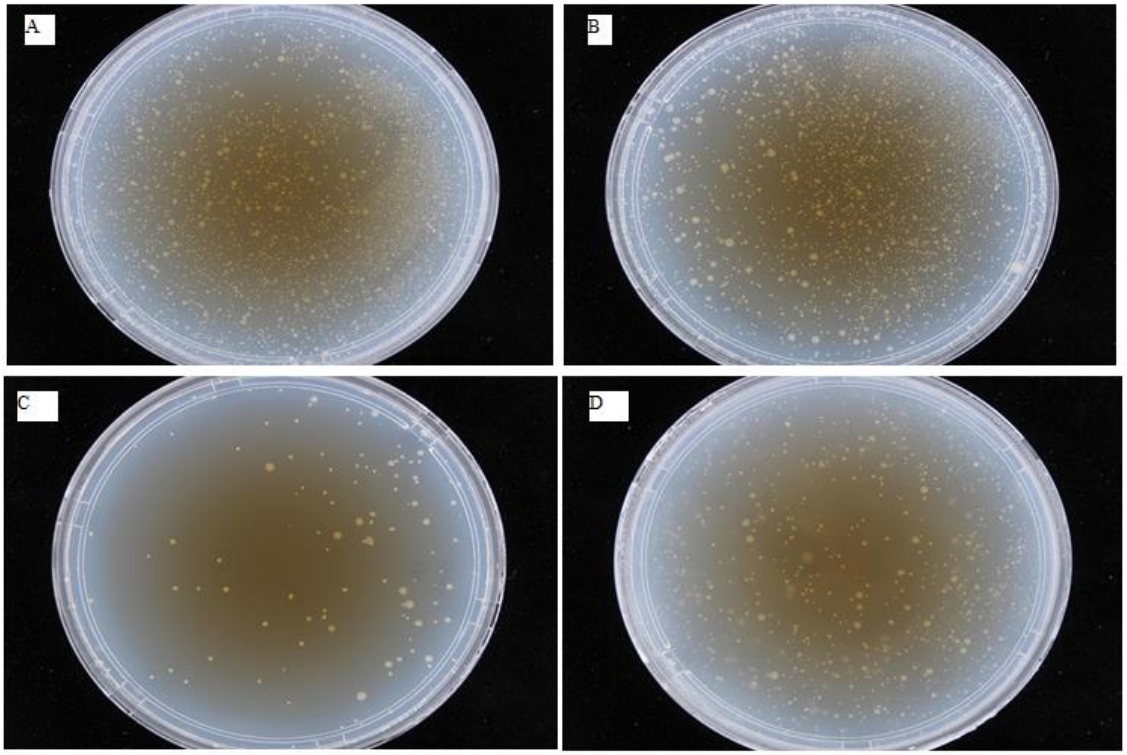

Figure 7: (A) Plate with T 100 showing revertant colonies,

(B) Plate with TA98 showing revertant colonies,

(C) Plate showing revertant colonies of compound **36c** against TA98 at 100µg/mL,

(D) Plate showing revertant colonies of compound **36i** at 1mg/mL against TA 100.

4.6 Conclusion

In this study, nine novel fused indolo [1, 8] naphthyridine derivatives were synthesized with evaluation of their biological activity. The Povarov reaction proved to be a feasible protocol with mild conditions, easy work up process, yielding complex and diverse heterocyclic compounds in a single step operation. The antibacterial assay showed significant inhibitory activity especially for compounds **4a, 4c** and **4i** with MIC value from 0.04687 - 0.09375 µM against *Bacillus cereus* and *Staphylococcus aureus*. Hence, these compounds are potential antibacterial agents. Furthermore, all the compounds showed no mutagenic effects against *Salmonella typhimurium* TA 98 and TA 100 strains hence, they can be investigated in future as potential medicinal drugs.

4. 7 Experimental

4.7.1 Typical Procedure for the Multi-Component Domino Synthesis of Novel Fused 1-Methyl-6-Phenyl-6, 6a, 7, 11b-Tetrahydro-5H-Indolo [2, 3- *c*] [1, 8] Naphthyridine Derivatives

A mixture of 2-amino picoline **34** (1 mmol), indole **35** (1 mmol) and benzaldehyde derivatives **33** (1 mmol) in acetonitrile (20 mL) was refluxed for 12 hours. The reaction product was poured into ice-water; thereafter the precipitate was collected by filtration, washed with water and dried. The resulting crude product was purified by column chromatography using a solvent composition of hexane: ethyl acetate (88:12) to isolate reddish brown solid compounds **36a-36i**. All synthesized compounds were characterized by infrared, nuclear magnetic resonance and mass spectrometry. The spectroscopic data for all nine synthesized derivatives are presented in the next page.

4.7.1.1 The Spectroscopic Analysis of 36a-h

1-methyl-6-phenyl-6, 7-dihydro-5H-indolo [3, 2-c] [1, 8] naphthyridine (36a)

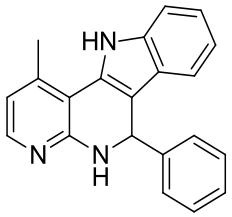

36a

Yield 88%, reddish brown solid, m.p. 184 - 186 ^{0}C. IR (KBr): ν 3390-3271 (N-H), 2854 (CH), 1675-1618 (N-H & C=C), 1479 (C-N) and 744 (N-H) cm $^{-1}$. ^{1}H NMR (400 MHz, DMSO-d_6): δ 10.80 (s, N-H) , 7.39 (1H, d, *J* = 8.1 Hz, H-15), 7.37 (2H, d, *J* = 8.1 Hz, H-5 & H-8), 7.32 (2H, d, *J* = 8.1 Hz, H-2'& H-6'), 7.29 (2H, t, *J* = 7.4 Hz, H-3' & H-5'), 7.17 (1H, t, *J* = 8.2 Hz, H-4'), 7.07 (1H, t, *J* = 7.8 Hz, H-7), 6.89 (1H, t, *J* = 7.8 Hz, H-6), 6.85 (1H, d, *J* = 8.1 Hz, H-14), 5.87 (s, H-2), 2.0 (s, CH_3). ^{13}C NMR (400 MHz, DMSO-d_6): δ 20.7, 39.7, 111.1, 111.4, 118.0, 118.2, 119.1, 120.9, 123.5, 125.8, 127.9, 128.2, 128.4, 131.0, 136.6, 138.4, 144.9 ppm. TOF-MS *m*/*z* found: 311.2 [M^+], TOF-MS *m*/*z* calculated: 311.3 [M^+]. Anal. calcd for $C_{21}H_{17}N_3$: C, 80.00; H, 5.50; N, 13.49; found: C, 80.06; H, 5.48; N, 13.46.

1-methyl-6-(p-tolyl)-6, 7-dihydro-5H-indolo [3, 2-c] [1, 8] naphthyridine (36b)

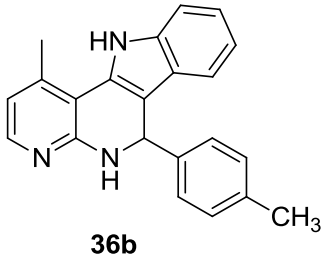

36b

Yield 83%, reddish brown solid, m.p. 188 - 190 ^{0}C. IR (KBr): ν 3419-3277 (N-H), 1618 (N-H & C=C), 1454 (C-N) and 744 (N-H) cm $^{-1}$. ^{1}H NMR (400 MHz, DMSO-d_6): δ 10.8 (s, N-H) , 7.40 (3H, d, *J* = 7.3 Hz, H-5, H-8 & H-15), 7.33 (2H, d, *J* = 7.3 Hz, H-2'& H-6'), 7.27 (2H, d, *J* = 8.0 Hz, H-3' & H-5'), 7.08 (1H, t, *J* = 7.3 Hz, H-7), 6.9 (1H, t, *J* = 7.3 Hz, H-6), 6.85 (1H, d, *J* = 7.2 Hz, H-14), 5.83 (s, H-2), 2.26 (s, CH_3) ppm. ^{13}C NMR (400 MHz, DMSO-d_6): δ 20.6, 39.5, 111.1, 118.2, 118.3, 119.1, 120.9, 123.5, 126.7, 128.5, 134.5, 136.6, 141.9 ppm. TOF-

MS *m/z* found: 325.2 [M^+], TOF-MS *m/z* calculated: 325.4 [M^+] . Anal. calcd for $C_{22}H_{19}N_3$: C, 81.20; H, 5.89; N, 12.91; found: C, 81.08; H, 5.82; N, 12.87.

6-(4-chlorophenyl)-1-methyl-6, 7-dihydro-5H-indolo [3, 2-c] [1, 8] naphthyridine (36c)

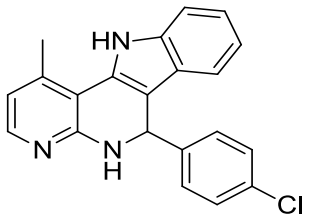

36c

Yield 88%, reddish brown solid, m.p. 194-196 ^{0}C. IR (KBr): ν 3401-3262 (N-H), 1618 (N-H & C=C), 1465 (C-N) and 744 (N-H) cm $^{-1}$. ^{1}H NMR (400 MHz, DMSO-d_6): δ 10.89 (s, N-H) , 7.40 (3H, d, *J* = 8.8 Hz, H-5, H-8 & H-15), 7.33 (2H, d, *J* = 8.5 Hz, H-2' & H-6'), 7.32 (2H, d, *J* = 8.4 Hz, H-3'& H-5'), 7.08 (1H, t, *J* = 7.2 Hz, H-7), 6.92 (1H, d, *J* = 7.3 Hz, H-6), 6.88 (1H, d, *J* = 7.6 Hz, H-14), 5.90 (s, H-2), 2.0 (s, CH_3) ppm. ^{13}C NMR (400 MHz, DMSO-d_6): δ 20.7, 39.8, 111.5, 117.6, 118.3, 119.0, 120.9, 123.6, 127.9, 130.1, 130.3, 136.6, 143.9 ppm. TOF-MS *m/z* found: 347.1 [M^+], TOF-MS *m/z* calculated: 345.8 [M^+]. Anal. calcd for $C_{21}H_{16}ClN_3$: C, 72.93; H, 4.66; N, 12.15; found: C, 72.51; H, 5.20; N, 12.08.

6-(4-fluorophenyl)-1-methyl-6, 7-dihydro-5H-indolo [3, 2-c] [1, 8] naphthyridine (36d)

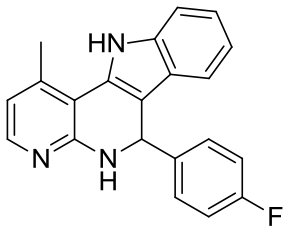

36d

Yield 79%, reddish brown solid, m.p. 189-191 ^{0}C. IR (KBr): ν 3408 (N-H), 1519 (N-H), 1454 (C-N), 1005 (C-F) and 742 (N-H) cm $^{-1}$. ^{1}H NMR (400 MHz, DMSO-d_6): δ 10.85 (s, N-H), 7.38 (3H, d, *J* = 8.6 Hz, H-5, H-8 & H-15), 7.30 (2H, d, *J* = 8.9 Hz, H-2'& H-6'), 7.08 (1H, t, *J* = 6.5 Hz, H-7), 7.03 (2H, d, *J* = 8.2 Hz, H-3' & H-5'), 6.89 (1H, d, *J* = 7.3 Hz, H-6), 6.83 (1H, d, *J* = 7.6 Hz, H-14), 5.87 (s, H-2), 1.99 (s, CH_3) ppm. ^{19}F NMR (400 MHz, DMSO-d_6): δ -117.6 ppm (Ar-F). ^{13}C NMR (400 MHz, DMSO-d_6): δ 20.9, 38.7, 111.5, 114.5, 117.9, 118.2,

119.0, 120.9, 123.5, 125.6, 126.5, 129.9, 136.6, 141.1, 159.3, 161.7 ppm. TOF-MS *m/z* found: 340.1 [M^++1], TOF-MS *m/z* calculated: 329.4 [M^+]. Anal. calcd for $C_{21}H_{16}FN_3$: C, 76.58; H, 4.90; N, 12.76; found: C, 76.56; H, 4.95; N, 12.68.

1-methyl-6-(4-(trifluoromethyl) phenyl)-6, 7-dihydro-5H-indolo [3, 2-c] [1, 8] naphthyridine (**36e)**

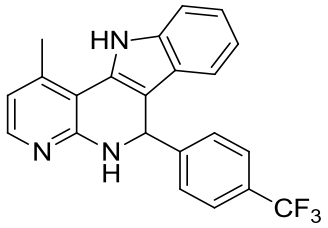

36e

Yield 86%, pink solid, m.p. 184-186 ^{0}C. IR (KBr): ν 3244 (N-H), 1615 (N-H & C=C), 1438 (C-N), 1339 (C-F) and 745 (N-H) cm $^{-1}$. ^{1}H NMR (400 MHz, DMSO-d_6): δ 10.89 (s, N-H), 7.64 (1H, d, *J* = 8.3 Hz, H-15), 7.58 (3H, d, *J* = 8.2 Hz, H-5, H-3'& H-5'), 7.37 (2H, d, *J* = 8.1 Hz, H-2'& H-6'), 7.30 (1H, d, *J* = 8.0 Hz, H-8), 7.07 (1H, t, *J* = 7.0 Hz, H-7), 6.90 (1H, d, *J* = 8.1 Hz, H-6), 6.86 (1H, d, *J* = 7.6 Hz, H-14), 5.97 (s, H-2), 1.98 (s, CH_3) ppm. ^{19}F NMR (400 MHz, DMSO-d_6): δ -60.6 ppm (Ar-CF_3). ^{13}C NMR (400 MHz, DMSO-d_6): δ 20.7, 39.7, 111.5, 117.1, 118.3, 118.9, 120.9, 123.7, 124.9, 126.4, 128.9, 136.6, 149.8 ppm. TOF-MS *m/z* found: 380.1 [M^++1], TOF-MS *m/z* calculated: 379.4 [M^+]. Anal. calcd for $C_{22}H_{16}F_3N_3$: C, 69.65; H, 4.25; N, 11.08; found: C, 69.62; H, 4.28; N, 11.11.

1-methyl-6-(4-nitrophenyl)-6, 6a, 7, 11b-tetrahydro-5H-indolo [3, 2-c] [1, 8] naphthyridine (**4f**)

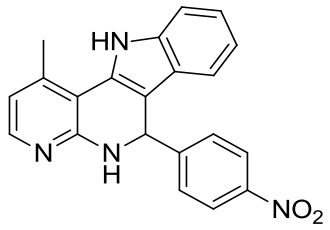

36f

Yield 84%, yellow solid, m.p. 238-240 ^{0}C. IR (KBr): ν 3386-3455 (N-H), 1594 (N-H & C=C), (C-N), 1340 (N-O) and 745 (N-H) cm $^{-1}$. ^{1}H NMR (400 MHz, DMSO-d_6): δ 10.93 (s, N-H), 8.15 (2H, d, *J* = 8.8 Hz, H-3' & H-5'), 7.61 (2H, d, *J* = 8.7 Hz, H-15 & H-5), 7.37 (2H, d, *J* = 8.1 Hz, H-2'& H-6'), 7.30 (1H, d, *J* = 7.9 Hz, H-8), 7.07 (1H, t, *J* = 7.1 Hz, H-7), 6.90 (1H, t, *J* = 7.0 Hz, H-6), 6.87 (1H, d, *J* = 7.9 Hz, H-14), 6.03 (s, H-2), 2.00 (s, CH_3) ppm. ^{13}C NMR (400 MHz, DMSO-d_6): δ 20.7, 39.6, 111.6, 116.6, 118.4, 118.9, 121.1, 123.3, 123.8, 126.3, 129.4, 136.6, 145.7, 151.3 ppm. TOF-MS *m*/*z* found: 357.1 [M^++1], TOF-MS *m*/*z* calculated: 356.4 [M^+]. Anal. calcd for $C_{21}H_{16}N_4O_2$: C, 70.77; H, 4.53; N, 15.72; found: C, 70.81; H, 5.76; N, 15.76.

6-(4-methoxyphenyl)-1-methyl-6, 6a, 7, 11b-tetrahydro-5H-indolo [3, 2-c] [1, 8]naphthyridine (**4g)**

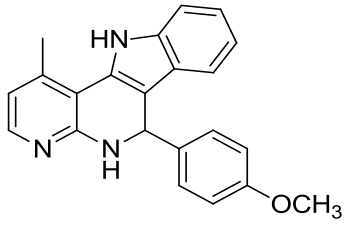

36g

Yield 70%, orange solid, m.p. 181-183 ^{0}C. IR (KBr): ν 3396 (N-H), 1610 (N-H & C=C), 1509 (C-N), 1093 (C-O-C) and 724 (N-H) cm $^{-1}$. ^{1}H NMR (400 MHz, DMSO-d_6):): δ 10.79 (s, N-H) , 7.35 (2H, d, *J* = 8.1 Hz, H-15 & H-5), 7.29 (1H, d, *J* = 8.0 Hz, H-8), 7.26 (2H, d, *J* = 8.4 Hz, H-2' & H-6'), 7.04 (1H, t, *J* = 7.2 Hz, H-7), 6.88 (1H, t, *J* = 7.2 Hz, H-6), 6.83 (2H, d, *J* = 8.7 Hz, H-3' & 5'), 6.81 (1H, d, *J* = 7.6 Hz, H-14), 5.78 (s, H-2), 3.69 (s, OCH_3), 2.00 (s, CH_3) ppm. ^{13}C NMR (400 MHz, DMSO-d_6): δ 20.7, 39.7, 54.9, 111.1, 113.3, 118.0, 118.4, 119.1, 120.8, 123.4, 126.6, 129.2, 136.6, 136.9, 157.2 ppm. TOF-MS *m*/*z* found: 342.1 [M^++1],

TOF-MS *m/z* calculated: 341.4 [M^+]. Anal. calcd for $C_{22}H_{19}N_3O$: C, 77.40; H, 5.61; N, 12.31; found: C, 77.37; H, 5.58; N, 12.29.

2-methoxy-4-(1-methyl-6, 6a, 7, 11b-tetrahydro-5H-indolo [3, 2-c] [1, 8] naphthyridin-6-yl) phenol (**36h)**

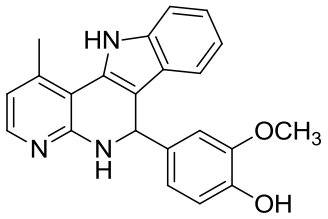

36h

Yield 73%, reddish brown solid, m.p. 195-197 ^{0}C. IR (KBr): ν 3485 (N-H), 3412 (OH), 1591 (N-H & C=C), 1454 (C-N), 1028 (C-O-C) and 745 (N-H) cm $^{-1}$. ^{1}H NMR (400 MHz, DMSO-d_6): δ 10.77 (s, N-H), 8.71 (s, OH), 7.36 (2H, d, *J* = 8.1 Hz, H-15 & H-5), 7.31 (1H, d, *J* = 7.9 Hz, H-8), 7.05 (1H, t, *J* = 7.1 Hz, H-7), 6.98 (1H, d, *J* = 7.6 Hz, H-5'), 6.87 (1H, t, *J* = 7.1 Hz, H-6), 6.83 (1H, d, *J* = 8.5 Hz, H-2'), 6.73 (1H, d, *J* = 7.6 Hz, H-14), 6.69 (1H, d, *J* = 7.6 Hz, H-6'), 5.75 (s, H-2), 3.67 (s, OCH_3), 2.21 (s, CH_3) ppm. ^{13}C NMR (400 MHz, DMSO-d_6): δ 20.9, 39.7, 55.6, 111.4, 112.8, 115.0, 118.0, 118.6, 119.1, 120.5, 120.8, 123.4, 126.7, 135.9, 136.6, 144.5, 147.2 ppm. TOF-MS *m/z* found: 358.1 [M^++1], TOF-MS *m/z* calculated: 357.4 [M^+]. Anal. calcd for $C_{22}H_{19}N_3O_2$: C, 73.93; H, 5.36; N, 11.76; found: C, 73.89; H, 5.42; N, 11.78.

2-bromo-6-methoxy-4-(1-methyl-6, 7-dihydro-5H-indolo [2, 3-c] [1, 8] naphthyridin-6-yl) phenol (**36i)**

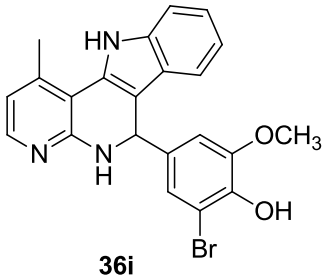

36i

Yield 81%, reddish brown solid, m.p. 205-207 ^{0}C. IR (KBr): v 3283 (OH), 1603 (N-H & C=C), 1494 (C-N), 1038 (C-O-C) and 741 (N-H) cm $^{-1}$. ^{1}H NMR (400 MHz, DMSO-d_6): δ 10.81 (s, N-H), 9.19 (s. OH), 7.38 (2H, d, *J* = 8.2 Hz, H-15 & H-5), 7.33 (1H, d, *J* = 7.9 Hz, H-8), 7.08 (1H, t, *J* = 8.0 Hz, H-7), 7.04 (1H, d, *J* = 7.6 Hz, H-2'), 6.99 (1H, d, *J* = 7.6 Hz, H-6'), 6.91 (1H, t, *J* = 7.1 Hz, H-6), 6.87 (1H, d, *J* = 7.2 Hz, H-14), 5.79 (s, H-2), 3.74 (s, OCH_3), 2.0 (s, CH_3) ppm. ^{13}C NMR (400 MHz, DMSO-d_6): δ 20.7, 39.7, 56.1, 108.9, 111.5, 111.8, 117.9, 118.2, 119.0, 120.9, 123.5, 126.6, 136.6, 137.1, 141.8, 148.2 ppm. TOF-MS *m*/*z* found: 435.1 [M^+], TOF-MS *m*/*z* calculated: 436.3 [M^+]. Anal. calcd for $C_{22}H_{18}BrN_3O_2$: C, 60.56; H, 4.16; N, 9.63; found: C, 60.59; H, 4.18; N, 9.59.

4.7.2 Antibacterial Activity

The antibacterial activity of the compounds was determined using the protocol described by Cos *et al*.(2006) using agar disc diffusion assay. The bacterial strains used in the study were collected from the culture collection at the Department of Biotechnology and Food Technology, Durban University of Technology, South Africa. The strains include *Staphylococcus aureus* (DBT), *Bacillus cereus* (DBT), *Citrobacter freundii* (DBT), *Serratia marcescens* (DBT), *Klebsiella pneumonia* (DBT) and *Micrococcus luteus* (DBT)

DBT: Durban University of Technology Culture collection reference based at the department of Biotechnology and Food Technology**.**

4.7.2.1 Typical Procedure

Stock cultures were sub-cultured to check their viability and stored using 50 % glycerol in micro bank vials (Davies Diagnostics, South Africa). For the assay, cultures were plated on Nutrient Agar (Biolab) and kept in the incubator for 24 hours at 37 °C, then grown in Nutrient Broth (Biolab) under the same conditions. The MacFarland standard of 0.5 absorbance corresponding to 10^8 cfu/mL was used to standardize the bacterial cell concentration. A suspension (100 µL of 10^8 cfu/mL) of the test bacteria was plated on Mueller Hinton Agar plates (Fluka, Biochemika). The Whatman No. 1 filter paper was cut into 5 mm disks and dried

in open sterile petri-dishes in a biosafety chamber (LabtecBioflow II, South Africa). The disks were impregnated with 10 µL of each compound at the concentration of 3 mg/mL then placed onto the pre-inoculated bacterial agar plates and incubated at 37 °C for 24 hours. The assay was carried out in triplicate. Ciprofloxacin (Fluka, Biochemika) (3 µM) was used as the positive control while DMSO (100 %) as a negative control.

The minimum inhibitory concentrations (MIC) were defined as the lowest concentration of a compound that inhibits the bacterial growth. A stock solution of the compounds was made in DMSO and diluted to a final concentration of 3, 1.5; 0.75; 0.37; 0.18; 0.09 µM.

4.7.3 Antifungal Activity Typical Procedure

The antifungal activity of the compounds was carried out using three yeast cultures, *Candida albicans* (DBT*_AB), *Candida utilis* (DBT*_AB), *Saccharomyces cerevisiae* (DBT*_R) and two species of mould, *Aspergillus flavus* (DBT*_AR) and *Aspergillus niger* (DBT*_AR). Sabouraud Dextrose broth was used to grow the yeast culture at 37 °C for 24 hours, and fungi incubation were carried out at 28 °C until sporulation for about 4-7 days using the same media. The spores that were produced were collected in sterile distilled water (10 mL), the concentration was adjusted to 10^6 spores/mL and then counted in a Neubauer counting chamber. Hundred microliter of sterile distilled water was inoculated with the fungal spores (10^6 spores/mL), then poured on the Sabouraud Dextrose Agar plate. The filter disks and samples were prepared as previously described in antibacterial assay. Inoculated disks were placed on the inoculated agar plates and incubated for 72 hours at 25°C. The assay was carried out in triplicate. Each reaction contained 3 µM of sample; amphotericin B (Fluka, Biochemika) was used as the positive control and 10 µL DMSO (100 %) as negative control.

4.7.4 Mutagenicity Studies Typical Procedure

The *Salmonella* mutagenicity experiment was conducted using the method described by Maron and Ames (1983), with few modifications. *Salmonella typhimurium* TA 98 and TA 100 strains. The test strains were obtained in disc cultures from the Medical Research Council, Durban (MRC). TA 100 test strain was retrieved from broth cultures that were initially supplied as

frozen disc cultures. The culture discs were aseptically removed and inoculated, using a flamed bacteriological needle, into a sterile 250 mL Erlenmeyer flask that contained 25 mL of nutrient broth (Oxoid) and 78 µL of Ampicillin (8 µM) (this was performed to maintain the stability of the bacterial plasmid). The flask was then incubated on a shaker (150 rpm) at 37 ºC for 16 hours. This was performed to obtain an optical density of between 1.2 and 1.4 at 660 nm.

In a sterile test tube, 100 µL of grown *Salmonella typhimurium* TA 100 and TA 98 culture was added to 2 mL of 0.05 mM histidine/0.05 mM biotin top agar. The tube was vortexed and plated onto a minimal glucose agar plate, followed by incubation at 37 ºC for 48 hours. Well separated colonies from plates were used as initial broth cultures. The cultures of *Salmonella typhimurium* were made by inoculating nutrient broth with the master plate colonies. These cultures were incubated on a shaker (150 rpm) at 37 ºC for 24 hours.

The fused indolo-naphthyridine compounds **36a-36i** were prepared for antimutagenicity tests by dissolving them in DMSO, so that respective concentrations of 10, 100 and 1000 µM were obtained. NaN_3, a highly mutagenic compound, was used as the positive control (Maron and Ames, 1983). The NaN_3 was dissolved in DMSO (5, 10and 20 µM). The negative control used was sterile distilled water.

For each concentration of test compound, three plates were used. In a sterile test tube, 100 µL bacterial culture, 100 µL test compound, and 2.9 mL soft agar at 45 ºC were added. The tube was briefly vortexed and poured onto glucose minimal agar plates. Once the agar overlay was solidified, plates were inverted and incubated at 37 ºC for 48 hours. Following incubation, revertant colonies (i.e. histidine dependant) were counted and the mutant frequency was determined. The mutant frequency was expressed as a fraction of the number of revertant colonies and the number of colonies in the negative control. (Maron and Ames, 1983: 173)

4.8 References

1. Kouznetsov V.V. 2009. Recent synthetic developments in a powerful imino Diels-Alder reaction (Povarov reaction): application to the synthesis of *N*-polyheterocycles and related alkaloids. *Tetrahedron*, 65: 2721-2750.
2. Bharate J.B., Vishwakarma R.A. and Bharate S.B. 2015. Metal-free domino one-pot protocols for quinoline synthesis. *Royal Society of Chemistry*: 1-35.
3. Buonora P., Olsen J.C. and Oh T. 2001. Recent developments in imino Diels-Alder reactions. *Tetrahedron*, 57: 6099-6138.
4. Glushkov V.A. and Tolstikov A.G. 2008. Synthesis of substituted 1,2,3,4-tetrahydroquinones by the Povarov reaction. New potentials of the classical reaction. *Russian Chemical Reviews*, 77(2): 137-159.
5. Nino P., Caba M., Aguilar N., Terricabras E., Albericio F. and Fernandez J.C. 2016. Povarov reaction, scope and limitations: Preparation of diversely heterocyclic tetrahydro-1-*H*-cyclopenta[*c*]quinolines. *Indian Journal of Chemistry*, 55B: 1117-1130.
6. Powell D.A. and Batey R.A. 2002. Total synthesis of the alkaloids martinelline and martinellic acid via a hetero Diels-Alder multicomponent coupling reaction. *Organic Letters*, 4(17): 2913-2916.
7. Alonso C., Fuertes M., Gonzalez M., Rubiales G., Tesauro C., Knudsen B.R. and Palacios F. 2016. Synthesis and biological evaluation of indeno[1,5]naphthyridines as topoisomerase I (TopI) inhibitors with antiprokiferative activity. *European Journal of Medicinal Chemistry*, 115: 179-190.
8. Tejeria A., Perez-Pertejo Y., Reguera R.M., Balana-Fouce R., Alonso C., Fuertes M., Gonzalez M., Rubiales G. and Palacios F. 2016. Antileishmanial effect of new indeno-1, 5-naphthyridines, selective inhibitors of Leishmania infantum type IB DNA topoisomerase. *European Journal of Medicinal Chemistry*, 124: 740-749.
9. Twin H. and Batey R.A. 2004. Intramolecular hetero Diels-Alder (Povarov) approach to the synthesis of alkaloids Luotonin A and Camptothecin. *Organic Letters*, 6 (26): 4913-4916.
10. Domingo L.R., Aurell M.J., Saez J.A. and Mekelleche S.M. 2014. Understanding the mechanism of the Povarov reaction. A DFT study. *The Royal Society of Chemistry*, 4: 25268-25278.
11. Belal Md., Das D.K. and Khan A.T. 2015. Synthesis of pyrido[2,3-*c*]coumarin derivatives by an intramolecular Povarov reaction. *New York Synthesis*, 47: A-H.

12. Min C., Sanchawala A. and Seidel D. 2014. Dual C-H functionalization of N-aryl amines: Synthesis of polycyclic amine via an oxidative Povarov approach. *Organic Letters*: A-D.
13. Khan A.T. and Khan M.M. 2011. Sequential three-component reactions: synthesis, regioselectivity and application of functionalized dihydropyridines (DHPs) for the creation of fused naphthyridines. *Tetrahedron Letters*, 52: 3455-3459.
14. Hostyn S., Maes B.U.W., Pieters L., Lemiere G.L.F. Matyus P., Hajos G. and Dommisse R.A. 2005. Synthesis of the benzo-beta-carboline isoneocryptolepine: the missing indoloquinoline isomer in the alkaloid series cryptolepine, neocryptolepine and isocryptolepine. *Tetrahedron*, 61: 1571-1577.
15. Sharma V., Kumar P. and Pathak D. 2010. Biological importance of the indole nucleus in recent years: A Comprehensive Review. *Journal of Heterocyclic Chemistry*, 47: 491-502.
16. Maron, D. M. & Ames, B. N. 1983. Revised methods for the Salmonella mutagenicity test. *Mutation Research/Environmental Mutagenesis and Related Subjects,* 113: 173-215.

Appendix - IV

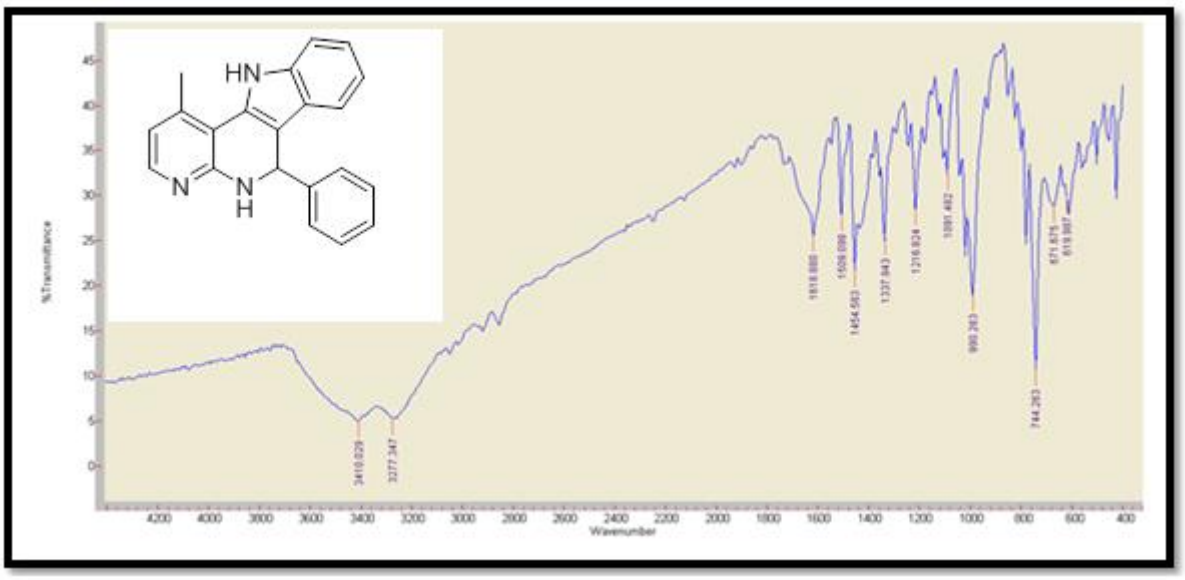

Appendix 4.1: IR spectrum for compound **36a**

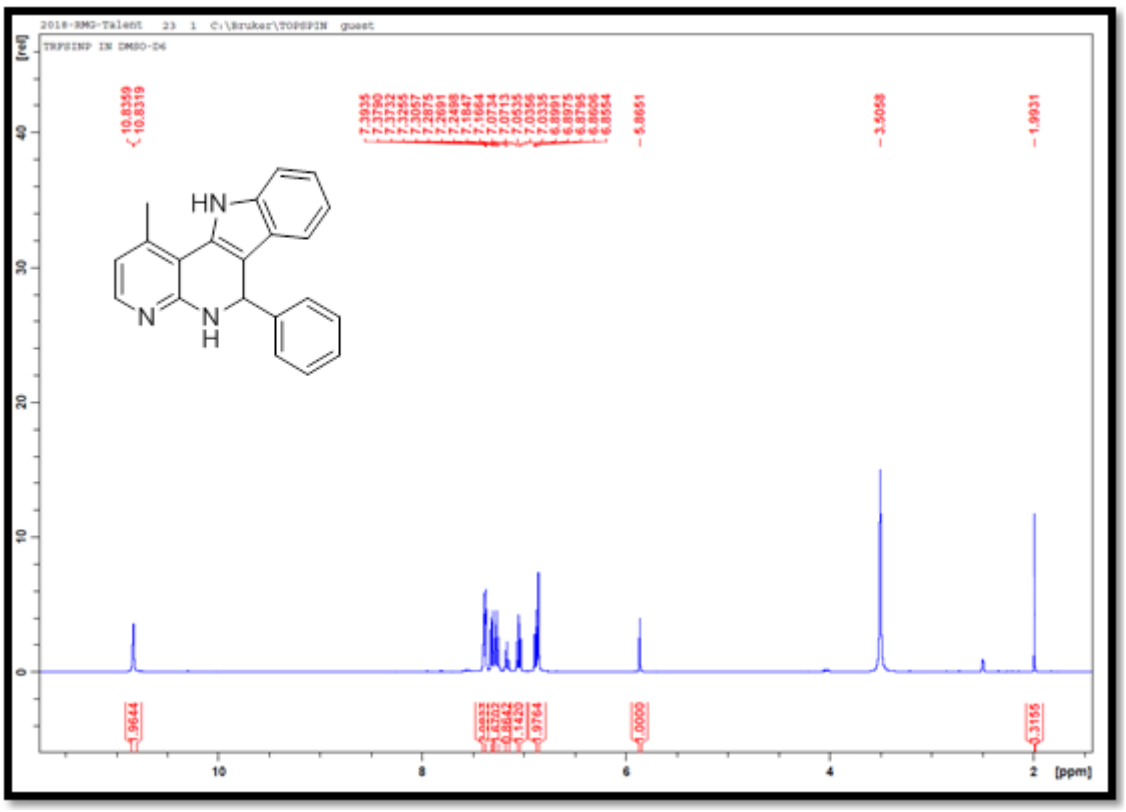

Appendix 4.2: ^{1}H NMR spectrum for compound **36a**

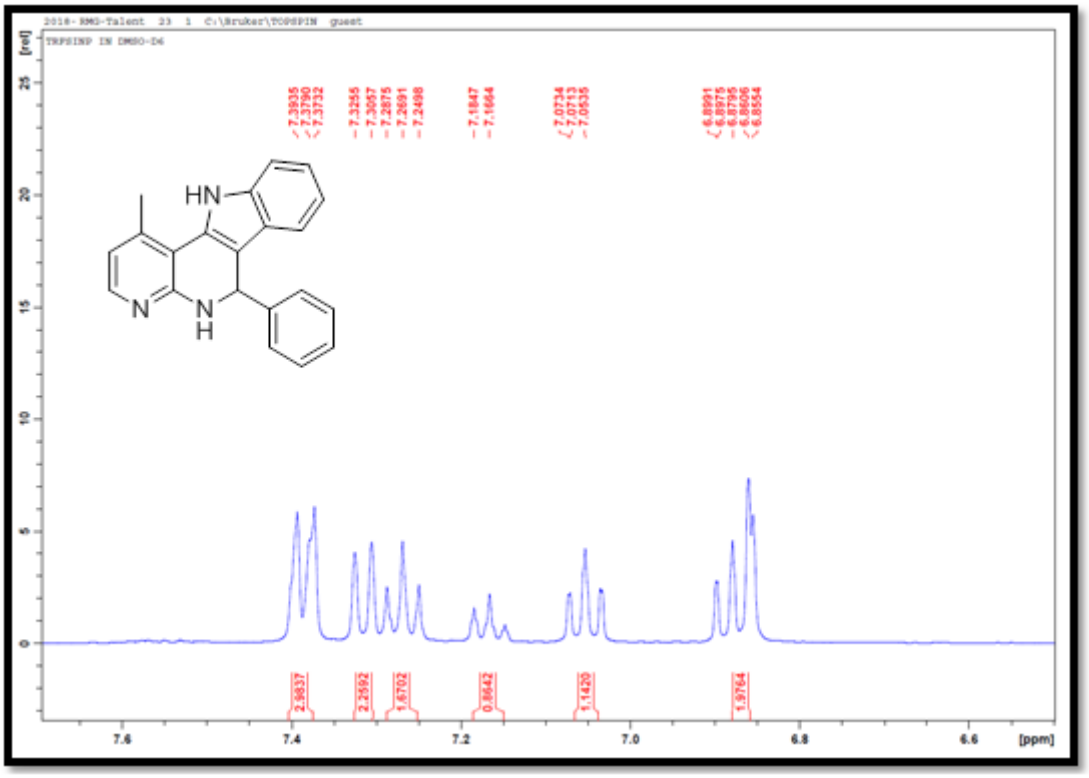

Appendix 4.3: Expanded ^{1}H NMR spectrum for compound **36a**

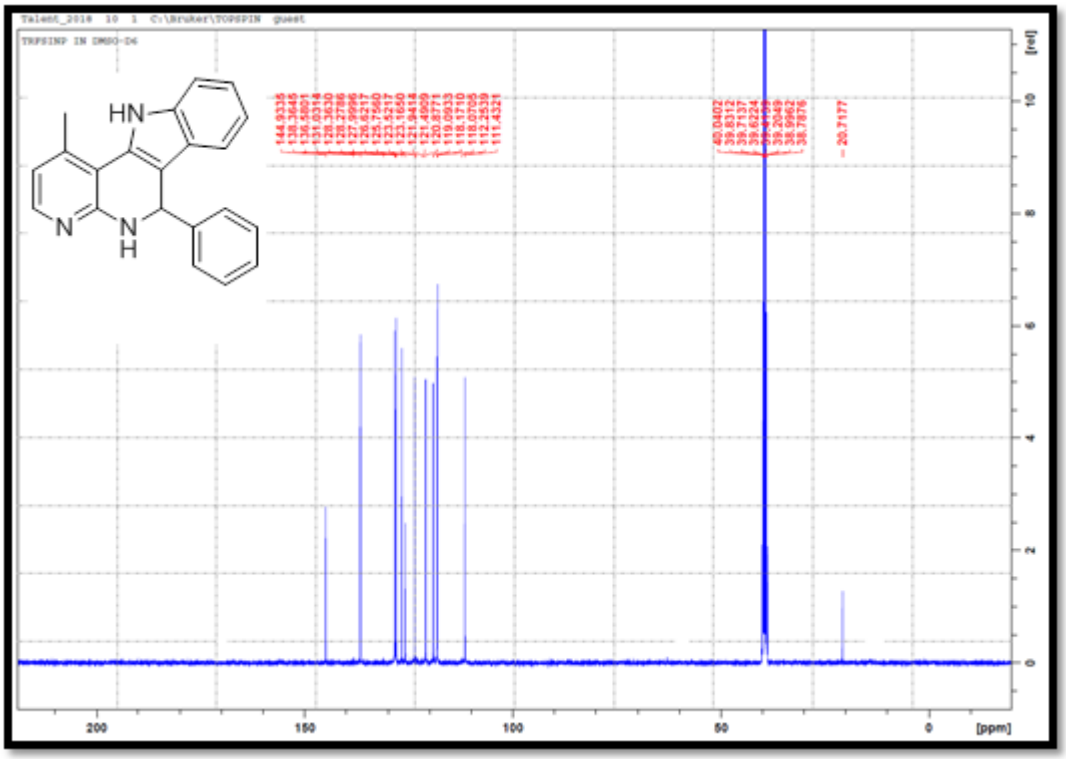

Appendix 4.4: ^{13}C NMR spectrum for compound **36a**

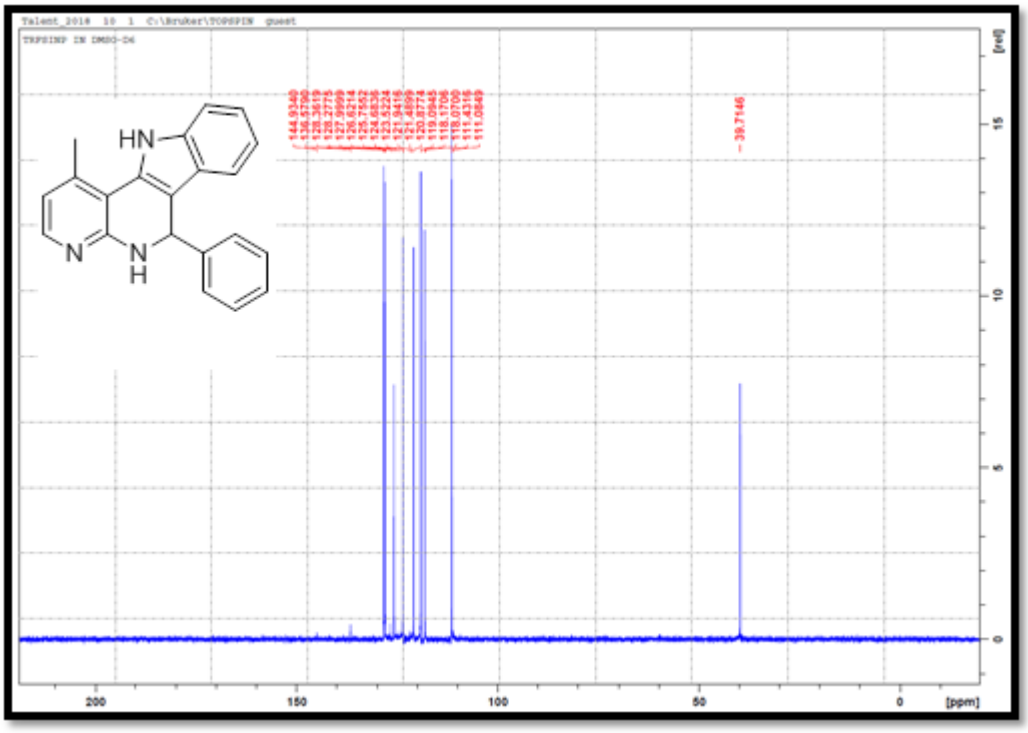

Appendix 4.5: 90^0 DEPT NMR spectrum for compound **36a**

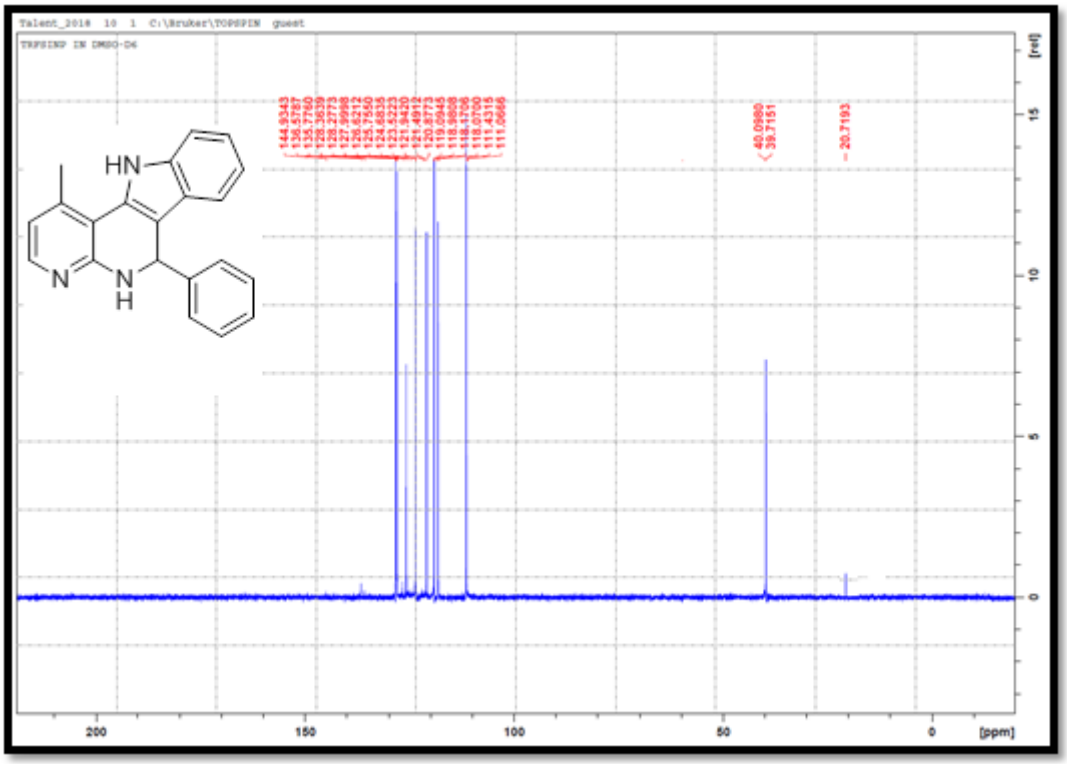

Appendix 4.6: 135^0 DEPT NMR spectrum for compound **36a**

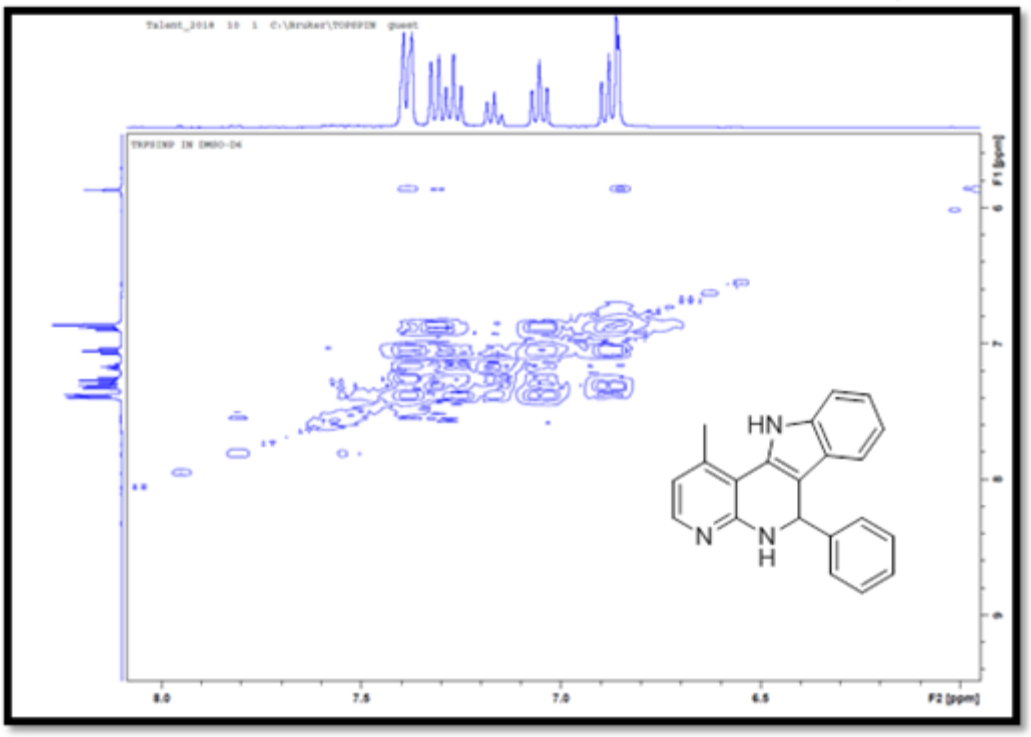

Appendix 4.7: ^{1}H COSY NMR spectrum for compound **36a**

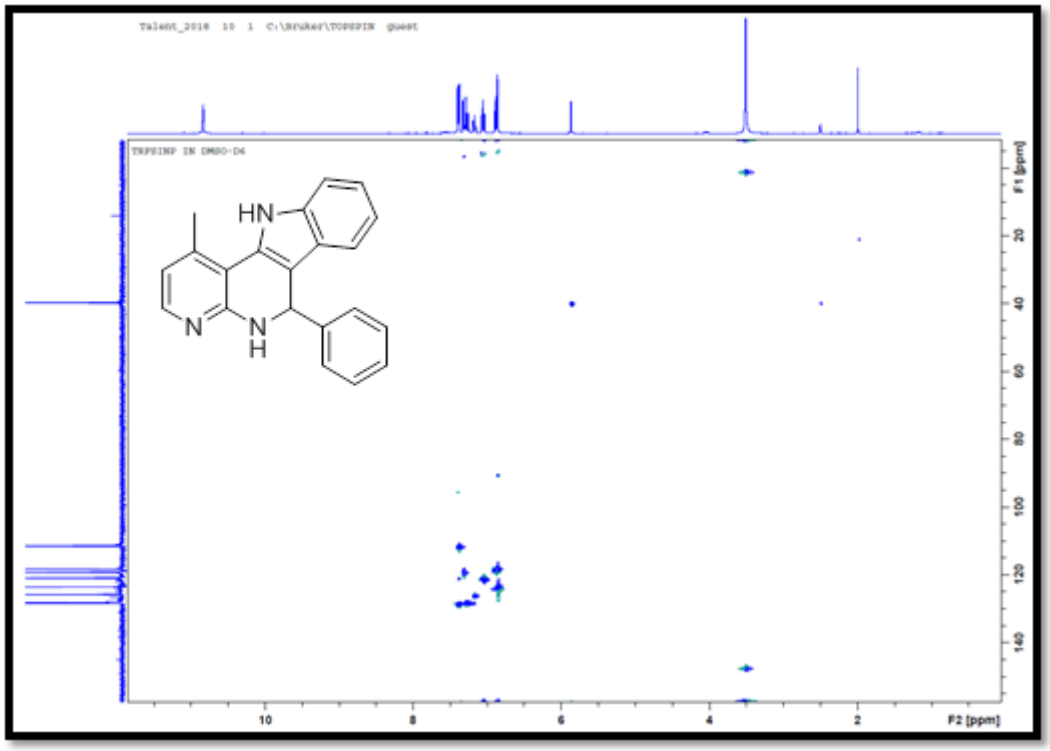

Appendix 4.8: HSQC NMR spectrum for compound **36a**

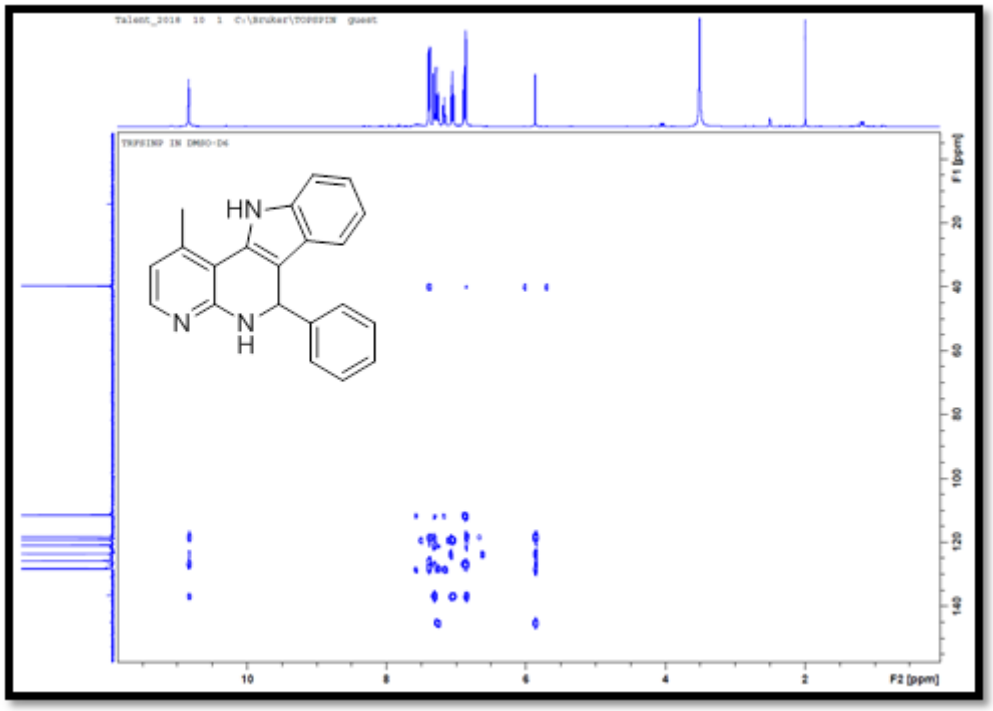

Appendix 4.9: HMBC NMR spectrum for compound **36a**

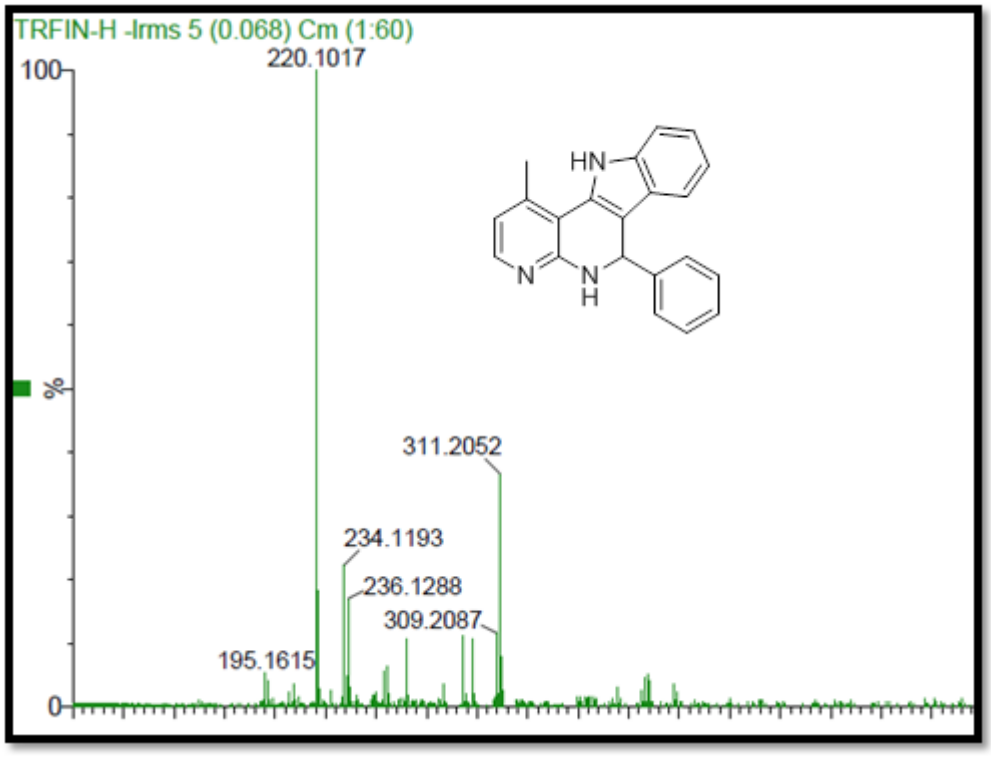

Appendix 4.10: TOF-MS spectrum for compound **36a**

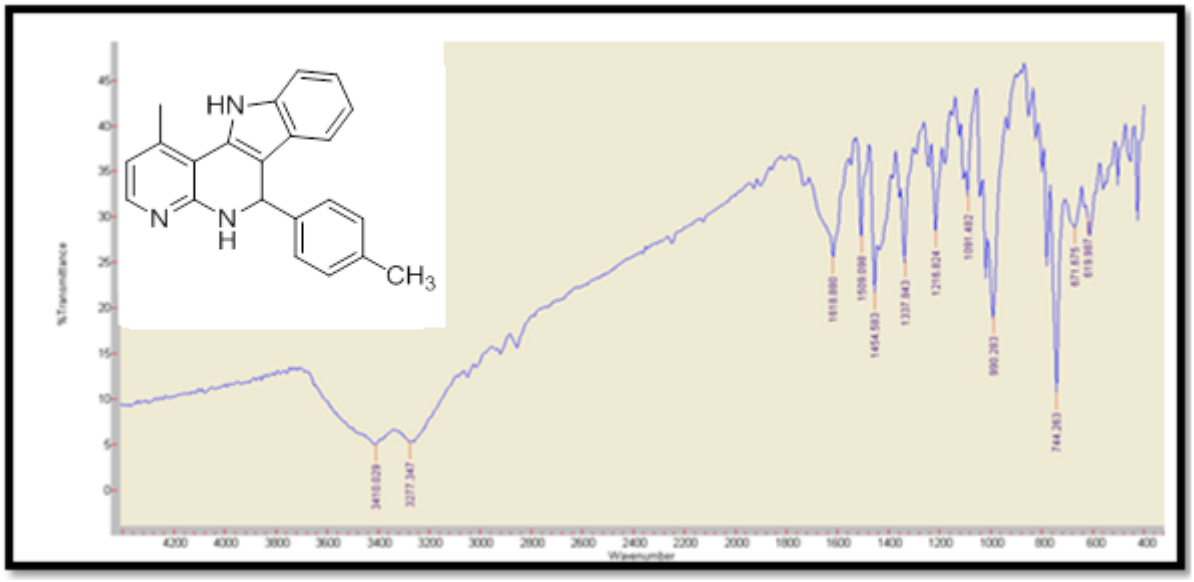

Appendix 4.11: IR spectrum for compound **36b**

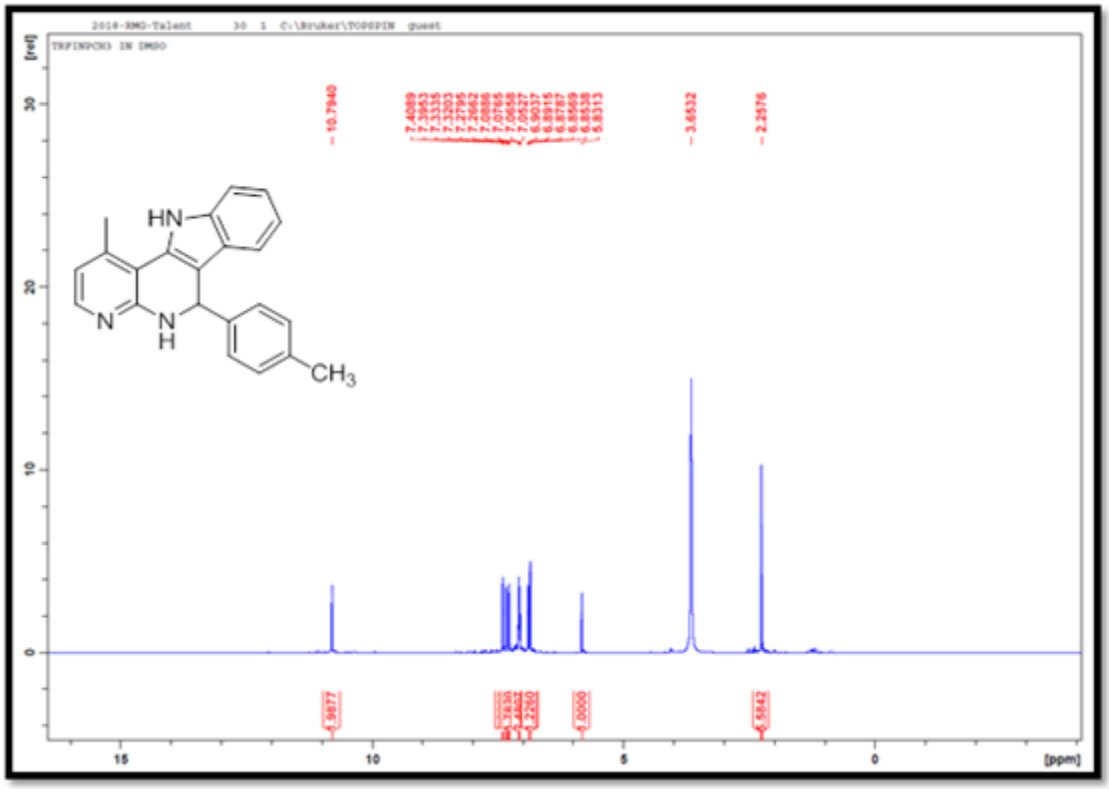

Appendix 4.12: ^{1}H NMR spectrum for compound **36b**

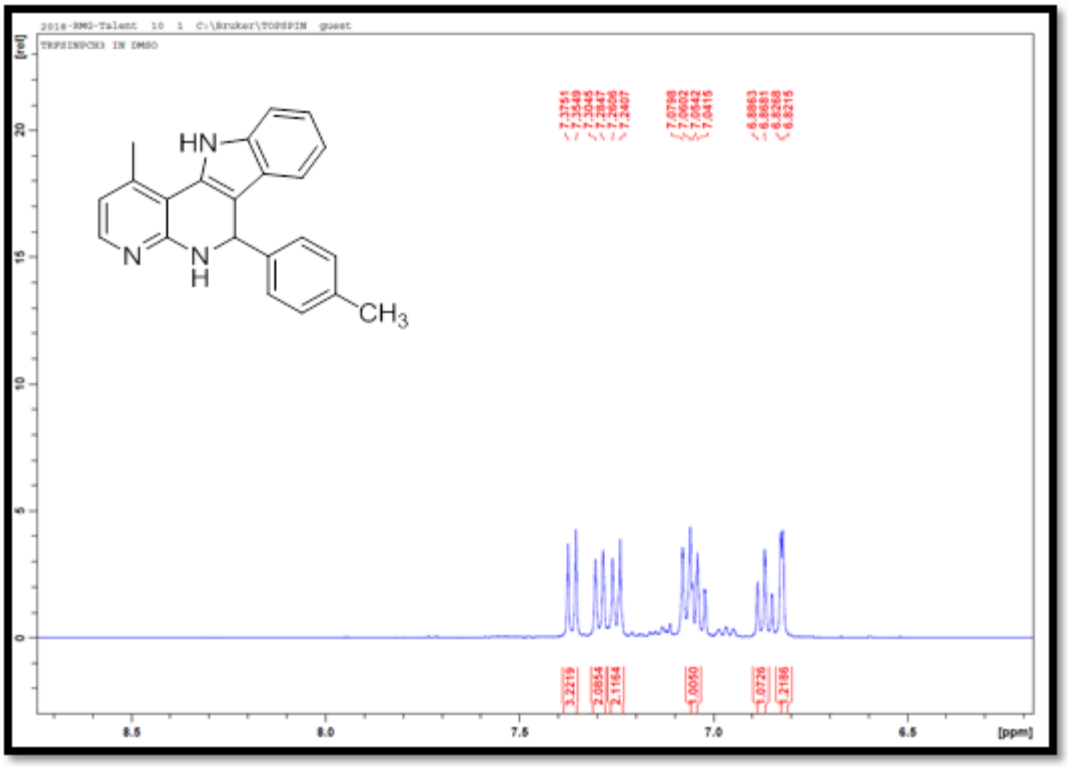

Appendix 4.13: ^{1}H NMR expanded spectrum for compound **36b**

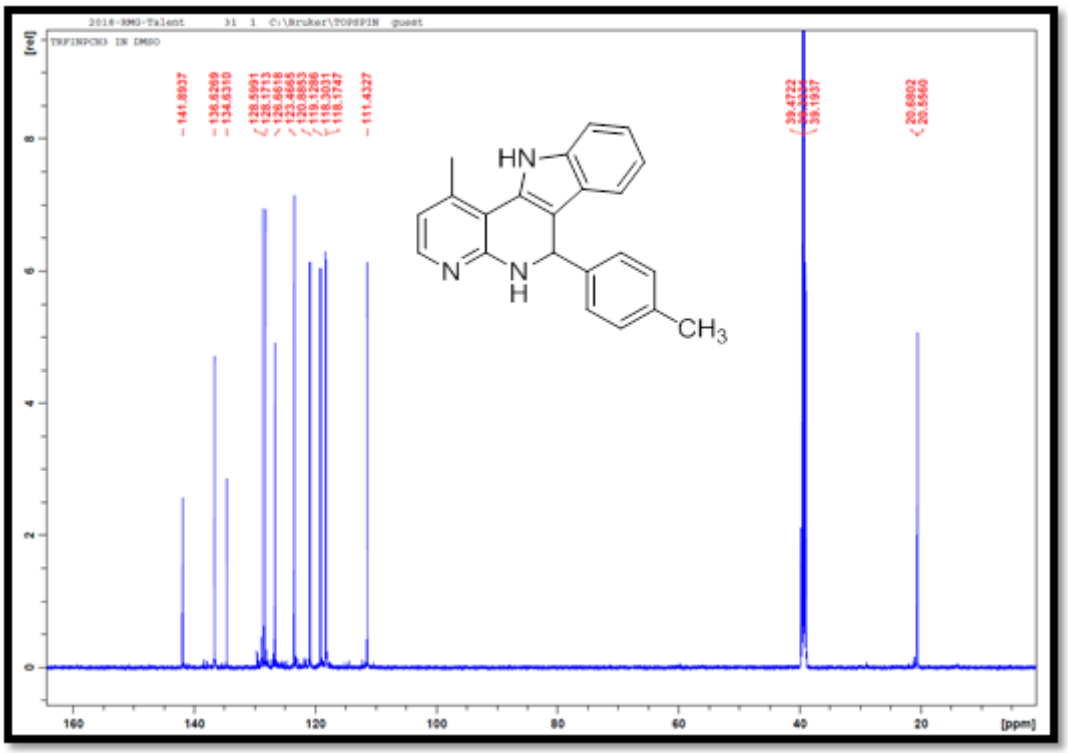

Appendix 4.14: ^{13}C NMR spectrum for compound **36b**

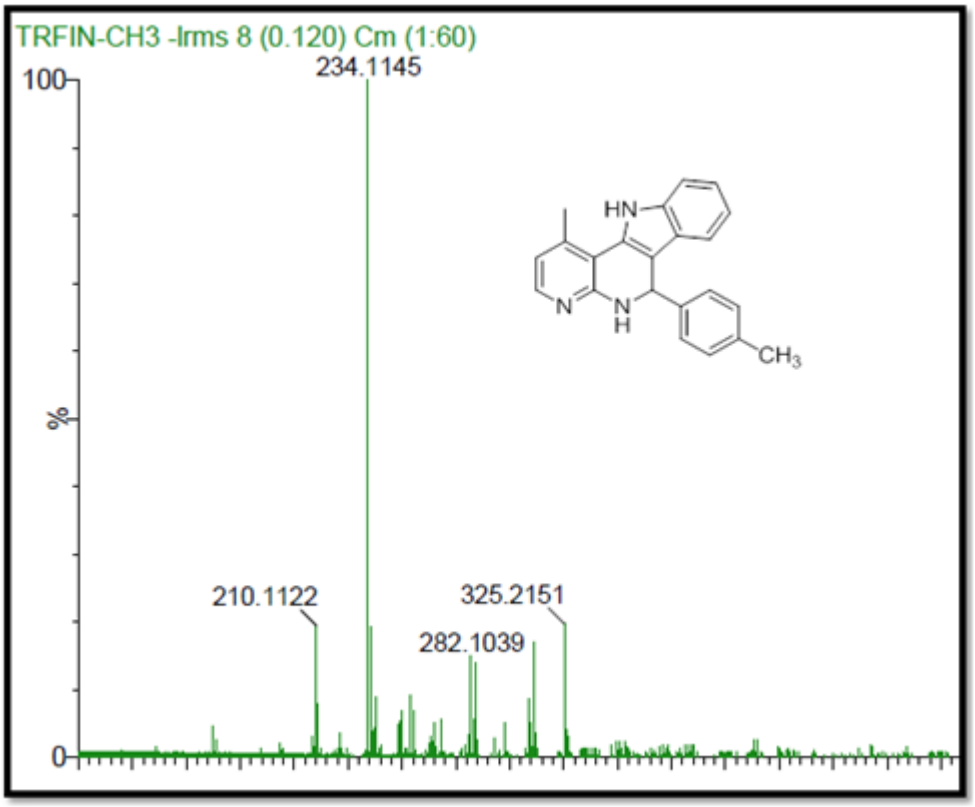

Appendix 4.15: TOF-MS spectrum for compound **36b**

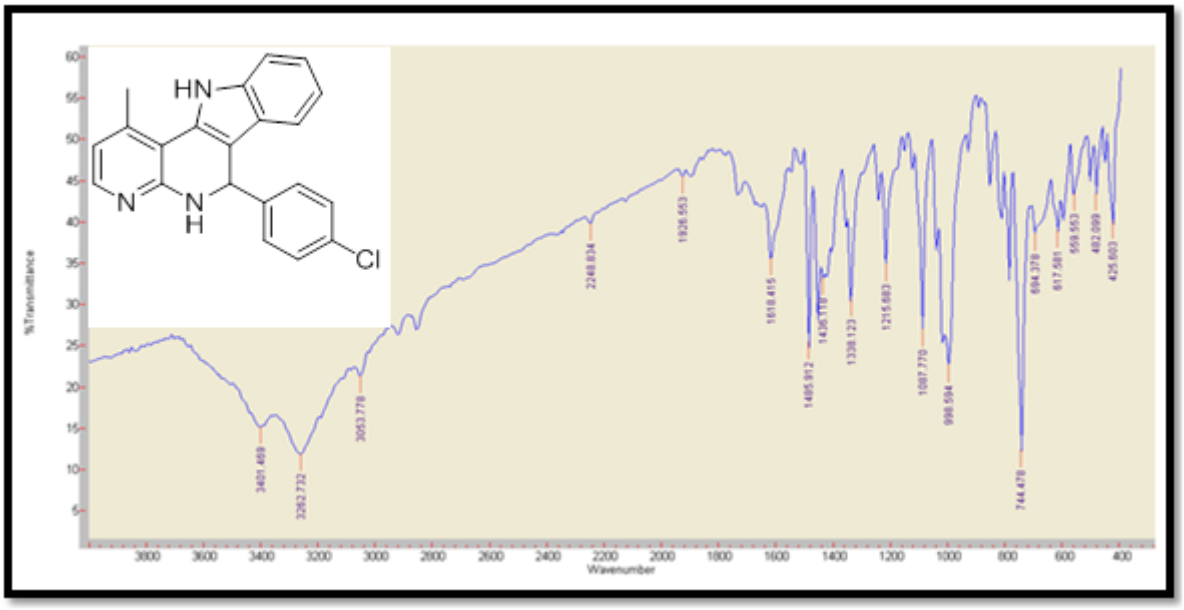

Appendix 4.16: IR spectrum for compound **36c**

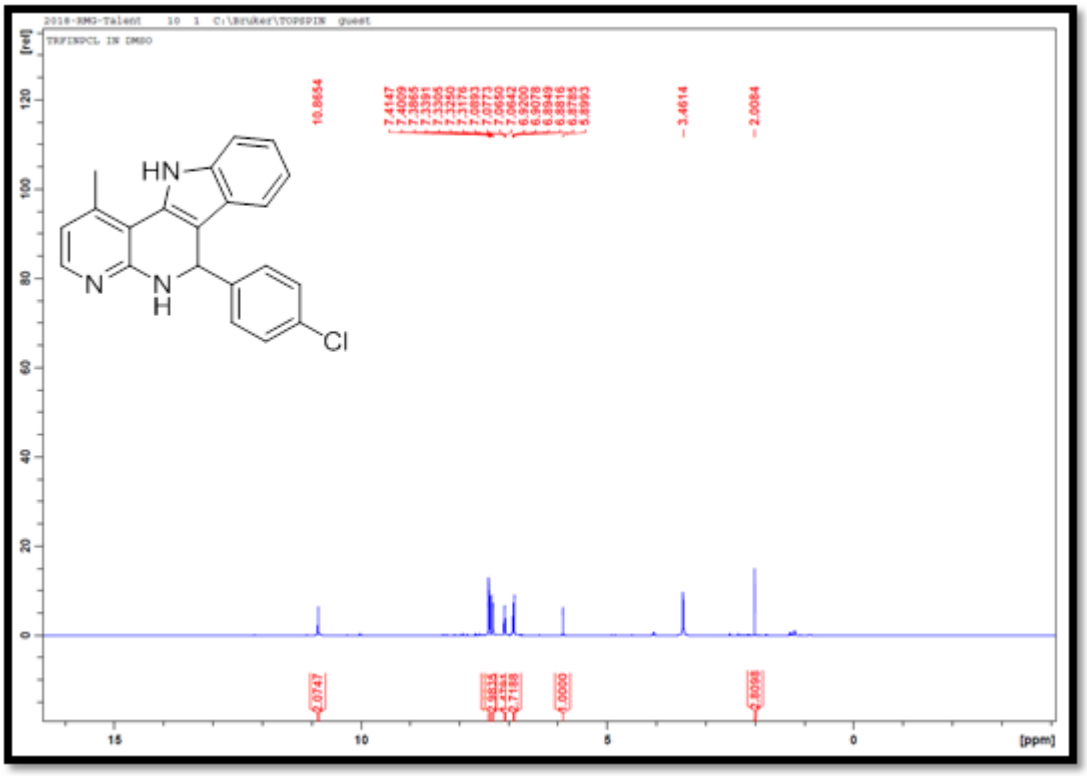

Appendix 4.17: ^{1}H NMR spectrum for compound **36c**

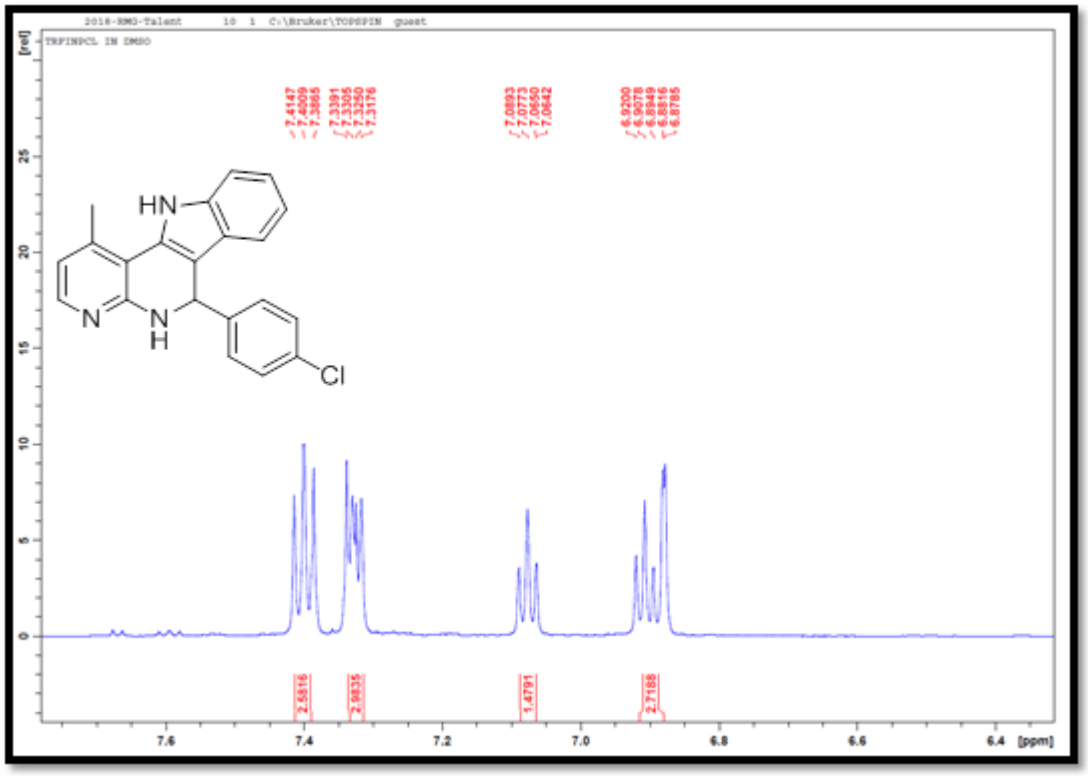

Appendix 4.18: ^{1}H NMR expanded spectrum for compound **36c**

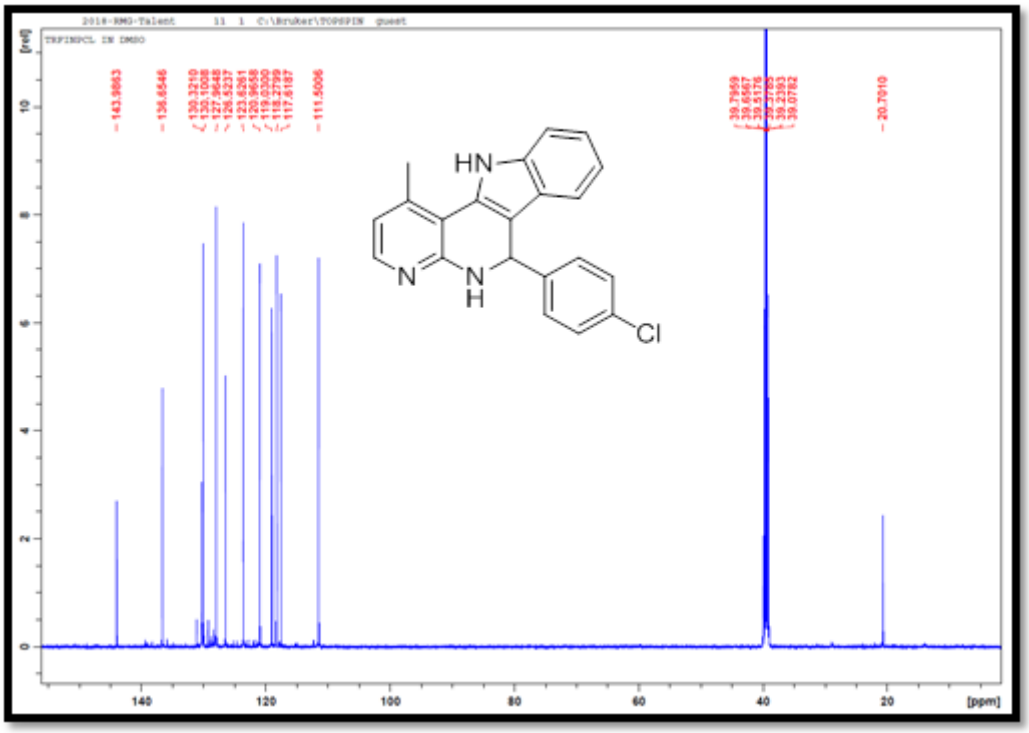

Appendix 4.19: ^{13}C NMR spectrum for compound **36c**

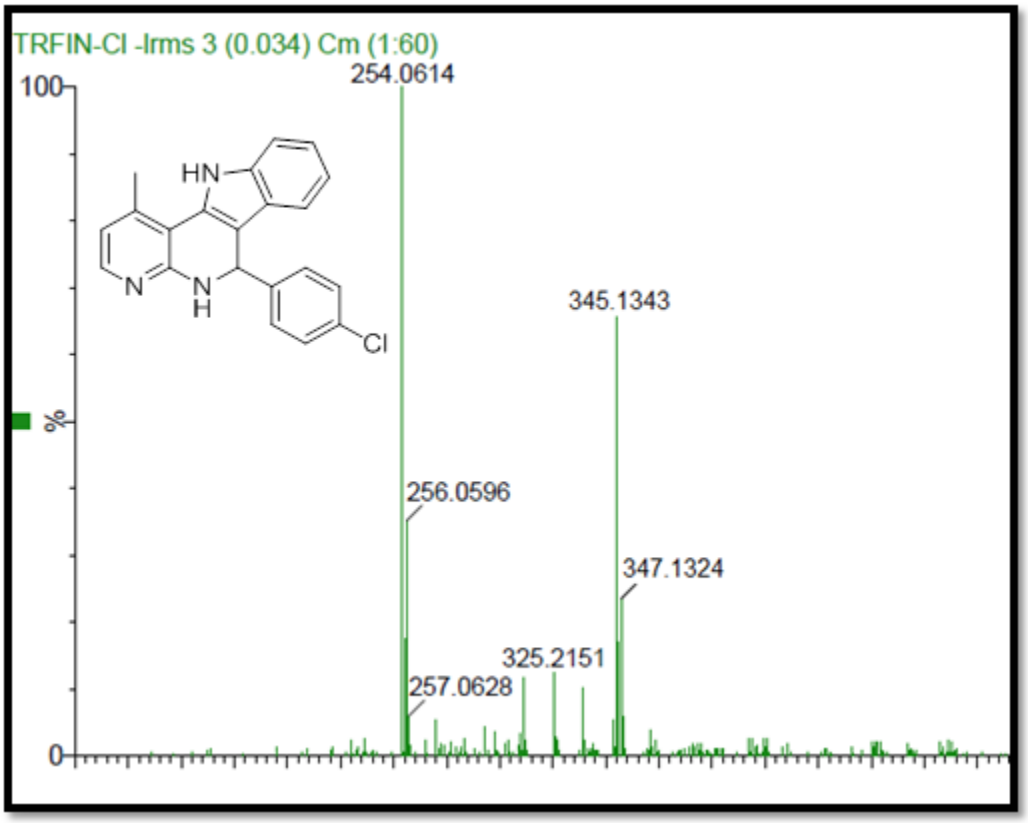

Appendix 4.20: TOF-MS spectrum for compound **36c**

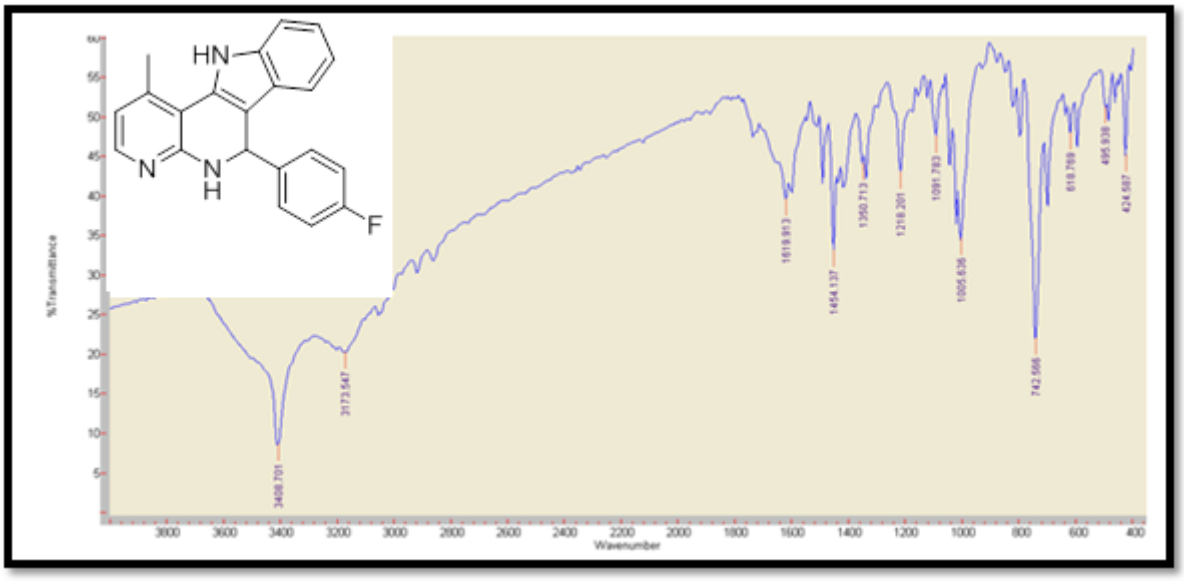

Appendix 4.21: IR spectrum for compound **36d**

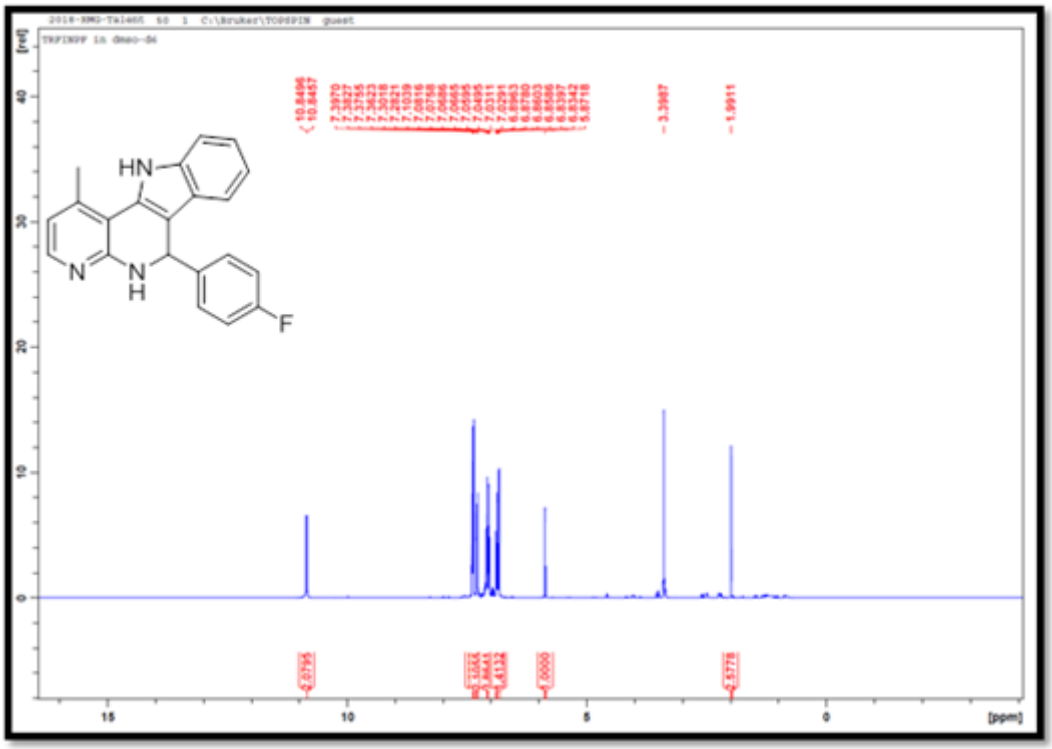

Appendix 4.22: ^{1}H NMR spectrum for compound **36d**

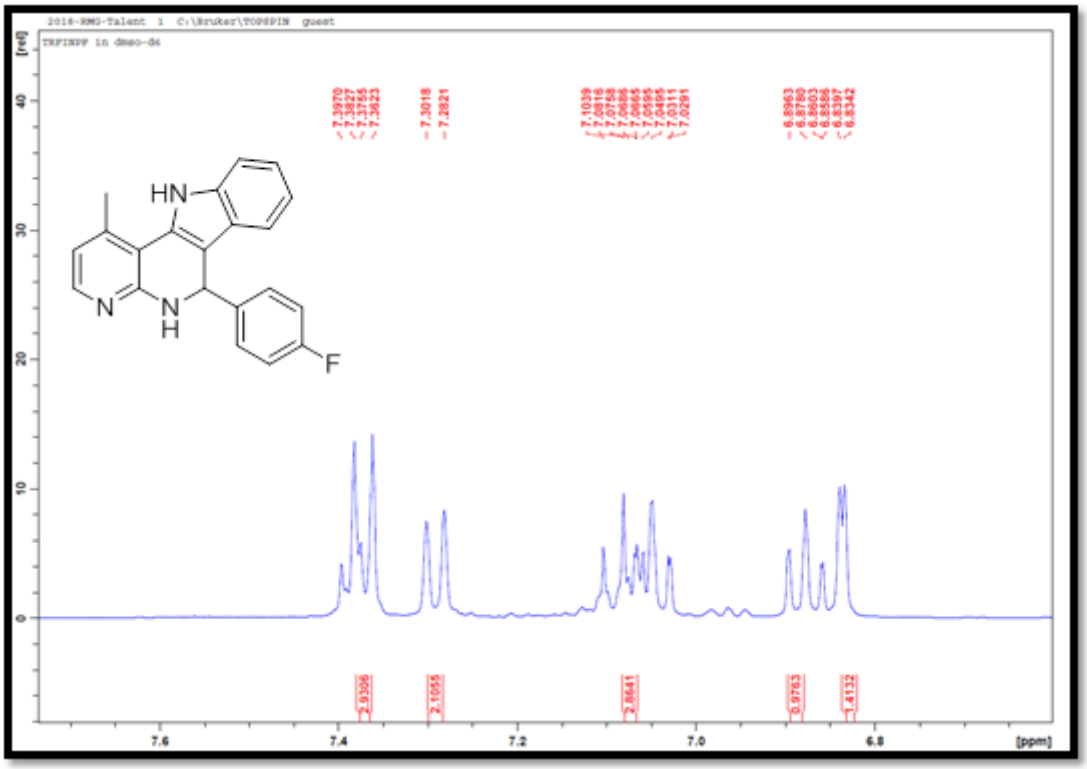

Appendix 4.23: ^{1}H NMR expanded spectrum for compound **36d**

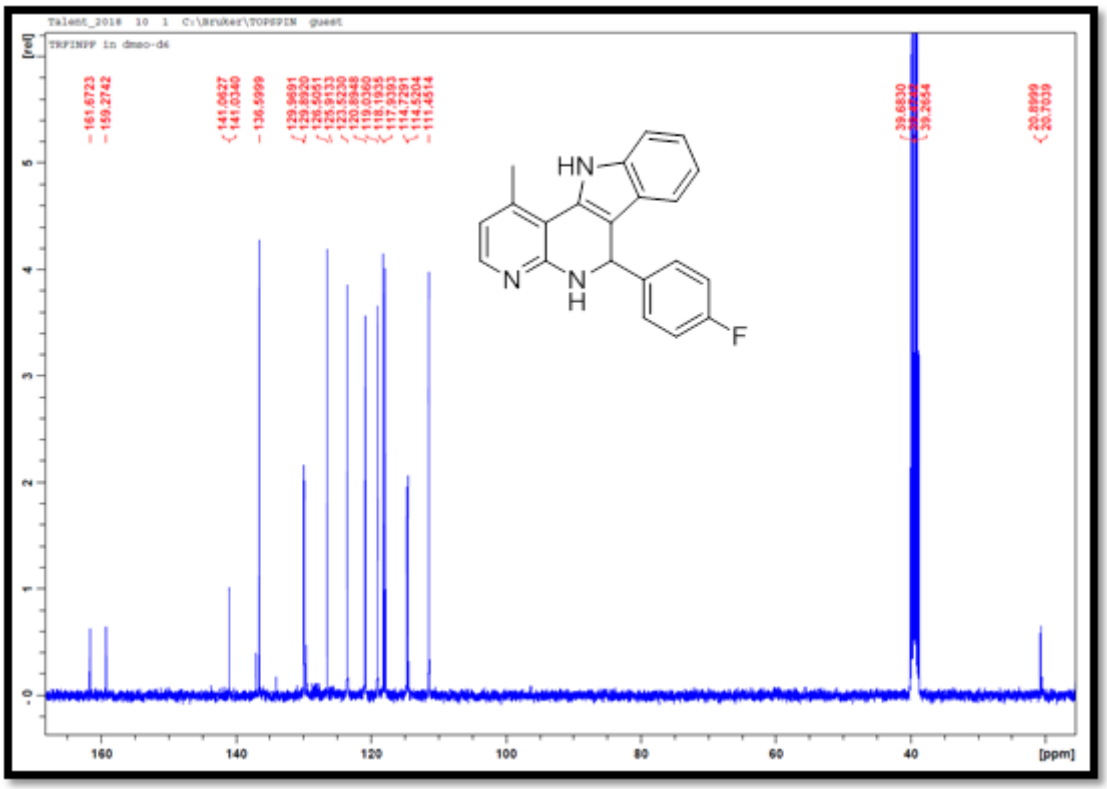

Appendix 4.24: ^{13}C NMR spectrum for compound **36d**

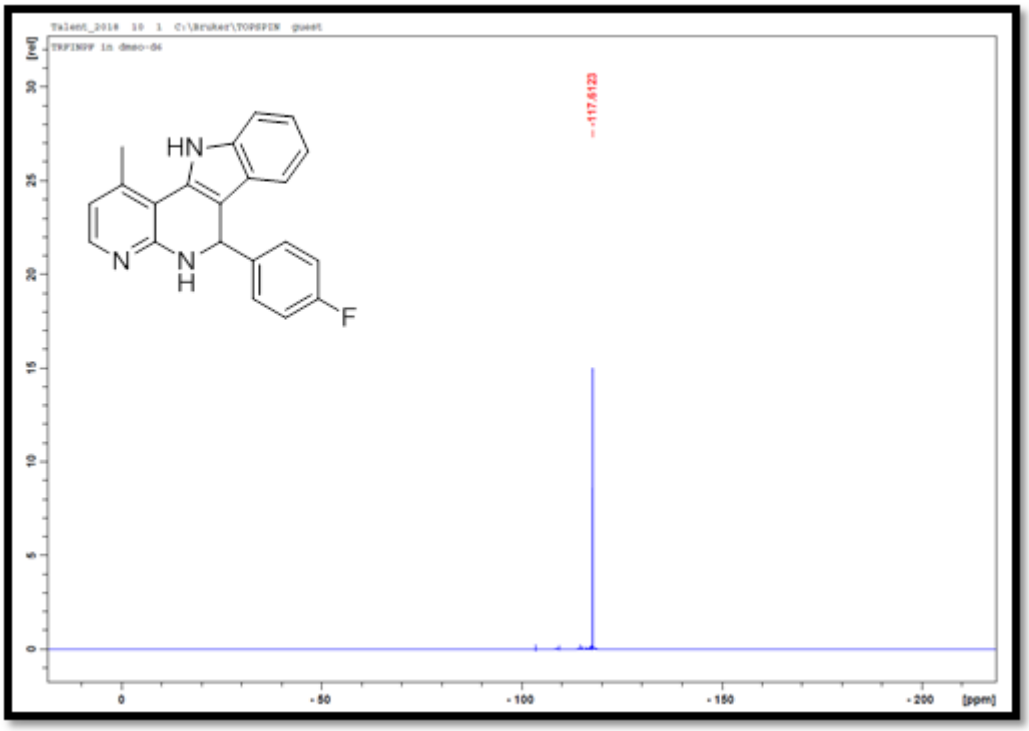

Appendix 4.25: ^{19}F NMR spectrum for compound **36d**

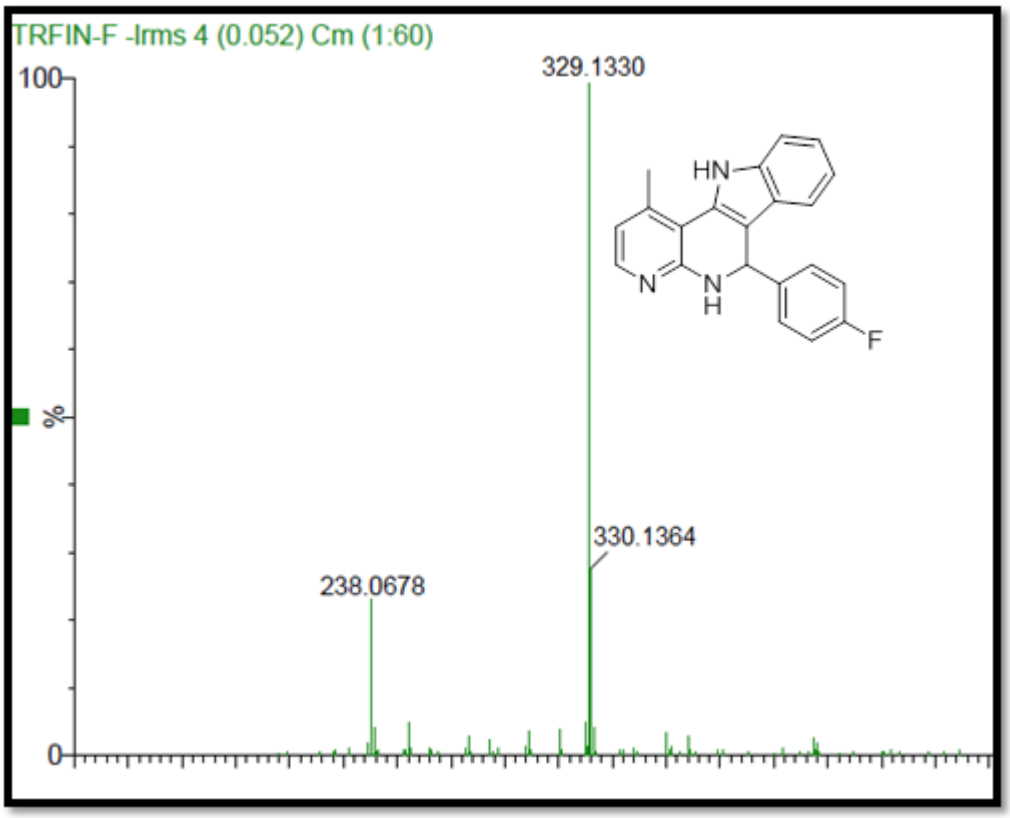

Appendix 4.26: TOF-MS spectrum for compound **36d**

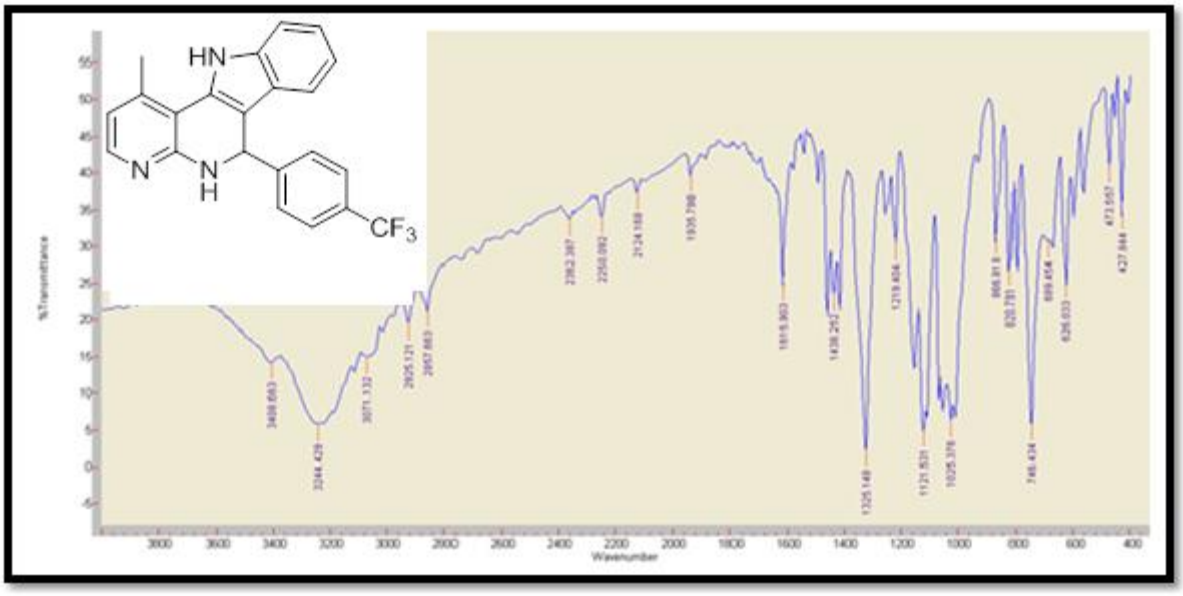

Appendix 4.27: IR spectrum for compound **36e**

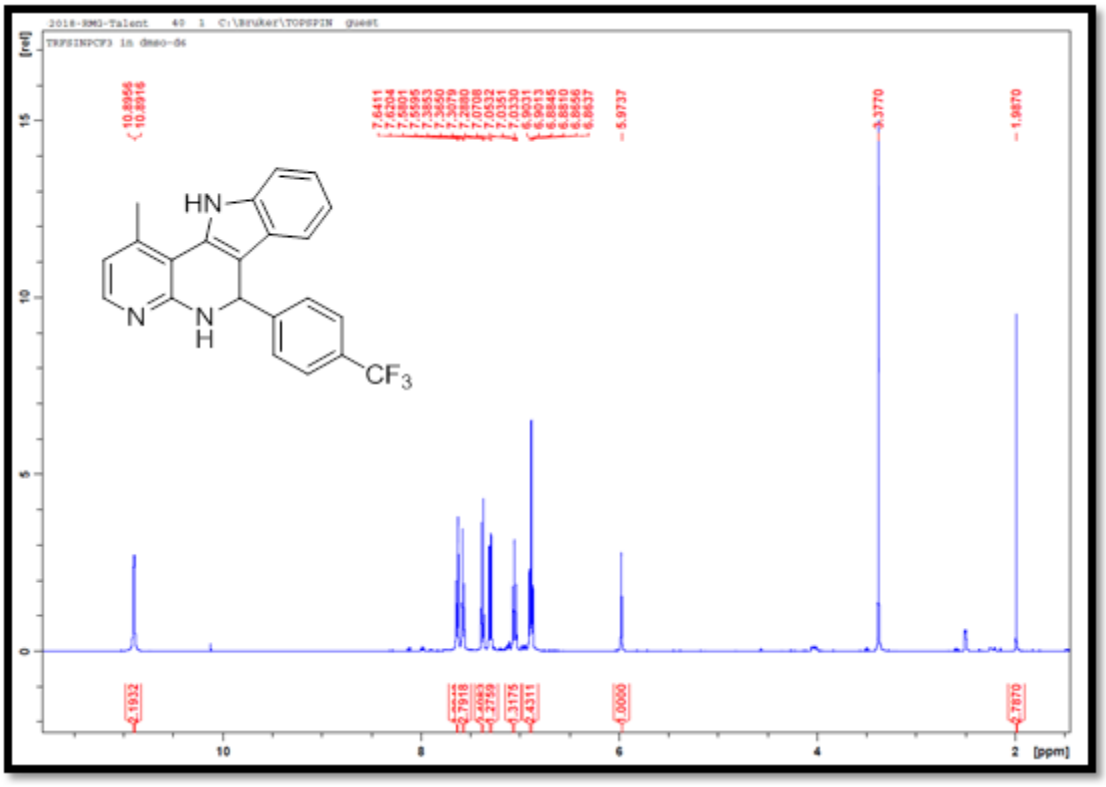

Appendix 4.28: ^{1}H NMR spectrum for compound **36e**

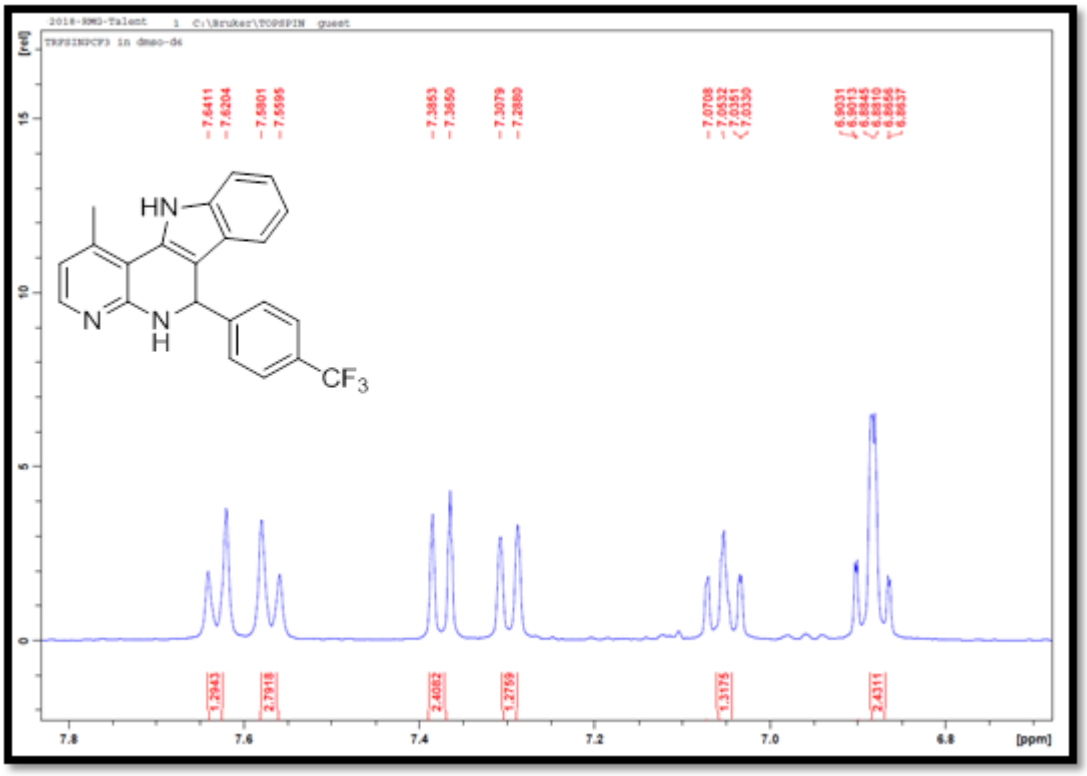

Appendix 4.29: ^{1}H NMR expanded spectrum for compound **36e**

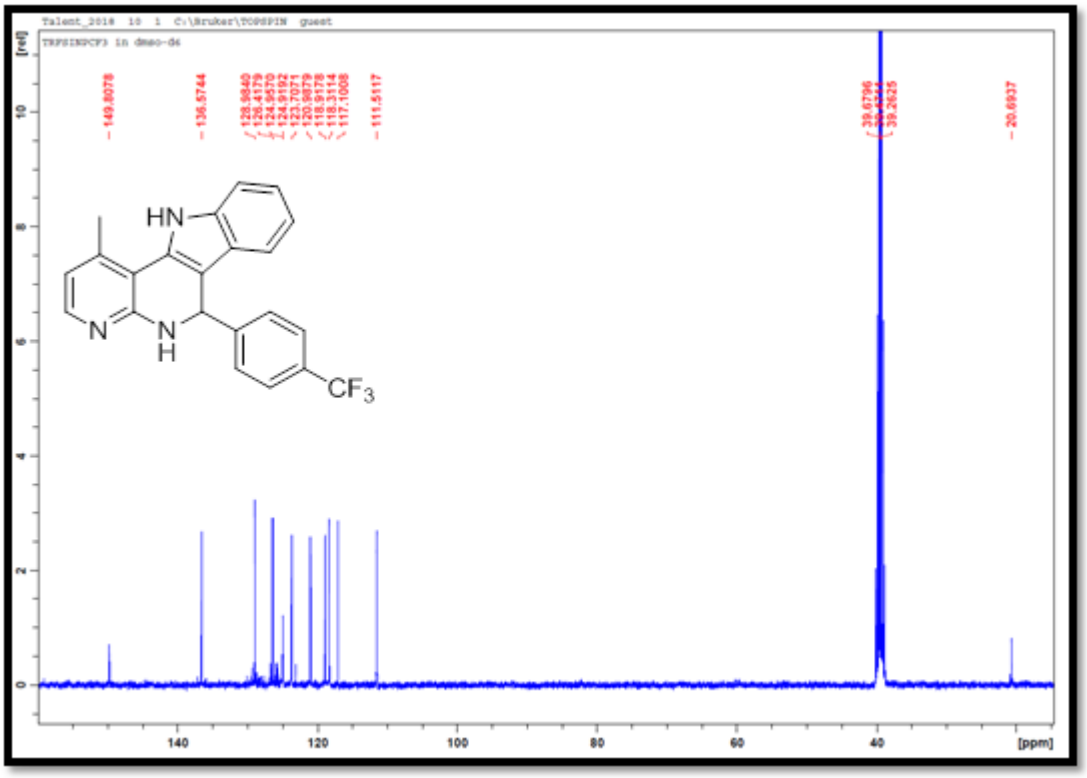

Appendix 4.30: ^{13}C NMR spectrum for compound **36e**

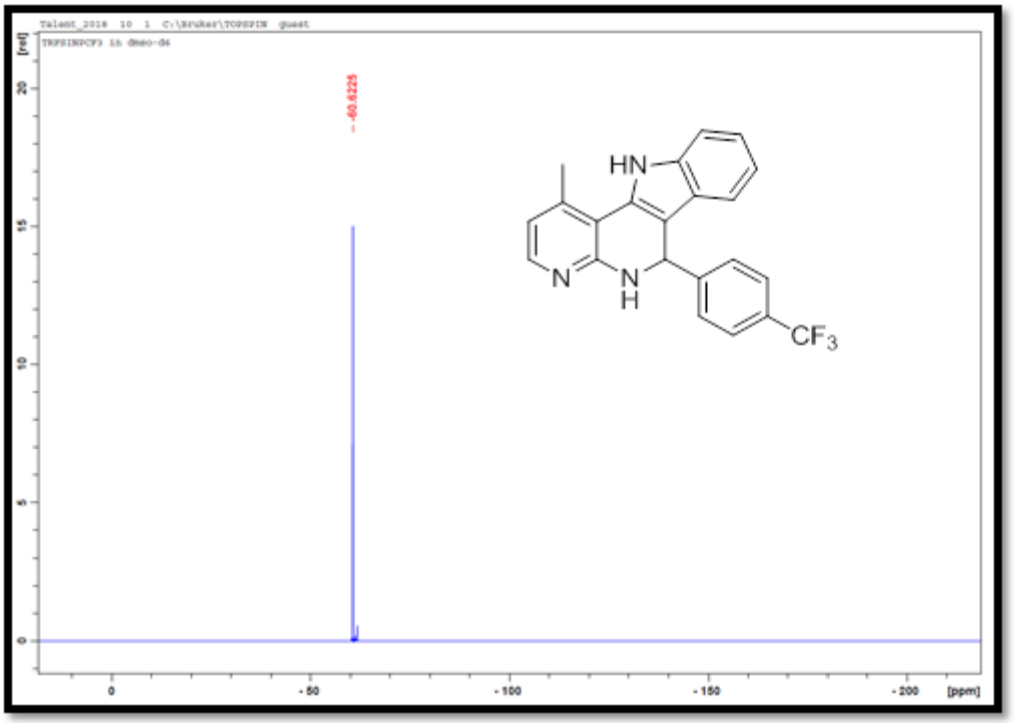

Appendix 4.31: ^{19}F NMR spectrum for compound **36e**

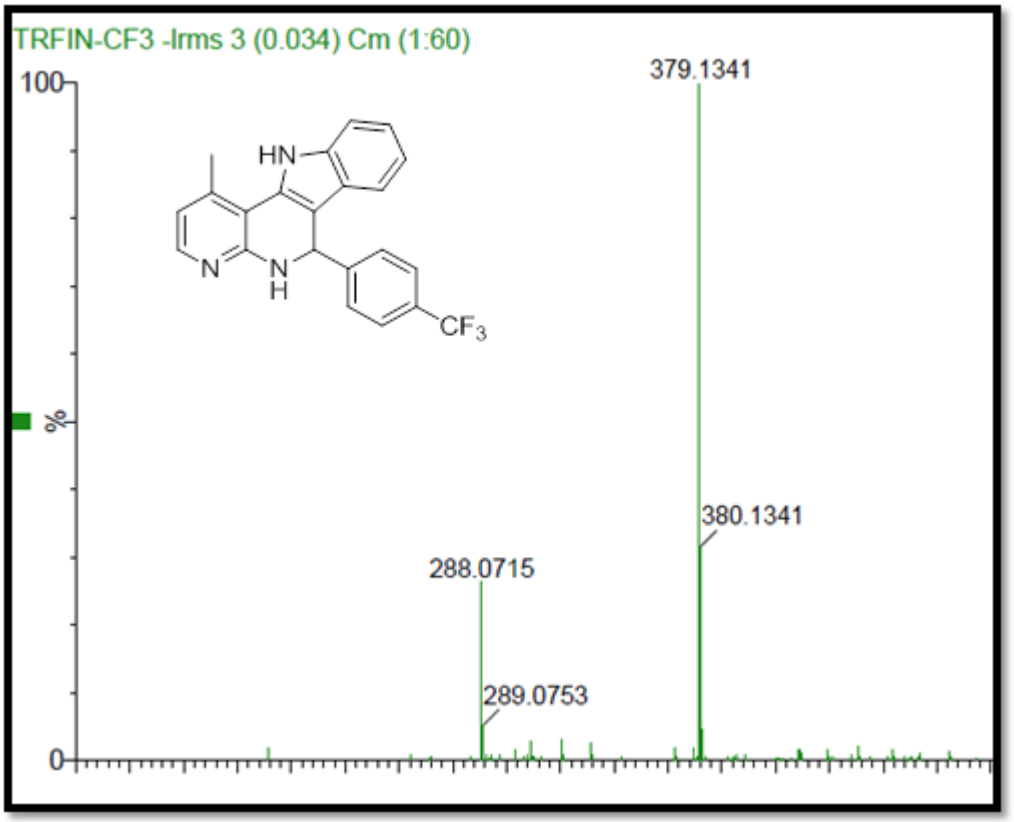

Appendix 4.32: TOF-MS spectrum for compound **36e**

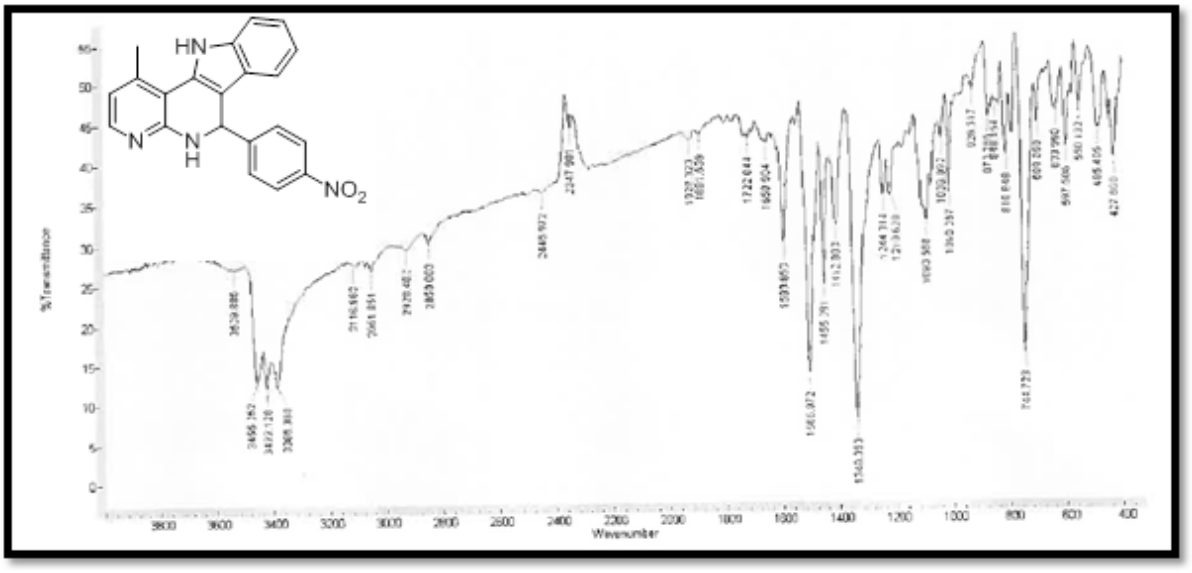

Appendix 4.33: IR spectrum for compound **36f**

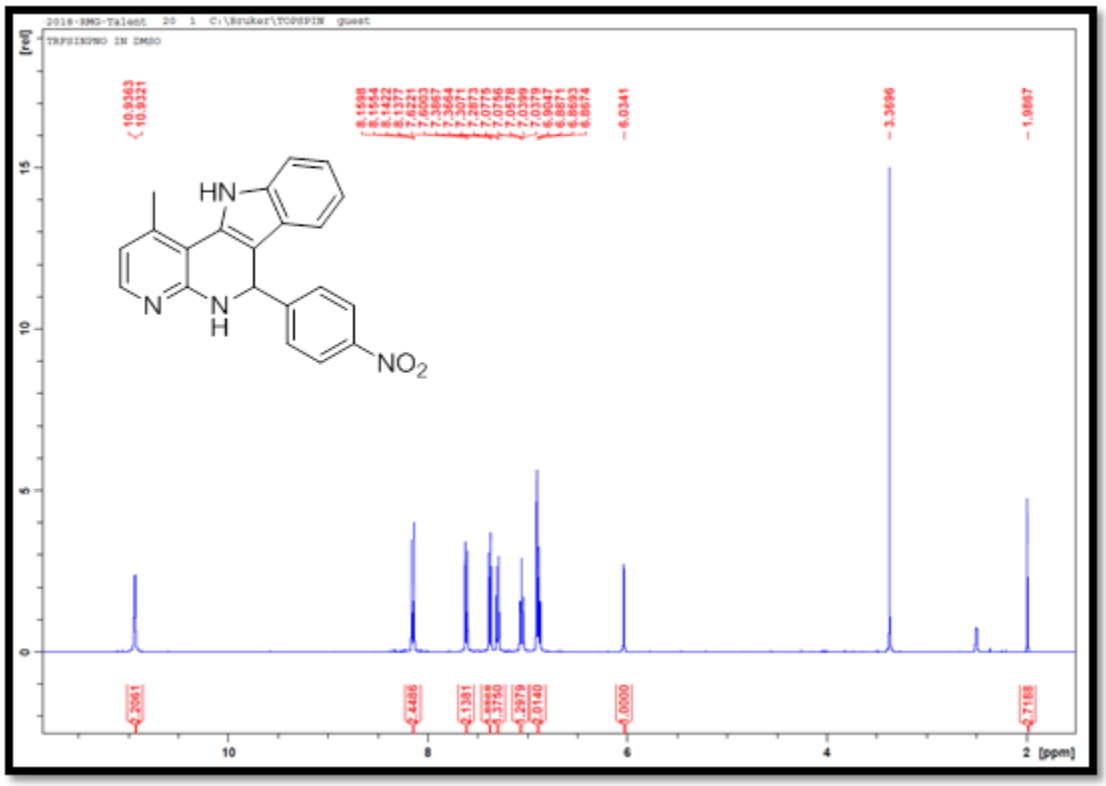

Appendix 4.34: ^{1}H NMR spectrum for compound **36f**

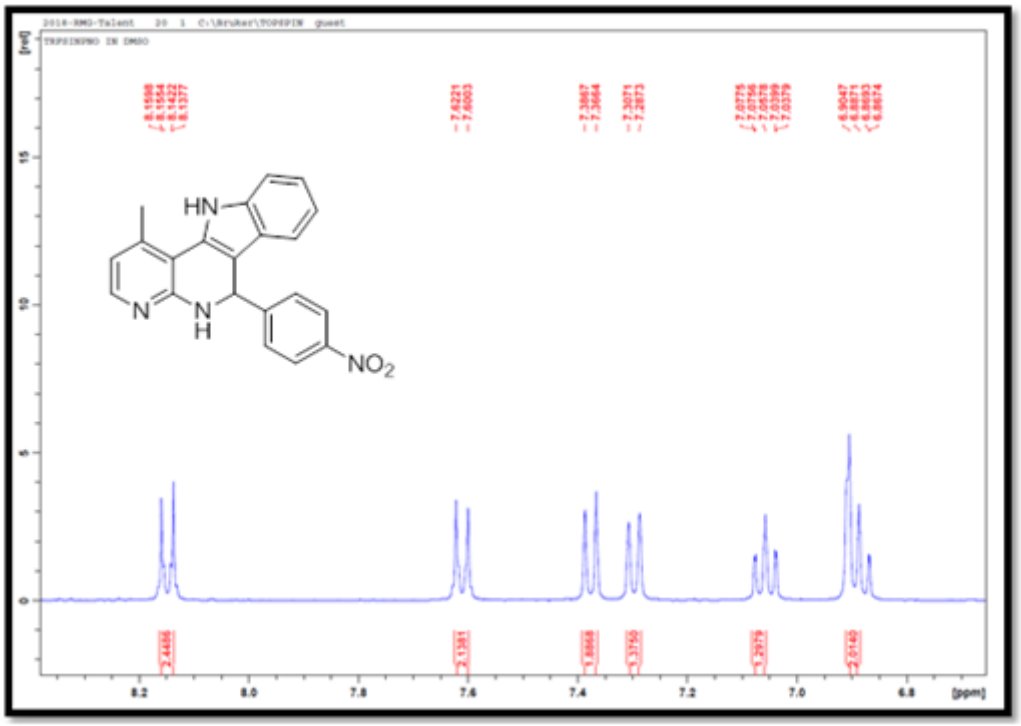

Appendix 4.35: ^{1}H NMR expanded spectrum for compound **36f**

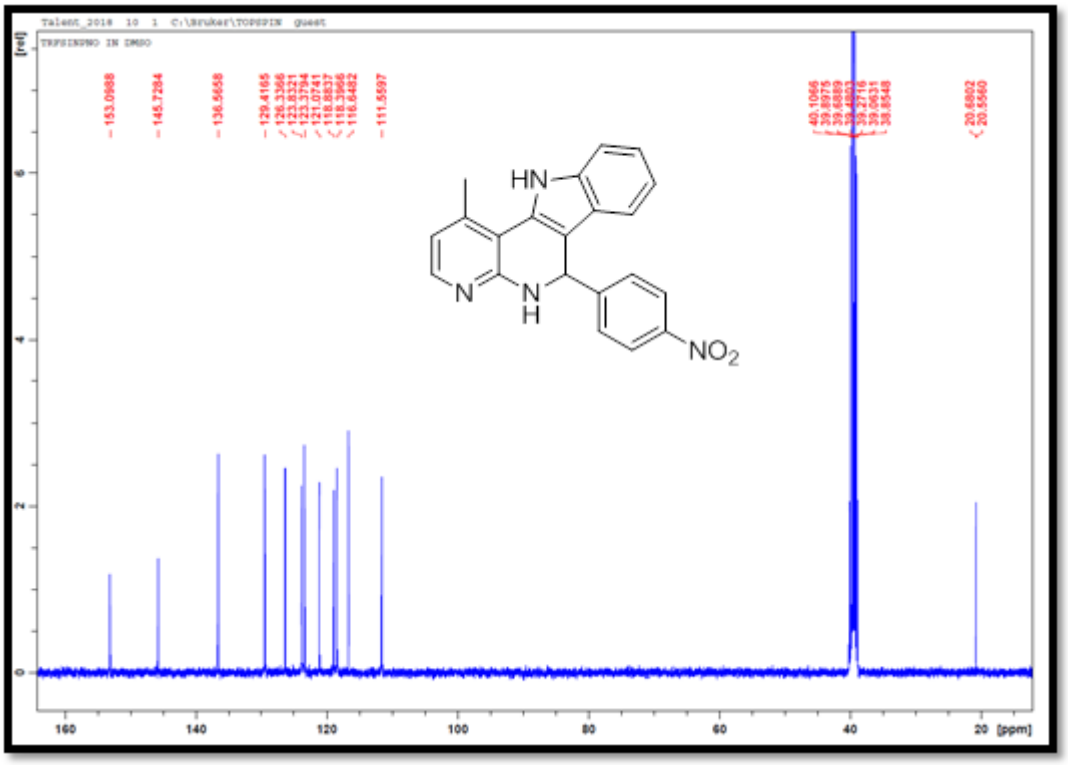

Appendix 4.36: ^{13}C NMR spectrum for compound **36f**

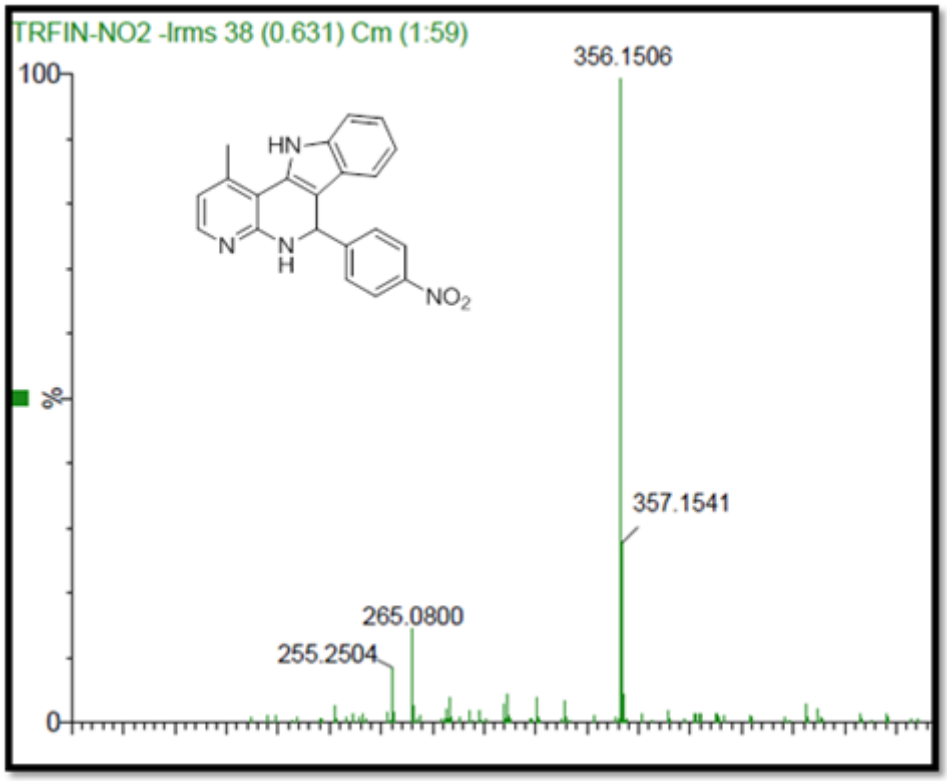

Appendix 4.37: TOF-MS spectrum for compound **36f**

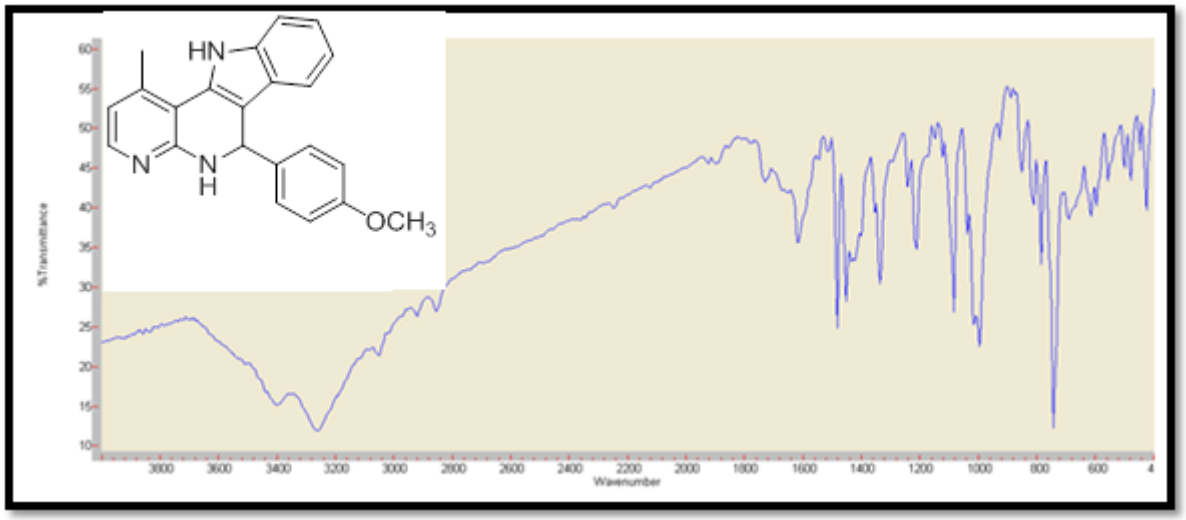

Appendix 4.38: IR spectrum for compound **36g**

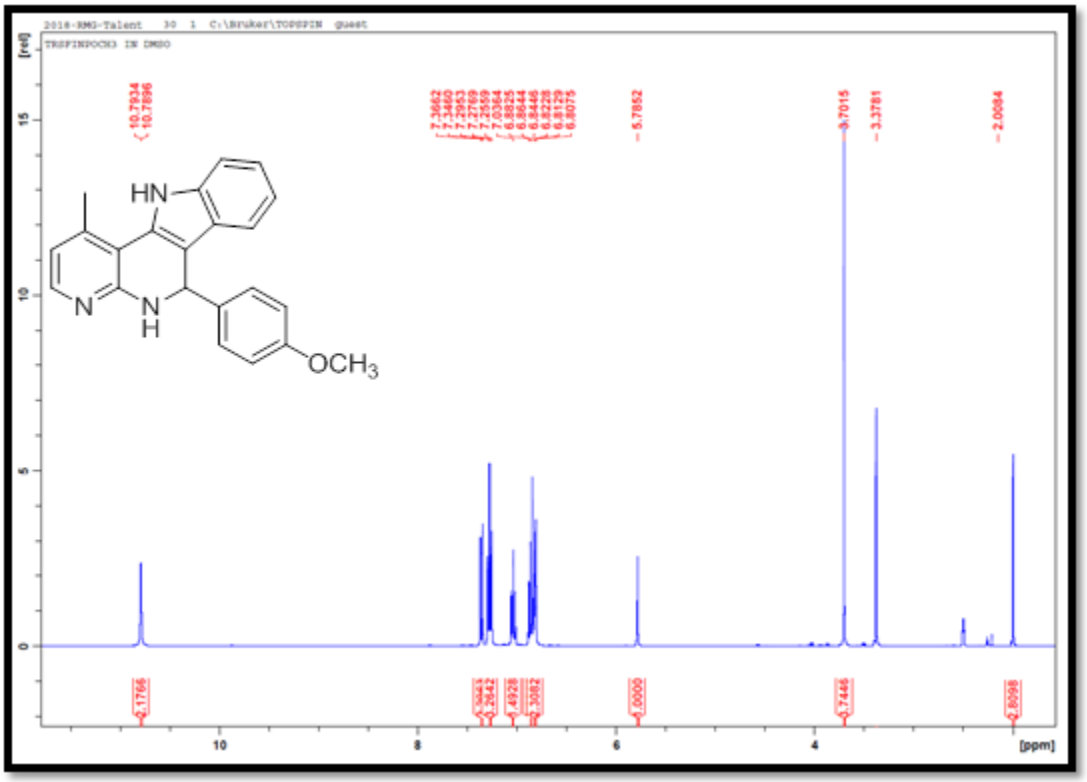

Appendix 4.39: ^{1}H NMR spectrum for compound **36g**

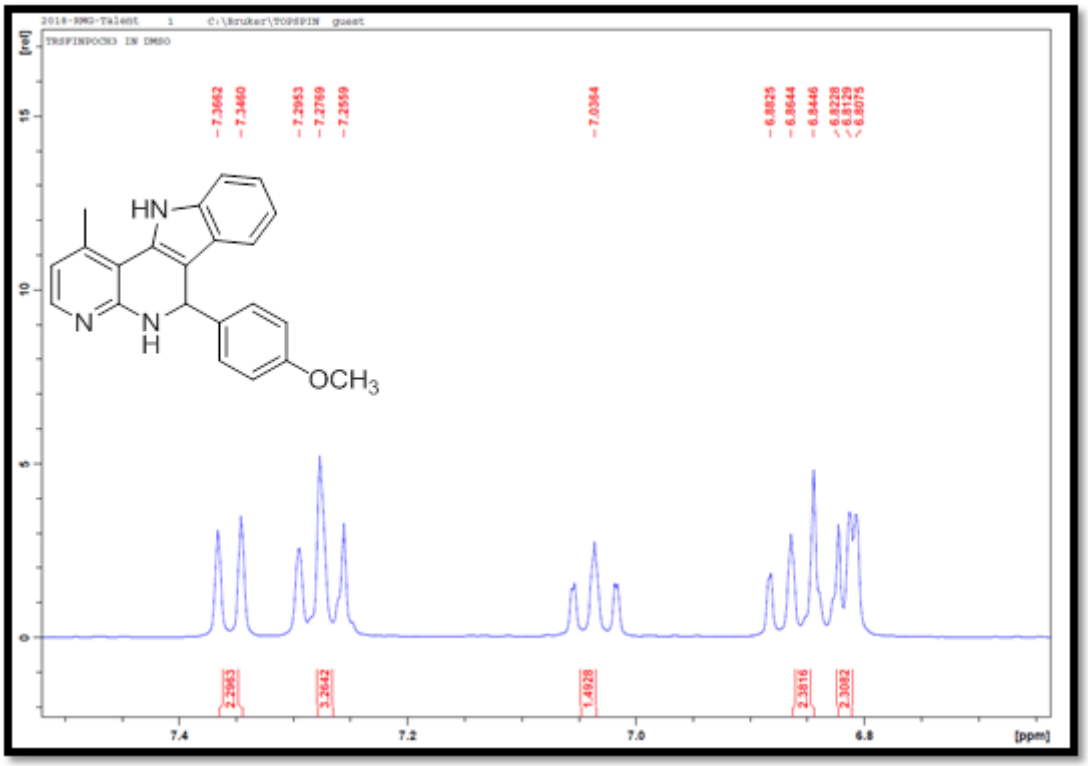

Appendix 4.40: ^{1}H NMR expanded spectrum for compound **36g**

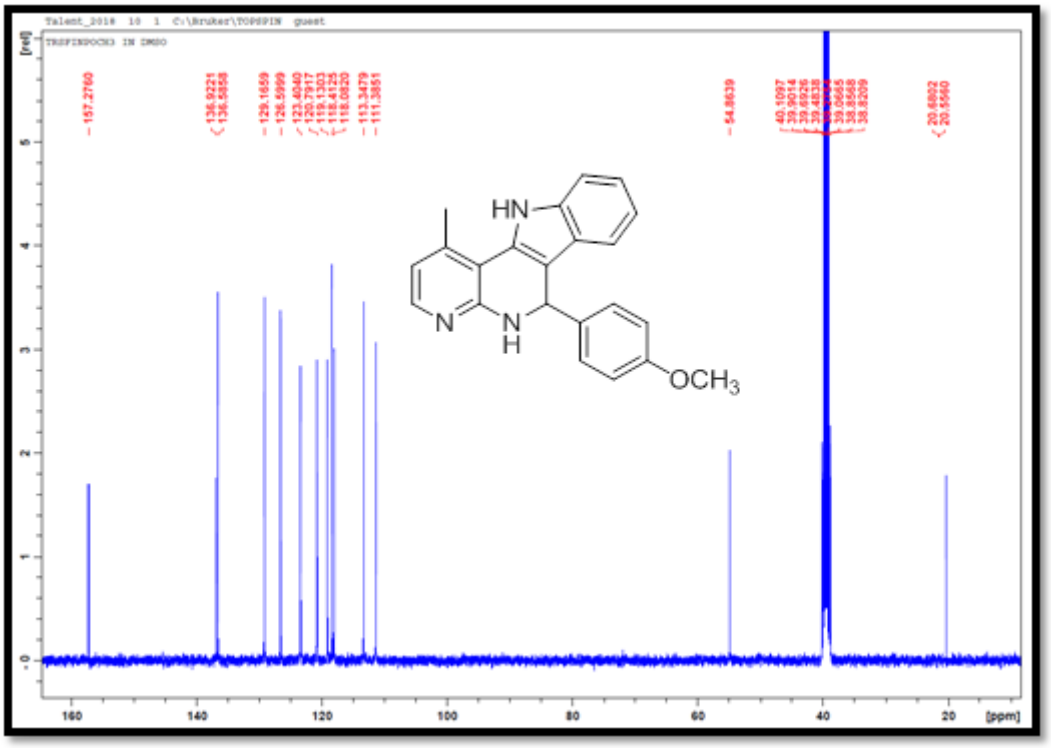

Appendix 4.41: ^{13}C NMR spectrum for compound **36g**

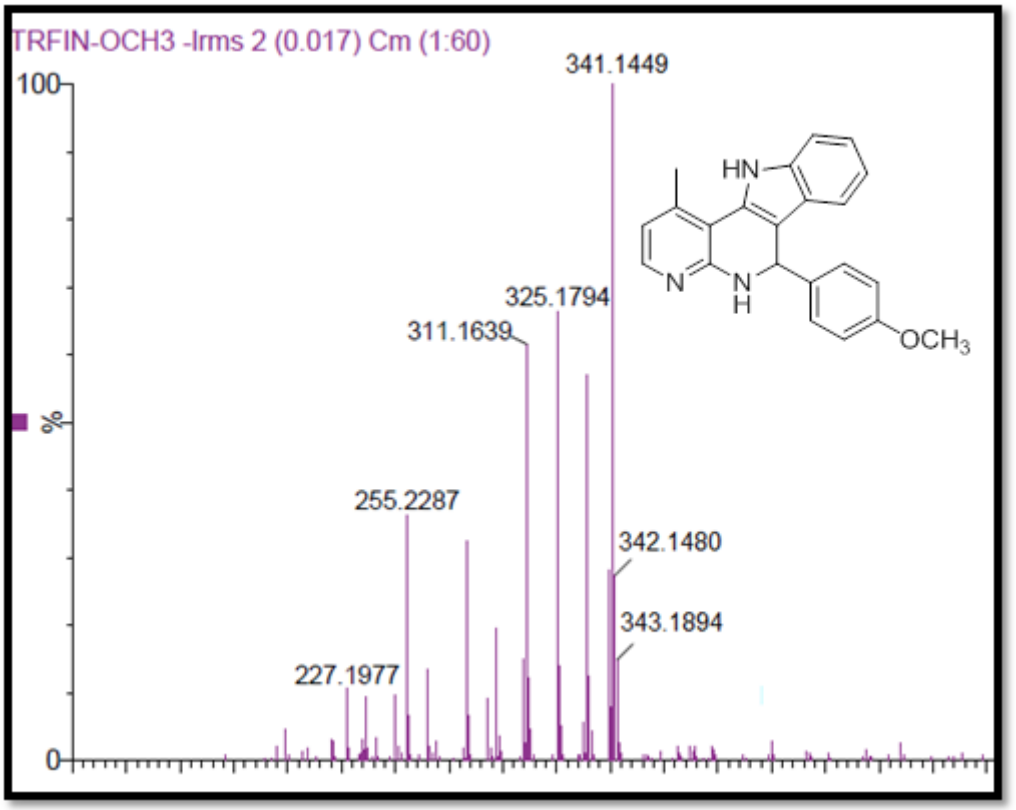

Appendix 4.42: TOF-MS spectrum for compound **36g**

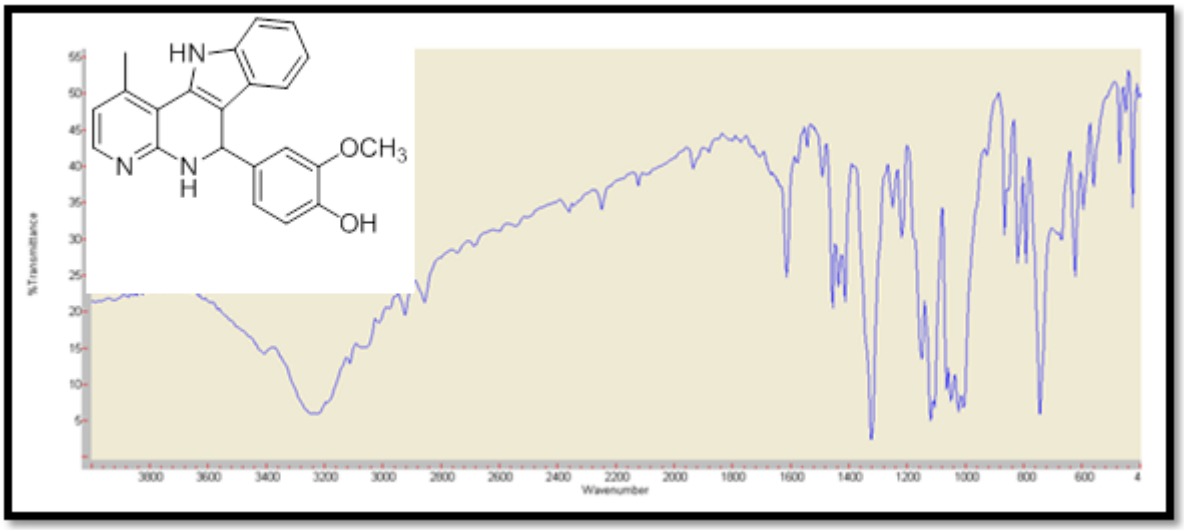

Appendix 4.43: IR spectrum for compound **36h**

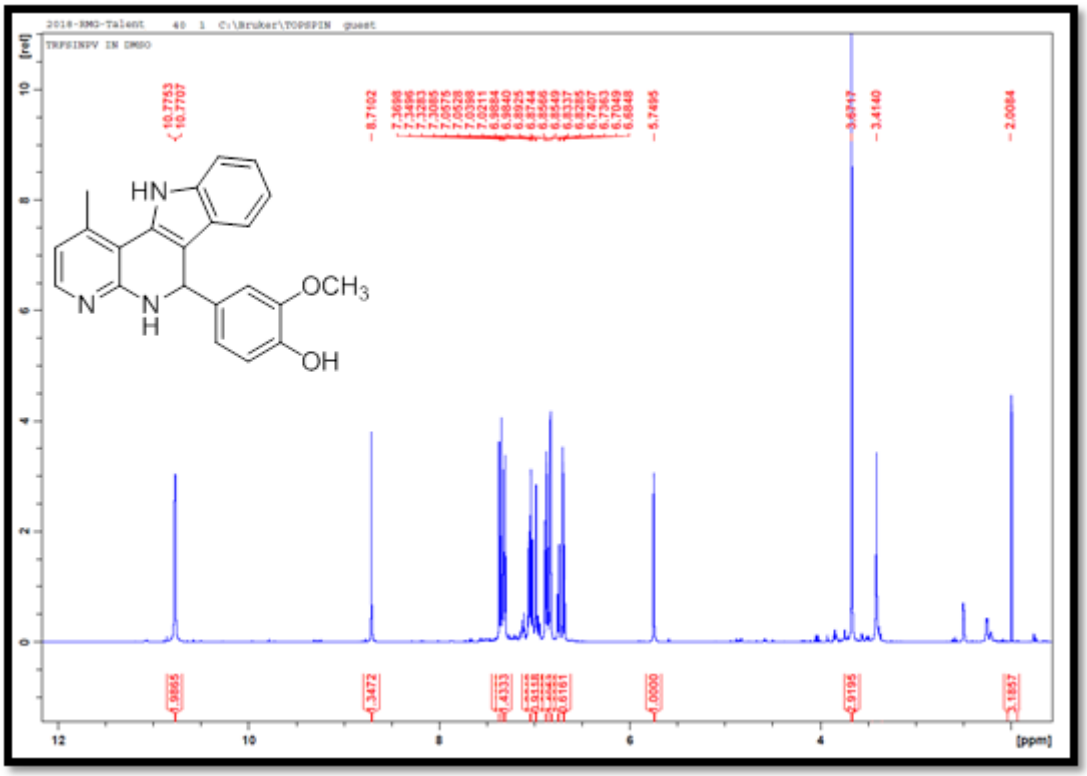

Appendix 4.44: ^{1}H NMR spectrum for compound **36h**

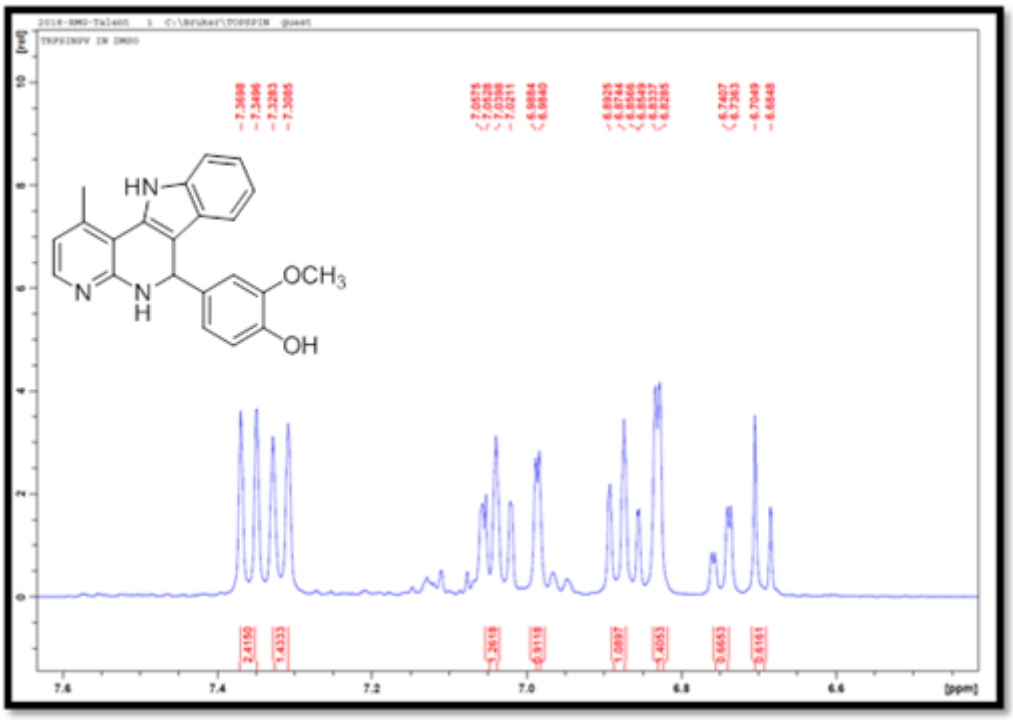

Appendix 4.45: ^{1}H NMR spectrum for compound **36h**

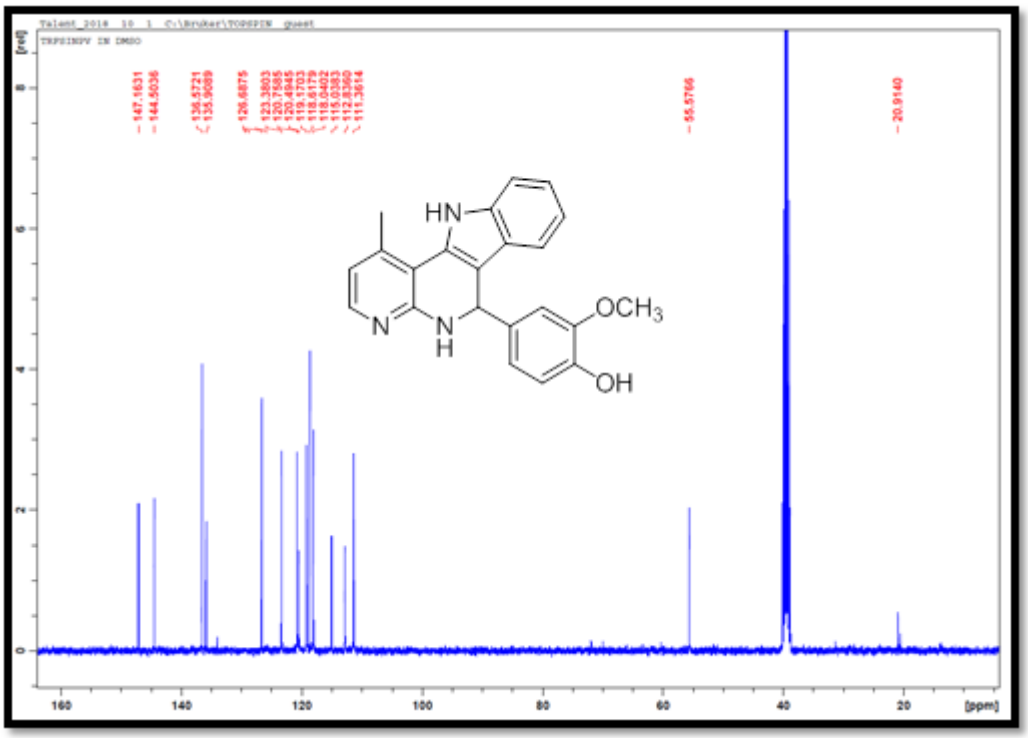

Appendix 4.46: ^{13}C NMR spectrum for compound **36h**

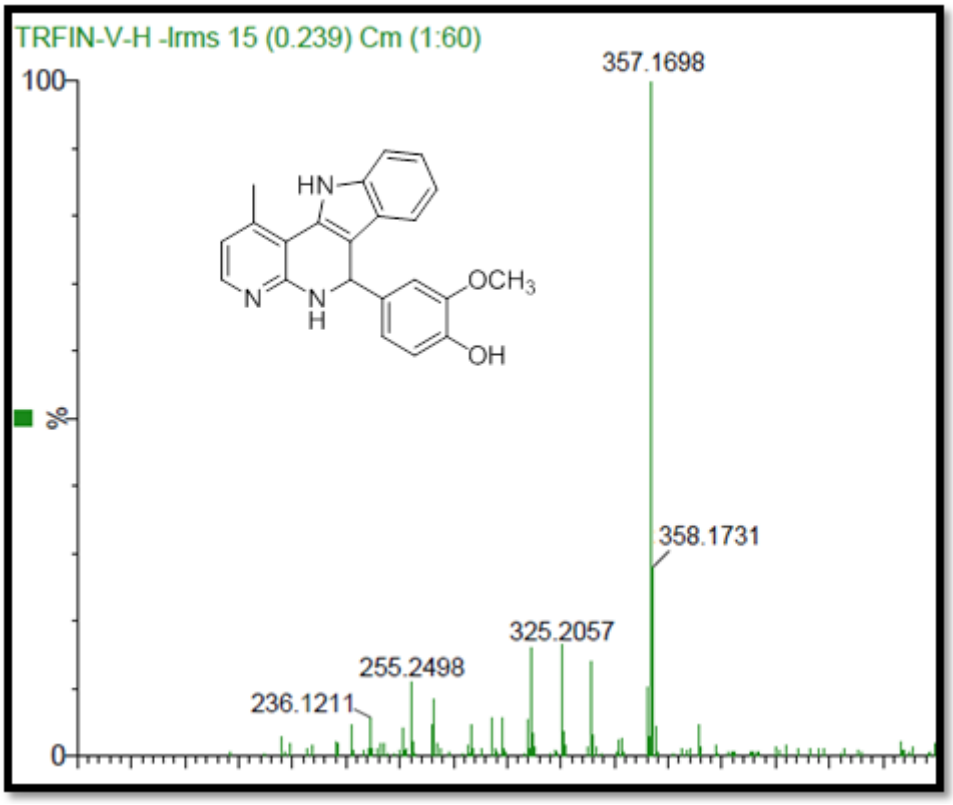

Appendix 4.47: TOF-MS spectrum for compound **36h**

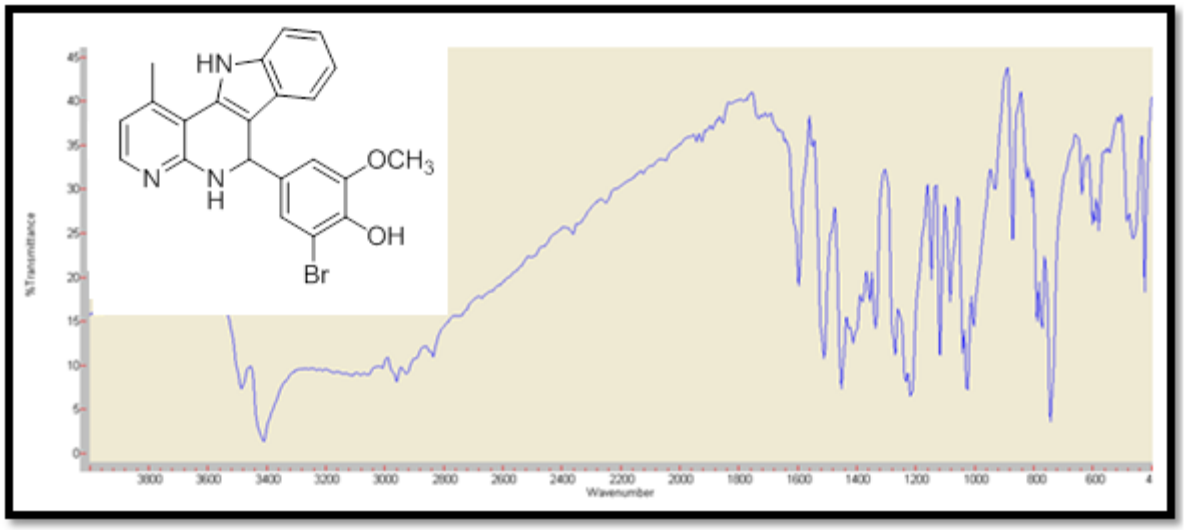

Appendix 4.48: IR spectrum for compound **36i**

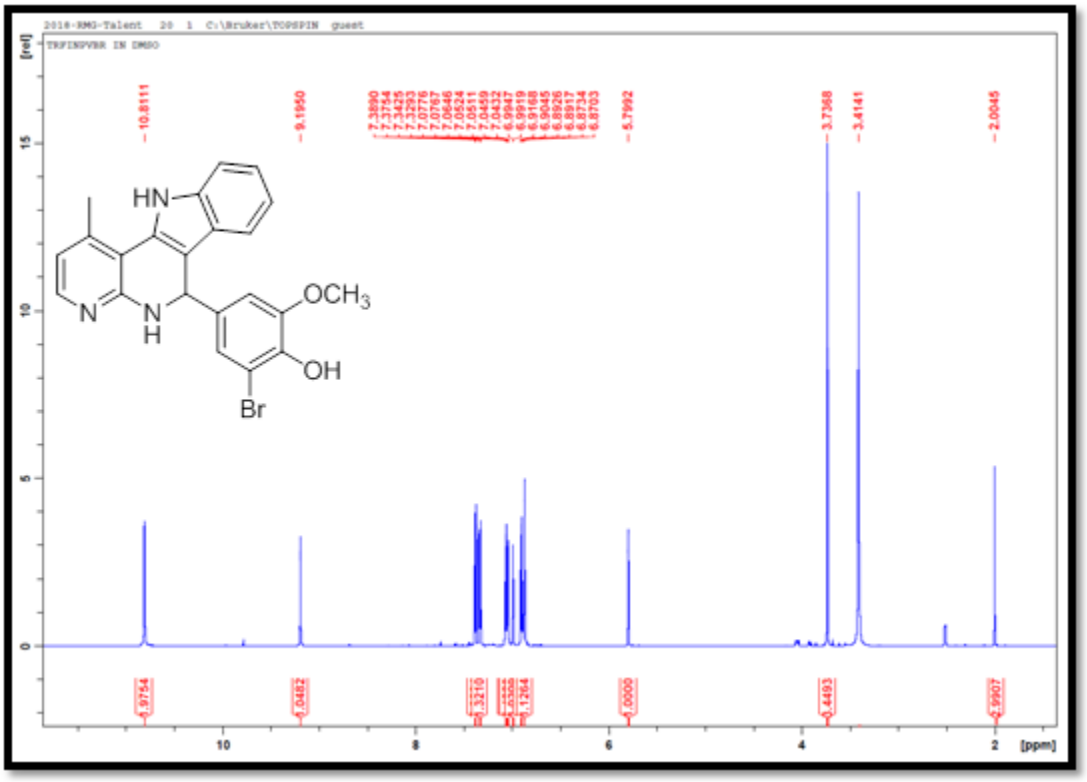

Appendix 4.49: ^{1}H NMR spectrum for compound **36i**

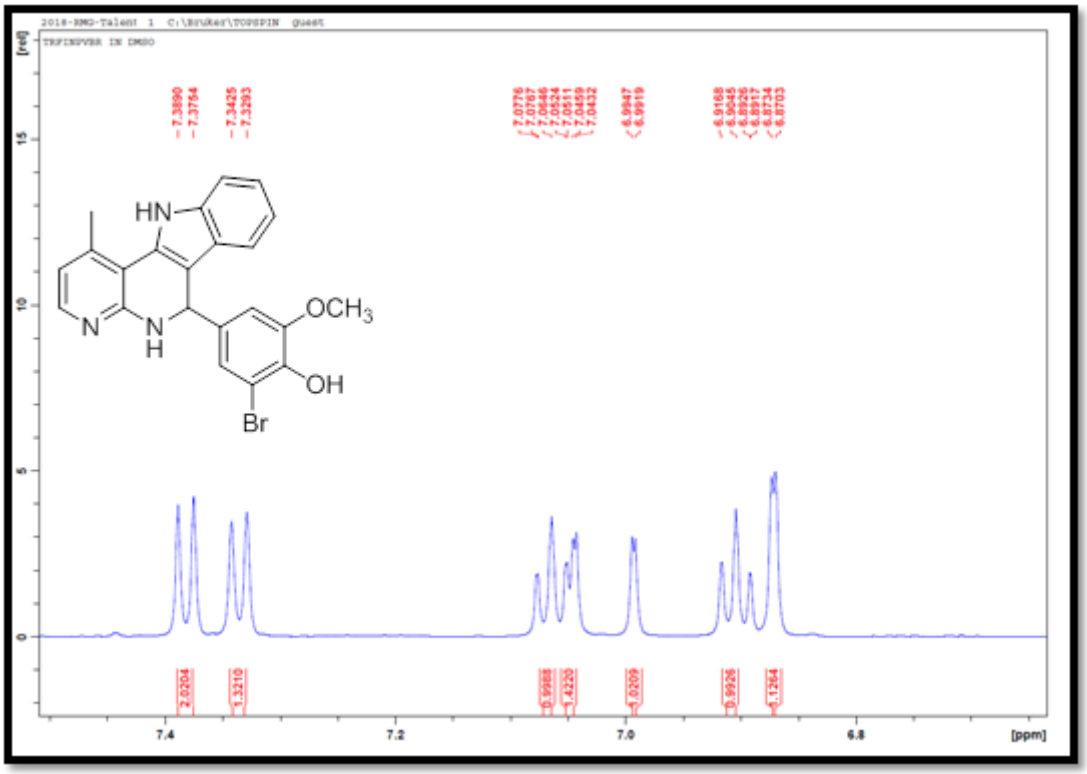

Appendix 4.50: ^{1}H NMR expanded spectrum for compound **36i**

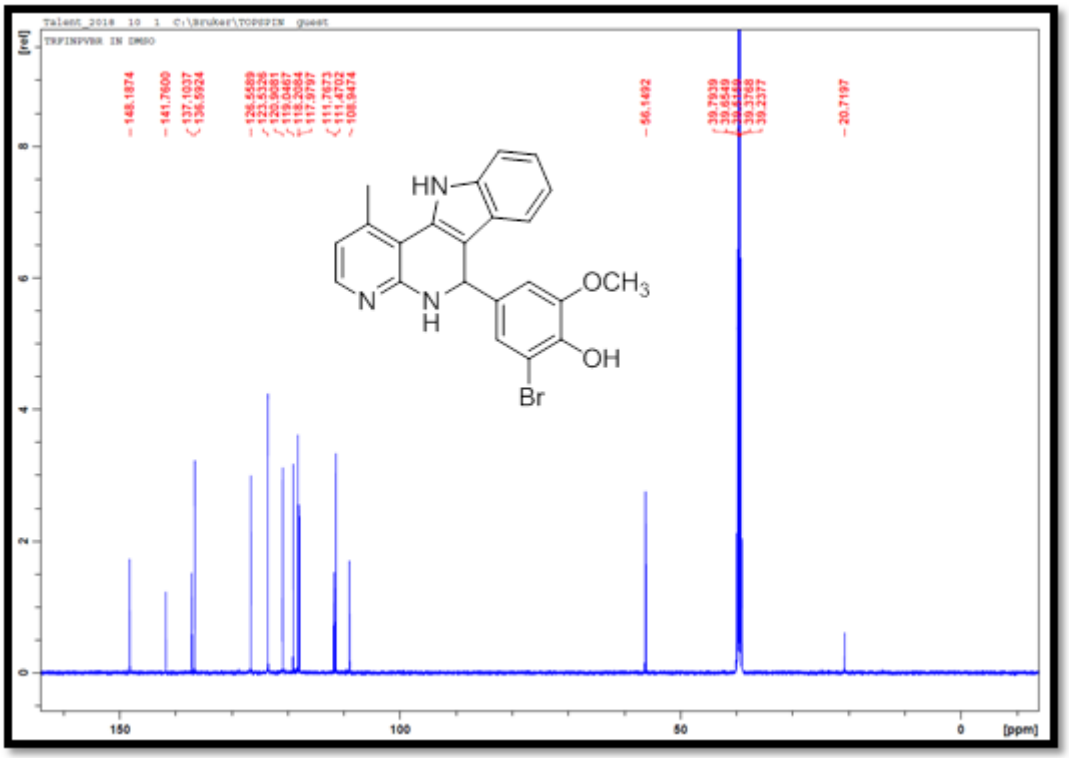

Appendix 4.51: ^{13}C NMR spectrum for compound **36i**

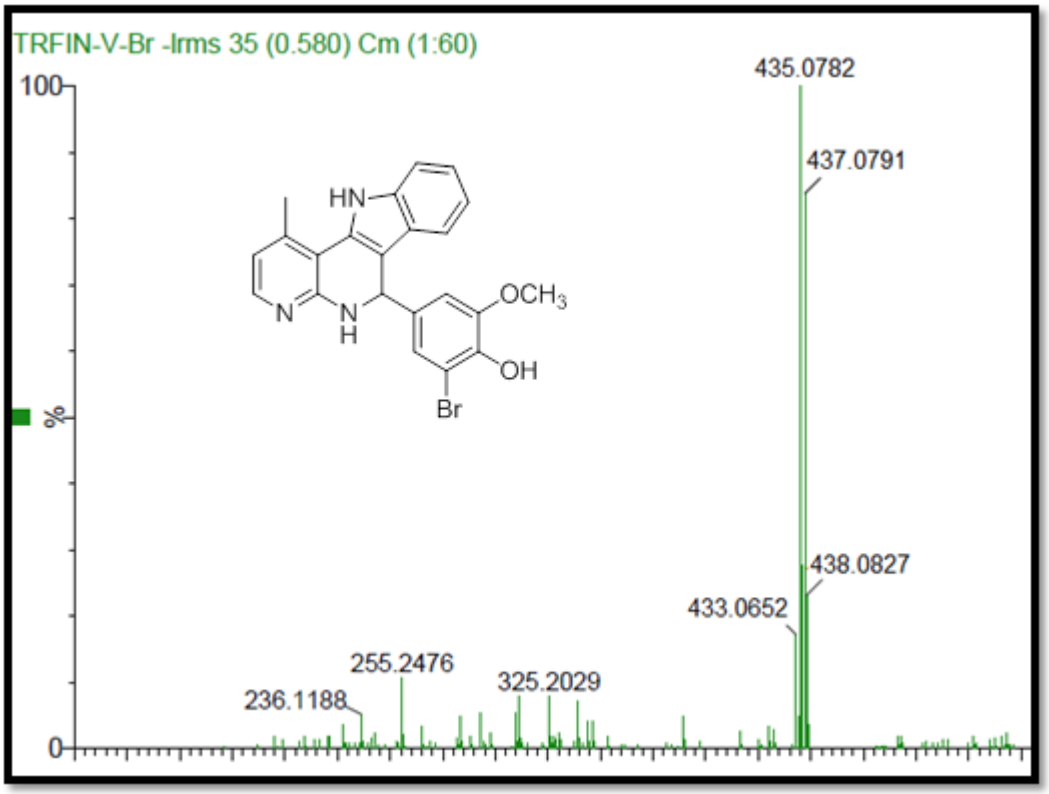

Appendix 4.52: TOF-MS spectrum for compound **36i**

Chapter Five

Multi-Component Synthesis of Novel Fused Indolo Pyrazoles via Povarov's Reaction and Study their Antimicrobial Activity

5.1 Abstract

A series of 36 novel fused indolo pyrazole derivatives were synthesized via a [3+2] Povarov's cycloaddition reaction using affordable starting material such as benzaldehyde, hydrazines (thiosemicarbazides, isoniazid) and indole in the presence of a catalytic amount of indium chloride. All synthesized compounds were characterized by FTIR, NMR and TOF-MS. These compounds were screened for antibacterial and antifungal activities against various strains of pathogenic bacteria and fungi. Compound **88t** showed good inhibitory effect against *Candida albicans* and *Candida utilis* with an inhibition diameter of 15 and 14 mm, respectively. The other compounds tested showed moderate to good antifungal activity against *Candida albicans, Candida utilis* and *Saccharomyces cerevisiae* whilst compounds **88r** and **88x** showed a significant antifungal activity against *Saccharomyces cerevisiae* with zone of inhibition diameter of 23 and 20 mm, respectively. Compounds **88o** and **88x** showed substantial potency against *Saccharomyces cerevisiae* with the MIC of 0.18 µM whereas compounds **88l** and **88u** displayed good potency against *Candida albicans, Candida utilis* and *Saccharomyces cerevisiae* with MIC of 1.5; 1.1 and 0.375 µM, respectively. Furthermore, compounds **88s** and **88t** showed significant potency MIC of 0.18 and 1.5 µM against *Candida albicans* and *Candida utilis,* respectively. These results indicated that all the compounds displayed significant antifungal activity however no antibacterial activity were recorded against *Citrobacter freundii, Citrobacter diversus, Serratia marcescens, Klebsiella pneumonia, Micrococcus luteus* and *Staphylococcus aureus*. Furthermore, the scope of the Povarov's reaction was investigated using isoniazid as a substrate to synthesized ten novel nicotinyl fused indolo pyrazole derivatives. Compounds **94e** and **94f** showed weak activity against *Streptococcus faecalis, Micrococcus luteus and Bacillus coagullans* with a zone inhibition diameter of 9 mm whilst compound **94j** also showed weak activity against *Micrococcus luteus* with a zone inhibition diameter of 9 mm. The MIC of **94e**, **94f** and **94j** was 0.75 µM. No antifungal activity was recorded against *Candida albicans, Candida utilis* and *Setaria cervi*. Furthermore, all synthesized compounds were tested for their toxicity against *Salmonella tyhphimurium* TA 98 and TA100 strains: none showed mutagenic activity.

5.2 Significance of Pyrazoles

Pyrazoles are five-membered aromatic heterocycles containing two nitrogen atoms adjacent to each other. This scaffold is an important template for designing and developing diverse therapeutic drugs (Kale *et al*., 2016: 906) since they exhibit several biological properties such as anti-hyperglycemic, analgesic, anti-inflammatory, antipyretic, antibacterial, hypoglycemic and sedative-hypnotic activities (Dadiboyena *et al*., 2011: 5258). Synthetic pyrazole based drugs which are extensively utilized in the pharmaceutical industry include Acomplia (**1**) to treat obesity, Celebrex (**2)** to treat inflammation and Viagra (**3**) to treat erectile dysfunction (Figure 1**)** (Kumar *et al*., 2013: 389 and Tewari *et al*., 2014: 8).

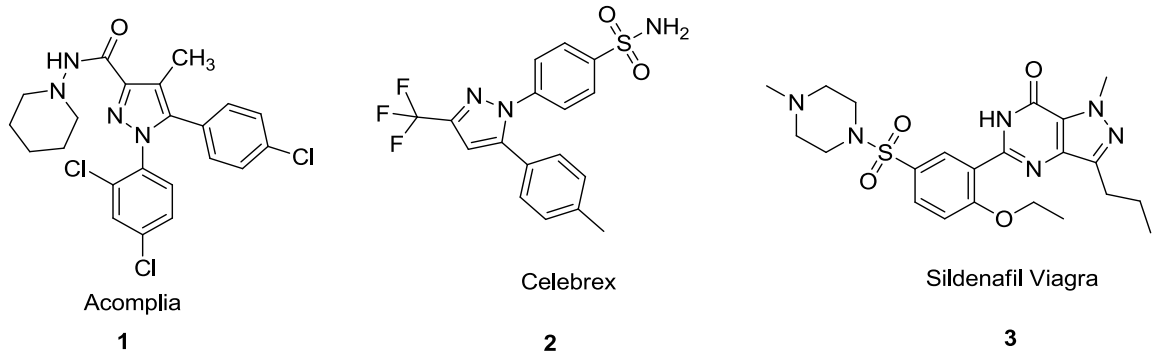

Figure 1: Some important synthetic pyrazole containing drugs

Although pyrazoles are available from natural sources, the synthetic molecules dominate the pharmaceutical industry because they can be synthesized from simple substrates whilst different methodologies are reported. The problem of obtaining pyrazoles from living organisms is their limited ability to metabolize molecules which possess two nitrogen atoms next to each other. Some important pyrazoles obtained as natural products are illustrated in Figure 2 (Kumar *et al.*, 2013:735).

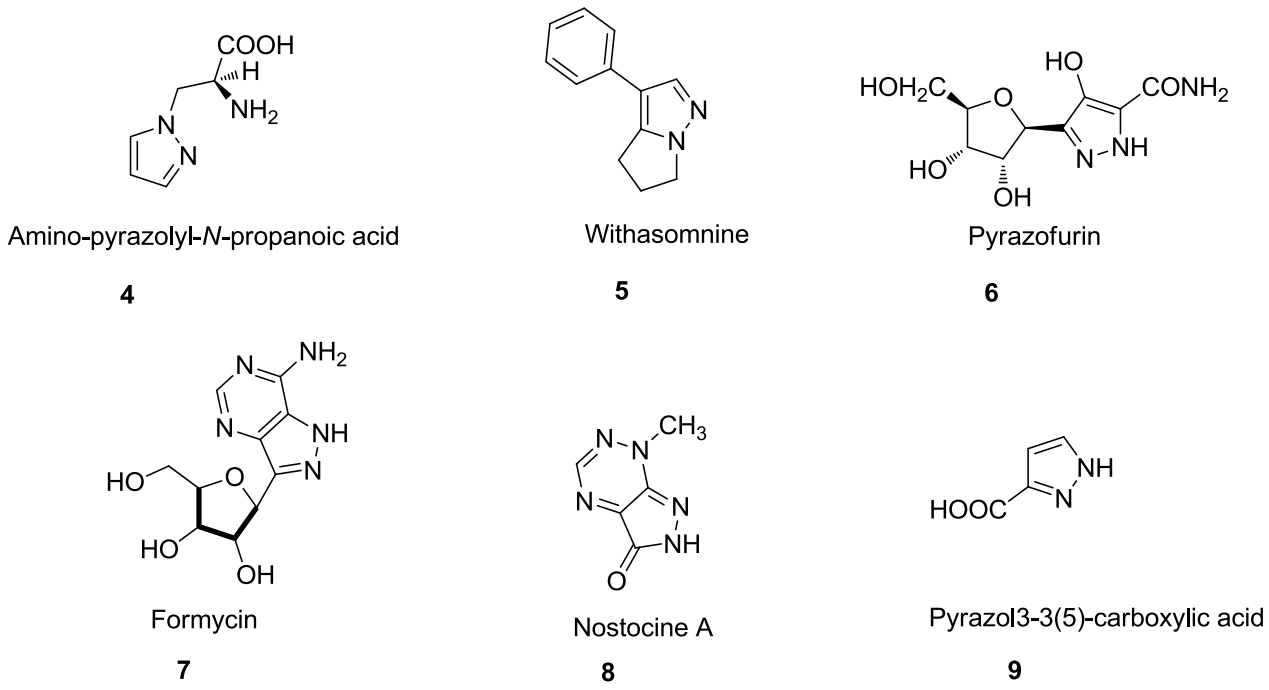

Figure 2: Some pyrazole containing natural products. (Kumar *et al*., 2013:735)

Due to the lack of sufficient natural products, researchers are focusing on increasing the library of pyrazoles by designing new synthetic routes to produce novel molecules which have potential bio-activity. This research area of synthesis is unlimited since the pyrazole scaffold can be fused to numerous substituted and un-substituted aromatic compounds thereby creating new molecules.

The aim of this research was to synthesize novel fused indolo-pyrazoles by multi-component reactions and investigate their antifungal and antibacterial activities.

5.3 The Synthesis of Pyrazole

Synthetic chemists have developed various methods such as the classical Knorr synthesis, Pechmann synthesis, Claisen-Schmidt condensation reaction, Vilsmeier Haack reaction (VHR) and a new strategy includes the multi-component reaction for the synthesis of new pyrazole derivatives (Shkineva *et al.*1995: 509 and Dadiboyena *et al*., 2011: 5258).

5.3.1 The Knorr Synthesis of Pyrazole

In 1883, Knorr synthesized pyrazoles **13** by using a substituted 1, 3-dicarbonyl compounds **10** and hydrazine **11** (Scheme 1).

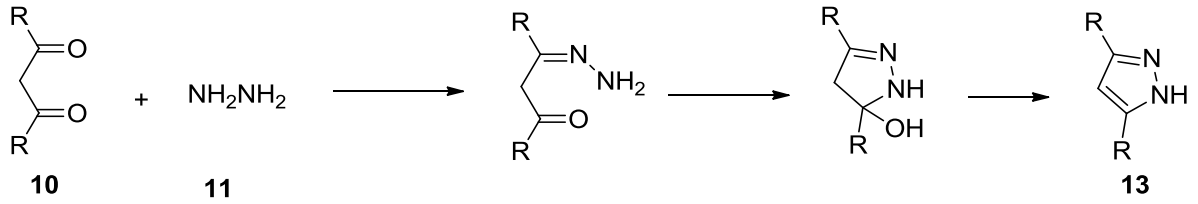

Scheme 1: Knorr pyrazole synthesis (Wang. 2010: 1631)

This reaction was named the Knorr pyrazole reaction which became a powerful strategy for the synthesis of thousands of new compounds bearing the pyrazole scaffold. Another notable development of Knorr pyrazole reaction was the synthesis of edaravone **16** using 1,3-dicarbonyl **14** and phenylhydrazine **15** (Scheme 2) (Wang. 2010: 1631).

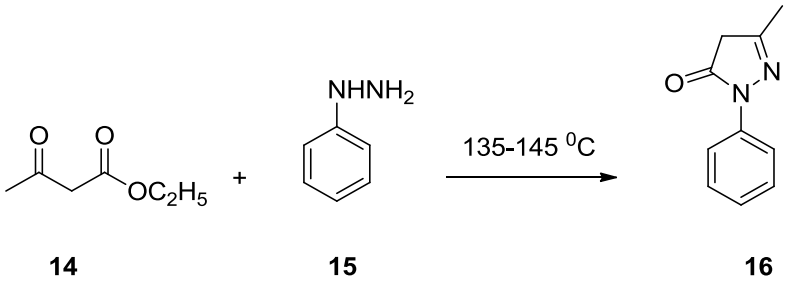

Scheme 2: Knorr synthesis of edaravone (Wang, 2010: 1631).

The scope of the Knorr synthesis was expanded through the use of substituted 2, 4-diketones **19** which was prepared from ketones **17** and acid chlorides **18** followed by an *in situ* reaction with hydrazine **20** to form pyrazole **21**.

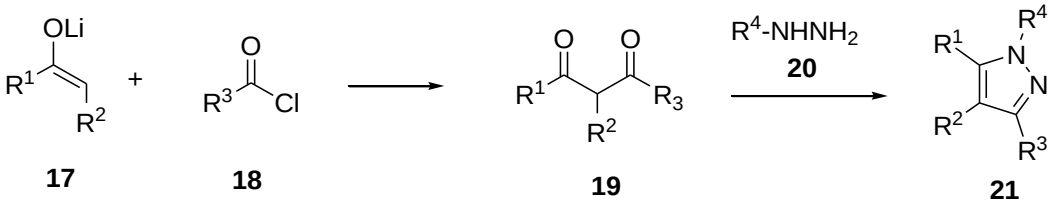

Scheme 3: Synthesis of pyrazoles from acid chlorides and ketones

(Heller *et al*., 2006: 2675)

5.3.2 The Pechmann's Synthesis of Pyrazole

In 1895, Pechmann developed another synthetic route for pyrazole through 1, 3-dipolar cycloaddition between acetylene **22** and diazomethane **23**. The general Pechmann's pyrazole synthesis involves acetylene and diazomethane (Scheme 4) (Wang, 2010: 2147).

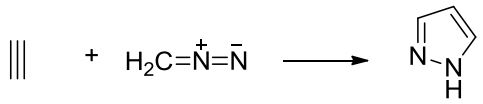

22 **23** **24**

Scheme 4: General Pechmann's reaction for pyrazole synthesis **24**

(Wang. 2010: 1631)

Other various substituted pyrazole derivatives were synthesized through substituted alkenes **25** and diazomethane (Scheme **5**).

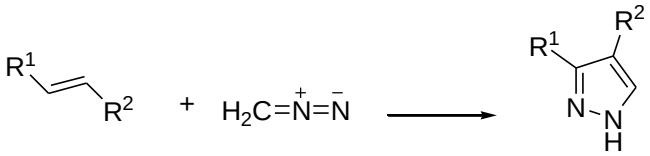

25 **23** **26**

R^1 = H, alkyl, phenyl
R^2 = H, alkyl

Scheme 5: Synthesis of substituted pyrazole derivatives **26**

(Wang. 2010: 1631)

Pechmann's pyrazoles synthesis was further explored using α, β-unsaturated carbonyl as an alternate route to synthesize substituted pyrazole derivatives. Hence, ethyl 2-butenoate **27** was treated with diazomethane to produce substituted pyrazoles **28** (Scheme 6) (Wang 2010: 2147).

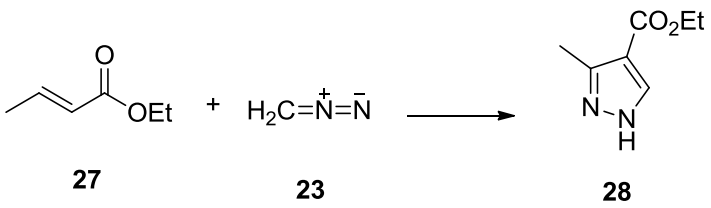

Scheme 6: Synthesis of substituted pyrazole from α, β-unsaturated carbonyls

(Wang. 2010: 1631)

5.3.3 The Synthesis of Pyrazole Through Claisen Schmidt Condensation

The synthesis of pyrazole via the Claisen Schmidt condensation occurred only during the past decade and was considered to be an effective route for generating substituted pyrazole derivatives. Briefly, using an aromatic aldehyde and ketone through a cross aldol condensation, a chalcone **31** was generated which then reacts with hydrazine or substituted hydrazine **32** by the Claisen Schmidt condensation to produce the corresponding pyrazole derivatives **33** (Scheme 7) (Ehsan *et al.*, 2012:195 and Nossier *et al*., 2017:1).

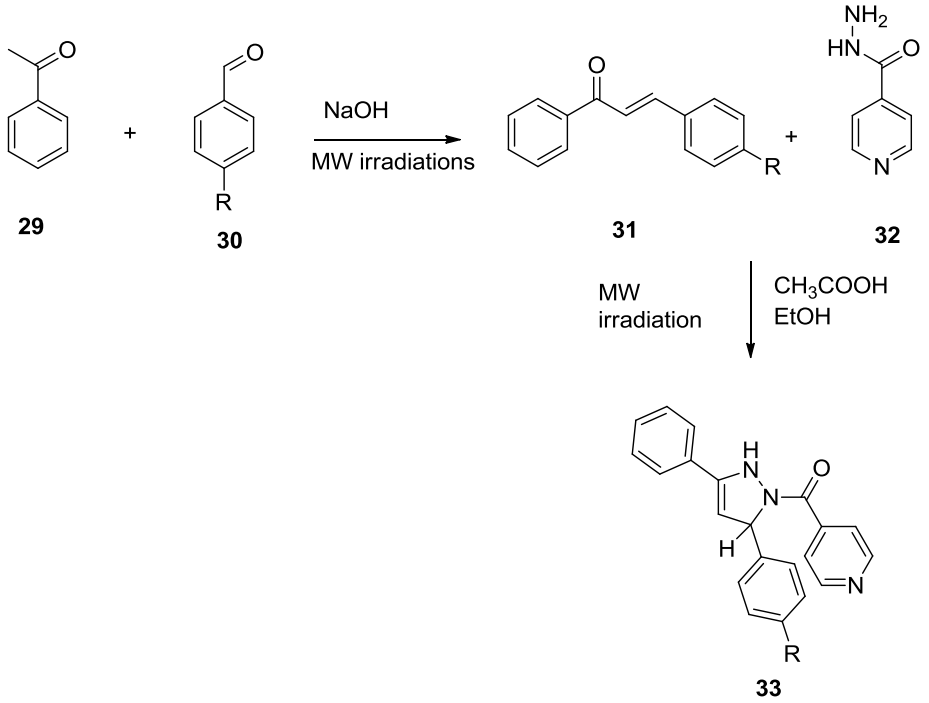

Scheme 7: Claisen Schmidt's synthesis of substituted pyrazole derivatives via chalcone.

(Ehsan *et al*., 2012:195)

5.3.4 The Use of the Vilsmeier-Haack Reaction for the Synthesis of Formylated Pyrazoles

In 1970, Kira and co-workers found that when they treated acetophenone phenylhydrazone **34** with two moles of DMF-$POCl_3$, under reflux in DMF, for 6 hours an immonium perchlorate intermediate **35** was produced (Scheme 8).

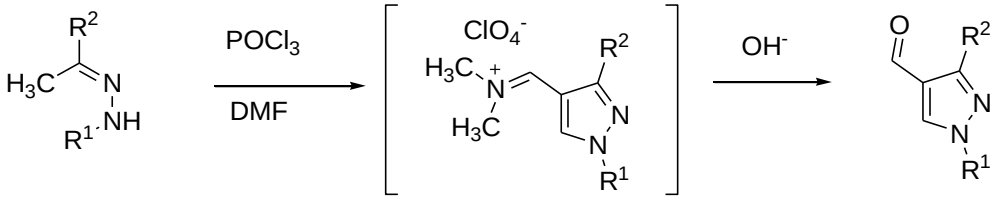

34 **35** **36**

Scheme 8: Synthesis of the first 1, 3-dialrylpyrazole-4-carboxaldehyde **36** via Vilsmeier-Haack reaction (Dar *et al*., 2015:1)

Subsequently, Dar and co-workers, 2015 used alkaline hydrolysis of **35** to produce 1, 3-diarylpyrazole-4-carboxaldehyde **36** which became a highly effective new procedure for the synthesis of pyrazoles. The cyclization of aryl hydrazones **37** using DMF-$POCl_3$ to generate substituted pyazoles **38** (Scheme 9) was also reported (Dar *et al*., 2015:1).

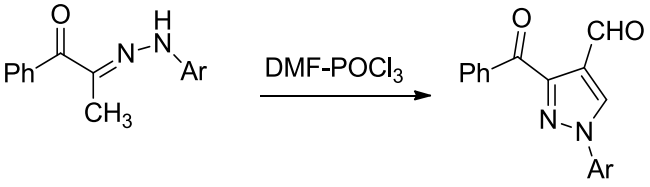

37 **38**

Scheme 9: Cyclization of aryl hydrazones under Vilmeier Haack conditions (Dar *et al*., 2015:1-5)

In 2012, Desai and co-workers, used the Vilmeier Haack reaction to synthesize the pyrazole **39** which was subsequently used in a cross aldol condensation reaction to yield a chalcone **4**1 bearing the pyrazole scaffold. The latter was reacted with thiosemicarbazide **42**, under reflux in alkaline ethanol, to yield bis pyrazole compounds **43** (Scheme 10): this was known as Claisen Schmidt condensation reaction. (Desai *et al.*, 2012: 67)

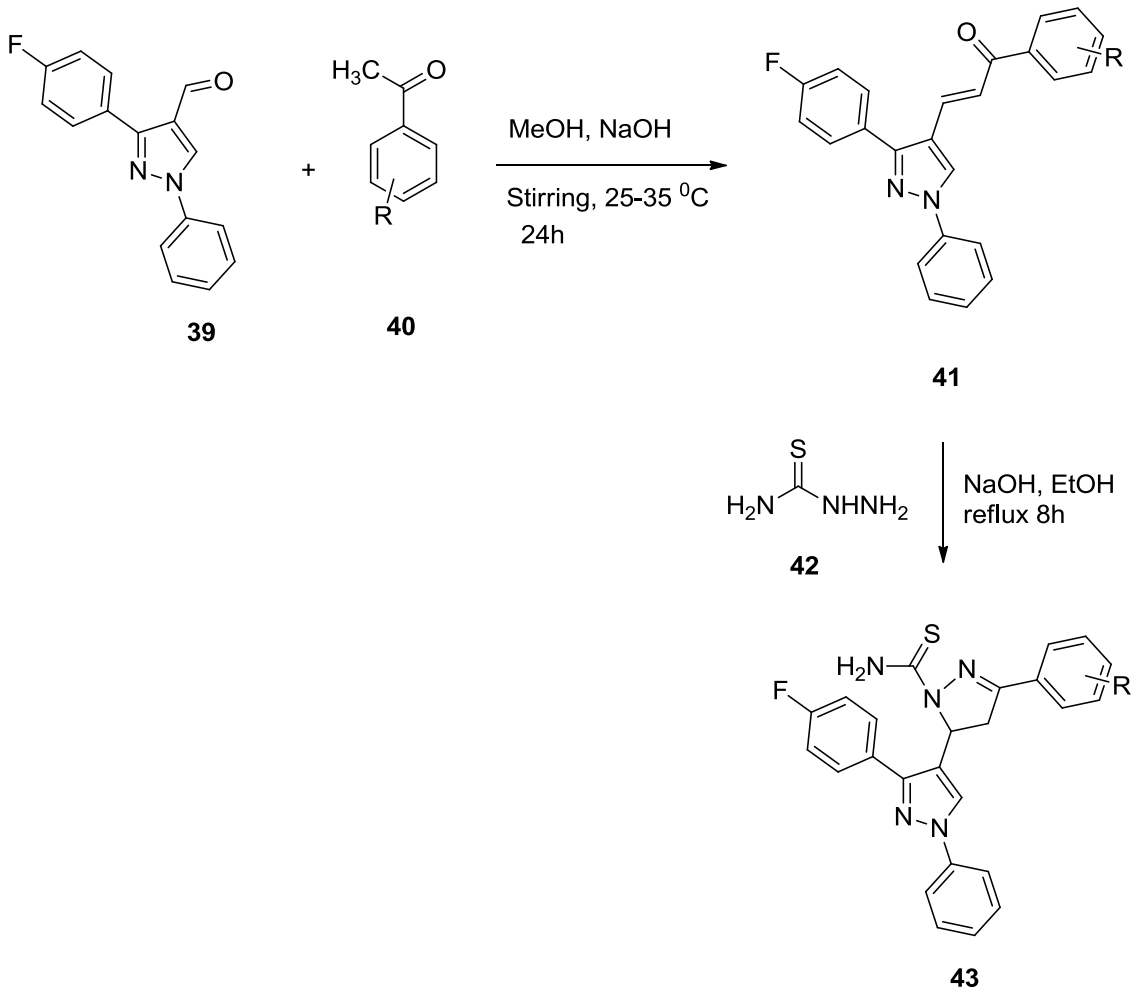

Scheme 10: Synthesis of bis-pyrazole through combination of Vilsmeier-Haack and Claisen condensation reactions. (Desai *et al.,* 2012: 67)

The Vilsmeier-Haack reaction has become important for the synthesis of new starting materials and hence has been applied for MCRs such as the Biginelli reaction, Hantzsch condensation and Ugi four component reaction (Viveka *et al*., 2015). Kumar and co-workers, in 2013, synthesized new functionalized pyrazole carboxylate derivatives **46** by reacting aryl hydrazones **44** with diethyl but-2-ynedioate **45** at 130 ^{0}C for 10 hours (Scheme 11) (Kumar *et al*., 2013: 389).

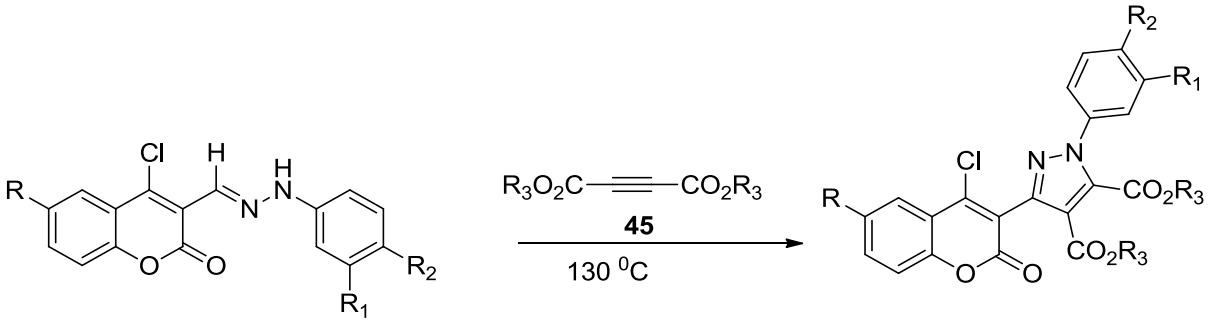

44 **46**

Scheme 11: Synthesis of substituted 2-oxo-2H-chromenylpyrazolecarboxylates

(Kumar *et al*., 2013: 389).

Also in 2013, Khalili reported the synthesis of sulfonyl pyrazoles **49** from arylsufonyl hydrazones **48** and dialkyl acetylenedicarboxylates **47** in the presence of nucleophilic compounds such as pyridine, isoquinoline, or triphenylphosphines (Scheme 12) (Khalil. 2013: 3170).

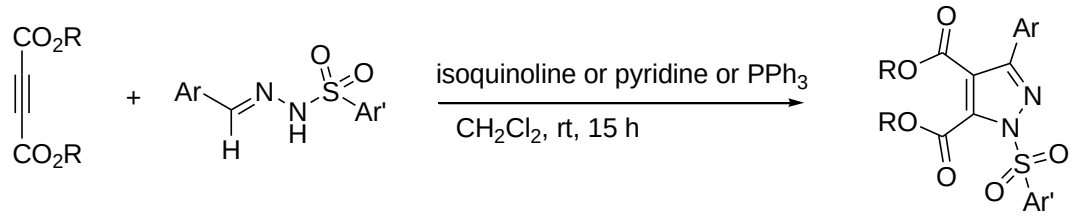

47 **48** **49**

Scheme 12: Synthesis of *N*-arylsulonyl pyrazoles (Khalil. 2013: 3170).

5.3.5 Sigmatropic Rearrangement / Cascade Cyclization in the Synthesis of Pyrazoles

In recent years, more interesting methods for the synthesis of the pyrazole moiety have been reported. Wen *et al*, 2014 reported a sigmatropic rearrangement or a cyclization cascade reaction to generate polysubstituted pyrazole **51** from *N*-propargylhydrazones **50** which was catalyzed by platinum (Wen *et al*., 2014:5940).

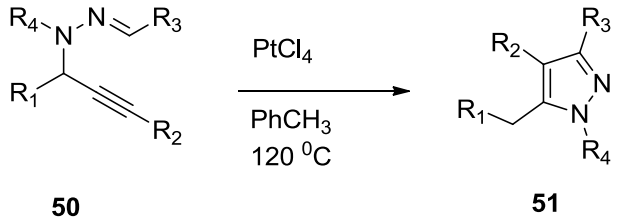

50 **51**

Scheme 13: Synthesis of polysubstituted pyrazoles by platinum-catalyzed sigmatropic rearrangement (Wen *et al*., 2014:5940).

5.3.6 Synthesis of Fused Indole-Pyrazoles

The chemistry of fused pyrazoles have attracted enormous attention because of their pharmacological importance in treating various health issues. Whilst several synthetic methods are available to synthesize fused pyrazoles through both linear synthesis and MCRs, the latter has recently gained prominence.

The construction of fused pyrazole indole compounds have been a long-standing interest for synthetic chemists ever since Katayama reported pyrazole [1, 5-*a*] indole **52** (Fig 3) with potent inhibitory activity against DNA topoisomerase I and II, and strong cytotoxic activity against cancer cells (Katayama *et al.,* 1994:214).

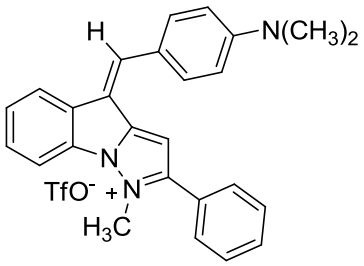

52

Figure 3: Bio-active pyrazolo [1, 5-*a*] indole derivative (Katayama *et al.,* 1994:214).

Hence, Zhu and co-worker, 2007 reported the synthesis of pyrazolo [1, 5-*a*] indole **55** from pyrazole derivative **54** via copper (I)-catalyzed intramolecular cyclization (Scheme 14) (Zhu *et al*., 2007: 6262).

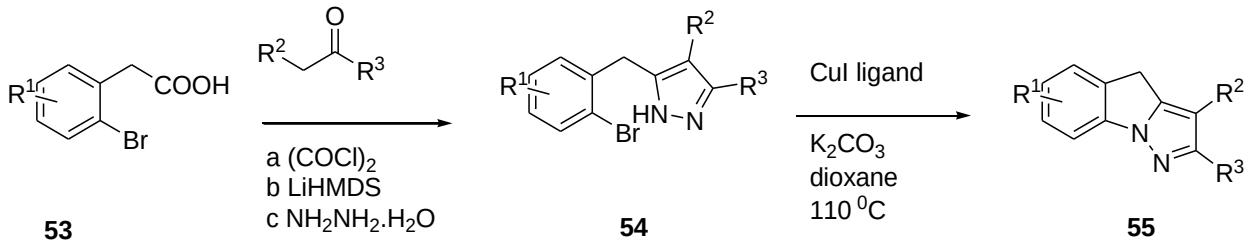

53 **54** **55**

Scheme 14: Synthesis of pyrazolo [1, 5-*a*] indole via intramolecular cyclization

(Zhu *et al*., 2007: 6262)

In 2014, Rahmouni and co-workers reported the synthesis of fused pyrazolopyrimidine derivatives **58** which resembled the purines. This reaction occurred through the nucleophilic addition followed by cyclization of 5-aminopyrazole-4-carbonitriles **56** with formamide **57** (Scheme 15) (Dadiboyena *et al*., 2011: 5258 and Rahmouni *et al*., 2014: 210).

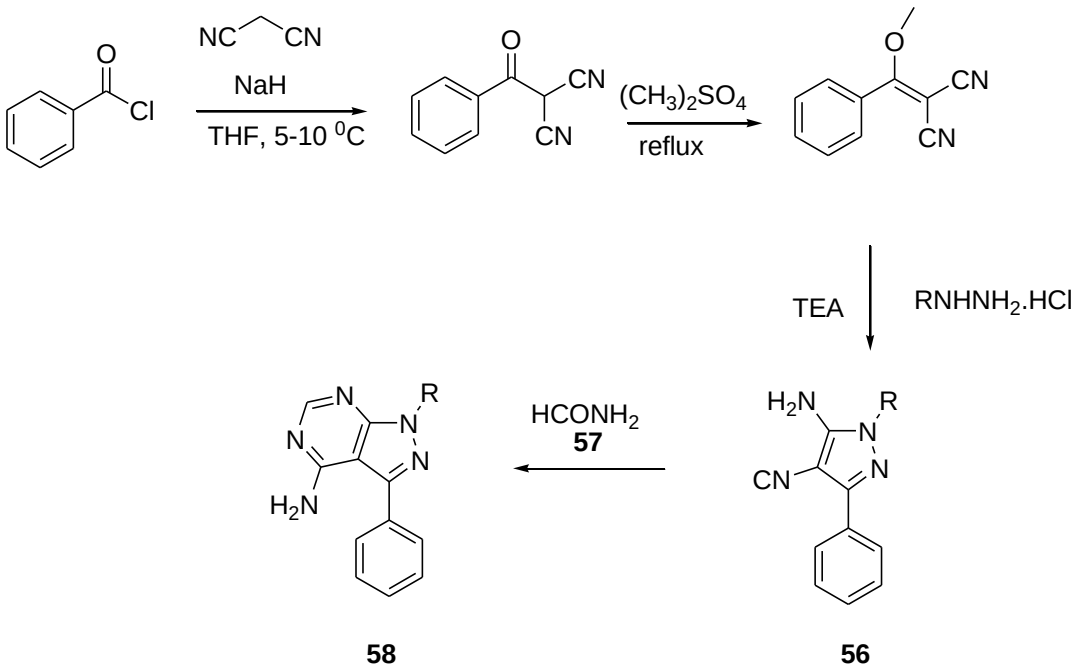

58 **56**

Scheme 15: Synthesis of fused pyrazolopyrimidine derivatives **58**

(Dadiboyena *et al*., 2011: 5258 and Rahmouni *et al*., 2014: 210).

As mentioned earlier, the pyrazoles are synthesized from chalcone through hydro-amination and Claisen-Schmidt condensation, Li and Dong, 2015 used a similar approach by using *o*-alkynylchalcones **59** with hydrazine **60** to yield fused pyrazoles **61** (Scheme 16) (Li *et al*., 2015: 623).

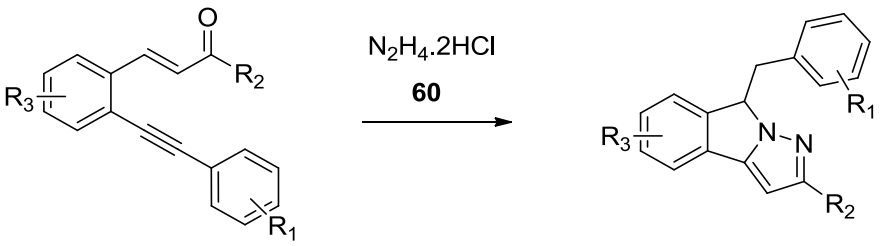

59 **61**

Scheme 16: Synthesis of fused pyrazole via simple cyclization of *o*-alknylchalcones

(Li *et al*., 2015: 623)

Compounds possessing the indole scaffold are also present in numerous natural products and they possess diverse biological properties such as anti-inflammatory, anticonvulsant, cardiovascular and antibacterial activities (El-Mekabaty *et al*., 2015: 894). Thus, the synthesis of fused indole-pyrazoles have attracted enormous interest by synthetic and medicinal chemists.

In 2015, El-Mekabaty and co-workers reported the synthesis of 3-amino-pyrazole bearing indole **65** which was subsequently reacted with 1,3-dicarbonyl derivatives to generate various fused pyrazolo [1, 5-*a*] pyrimidines **66**, **67**, **68** and **69** derivatives containing an indole moiety (Scheme 17) (El-Mekabaty *et al*., 2015: 894).

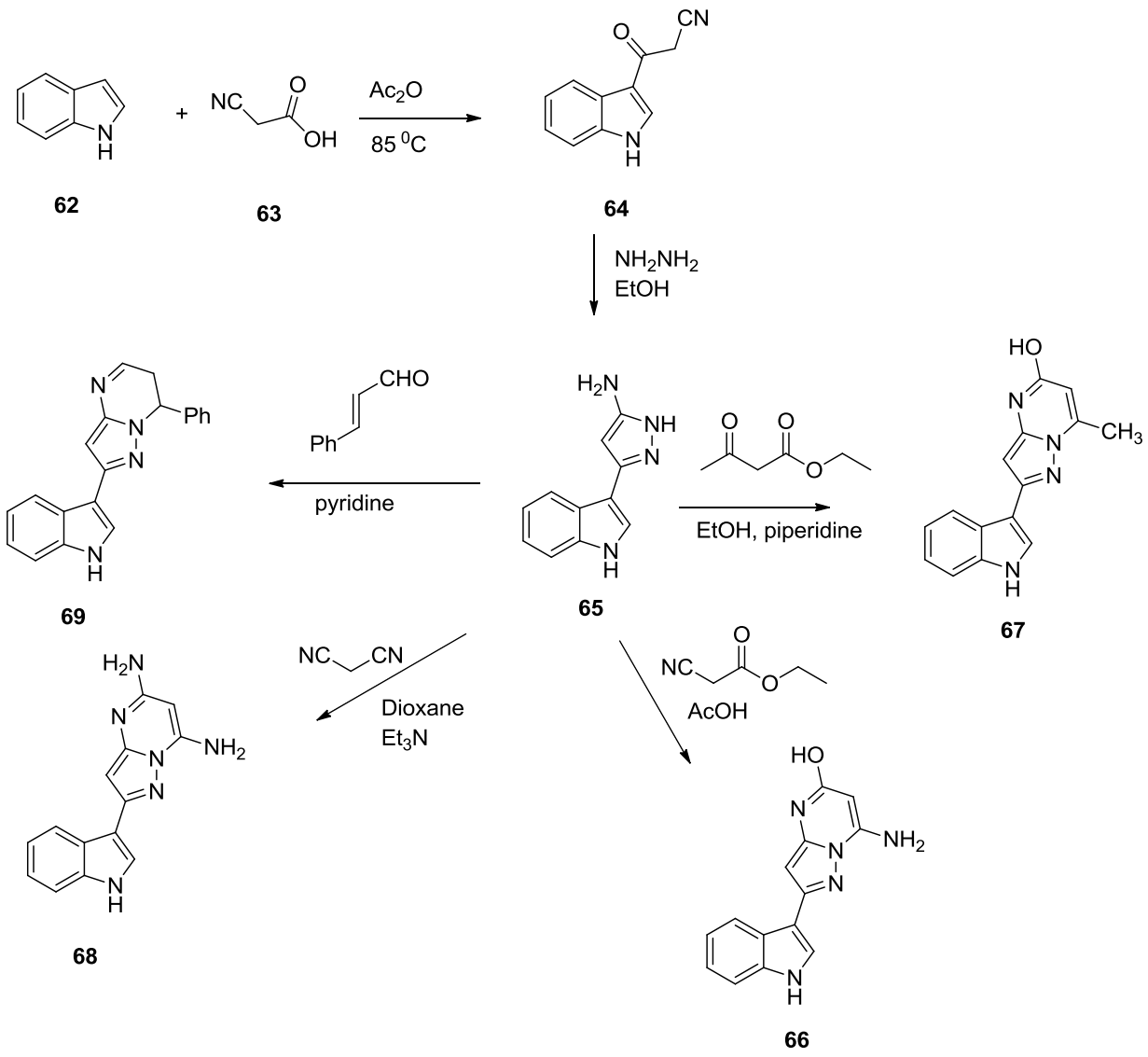

Scheme 17: Synthesis of pyrazolo [1, 5-*a*] pyrimidines (El-Mekabaty *et al*., 2015: 894)

5.3.7 Multi-Component Reaction in the Synthesis of Pyrazoles

In 2012, Hao and co-workers used a 3 component reaction: synthesis of pentacyclic pyrazole-fused naphtho [1, 8-*fg*]-isoquinolines **73** was achieved from a mixture of acenaphthylene-1, 2-dione **70**, diaroylmethanes **71** and electron-rich pyrazol-5-amines **72** in acetic acid (Scheme 18). This reaction was efficient and the work-up process was easy (Hao *et al*., 2012: 4894).

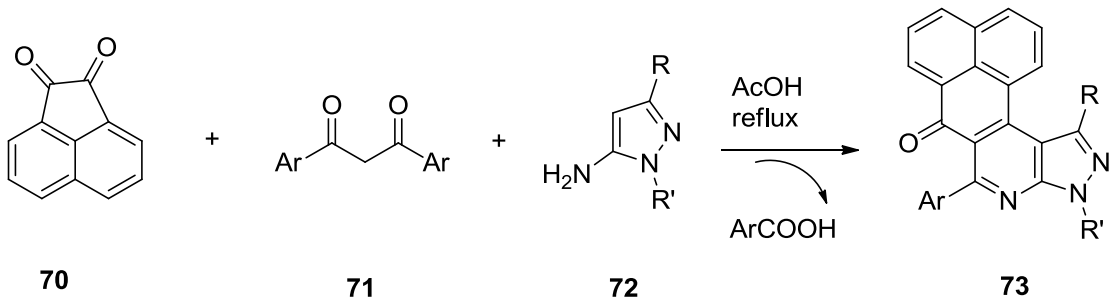

70 71 72 73

Scheme 18: Multi-component synthesis of pentacyclic pyrazole-fused naphtho [1, 8-*fg*]-isoquinolines (Hao *et al*., 2012: 4894)

In the same year, Suzuki *et al.*, reported a Mannich-type coupling of alkynes **74** with *N*, *N*-disubstituted hydrazines **76** and aldehydes/ketones **75** through intramolecular hydro-amination followed by cascade cyclization employing 1, 2-dialkynylbenzene **78** derivatives to yield fused tricyclic dihydropyrazoles **79** (Scheme 19). This sequential reaction occurred in one-pot through a three component reaction which was catalyzed by gold (Suzuki *et al*., 2012: 326).

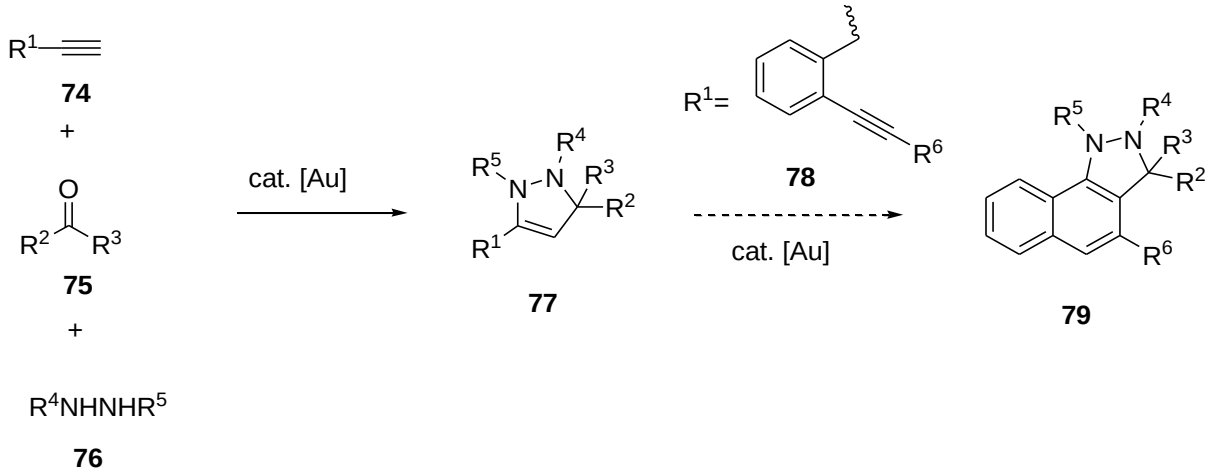

Scheme 19: Gold catalyzed synthesis of dihydropyrazoles via three-component annulation reaction. (Suzuki *et al*., 2012: 326)

In the last decade, several studies were devoted towards developing and discovering more efficient strategies for the preparation of pyrazole-containing compounds. Hence, exciting and attractive protocols and new routes have been documented which led to the rapid advancement

of the synthetic chemistry of pyrazoles. Recently Tekale *et al*., 2013 reported an eco-friendly method through four component synthesis to yield pyrano-pyrazole **84** using a heterogenous catalyst nano-ZnO (Scheme 20). This protocol was an inspiring development in organic synthesis which can catalyze the synthesis of more highly complex pyrazole derivatives (Tekale *et al*., 2013:1).

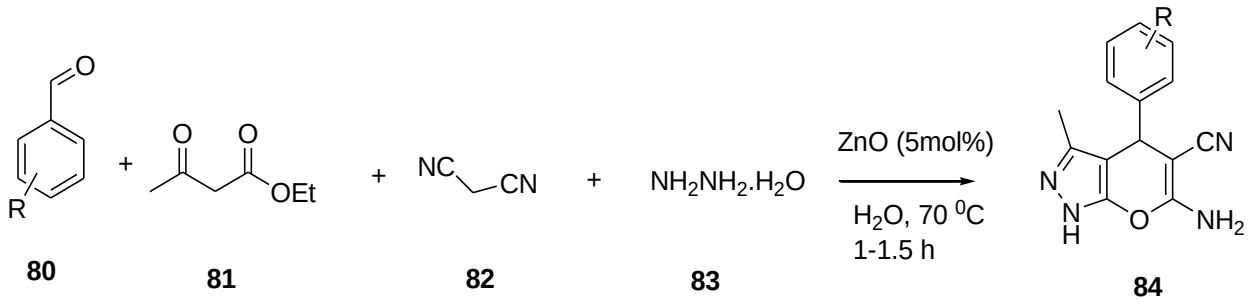

80 **81** **82** **83** **84**

Scheme 20: ZnO nanoparticle catalyzed one-pot four-component green synthesis of pyranopyrazole (Tekale *et al.*, 2013:1)

Despite the advanced developments documented in literature, more flexible synthetic routes to target a variety of fused pyrazole derivatives are needed. The approach that can readily give access to highly functionalized fused pyrazole derivatives are still of high priority. In the previous chapter, a very interesting transformation was demonstrated when Povarov's strategy was used to synthesize novel fused indole [1, 8] naphthyridine derivatives through [4+2] cyclo-addition. From this strategy, a hypothesis was pursued through a feasible reaction between aryl hydrazones derived from semicarbizide and benzaldehyde which can react with an indole moiety via a Povarov's [3+2] cycloaddition. In this study, the aryl hydrazone was predicted to behave as a diene due to the high nucleophilicity of nitrogen atoms of aryl hydrazones whilst the indole may act as an electron rich dienophile. This reaction would enable the formation of fused indolo-pyrazoles.

5.4 Results and Discussions

Part A: Investigating semicarbazide derivaives in Povaro'v reaction

5.4.1A Synthesis and Characterization of A Novel Fused 3-Phenyl-2, 3-Dihydropyrazolo [3, 4-*b*] Indole-1(4H)-Carbothioamide (88a)

A mixture containing benzaldehyde **85**, thio-semicarbazide **86** and indole **87** was refluxed in the presence of indium chloride, as a Lewis acid catalyst. The product obtained was 3-phenyl-2, 3-dihydropyrazolo [3, 4-*b*] indole-1(4H)-carbothioamide **88a** which was fully characterized by FT-IR, NMR and TOF-MS. Thereafter, different derivatives of benzaldehyde and thio-semicarbazide were used (Figure 4) to synthesize 26 derivatives (Figure 5).

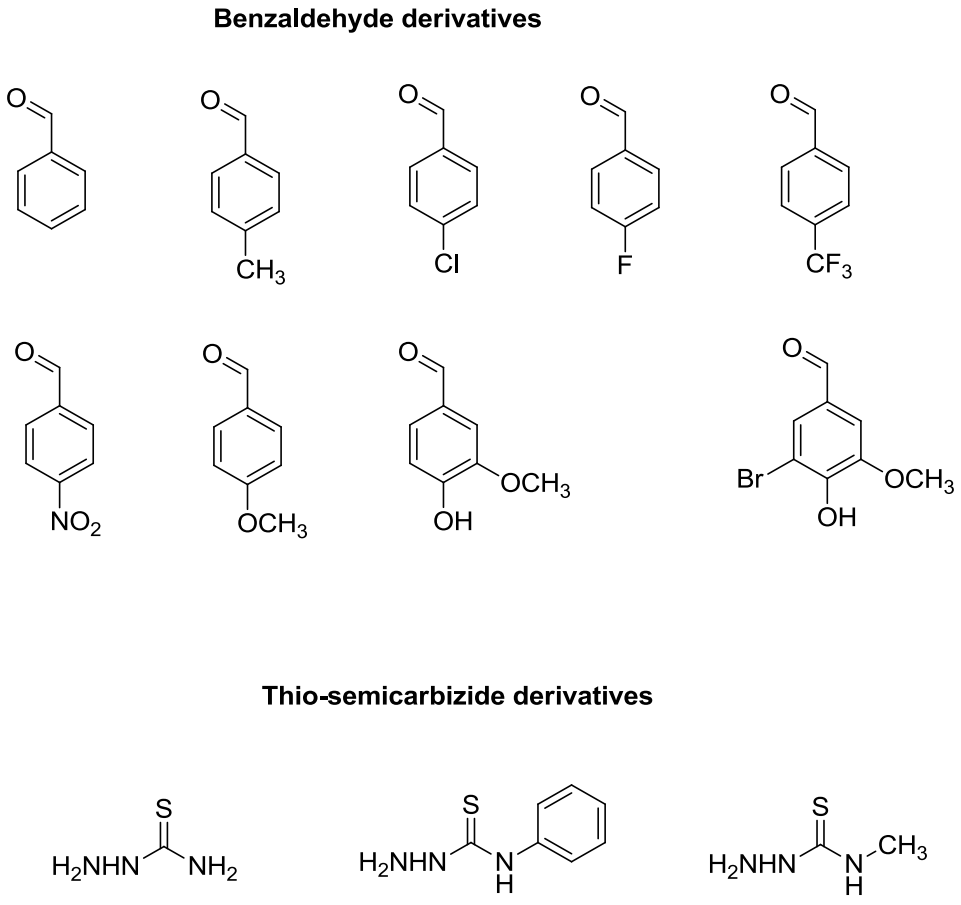

Figure 4: Benzaldehyde and thio-semicarbized derivatives

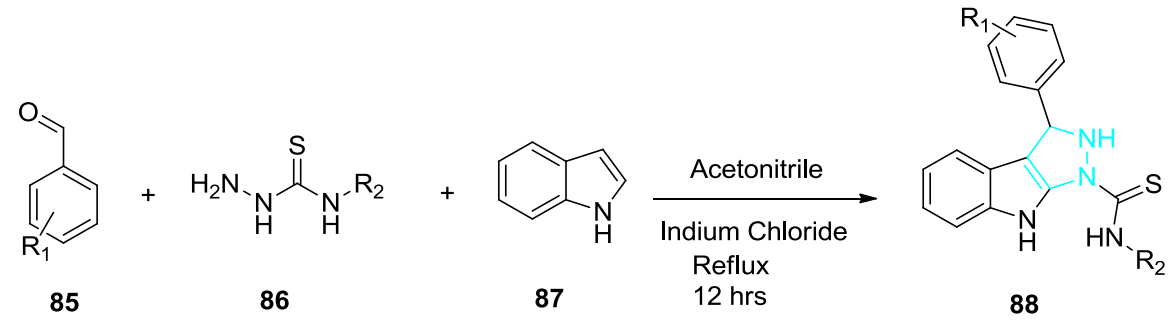

85 **86** **87** **88**

Key: R_1 = H, *p*-CH_3, *p*-Cl, *p*-F, *p*-CF_3, *p*-NO_2, *p*-OCH_3, *m* -OCH_3-*p*-OH, *m* -OCH_3-*p*-OH-*m*Br
R_2 = H (**86a**),Ph (**86i**), CH_3 (**86r**)

Scheme 21. Synthetic route for the titled compounds **88a- 88z**

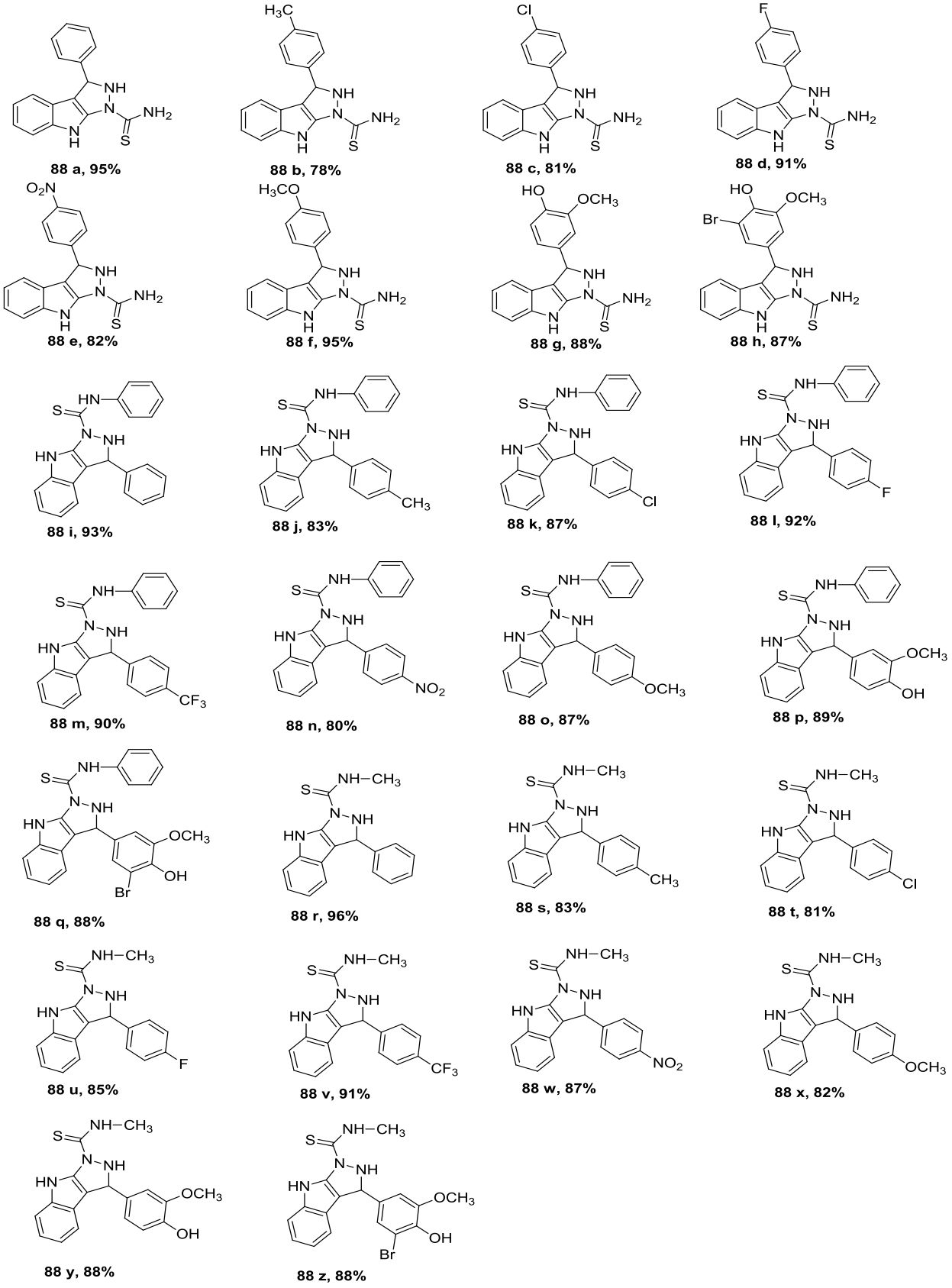

Figure 5: Synthesized novel fused indolo-pyrazole derivatives

The mechanism for the 3+2 cycloaddition reaction is presented in Scheme 22. It involves an interaction between a diene and dienophiles.

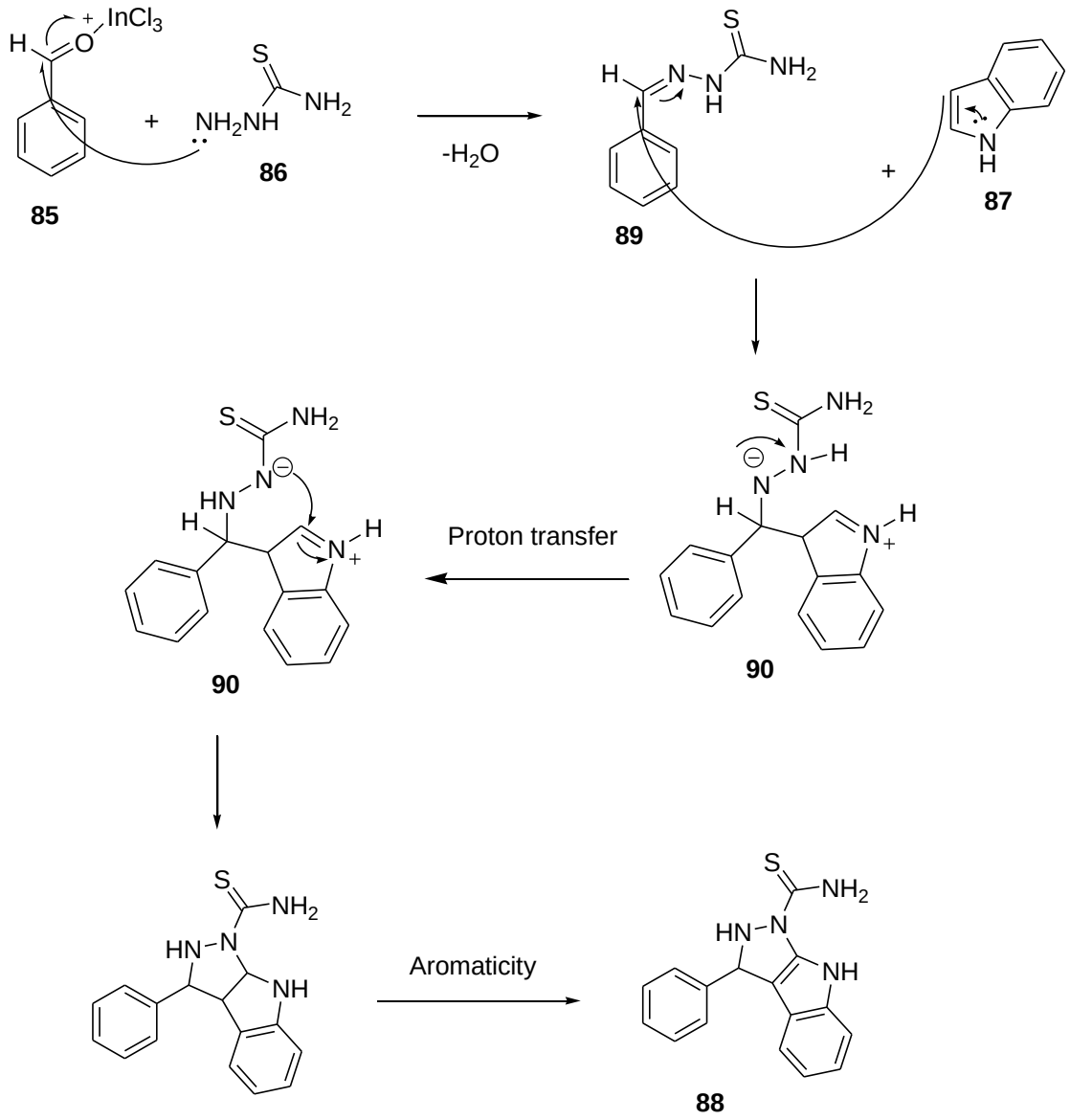

Scheme 22: Plausible mechanism for Povarov [3+2] cycloaddition reaction for the synthesis of **88**.

The above mechanism was triggered by the Schiff base reaction occurred between benzalydehyde **85** and hydrazine moiety **86** which yielded an imine product **89**. The latter was attacked by the lone pairs from indole nitrogen **87** due to nucleophilicity of enamines to yield an intermediate product **90**. At this stage compound **90** was unstable hence the delocalization of the lone pair from nitrogen causes a high electron density on the nitrogen atom which eventually causes proton transfer to make the adjacent nitrogen to be nucleophilic. This

instigated the attack of the electrophilic carbon from indole while compelling the hydrogen to depart. That hydrogen migrated and became attached to the nucleophilic adjacent nitrogen to stabilize it. Thereafter, aromaticity occurred to yield a stable desired compound **88.**

5.4.2A The Synthesis and Characterization of Novel 3-Phenyl-2, 3-Dihydropyrazolo [3, 4-*b*] Indole-1(4H)-Carbothioamide (88a-88h)

In the synthesis of the first series of pyrazole-indoles **88a-88h**, benzaldehyde derivatives **85** were selected with thio-semicarbazide **86a** and indole **87**. After completion of the reaction followed by the usual-work up and purification, pure red-brown solids were obtained in high yield. Compound **88a** with a yield of 95 %, a reddish brown solid with a melting point of 111 - 113 ^{0}C, was chosen as a template to discuss its unambiguous characterization.

The FT-IR spectrum (Appendix 5.1A) showed stretching absorption (cm $^{-1}$) at 3456, 1504, 1333 and out of plan bend at 726 cm $^{-1}$ which was assigned to secondary N-H, C=S, C-N and N-H, respectively. The numbers for peripheral atoms depicted in Figure 6 were used to facilitate the assigning of proton and carbon for NMR spectral interpretation.

The ^{1}H NMR spectrum (Appendix 5.2A – 5.3A) showed signals at δ 10.89 for overlapping NH-4 indole and NH-1 pyrazole whilst at 2.0 showed signal for NH-13 thioamde. Aromatic protons at δ 7.46 (1H, d, *J* = 8.2 Hz, H-5), 7.45 (1H, d, *J* = 8.2 Hz, H-8), 7.11 (1H, t, *J* = 7.5 Hz, H-6) and 6.92 (1H, d, *J* = 7.2 Hz, H-7) corresponded to indole –CH. The signal at δ 5.94 (s, H-11) exhibited the presence of –CH (sp^{3}) aliphatic proton which confirmed the formation of a new pyrazole ring. The phenyl ring exhibited five protons as triplets at δ 7.19 (1H, t, *J* = 8.2 Hz, H-4') while doublets appeared at δ 7.40 (2H, d, *J* = 8.0 Hz, H-2'& H-6') and δ 7.29 (2H, d, *J* = 7.6 Hz, H-3' & H-5'), see (Figure6).

The ^{13}C NMR (Appendix 5.4A), DEPT (Appendix 5.5A-5.6A) and HSQC (Appendix 5.8A) spectra showed the presence of ten CH carbons at δ 39.7 (C11), 111.1 (C5), 118.1 (C7), 120.9 (C6), 123.6 (C8), 125.8 (4'), 126.7 (C2' & C6') and 128.0 (3' & C5'). Whilst six quaternary carbons resonated at δ 118.2 (C10a), 119.2 (C9a), 136.7 (C3a & C4a), 144.9 (C1') and 170.4 (C12), see (Figure 6).

The 2-D NMR analysis of COSY (Appendix 5.7A) and HMBC (Appendix 5.9A – 5.10A) were used to confirm the identity of compound **88a** through correlation between proton and carbon as presented in Figure 7.

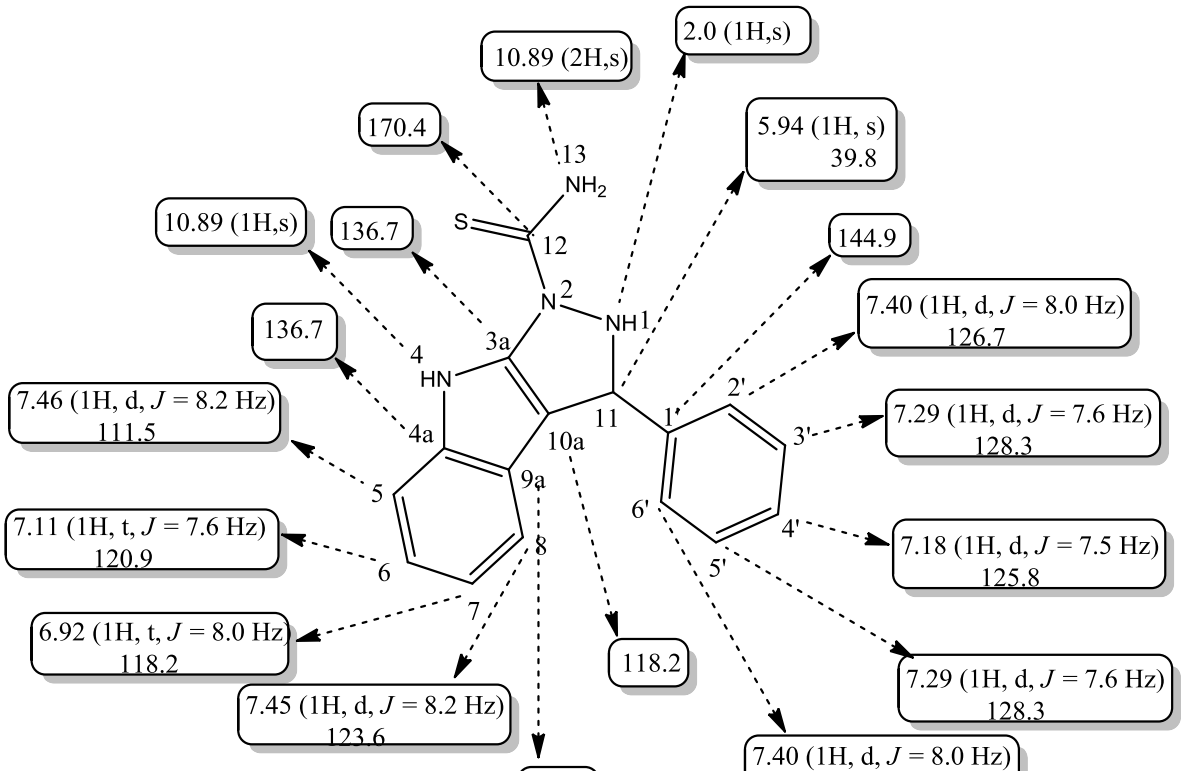

Figure 6: ^{1}H and ^{13}C NMR chemical shifts of **88a**.

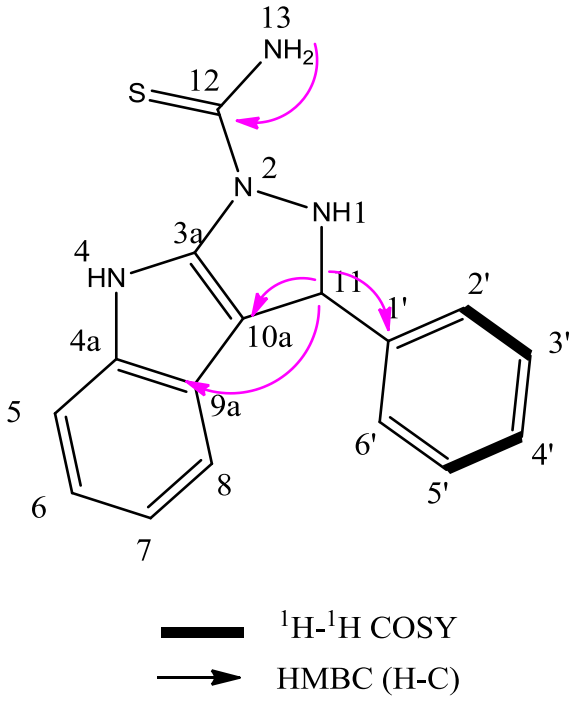

Figure 7: COSY and HMBC correlations of compound **88a.**

The ^{1}H, ^{1}H-COSY spectrum showed strong coupling between H-7 (δ 6.9) and H-6 (δ 7.11). Another strong coupling occurred between H-7 (δ 6.9) and H-8 (δ 7.45). There are strong coupling occurred between the phenyl proton: H-2' (δ 7.40) and H-3' (δ 7.29); H-6' (δ 7.40) and H-5' (δ 7.29). Another strong coupling occurred between phenyl proton: H-4' (δ 7.18) and H-3' (δ 7.29); H-4' (δ 7.18) and H-5' (δ 7.29).

The HMBC spectrum showed the proton and quaternary carbon coupling: H-11 (δ 5.94) coupled with C1' (δ 144.9), C10a (δ 118.2) and C9a (δ 119.2). H-13 (δ 2.0) coupled with C12 (δ 170.4).

Finally the mass spectrum (Appendix 5.11A) TOF-MS showed 319.1 [M^{+} + Na] for the molecular ion confirming compound **88a** as 3-phenyl-2, 3-dihydropyrazolo [3, 4-*b*] indole-1(4H)-carbothioamide. Scheme 23 depicts other fragments resulted after the loss of phenyl group, thio-amide and hydrogen from amines.

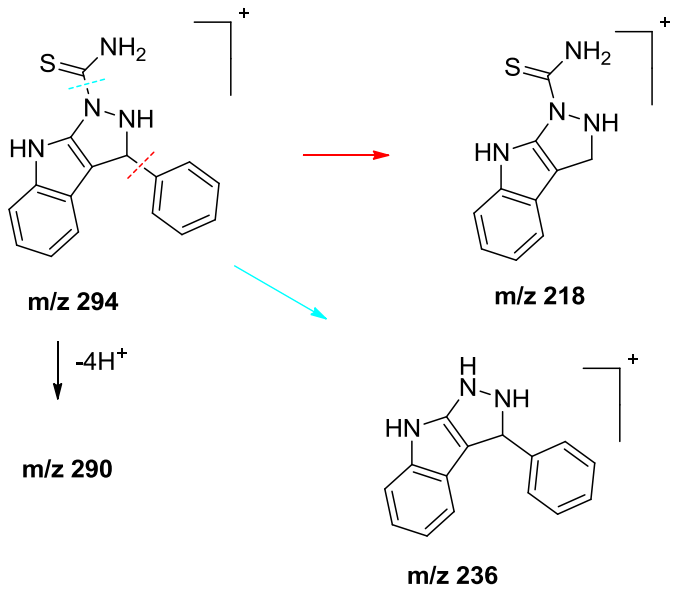

Scheme 23: Proposed fragmentation of compound **88a**.

5.4.3A The Synthesis and Characterization of Novel N, 3-Diphenyl-2, 3-Dihydropyrazolo [3, 4-*b*] Indole-1(4H)-Carbothioamide (88i-88p)

In the synthesis of the second series of pyrazole-indoles **88i-88p**, benzaldehyde derivatives **85** were selected together with N-phenyl thio-semicarbazide **86b** and indole **87**. After completion of the reaction and purification, compound **88i** was obtained with a yield of 93 %. It was a reddish brown solid with a melting point 138 - 140 ^{0}C: this was chosen as a template to discuss its unambiguous characterization.

The FT-IR spectrum (Appendix 5.41A) showed stretching absorptions (cm $^{-1}$) at 3383, 1503, 1336 and out of plane bend at 736 cm $^{-1}$ which were assigned to N-H, C=S, C-N and N-H, respectively.

The ^{1}H NMR spectrum (Appendix 5.42A – 5.43A) showed three N-H signals resonated at δ 11.8 for NH13, 10.8 for NH4 and 10.1 NH1which were assigned thio-amide, indole and pyrazole ring, respectively. Aromatic protons at δ 7.59 (1H, d, *J* = 7.6 Hz, H-5), 7.43 (1H, d, *J* = 7.2 Hz, H-8), 7.03 (1H, t, *J* = 7.5 Hz, H-6) and 6.82 (1H, d, *J* = 7.2 Hz, H-7) corresponded to indole –CH. The signal at δ 5.83 (s, H-11) exhibited the presence of –CH (sp^{3}) aliphatic proton which confirmed the formation of a new pyrazole ring. The phenyl ring exhibited five protons as triplets at δ 7.29 (1H, t, *J* = 8.0 Hz, H-4') while doublets appeared at δ 7.38 (2H, d, *J* = 7.7 Hz, H-2'& H-6') and δ 7.34 (2H, d, *J* = 7.8 Hz, H-3' & H-5'). Another phenyl ring exhibited five protons as triplets at δ 6.88 (1H, t, *J* = 7.8 Hz, H-10') while doublets appeared at δ 7.92 (2H, d, *J* = 7.6 Hz, H-8'& H-12') and δ 7.26 (2H, d, *J* = 7.9 Hz, H-9' & H-11'), (Figure 8).

The ^{13}C NMR (Appendix 5.44A), DEPT (Appendix 5.45A – 5.46A) and HSQC (Appendix 5.48A) spectra showed the presence of fifteen CH carbons at δ 39.7 (C11), 111.4 (C5), 118.1 (C7), 120.8 (C6), 123.4 (C8), 126.6 (4'), 127.6 (C2' & C6'), 128.6 (3' & C5'), 128.3 (10'), 125.8 (C12' & C8') and 129.9 (9' & C11'). Whilst seven quaternary carbons resonated at δ 118.0 (C10a), 119.1 (C9a), 136.5 (C3a) 133.9 (C4a), 142.9 (C7'), 144.9 (C1') and 176.0 (C12), see (Figure 8).

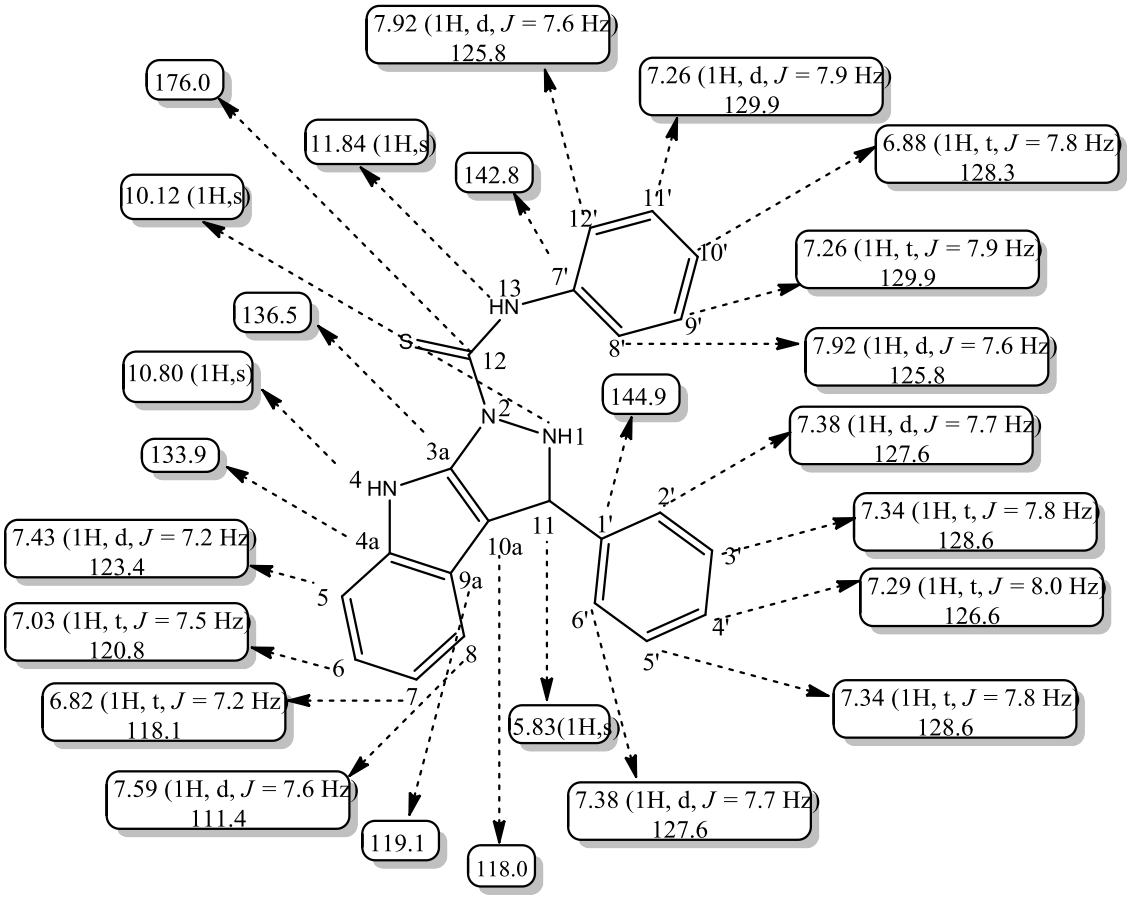

Figure 8: ^{1}H and ^{13}C NMR chemical shifts of **88i**.

The 2-D NMR analysis of COSY (Appendix 5.47A) and HMBC (Appendix 5.49A) were used to confirm the identity of compound **88i** through correlation between proton and carbon as presented in Figure 9 below.

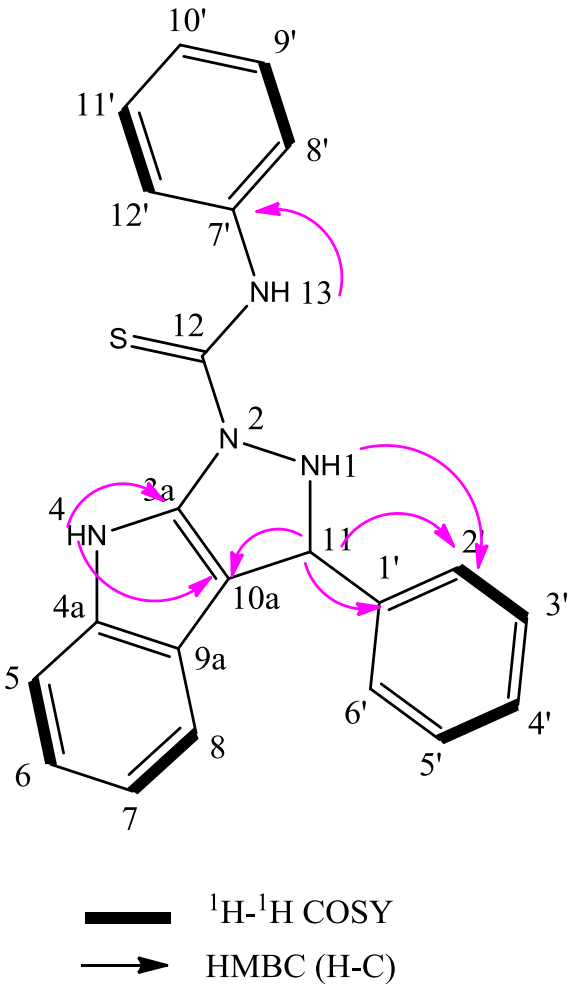

Figure 9: COSY and HMBC correlations of compound **88i.**

The ^{1}H, ^{1}H-COSY spectrum showed strong coupling between indole aromatic protons H-5(δ 7.43) and H-6(δ 7.03). Another strong coupling occurred between indole aromatic protons H-7(δ 6.82) and H-8 (δ 7.59). A strong coupling occurred between phenyl protons H-2' (δ 7.38) and H-3' (δ 7.34). Another strong coupling occurred between phenyl protons H-4' (δ 7.29) and H-5' (δ 7.34.). A strong coupling occurred between phenyl protons H-8' (δ 7.92) and H-9' (δ 7.29).

The HMBC spectrum showed the proton and quaternary carbon coupling: H-11 (δ 5.83) coupled with C10a (δ 118.0), C1' (δ 144.5) and C2' (δ 127.6); H-4 (δ 10.81) coupled with C10a (δ 118.0) and C3a (δ 136.5); H-1 (δ 10.12) coupled with C2' (δ 127.6); H-14 (δ 11.84) coupled with C7' (δ 142.9).

Finally the mass spectrum (Appendix 5.50A) TOF-MS showed 370.1 [M^+] for the molecular ion confirming compound **88**i as N, 3-diphenyl-2, 3-dihydropyrazolo [3, 4-*b*] indole-1(4H)-carbothioamide. Scheme 24 depicts other fragments resulted after the loss of phenyl groups and hydrogen from amines.

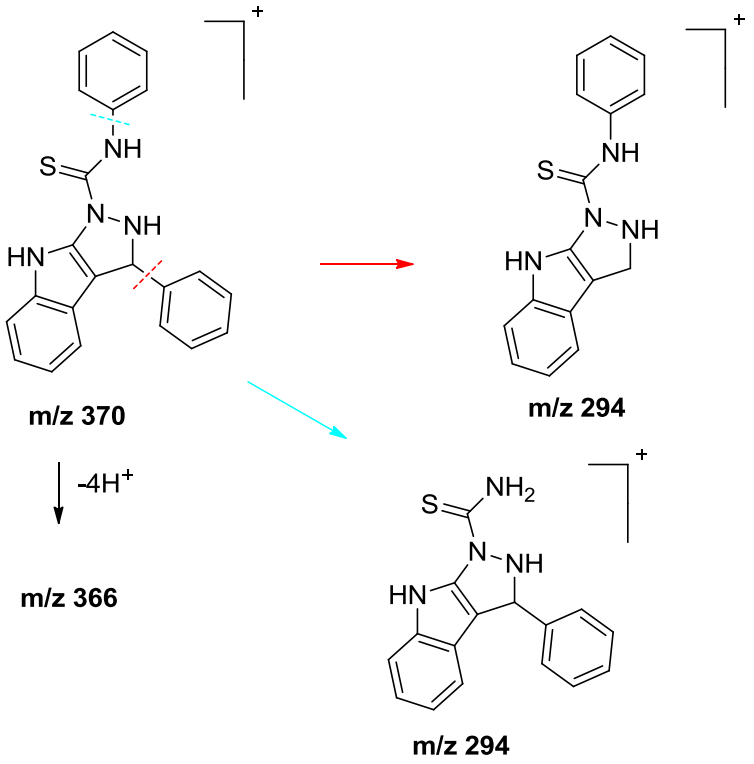

Scheme 24: Proposed fragmentation of compound **88i**.

5.4.4A The Synthesis and Characterization of Novel N-Methyl-3-Phenyl-2, 3-Dihydropyrazolo [3, 4-*b*] Indole-1(4H)-Carbothioamide (88r-88z)

In the synthesis of the third series of pyrazole-indoles **88r-88z**, benzaldehyde derivatives **85** were selected together with N-methyl thio-semicarbazide **86c** and indole **87**. After the reaction followed by the usual-work up and purification, pure red-brown solids were obtained in high yield. Compound **88r** with a yield of 96 %, a reddish brown solid with a melting point of 122 - 124 ^{0}C was chosen as a template to discuss its unambiguous characterization.

The FT-IR spectrum (Appendix 5.85A) showed stretching absorption (cm $^{-1}$) at 3484, 1504, 1334 and out of plane bend at 735 cm $^{-1}$ which was assigned to N-H, C=S, C-N and N-H respectively.

The ^{1}H NMR spectrum (Appendix 5.86A – 5.87A) showed three N-H signals resonated at δ 11.5, 10.8, 8.6 which were assigned to NH1 from pyrazole ring, NH4 from indole and NH13 from thio-amide, respectively. Aromatic protons at δ 7.40-7.38 (2H, d, *J* = 7.8 Hz, H-5& H-8), 7.08 (1H, t, *J* = 7.1 Hz, H-6) and 6.86 (1H, d, *J* = 8.8 Hz, H-7) corresponded to indole –CH.

The signal at δ 5.87 (s, H-11) exhibited the presence of –CH (sp^3) aliphatic proton which confirmed the formation of a new pyrazole ring whilst methyl protons appeared as doublets a δ 3.08 (3H, d, *J* = 4.6 Hz, H-14). The phenyl ring exhibited five protons as triplets at δ 7.16 (1H, t, *J* = 7.4 Hz, H-4') while doublets appeared at δ 7.33 (2H, d, *J* = 7.8 Hz, H-2'& H-6') and δ 7.29 (2H, t, *J* = 7.9 Hz, H-3' & H-5'), (Figure10).

The ^{13}C NMR (Appendix 5.88A), DEPT (Appendix 5.89A-5.90A) and HSQC (Appendix 5.93A) spectra showed the presence of eleven CH and CH_3 carbons at δ 30.8 (C14), 39.7 (C11), 111.4 (C5), 118.2 (C7), 120.9 (C6), 123.6 (C8), 126.6 (4'), 127.2 (C2' & C6') and 128.6 (3' & C5'). Whilst six quaternary carbons resonated at δ 118.1 (C10a), 119.4 (C9a), 136.6 (C4a), 134.3(C3a), 144.9 (C1') and 177.8 (C12), see (Figure10).

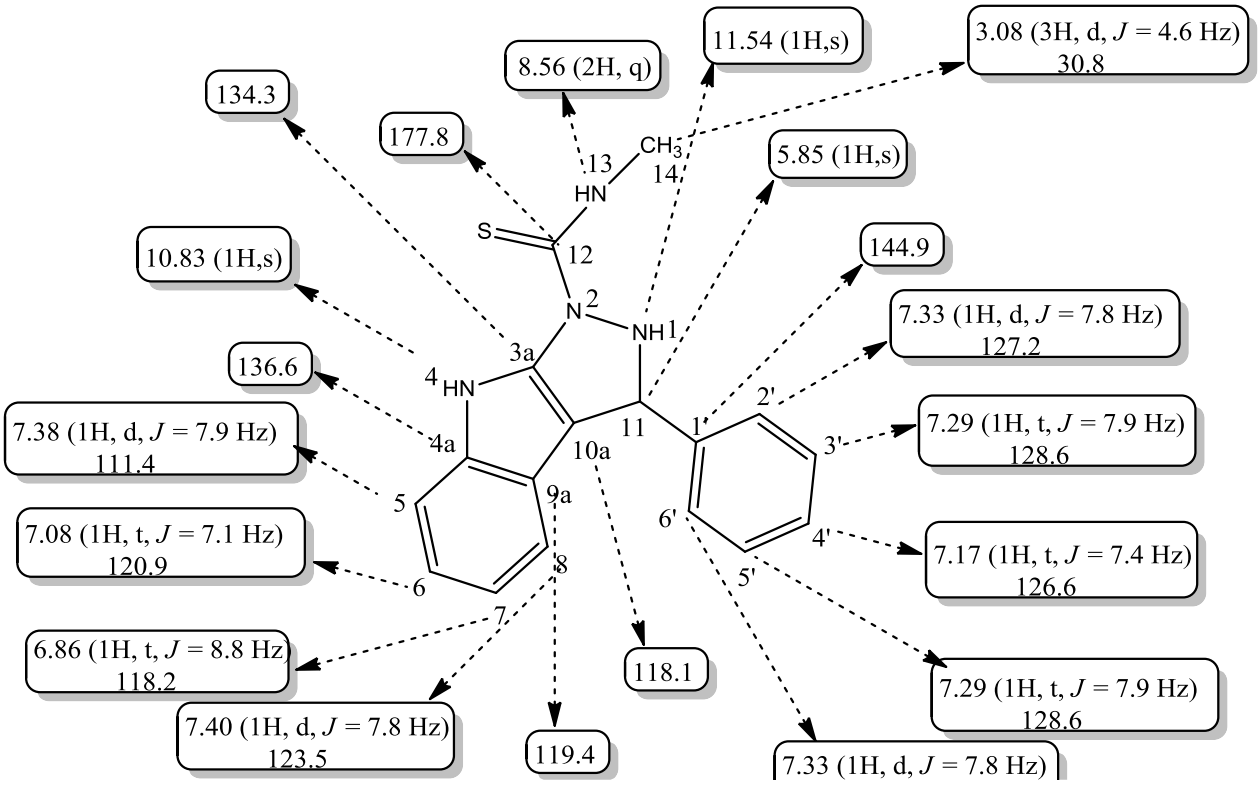

Figure 10: ^1H and ^{13}C NMR chemical shifts of **88r.**

The 2-D NMR analysis of COSY (Appendix 5.91A – 5.92A) and HMBC (Appendix 5.94A) were used to confirm the identity of compound **88r** through correlation between proton and carbon as presented in Figure 11.

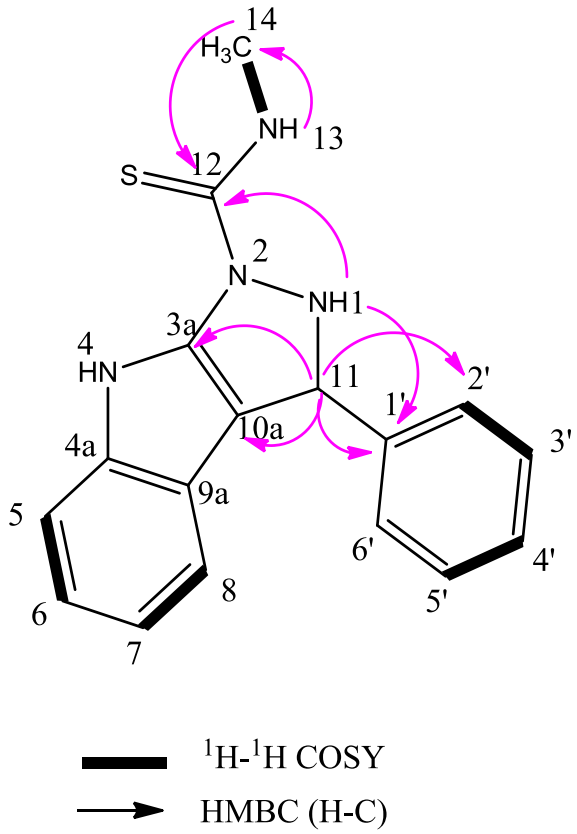

Figure 11: COSY and HMBC correlations of compound **88r.**

The ^{1}H, ^{1}H-COSY spectrum showed strong coupling between H14 (δ 3.08) methyl and NH-13 (δ 8.56) thio-amide protons. A strong coupling oocurred between indole aromatic protons H-8 (δ 7.40) and H-7 (δ 6.86). Another strong coupling occurred between indole aromatic protons H-6 (δ 7.08) and H-5 (δ 7.38). A strong coupling occurred between phenyl protons H-2' (δ 7.33) and H-3' (δ 7.29). Another strong coupling occurred between phenyl protons H-4' (δ 7.17) and H-5' (δ 7.29).

The HMBC spectrum showed the proton and quaternary carbon coupling: H-11 (δ 5.87) coupled with C10a (δ 118.1); H-11 (δ 5.87) coupled with C3a (δ 134.3); H-11 (δ 5.87) coupled with C1' (δ 144.9); H-11 (δ 5.87) coupled with C2' (δ 127.2); NH1 (δ 11.54) pyrazole coupled with C-1' (δ 144.9) and C12 (δ 177.8) ; NH14 (δ 8.56) thio-amide coupled with C12 (δ 177.8).

Finally the mass spectrum (Appendix 5.95A) TOF-MS showed 333.9 [M^{+}+ Na] for the molecular ion confirming compound **88r** as N-methyl-3-phenyl-2, 3-dihydropyrazolo [4, 3-b] indole-1(4H)-carbothioamide. **Scheme 25** depicts other fragments resulted after the loss of phenyl groups.

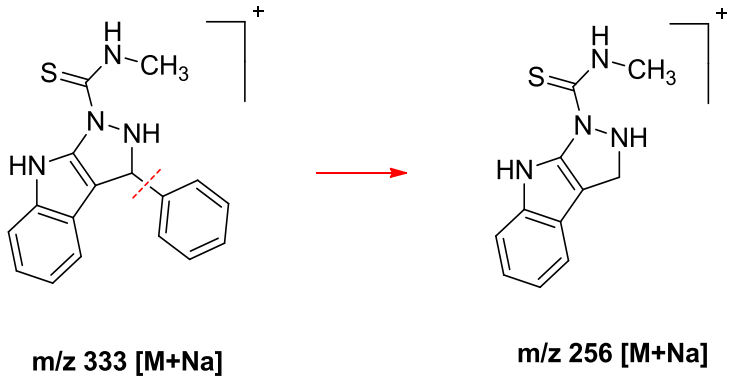

Scheme 25: Proposed fragmentation of compound **88r**.

5.4.5A Antibacterial Activity

The antibacterial activity of synthesized compounds **88a-88z** was performed against bacteria organisms which were *Staphylococcus* aureus, *Citrobacter freundii, Citrobacter diversus, Serratia marcescens, Klebsiella pneumonia and Micrococcus luteus* using Ciprofloxacin as positive and DMSO as negative control. The data is presented in Table 1. The activity was evaluated based on zone of inhibition in millimetre: the compounds observed with zone of inhibition diameter greater than eight (>8mm) were considered as active compounds.

Table 1: Antibacterial activity of compound **88a-88z.**

	Bacteria organisms- zones of inhibition (mm)					
Compounds	**Citrobacter freundii**	**Citrobacter diversus**	**Serratia marcescens**	**Klebsiella pneumoniae**	**Micrococcus luteus**	**Staphylococcus aureus**
88a	0	0	0	0	**0**	0
88b	0	0	0	0	**0**	0
88c	0	0	0	0	**0**	7**±0**
88d	0	6**±0.0**	0	0	**6±0.0**	0
88e	0	0	0	6**±0.0**	**0**	6**±0**
88f	0	0	0	0	**0**	0
88g	6**±0.0**	0	0	0	**0**	0
88h	6**±0.0**	0	0	0	**0**	0
88i	0	0	0	0	**0**	6**±0**
88j	0	0	6**±0.0**	0	**0**	6**±0**
88k	0	0	0	0	**0**	0
88l	6**±0.0**	0	0	0	**7±0.5**	0
88m	0	0	0	0	**0**	0
88n	0	0	0	0	**0**	0
88o	0	0	6**±0.5**	0	**0**	0
88p	0	0	0	6**±0.0**	**0**	0
88q	0	0	0	6**±0.0**	**0**	0
88r	0	0	0	0	**6±0.0**	0
88s	0	0	0	0	0	0
88t	0	0	0	0	**6±0.0**	0
88u	0	0	0	0	0	0
88v	0	0	0	0	**0**	0
88w	0	0	0	0	0	0
88x	0	0	0	0	0	0
88y	0	0	0	0	**6±0.0**	0
88z	0	0	0	0	**7±0.0**	0
Ciprofloxacin	35±0.7	36±0.7	35±0.7	28±1.4	30±0.7	25**±1**

Values are mean ±SD, number of sample (n=3)

Table 1 shows that no inhibitory activity against *Citrobacter freundii*, *Citrobacter diversus*, *Serratia marcescens*, *Klebsiella pneuminiae*, *Micrococcus luteus* and *Staphylococcus aureus.*

5.4.6A Antifungal Activity

The antifungal activity of synthesized compounds **88a-88z** was conducted against fungal organisms such as *Candida albicans, Candida utilis, Saccharomyces cerevisiae, Aspergillus flavus, Aspergillus niger* using Ciprofloxacin as positive and DMSO as negative control. The data is presented in Table 2. The activity was evaluated based on zone of inhibition in millimetre: the compounds observed with zone of inhibition diameter greater than eight (>8mm) were considered as active compounds.

Table 2: Antifungal activity of compound **88a-z**.

	Fungal organism- zones of inhibition (mm)				
Compounds	**Candida albicans**	**Candida utilis**	**Saccharomyces cerevisiae**	**Aspergillus flavus**	**Aspergillus niger**
88a	0	0	0	0	0
88b	0	0	0	0	0
88c	0	0	8±**0.6**	6±**1.5**	0
88d	0	0	0	0	0
88e	0	0	0	0	0
88f	0	0	0	0	0
88g	0	0	0	0	0
88h	0	0	0	0	0
88i	0	12±**0.6**	6±**1.3**	0	6±**0.4**
88j	10±**0.5**	0	0	7±**1.6**	0
88k	0	0	8±**0.6**	6±**1.5**	0
88l	9±**0.6**	11±**0.5**	12±**1.2**	6±**1**	6±**1.4**
88m	0	0	0	0	0
88n	0	0	0	0	0
88o	7±**0**	7±**0.5**	12±**0.6**	6±**0.8**	7±**1.2**
88p	0	0	0	0	0
88q	0	0	0	0	
88r	**7±0.6**	**12±0.6**	**23±1.5**	0	0
88s	**13±0.6**	**9±1.0**	0	0	0
88t	**15±0.6**	**14±1.0**	0	0	0
88u	**8±1.2**	**8±0.6**	**12±1.0**	0	0
88v	**8±1.2**	**8±0.6**	**12±1.0**	0	0
88w	0	0	0	0	0
88x	0	0	**20±1.5**	0	0
88y	0	0	0	0	0
88z	0	0	0	0	0
Amphotericin b	32±**0.2**	30±**0.6**	29±**0.0**	25±**1.6**	22±**1.5**

Values are mean ±SD, number of sample (n=3), 0= no activity

From the Table 2 above, some synthesized compound showed moderate antifungal activity against *Candida albicans, Candida utilis* and *Saccharomyces cerevisiae*. Compound **88t** showed good potency against *Candida albicans* and *Candida utilis* with an inhibition diameter of 15 and 14 mm respectively (Figure 12).

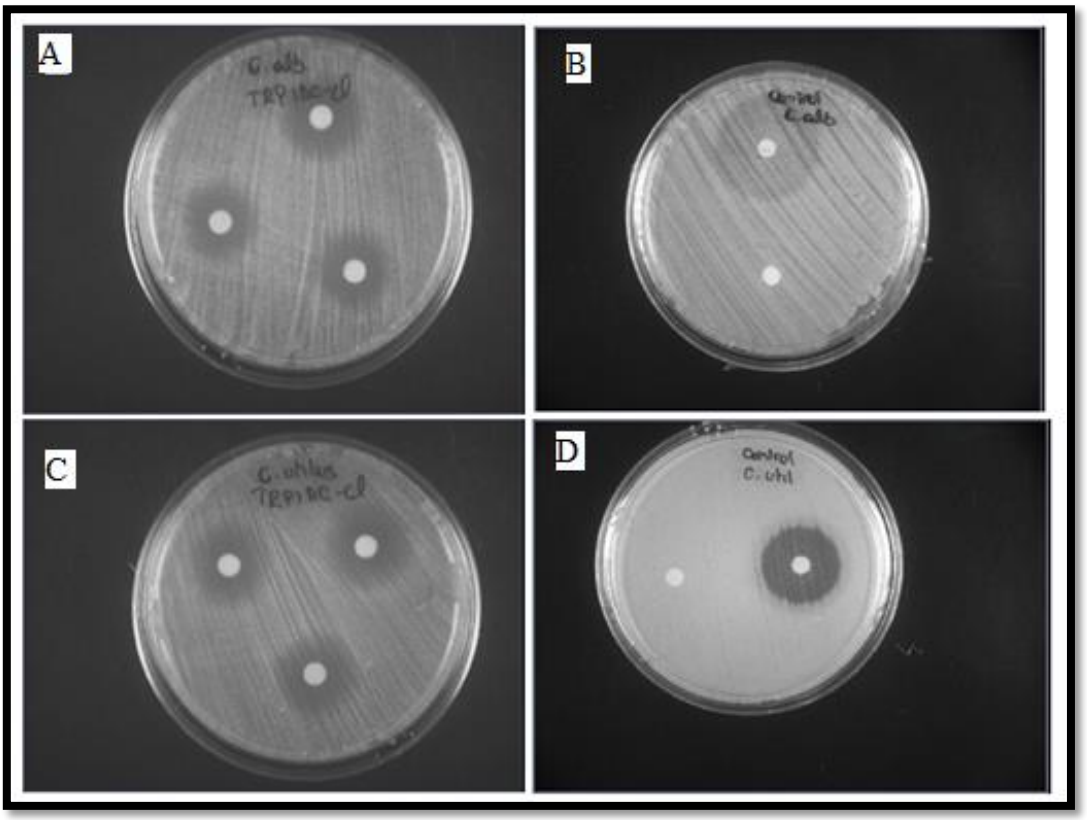

Figure 12: Present moderate zone inhibition activity:

(A) 88t versus (B) *Candadi albicans* (control);

(C) 88t versus (D) *Candida utilus* (control).

Compound **88r** and **88x** showed significant antifungal activity against *Saccharomyces cerevisiae* exhibiting a zone inhibition of 23 and 20 mm respectively (Figure 13).

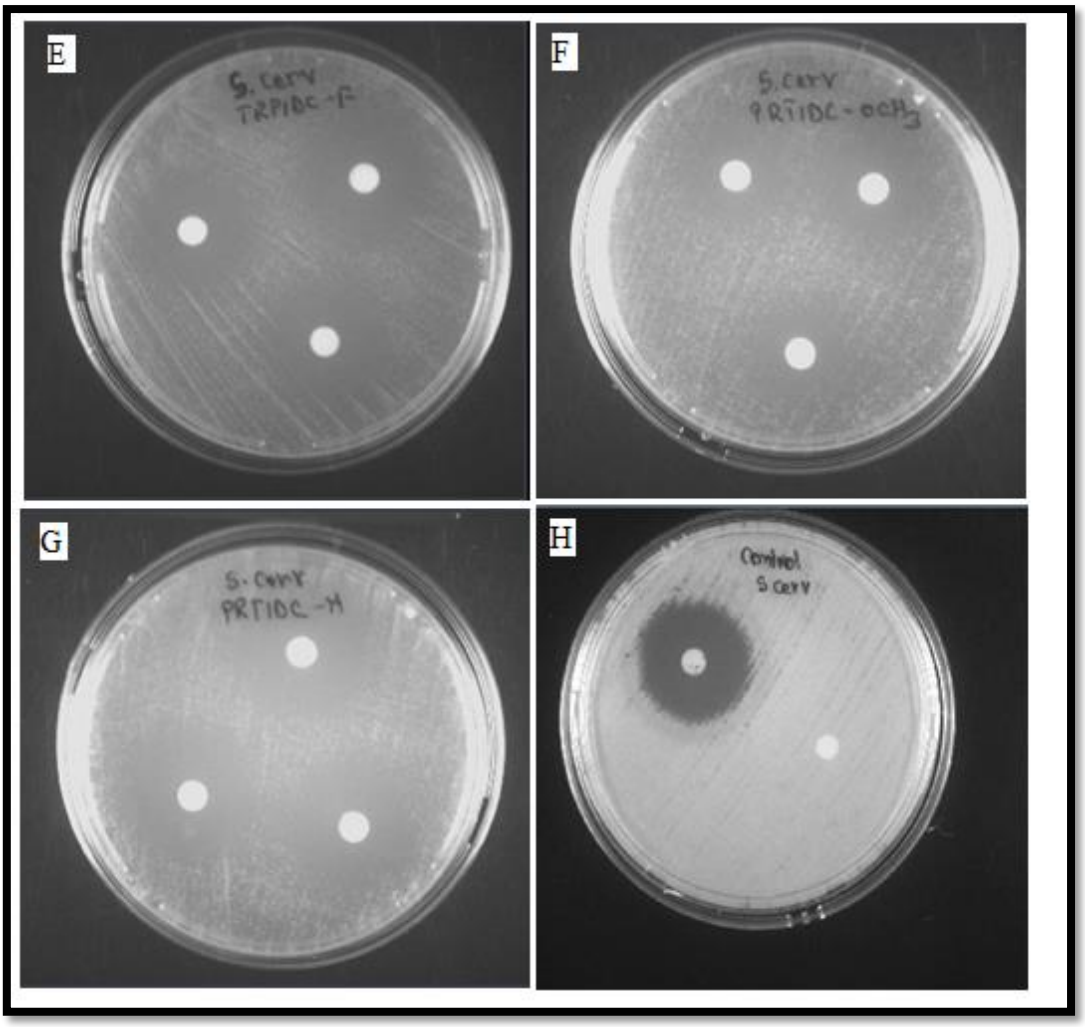

Figure 13: Present antifungal zone inhibition activity:

(E) **88u**, (F) **88x**,

(G) **88r** and (H) *Saccharomyces cerevisiae* (control)

These active compounds closely matched the antifungal activity of the positive control but no inhibitory activity observed against *Aspergillus flavus* and *Aspergillus niger.*

Table3: Antifungal Minimum Inhibition Concentration (MIC) of compound **88i-88x**

	Fungal organism MIC (µM)		
Compounds	**Candida albicans**	**Candida utilis**	**Saccharomyces cerevisiae**
88i	-	0.37	-
88j	0.75	-	-
88k	-	-	1.5
88l	1.5	1.1	0.375
88o	-	-	0.75
88r	-	0.375	0.18
88s	0.75	1.5	-
88t	0.37	0.18	-
88u	1.5	1.5	0.375
88x	-	-	0.18

5.4.7A Mutagenicity Studies

The mutagenic activity of the synthesized compounds was studied to determine their suitability for *in vivo* biological applications. Table 4 & 5 on page 178 and 179, showed that the compounds had no mutagenic activity against *Salmonella tyhphimurium TA* 98 and TA100 strains. None of the tested compounds induced any significant increase in the number of revertant colonies in comparison with the control, sodium azide.

Table 4: Mutagenicity assay of compound **88a-88m**.

Compounds	Mutant Frequency of revertant at different concentrations (µM)				
	5	10	20	100	1000
88a	na	0.08±0.04	na	0.3±0.08	0.631±0.06
	na	0	na	0.06±0.134	0.251±0.14
88b	na	0.08±0.04	na	0.3±0.08	0.631±0.06
	na	0	na	0.06±0.134	0.251±0.14
88c	na	0.2±0.102	na	1±0.342	1.22±0.222
	na	0.2±0.1	na	0.6±0.31	0.82±0.17
88d	na	0.04±0.02	na	0.1±0.09	0.26±0.13
	na	0.35±	na	0.98±0.18	1.5±0.15
88e	na	00.2±0.04	na	0.1±0.07	0.312±0.3
	na	0.1±0.04	na	0.92±0.26	1.41±0.17
88f	na	00.2±0.04	na	0.1±0.07	0.312±0.3
	na	0.1±0.04	na	0.92±0.26	1.41±0.17
88g	na	0.08±0.04	na	0.3±0.08	0.631±0.06
	na	0	na	0.06±0.134	0.251±0.14
88h	na	0.6±0.02		1.0±0.16	1.32±0.1
	na	0	na	0.05±0.02	0.145±0.09
88i	na	0.13±0.17	na	0.56±0.28	0.84±0.8
	na	0.02±0.06	na	0.35±0.9	0.72±0.06
88j	na	0.03±0.3	na	0.1±0.039	0.17±0.23
	na	0.09±0.014	na	0.38±0.047	0.69±0.1
88k	na	0.2±0.102	na	1±0.342	1.22±0.222
	na	0.2±0.1	na	0.6±0.31	0.82±0.17
88l	na	0.13±0.08	na	0.95±0.035	1.11±0.013
	na	0.2±0.06	na	0.86±0.02	1.14±0.017
88m	na	0.02±0.05	na	0.85±0.2	1.18±0.12
	na	0	na	0	0.12±0.03
Sodium Azide	1.056±0.474	2.060±0.5	3.920±0.27	na	na
	1.065±0.26	2.173±0.3	4.50±0.6	na	na

Values are expressed as Mean (±SD), n=3, TA100: Black, TA98: Red, na: not applicable, 0 = no activity

Table 5: Mutagenicity assay of compound **88n-88z**

Compounds	Mutant Frequency of revertant at different concentrations (µM)				
	5	10	20	100	1000
88n	na	00.2±0.04	na	0.1±0.07	0.312±0.3
	na	0.1±0.04	na	0.92±0.26	1.41±0.17
88o	na	0.1±0.03	na	0.3±0.015	0.6±0.017
	na	0.14±0.5	na	0.23±0.019	0.55±0.026
88p	na	0	na	0	0.2±0.01
	na	0	na	0	0.16±0.04
88q	na	0.08±0.04	na	0.3±0.08	0.631±0.06
	na	0	na	0.06±0.134	0.251±0.14
88r	na	0.05±0.97	na	0.1±0.4	0.19±0.7
	na	0.08±0.9	na	0.32±0.4	0.28±0.6
88s	na	0.02±0.6	na	0.51±0.8	0.9±0.3
	na	0.04±0.1	na	0.8±0.41	1.1±0.7
88t	na	0.01±0.045	na	0.16±0.036	0.31±0.05
	na	0.1±0.2	na	0.23±0.052	0.65±0.016
8888u	na	0.09±0.35	na	0.12±0.7	0.39±0.1
	na	0.06±0.9	na	0.14±0.23	0.2±0.12
88v	na	0.09±0.35	na	0.12±0.7	0.39±0.1
	na	0.06±0.9	na	0.14±0.23	0.2±0.12
88w	na	00.2±0.04	na	0.1±0.07	0.312±0.3
	na	0.1±0.04	na	0.92±0.26	1.41±0.17
88x	na	0.4±0.6	na	0.9±0.52	1.3±0.2
	na	0.24±0.51	na	0.63±0.3	0.89±0.8
88y	na	0.05±0.22	na	0.18±0.154	0.4±0.431
	na	0.07±0.563	na	0.5±0.234	0.91±0.322
88z	na	0.09±0.4	na	0.29±	0.8±1.2
		0.08±0.03	na	0.41±0.9	0.79±0.6
Sodium Azide	1.056±0.474	2.060±0.5	3.920±0.27	na	na
	1.065±0.26	2.173±0.3	4.50±0.6	na	na

Values are expressed as Mean (±SD), n=3, TA100: Black, TA98: Red, na: not applicable, 0=no activity

NaN_3 was used to confirm the revertant colonies, if any, in the experiment. In this experiment, it was taken that an increase in the number of revertant colonies was in direct proportion to the concentration.

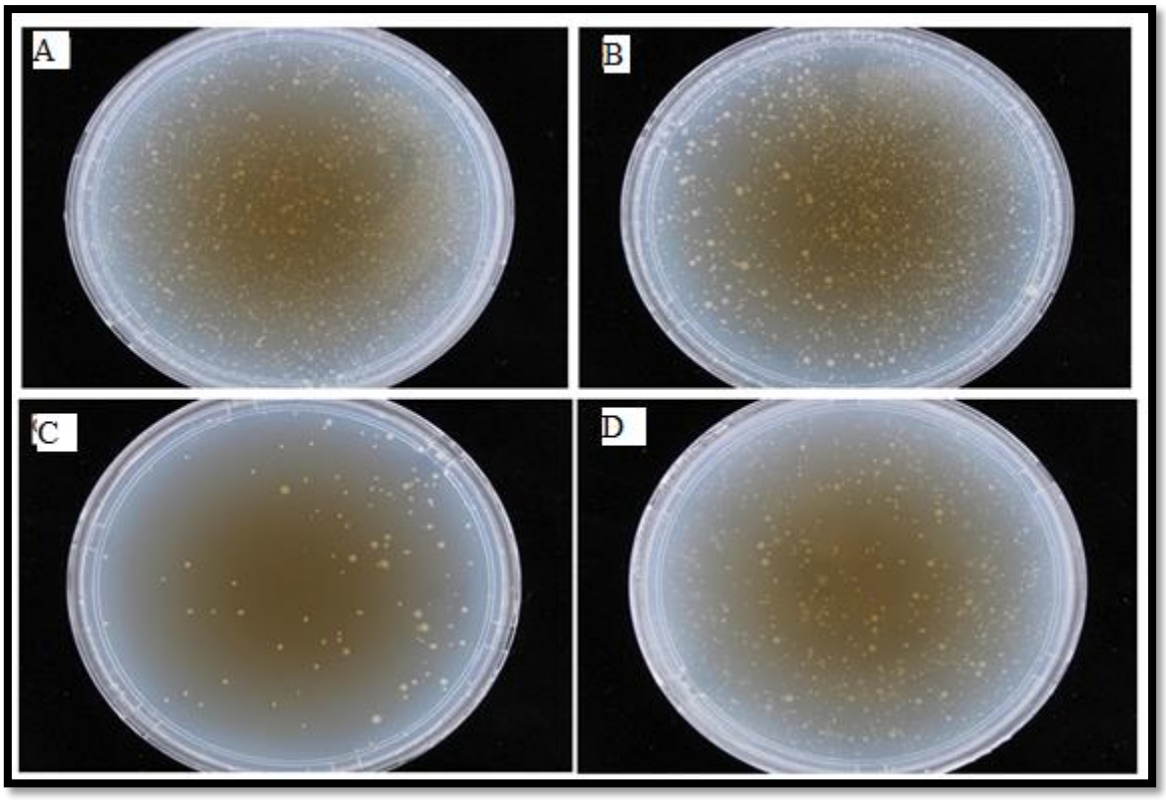

Figure 14: (A) Plate with T 100 showing revertant colonies,

(B) Plate with TA98 showing revertant colonies,

(C) Plate showing revertant colonies of compound **88y** against TA98 at 100 µM,

(D) Plate showing revertant colonies of compound **88h** at 1mg/mL against TA 100.

Part B: **Investigating the generality of the Povarov's reaction using Isoniazid**

Isoniazid **91**, a derivative of pyridine carboxylic acid **93**, was first synthesized in 1912, however, it was only used in 1952 to treat TB (Judge *et al*., 2012: 3940). Since then, **91** has been used as a first line anti-TB drug. Pyridine carboxylic acid, also known as nicotinic acid, is an important class of heterocyclic compounds with diverse biological applications such as Nevirapine **92,** an anti-HIV agent whilst vitamin B3 (Niacin) , plays a pivotal role in various biological processes (Rodrigues *et al*., 2013: 21) (Figure 15). However, **91** is still considered as the magic molecule due to the presence of a hydrazone moiety which has attracted the attention of several researchers owing to its structural reactivity and flexibility (Pahlavani *et al*., 2015: 1). Thus, there are numerous reports about the application of **91** as a key starting material to synthesize different types of derivatives via chalcones, Schiff base and various types of condensation reactions (Judge *et al*., 2012: 3940). It was envisaged that the application of **91** in a Povarov reaction through [3+2] cycloaddition generates new target compounds. This hybridization approach might enable the formation of new drugs with high potential of improved biological activity with respect to the corresponding lead compounds.

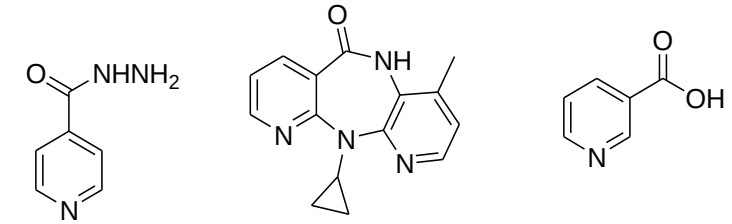

Isoniazid **91** **Nevirapine** **92** **Vitamin B3** **93**

Figure 15: Chemical structures of biological active heterocyclic compounds

(Rodrigues *et al*., 2013: 21-28)

5.4.8B Synthesis and Characterization of (3-Phenyl-2,3-Dihydropyrazolo[3,4-*b*]Indol-1(4H)-yl)(Pyridin-4-yl)Methanone

In this study Povarov's [3+2] cycloaddition approach was used for the synthesis of a novel nicotinyl fused indolo-pyrazole **94a**. A mixture containing benzaldehyde **85**, isoniziad **91** and indole **87** was refluxed in the presence of indium chloride, a Lewis acid catalyst. A reddish brown solid with a melting point of 111 - 113 ^{0}C and 95% yield was obtained: FT-IR, NMR and TOF-MS were successfully used to characterize the compound. Thereafter, different derivatives of benzaldehyde were used to synthesize 10 new derivatives (Scheme 26**)**.

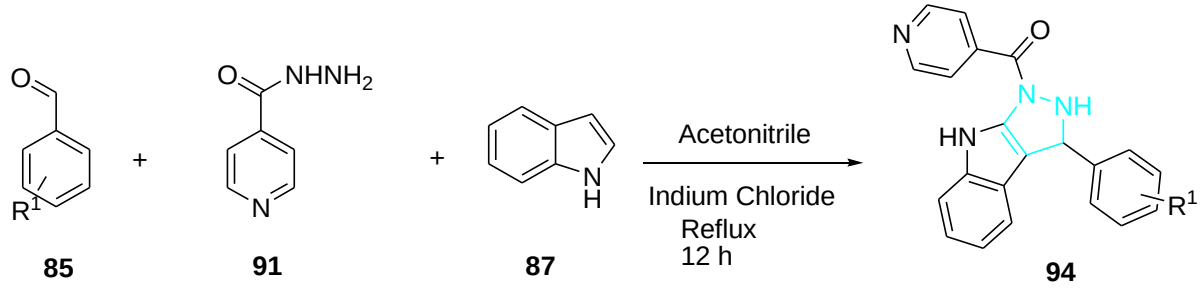

85 **91** **87** **94**

Key: R_1 = H(**6a**), *p*-CH_3(**6b**), *p*-Cl(**6c**), *p*-F(**6d**), *p*-NO_2(**6e**),*o*-NO_2(**6f**), *o*-OH(**6g**), *p*-OCH_3(**6h**), *m* -OCH_3-*p*-OH(**6i**), *m* -OCH_3-*p*- OH-*m*Br(**6j**)

Scheme 26. Synthetic route for the titled compounds **94a- 94j**

94a was chosen as a template to discuss its unambiguous characterization that could be used to authenticate all the other synthesized derivatives.

The FT-IR spectrum (Appendix 5.1B) showed stretching absorptions (cm^{-1}) at 3390, 2929, 1687, 1600, 1415 and 742 cm^{-1} which were assigned to N-H (stretch), C-H (stretch), C=O (stretch), N-H (bend), C-N (stretch) and N-H (out of plane bend), respectively.

The ^{1}H NMR spectrum (Appendix 5.2B – 5.3B) showed singlets at δ (ppm) 10.8 which was assigned to overlapping N-H for the indole and pyrazole moieties, respectively (Figure 2). The aromatic proton C15-CH, C17-CH, C14-CH and C18-CH appeared as multiplets at δ 7.39-7.34) (4H, m) corresponded to the pyridine –CH. The phenyl ring exhibited five protons: C4'-CH appeared as a triplet at 7.18 (1H, t, *J* = 7.4 Hz), C3'-CH and C5'-CH appeared as a triplet at 7.05-7.01 (2H, t, *J* = 7.5 Hz), C2'-CH and C6'-CH appeared as doublets at δ 7.30 (2H, d, *J* = 7.5 Hz). Whilst the indole ring exhibited four protons: C8-CH appeared as doublets at δ 7.30 (1H, d, *J* = 7.5 Hz), C7-CH appeared as triplets at 6.9 (1H, t, *J* = 7.6 Hz), C6-CH appeared as a triplet at δ 7.05 (1H, t, *J* = 8.0 Hz), and C5-CH

appeared as doublets at 6.9 (1H, d, *J* = 7.6 Hz). Aliphatic proton C11-CH appeared as singlet at δ 5.9 (1H, s), see Figure 2.

The ^{13}C NMR (Appendix 5.4B), DEPT (Appendix 5.5B) and HSQC (Appendix 5.7B) spectra showed the presence of thirteen CH carbons at δ 39.8 (C11), 111.9 (C5), 119.6 (C7 & C8), 121.3 (C6), 126.3 (C4'), 127.0 (C2' & C6'), 129.0 (3' & C5'), 129.0 (C14-C18). Also seven quaternary carbons resonated at δ 118.6 (C10a), 119.6 (C9a), 137.1 (C3a & C4a), 145.4 (C1' & C13) and 172.5 (C12), see Figure 16.

The 2-D NMR analysis of COSY (Appendix 5.6B) and HMBC (Appendix 5.8B) were used to confirm the identity of compound **6a** through correlation between proton and carbon as presented in Figure 17.

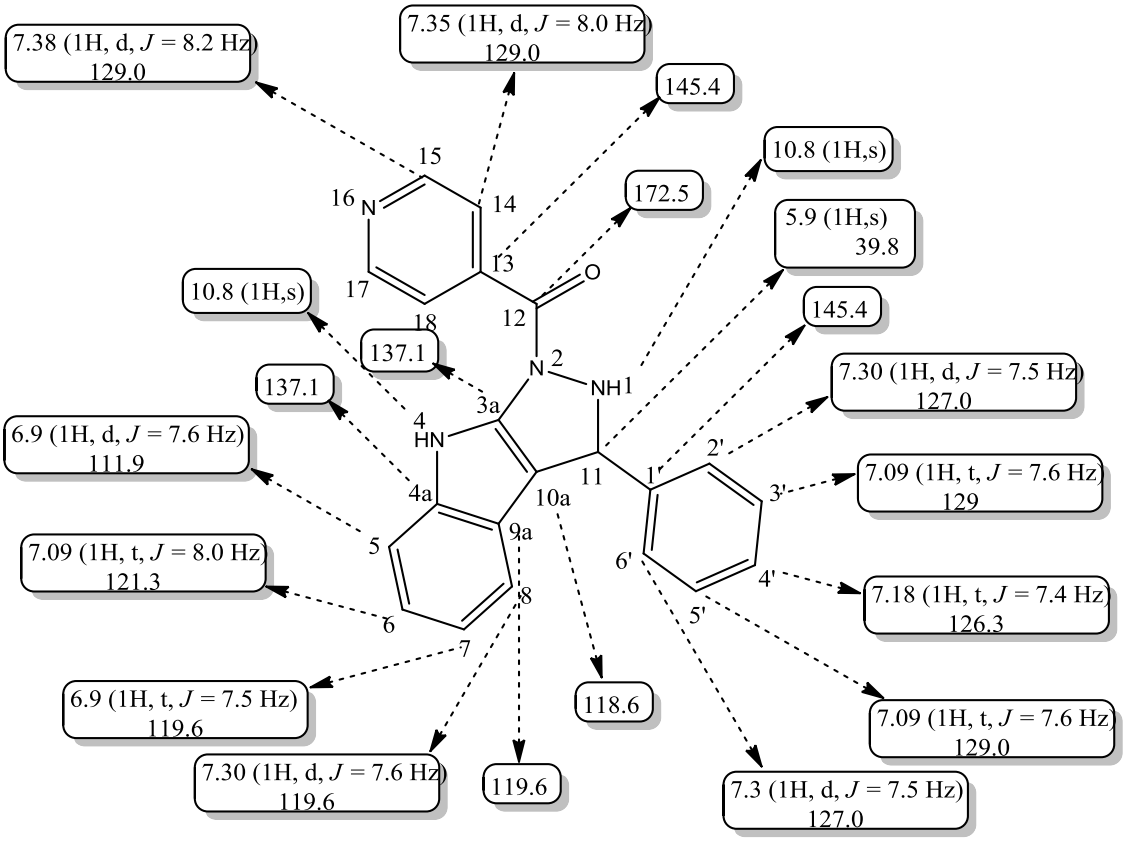

Figure 16: ^{1}H and ^{13}C NMR chemical shifts of **6a**.

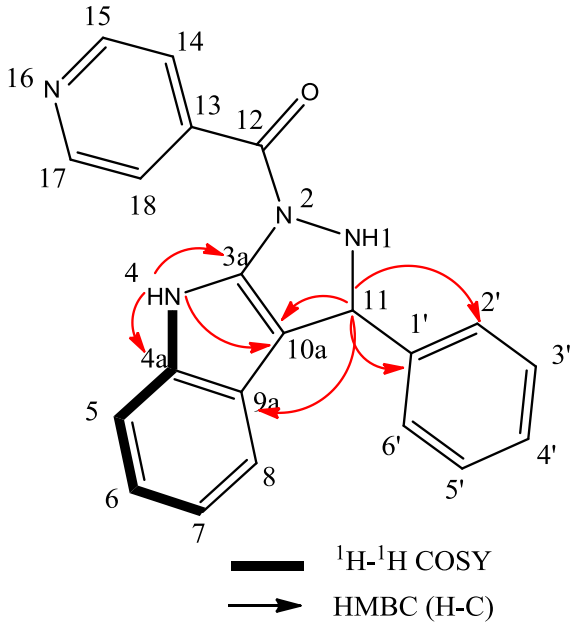

Figure 17: COSY and HMBC correlations of compound **94a.**

The ^{1}H, ^{1}H-COSY spectrum showed strong coupling between H-5 (δ 6.9) and H-6 (δ 7.0). Another strong coupling occurred between H-6 (δ 7.0) and H-7 (δ 6.9). Strong coupling occurred between the indole NH-4 (δ 10.8) and H-5 (δ 6.9). The HMBC spectrum showed the proton and quaternary carbon coupling: H-11 (δ 5.9) coupled with C1' (δ 145.4); H-11 (δ 5.9) coupled with C2' (δ 127.0) and C6' (δ 127.0); H-11 (δ 5.9) coupled with C9a (δ 118.6); H-11 (δ 5.9) coupled with C10a (δ 119.6); H-14 (δ 10.8) coupled with C3a (δ 137.7), C4a (δ 137.7) and C10a (δ 118.6). Finally in the mass spectrum (Appendix 5.9B) TOF-MS showed 341.1 [M^+] for the molecular ion confirming **94a** as (3-phenyl-2,3-dihydropyrazolo[3,4-*b*]indol-1(4H)-yl)(pyridin-4-yl)methanone. As mentioned earlier, after characterizing **94a**, different derivatives of benzaldehyde were used (Figure 4) to synthesize another nine other new compounds.

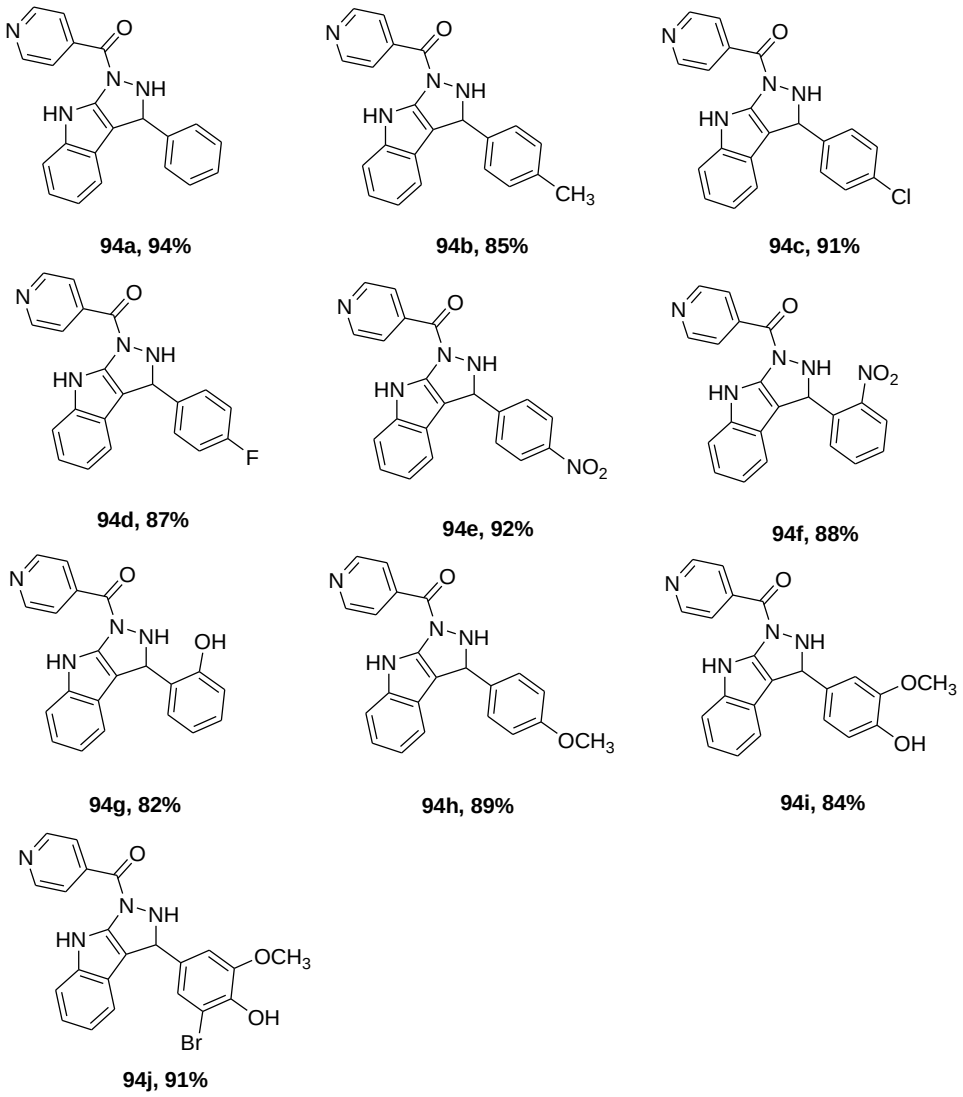

Figure 18: Novel synthesized nicotinyl fused indolo-pyrazole derivatives

5.4.9B Antibacterial Activity

The antibacterial activity of **94a**-**94j** was assessed against bacterial organisms *Bacillus cereus, Bacillus coagullans, Escherichia coli, Streptococcus faecalis and Micrococcus luteus* using Ciprofloxacin as positive and DMSO as negative control. The data as presented in Table 6. The antibacterial activity was evaluated based on zone of inhibition in millimetre: the compounds with zone of inhibition diameter greater than eight (>8mm) were considered as active compounds.

Table 6: Antibacterial activity of compound **94a-94j.**

	Bacteria organisms- zones of inhibition (mm)				
Compounds	**Bacillus. cerieus**	**Bacillus. coagullans**	**Escherichia. coli**	**Micrococcus. luteus**	**Streptococcus. faecalis**
94a					
94b			7±0.4		
94c					
94d					
94e	8±0.4	9±0.6		9±0.4	9±0.4
94f	8±0.3	9±0.8		9±0.2	9±0.3
94g					
94h					
94i	8±0.2		6±0.8		8±0.3
94j				9±0.4	
Ciprofloxacin	35±0.6	36±0.8	35±0.6	28±1.4	30±0.4

Values are mean ±SD, number of sample (n=3)

From the Table 6 above, compounds **94e** and **94f** showed slight antibacterial activity against *Bacillus cerieus, Bacillus coagullans, Micrococcus luteus* and *Streptococcus faecalis* with a zone of inhibition diameter ranging from 8 - 9 mm whilst **94j** only showed antibacterial activity against *Micrococcus luteus* with a zone of inhibition diameter of 9 mm (Figure 19).

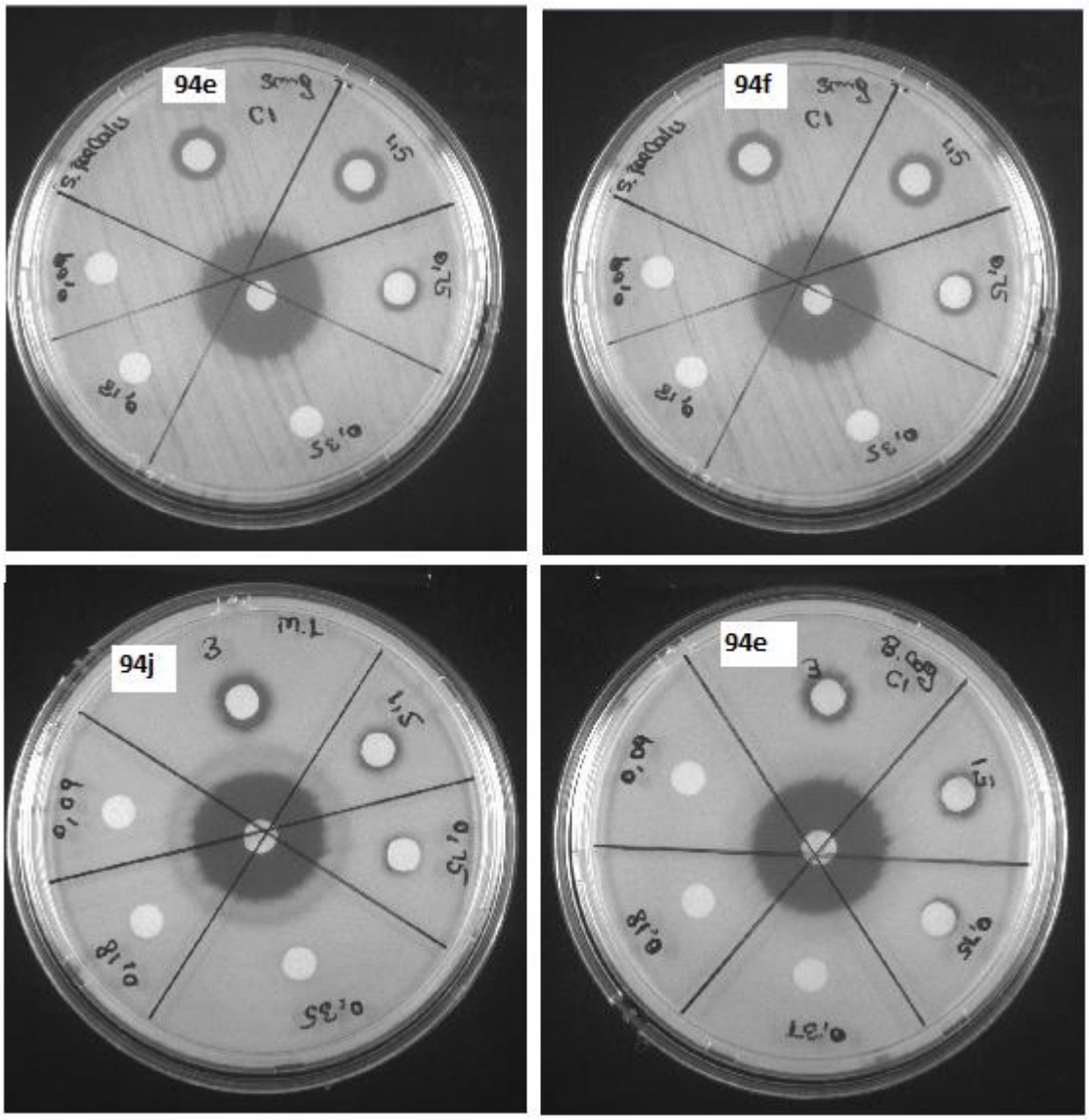

Figure 19: Present moderate zone of inhibitory activity for:

Compound **94e** and **94f** against *Streptococcus faecalis*,

Compound **94e** against *Bacillus coagullans*,

Compound **94j** against *Micrococcus luteus.*

Figure 19 above, shows the zone of inhibition for the active compounds and also illustrates their MIC values which was 0.75 µM for all active compounds.

5.4.10B Antifungal Activity

The antifungal activity of **94a-94j** was conducted against fungal organisms such as *Candida albicans, Candida utilis and Setaria cervi* using Amphotericin B as positive and DMSO as negative control. The activity was evaluated based on zone of inhibition in millimetre: the compounds with zone of inhibition diameter greater than eight (>8mm) were considered as active compounds. There was no inhibitory activity observed against tested fungal organisms (Figure 20).

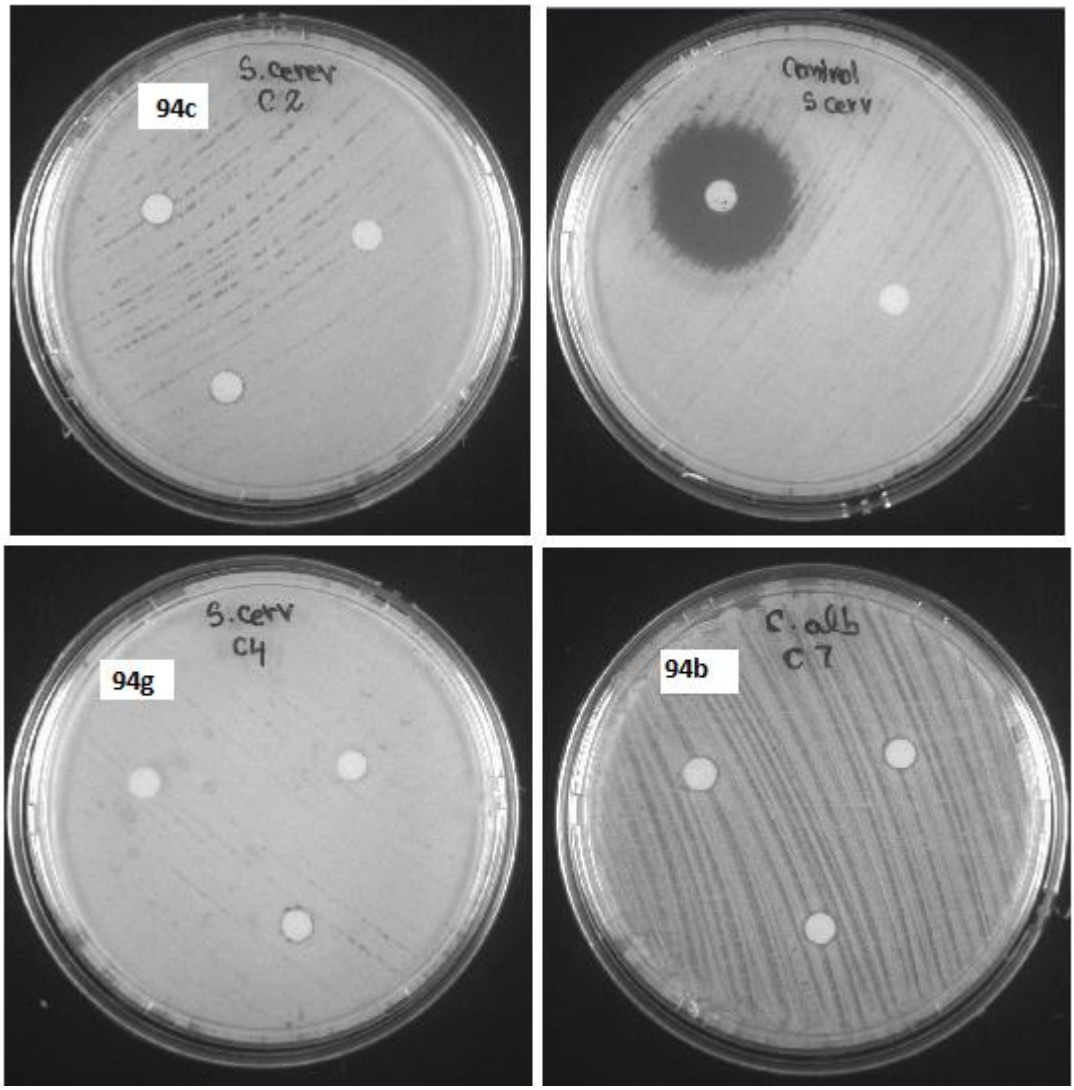

Figure 20: Present no inhibitory activity for the synthesized compound against *Setaria cervi*, and

Candida albicans

5.4.11B Mutagenicity Studies

The mutagenic activity of **94a-94j** was studied to determine their suitability for *in vivo* biological applications. Table 7 showed that the compounds had no mutagenic activity against *Salmonella typhimurium* TA 98 and TA100 strains. None of the tested compounds induced any significant increase in the number of revertant colonies in comparison with the control, sodium azide.

Table 7: Mutagenicity assay of compound **94a-94j**

Compounds	**Mutant Frequency of revertant at different concentrations (µM)**				
	5	10	20	100	1000
94a	na	0.4±0.6	na	0.9±0.52	1.3±0.2
	na	0.24±0.51	na	0.63±0.3	0.89±0.8
94b	na	0.05±0.22	na	0.18±0.154	0.4±0.431
	na	0.07±0.563	na	0.5±0.234	0.91±0.322
94c	na	0.09±0.4	na	0.29±	0.8±1.2
		0.08±0.03	na	0.41±0.9	0.79±0.6
94d	na	0.08±0.04	na	0.3±0.08	0.631±0.06
	na	0	na	0.06±0.134	0.251±0.14
94e	na	0.05±0.97	na	0.1±0.4	0.19±0.7
	na	0.08±0.9	na	0.32±0.4	0.28±0.6
94f	na	0.02±0.6	na	0.51±0.8	0.9±0.3
	na	0.04±0.1	na	0.8±0.41	1.1±0.7
94g	na	0.01±0.045	na	0.16±0.036	0.31±0.05
	na	0.1±0.2	na	0.23±0.052	0.65±0.016
94h	na	0.09±0.35	na	0.12±0.7	0.39±0.1
	na	0.06±0.9	na	0.14±0.23	0.2±0.12
94i	na	0.09±0.35	na	0.12±0.7	0.39±0.1
	na	0.06±0.9	na	0.14±0.23	0.2±0.12
94j	na	00.2±0.04	na	0.1±0.07	0.312±0.3
	na	0.1±0.04	na	0.92±0.26	1.41±0.17
Sodium Azide	1.056±0.474	2.060±0.5	3.920±0.27	na	na
	1.065±0.26	2.173±0.3	4.50±0.6	na	na

Values are expressed as Mean (±SD), n=3, TA100: Black, TA98: Red, na: not applicable, 0 = no activity

5.5 Conclusion

In this study, Povarov's reaction via [3+2] cycloaddition was used to synthesize 36 novel fused indolo-pyrazole compounds. This approach enabled a one pot synthesis of fused indolo-pyrazole from readily available substrates viz. benzaldehyde, indole and semicarbazide.
All synthesized compound were screened against bacterial and fungal organisms. Compounds **88r** and **88x** showed a significantly good antifungal activity against *Saccharomyces cerevisiae* with zone of inhibition diameter of 23 and 20 mm, respectively. However, no antibacterial activity were observed against *Citrobacter freundii, Citrobacter diversus, Serratia marcescens, Klebsiella pneumonia, Micrococcus luteus* and *Staphylococcus aureus*. In addition, Povarov reaction via a [3+2] cycloaddition was further investigated to demonstrate it generality by using isoniziad, benzaldehyde and indole. This approach enabled a one pot synthesis of ten nicotinyl fused indolo-pyrazole derivatives in good yield. Antimicrobial activity were conducted on the synthesized compounds using bacterial and fungal organisms. Compounds **94e** and **94f** showed weak antibacterial activity against *Streptococcus faecalis, Micrococcus luteus and Bacillus coagullans* with a zone of inhibition diameter of 9 mm. Compound **94j** also showed weak activity against *Micrococcus luteus* with a zone inhibition diameter of 9 mm. The MIC of these slightly active compounds was 0.75 µM. No antifungal activity was observed against *Candida albicans, Candida utilis* and *Setaria cervi*. All the synthesized compounds showed no mutagenic activity against *Salmonella tyhphimurium* TA 98 and TA100 strains. Hence, all the synthesized compounds can be safely used for further biological screening.

5.6A Experimental

5.6.1A Typical Procedure for the Multi-Component Synthesis of Fused Novel 3-Phenyl-2, 3-Dihydropyrazolo [3, 4-*b*] Indole-1(4H)-Carbothioamide (88a-88h)

A mixture of benzaldehyde derivatives **85** (1 mmol), thio-semicarbazide **86a** (1 mmol) and indole **87** (1 mmol), in acetonitrile (20 mL), was refluxed for 12 hours. The reaction product was poured into ice-water and the precipitate was collected by filtration, washed with water and dried. The resulting crude product was purified by column chromatography using a solvent system of hexane: ethyl acetate (88:12) to isolate a reddish brown solid compounds **88a-88h**

with good yields. All synthesized compounds were characterized by FTIR, NMR and TOF-MS. The spectroscopic data for all synthesized derivatives is presented below.

5.6.1.1A The Spectroscopic Analysis of 88a-88h

3-phenyl-2,3-dihydropyrazolo[3,4-*b*]indole-1(4H)-carbothioamide (88a)

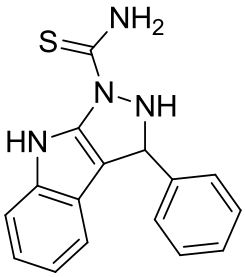

88a

Yield 93%, reddish brown solid, m.p. 111 - 113 ^{0}C. **IR (KBr):** ν 3456-3384 (N-H), 1504 (C=S), 1333 (C-N) and 726 (N-H) cm $^{-1}$. **^{1}H NMR (400 MHz, DMSO-d$_6$):** δ 10.9 (s, N-H) indole & pyrazole, 2.0 (s, N-H) thioamide, 7.5 (2H, d, *J* = 8.2 Hz), 7.4 (2H, d, *J*= 8.2 Hz), 7.3 (2H, t, *J* = 7.6 Hz), 7.2 (1H, t, *J* = 7.6 Hz), 7.1 (1H, t, *J* = 7.6 Hz), 6.9 (1H, t, *J* = 7.6 Hz), 5.8 (1H,s) ppm. **^{13}C NMR (400 MHz, DMSO-d$_6$):** δ 39.8, 111.5, 118.2, 119.2, 120.9, 123.6, 125.8, 126.7, 128.3, 136.7, 145.0, 170.4 ppm. **TOF-MS** found: 319.1 [M^{+}+ Na], **TOF-MS** calculated: 294.4[M^{+}].

3-(p-tolyl)-2,3-dihydropyrazolo[3,4-*b*]indole-1(4H)-carbothioamide (88b)

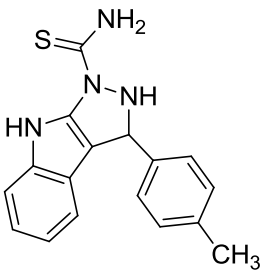

88b

Yield 78%, reddish brown solid, m.p. 114 - 116 ^{0}C. **IR (KBr)**: ν 3456-3383 (N-H), 1505 (C=S), 1334 (C-N) and 726 (N-H) cm $^{-1}$. **^{1}H NMR (400 MHz, DMSO-d$_6$)**: δ 10.9 (s, N-H)

indole & thio-amide, 2.0 (s, N-H) pyrazole , 7.5 (1H, d, *J* = 7.6 Hz), 7.4 (1H, d, *J* = 7.6 Hz), 7.3 (2H, d, *J* = 7.6 Hz), 7.1 (2H, d, *J* = 7.6 Hz), 7.1 (1H, t, *J* = 8.0 Hz), 6.9 (1H, t, *J* = 8.0 Hz), 5.8 (1H, s), 2.3 (s, CH_3) ppm. **^{13}C NMR (400 MHz, DMSO-d$_6$)**: δ 20.6, 39.8, 111.4, 118.2, 118.3, 119.2, 120.8, 123.5, 126.7, 128.8, 134.6, 136.7, 141.9, 170.4 ppm. **TOF-MS** found: 333.1 [M^++ Na], **TOF-MS** calculated: 308.4 [M^+].

3-(4-chlorophenyl)-2,3-dihydropyrazolo[3,4-*b*]indole-1(4H)-carbothioamide (88c)

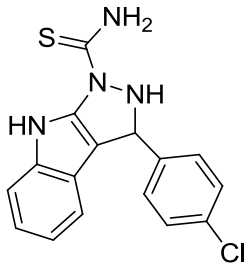

88c

Yield 81%, reddish brown solid, m.p. 132 - 134 ^{0}C. **IR (KBr)**: ν 3390 (N-H), 1505 (C=S), 1333 (C-N) and 726 (N-H) cm $^{-1}$. **^{1}H NMR (400 MHz, DMSO-d$_6$)**: δ 10.9 (s, N-H) indole & thio-amide, 2.0 (s, N-H) pyrazole , 7.4 (2H, d, *J* = 7.6 Hz), 7.3 (2H, d, *J*= 7.6 Hz), 7.1 (2H, d, *J* = 7.6 Hz), 6.9 (1H, t, *J* = 8.0 Hz), 6.8 (1H, t, *J* = 8.0 Hz), 5.9 (1H, s) ppm. **^{13}C NMR (400 MHz, DMSO-d$_6$)**: δ 39.9, 111.5, 117.6, 118.3, 119.0, 120.9, 123.6, 128.0, 128.8, 130.0, 136.6, 137.1, 143.9, 170.3 ppm. **TOF-MS** found: 351.0 [M^+ + Na], **TOF-MS** calculated: 328.8 [M^+].

3-(4-fluorophenyl)-2,3-dihydropyrazolo[3,4-*b*]indole-1(4H)-carbothioamide (88d)

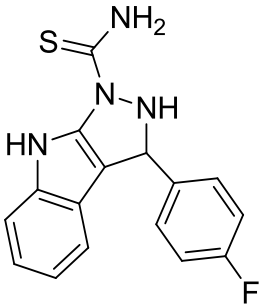

88d

Yield 91%, reddish brown solid, m.p. 117 - 119 ^{0}C. **IR (KBr)**: ν 3388 (N-H), 1506 (C=S), 1335 (C-N) and 811 (N-H) cm $^{-1}$. **^{1}H NMR (400 MHz, DMSO-d$_6$)**: δ 10.9 (s, N-H) indole & thio-amide, 2.0 (s, N-H) pyrazole , 7.5 (1H, d, *J* = 7.6 Hz), 7.4 (1H, d, *J*= 7.6 Hz), 7.3 (2H, t, *J*

= 8.0 Hz), 7.1 (2H, d, *J* = 7.6 Hz), 7.1 (1H, t, *J* = 8.0 Hz), 6.9 (1H, t, *J* = 8.0 Hz), 5.9 (s, CH) ppm. **^{13}C NMR (400 MHz, DMSO-d$_6$)**: δ 39.8, 111.5, 114.5, 118.0, 118.3, 119.1, 121.0, 123.6, 129.9, 130.0, 136.7, 141.1, 161.8, 170.5 ppm. **^{19}F NMR (400 MHz, DMSO-d$_6$)**: δ -61.6 ppm (Ar-F). **TOF-MS** found: 337.0 [M^+ + Na], **TOF-MS** calculated: 312.4 [M^+].

3-(4-nitrophenyl)-2,3-dihydropyrazolo[3,4-*b*]indole-1(4H)-carbothioamide (88e)

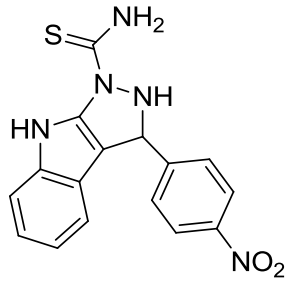

88e

Yield 82%, reddish brown solid, m.p. 116 - 118 ^{0}C. **IR (KBr)**: ν 3385 (N-H), 1503 (C=S), 1335 (C-N) and 744 (N-H) cm $^{-1}$. **^{1}H NMR (400 MHz, DMSO-d$_6$)**: δ 10.9 (s, N-H) indole & thio-amide, 2.0 (s, N-H)pyrazole, 8.2 (2H, d, *J* = 7.6 Hz), 8.1 (1H, d, *J* = 7.6 Hz), 7.6 (2H, d, *J* = 7.6 Hz), 7.4 (1H, d, *J* = 7.6 Hz), 7.1 (1H, t, *J* = 8.0 Hz), 6.9 (1H, t, *J* = 8.0 Hz), , 6.0 (s, CH) ppm. **^{13}C NMR (400 MHz, DMSO-d$_6$)**: δ 39.8, 111.6, 116.6, 118.4, 118.9, 121.1, 123.4, 123.8, 126.3, 129.4, 136.6, 145.7, 153.1, 170.4 ppm. **TOF-MS** found: 366.1 [M^++ Na], **TOF-MS** calculated: 339.4 [M^+].

3-(4-methoxyphenyl)-2, 3-dihydropyrazolo [3, 4-*b*] indole-1(4H)-carbothioamide (**88f)**

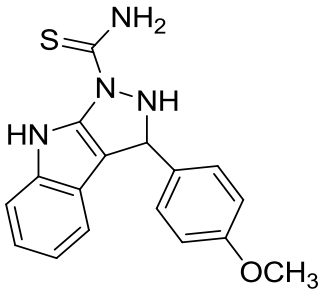

88f

Yield 84%, reddish brown solid, m.p. 114 - 116 ^{0}C. **IR (KBr)**: ν 3445 (N-H), 1503 (C=S), 1333 (C-N), 1070 (C-O) and 744 (N-H) cm $^{-1}$. **^{1}H NMR (400 MHz, DMSO-d$_6$)**: δ 10.9 (s, N-H) indole & thio-amide, 2.0 (s, N-H)pyrazole , 7.4 (1H, d, *J* = 7.6 Hz), 7.3 (3H, d, *J* = 7.6 Hz),

7.1 (1H, t, *J* = 8.0 Hz), 6.9 (1H, d, *J* = 8.0 Hz), 6.8 (1H, t, *J* = 8.0 Hz), 5.8 (s, CH), 3.7 (s, OCH_3) ppm. **^{13}C NMR (400 MHz, DMSO-d$_6$)**: δ 39.8, 54.8, 111.4, 113.4, 118.1, 118.5, 119.2, 120.8, 123.4, 126.7, 129.2, 136.6, 136.9, 157.3, 170.3 ppm. **TOF-MS** found: 349.0 [M^+ + Na], **TOF-MS** calculated: 324.4 [M^+].

3-(4-hydroxy-3-methoxyphenyl)-2, 3-dihydropyrazolo [3, 4-*b*] indole-1(4H)-carbothioamide (88g)

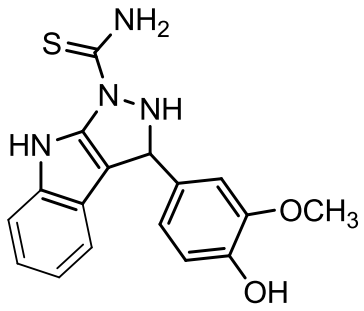

88g

Yield 88%, reddish brown solid, m.p. 127 - 129 ^{0}C. **IR (KBr)**: ν 3388 (N-H), 1504 (C=S), 1333 (C-N), 1010 (C-O) and 734 (N-H) cm $^{-1}$. **^{1}H NMR (400 MHz, DMSO-d$_6$)**: δ 10.9 (s, N-H) indole & thio-amide, 2.0 (s, N-H)pyrazole, 8.7 (s, OH), 7.4 (1H, d, *J* = 7.6 Hz), 7.3 (1H, d, *J* = 7.6 Hz), 7.1 (1H, t, *J* = 8.0 Hz), 7.0 (1H, d, *J* = 8.0 Hz), 6.9 (1H, s), 6.8 (1H, d, *J* = 7.6 Hz), 6.7 (1H, t, *J* = 8.0 Hz), 5.8 (1H, s), 3.7 (s, OCH_3) ppm. **^{13}C NMR (400 MHz, DMSO-d$_6$)**: δ 39.8, 55.6, 111.4, 112.8, 115.0, 118.0, 118.6, 119.2, 120.5, 120.8, 123.4, 135.9, 136.6, 144.5, 147.2, 170.3 ppm. **TOF-MS** found: 365.1 [M^++ Na], **TOF-MS** calculated: 340.4 [M^+].

3-(3-bromo-4-hydroxy-5-methoxyphenyl)-2, 3-dihydropyrazolo [3, 4-*b*] indole- 1(4H)-carbothioamide (88h)

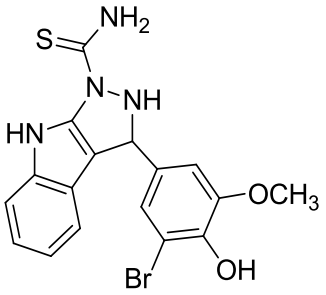

88h

Yield 87%, reddish brown solid, m.p. 131 - 133 ^{0}C. **IR (KBr)**: ν 3386 (N-H), 1506 (C=S), 1335 (C-N), 1040 (C-O) and 744 (N-H) cm $^{-1}$. **^{1}H NMR (400 MHz, DMSO-d$_6$)**: δ 10.9 (s, N-H) indole & thio-amide, 2.0 (s, N-H)pyrazole , 9.2 (s, OH), 7.4 (2H, m), 7.1 (1H, t, *J* = 8.0 Hz), 7.0 (1H, d, *J* = 8.0 Hz), 6.9 (1H, d, *J* = 8.0 Hz), 6.8 (1H, t, *J* = 8.0 Hz), 5.8 (s, CH), 3.7 (s, OCH_3) ppm. **^{13}C NMR (400 MHz, DMSO-d$_6$)**: δ 39.8, 55.1, 108.9, 111.4, 111.7, 117.9, 118.2, 119.0, 120.9, 123.5, 125.9, 136.5, 137.1, 141.7, 148.1, 170.3 ppm. **TOF-MS** found: 443.0 [M^+ + Na], **TOF-MS** calculated: 419.3 [M^+].

5.6.2A Typical Procedure for the Multi-Component Domino Synthesis of Novel N, 3-Diphenyl-2, 3-Dihydropyrazolo [3, 4-*b*] Indole-1(4H)-Carbothioamide (88i-88q)

A mixture of benzaldehyde derivatives **85** (1 mmol), N-phenyl thio-semicarbizide **86b** (1 mmol) and indole **87** (1 mmol) in acetonitrile (20 mL) was refluxed for 12 hours. The reaction product was poured into ice-water and the precipitate was collected by filtration, washed with water and dried. The resulting crude product was purified by column chromatography using a solvent system of hexane: ethyl acetate (88:12) to isolate reddish brown solid compounds **88i-88q** with good yields. All synthesized compounds were characterized by Infrared, Nuclear Magnetic Resonance and Mass Spectroscopy. The spectroscopic data for all synthesized derivatives is presented below.

5.6.2.1A The Spectroscopic Analysis of 88i-88q

N, 3-diphenyl-2,3-dihydropyrazolo[3,4-*b*]indole-1(4H)-carbothioamide (88i)

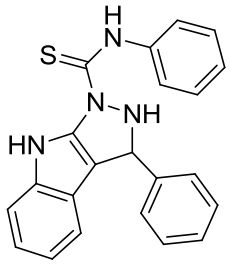

88i

Yield 93%, reddish brown solid, m.p. 138 - 140 ^{0}C. **IR (KBr):** ν 3383 (N-H), 1503 (C=S), 1336 (C-N) and 736 (N-H) cm $^{-1}$. **^{1}H NMR (400 MHz, DMSO-d$_6$):** δ 11.8 (s, N-H) thio-amide, 10.8 (s, N-H) indole, 10.1 (s, N-H) pyrazole, 7.9 (2H, d, *J* = 7.6 Hz), 7.6 (1H, d, *J* = 7.6 Hz), 7.4 (1H, d, *J* = 7.6 Hz), 7.4 (2H, d, *J* = 7.6 Hz), 7.3 (2H, d, *J* = 7.6 Hz), 7.2 (2H, d, *J* = 7.6 Hz), 7.2 (1H, t, *J* = 8.0 Hz), 7.0 (1H, t, *J* = 8.0 Hz), 6.9 (1H, t, *J* = 8.0 Hz), 6.8 (1H, t, *J* = 8.0 Hz), 5.8 (s, CH) ppm. **^{13}C NMR (400 MHz, DMSO-d$_6$):** δ 39.9, 111.4, 118.0, 118.1, 119.1, 120.8, 123.4, 125.8, 126.6, 127.9, 128.3, 128.6, 129.9, 133.9, 136.5, 142.0, 144.9, 176.0 ppm. **TOF-MS** found: 370.1 [M^{+}], **TOF-MS** calculated: 370.7 [M^{+}].

N-phenyl-3-(*p*-tolyl)-2, 3-dihydropyrazolo [3, 4-*b*] indole-1(4H)-carbothioamide (88j)

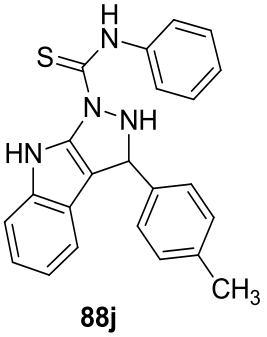

88j

Yield 83%, reddish brown solid, m.p. 141 - 143 ^{0}C. **IR (KBr):** ν 3378 (N-H), 1505 (C=S), 1336 (C-N) and 736 (N-H) cm $^{-1}$. **^{1}H NMR (400 MHz, DMSO-d$_6$):** δ 11.8 (s, N-H) thio-amide , 10.8 (s, N-H) indole, 10.1 (s, N-H) pyrazole, 7.8 (2H, d, *J* = 7.6 Hz), 7.6 (1H, d, *J* = 7.6 Hz), 7.4 (1H, d, *J* = 7.6 Hz), 7.3 (2H, d, *J* = 7.6 Hz), 7.3 (2H, d, *J* = 7.6 Hz), 7.2 (2H, d, *J* = 7.6 Hz), 7.1 (1H, t, *J* = 8.0 Hz), 6.9 (1H, t, *J* = 8.0 Hz), 6.8 (1H, d, *J* = 8.0 Hz), 5.8 (s, CH), 2.5 (s, CH_3) ppm. **^{13}C NMR (400 MHz, DMSO-d$_6$):** δ 21.0, 39.8, 111.4, 118.0, 118.2, 119.1, 120.7,

123.4, 125.8, 126.6, 127.5, 128.6, 129.6, 134.5, 136.6, 139.8, 143.0, 175.9 ppm. **TOF-MS** found: 380.0 [M^+], **TOF-MS** calculated: 384.5 [M^+]..

3-(4-chlorophenyl)-N-phenyl-2, 3-dihydropyrazolo [3, 4-*b*] indole-1(4H)- carbothioamide (88k)

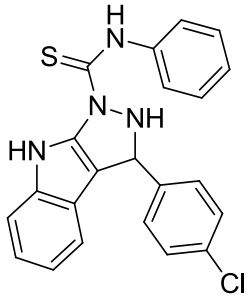

88k

Yield 87%, reddish brown solid, m.p. 136 - 138 ^{0}C. **IR (KBr):** ν 3385 (N-H), 1504 (C=S), 1334 (C-N) and 736 (N-H) cm $^{-1}$. **^{1}H NMR (400 MHz, DMSO-d$_6$):** δ 11.9 (s, N-H) thio-amide , 10.8 (s, N-H) indole, 10.2 (s, N-H) pyrazole, 7.9 (2H, d, *J* = 7.6 Hz), 7.6 (1H, d, *J* = 7.6 Hz), 7.5 (1H, d, *J* = 7.6 Hz), 7.4 (2H, d, *J* = 7.6 Hz), 7.3 (2H, d, *J* = 7.6 Hz),7.2 (2H, d, *J*= 7.6 Hz), 7.1 (1H, t, *J* = 8.0 Hz), 6.9 (1H, t, *J* = 8.0 Hz), 6.8 (1H, t, *J* = 8.0 Hz), 5.9 (s, CH) ppm. **^{13}C NMR (400 MHz, DMSO-d$_6$):** δ 39.7, 111.5, 117.5, 118.2, 118.9, 120.9, 123.6, 126.4, 127.9, 128.0, 128.7, 129.2, 133.0, 134.4, 136.6, 139.0, 141.5, 176.1 ppm. **TOF-MS** found: 404.1 [M^+], **TOF-MS** calculated: 404.9 [M^+].

3-(4-fluorophenyl)-N-phenyl-2, 3-dihydropyrazolo [3, 4-*b*] indole-1(4H)- carbothioamide (88l)

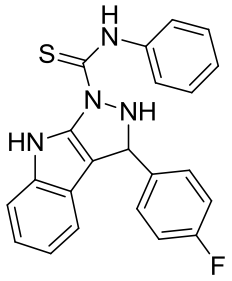

88l

Yield 92%, reddish brown solid, m.p. 147 - 149 ^{0}C. **IR (KBr):** ν 3390 (N-H), 1502 (C=S), 1335 (C-N) and 743 (N-H) cm $^{-1}$. **^{1}H NMR (400 MHz, DMSO-d$_6$):** δ 11.8 (s, N-H) thio-amide, 10.8 (s, N-H) indole, 10.1 (s, N-H) pyrazole, 7.9 (2H, d, *J* = 7.6 Hz), 7.6 (1H, d, *J* = 7.6 Hz), 7.4 (1H, d, *J* = 7.6 Hz), 7.4 (2H, d, *J* = 7.6 Hz), 7.3 (2H, d, *J* = 7.6 Hz),7.2 (2H, d, *J*= 7.6 Hz), 7.1 (1H, t, *J* = 8.0 Hz), 6.9 (1H, t, *J* = 8.0 Hz), 6.8 (1H, t, *J* = 8.0 Hz), 5.9 (s, CH) ppm. **^{13}C NMR (400 MHz, DMSO-d$_6$):** δ 39.7, 111.4, 115.7, 117.9, 118.2, 119.0, 120.9, 123.5, 126.5, 128.0, 129.8, 129.9, 130.7, 136.6, 139.0, 141.7, 161.9, 176.0 ppm. **^{19}F NMR (400 MHz, DMSO-d$_6$)**: δ -117.6 ppm (Ar-F). **TOF-MS** found: 385.1 [M^{+}], **TOF-MS** calculated: 388.5 [M^{+}].

N-phenyl-3-(4-(trifluoromethyl) phenyl)-2, 3-dihydropyrazolo [3, 4-*b*] indole-1(4H)-carbothioamide (88m)

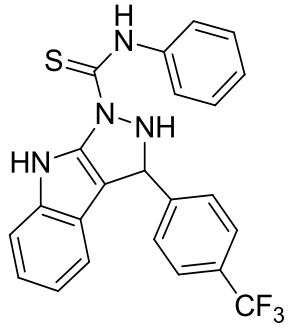

88m

Yield 90%, reddish brown solid, m.p. 152 - 154 ^{0}C. **IR (KBr):** ν 3392 (N-H), 1505 (C=S), 1337 (C-N) and 741 (N-H) cm $^{-1}$. **^{1}H NMR (400 MHz, DMSO-d$_6$):** δ 11.9 (s, N-H) pyrazole, 10.9 (s, N-H) indole, 10.3 (s, N-H) thio-amide, 7.8 (2H, d, *J* = 7.6 Hz), 7.6 (1H, d, *J* = 7.6 Hz), 7.5 (2H, d, *J* = 7.6 Hz), 7.4 (1H, d, *J* = 7.6 Hz),7.3 (2H, d, *J* = 7.6 Hz), 7.2 (2H, d, *J* = 7.6 Hz), 7.1 (1H, t, *J* = 8.0 Hz), 6.9 (2H, t, *J* = 8.0 Hz), 5.9 (s, CH) ppm. **^{13}C NMR (400 MHz, DMSO-**

d_6): δ 39.9, 111.5, 117.1, 118.3, 118.9, 120.8, 123.7, 124.9, 126.7, 128.0, 128.9, 129.0, 130.1, 136.6, 140.9, 149.8, 166.2, 176.4 ppm. **^{19}F NMR (400 MHz, DMSO-d_6)**: δ -61.6 ppm (Ar-F). **TOF-MS** found: 437.0 [M^+], **TOF-MS** calculated: 438.5 [M^+].

3-(4-nitrophenyl)-N-phenyl-2, 3-dihydropyrazolo [3, 4-*b*] indole-1(4H)-carbothioamide (88n)

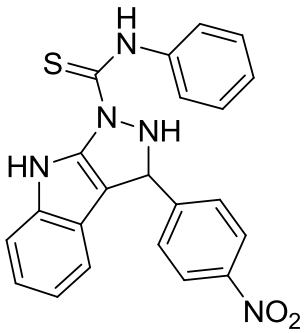

88n

Yield 80%, yellow solid, m.p. 191 - 193 ^{0}C. **IR (KBr):** ν 3387 (N-H), 1504 (C=S), 1333 (C-N) and 737 (N-H) cm $^{-1}$. **^{1}H NMR (400 MHz, DMSO-d_6):** δ 12.1 (s, N-H) pyrazole, 10.9 (s, N-H) indole, 10.3 (s, N-H) thio-amide, 8.2 (2H, d, *J* = 7.6 Hz), 7.6 (3H, d, *J* = 7.6 Hz), 7.5 (2H, d, *J* = 7.6 Hz), 7.4 (1H, d, *J* = 7.6 Hz),7.3 (2H, d, *J*= 7.6 Hz), 7.1 (1H, t, *J* = 8.0 Hz), 6.9 (2H, t, *J* = 8.0 Hz), 6.0 (s, CH) ppm. **^{13}C NMR (400 MHz, DMSO-d_6):** δ 39.9, 111.5, 116.6, 118.3, 118.9, 121.1, 123.7, 126.4, 128.1, 128.4, 129.4, 136.5, 138.9, 140.5, 145.7, 147.7, 176.5 ppm. **TOF-MS** found: 415.1 [M^+], **TOF-MS** calculated: 415.5 [M^+].

3-(4-methoxyphenyl)-N-phenyl-2, 3-dihydropyrazolo [3, 4-*b*] indole-1(4H)-carbothioamide (88o)

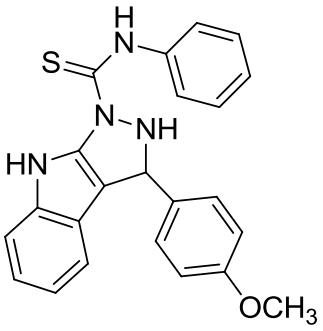

88o

Yield 87%, reddish brown solid, m.p. 115 - 117 ^{0}C. **IR (KBr):** ν 3387 (N-H), 1504 (C=S), 1333 (C-N) and 737 (N-H) cm $^{-1}$. **^{1}H NMR (400 MHz, DMSO-d$_6$):** δ 11.7 (s, N-H) pyrazole, 10.8 (s, N-H) indole, 10.0 (s, N-H) thio-amide, 7.9 (2H, d, *J* = 7.6 Hz), 7.6 (1H, d, *J* = 7.6 Hz), 7.4 (3H, d, *J* = 7.6 Hz), 7.2 (2H, d, *J* = 7.6 Hz), 7.1 (1H, t, *J* = 8.0 Hz), 7.0 (2H, d, *J* = 7.6 Hz), 6.9 (1H, t, *J* = 8.0 Hz), 6.8 (1H, t, *J* = 8.0 Hz), 5.8 (s, CH), 3.8 (s, OCH_3) ppm. **^{13}C NMR (400 MHz, DMSO-d$_6$):** δ 39.9, 55.3, 111.4, 113.3, 118.0, 118.4, 119.1, 120.8, 123.4, 126.6, 127.9, 129.1, 136.6, 139.1, 142.9, 157.3, 175.6 ppm. **TOF-MS** found: 398.0 [M^+], **TOF-MS** calculated: 400.5 [M^+].

3-(4-hydroxy-3-methoxyphenyl)-N-phenyl-2, 3-dihydropyrazolo [3, 4-*b*] indole-1(4H)-carbothioamide (**88p)**

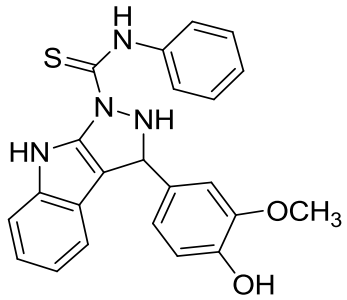

88p

Yield 89%, reddish brown solid, m.p. 125 - 127 ^{0}C. **IR (KBr):** ν 3385 (N-H), 1505 (C=S), 1336 (C-N), 1000 (C-O-C) and 737 (N-H) cm $^{-1}$. **^{1}H NMR (400 MHz, DMSO-d$_6$):** δ 11.7 (s, N-H) pyrazole, 10.7 (s, N-H) indole, 10.0 (s, N-H) thio-amide, 9.5 (s, OH), 8.7 (s, 1H), 7.6 (2H, d, *J* = 7.6 Hz), 7.5 (1H, d, *J* = 7.6 Hz), 7.4 (1H, d, *J* = 7.6 Hz), 7.3 (2H, d, *J* = 7.6 Hz), 7.0 (1H, t, *J* = 8.0 Hz), 6.8 (2H, m) , 6.7 (1H, d, *J* = 7.6 Hz), 6.6 (2H, m) 5.7 (s, CH), 3.7 (s, OCH_3) ppm. **^{13}C NMR (400 MHz, DMSO-d$_6$):** δ 39.7, 55.9, 111.3, 112.8, 115.3, 116.8, 118.0, 118.6, 119.1, 120.7, 121.7, 123.3, 126.7, 128.0, 128.9, 135.9, 136.5, 139.2, 141.2, 144.5, 147.1, 175.5 ppm. **TOF-MS** found: 416.1 [M^+], **TOF-MS** calculated: 416.5 [M^+].

3-(3-bromo-4-hydroxy-5-methoxyphenyl)-N-phenyl-2, 3-dihydropyrazolo [3, 4-*b*] indole-1(4H)-carbothioamide (88q)

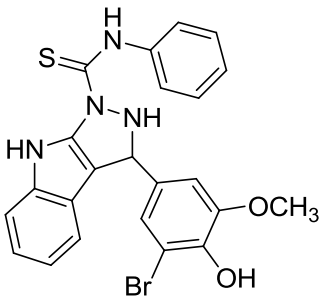

88q

Yield 88%, reddish brown solid, m.p. 123 - 125 ^{0}C. **IR (KBr):** ν 3389 (N-H), 1505 (C=S), 1337 (C-N), 1010 (C-O-C) and 737 (N-H) cm $^{-1}$. **^{1}H NMR (400 MHz, DMSO-d$_6$):** δ 11.8 (s, N-H) pyrazole, 10.8 (s, N-H) indole, 10.1 (s, N-H) thio-amide, 8.7 (s, OH), 8.0 (s, 1H), 7.6 (2H, d, *J* = 7.6 Hz), 7.5 (1H, d, *J* = 7.6 Hz), 7.4 (1H, d, *J* = 7.6 Hz), 7.3 (2H, d, *J* = 7.6 Hz), 7.0 (1H, t, *J* = 8.0 Hz), 6.9 (2H, m) , 6.8 (2H, m), 5.8 (s, CH), 3.7 (s, OCH_3) ppm. **^{13}C NMR (400 MHz, DMSO-d$_6$):** δ 39.7, 56.5, 111.4, 111.7, 116.8, 117.9, 118.2, 119.0, 120.9, 123.5, 125.4, 126.7, 128.0, 128.9, 136.5, 137.1, 139.2, 141.7, 142.0, 155.7, 175.8 ppm. **TOF-MS** found: 496.0 [M^+], **TOF-MS** calculated: 495.4 [M^+].

5.6.3A Typical Procedure for the Multi-Component Synthesis of Novel N-Methyl-3-Phenyl-2, 3-Dihydropyrazolo [3, 4-*b*] Indole-1(4H)-Carbothioamide (88r-88z)

A mixture of benzaldehyde derivatives **85** (1 mmol), N-methyl thio-semicarbizide **86c** (1 mmol) and indole **87** (1 mmol), in acetonitrile (20 mL) was refluxed for 12 hours. The reaction product was poured into ice-water and the precipitate was collected by filtration, washed with water and dried. The resulting crude product was purified by column chromatography using a solvent system of hexane: ethyl acetate (88:12) to isolate reddish brown solid compounds **88r-88z** with good yields. All synthesized compounds were characterized by Infrared, Nuclear Magnetic Resonance and Mass Spectroscopy. The spectroscopic data for all synthesized derivatives is presented below.

5.6.3.1A The spectroscopic analysis of 88r-88z

N-methyl-3-phenyl-2, 3-dihydropyrazolo [3, 4-*b*] indole-1(4H)-carbothioamide (88r)

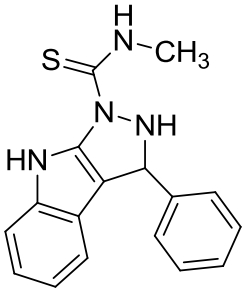

88r

Yield 96%, reddish brown solid, m.p. 122 - 124 ^{0}C. **IR (KBr):** ν 3484 (N-H), 1504 (C=S), 1334 (C-N) and 735 (N-H) cm $^{-1}$. **^{1}H NMR (400 MHz, DMSO-d$_6$):** δ 11.5 (s, N-H) pyrazole, 10.8 (s, N-H) indole, 8.6 (s, N-H) thio-amide, 7.4 (2H, d, *J* = 7.8 Hz), 7.3 (2H, d, *J* = 7.8 Hz), 7.29 (2H, t, *J* = 7.1 Hz), 7.16 (1H, t, *J* = 7.1 Hz), 7.08 (1H, t, *J* = 7.1 Hz), 6.9 (1H, t, *J* = 7.1 Hz), 5.9 (s, CH), 3.1 (3H, d, *J* = 4.6 Hz, CH_3) ppm. **^{13}C NMR (400 MHz, DMSO-d$_6$):** δ 30.9, 39.7, 111.4, 118.1, 118.2, 119.4, 120.9, 123.5, 126.6, 127.2, 128.6, 134.3, 136.6, 144.9, 177.8 ppm. **TOF-MS** found: 333.9 [M^++ Na], **TOF-MS** calculated: 308.4 [M^+].

N-methyl-3-(p-tolyl)-2, 3-dihydropyrazolo [3, 4-*b*] indole-1(4H)-carbothioamide (88s)

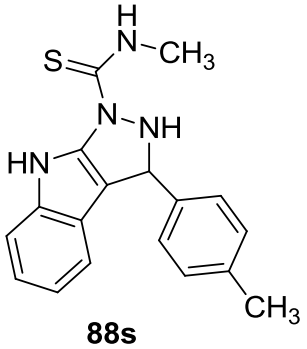

88s

Yield 83%, reddish brown solid, m.p. 144 - 146 ^{0}C. **IR (KBr):** ν 3388 (N-H), 1505 (C=S), 1336 (C-N) and 742 (N-H) cm $^{-1}$. **^{1}H NMR (400 MHz, DMSO-d$_6$):** δ 11.4 (s, N-H) pyrazole, 10.8 (s, N-H) indole, 8.5 (s, N-H) thio-amide, 7.4 (2H, d, *J* = 7.6 Hz), 7.3 (2H, d, *J* = 7.6 Hz), 7.2 (2H, d, *J* = 7.6 Hz), 7.1 (1H, t, *J* = 8.0 Hz), 6.9 (1H, t, *J* = 8.0 Hz), 5.8 (s, CH), 3.0 (3H, d, *J* = 4.6 Hz, CH_3), 2.3 (s, CH_3) ppm. **^{13}C NMR (400 MHz, DMSO-d$_6$):** δ 20.9, 30.8, 39.9,

111.4, 118.1, 118.2, 119.1, 120.8, 123.4, 126.0, 128.1, 134.5, 136.6, 141.8, 177.7 ppm. **TOF-MS** found: 322.1 [M^+], **TOF-MS** calculated: 322.4 [M^+].

3-(4-chlorophenyl)-N-methyl-2, 3-dihydropyrazolo [3, 4-*b*] indole-1(4H)-carbothioamide (88t)

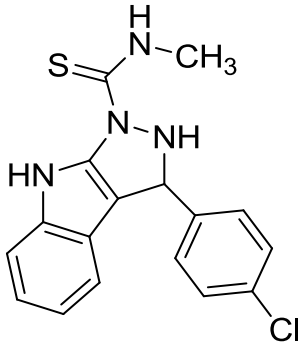

88t

Yield 81%, reddish brown solid, m.p. 141 - 143 ^{0}C. **IR (KBr):** ν 3385 (N-H), 1506 (C=S), 1334 (C-N) and 743 (N-H) cm $^{-1}$. **^{1}H NMR (400 MHz, DMSO-d$_6$):** δ 11.5 (s, N-H) pyrazole, 10.8 (s, N-H) indole, 8.6 (s, N-H) thio-amide, 7.5 (2H, d, *J* = 7.6 Hz), 7.4 (2H, d, *J* = 7.6 Hz), 7.3 (2H, d, *J* = 7.6 Hz), 7.1 (1H, t, *J* = 8.0 Hz), 6.8 (1H, t, *J* = 8.0 Hz), 5.9 (s, CH), 3.0 (3H, d, *J* = 4.6 Hz, CH_3) ppm. **^{13}C NMR (400 MHz, DMSO-d$_6$):** δ 30.8, 39.9, 111.5, 117.5, 118.2, 118.9, 120.9, 123.5, 128.6, 128.8, 133.3, 134.1, 136.6, 143.9, 177.8 ppm. **TOF-MS** found: 365.0 [M^+ + Na], **TOF-MS** calculated: 342.9 [M^+] .

3-(4-fluorophenyl)-N-methyl-2, 3-dihydropyrazolo [3, 4-*b*] indole-1(4H)- carbothioamide (88u)

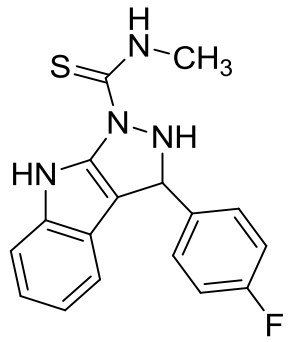

88u

Yield 85%, reddish brown solid, m.p. 128 - 130 ^{0}C. **IR (KBr):** ν 3389 (N-H), 1504 (C=S), 1334 (C-N) and 745 (N-H) cm $^{-1}$. **^{1}H NMR (400 MHz, DMSO-d$_6$):** δ 11.4 (s, N-H) pyrazole, 10.8 (s, N-H) indole, 8.5 (s, N-H) thio-amide, 7.4 (2H, d, *J* = 7.6 Hz), 7.3 (2H, d, *J* = 7.6 Hz),7.2 (2H, d, *J* = 7.6 Hz), 7.1 (1H, t, *J* = 8.0 Hz), 6.8 (1H, t, *J* = 8.0 Hz), 5.8 (s, CH), 3.0 (3H, d, *J* = 4.6 Hz, CH_3) ppm. **^{13}C NMR (400 MHz, DMSO-d$_6$):** δ 30.8, 39.7, 111.4, 115.6, 117.9, 118.2, 118.9, 120.9, 123.4, 129.8, 130.8, 136.5, 140.9, 161.7, 177.7 ppm. **^{19}F NMR (400 MHz, DMSO-d$_6$)**: δ -117.6 ppm (Ar-F). **TOF-MS** found: 326.1 [M^+], **TOF-MS** calculated: 326.4 [M^+].

N-methyl-3-(4-(trifluoromethyl) phenyl)-2, 3-dihydropyrazolo [3, 4-*b*] indole-1(4H)-carbothioamide (88v)

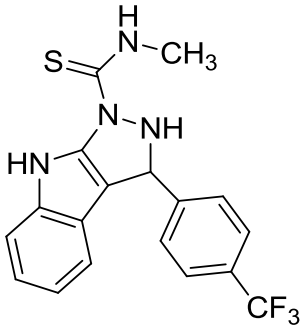

88v

Yield 91%, reddish brown solid, m.p. 204 - 1206 ^{0}C. **IR (KBr):** ν 3425 (N-H), 1505 (C=S), 1337 (C-N) and 742 (N-H) cm $^{-1}$. **^{1}H NMR (400 MHz, DMSO-d$_6$):** δ 11.7 (s, N-H) pyrazole, 10.9 (s, N-H) indole, 8.7 (s, N-H) thio-amide, 8.0 (2H, d, *J* = 7.6 Hz), 7.7 (1H, d, *J* = 7.6 Hz), 7.6 (1H, d, *J* = 7.6 Hz), 7.3 (2H, d, *J* = 7.6 Hz), 7.1 (1H, t, *J* = 8.0 Hz), 6.9 (1H, t, *J* = 8.0 Hz), 5.9 (s, CH), 3.0 (3H, d, *J* = 4.6

Hz, CH_3) ppm. **^{13}C NMR (400 MHz, DMSO-d$_6$):** δ 30.8, 39.8, 111.5, 117.1, 118.3, 118.9, 120.9, 123.6, 124.9, 129.3, 130.0, 136.6, 138.3, 139.7, 177.9 ppm. **^{19}F NMR (400 MHz, DMSO-d$_6$)**: δ -61.2 ppm (Ar-F). **TOF-MS** found: 401.1 [M^++ Na], **TOF-MS** calculated: 376.4 [M^+] .

N-methyl-3-(4-nitrophenyl)-2, 3-dihydropyrazolo [3, 4-*b*] indole-1(4H)-carbothioamide (88w)

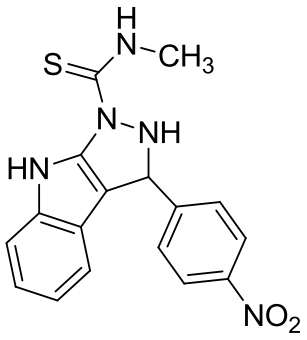

88w

Yield 87%, reddish brown solid, m.p. 189 - 191 ^{0}C. **IR (KBr):** ν 3383 (N-H), 1506 (C=S), 1336 (C-N) and 736 (N-H) cm $^{-1}$. **^{1}H NMR (400 MHz, DMSO-d$_6$):** δ 11.8 (s, N-H) pyrazole, 10.9 (s, N-H) indole, 8.8 (s, N-H) thio-amide, 8.1 (2H, d, *J* = 7.6 Hz), 7.6 (2H, d, *J* = 7.6 Hz), 7.4 (1H, d, *J* = 7.6 Hz), 7.3 (1H, d, *J* = 7.6 Hz),7.1 (1H, t, *J* = 8.0 Hz), 6.9 (1H, t, *J* = 8.0 Hz), 6.0 (s, CH), 3.0 (3H, d, *J* = 4.6 Hz, CH_3) ppm. **^{13}C NMR (400 MHz, DMSO-d$_6$):** δ 30.8, 39.8, 111.6, 116.6, 118.4, 118.9, 121.1, 123.3, 123.8, 127.9, 129.4, 136.6, 145.7, 147.5, 177.9 ppm. **TOF-MS** found: 376.0 [M^+ + Na], **TOF-MS** calculated: 353.4 [M^+].

3-(4-methoxyphenyl)-N-methyl-2, 3-dihydropyrazolo [3, 4-*b*] indole-1(4H)-carbothioamide (88x)

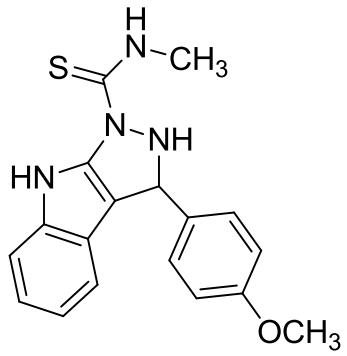

88x

Yield 82%, reddish brown solid, m.p. 165 - 167 ^{0}C. **IR (KBr):** ν 3383 (N-H), 1505 (C=S), 1335 (C-N), 1011 (C-O-C) and 735 (N-H) cm $^{-1}$. **^{1}H NMR (400 MHz, DMSO-d$_6$):** δ 11.4 (s, N-H) pyrazole, 10.8 (s, N-H) indole, 8.4 (s, N-H) thio-amide, 7.4 (2H, d, *J* = 7.6 Hz), 7.3 (2H, d, *J* = 7.6 Hz), 7.0 (1H, t, *J* = 8.0 Hz), 6.9 (2H, d, *J* = 7.6 Hz), 6.8 (1H, t, *J* = 8.0 Hz), 5.8 (s, CH), 3.8 (s,OCH_3), 3.0 (3H, d, *J* = 4.6 Hz, CH_3) ppm. **^{13}C NMR (400 MHz, DMSO-d$_6$):** δ 30.7, 39.9, 55.2, 111.4, 114.1, 118.1, 118.4, 119.1, 120.8, 123.4, 128.8, 129.2, 136.6, 136.9, 141.7, 157.3, 177.5 ppm. **TOF-MS found**: 336.0 [M^+], **TOF-MS** calculated: 338.4 [M^+].

3-(4-hydroxy-3-methoxyphenyl)-N-methyl-2, 3-dihydropyrazolo [3, 4-*b*] indole-1(4H)-carbothioamide (88y)

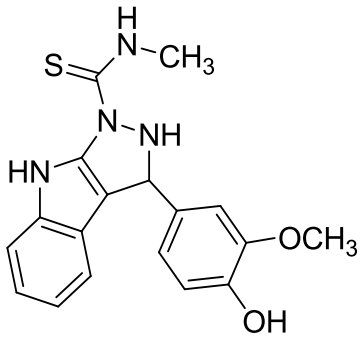

88y

Yield 88%, reddish brown solid, m.p. 186 - 188 ^{0}C. **IR (KBr):** ν 3388 (N-H), 1503 (C=S), 1333 (C-N), 1009 (C-O-C) and 736 (N-H) cm $^{-1}$. **^{1}H NMR (400 MHz, DMSO-d$_6$):** δ 11.4 (s, N-H) pyrazole, 10.8 (s, N-H) indole, 8.8 (s, N-H) thio-amide, 8.0 (s, OH), 7.4 (2H, d, *J* = 7.6 Hz), 7.1 (1H, t, *J* = 8.0 Hz), 6.9 (1H, s), 6.8 (1H, d, *J* = 7.6 Hz), 6.7 (2H, m), 5.8 (s, CH), 3.7

(s,OCH_3), 3.1 (3H, d, *J* = 4.6 Hz, CH_3) ppm. **^{13}C NMR (400 MHz, DMSO-d$_6$):** δ 30.8, 39.6, 55.6, 111.4, 112.8, 115.4, 118.7, 119.2, 120.5, 120.8, 123.4, 135.9, 136.6, 142.5, 147.2, 148.8, 177.4 ppm. **TOF-MS** found: 354.1 [M^+], **TOF-MS** calculated: 354.4 [M^+].

3-(3-bromo-4-hydroxy-5-methoxyphenyl)-N-methyl-2, 3-dihydropyrazolo [3, 4-*b*] indole-1(4H)-carbothioamide (88z)

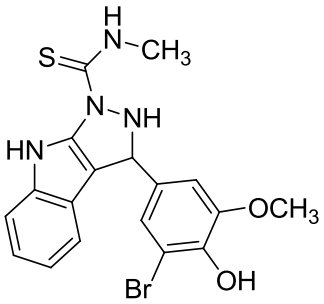

88z

Yield 88%, reddish brown solid, m.p. 218 - 220 ^{0}C. **IR (KBr):** ν 3420 (N-H), 1505 (C=S), 1335 (C-N), 1005 (C-O-C) and 745 (N-H) cm $^{-1}$. **^{1}H NMR (400 MHz, DMSO-d$_6$):** δ 11.4 (s, N-H) pyrazole, 10.8 (s, N-H) indole, 9.2 (s, OH), 8.8 (s, N-H) thio-amide, 7.4 (2H, d, *J* = 7.6 Hz), 7.1 (1H, t, *J* = 8.0 Hz), 6.9 (3H, m), 5.8 (s, CH), 3.7 (s,OCH_3), 3.1 (3H, d, *J* = 4.6 Hz, CH_3) ppm. **^{13}C NMR (400 MHz, DMSO-d$_6$):** δ 30.8, 39.6, 55.6, 111.4, 112.8, 115.4, 118.7, 119.2, 120.5, 120.8, 123.4, 135.9, 136.6, 142.5, 147.2, 148.8, 177.4 ppm. **TOF-MS** found: 434.0 [M^+], **TOF-MS** calculated: 433.3 [M^+].

5.7B Experimental

5.7.1B Typical Procedure for the Multi-Component Synthesis of Fused Novel {3-Phenyl-2,3-Dihydropyrazolo[3,4-*b*]Indol-1(4h)-yl)(Pyridin-4-yl}Methanone (94a-94j)

A mixture of benzaldehyde derivatives **4** (1 mmol), isoniazid **1** (1 mmol) and indole **5** (1 mmol), in acetonitrile (20 mL) was refluxed for 12 hours. The reaction product was poured into ice-water and the precipitate was collected by filtration, washed with water and dried. The resulting crude product was purified by column chromatography using solvent system of hexane: ethyl acetate (88:12) to isolate reddish brown solid compounds **94a-94j** with good yields. All synthesized compounds were characterized by FT-IR, NMR and TOF-MS: the spectroscopic data for all synthesized derivatives is presented below.

5.7.1.1B The Spectroscopic Analysis of 94a-94j

{3-phenyl-2,3-dihydropyrazolo[3,4-*b*]indol-1(4H)-yl)(pyridin-4-yl}methanone (94a)

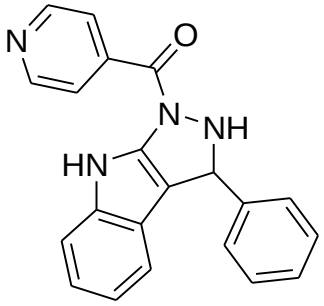

94a

Yield 94%, reddish brown solid, m.p. 89 - 91 ^{0}C. **IR (KBr):** ν 3390 (N-H), C-H (2929), 1687(C=O), 1600 (N-H), 1415 (C-N) and 742 (N-H) cm $^{-1}$. **^{1}H NMR (400 MHz, DMSO-d$_6$):** δ 10.80 (2H, s, N-H) indole and pyrazole, 7.40 (4H, m), 7.31 (3H, d, *J* = 8.4 Hz), 7.20 (1H, t, *J* = 7.3 Hz), 7.10 (3H, t, *J* = 7.3 Hz), 6.90 (1H, t, *J* = 7.3 Hz), 6.90 (1H, d, *J* = 8.4 Hz), 5.90 (1H, s) ppm. **^{13}C NMR (400 MHz, DMSO-d$_6$):** δ 39.8, 111.9, 118.6, 119.6, 121.4, 126.3, 127.1, 128.9, 137.1, 145.4, 172.5 ppm. **TOF-MS** found: 341.1 [M^{+}], **TOF-MS** calculated: 340.4 [M^{+}].

{3-(*p*-tolyl)-2,3-dihydropyrazolo[3,4-*b*]indol-1(4H)-yl)(pyridin-4-yl}methanone (94b)

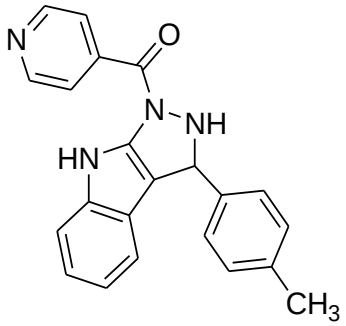

94b

Yield 88%, reddish brown solid, m.p. 85 - 87 ^{0}C. **IR (KBr)**: ν 3413 (N-H), C-H (2918), 1728 (C=O), 1583 (N-H), 1456 (C-N) and 742 (N-H) cm $^{-1}$. **^{1}H NMR (400 MHz, DMSO-d$_6$):** δ 10.85 (2H, s, N-H) indole and pyrazole, 7.40 (4H, d, *J* = 7.2 Hz), 7.31 (3H, d, *J* = 7.2 Hz), 7.29

(2H, t, *J* = 7.9), 7.06 (1H, t, *J* = 7.9 Hz), 6.90 (1H, d, *J* = 7.2 Hz), 6.80 (1H, d, *J* = 7.2 Hz), 5.90 (1H, s), 1.99 (3H, s) ppm. **^{13}C NMR (400 MHz, DMSO-d$_6$):** δ 14.2, 39.8, 111.9, 118.6, 119.6, 121.3, 123.9, 127.1, 128.6, 1289.1, 129.6, 129.8, 135.1, 137.1, 142.4, 170.8 ppm. **TOF-MS** found: 353.1 [M$^+$], **TOF-MS** calculated: 354.4 [M$^+$].

{3-(4-chlorophenyl)-2,3-dihydropyrazolo[3,4-*b*]indol-1(4H)-yl)(pyridin-4- yl}methanone (94c)

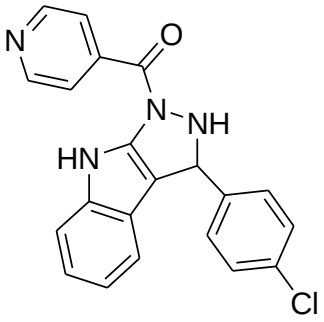

94c

Yield 81%, reddish brown solid, m.p. 132 - 134 ^{0}C. **IR (KBr)**: ν 3397 (N-H), C-H (2918), 1717 (C=O), 1609 (N-H), 1415 (C-N) and 741 (N-H) cm $^{-1}$. **^{1}H NMR (400 MHz, DMSO-d$_6$):** δ 10.8 (2H, s, N-H) indole and pyrazole, 7.40 (4H, d, *J* = 8.2 Hz), 7.29 (2H, d, *J* = 8.2 Hz), 7.25 (1H, d, *J* = 8.2 Hz), 7.08(1H, t, *J* = 7.7 Hz), 7.00 (2H, t, *J* = 7.7 Hz), 6.90 (1H, d, *J* = 8.2 Hz), 6.80 (1H, d, *J* = 8.2 Hz), 5.80 (1H, s) ppm. **^{13}C NMR (400 MHz, DMSO-d$_6$):** δ 39.8, 111.9, 118.6, 119.6, 121.3, 123.9, 127.1, 128.6, 1289.1, 129.6, 129.8, 135.1, 137.1, 142.4, 170.8 ppm. **TOF-MS** found: 375.3 [M$^+$], **TOF-MS** calculated: 374.8 [M$^+$].

{3-(4-fluorophenyl)-2,3-dihydropyrazolo[3,4-*b*]indol-1(4H)-yl)(pyridin-4-yl}methanone (94d)

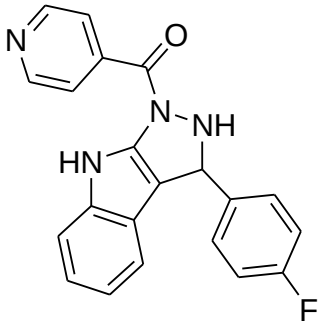

94d

Yield 91%, reddish brown solid, m.p. 104 - 106 ^{0}C. **IR (KBr)**: ν 3395 (N-H), C-H (2874), 1742 (C=O & N-H), 1457 (C-N) and 743 (N-H) cm $^{-1}$. **^{1}H NMR (400 MHz, DMSO-d$_6$):** δ 10.80 (2H, s, N-H) indole and pyrazole, 7.40 (4H, d, *J* = 8.3 Hz), 7.30 (3H, d, *J* = 8.3 Hz), 7.10 (2H, d, *J* = 8.3 Hz), 7.06 (1H, t, *J* = 8.8 Hz), 6.90 (1H, d, *J* = 8.3 Hz), 6.80 (1H, d, *J* = 8.3 Hz), 5.90 (1H, s) ppm. **^{13}C NMR (400 MHz, DMSO-d$_6$):** δ 39.8, 111.9, 115.0, 118.5, 118.7, 119.6, 121.4, 124.0, 127.0, 130.4, 137.1, 141.6, 160.2, 161.8, 170.8 ppm. **^{19}F NMR (400 MHz, DMSO-d$_6$)**: δ -117.6 ppm (Ar-F). **TOF-MS** found: 360.0 [M^{+}], **TOF-MS** calculated: 358.4 [M^{+}].

{3-(4-nitrophenyl)-2,3-dihydropyrazolo[3,4-*b*]indol-1(4H)-yl)(pyridin-4-yl}methanone (94e)

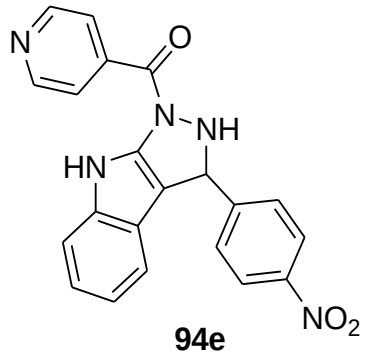

94e

Yield 86%, reddish brown solid, m.p. 241 - 243 ^{0}C. **IR (KBr)**: ν 3386 (N-H), C-H (2929), 1736 (C=O & N-H), 1337 (C-N) and 743 (N-H) cm $^{-1}$. **^{1}H NMR (400 MHz, DMSO-d$_6$):** δ 10.90 (2H, s, N-H) indole and pyrazole, 8.20 (2H, d, *J* = 7.9 Hz), 7.60 (2H, d, *J* = 7.9 Hz), 7.40 (3H, d, *J* = 7.9), 7.09 (1H, t, *J* = 7.4 Hz), 6.90 (2H, d, *J* = 7.9 Hz), 6.10 (1H, s) ppm. **^{13}C NMR (400 MHz, DMSO-d$_6$):** δ 39.8, 112.1, 117.2, 118.9, 119.4, 121.6, 123.9, 124.3, 126.9, 129.9, 137.1, 146.3, 153.6, 170.8 ppm. **TOF-MS** found: 386.1 [M^{+}], **TOF-MS** calculated: 385.4 [M^{+}].

{3-(2-nitrophenyl)-2,3-dihydropyrazolo[3,4-*b*]indol-1(4H)-yl)(pyridin-4-yl}methanone (94f)

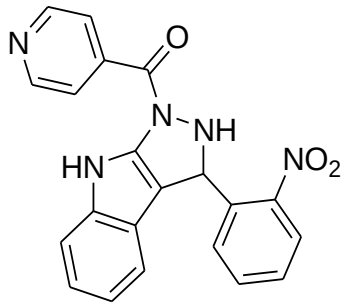

94f

Yield 80%, reddish brown solid, m.p. 241 - 243 ^{0}C. **IR (KBr)**: ν 3393 (N-H), C-H (2918), 1733 (C=O & N-H), 1521 (C-N) and 739 (N-H) cm $^{-1}$. **^{1}H NMR (400 MHz, DMSO-d$_6$):** δ 10.90 (2H, s, N-H) indole and pyrazole, 7.90 (1H, d, *J* = 8.1 Hz), 7.50 (1H, t, *J* = 7.6 Hz), 7.46 (3H, t, *J* = 7.6), 7.40 (2H, d, *J* = 8.1 Hz), 7.27 (2H, d, *J* = 8.1 Hz), 7.1 (1H, t, *J* = 7.6 Hz), 6.9 (1H, t, *J* = 7.6 Hz), 6.8 (1H, d, *J* = 7.6 Hz), 6.5 (1H, s) ppm. **^{13}C NMR (400 MHz, DMSO-d$_6$):** δ 39.8, 111.6, 116.0, 118.5, 121.2, 123.9, 124.1, 126.4, 127.5, 130.5, 132.5, 136.7, 137.7, 149.5, 170.8 ppm. **TOF-MS** found: 386.1 [M^{+}], **TOF-MS** calculated: 385.4 [M^{+}].

{3-(2-hydroxyphenyl)-2,3-dihydropyrazolo[3,4-*b*]indol-1(4H)-yl)(pyridin-4-yl}methanone (**94g)**

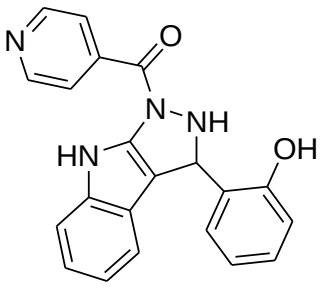

94g

Yield 84%, reddish brown solid, m.p. 120 - 122 ^{0}C. **IR (KBr)**: ν 3416 (N-H & OH), C-H (2928), 1719 (C=O & N-H), 1454 (C-N), 1217 (C-O) and 736 (N-H) cm $^{-1}$. **^{1}H NMR (400 MHz, DMSO-d$_6$):** δ 10.7 (2H, s, N-H) indole and pyrazole, 9.4 (1H, s, OH), 7.40 (3H, d, *J* = 8.1 Hz), 7.30 (2H, d, *J* = 8.1 Hz), 7.1 (1H, d, *J* = 8.1), 7.07 (2H, t, *J* = 7.3 Hz), 7.02 (1H, t, *J* = 7.3 Hz), 6.90 (2H, m), 6.80 (1H, d, *J* = 8.1 Hz), 6.70 (1H, t, *J* = 7.3 Hz), 6.20 (1H, s) ppm. **^{13}C**

NMR (400 MHz, DMSO-d$_6$): δ 39.8, 111.4, 115.0, 118.0, 118.2, 118.6, 119.0, 120.8, 123.5, 126.6, 129.3, 130.9, 136.6, 154.3, 170.4 ppm. **TOF-MS** found: 357.1 [M^+], **TOF-MS** calculated: 356.4 [M^+] .

{3-(4-methoxyphenyl)-2,3-dihydropyrazolo[3,4-*b*]indol-1(4H)-yl)(pyridin-4-yl}methanone (**94h)**

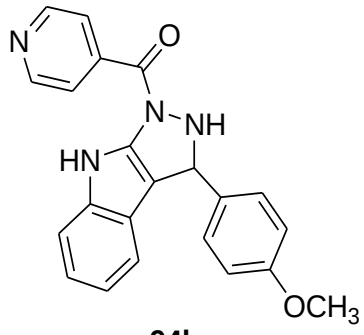

94h

Yield 94%, reddish brown solid, m.p. 189 - 191 ^{0}C. **IR (KBr)**: ν 3395 (N-H), C-H (2972), 1747 (C=O & N-H), 1455 (C-N), 1010 (C-O) and 739 (N-H) cm $^{-1}$. **^{1}H NMR (400 MHz, DMSO-d$_6$):** δ 10.8 (2H, s, N-H) indole and pyrazole, 7.40 (2H, d, *J* = 8.1 Hz), 7.30 (5H, m), 7.07 (1H, t, *J* = 7.3 Hz), 6.90 (2H, t, *J* = 7.3 Hz), 6.80 (2H, m), 5.80 (1H, s), 3.70 (3H, s) ppm. **^{13}C NMR (400 MHz, DMSO-d$_6$):** δ 39.8, 54.9, 111.4, 113.4, 118.1, 118.4, 119.1, 120.8, 123.4, 126.6, 129.2, 136.7, 157.3, 170.8 ppm. **TOF-MS** found: 371.1 [M^+], **TOF-MS** calculated: 370.4 [M^+].

{3-(3-hydroxy-4-methoxyphenyl)-2,3-dihydropyrazolo[3,4-*b*]indol-1(4H)-yl)(pyridin-4-yl}methanone (94i)

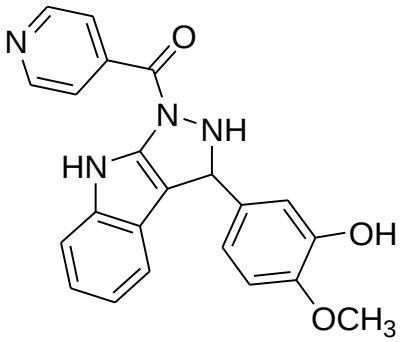

94i

Yield 88%, reddish brown solid, m.p. 149 - 151 ^{0}C. **IR (KBr)**: ν 3433 (OH & N-H), C-H (2925), 1739(C=O & N-H), 1453 (C-N), 1201 (C-O) and 735 (N-H) cm $^{-1}$. **^{1}H NMR (400 MHz, DMSO-d$_6$):** δ 10.80 (2H, s, N-H) indole and pyrazole, 8.70 (1H, s, OH), 7.40 (3H, d, *J* = 8.1 Hz), 7.34 (2H, d, *J* = 8.1 Hz), 7.07 (1H, t, *J* = 7.3 Hz), 7.0 (1H, s), 6.90 (1H, t, *J* = 7.3 Hz), 6.80 (2H, d, *J* = 8.1 Hz), 6.70 (1H, d, *J* = 8.1 Hz), , 5.80 (1H, s), 3.70 (3H, s) ppm. **^{13}C NMR (400 MHz, DMSO-d$_6$):** δ 39.8, 55.6, 111.4, 112.9, 115.1, 118.0, 118.7, 119.2, 120.5, 123.4, 126.7, 135.9, 136.6, 144.5, 147.2, 170.3 ppm. **TOF-MS** found: 389.0 [M^{+}], **TOF-MS** calculated: 386.4 [M^{+}].

{3-(3-bromo-5-hydroxy-4-methoxyphenyl)-2,3-dihydropyrazolo[3,4-*b*]indol-1(4H)-yl)(pyridin-4-yl}methanone (94j)

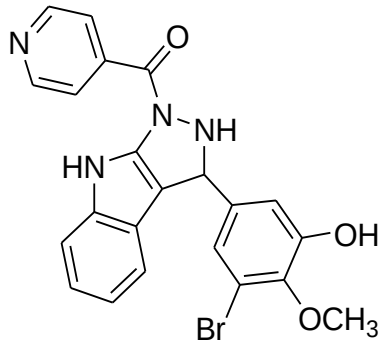

94j

Yield 87%, reddish brown solid, m.p. 131 - 133 ^{0}C. **IR (KBr)**: ν 3391 (OH & N-H), C-H (2968), 1739(C=O & N-H), 1368 (C-N), 1214 (C-O) and 738 (N-H) cm $^{-1}$. **^{1}H NMR (400 MHz, DMSO-d$_6$):** δ 10.8 (2H, s, N-H) indole and pyrazole, 9.20 (1H, s, OH), 7.40 (3H, d, *J* = 8.1 Hz), 7.3 (3H, d, *J* = 8.1 Hz), 7.07 (1H, t, *J* = 7.3 Hz), 7.0 (1H, s), 6.99 (1H, s), 6.90 (1H, t, *J* = 7.3 Hz), 6.80 (1H, d, *J* = 8.1 Hz), 5.8 (1H, s), 3.70 (1H,s) ppm. **^{13}C NMR (400 MHz, DMSO-d$_6$):** δ 39.8, 56.1, 108.9, 111.5, 117.9, 118.2, 119.0, 120.9, 123.5, 126.6, 136.6, 137.1, 141.8, 148.2, 170.3 ppm. **TOF-MS** found: 462.0 [M^{+}], **TOF-MS** calculated: 465.3 [M^{+}].

Experimental procedure for anti-bacterial studies, anti-fungal studies and mutagenicity will be found in Chapter 4 under 4.7.2 (page 113), 4.7.3 (page 114) and 4.7.4 (page 114).

5.8 References

1. Kale S.S., Pawari R.R. and Kale A.S. 2016. Imidazole, its derivatives and their importance. *International Journal of Current Advanced Research*, 5 (5): 906-911.
2. Dadiboyena S. and Nefzi A. 2011. Synthesis of functionalized tetrasubstituted pyrazolyl heterocycles. *European Journal of Medicinal Chemistry*, 46: 5258-5275.
3. Kumar V., Kaur K., Gupta G.K. and Sharma A.K. 2013. Pyrazole containing natural products: Synthetic preview and biological significance. *European Journal of Medicinal Chemistry*, 69: 735-753.
4. Tewari A.K., Singh V.P., Yadav P., Gupta G., Singh A., Goel R.K., Shinde P. and Mohan G. 2014. Synthesis, biological evaluation and molecular modelling study of pyrazole derivatives as selective COX-2 inhibitors and anti-inflammatory agents. *Bioorganic Chemistry*, 56: 8-15.
5. Shkineva T.K., Dalinger I.L. and Shevelev S.A. 1995. Synthesis of compounds with two or more pyrazole rings linked to each other (review). *Chemistry of Heterocyclic Compounds*, 31 (5): 509 – 529.
6. Wang Z. 2010. Comprehensive ornanic name reactions and reagents. *John Wiley & Sons*: 1631-1633.
7. Wang Z. 2010. Comprehensive ornanic name reactions and reagents. *John Wiley & Sons*: 2147-2150.
8. Heller S.T. and Natarajan S.R. 2006. 1,3-Diketones from acid chlorides and ketones: A rapid and general one-pot synthesis of pyrazoles. *Organic Letters*, 8 (13): 2675-2678.
9. Nossier E.S., Fahmy H.H., Khalifa N.M., El-Eraky W.I. and Baset M.A. 2017. Design and synthesis of novel pyrazole-substituted different nitrogenous heterocyclic ring systems as potential anti-imflammatory agents. *Molecules*, 22 (512): 1-16.
10. Ehsan S., Ghafoor S. and Khan B. 2012. Microwave assisted synthesis of nitrogen and hydroxyl containing bioactive compounds as drugs motif. *International Journal of Science and Research*, 3 (9): 195-199.
11. Dar A.M. and Shamsuzzaman. 2015. A concise review on the synthesis of pyrazole heterocycles. *Journal of Nuclear Medicine and Radiation Therapy*, 6 (5): 1-5.
12. Desai N.C., Joshi V.V., Rajpara K.M., Vaghani H.V. and Satodiya H.M. 2012. Facile synthesis of novel fluorine containing pyrazole based thiazole derivatives and evaluation of antimicrobial activity. *Journal of Fluorine Chemistry*, 142: 67-78.

13. Viveka S., Dinesha, Madhu L.N. and Nagaraja G.K. 2015. Synthesis of new pyrazole derivatives via multicomponent reaction and evaluation of their antimicrobial and antioxidant activities. *Monatsh Chem*, 146: 1547-1565.
14. Kumar J.A., Saidachary G., Mallesham G., Sridhar B., Jain N., Kalivendi S.V., Rao J. and Raju B.C. 2013. Synthesis, anticancer activity and photophysical properties of novel substituted 2-oxo-2H-chromenylpyrazolecarboxylates. *European Journal of Medicinal Chemistry*, 65: 389-402.
15. Khalili G. 2013. Multicomponent reaction for synthesis of N-arylsulfonyl pyrazoles. *Synthetic Communications*, 43 (23):3170-3174.
16. Katayama H and Shen J.K. 1994. Preparation and reactions of 3*H*-pyrazolo[1,5-a]indole derivatives. *Chem.Pharm.Bull,* 42 (2): 214-221.
17. Wen J., Tang H., Xiong K., Ding Z. and Zhan Z. 2014. Synthesis of polysubstituted pyrazoles by a plantinum-catalyzed sigmatropic reaarangement/cyclization cascade. *Organic Letters*, 15: 5940-5943.
18. Zhu Y., Qin L., Liu R., Ji S. and Katayama H. 2007. Synthesis of pyrazolo[1,5-a]indoles via copper(I)-catalyzed intramolecular amination. *Tetrahedron Letters*, 28: 6262-6266.
19. Rahmount A., Romdhane A., Ben Said A., Majouli K. and Ben Jannet H. 2014. Synthesis of new pyrazole and antibacterial pyrazolopyrimidine derivatives. *Turkish Journal of Chemistry*, 38: 210-221.
20. Li Y. and Dong C. 2015. Efficient synthesis of fused pyrazoles via simple cyclization of *o*-alkynylchalcones with hydrazine. *Chinese Chemical Letters*, 26: 623-626.
21. El-Mekabaty A., Etman H.A. and Mosbah A. 2015. Synthesis of some new fused pyrazole derivatives bearing indole moiety as antioxidant agents. *Journal of Heterocyclic Chemistry*, 53: 894-900.
22. Hao W., Xu X., Bai H., Wang S. and Ji S. 2012. Efficient multicomponent strategy to pentacyclic pyrazole-fused naphtho[1,8-fg]-isoquinolines through cleavage of two carbon-carbon bonds. *Organic Letters*, 14 (18): 4894-4897.
23. Suzuki Y., Naoe S., Oishi S., Fujii N. and Ohno H. 2012. Gold-catalyzed three component annulation: Efficient synthesis of highly functionalized dihydropyrazoles from alkynes, hydrazines, and aldehydes or ketones. *Organic Letters*, 14 (1): 326-329.
24. Tekale S.U., Kauthale S.S., Jadhav K.M. and Pawar R.P. 2013. Nano-ZnO catalyzed green and efficient one-pot four-component synthesis of pyranopyrazoles. *Hindawi Journal of Chemistry*: 1-8.

25. Judge V., Narasimhan B. and Ahuja M. 2012. Isoniazid: the magic molecule. *Medical Chemistry Research*, 21: 3940-3957.
26. Rodrigues F.A., Oliveira A.C.A., Calvalcanti B.C., Pessoa C., Pinheiro A.C. and de Souza M.V.N. 2013. Biological evaluation of isoniazid derivatives as an anticancer class. *Scientia Pharmaceutica*, 82: 21-28.
27. Pahlavani E., Kargar H. and Rad N.S. 2015. A study on antitubercular and antimicrobial activity of isoniazid derivative. *Journal Research Medical Science*, 7: 1-4.

Appendix – V

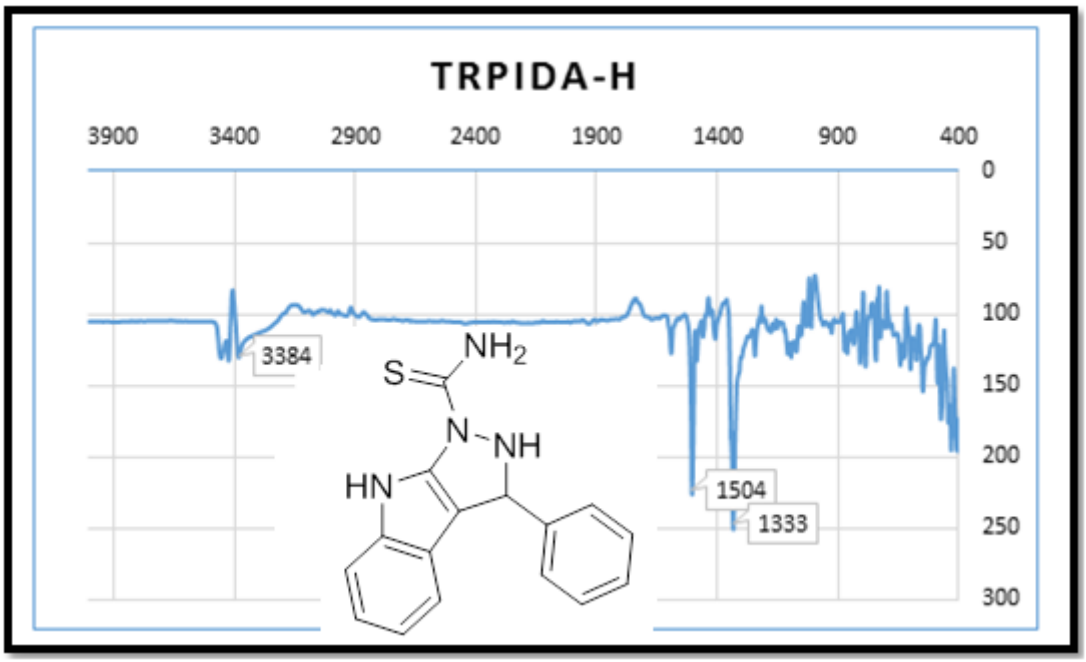

Appendix 5.1A: IR spectrum for compound **88a**

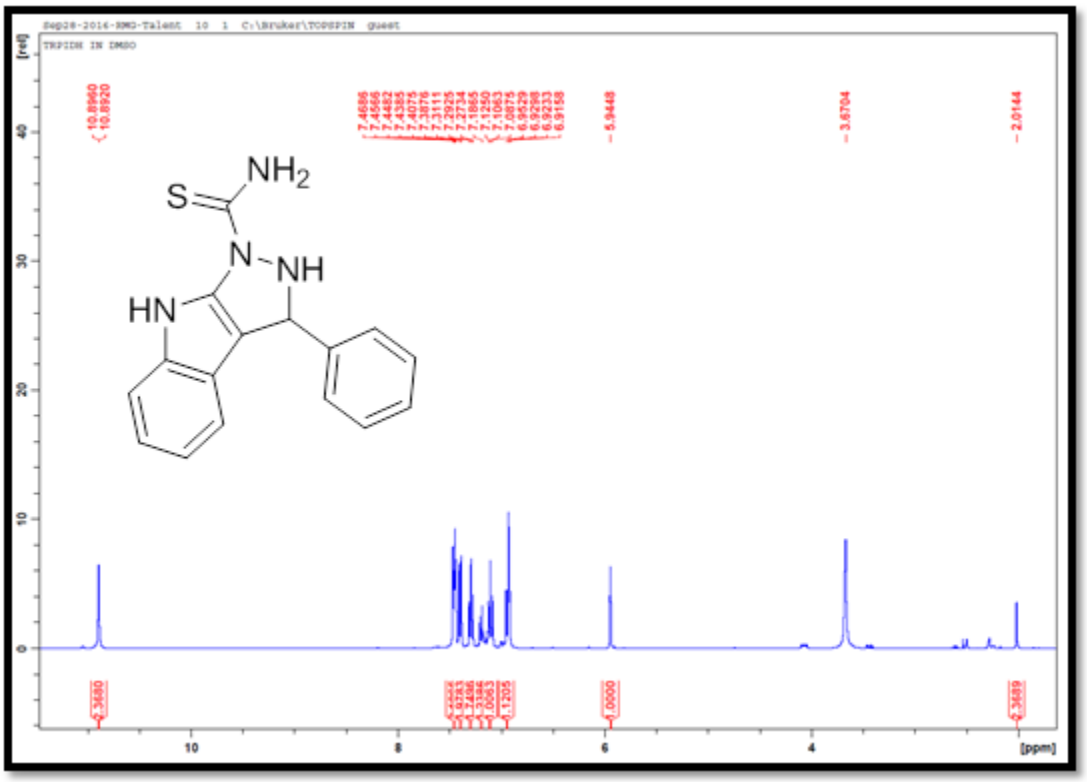

Appendix 5.2A: ^{1}H NMR spectrum for compound **88a**

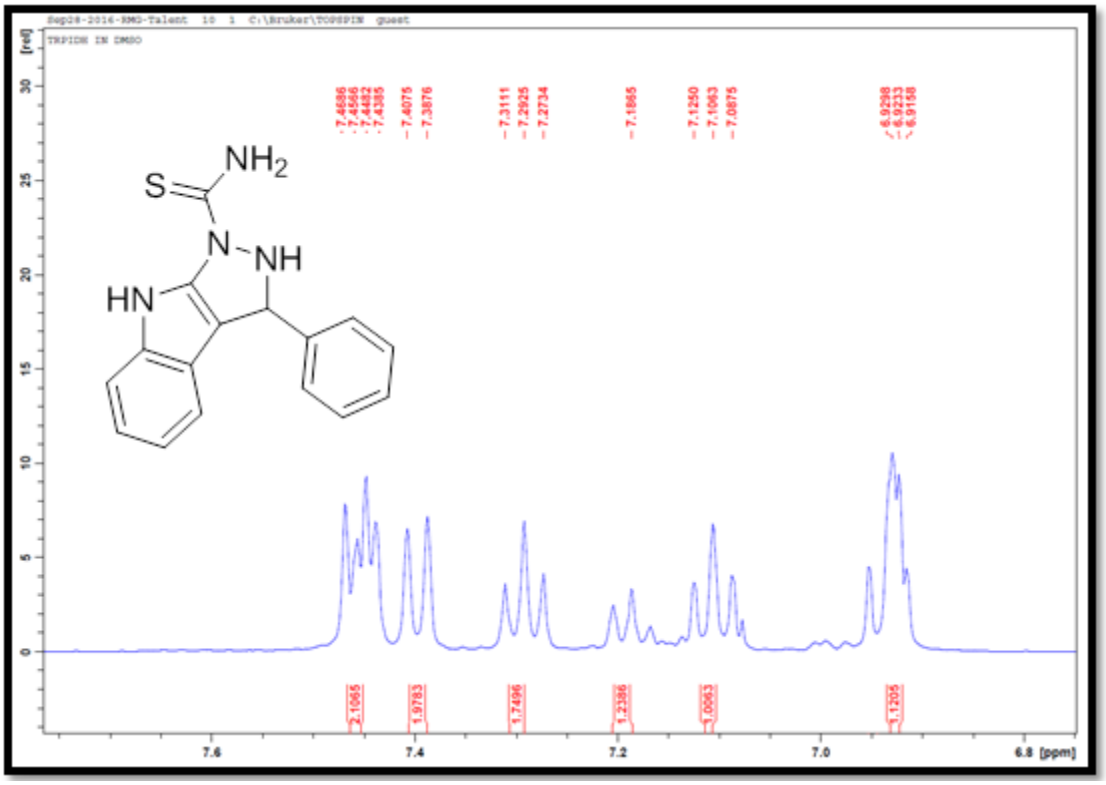

Appendix 5.3A: Expanded ^{1}H NMR spectrum for compound **88a**

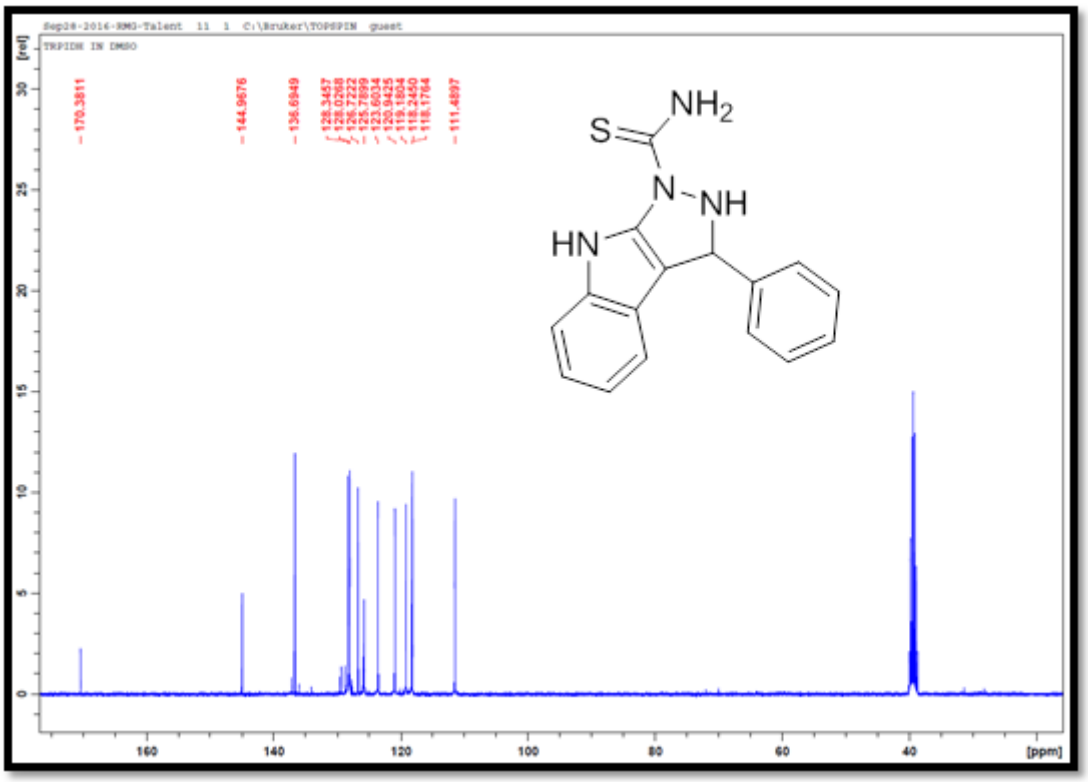

Appendix 5.4A: ^{13}C NMR spectrum for compound **88a**

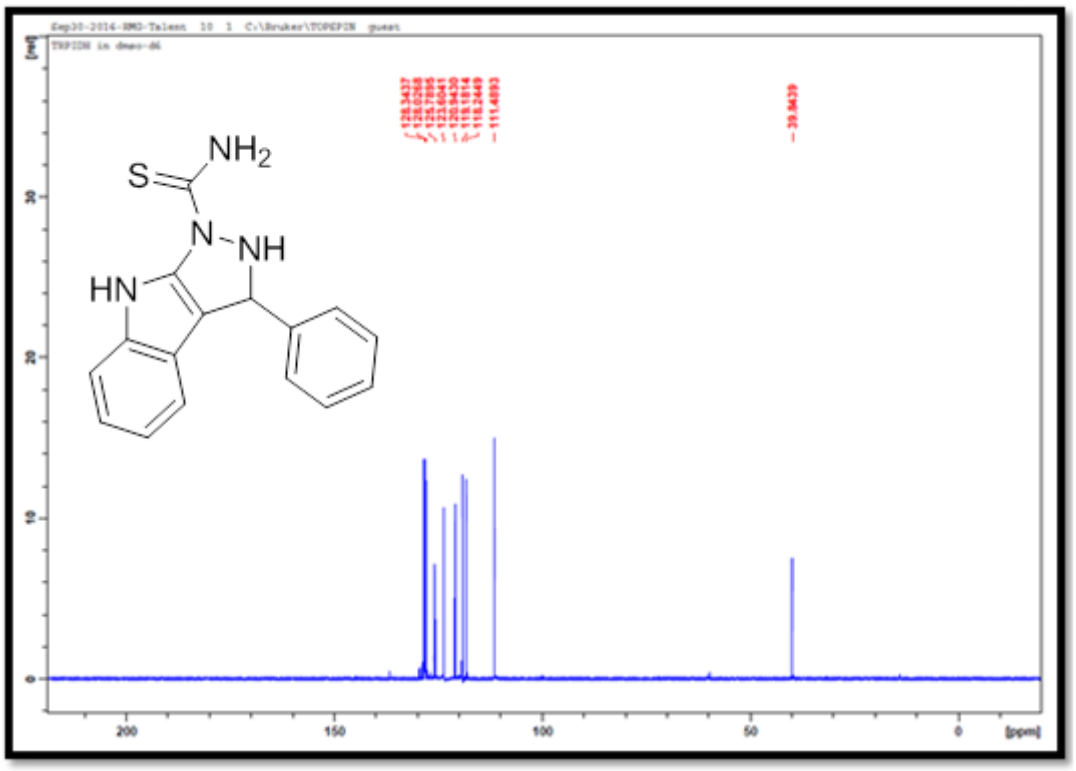

Appendix 5.5A: 90^0 DEPT NMR spectrum for compound **88a**

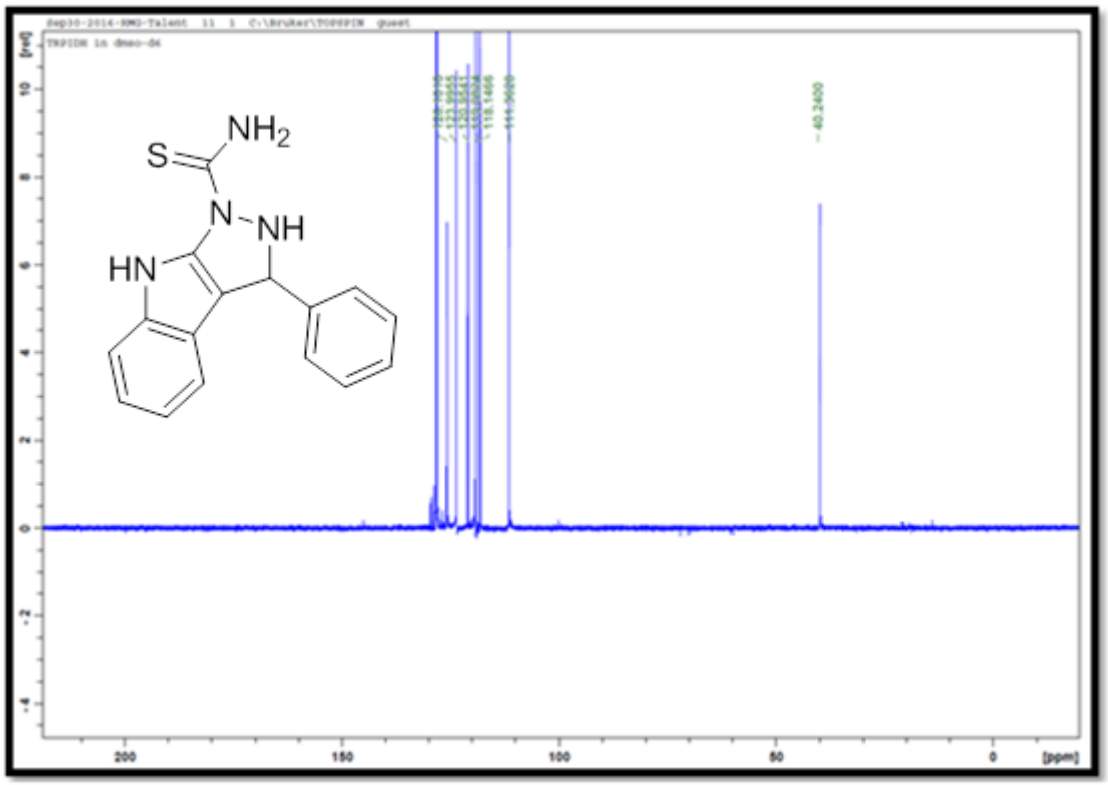

Appendix 5.6A: 135^0 DEPT NMR spectrum for compound **88a**

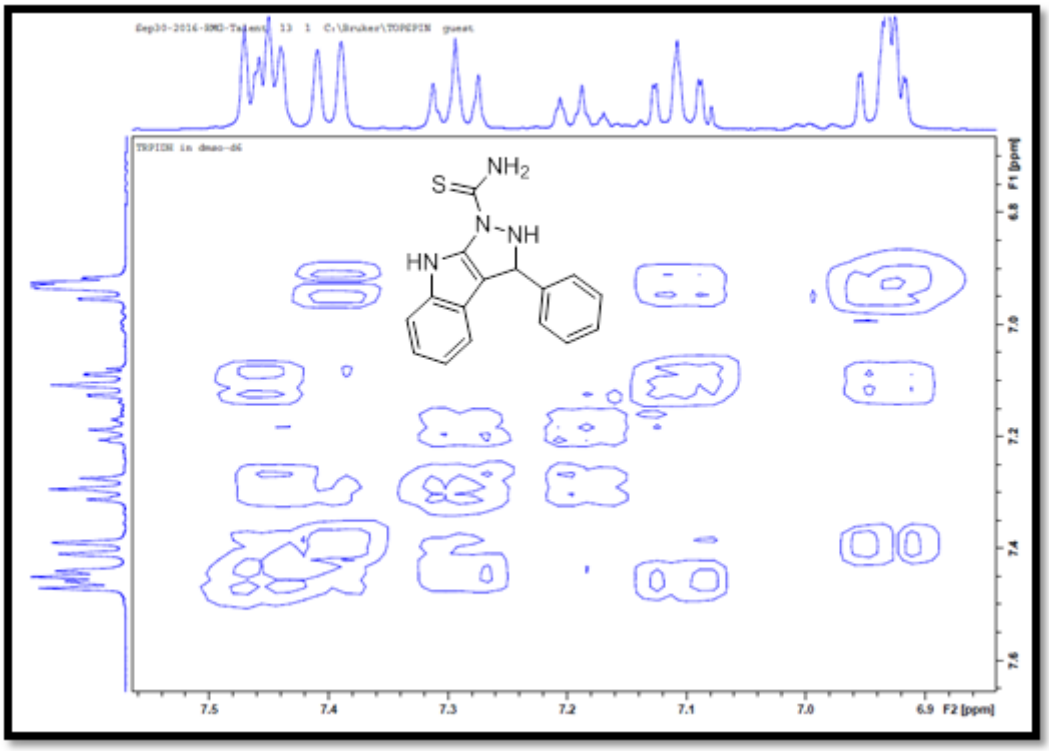

Appendix 5.7A: Expanded COSY NMR spectrum for compound **88a**

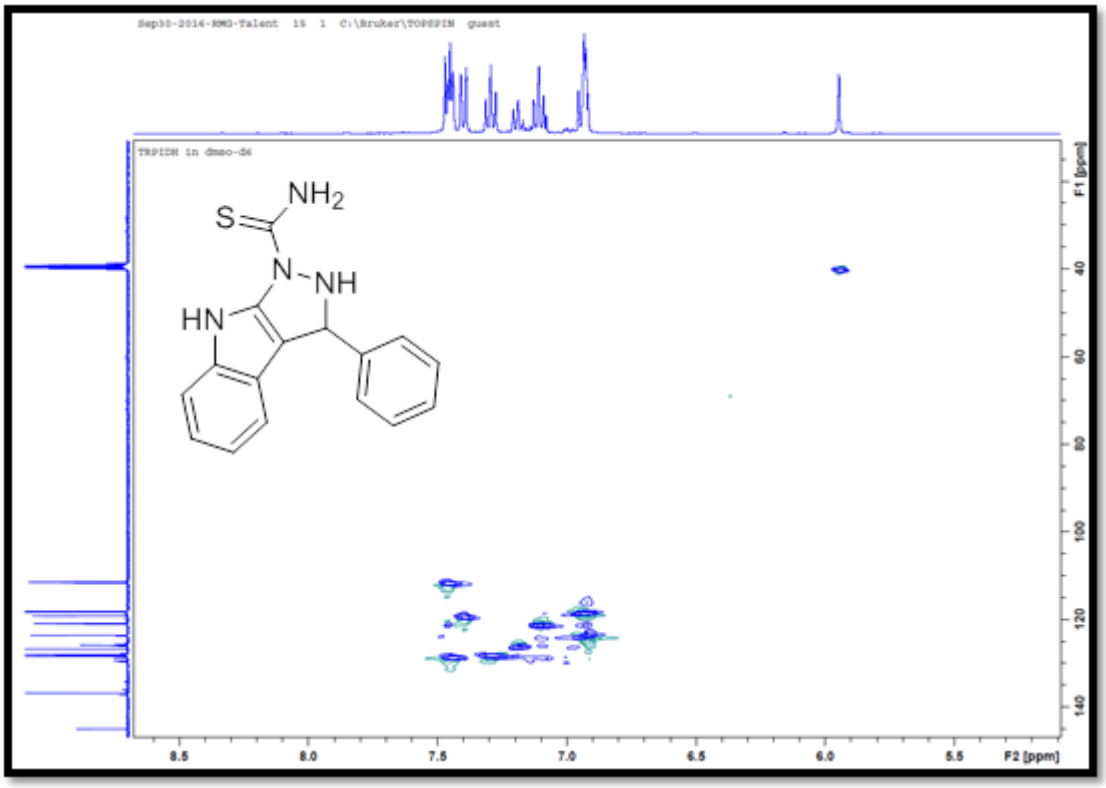

Appendix 5.8A: HSQC NMR spectrum for compound **88a**

Appendix 5.9A: HMBC NMR spectrum for compound **88a**

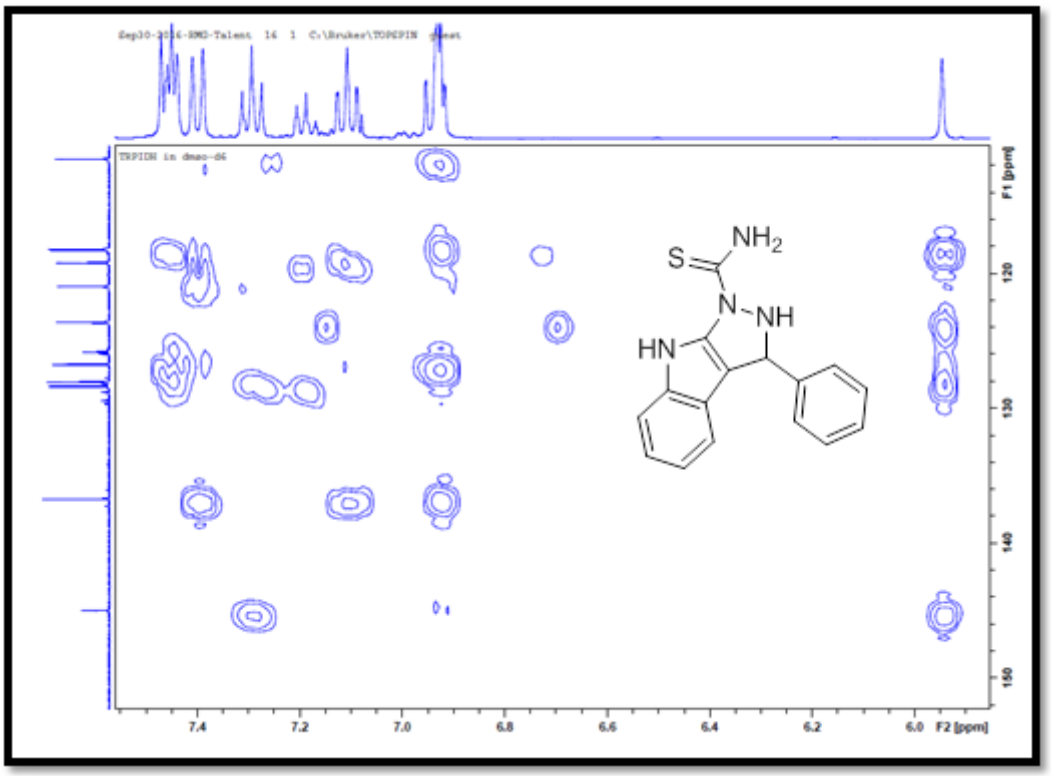

Appendix 5.10A: Expanded HMBC NMR spectrum for compound **88a**

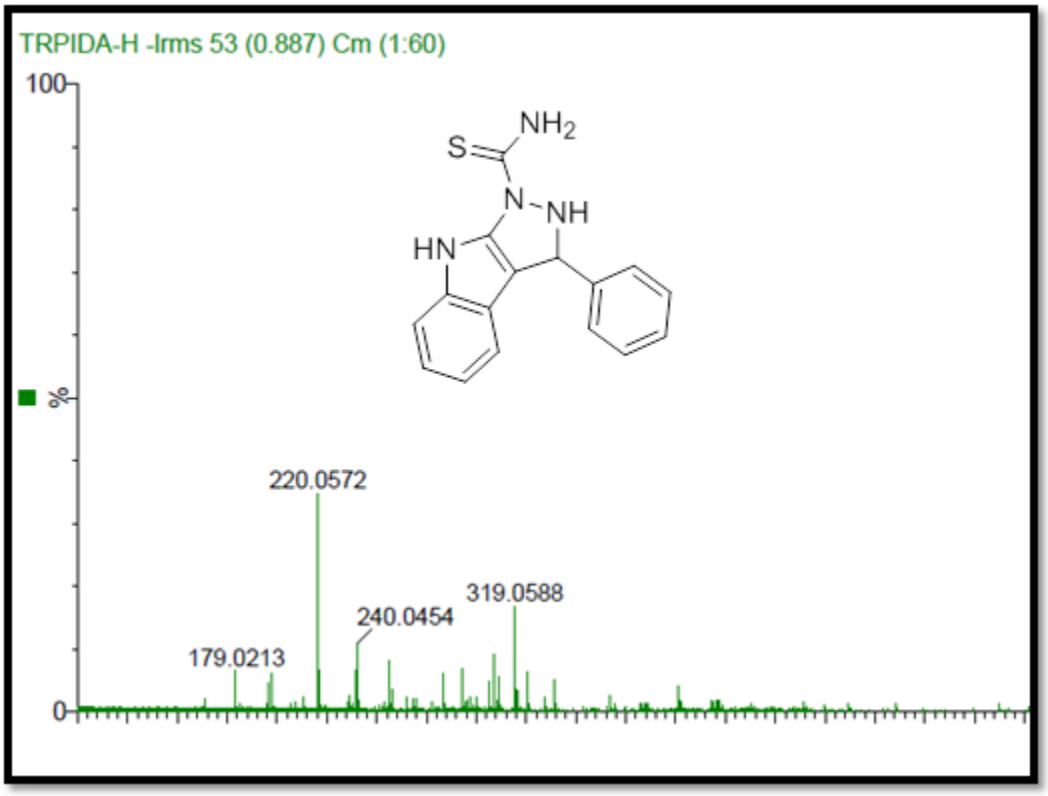

Appendix 5.11A: TOF-MS spectrum for compound **88a**

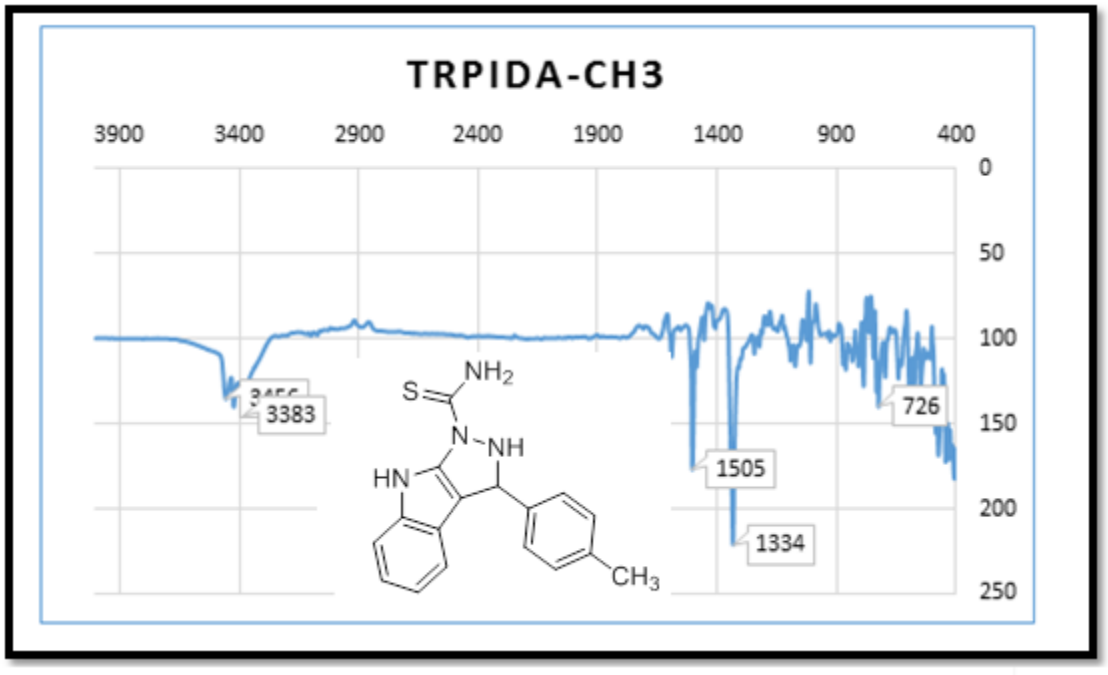

Appendix 5.12A: IR spectrum for compound **88b**

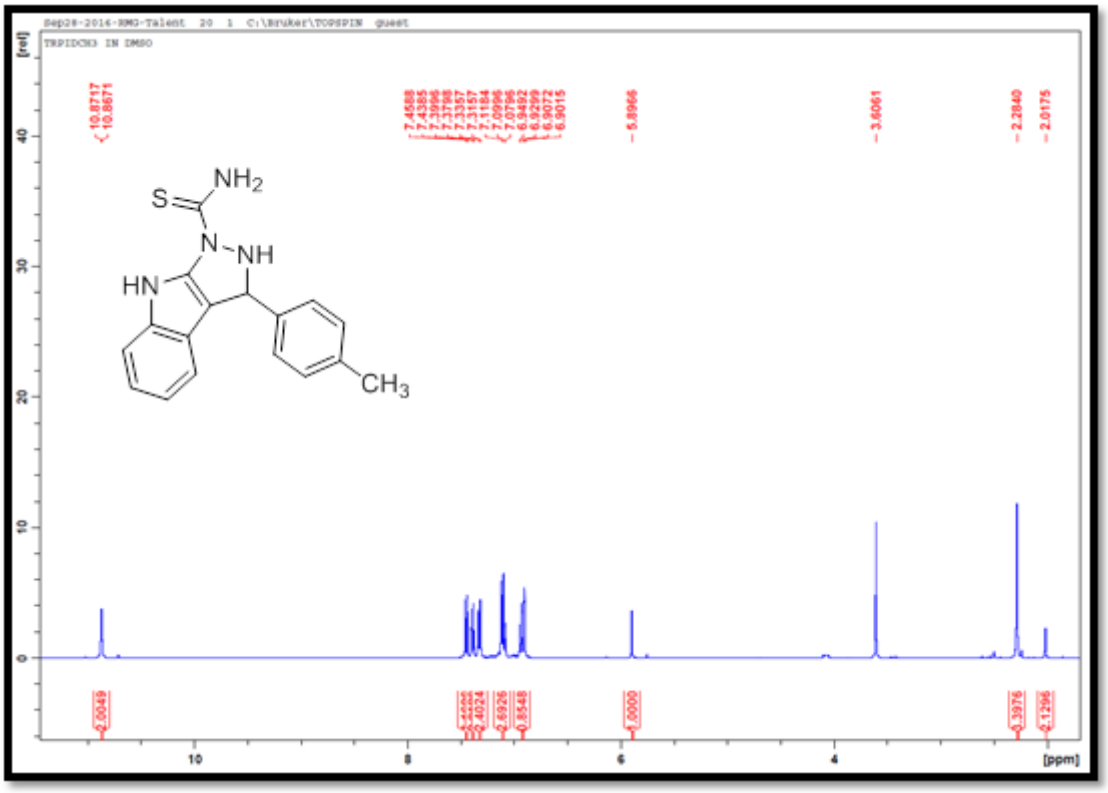

Appendix 5.13A: ^{1}H NMR spectrum for compound **88b**

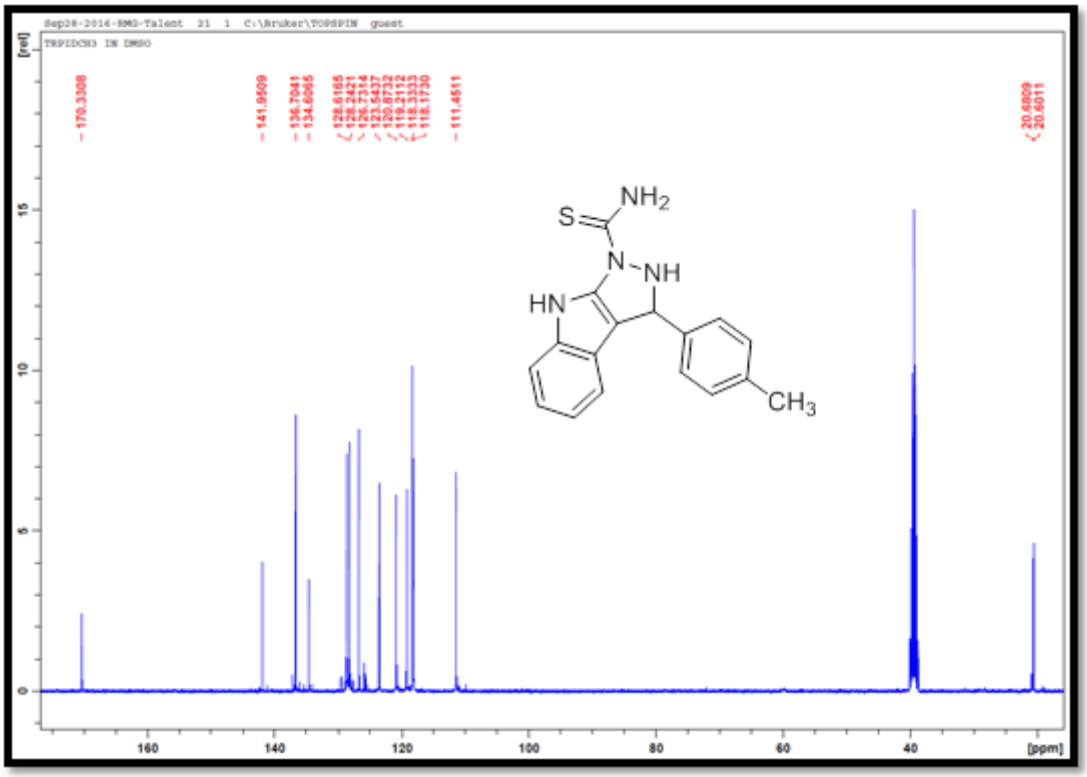

Appendix 5.14A: ^{13}C NMR spectrum for compound **88b**

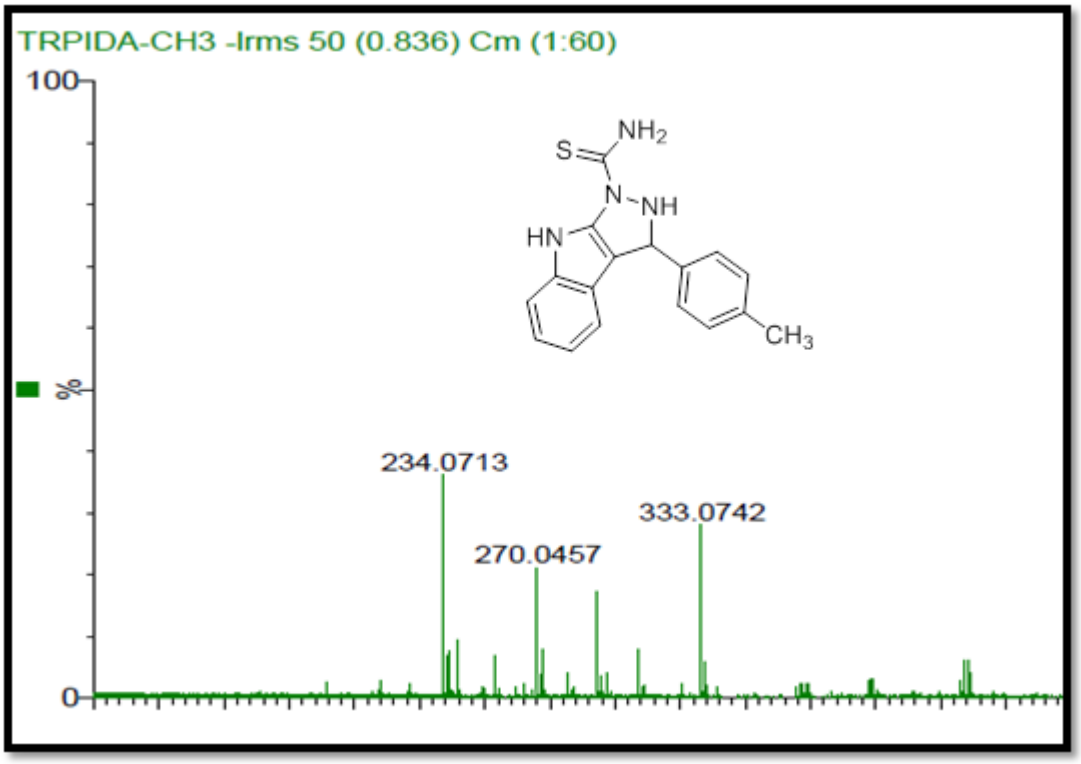

Appendix 5.15A: TOF-MS spectrum for compound **88b**

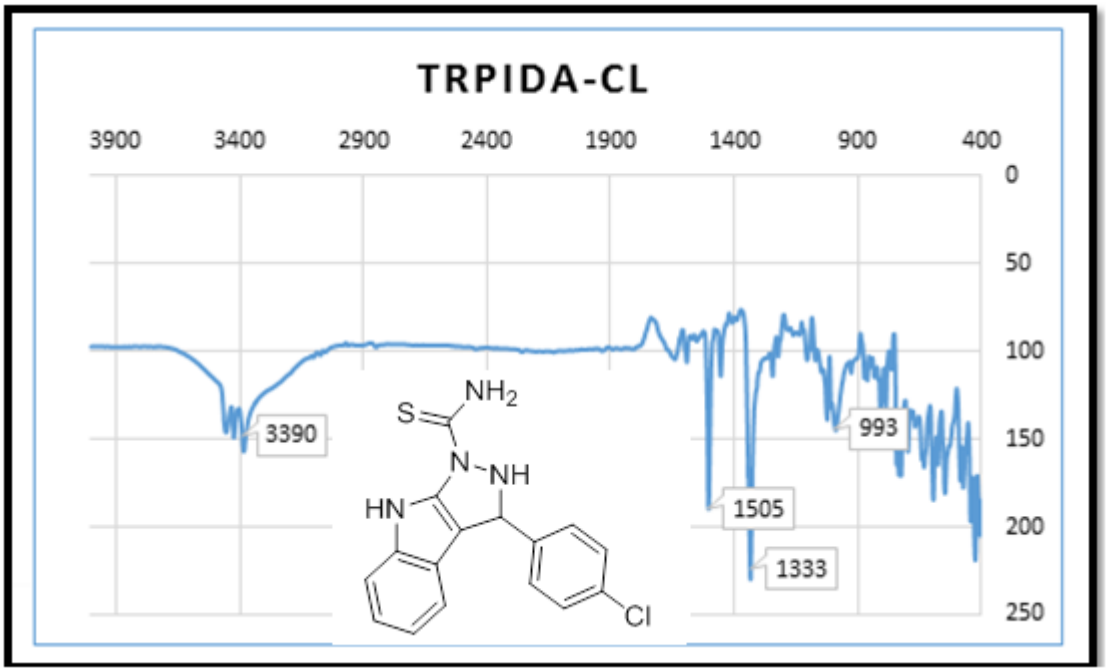

Appendix 5.16A: IR spectrum for compound **88c**

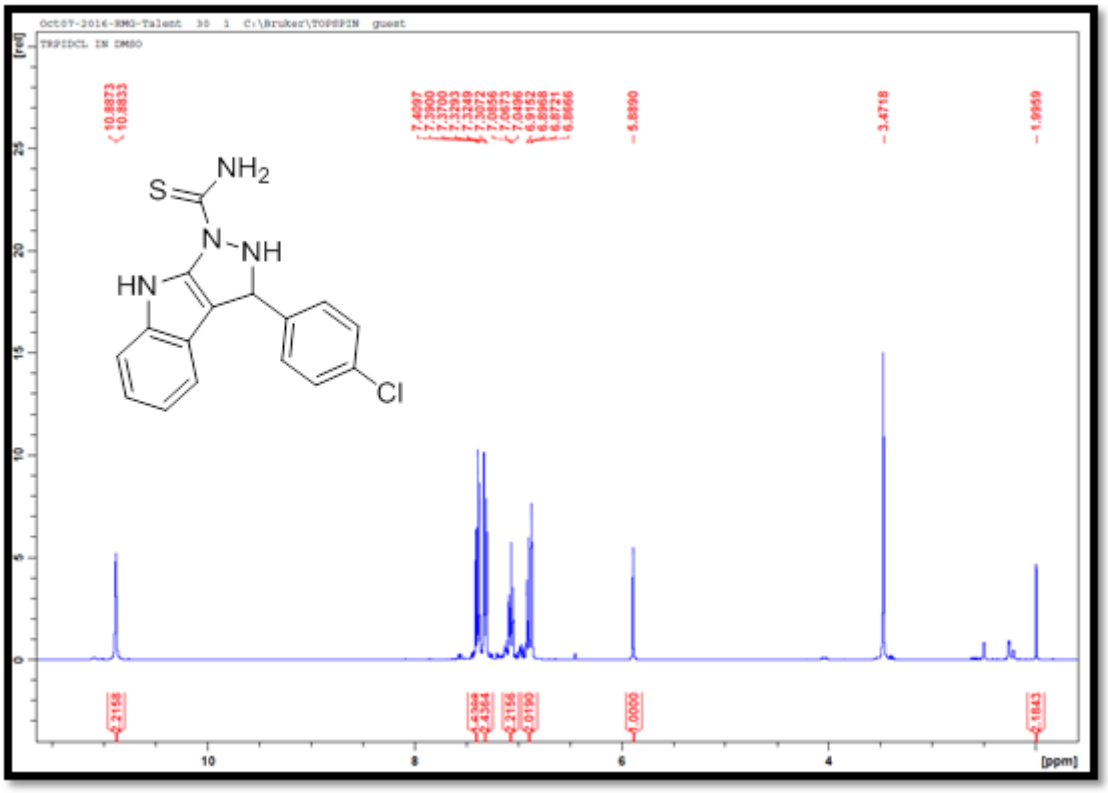

Appendix 5.17A: ^{1}H NMR spectrum for compound **88c**

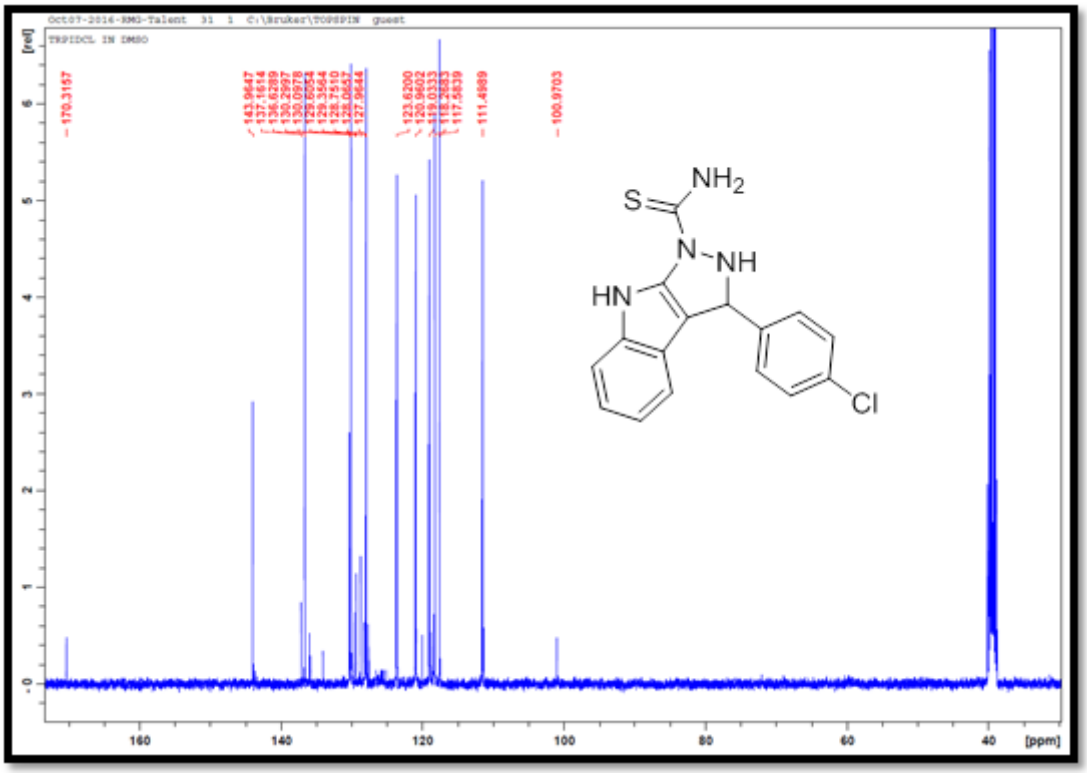

Appendix 5.18A: ^{13}C NMR spectrum for compound **88c**

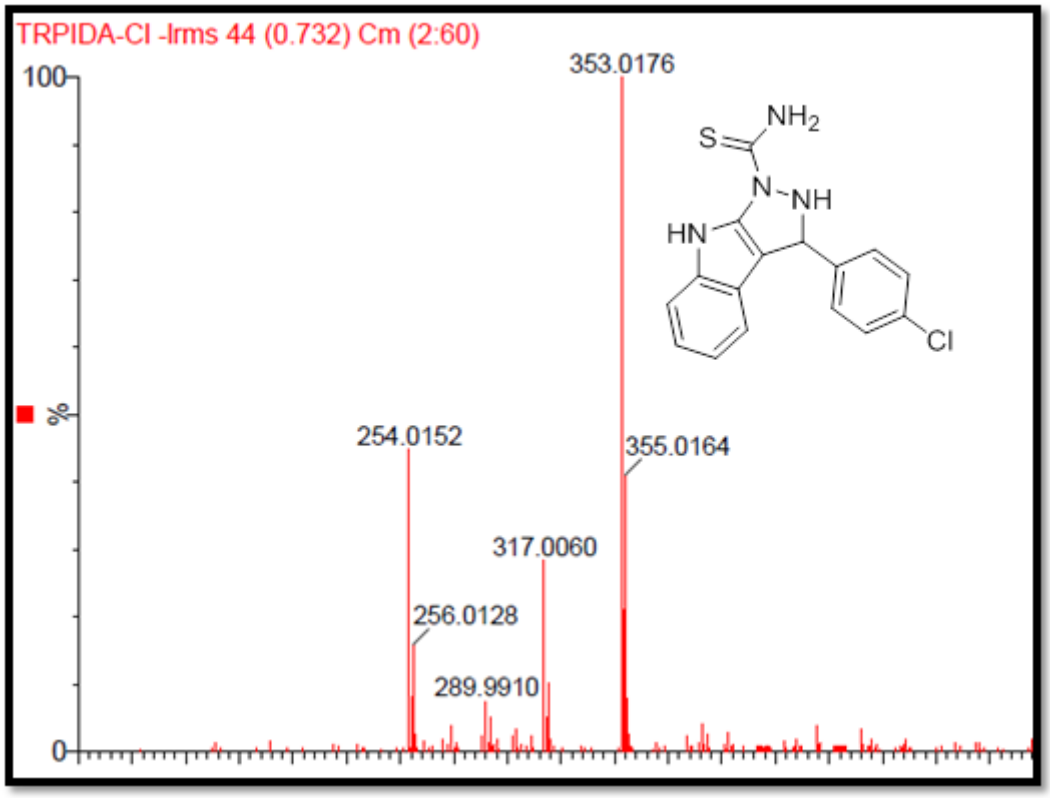

Appendix 5.19A: TOF-MS spectrum for compound **88c**

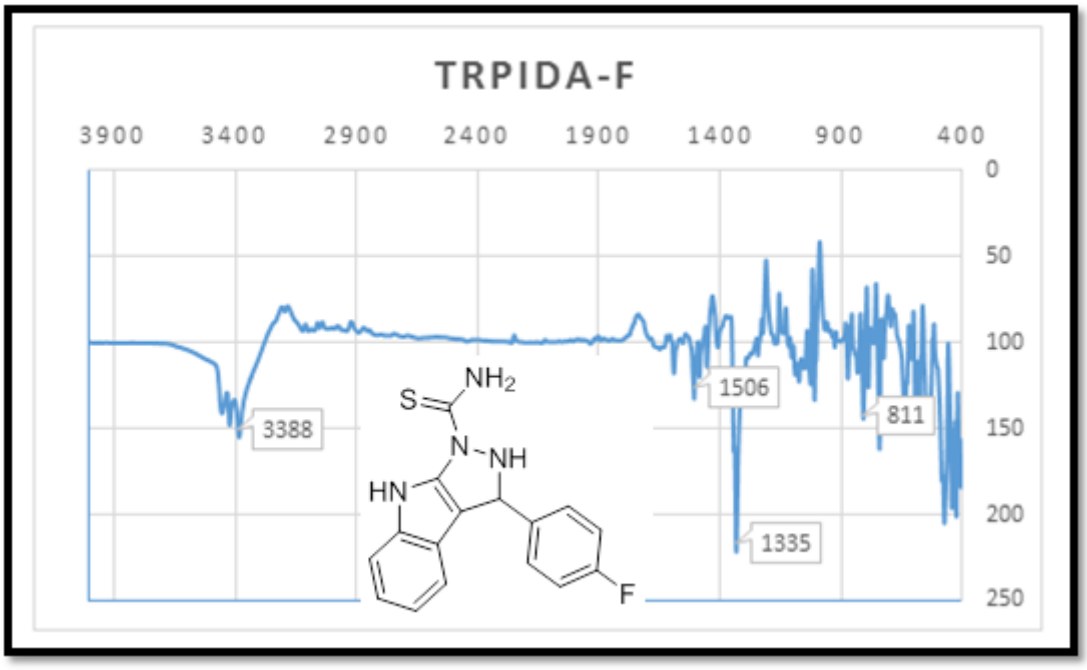

Appendix 5.20A: IR spectrum for compound **88d**

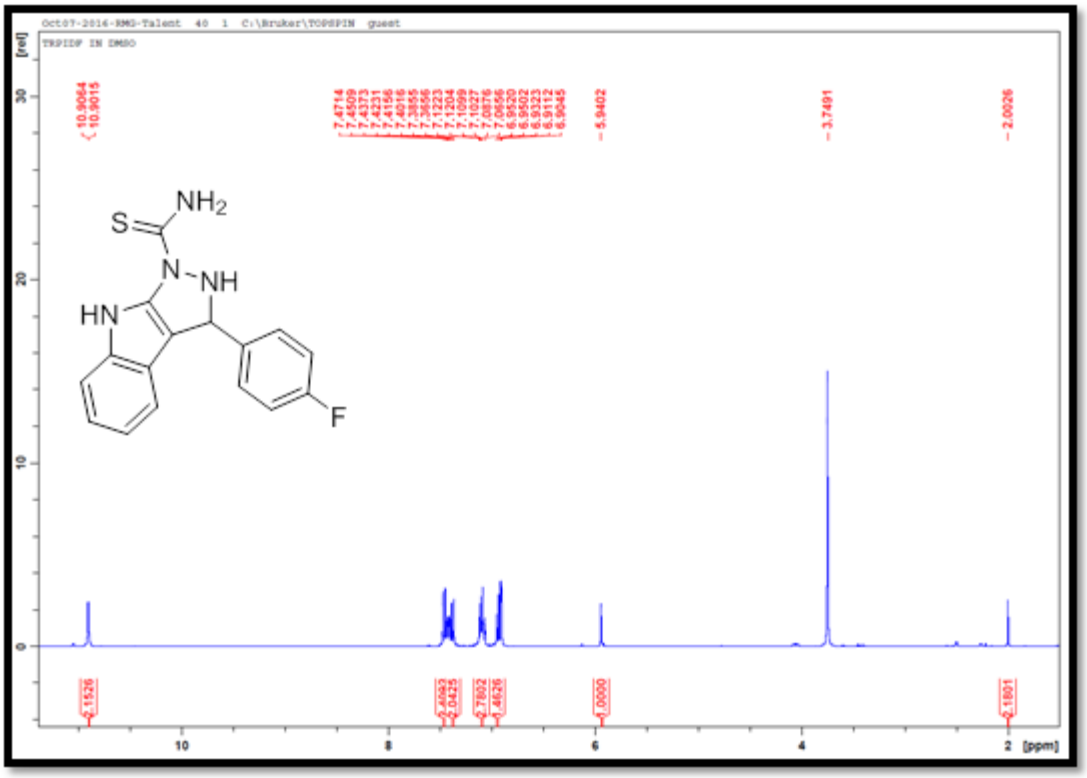

Appendix 5.21A: ^{1}H NMR spectrum for compound **88d**

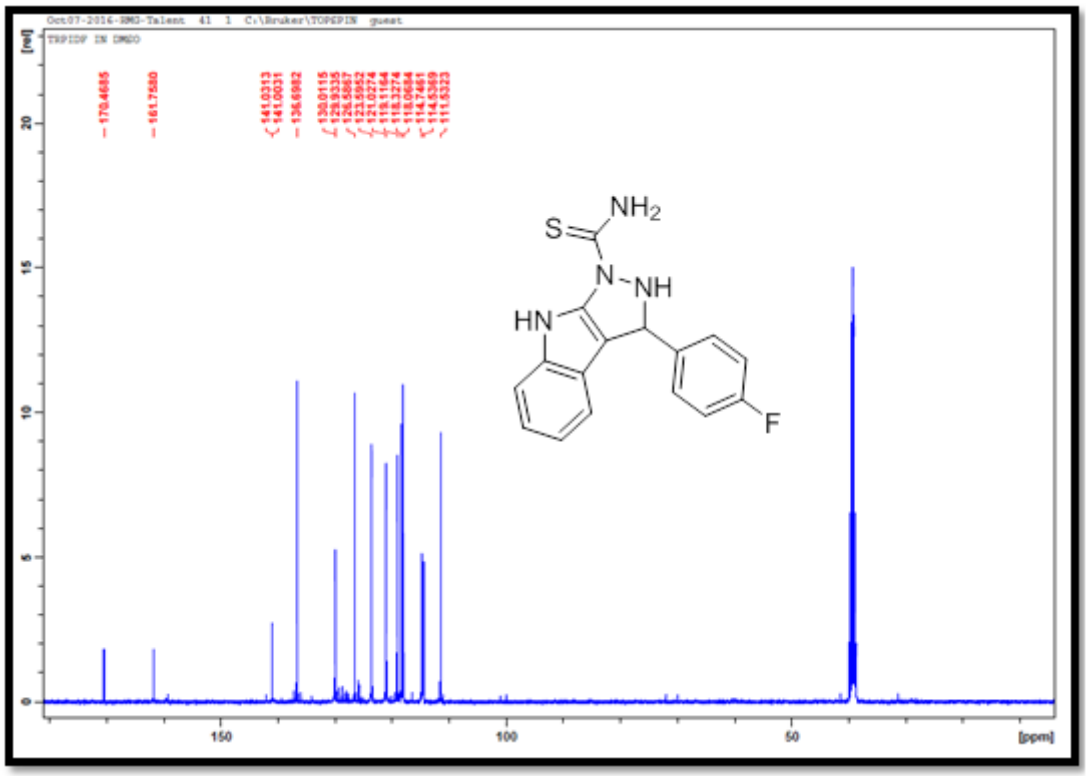

Appendix 5.22A: ^{13}C NMR spectrum for compound **88d**

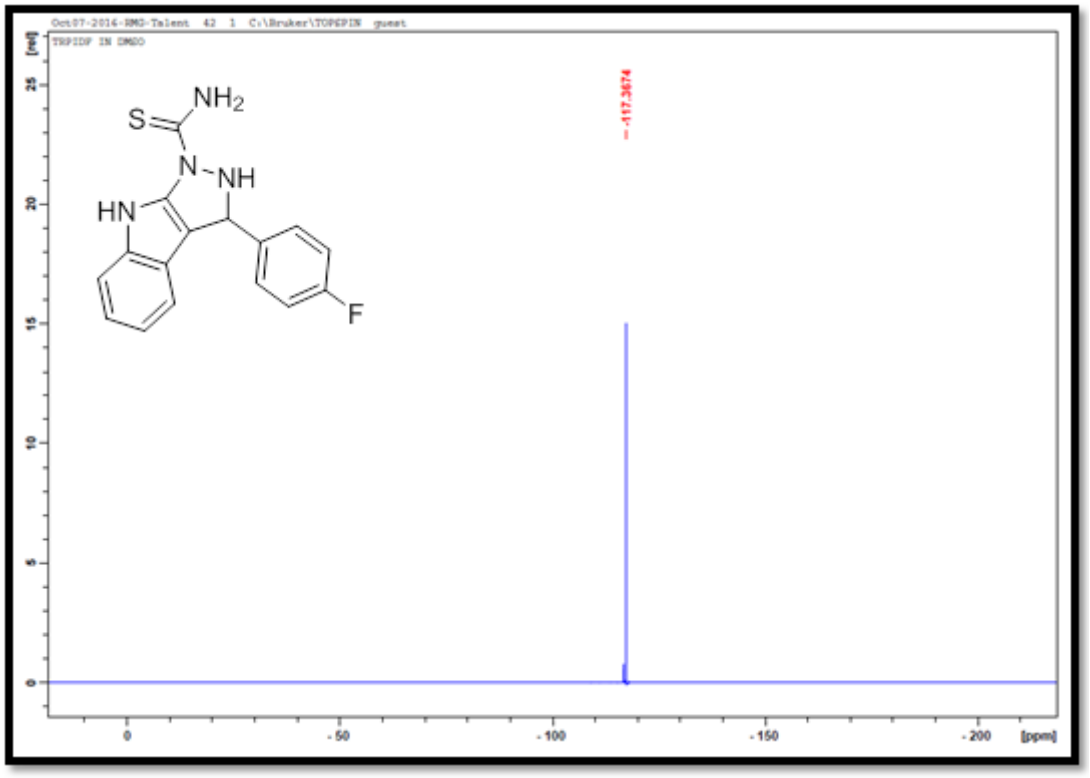

Appendix 5.23A: ^{19}F NMR spectrum for compound **88d**

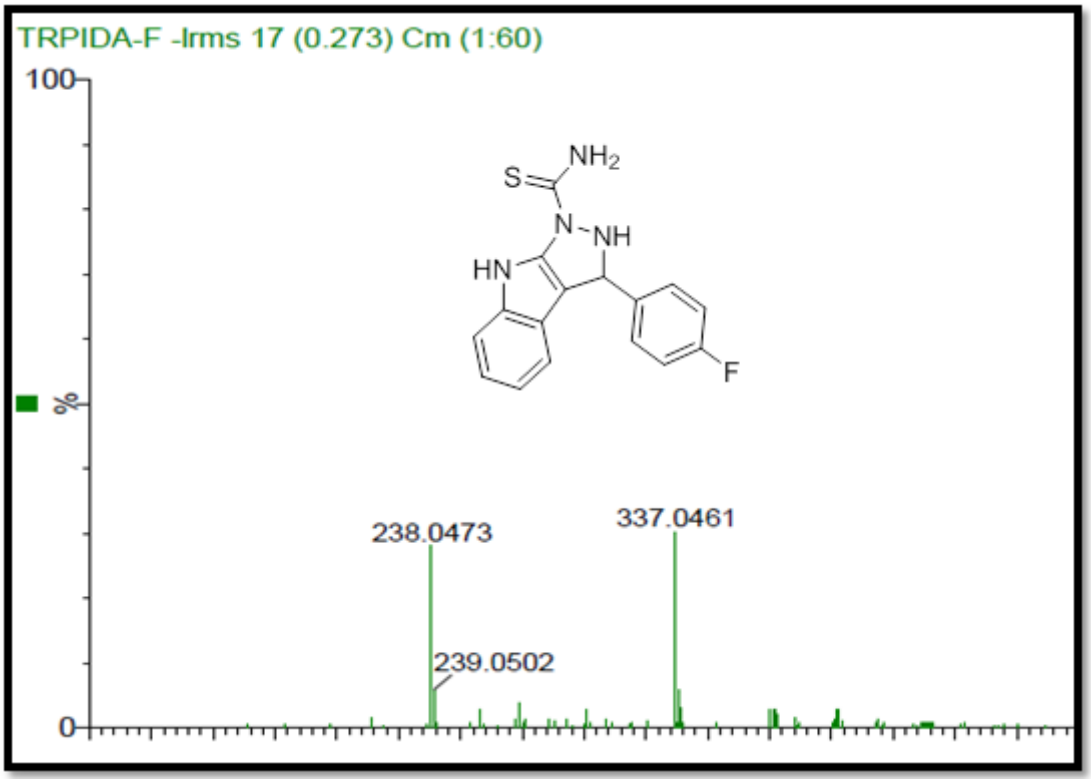

Appendix 5.24A: TOF-MS spectrum for compound **88d**

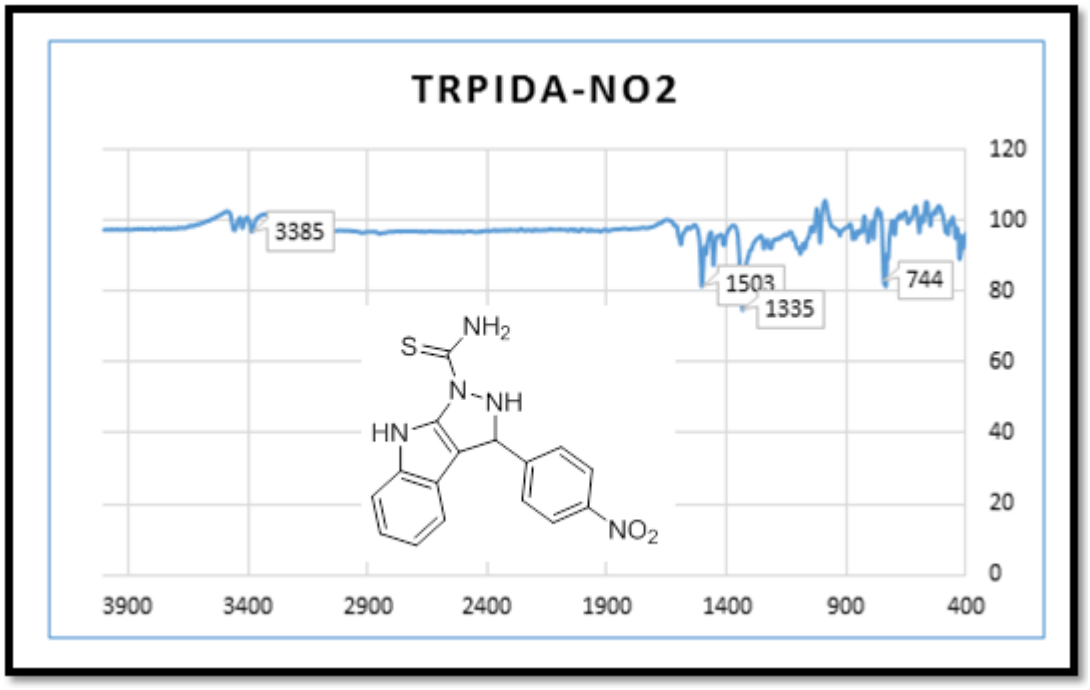

Appendix 5.25A: IR spectrum for compound **88e**

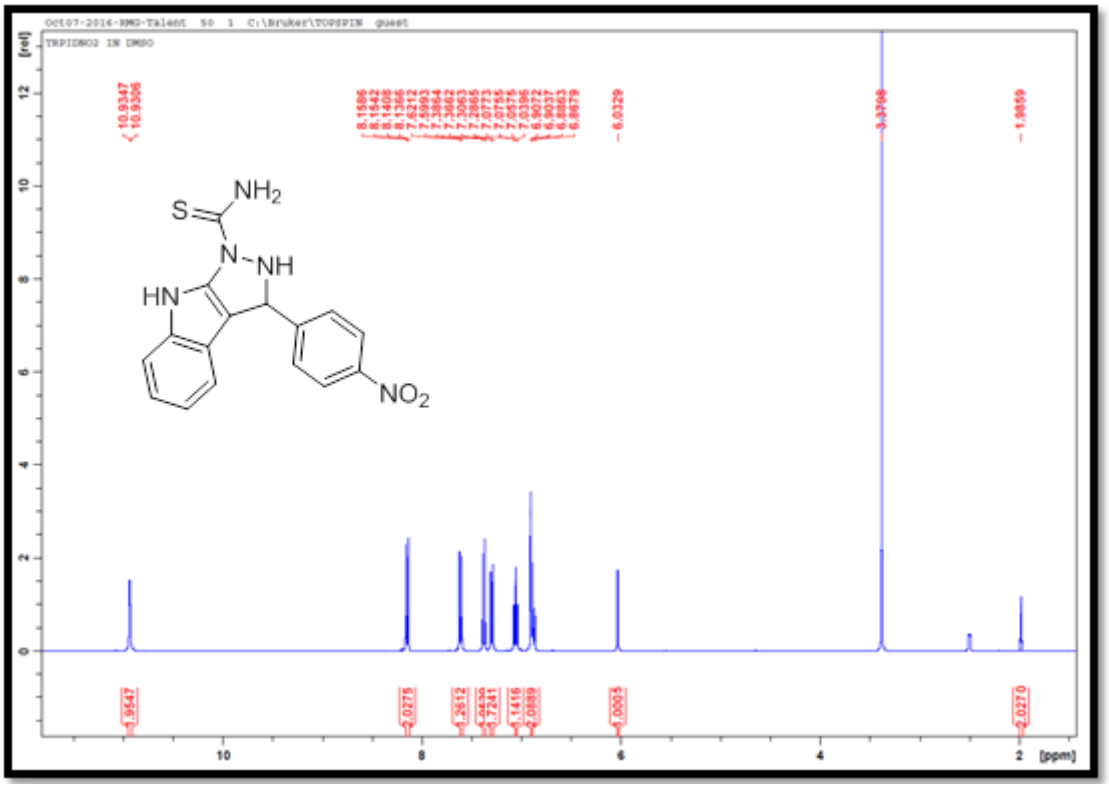

Appendix 5.26A: ^{1}H NMR spectrum for compound **88e**

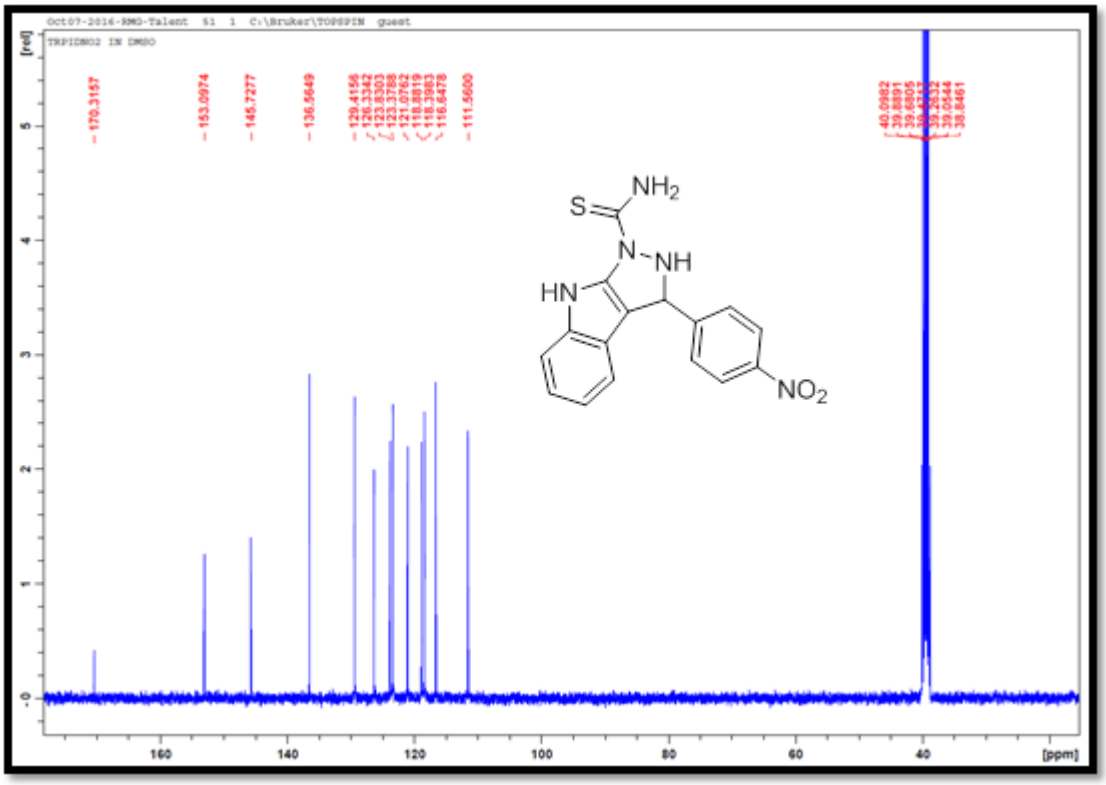

Appendix 5.27A: ^{13}C NMR spectrum for compound **88e**

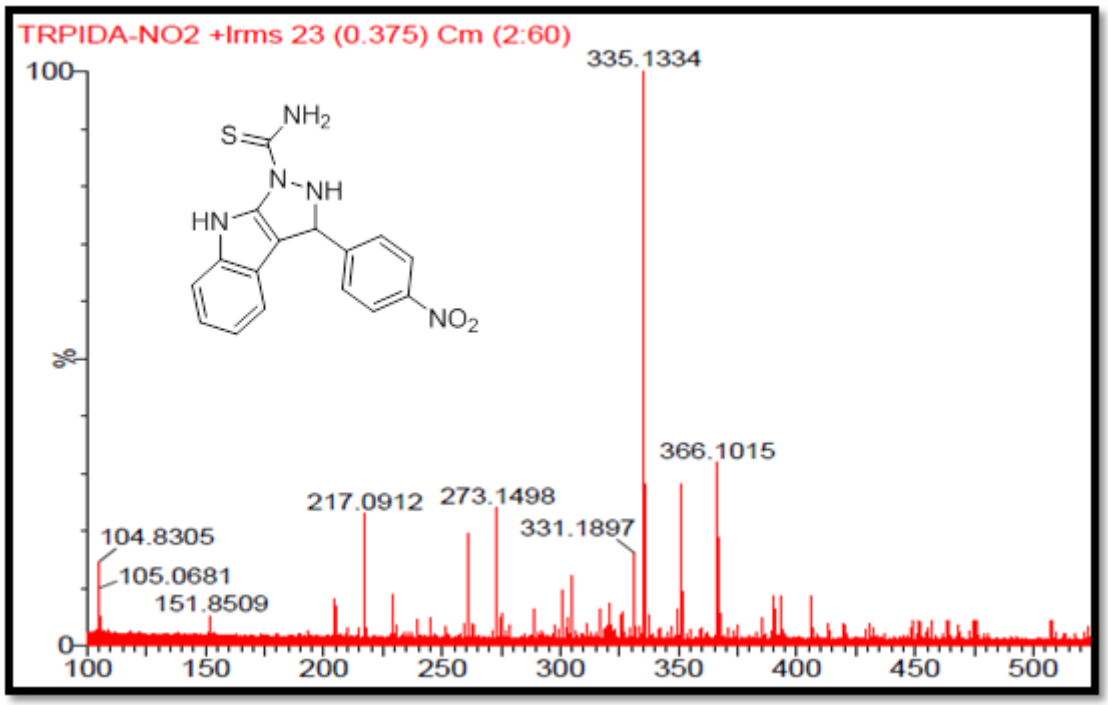

Appendix 5.28A: TOF-MS spectrum for compound **88e**

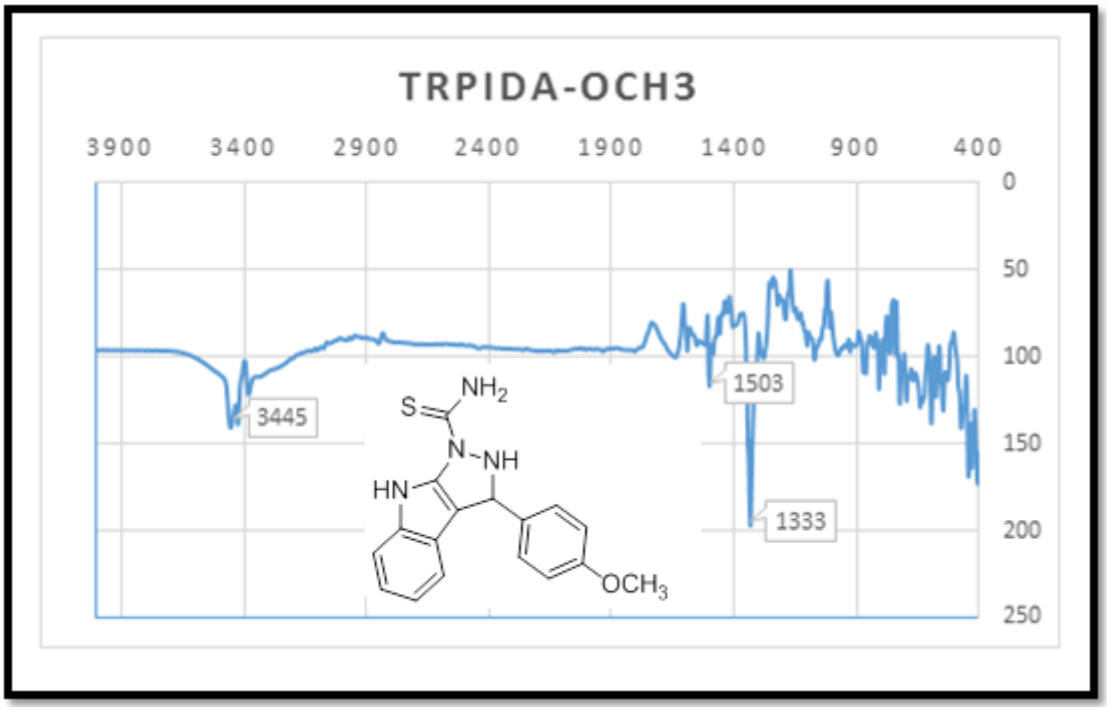

Appendix 5.29A: IR spectrum for compound **88f**

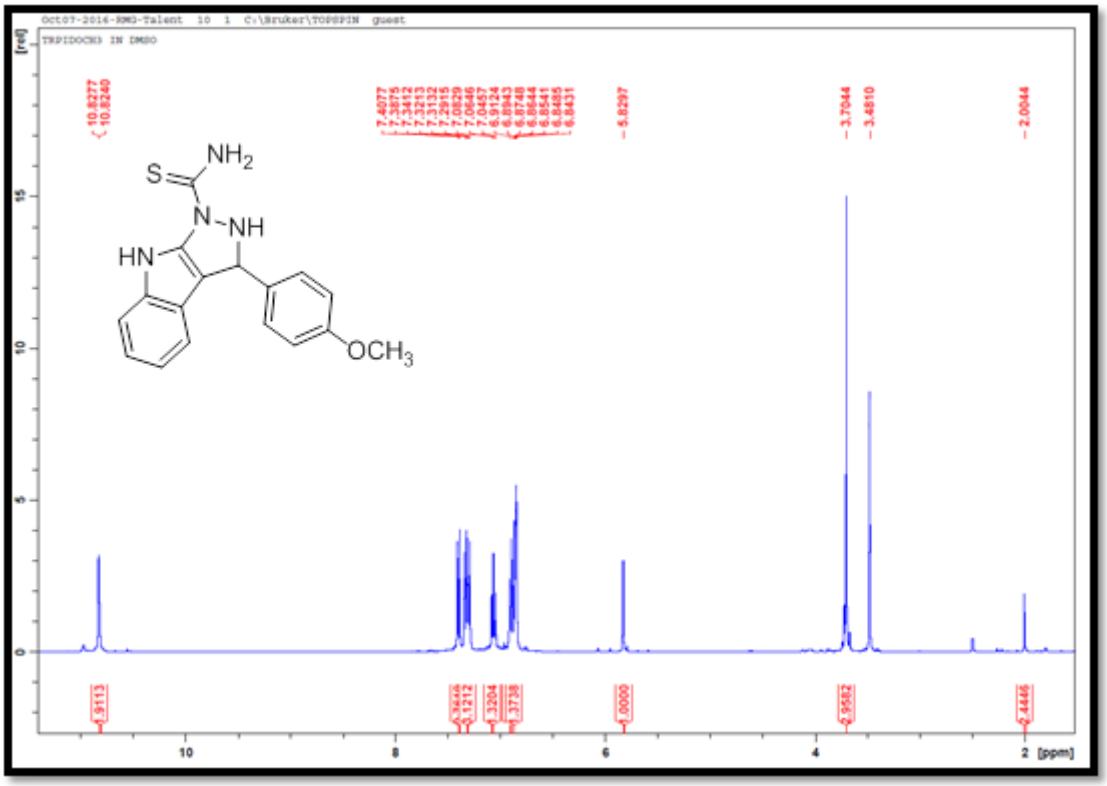

Appendix 5.30A: ^{1}H NMR spectrum for compound **88f**

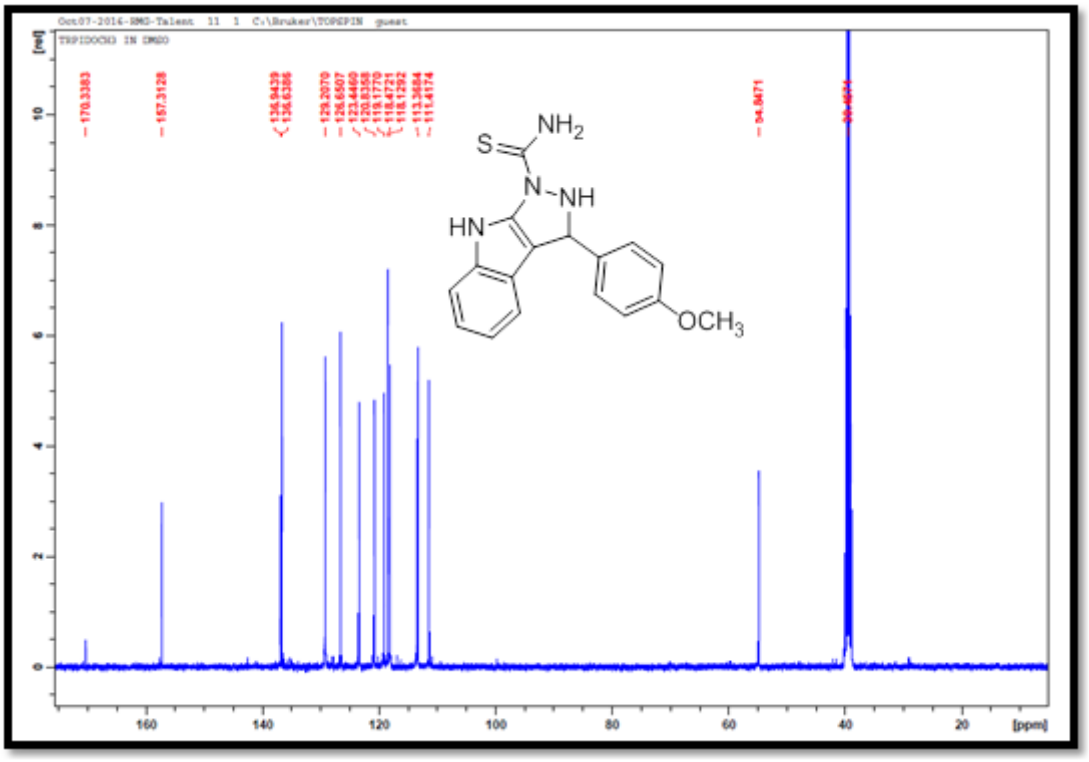

Appendix 5.31A: ^{13}C NMR spectrum for compound **88f**

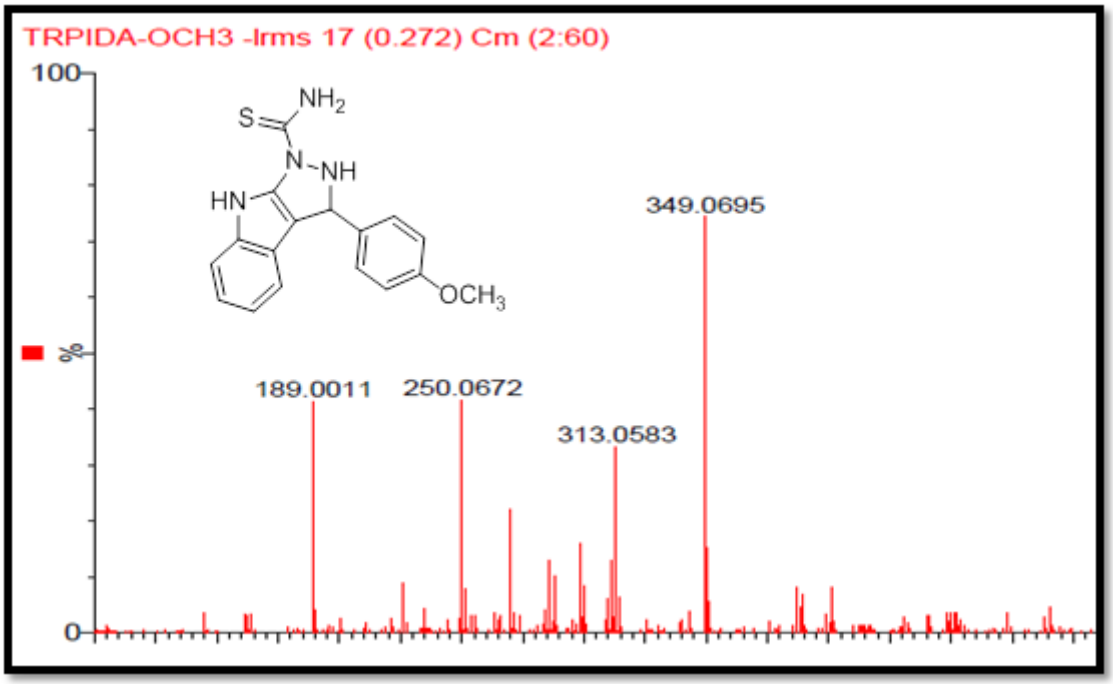

Appendix 5.32A: TOF-MS spectrum for compound **88f**

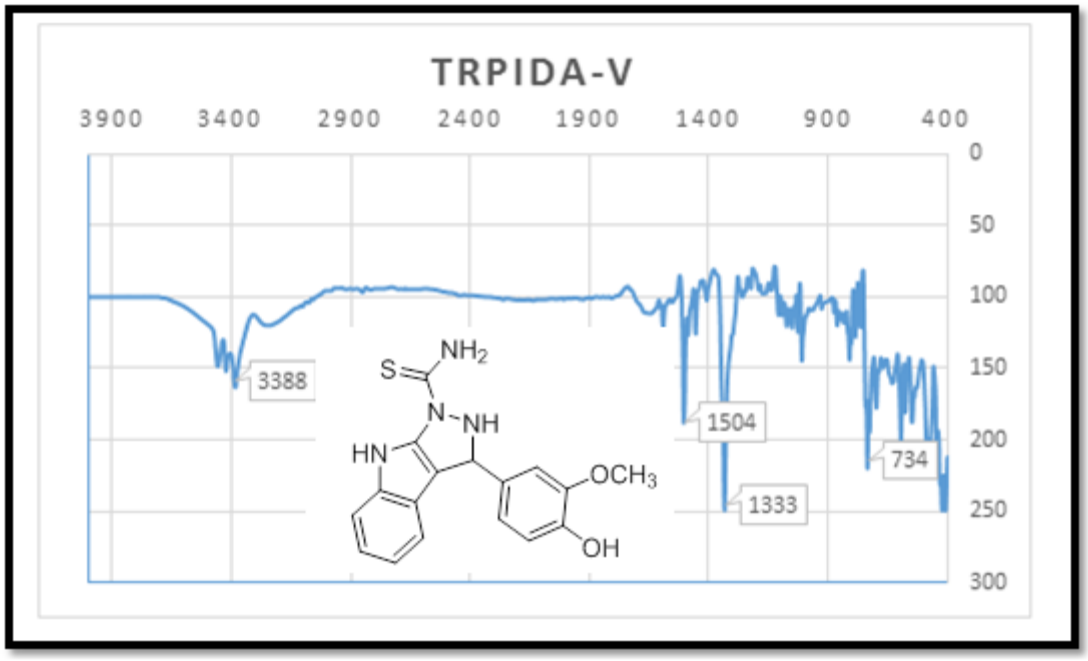

Appendix 5.33A: IR spectrum for compound **88g**

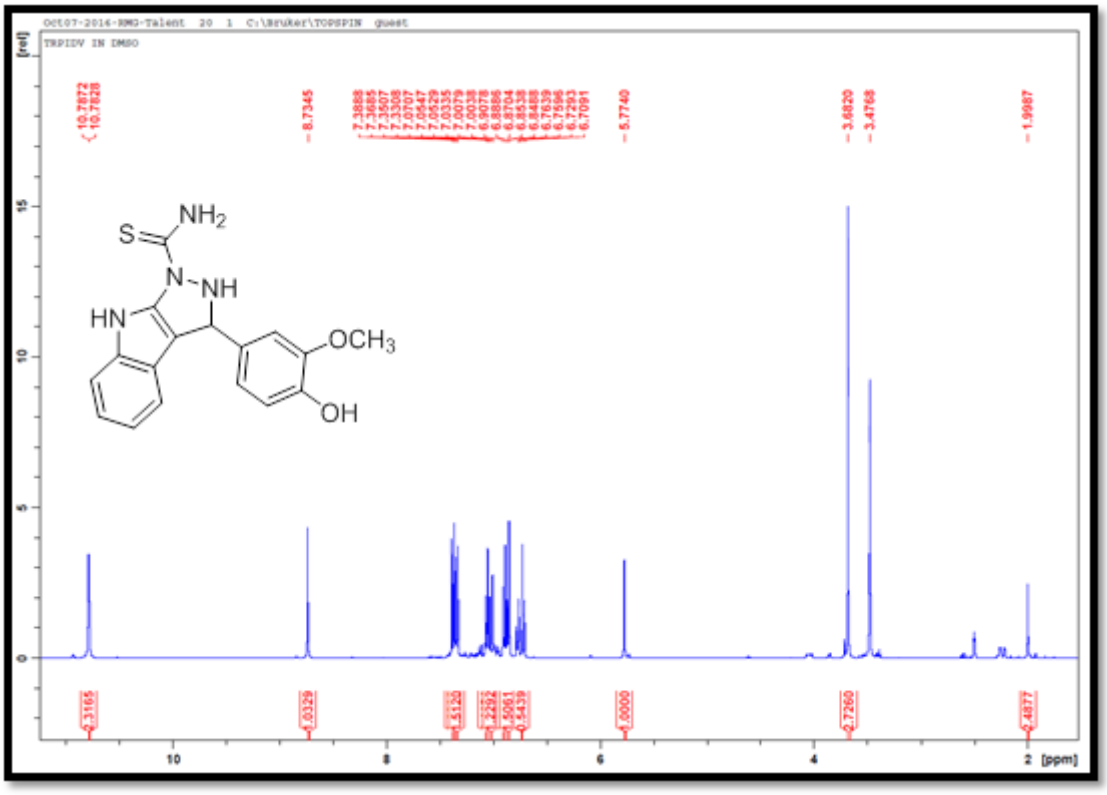

Appendix 5.34A: ^{1}H NMR spectrum for compound **88g**

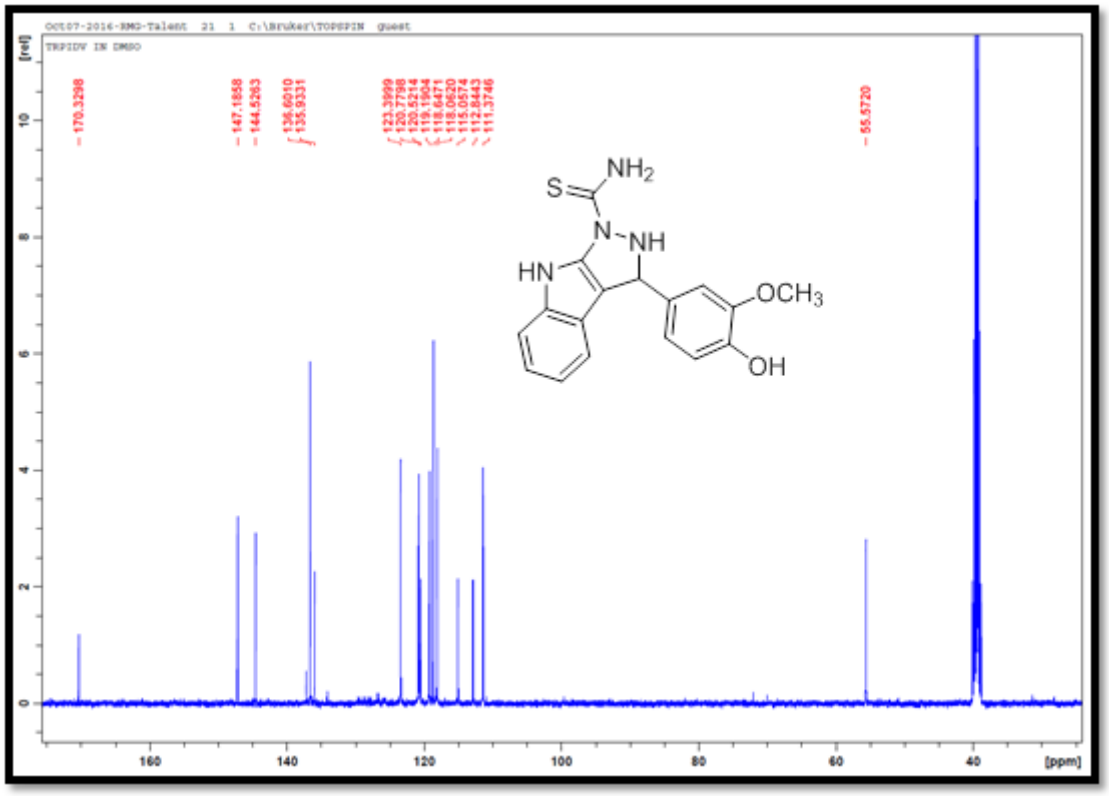

Appendix 5.35A: ^{13}C NMR spectrum for compound **88g**

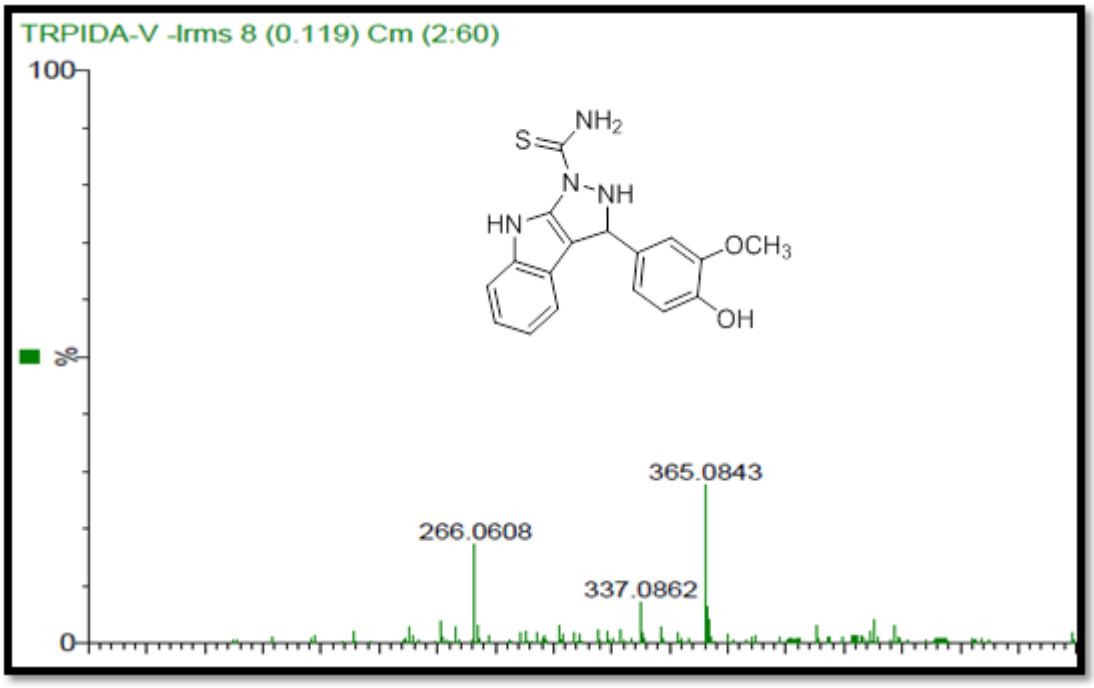

Appendix 5.36A: TOF-MS spectrum for compound **88g**

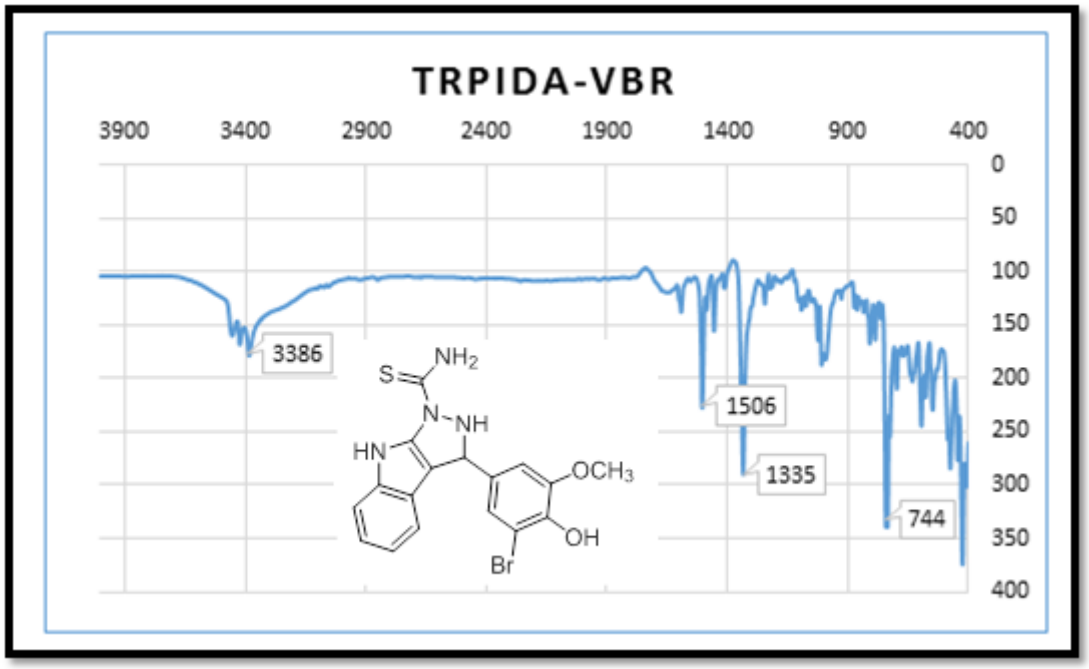

Appendix 5.37A: IR spectrum for compound **88h**

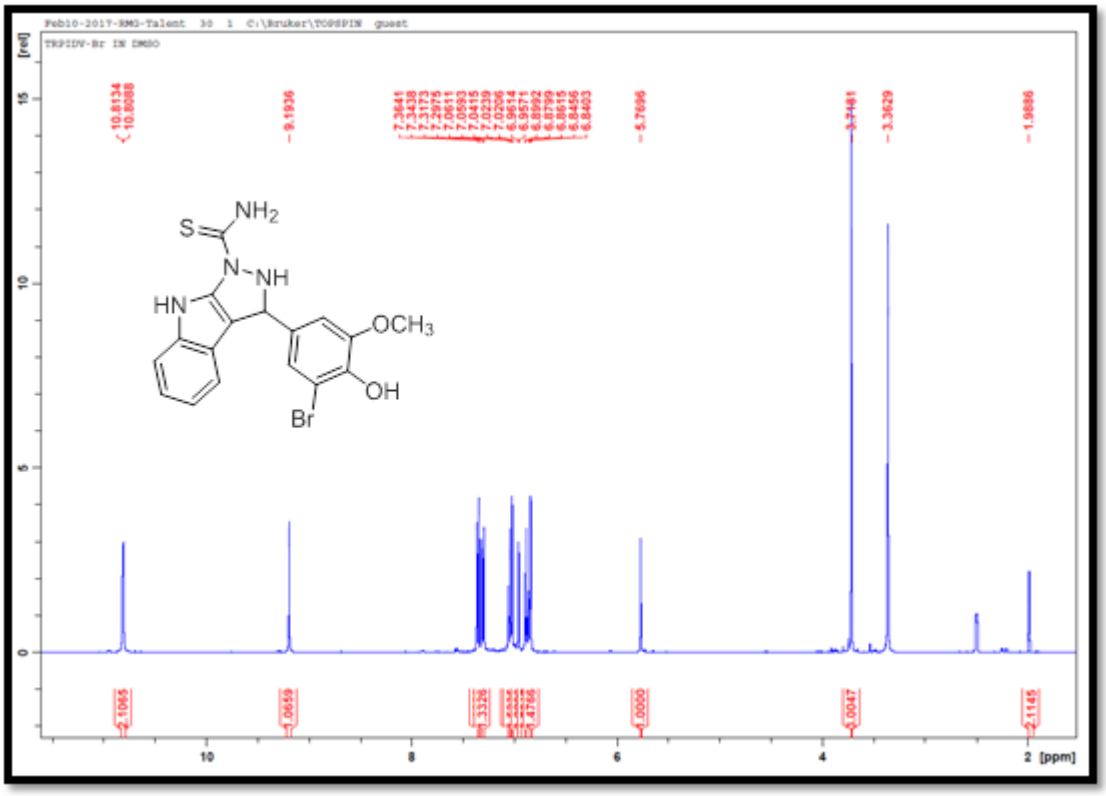

Appendix 5.38A: ^{1}H NMR spectrum for compound **88h**

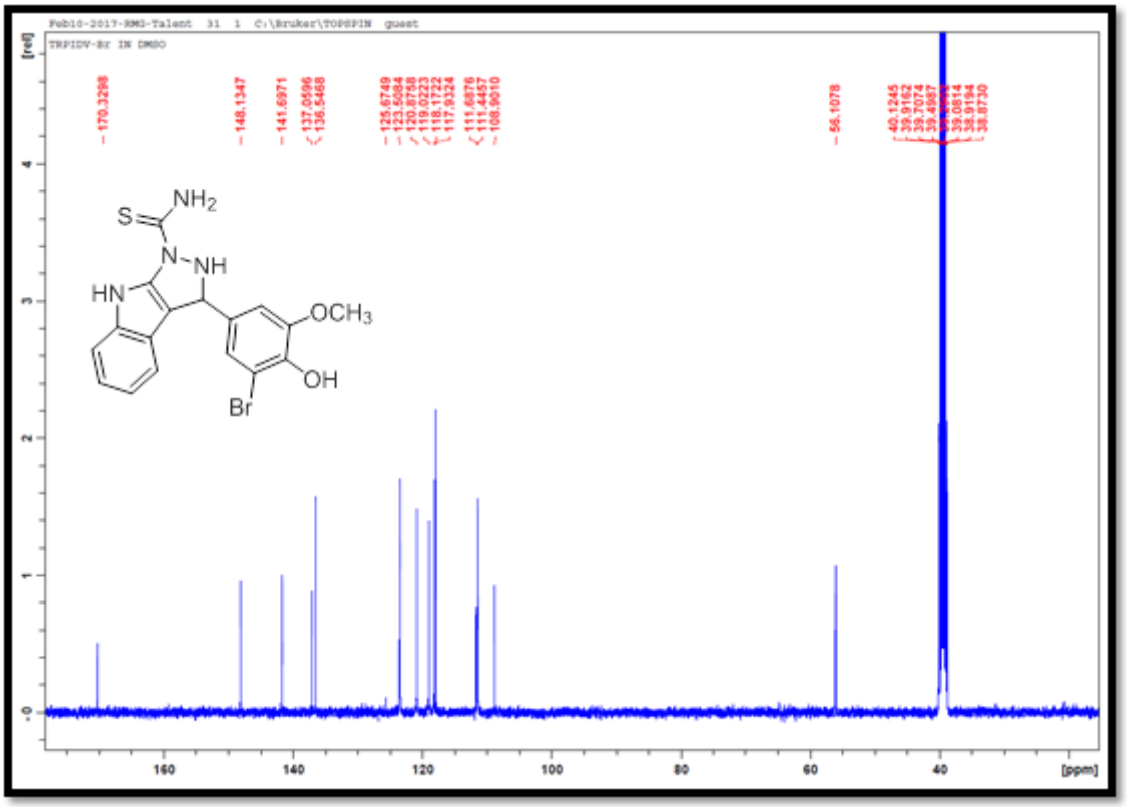

Appendix 5.39A: ^{13}C NMR spectrum for compound **88h**

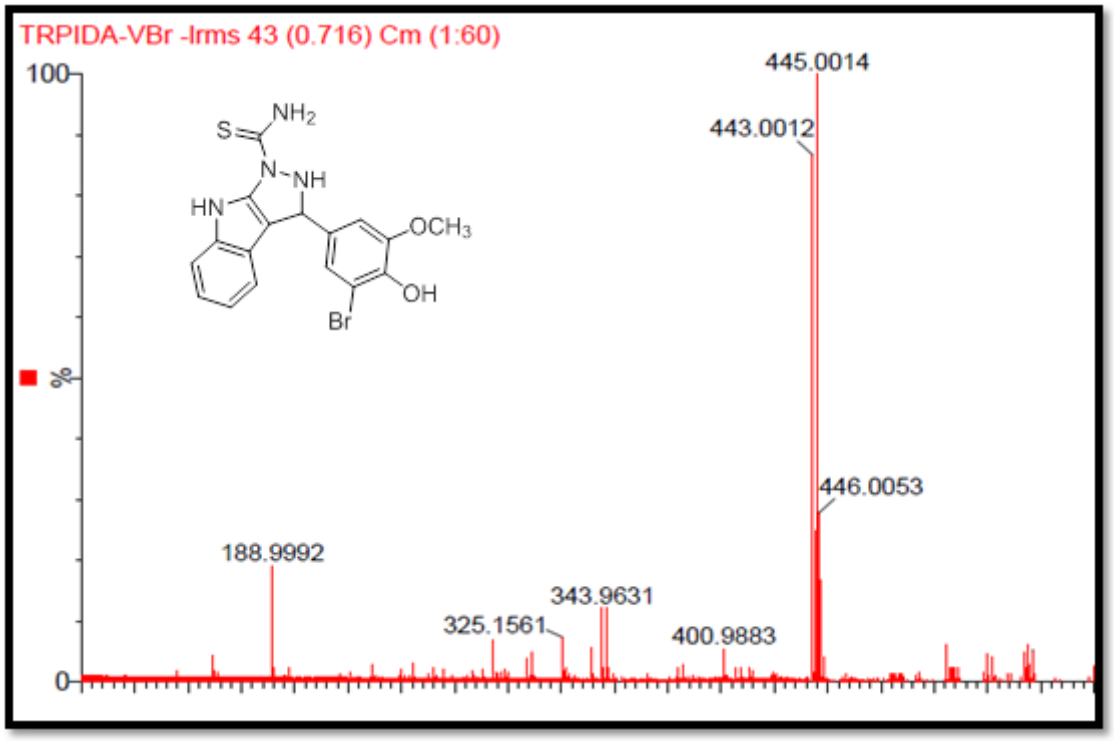

Appendix 5.40A: TOF-MS spectrum for compound **88h**

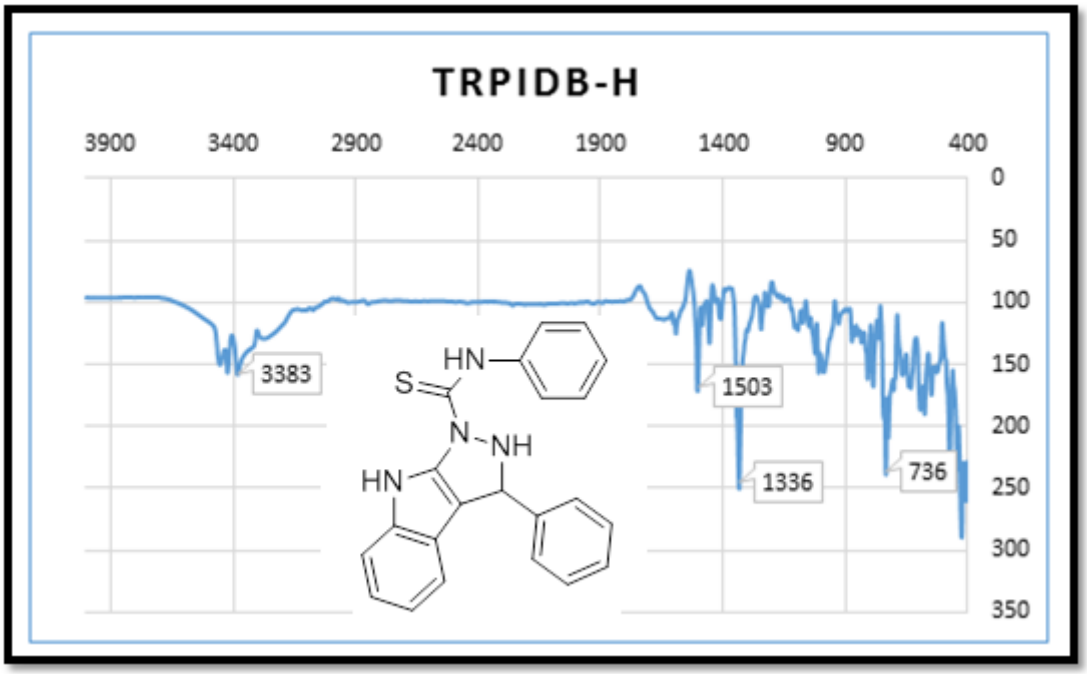

Appendix 5.41A: IR spectrum for compound **88i**

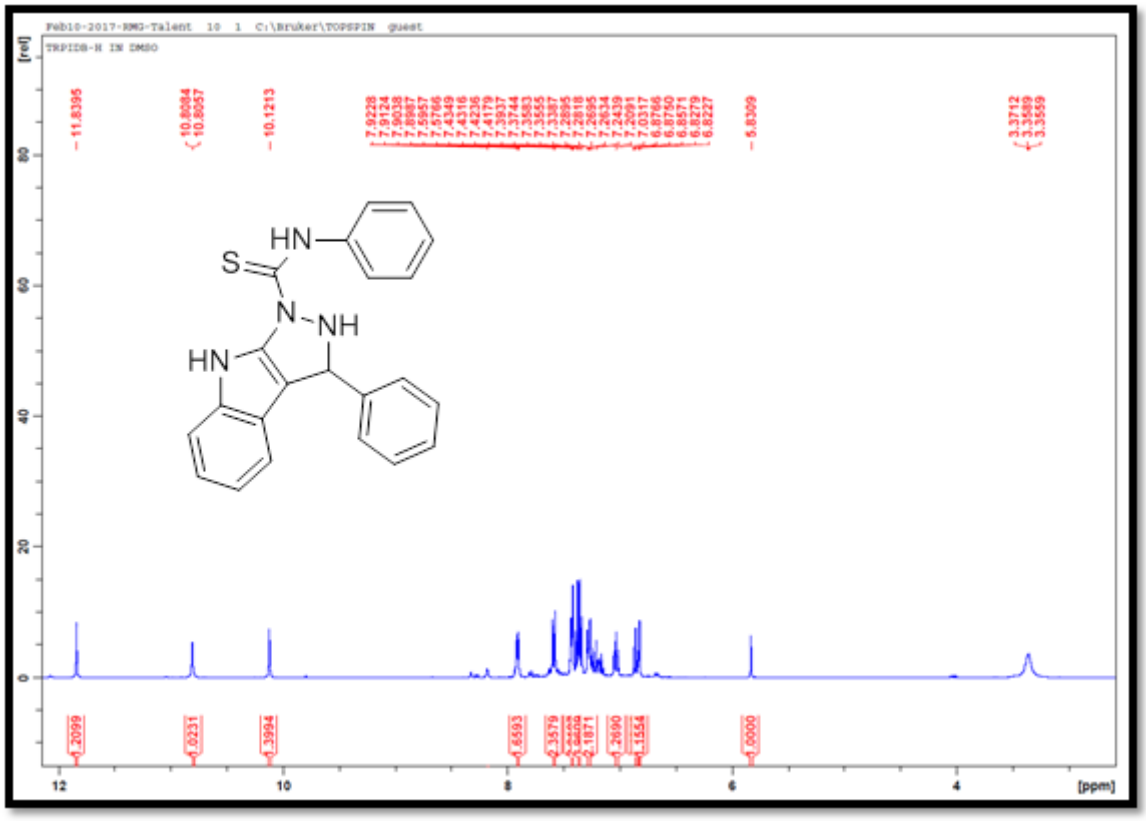

Appendix 5.42A: ^{1}H NMR spectrum for compound **88i**

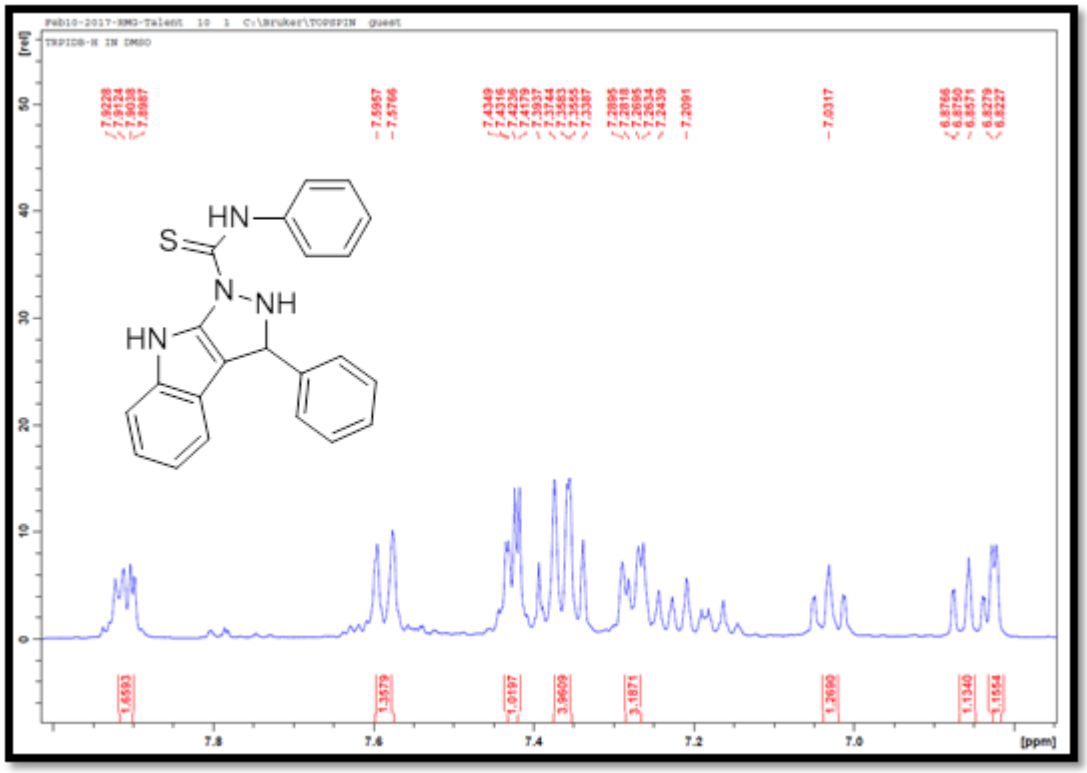

Appendix 5.43A: Expanded ^{1}H NMR spectrum for compound **88i**

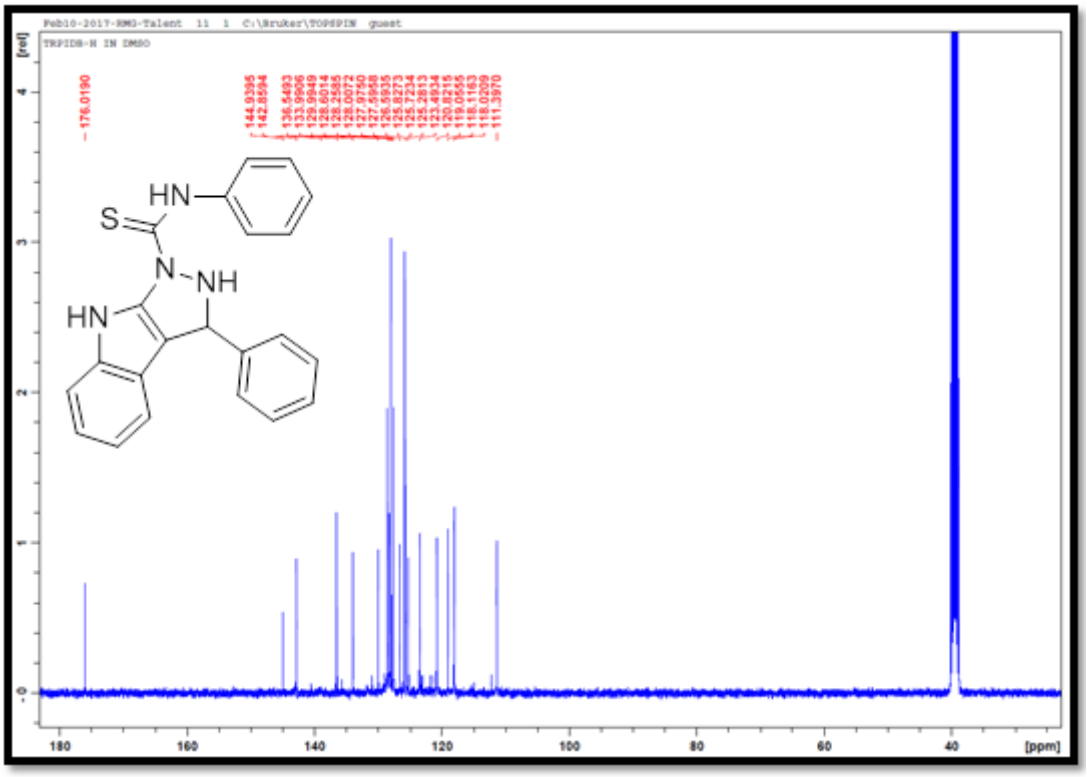

Appendix 5.44A: ^{13}C NMR spectrum for compound **88i**

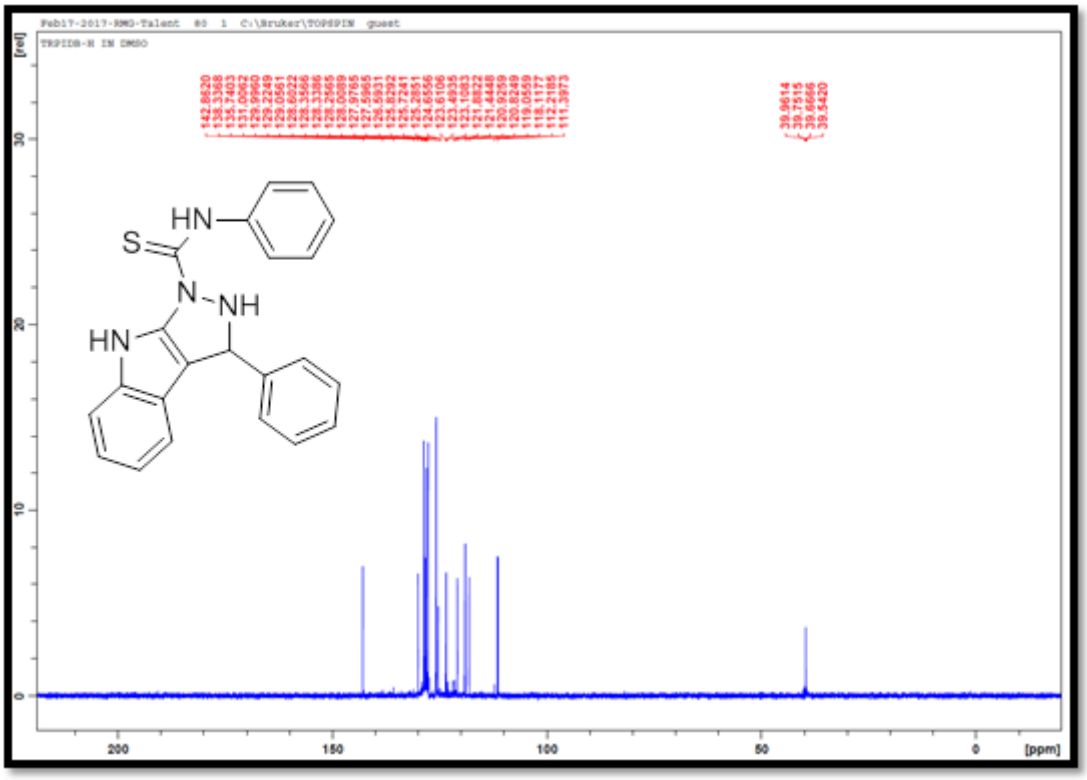

Appendix 5.45A: 90^0 DEPT NMR spectrum for compound **88i**

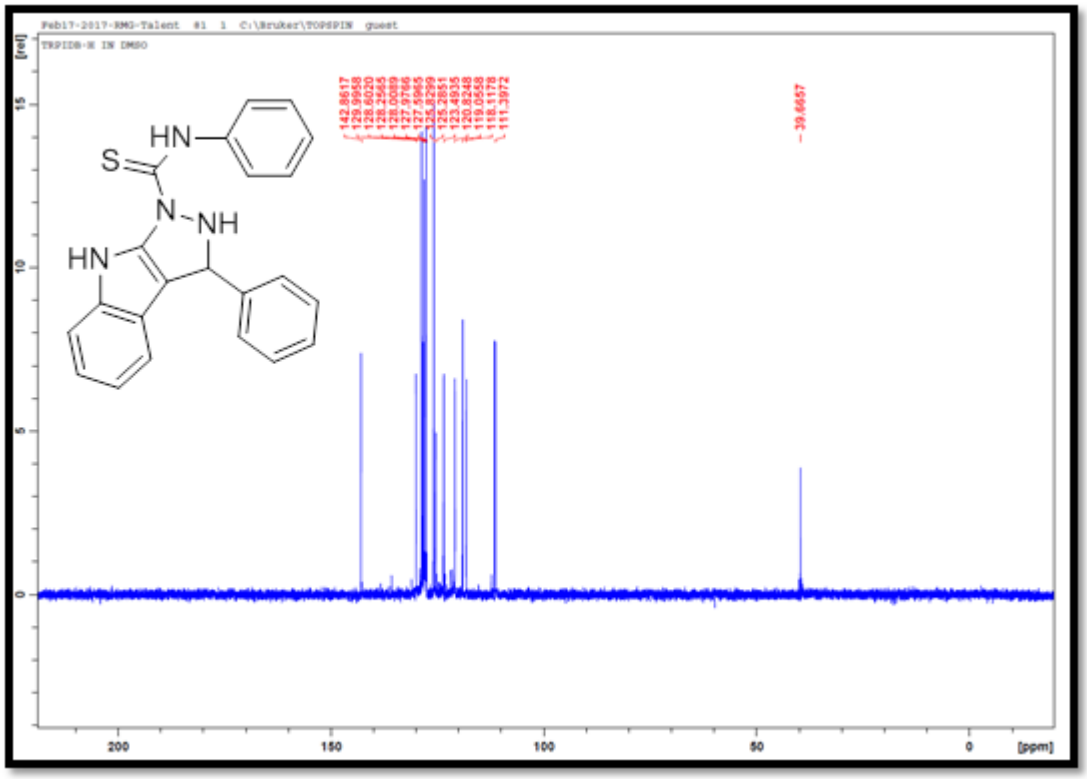

Appendix 5.46A: 135^0 DEPT NMR spectrum for compound **88i**

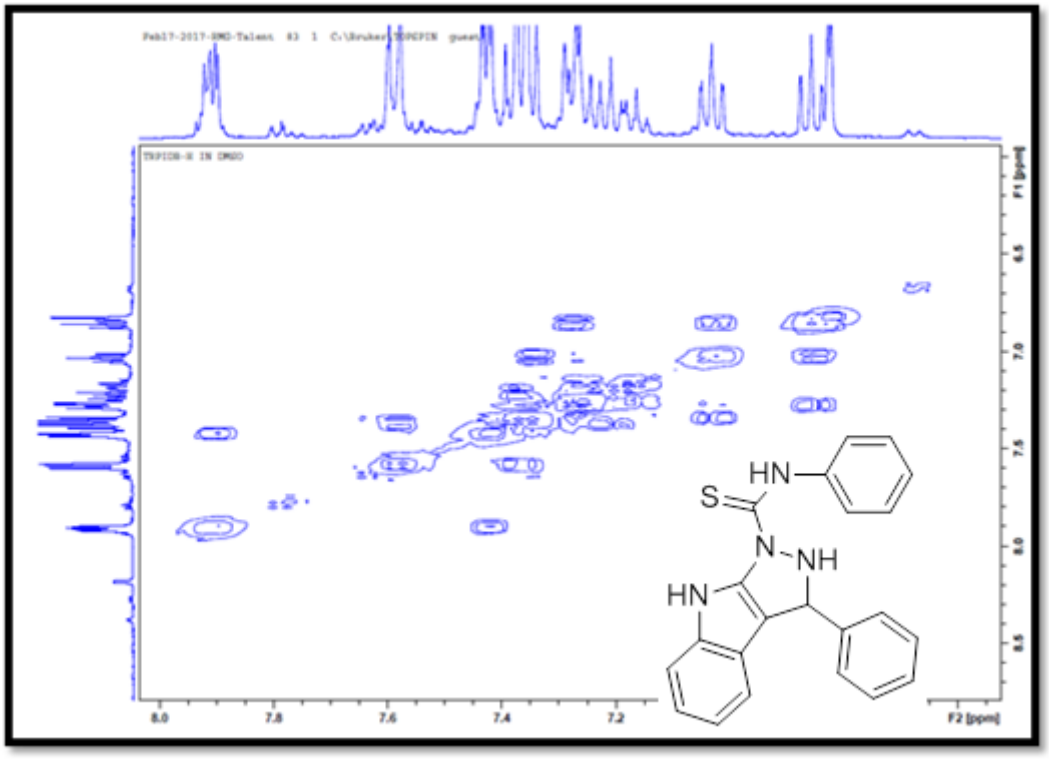

Appendix 5.47A: Expanded COSY NMR spectrum for compound **88i**

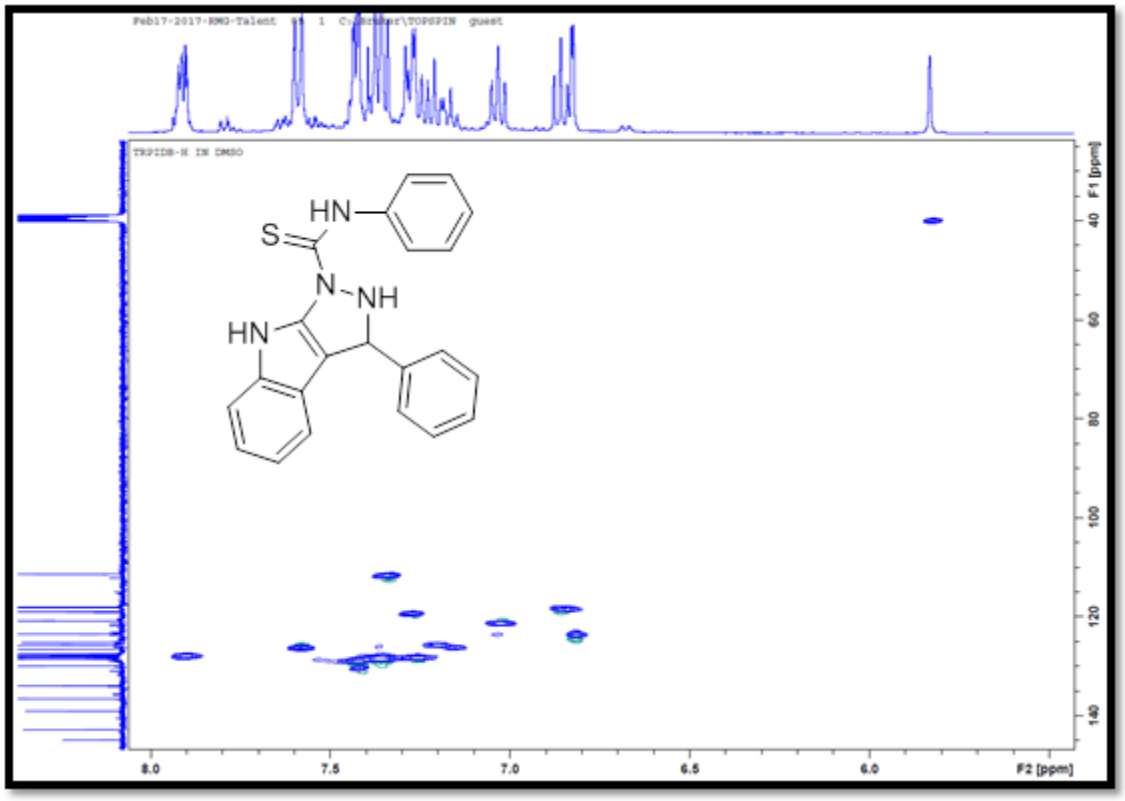

Appendix 5.48A: HSQC NMR spectrum for compound **88i**

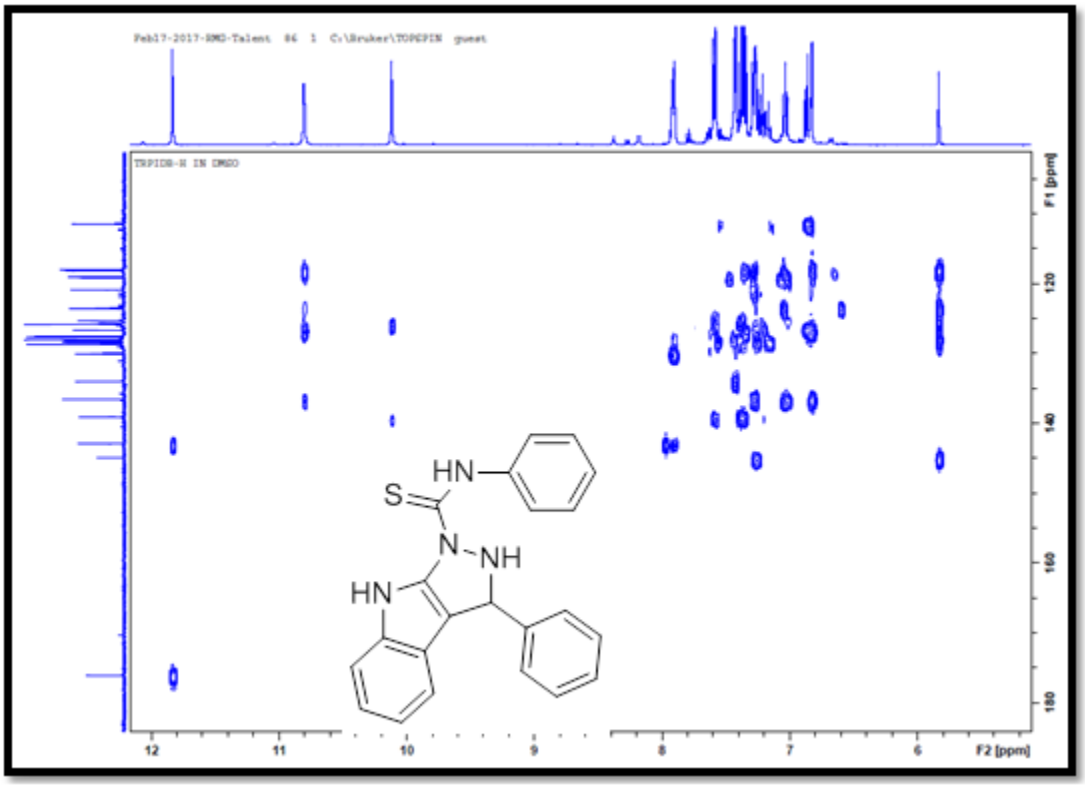

Appendix 5.49A: HMBC NMR spectrum for compound **88i**

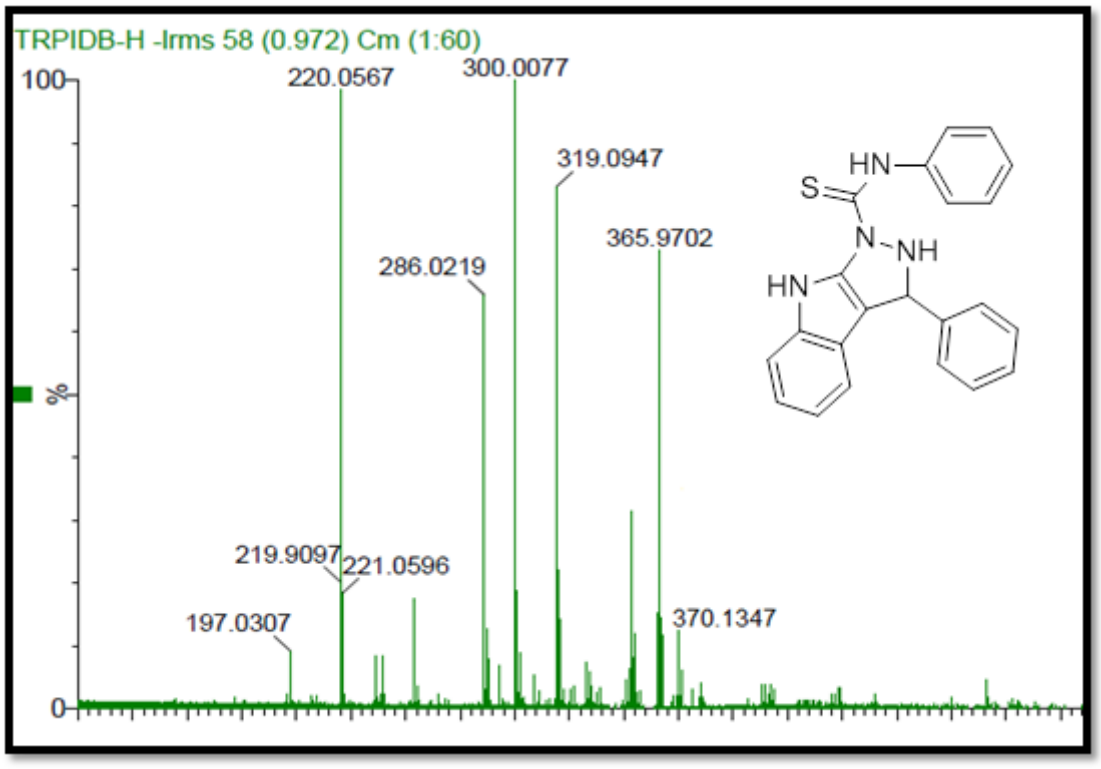

Appendix 5.50A: TOF-MS spectrum for compound **88i**

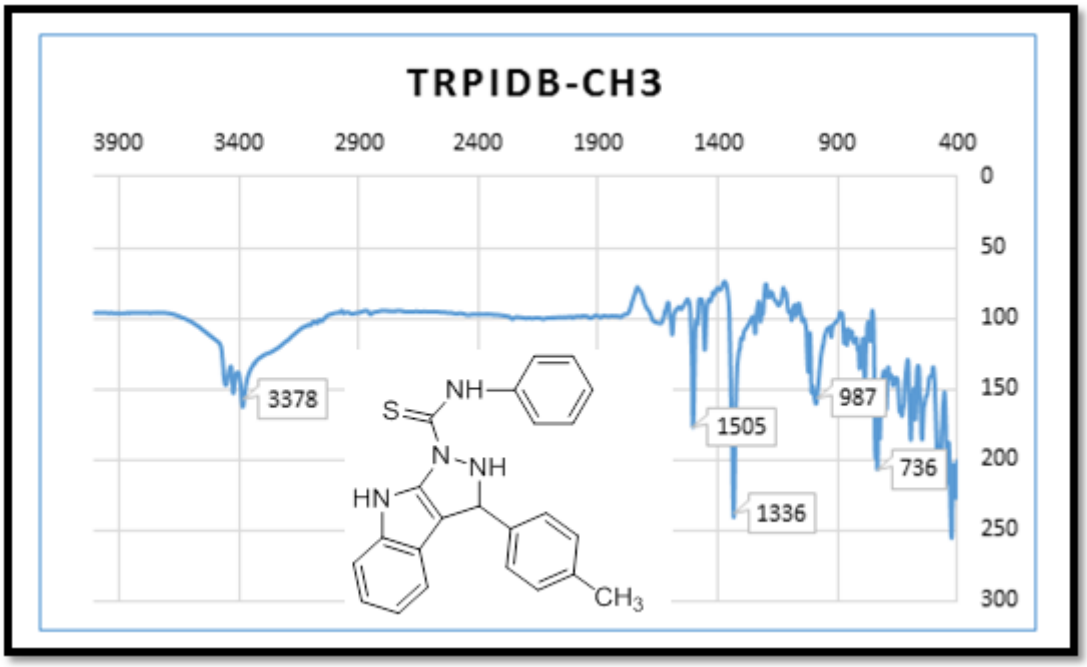

Appendix 5.51A: IR spectrum for compound **88j**

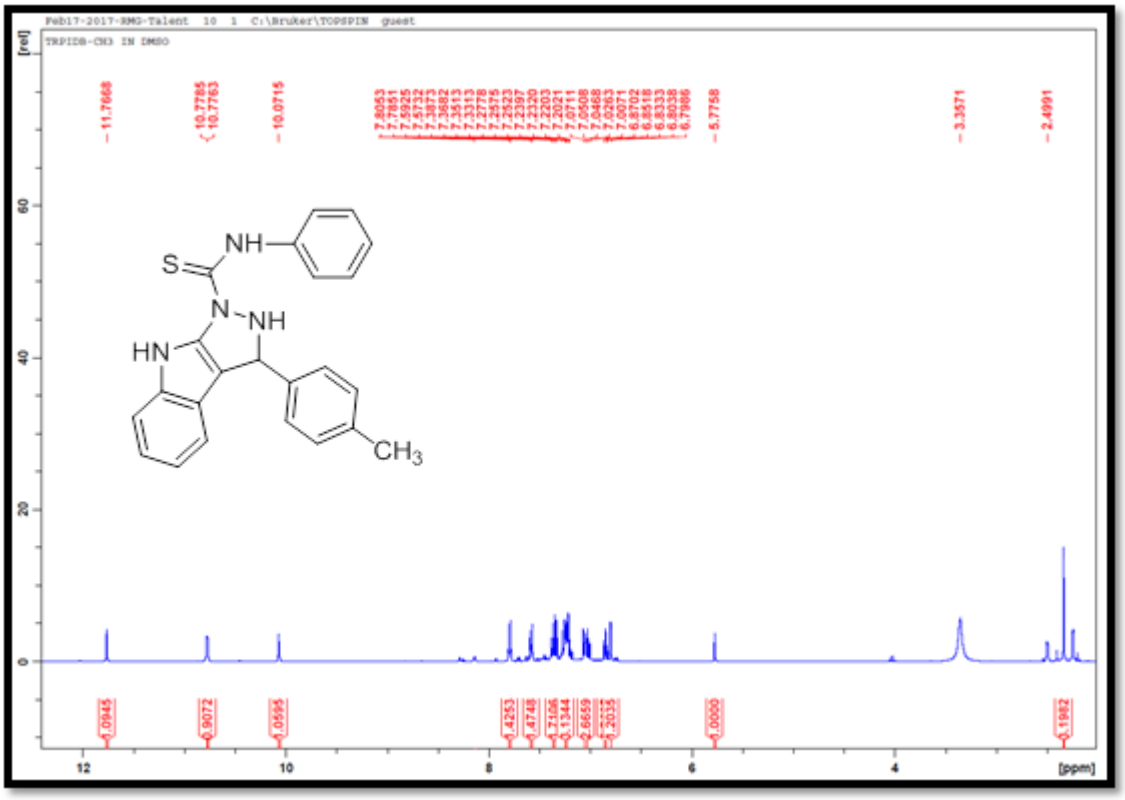

Appendix 5.52A: ^{1}H NMR spectrum for compound **88j**

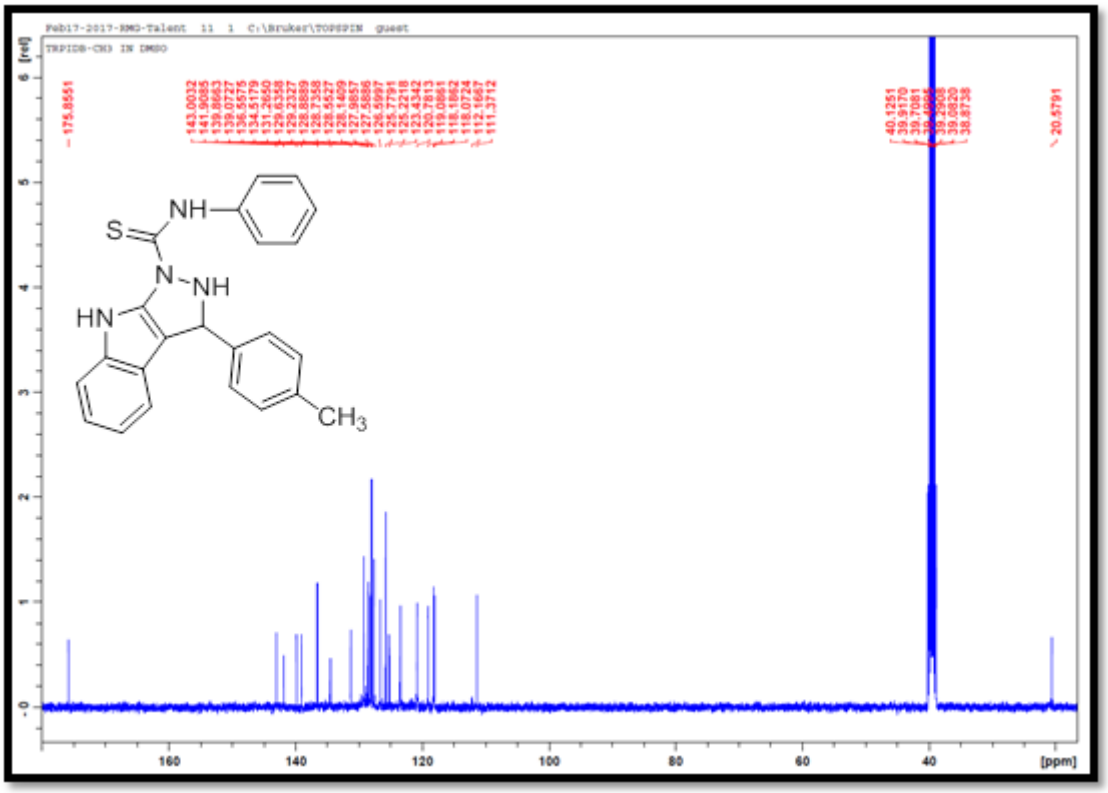

Appendix 5.53A: ^{13}C NMR spectrum for compound **88j**

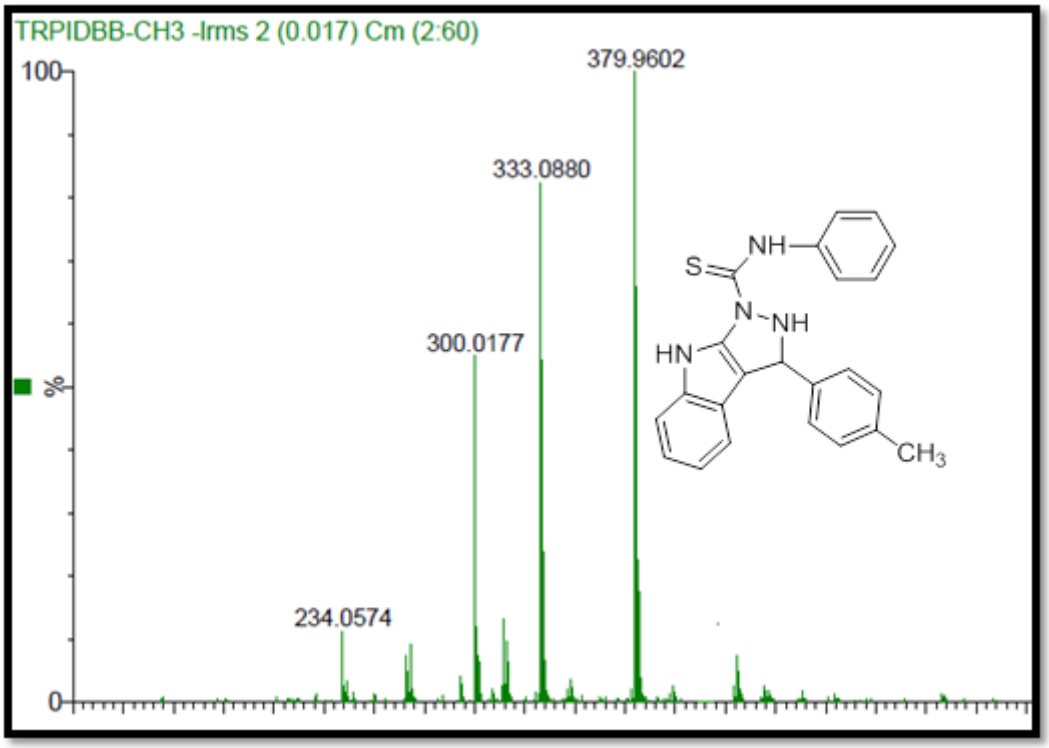

Appendix 5.54A: TOF-MS spectrum for compound **88j**

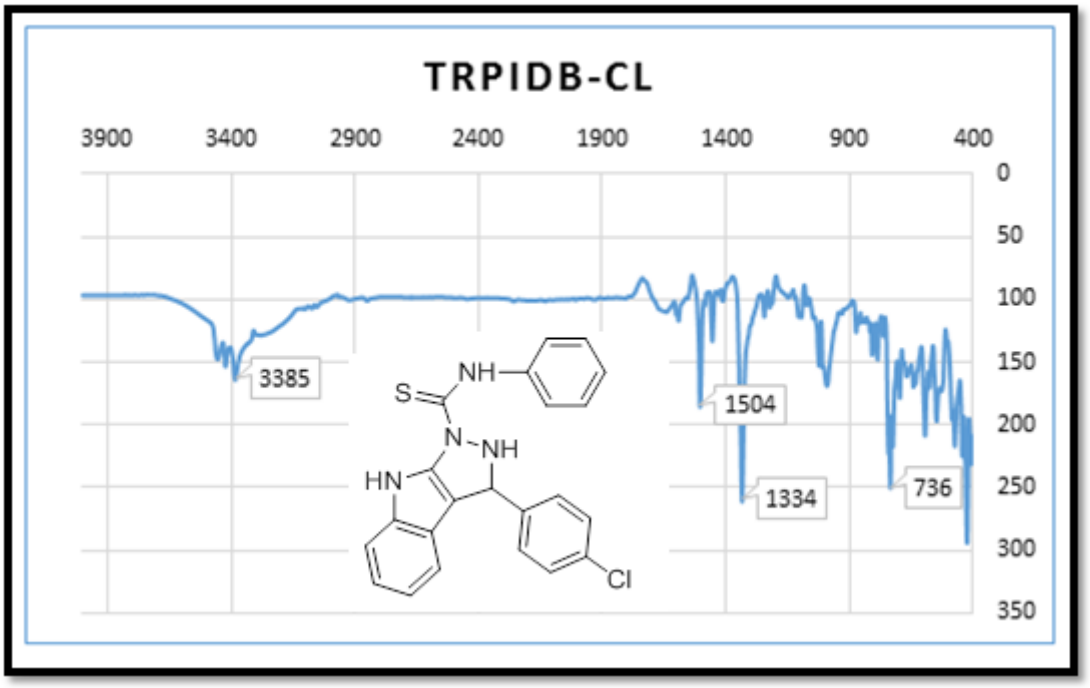

Appendix 5.55A: IR spectrum for compound **88k**

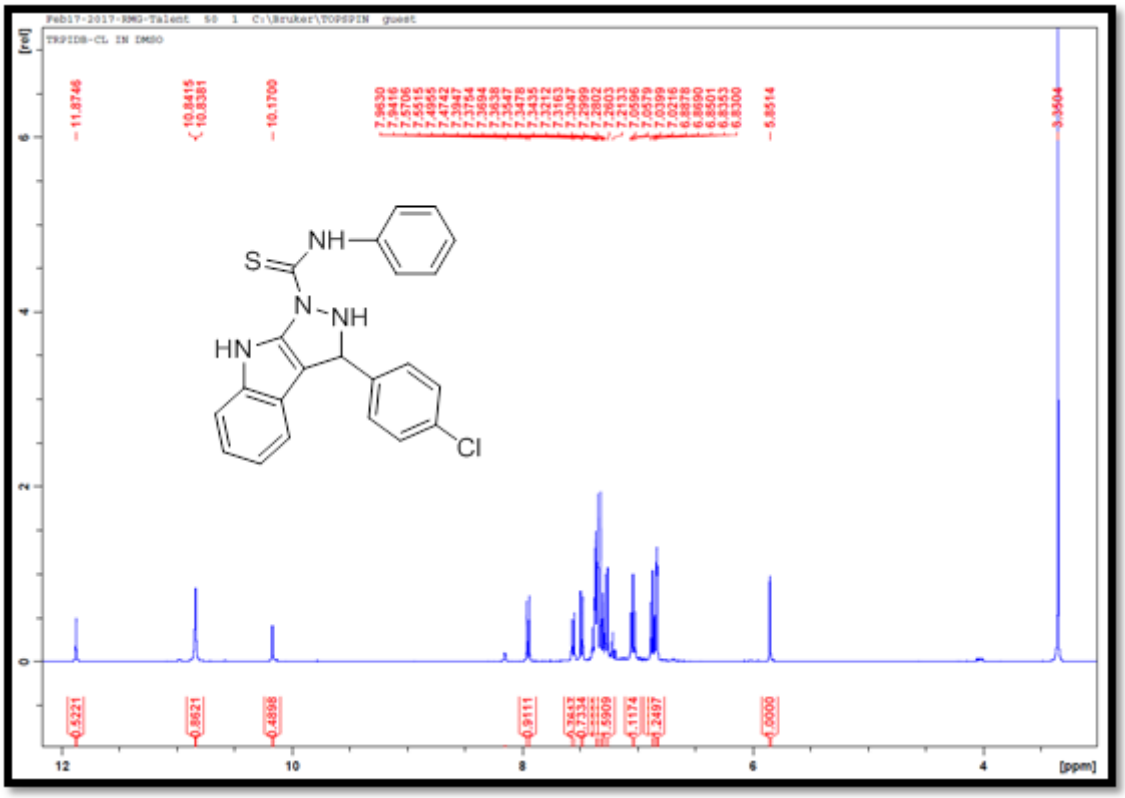

Appendix 5.56A: ^{1}H NMR spectrum for compound **88k**

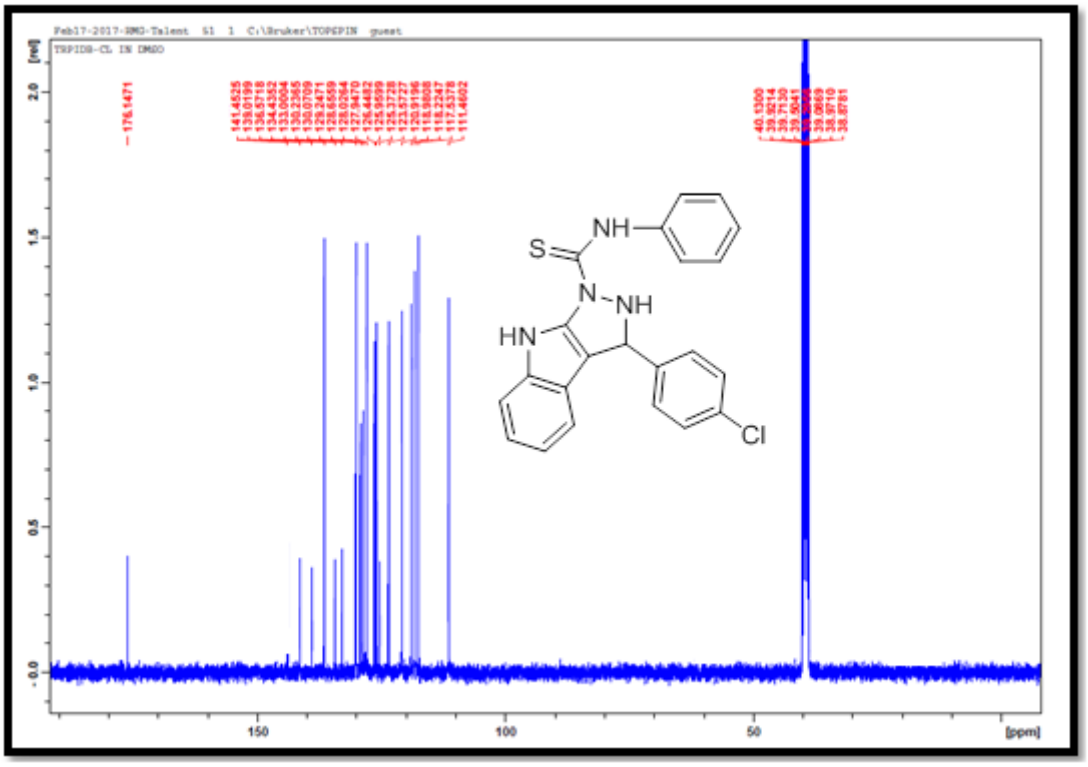

Appendix 5.57A: ^{13}C NMR spectrum for compound **88k**

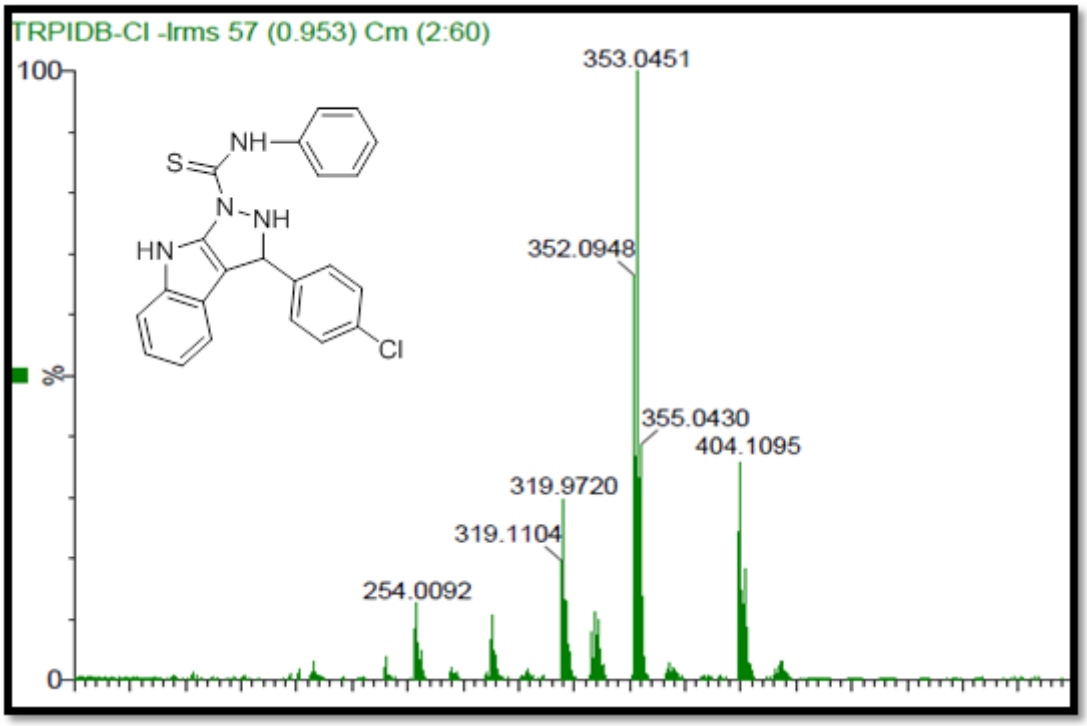

Appendix 5.58A: TOF-MS spectrum for compound **88k**

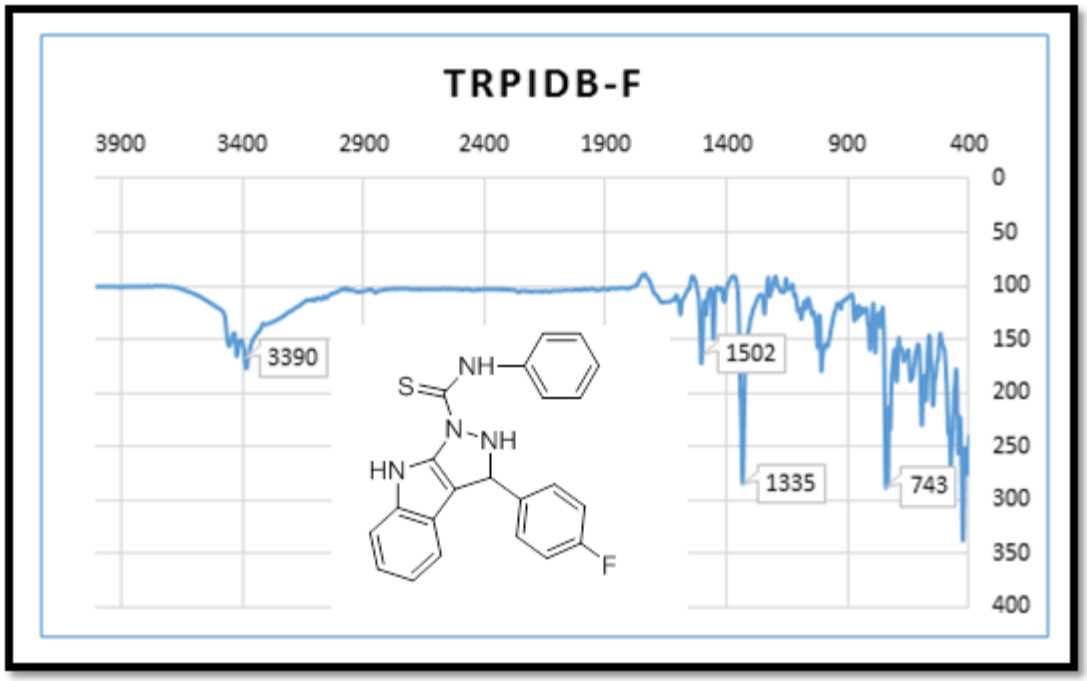

Appendix 5.59A: IR spectrum for compound **88l**

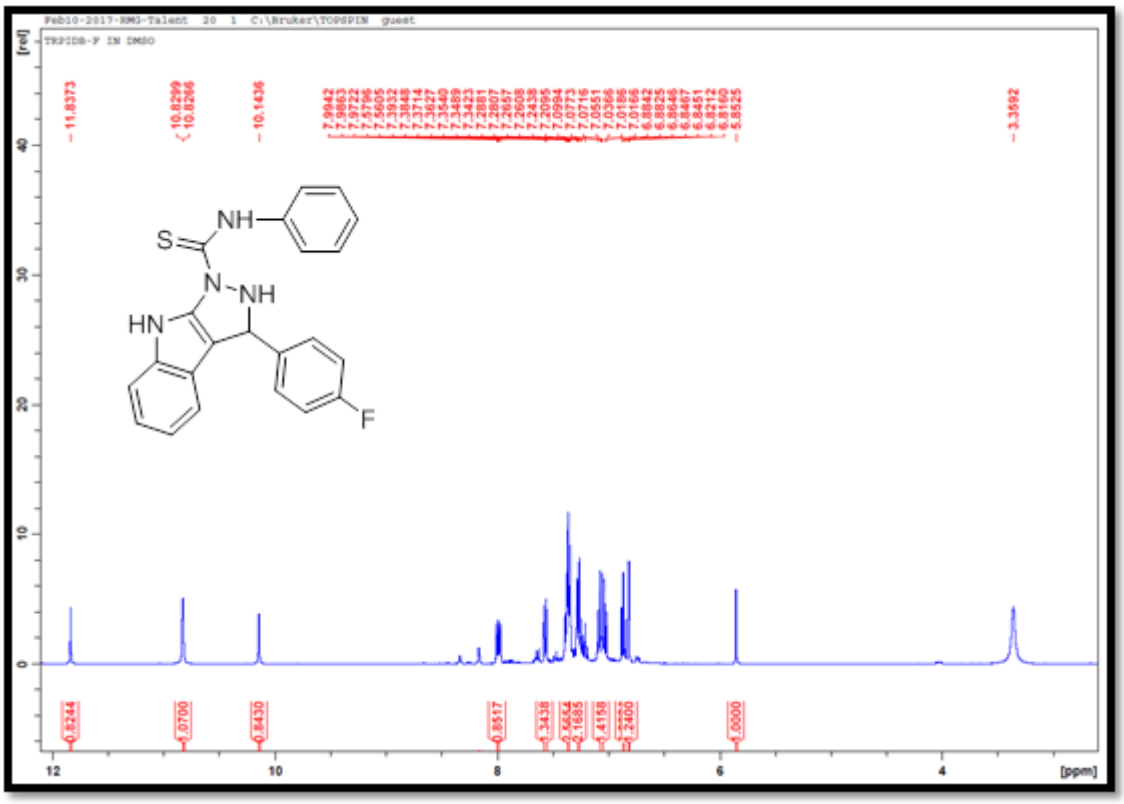

Appendix 5.60A: ^{1}H NMR spectrum for compound **88l**

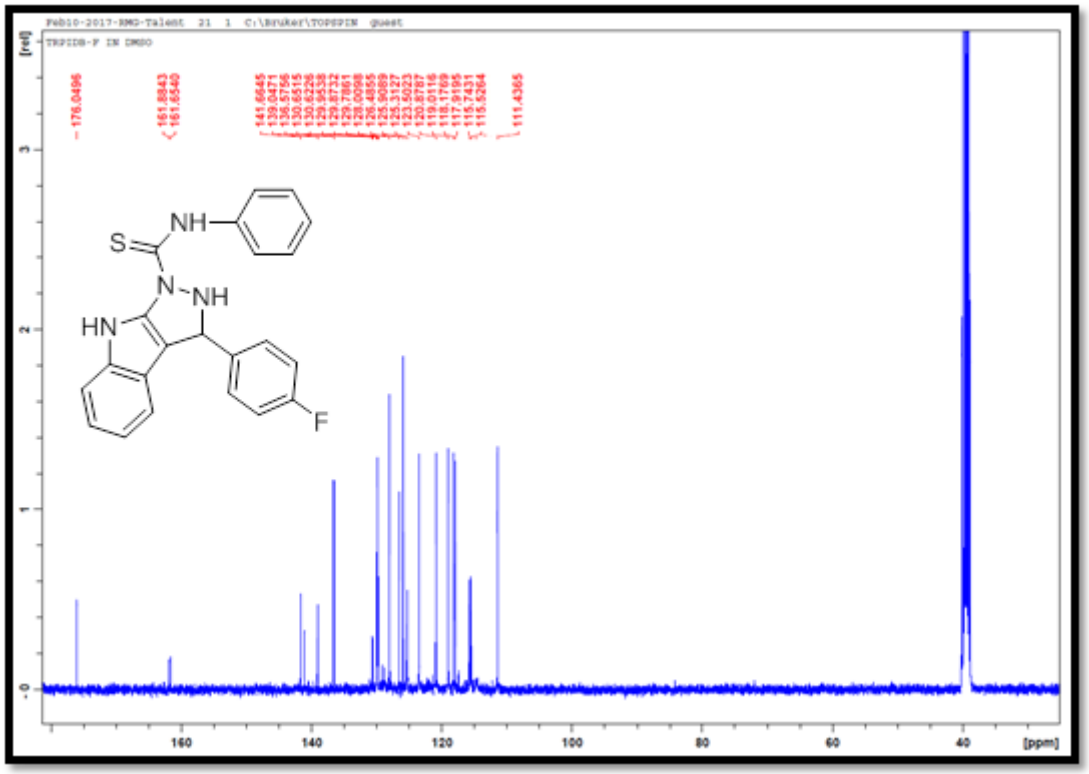

Appendix 5.61A: ^{13}C NMR spectrum for compound **88l**

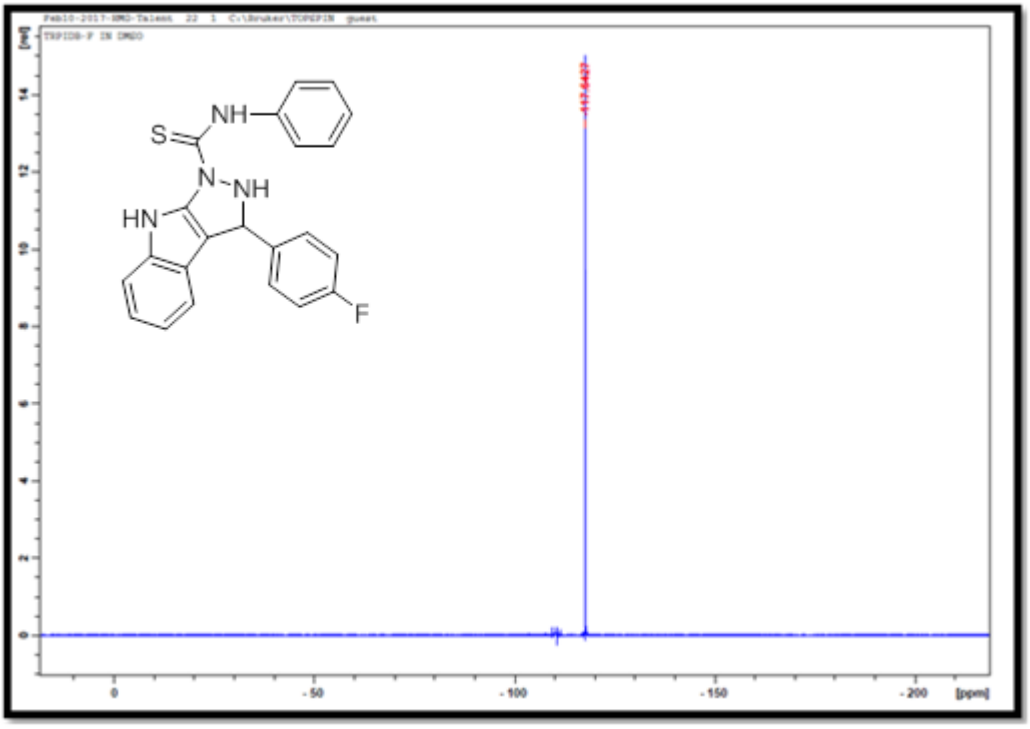

Appendix 5.62A: ^{19}F NMR spectrum for compound **88l**

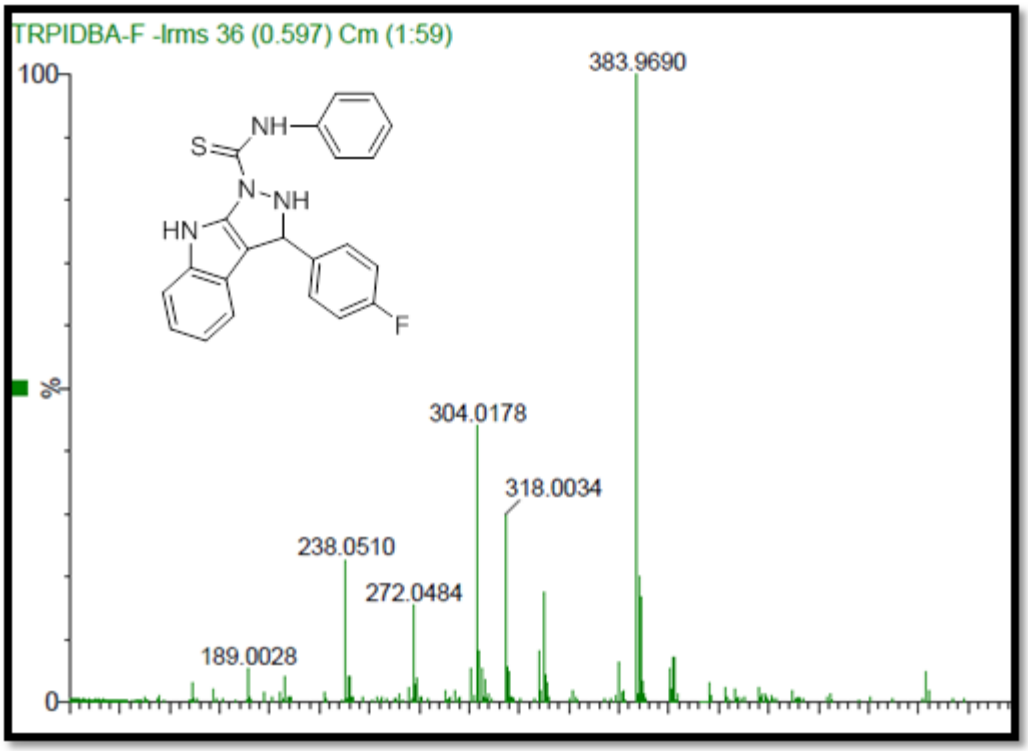

Appendix 5.63A: TOF-MS spectrum for compound **88l**

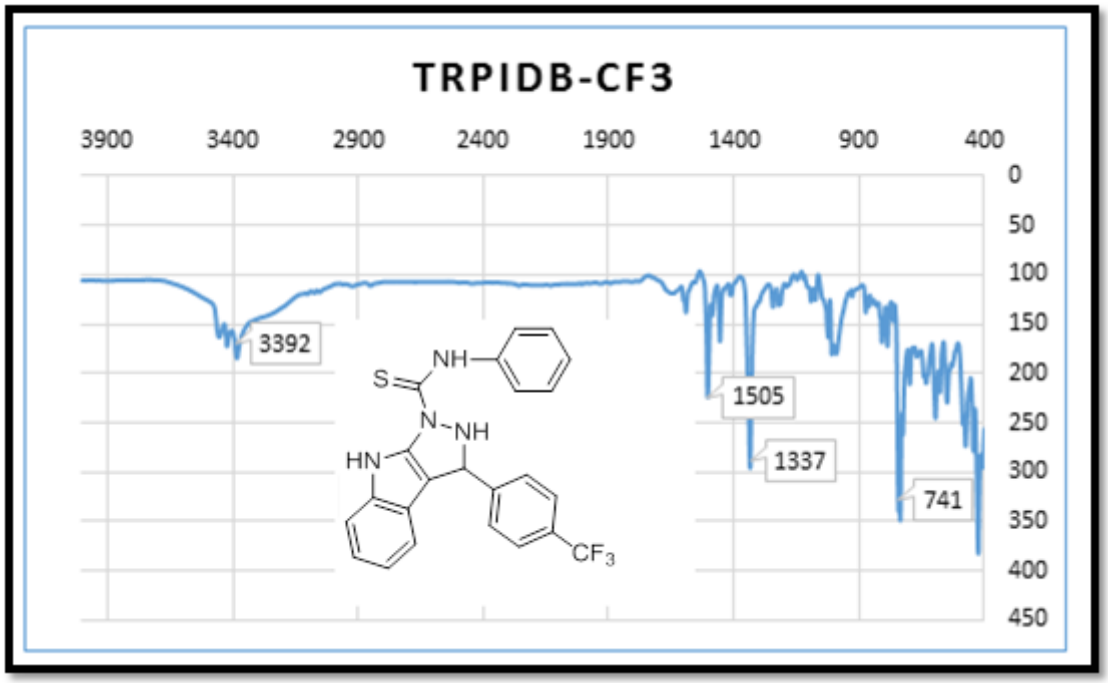

Appendix 5.64A: IR spectrum for compound **88m**

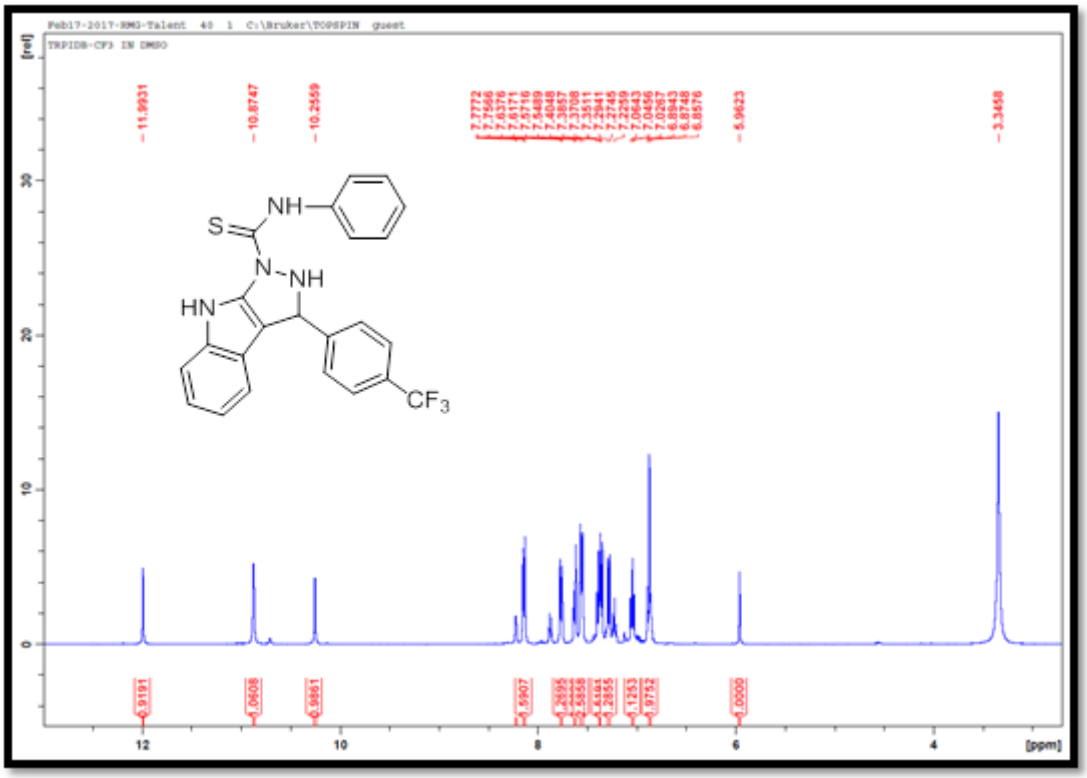

Appendix 5.65A: ^{1}H NMR spectrum for compound **88m**

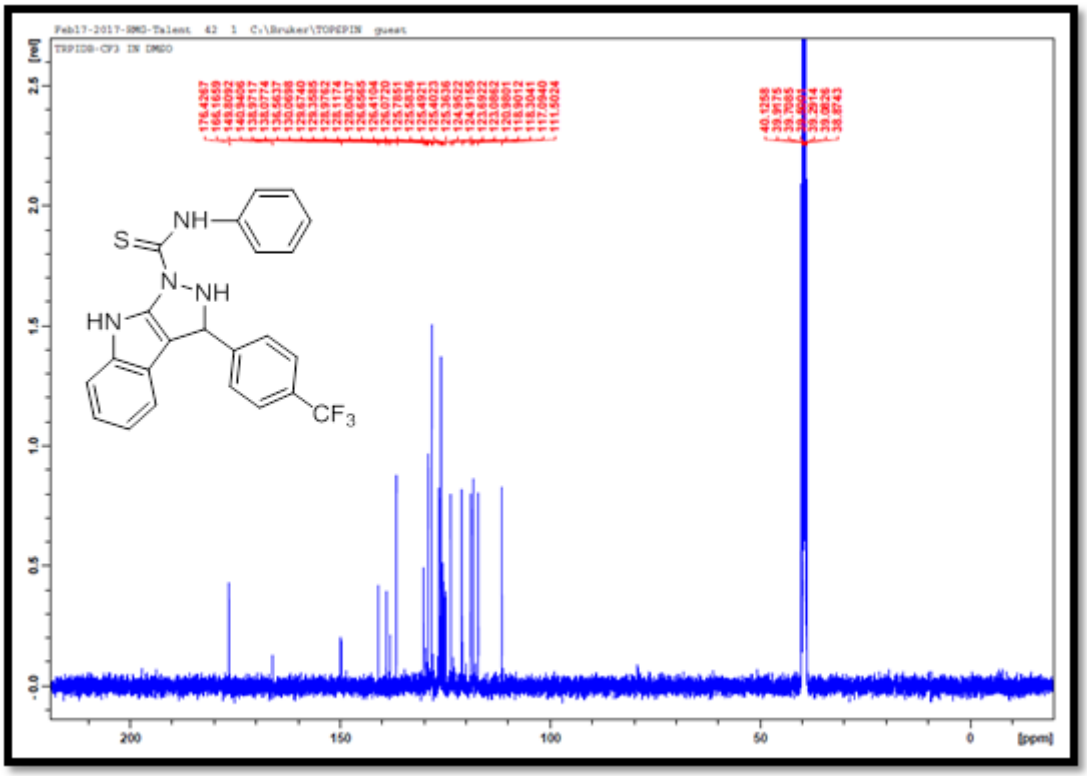

Appendix 5.66A: ^{13}C NMR spectrum for compound **88m**

Appendix 5.67A: ^{19}F NMR spectrum for compound **88m**

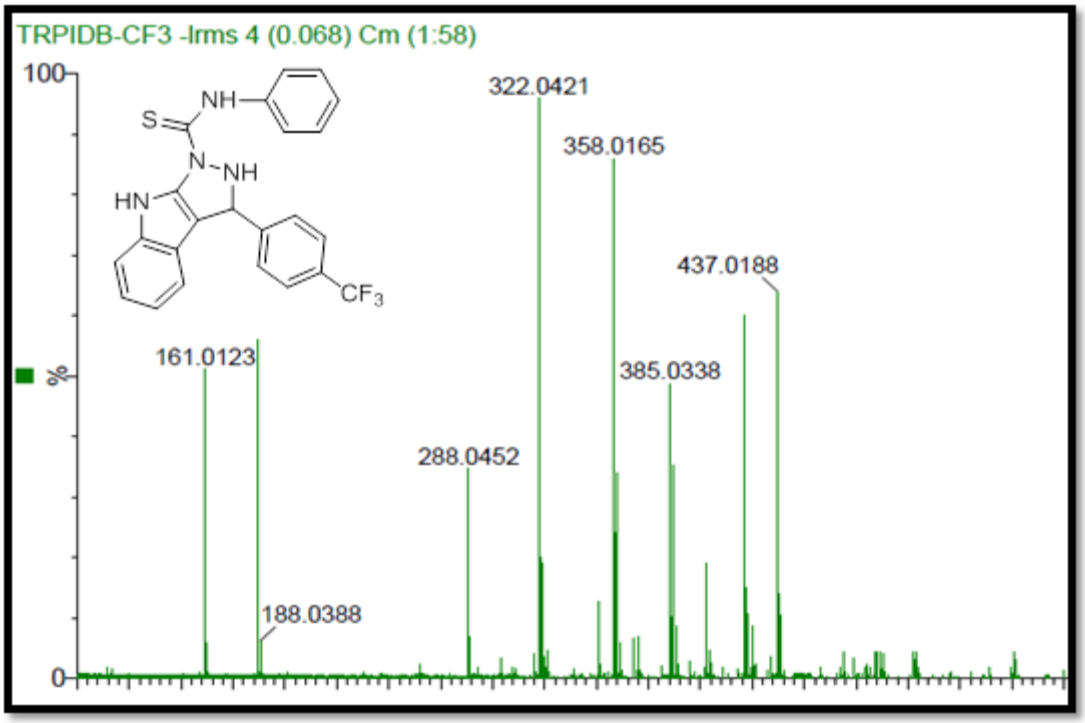

Appendix 5.68A: TOF-MS spectrum for compound **88m**

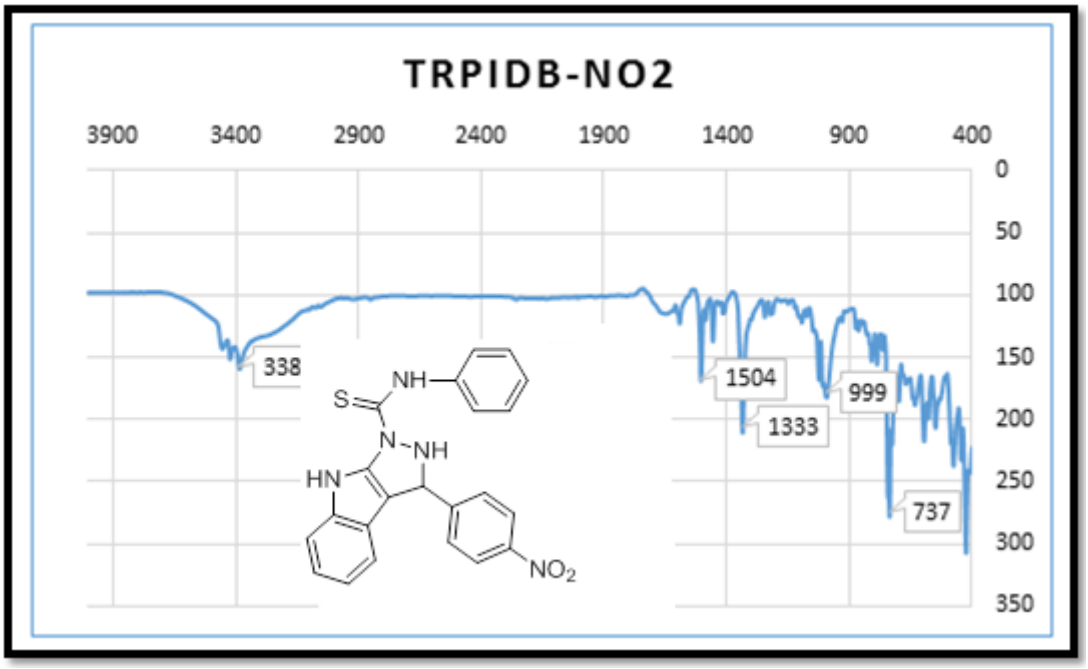

Appendix 5.69A: IR spectrum for compound **88n**

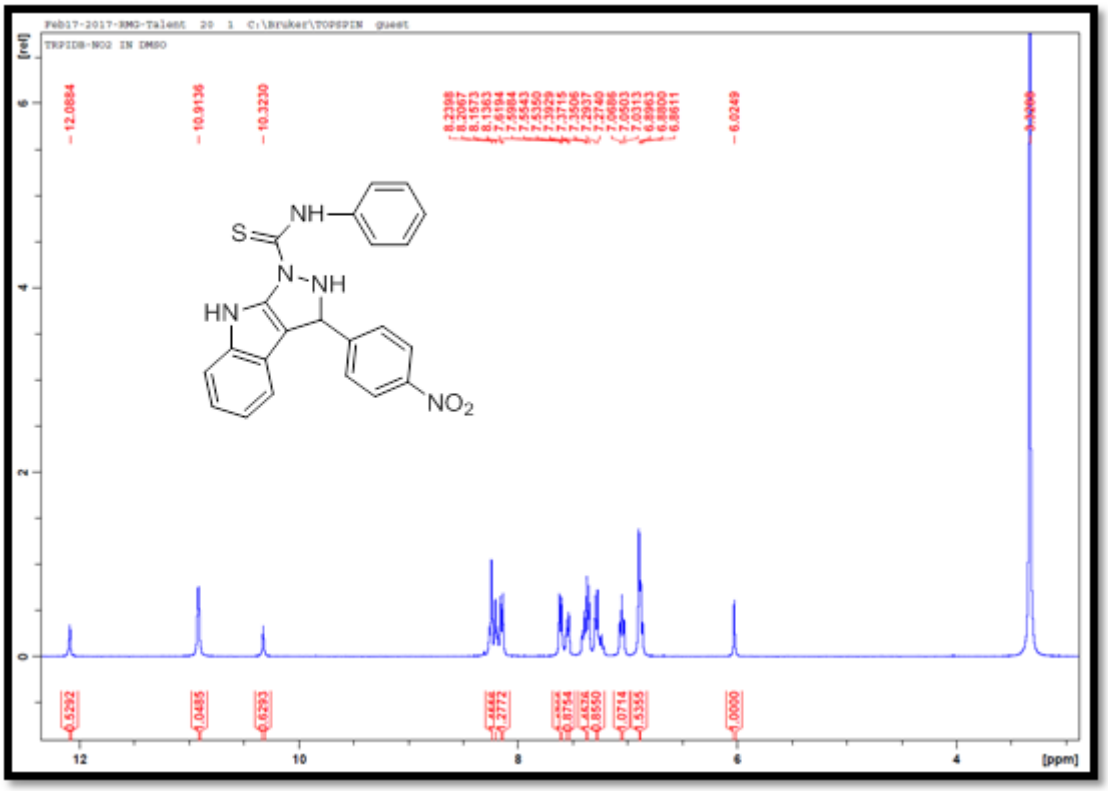

Appendix 5.70A: ^{1}H NMR spectrum for compound **88n**

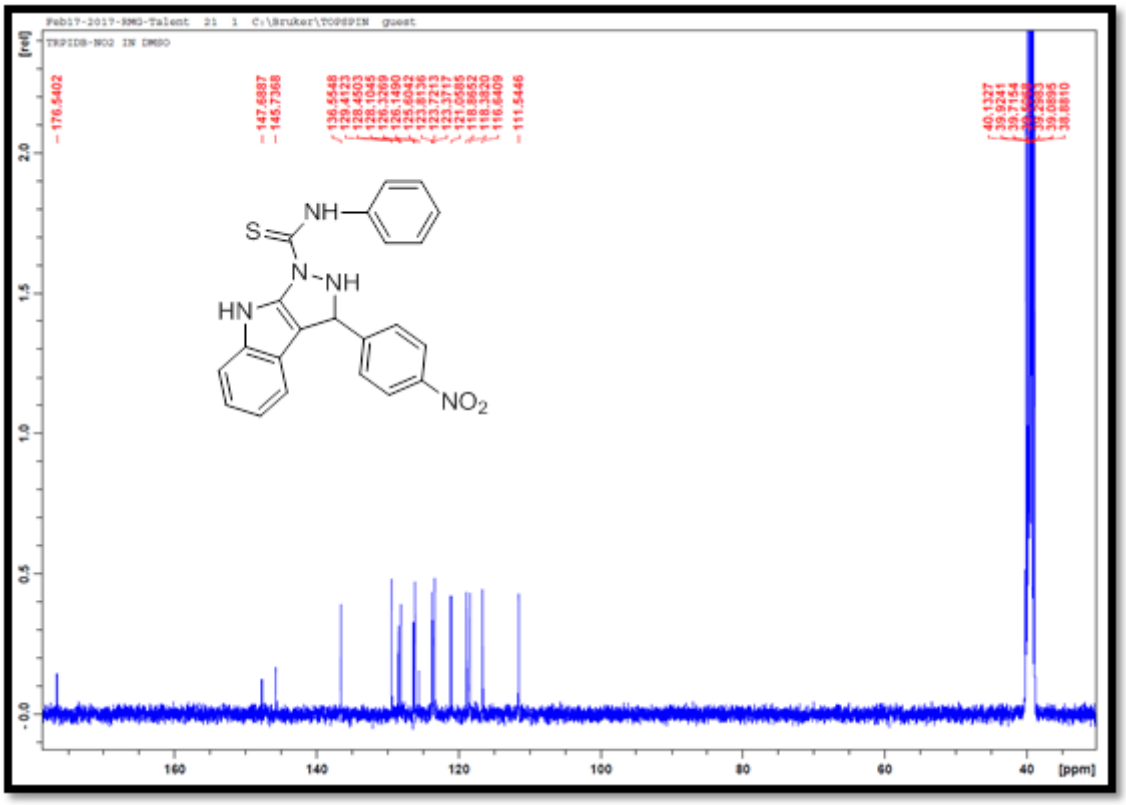

Appendix 5.71A: ^{13}C NMR spectrum for compound **88n**

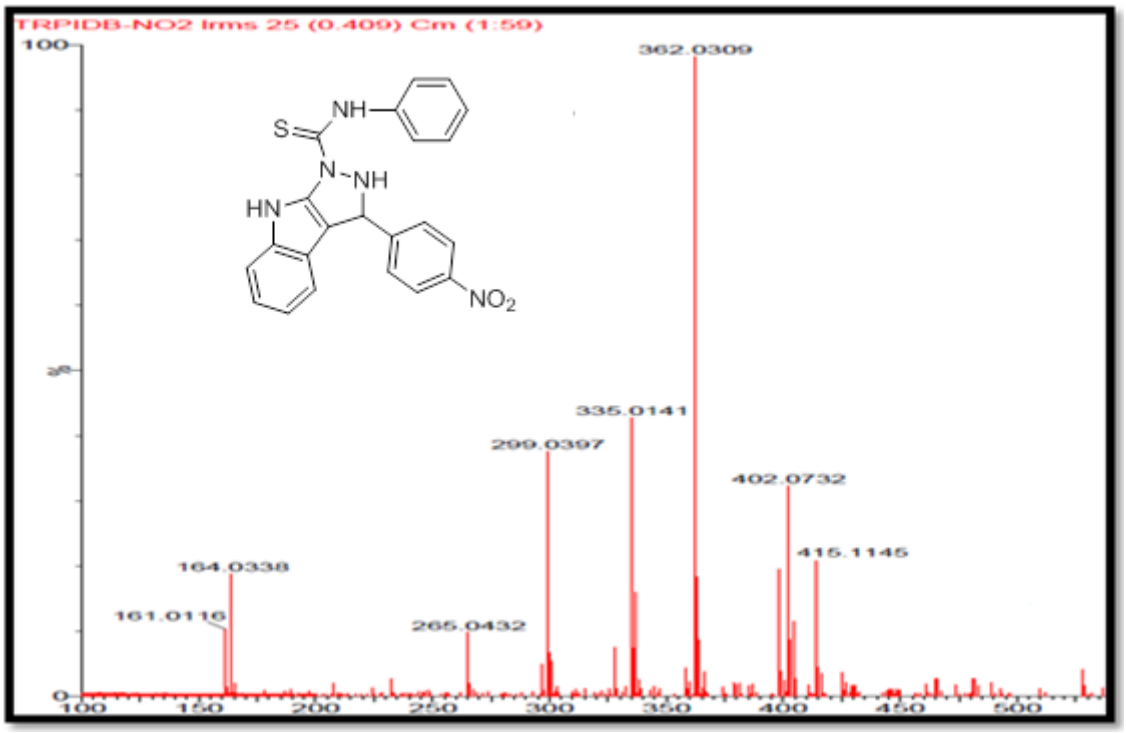

Appendix 5.72A: TOF-MS spectrum for compound **88n**

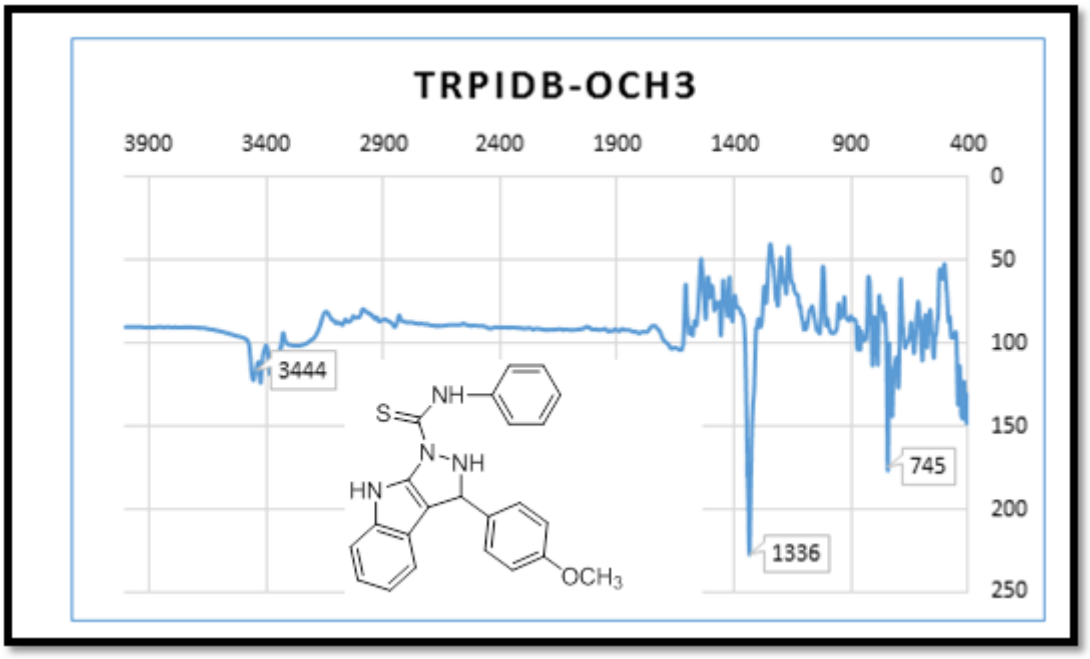

Appendix 5.73A: IR spectrum for compound **88o**

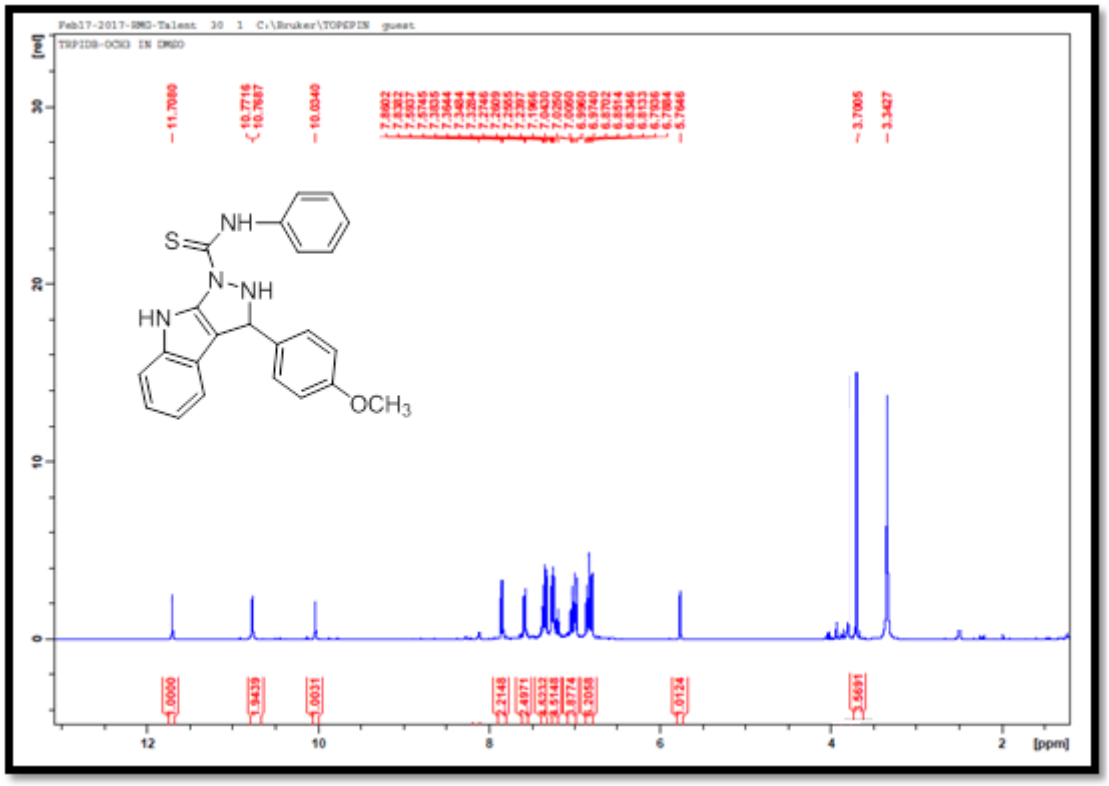

Appendix 5.74A: ^{1}H NMR spectrum for compound **88o**

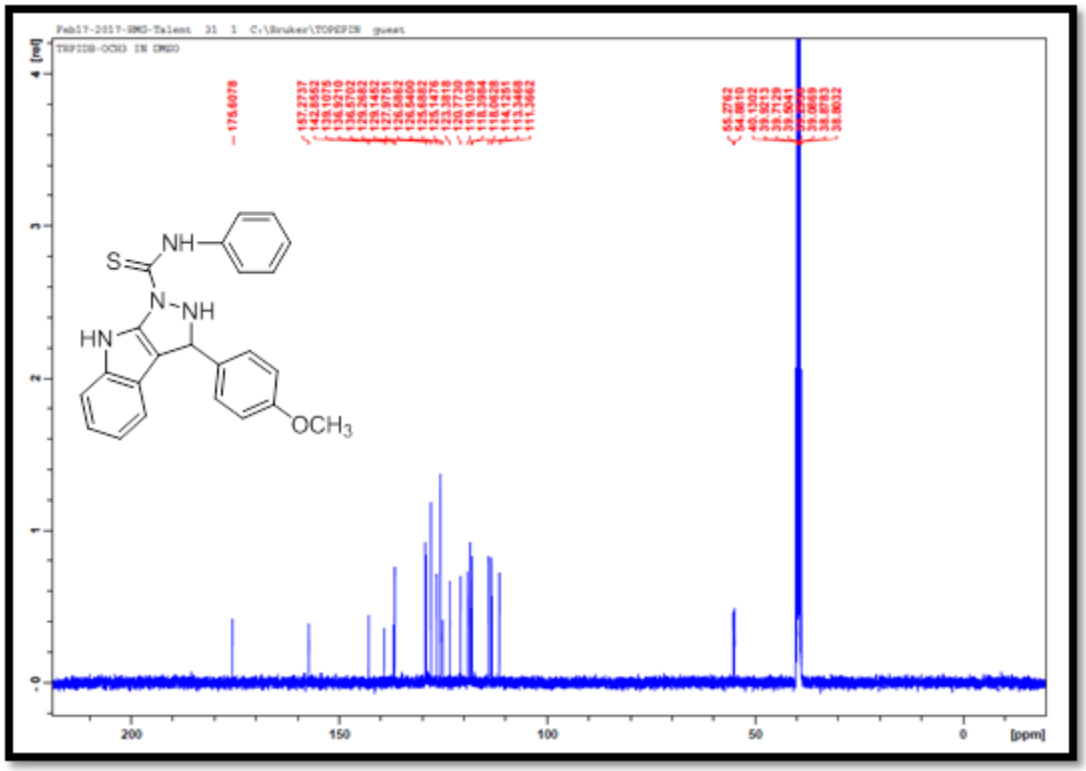

Appendix 5.75A: ^{13}C NMR spectrum for compound **88o**

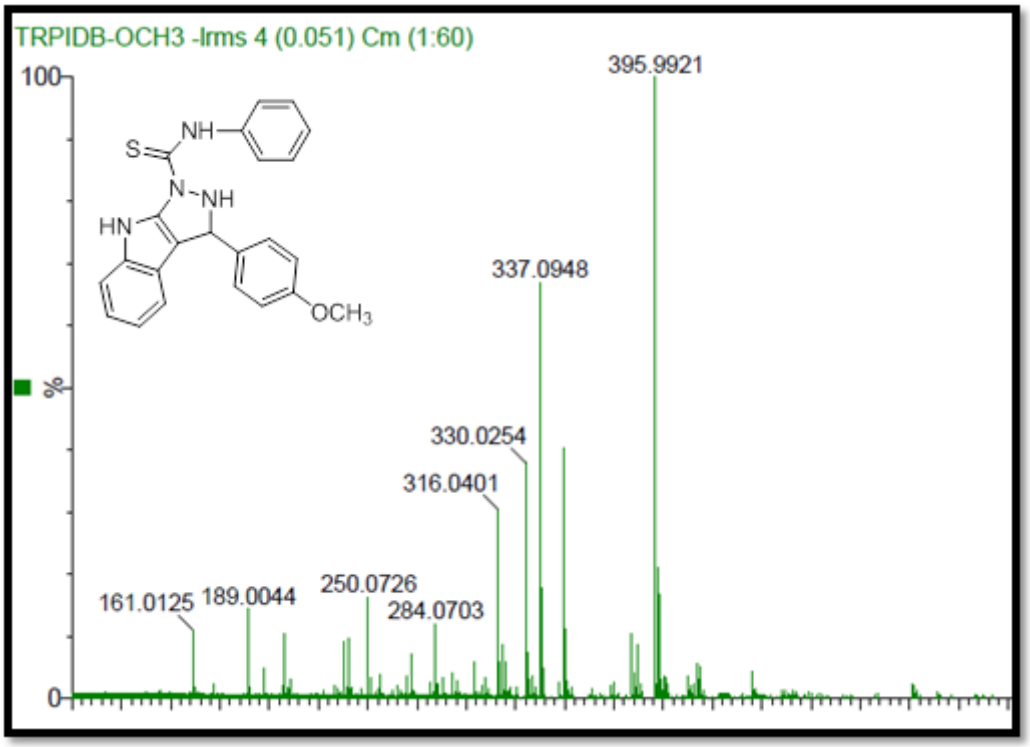

Appendix 5.76A: TOF-MS spectrum for compound **88o**

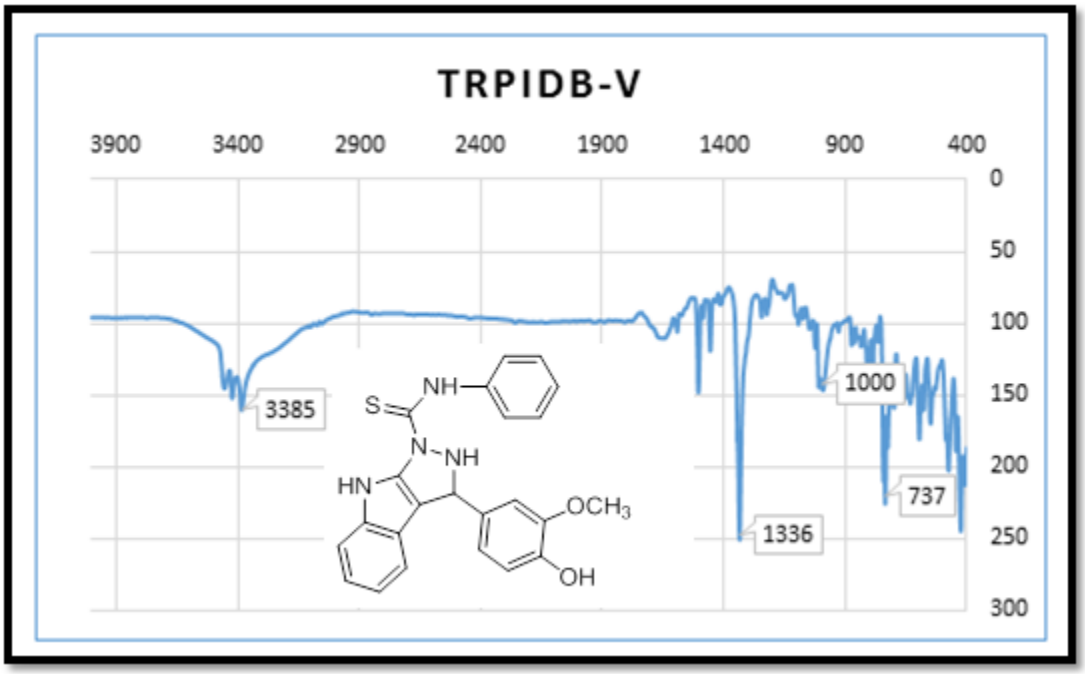

Appendix 5.77A: IR spectrum for compound **88p**

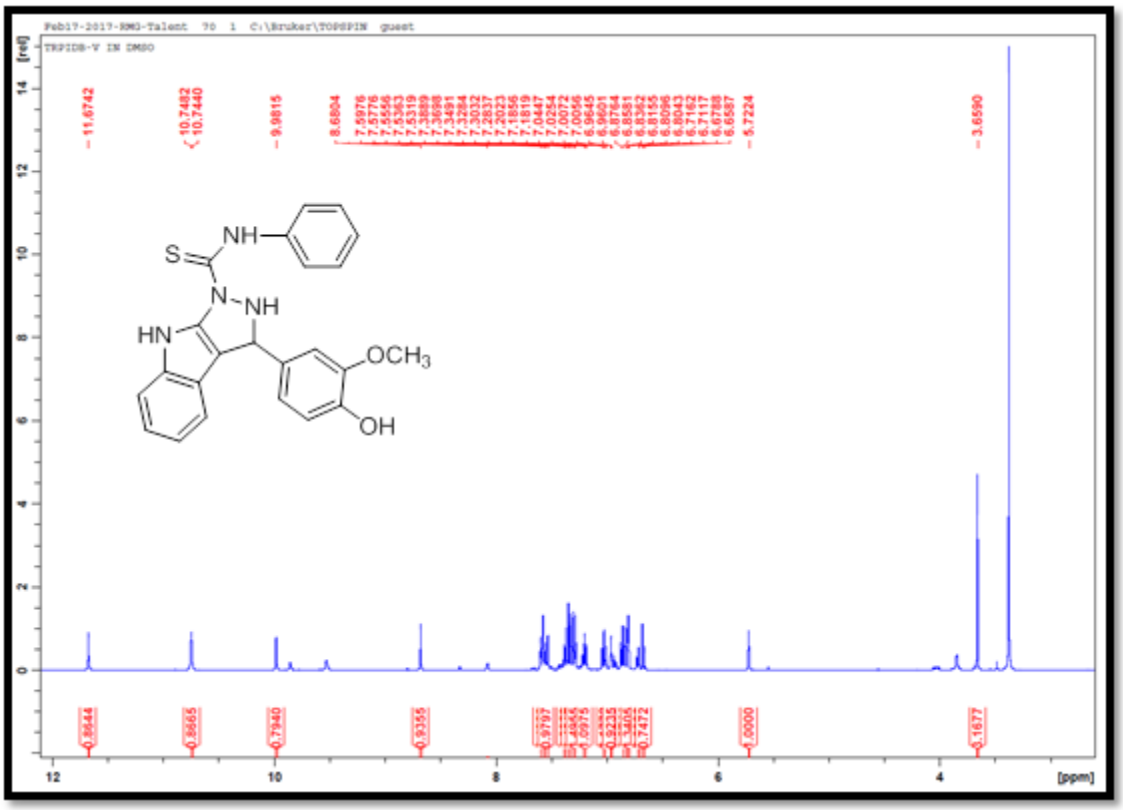

Appendix 5.78A: ^{1}H NMR spectrum for compound **88p**

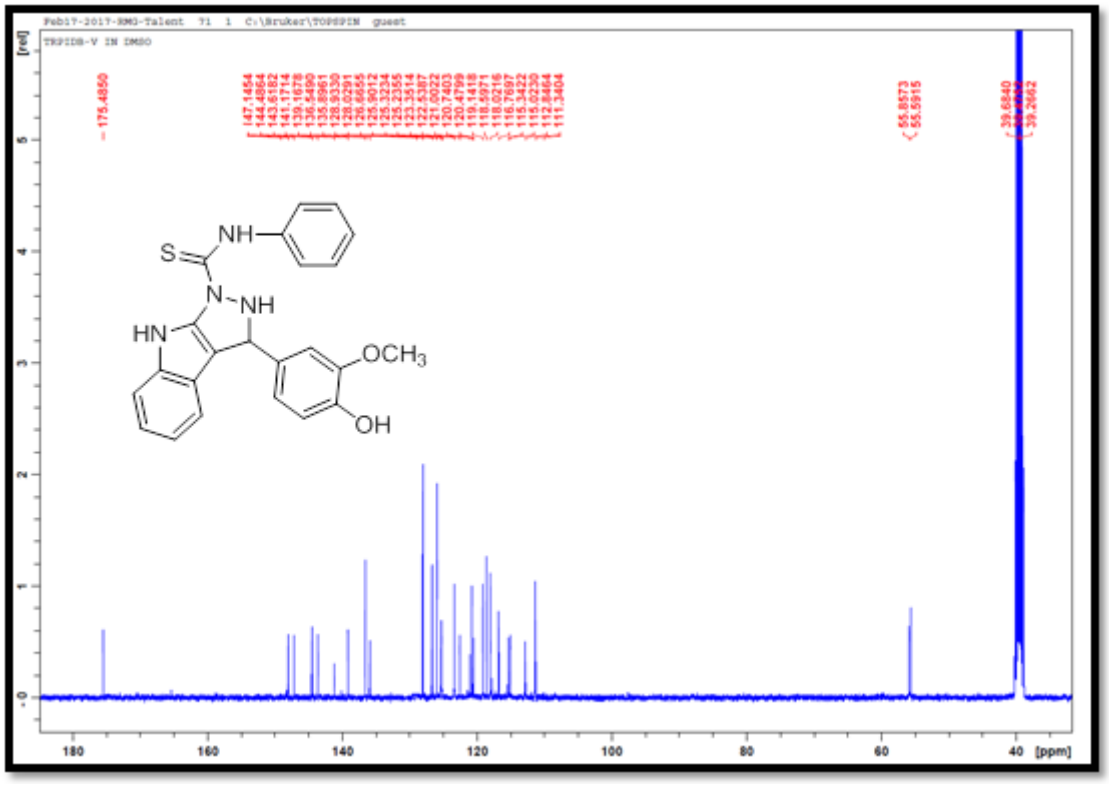

Appendix 5.79A: ^{13}C NMR spectrum for compound **88p**

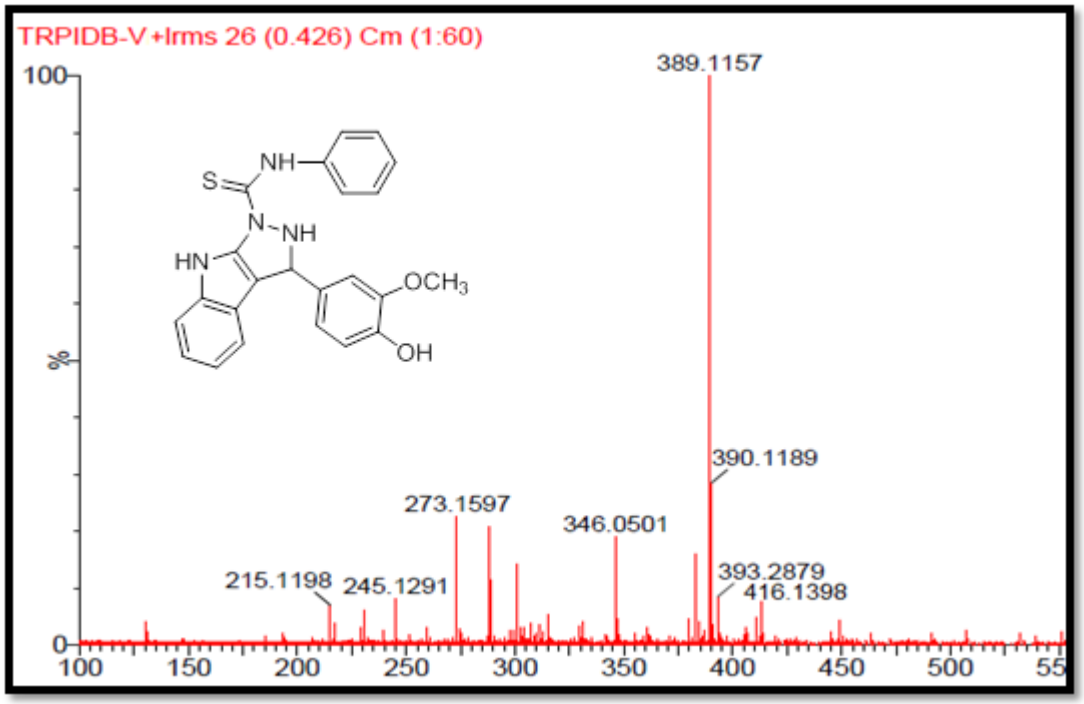

Appendix 5.80A: TOF-MS spectrum for compound **88p**

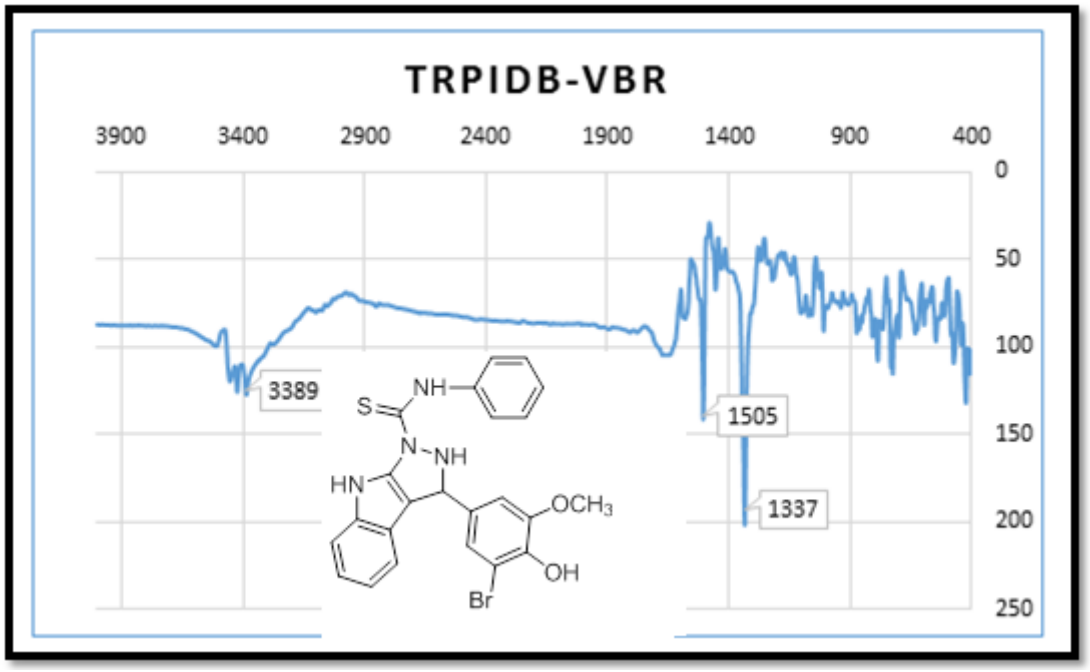

Appendix 5.81A: IR spectrum for compound **88q**

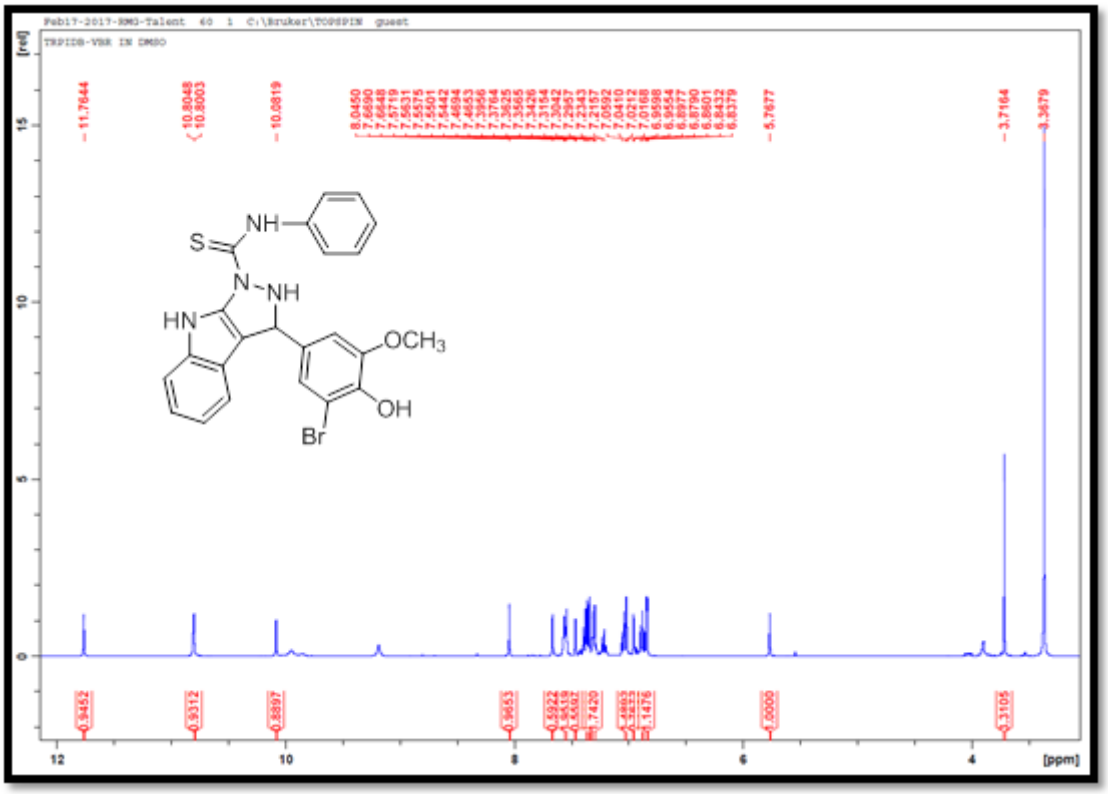

Appendix 5.82A: ^{1}H NMR spectrum for compound **88q**

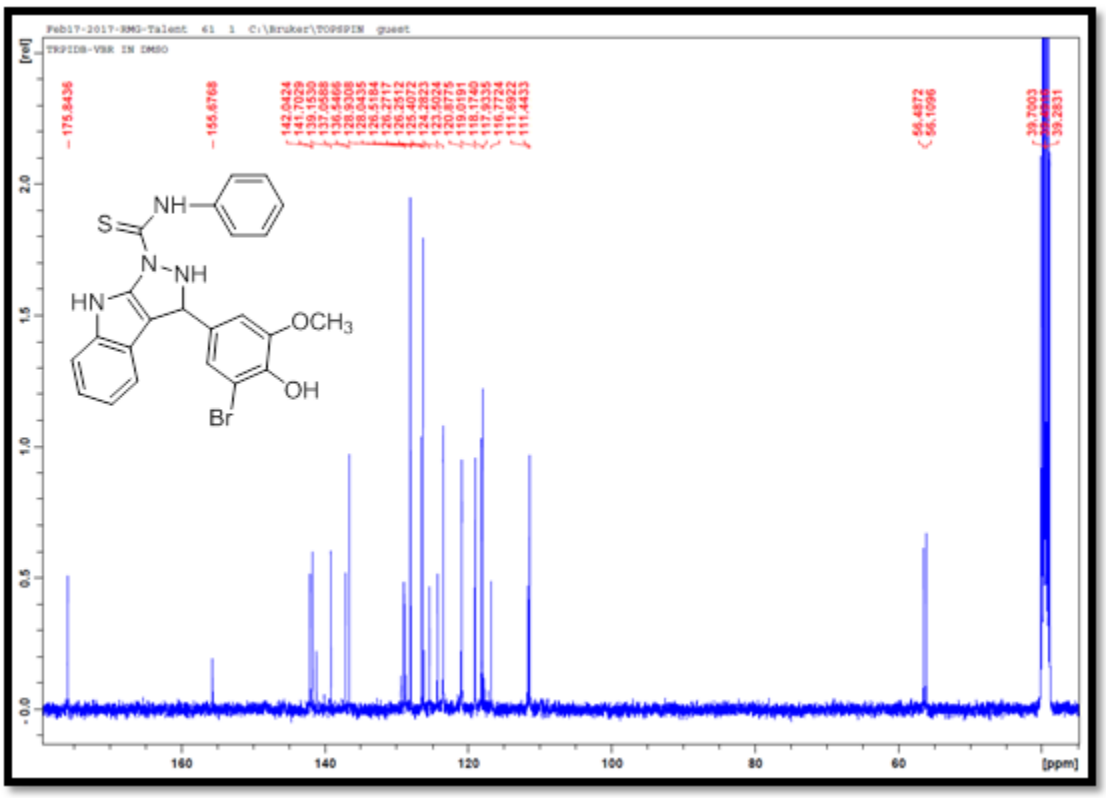

Appendix 5.83A: ^{13}C NMR spectrum for compound **88q**

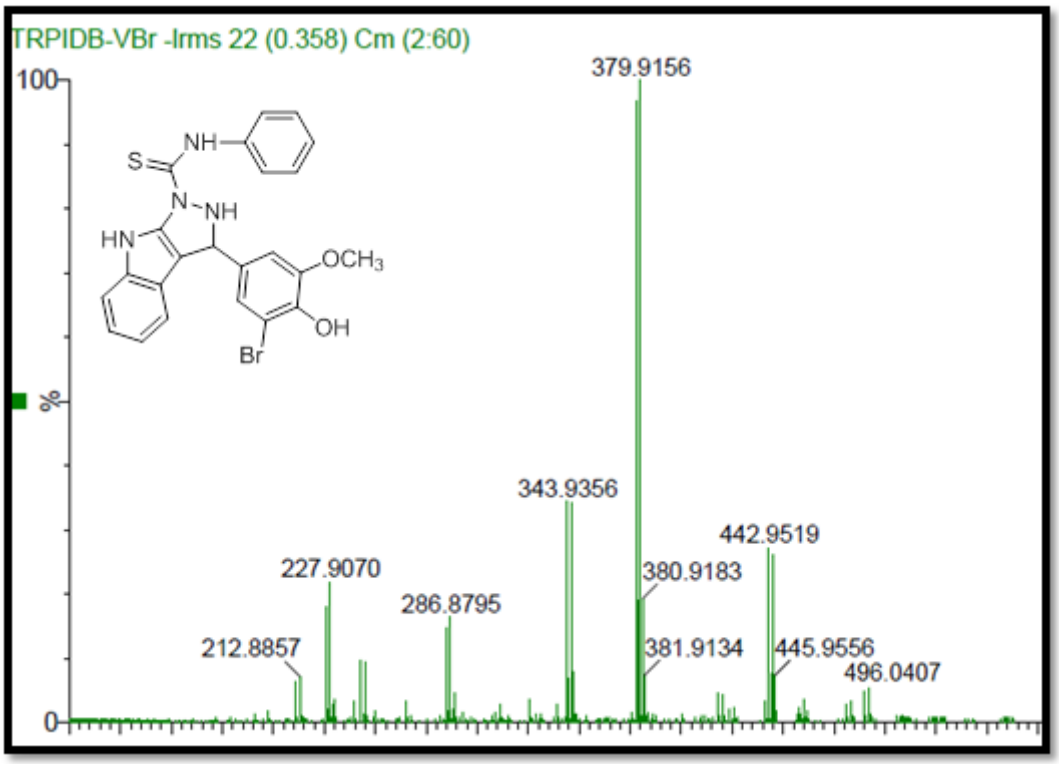

Appendix 5.84A: TOF-MS spectrum for compound **88q**

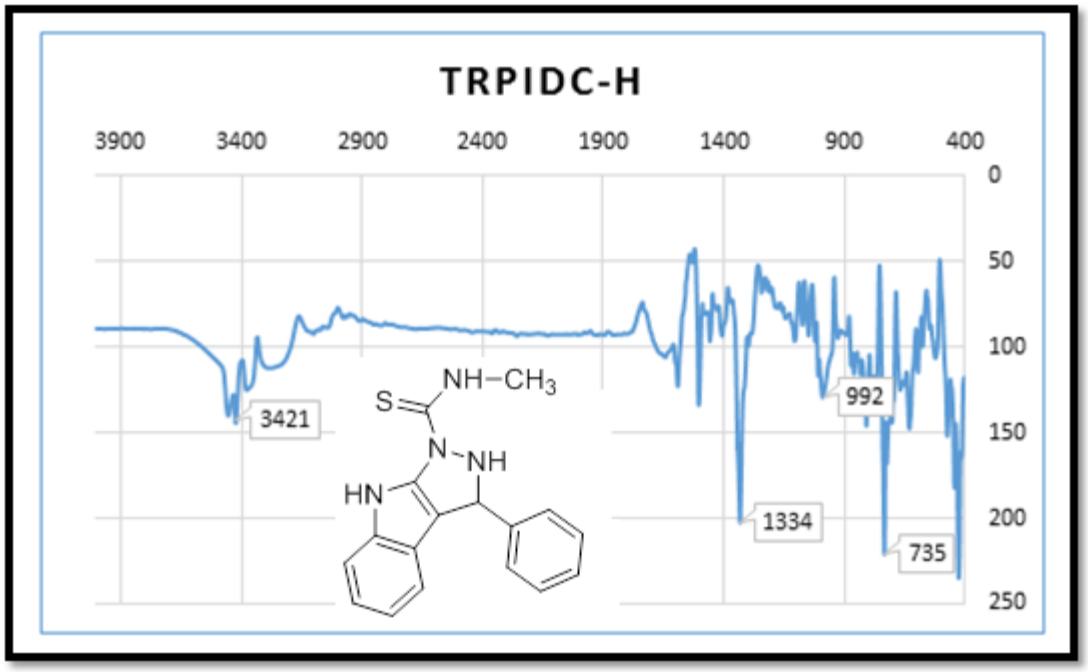

Appendix 5.85A: IR spectrum for compound **88r**

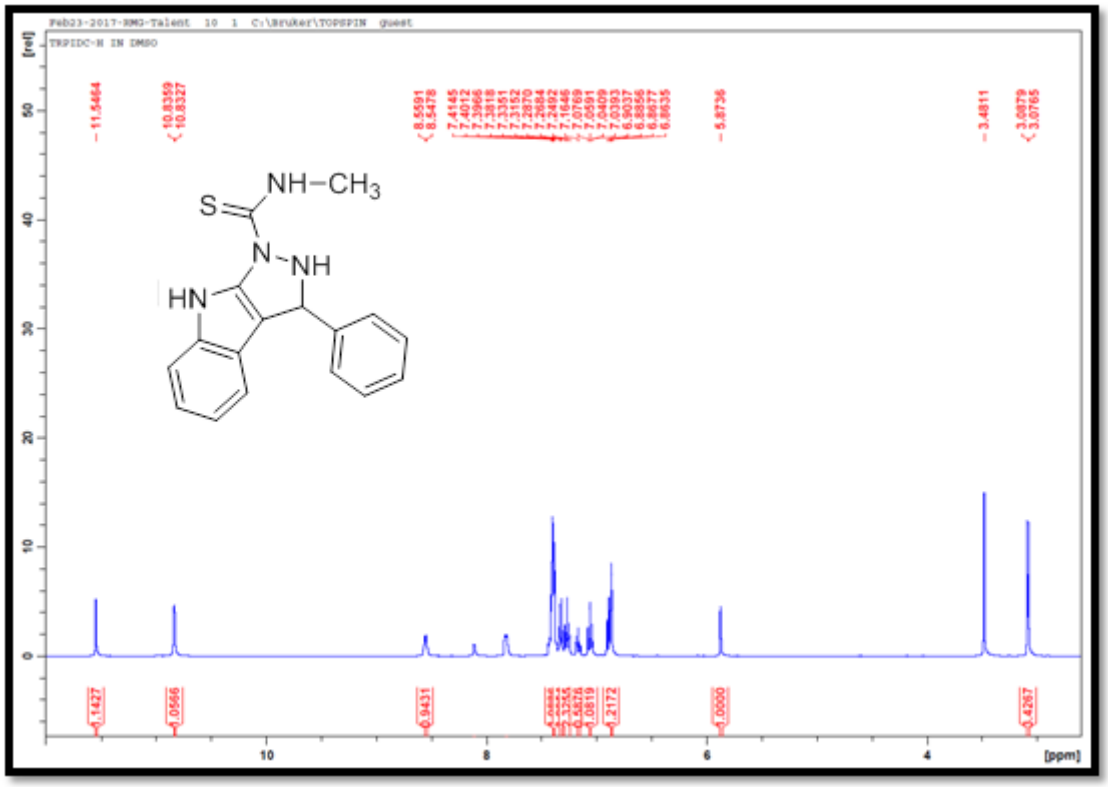

Appendix 5.86A: ^{1}H NMR spectrum for compound **88r**

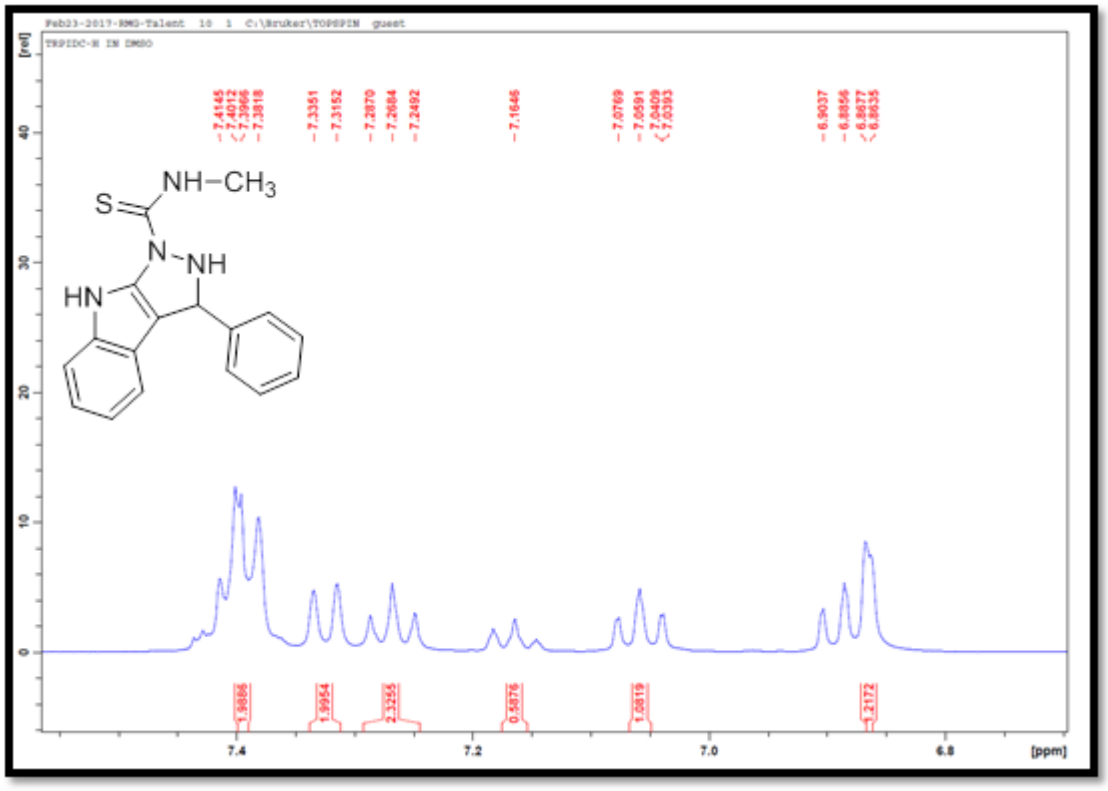

Appendix 5.87A: Expanded ^{1}H NMR spectrum for compound **88r**

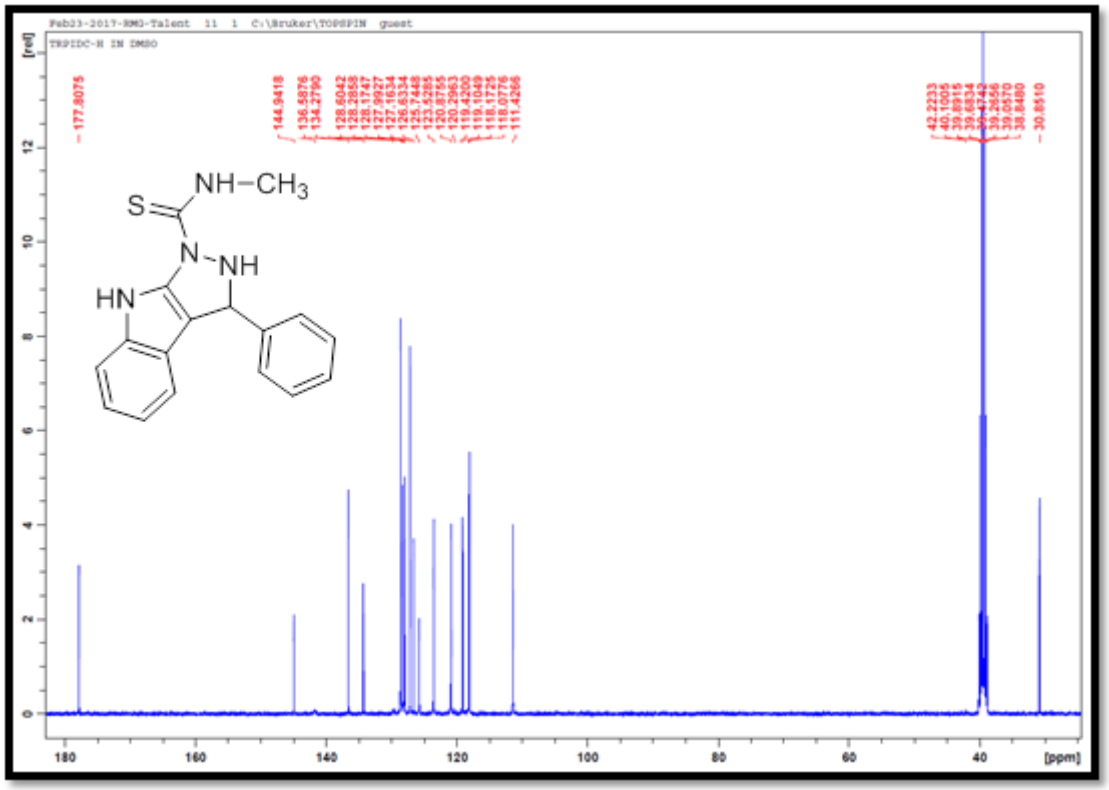

Appendix 5.88A: ^{13}C NMR spectrum for compound **88r**

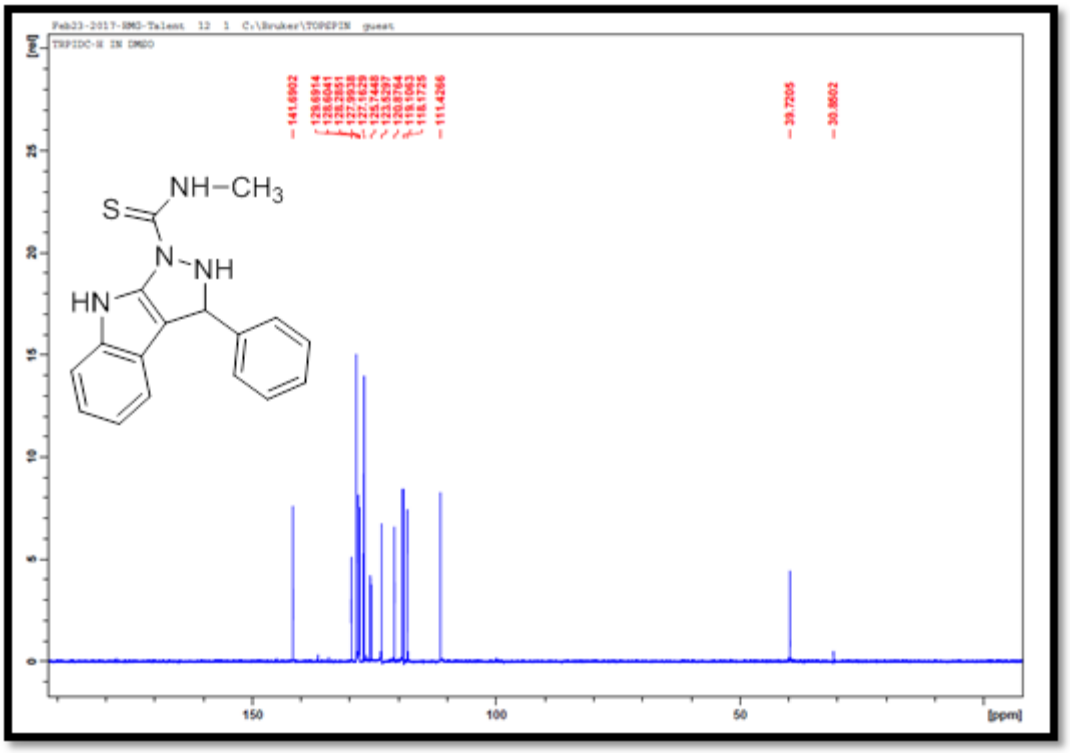

Appendix 5.89A: 90^0 DEPT NMR spectrum for compound **88r**

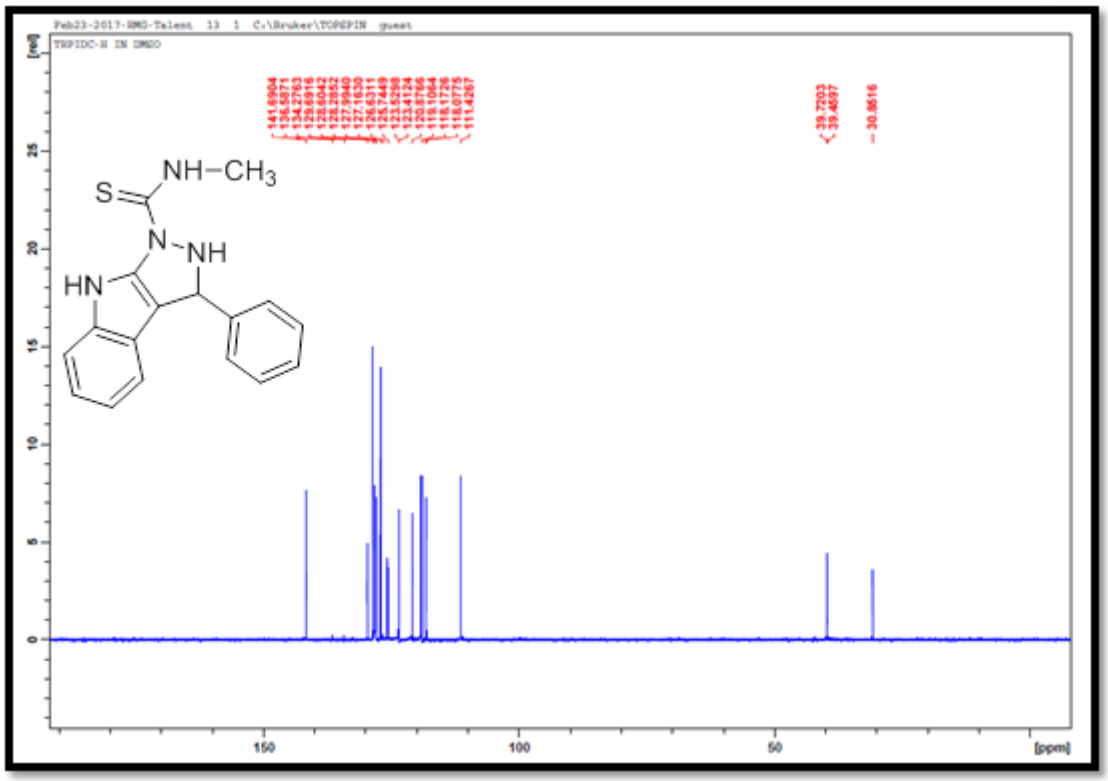

Appendix 5.90A: 135^0 DEPT NMR spectrum for compound **88r**

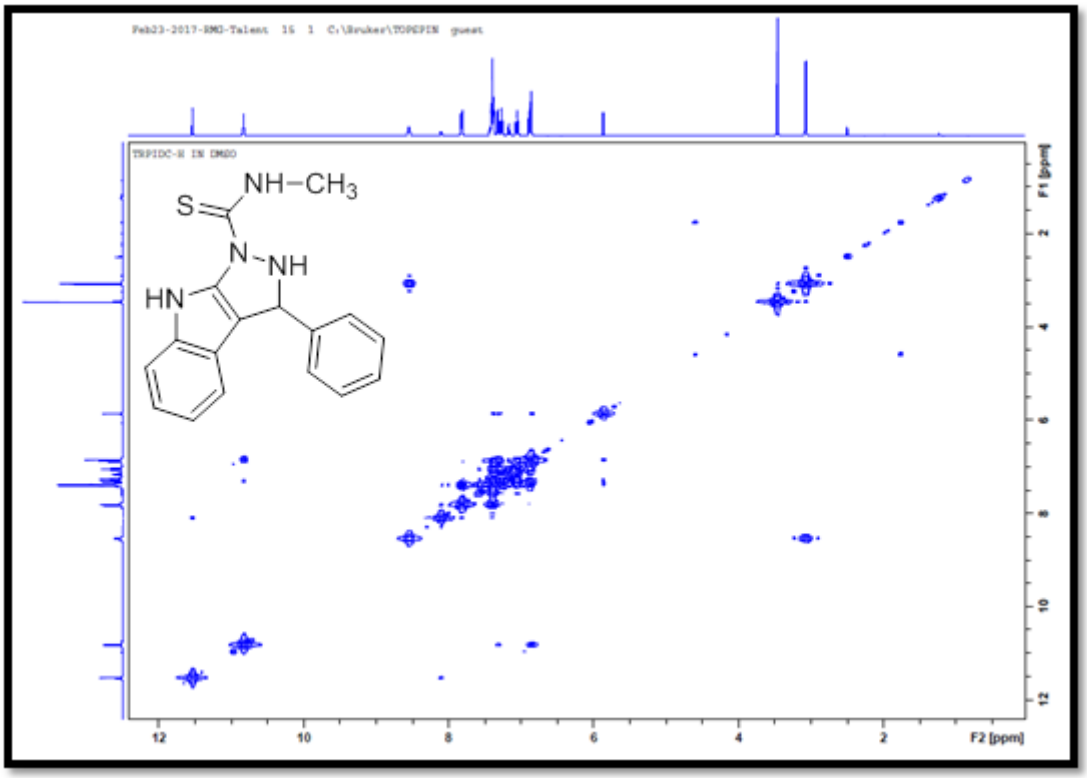

Appendix 5.91A: COSY NMR spectrum for compound **88r**

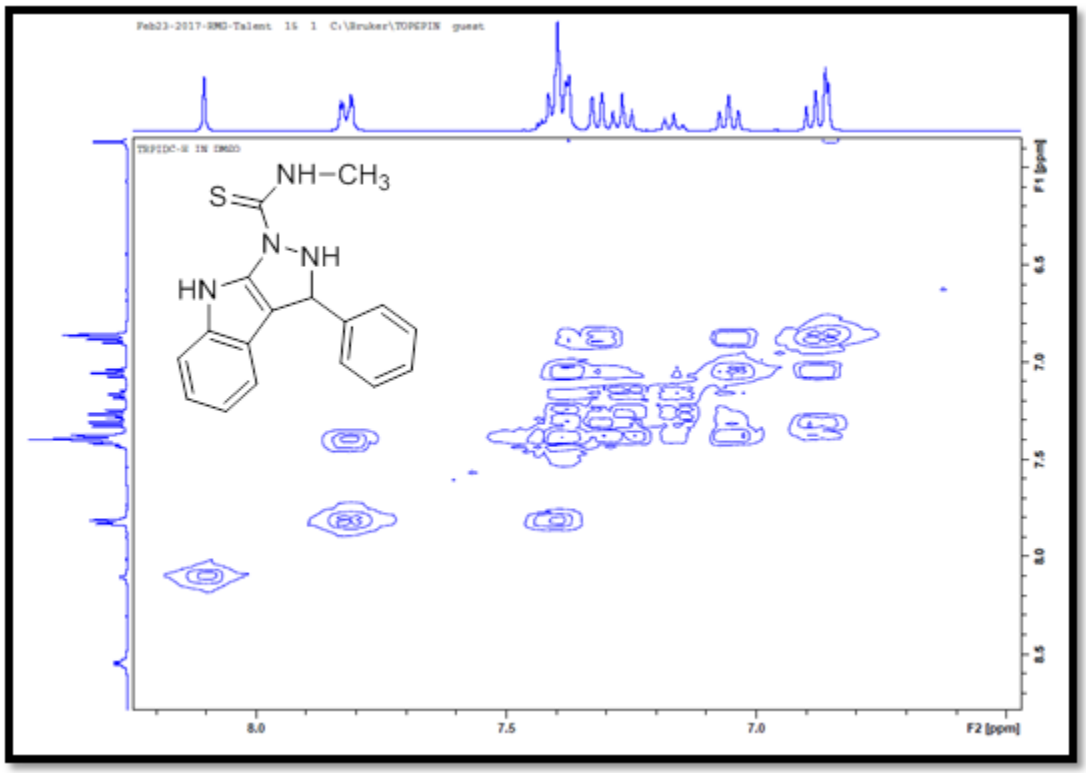

Appendix 5.92A: Expanded COSY NMR spectrum for compound **88r**

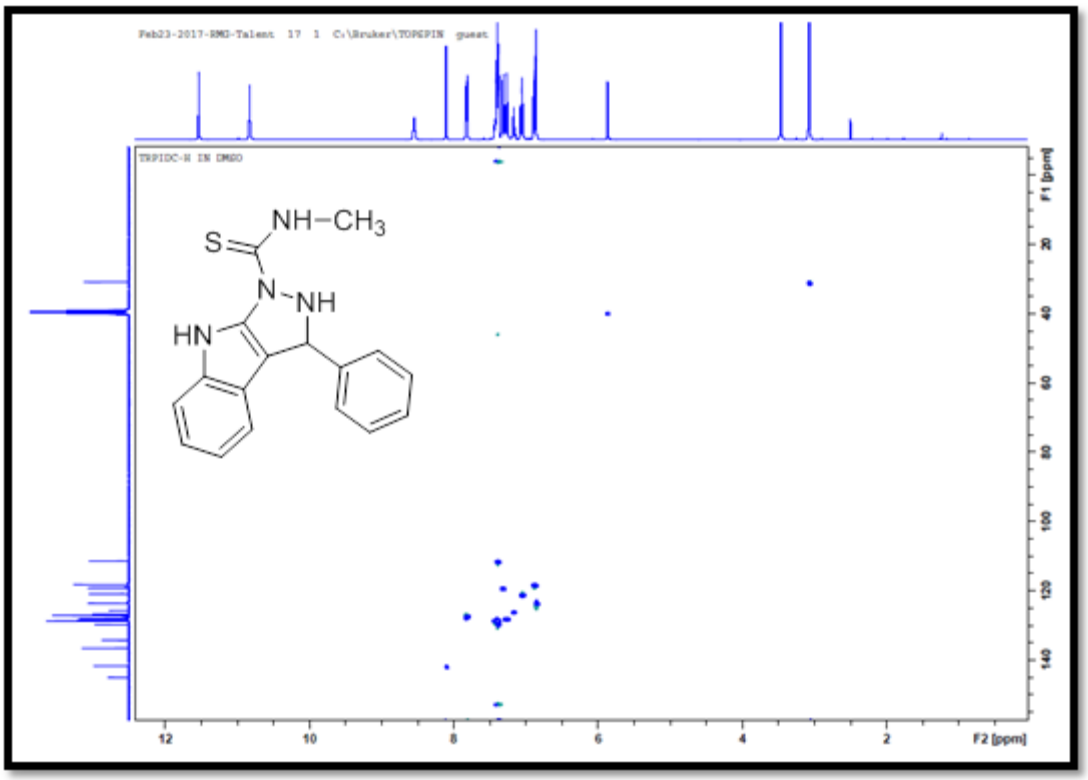

Appendix 5.93A: HSQC NMR spectrum for compound **88r**

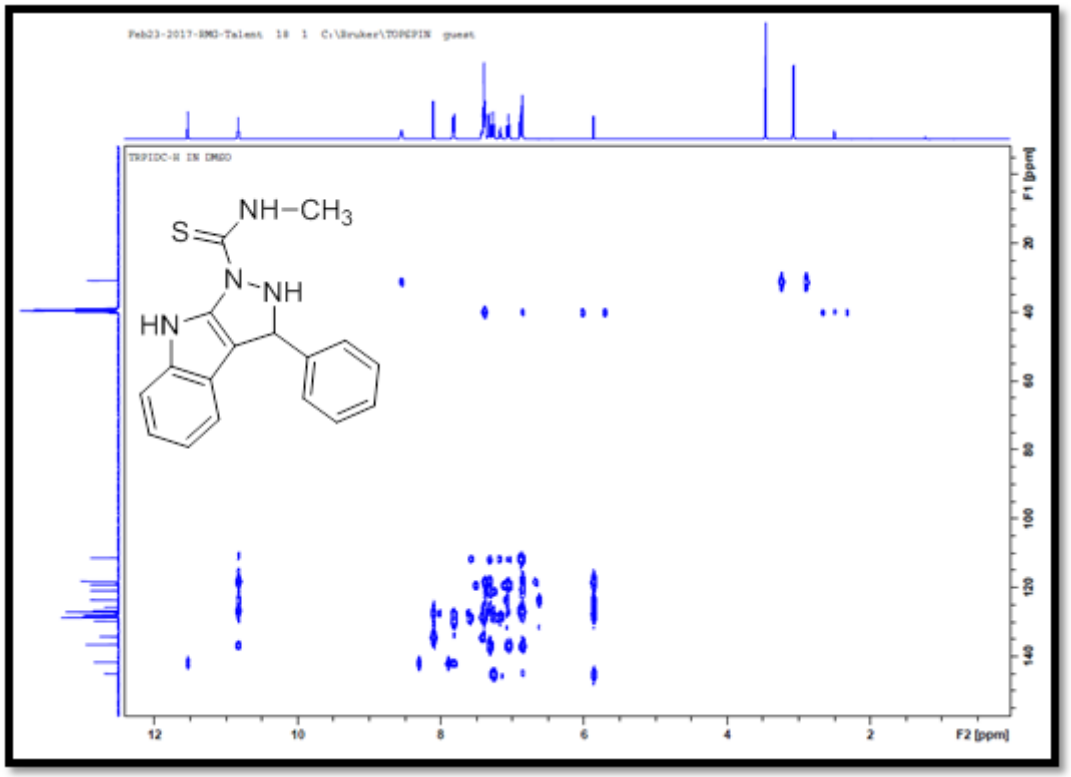

Appendix 5.94A: HMBC NMR spectrum for compound **88r**

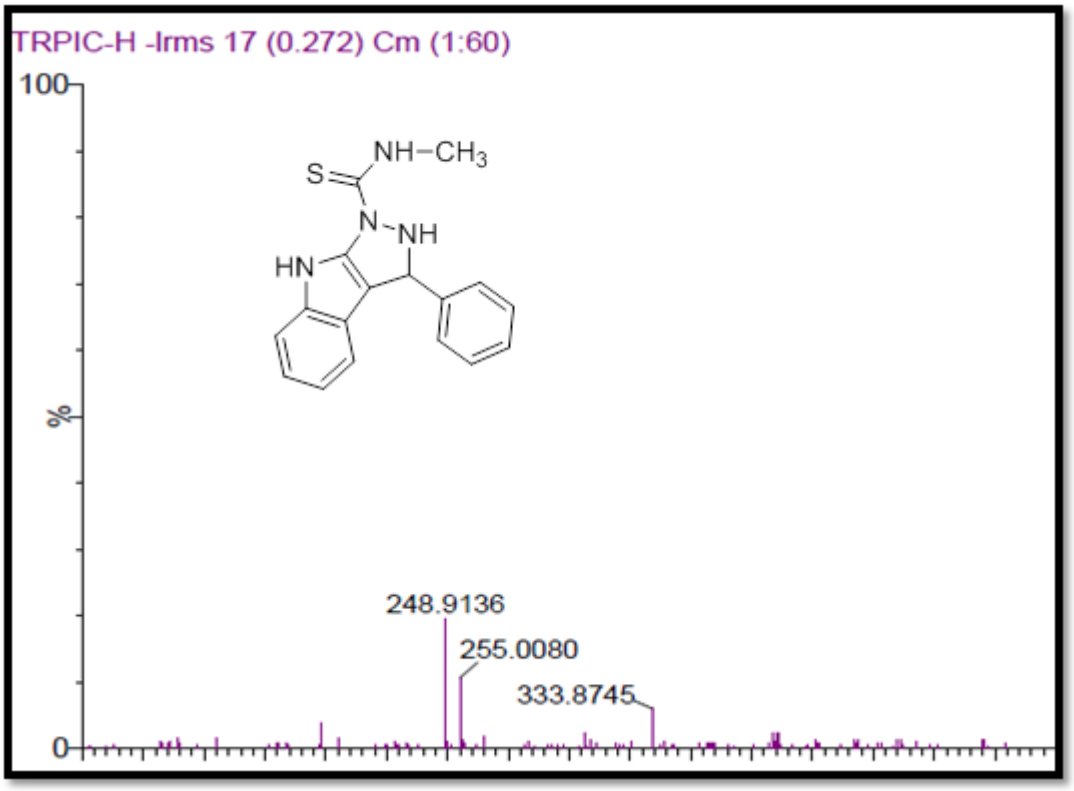

Appendix 5.95A: TOF-MS spectrum for compound **88r**

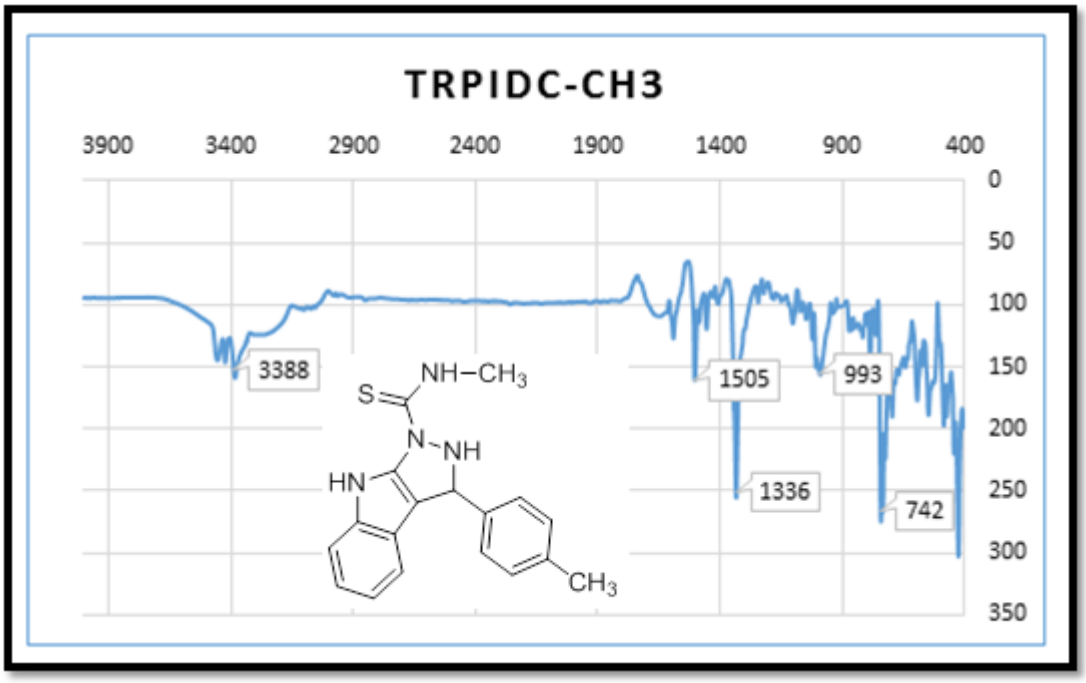

Appendix 5.96A: IR spectrum for compound **88s**

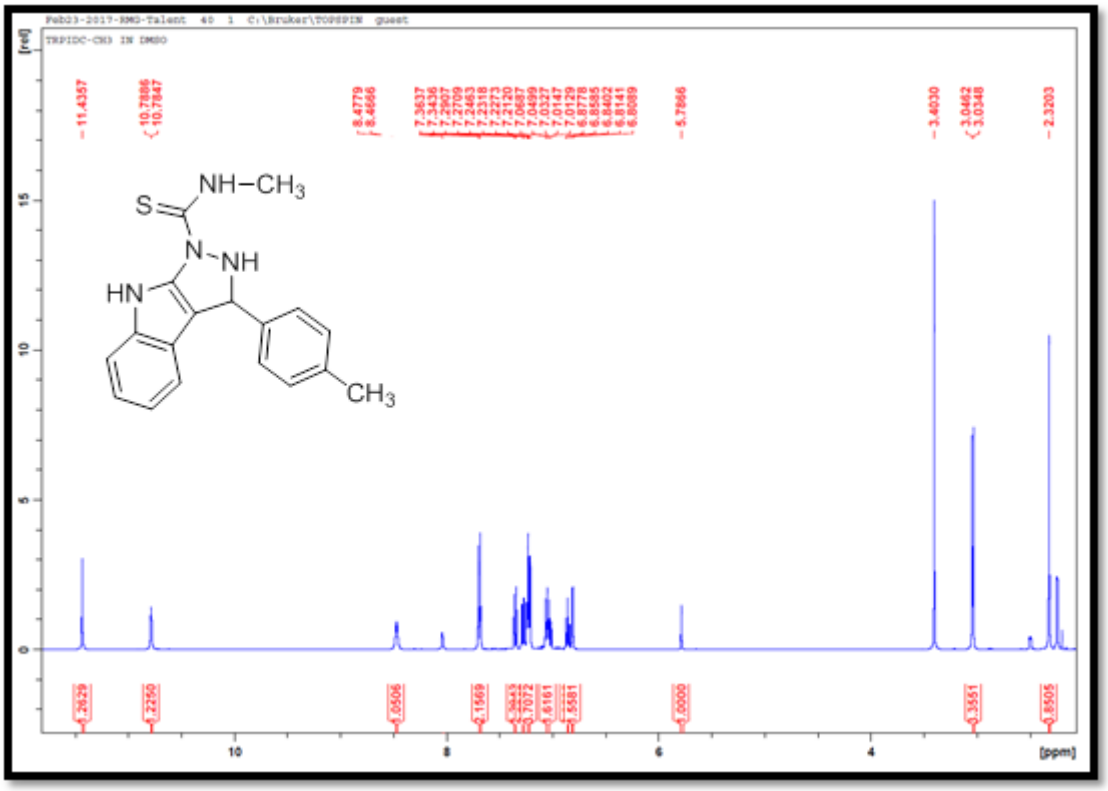

Appendix 5.97A: ^{1}H NMR spectrum for compound **88s**

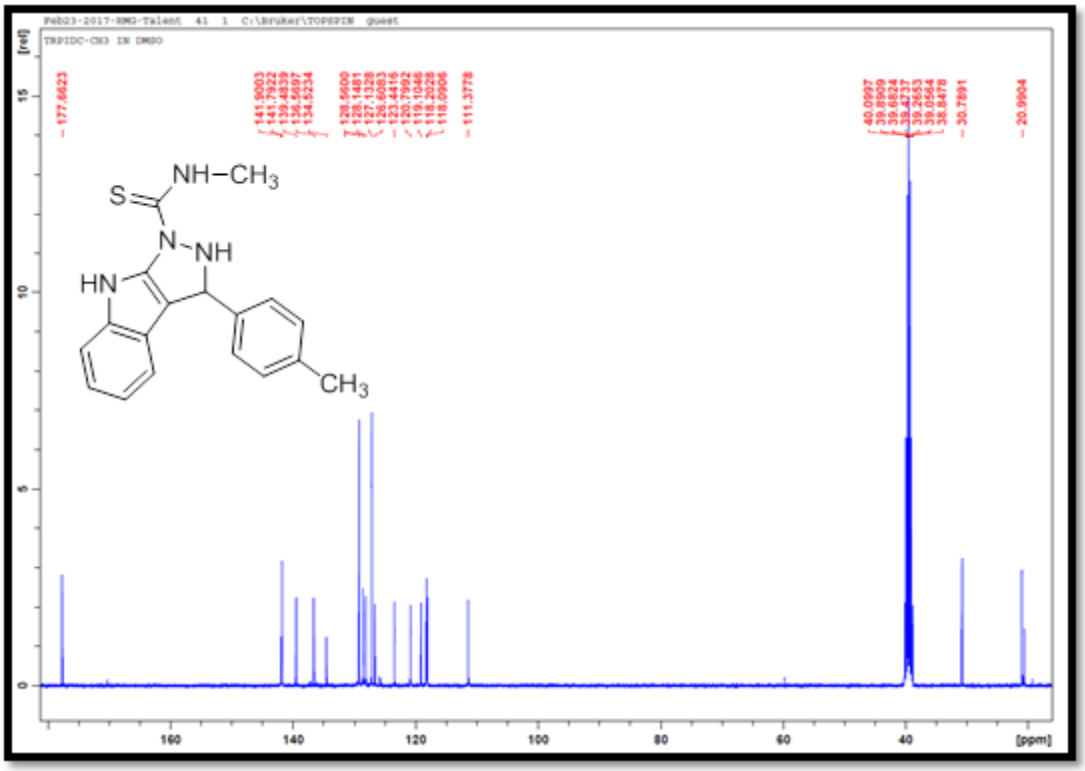

Appendix 5.98A: ^{13}C NMR spectrum for compound **88s**

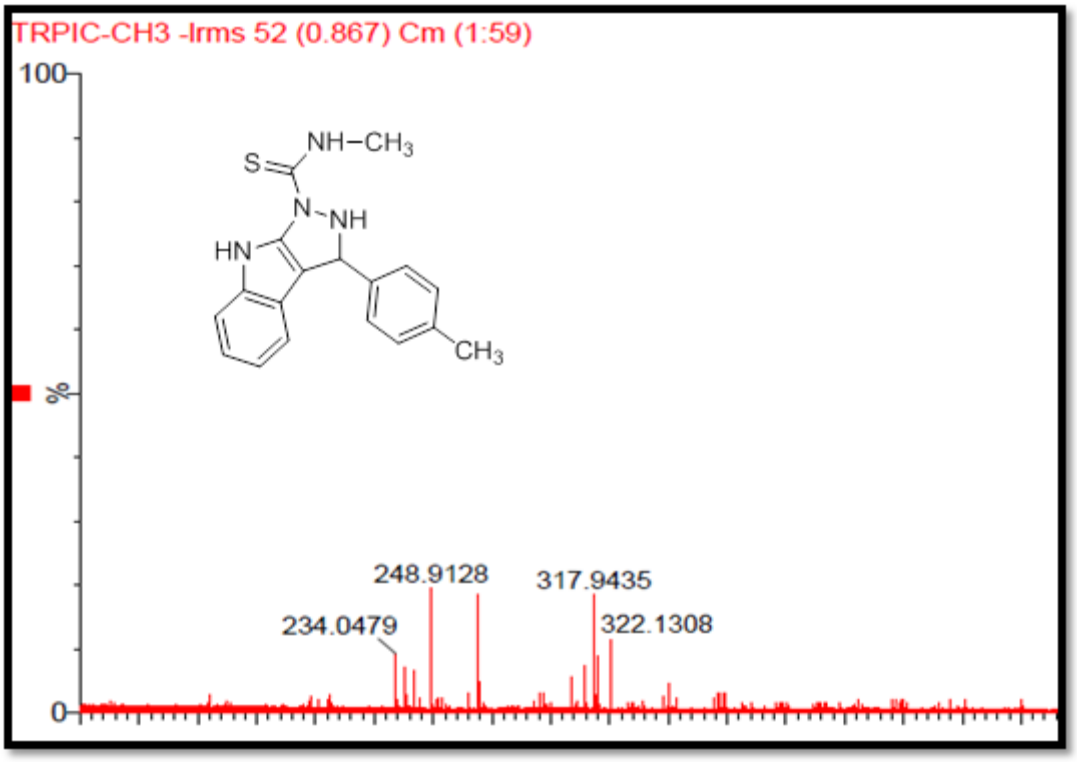

Appendix 5.99A: TOF-MS spectrum for compound **88s**

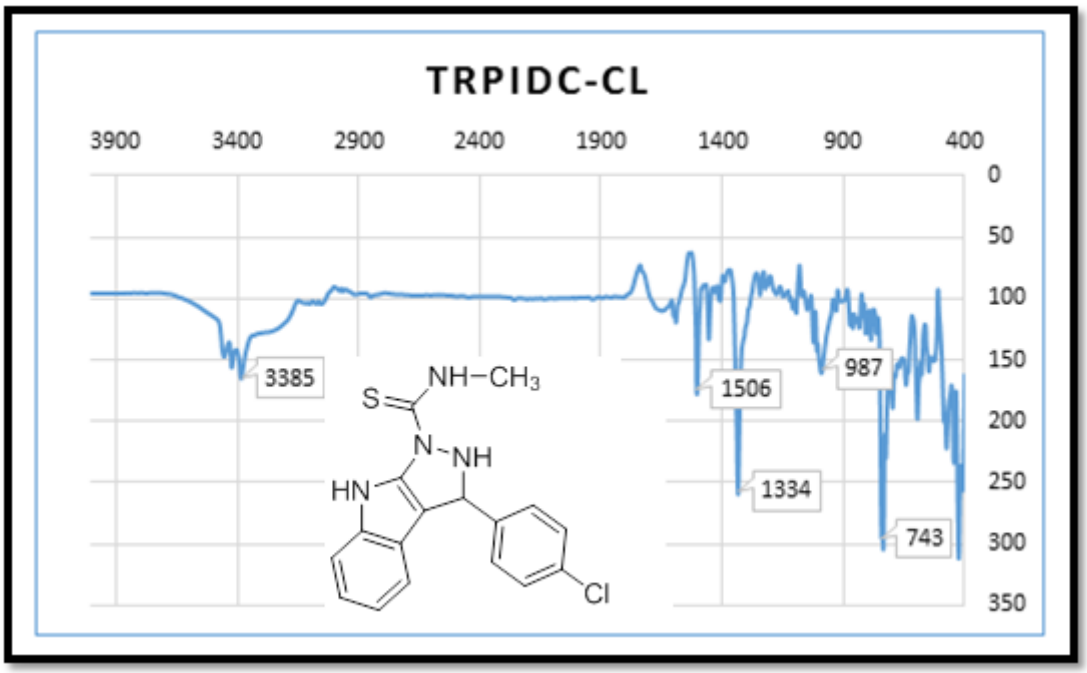

Appendix 5.100A: IR spectrum for compound **88t**

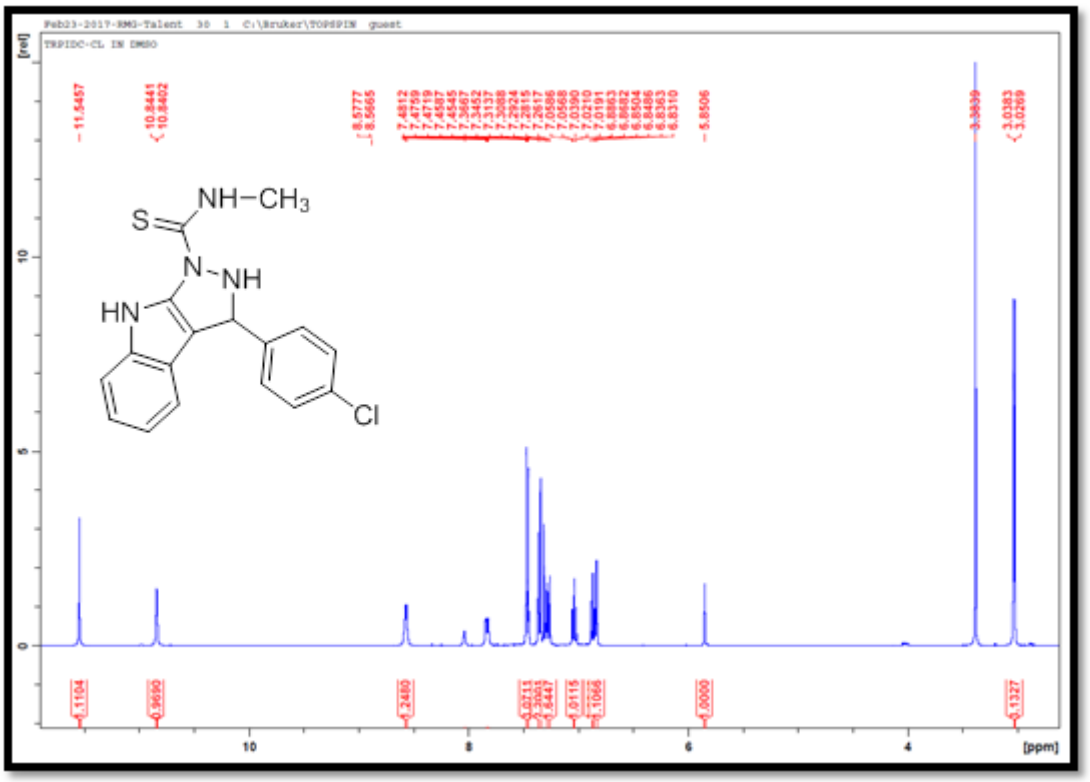

Appendix 5.101A: ^{1}H NMR spectrum for compound **88t**

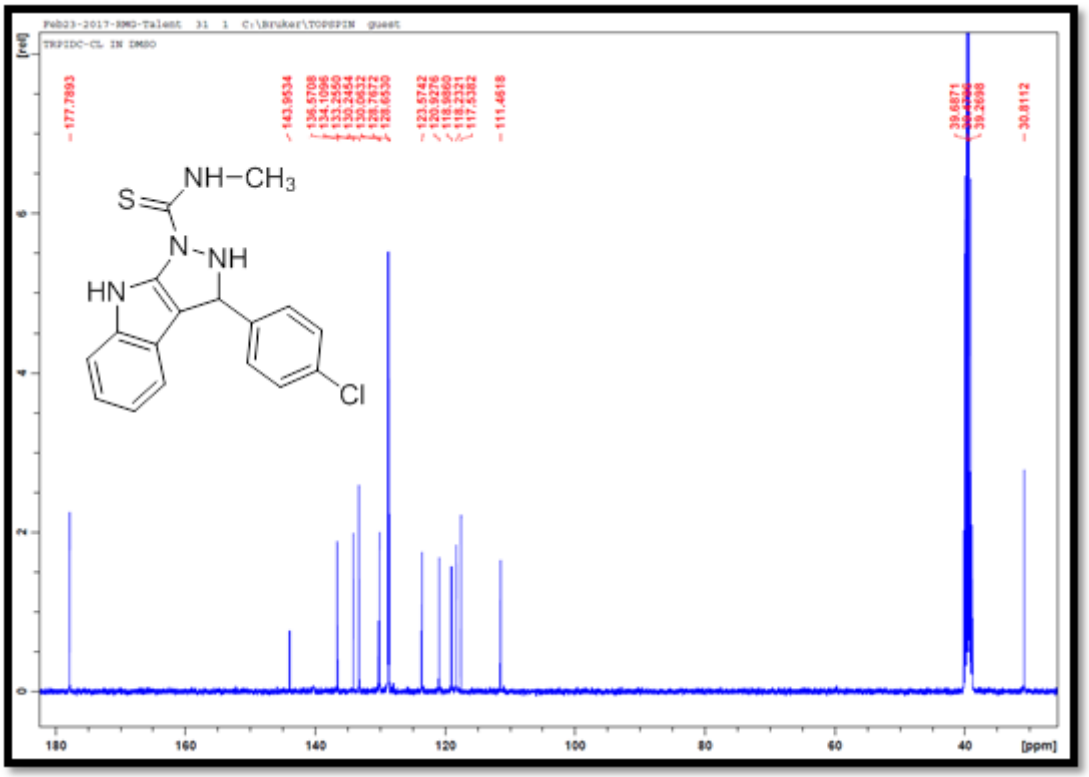

Appendix 5.102A: ^{13}C NMR spectrum for compound **88t**

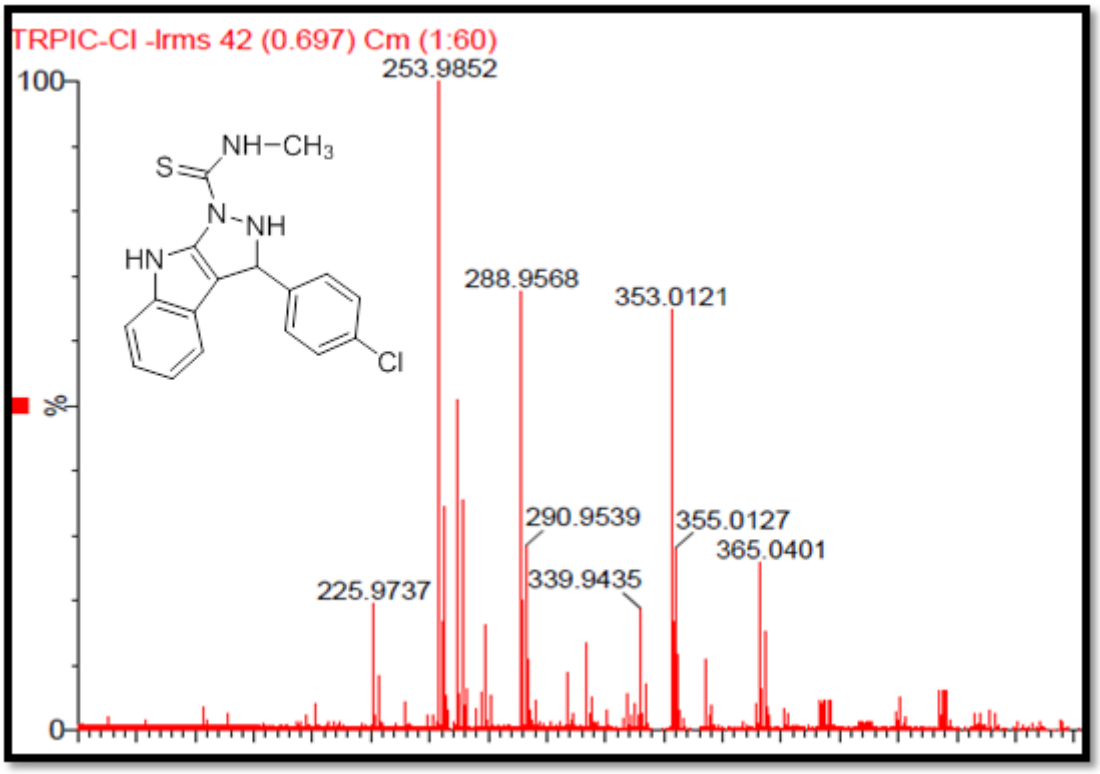

Appendix 5.103A: TOF-MS spectrum for compound **88t**

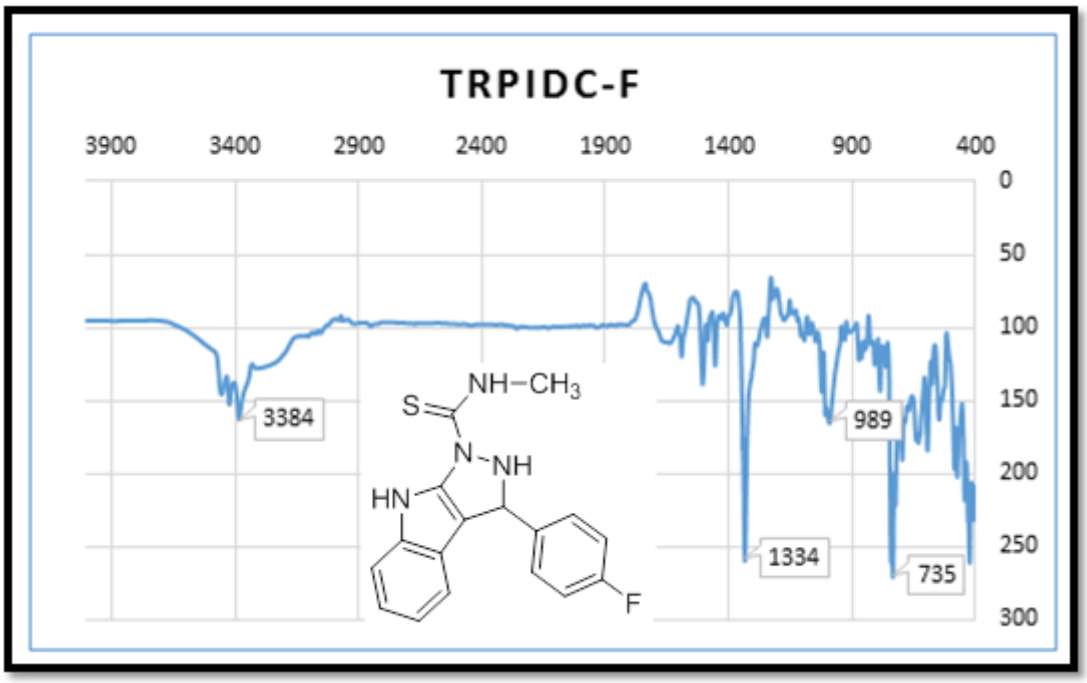

Appendix 5.104A: IR spectrum for compound **88u**

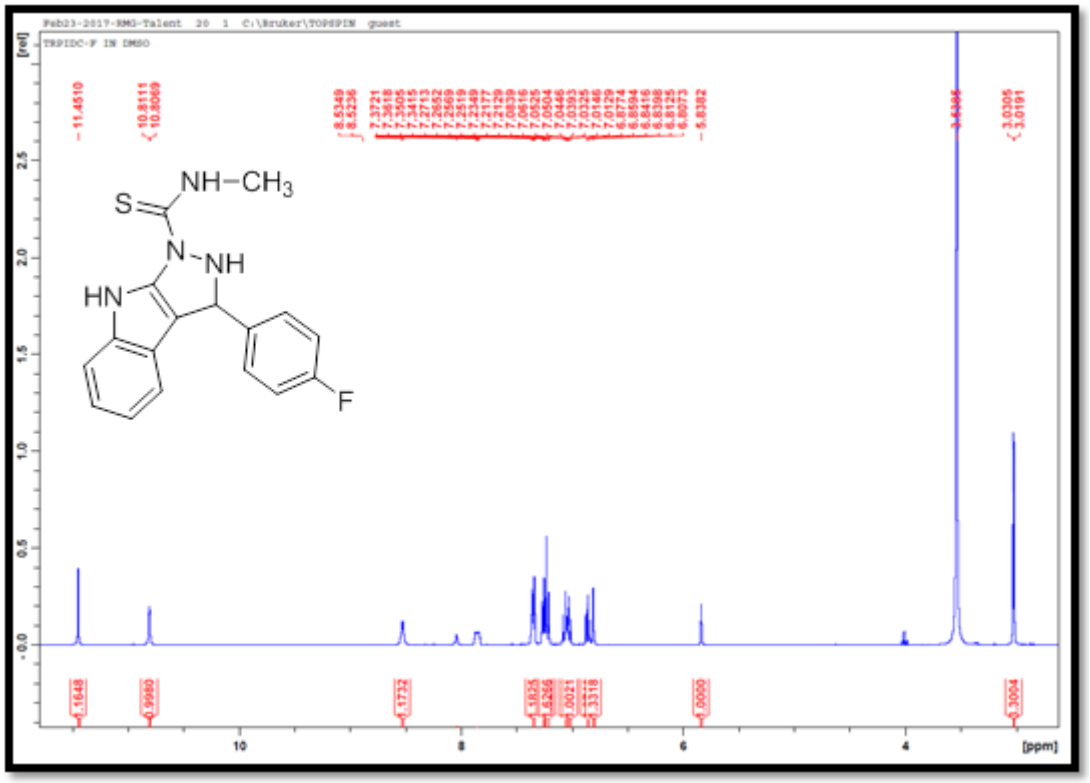

Appendix 5.105A: ^{1}H NMR spectrum for compound **88u**

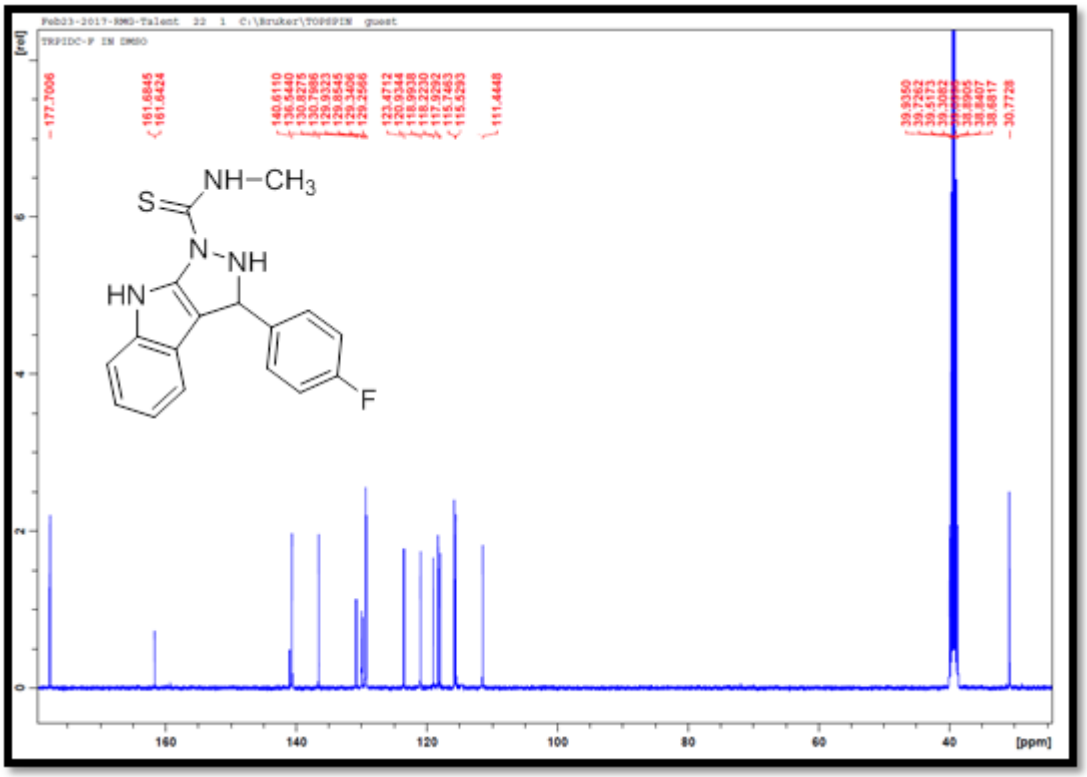

Appendix 5.106A: ^{13}C NMR spectrum for compound **88u**

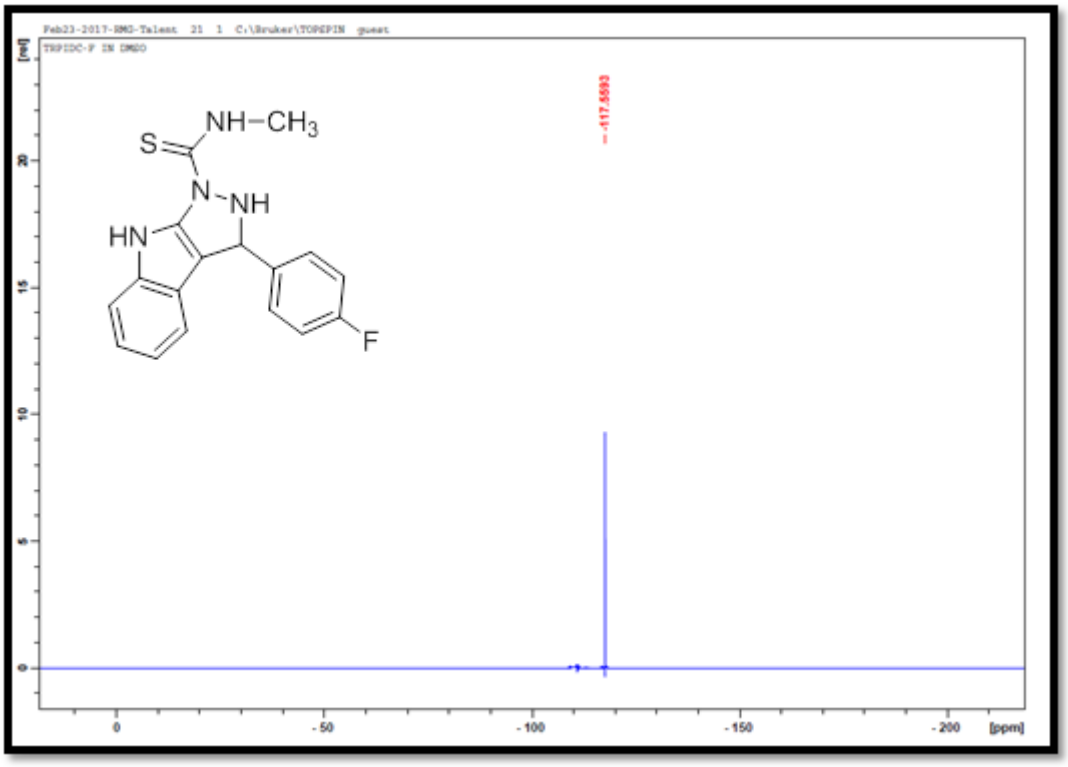

Appendix 5.107A: ^{19}F NMR spectrum for compound **88u**

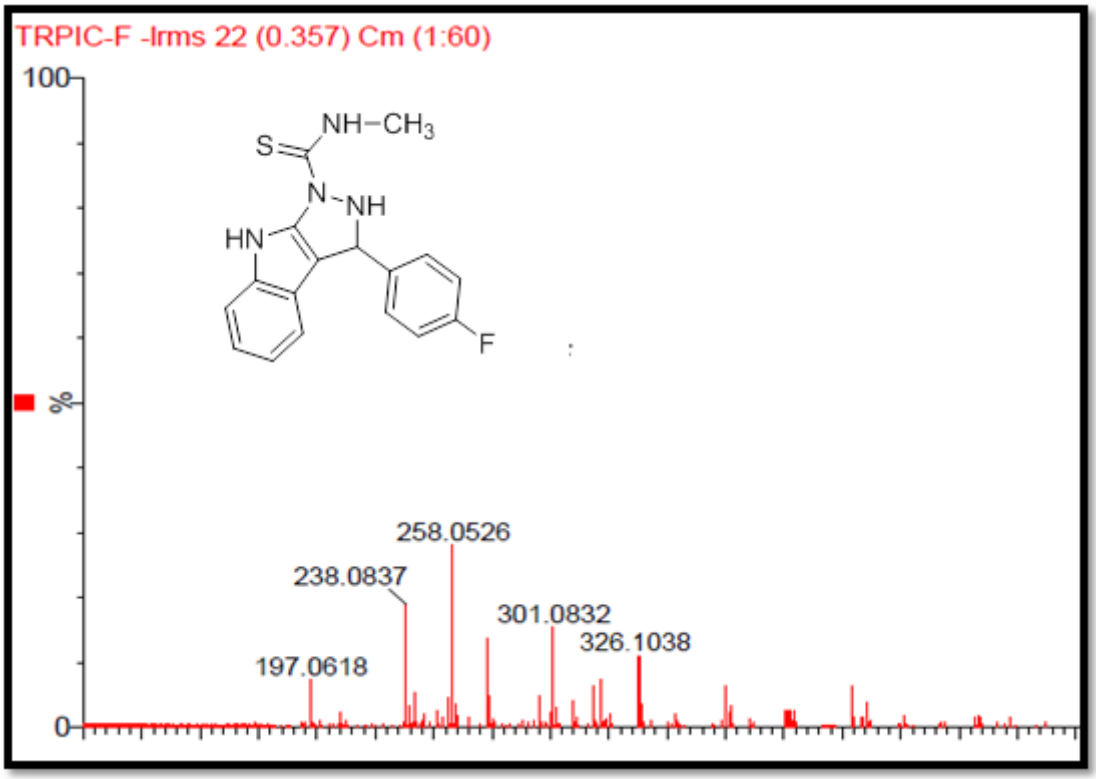

Appendix 5.108A: TOF-MS spectrum for compound **88u**

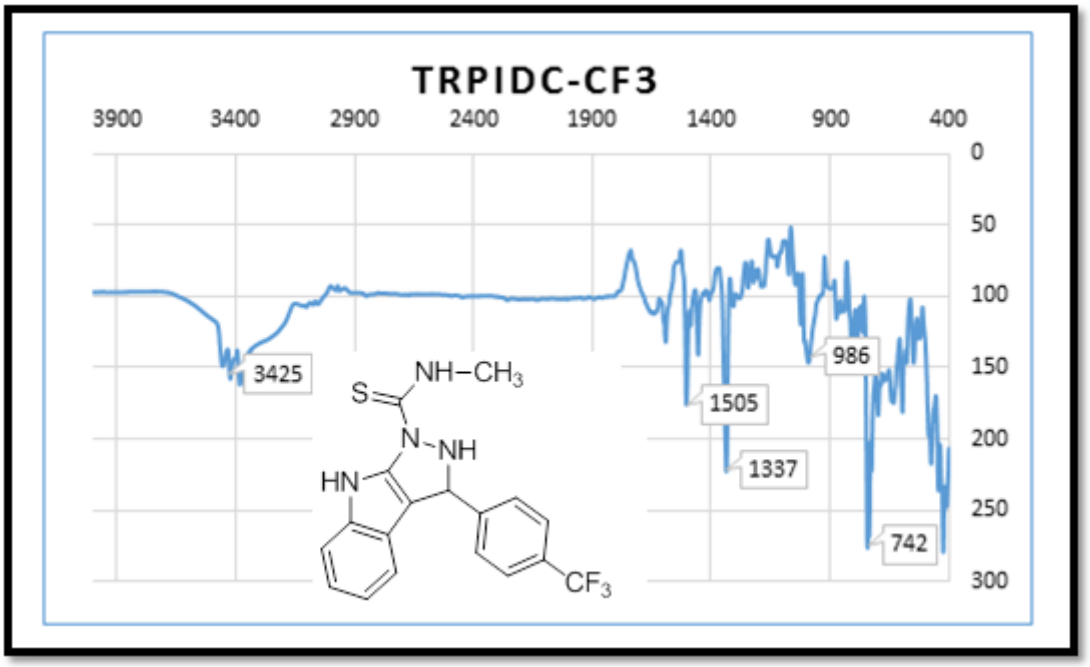

Appendix 5.109A: IR spectrum for compound **88v**

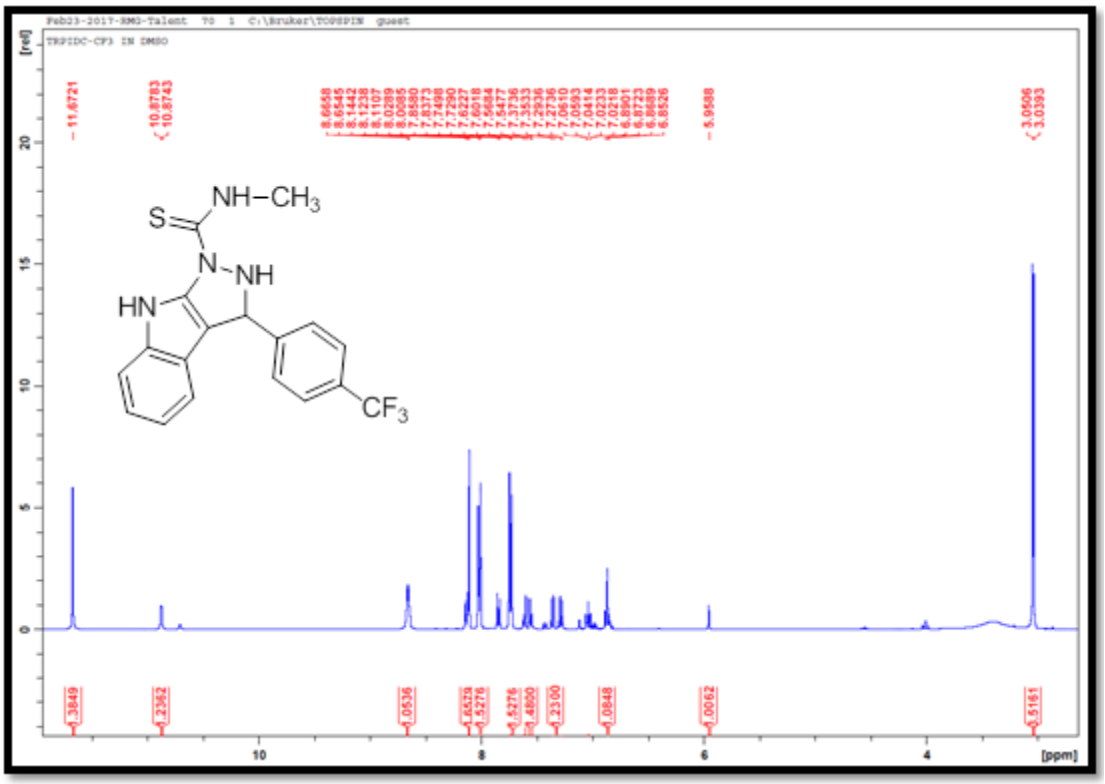

Appendix 5.110A: ^{1}H NMR spectrum for compound **88v**

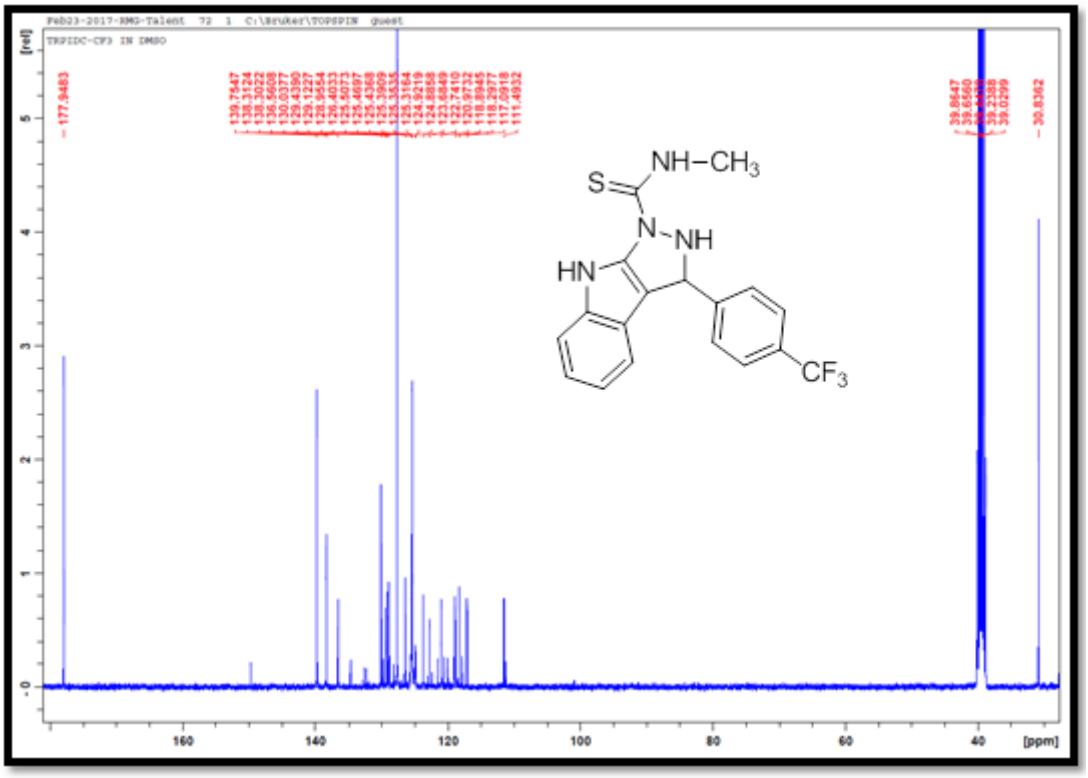

Appendix 5.111A: ^{13}C NMR spectrum for compound **88v**

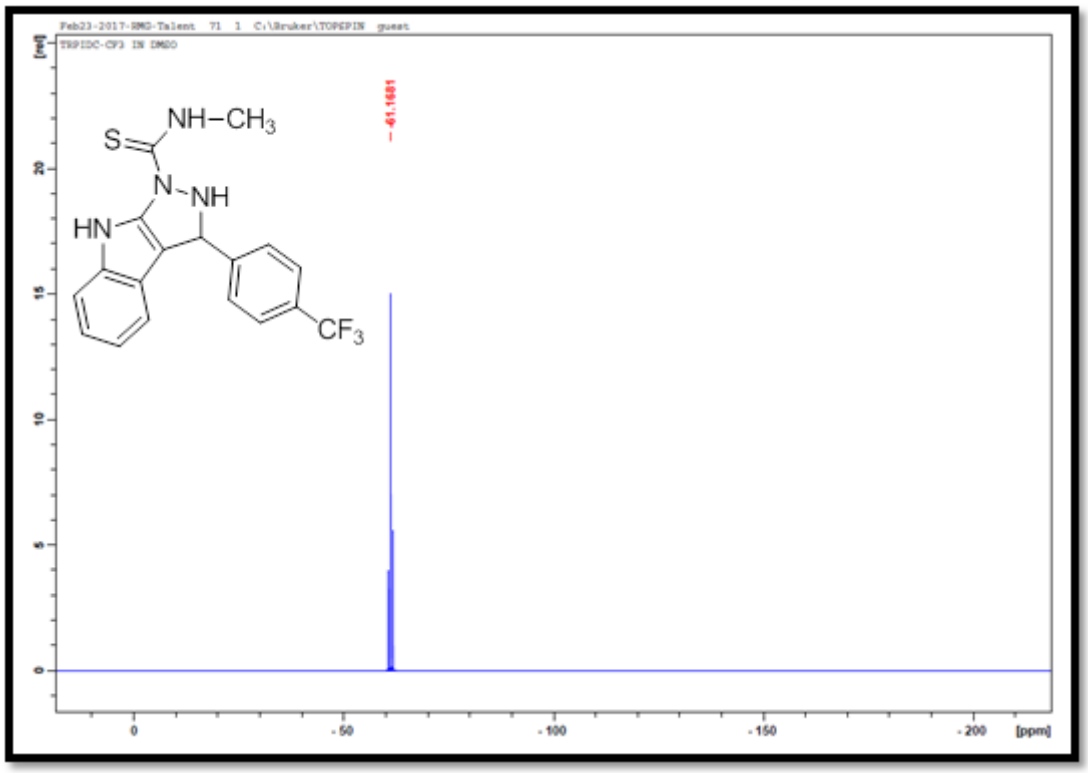

Appendix 5.112A: ^{19}F NMR spectrum for compound **88v**

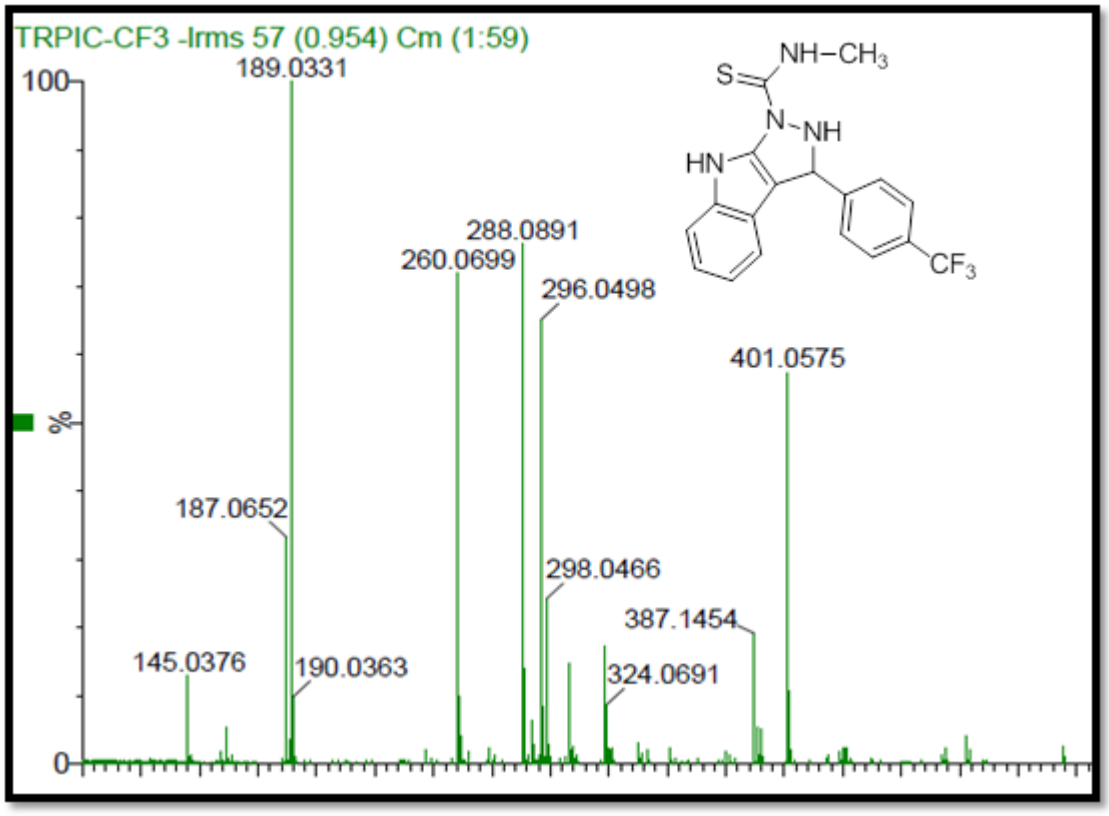

Appendix 5.113A: TOF-MS spectrum for compound **88v**

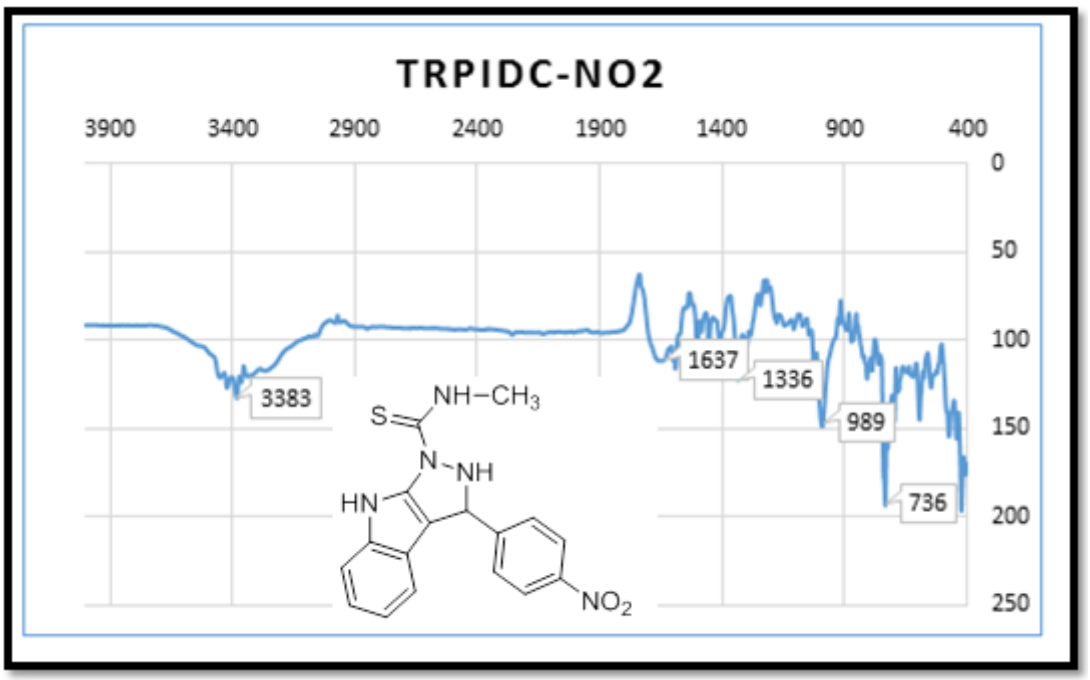

Appendix 5.114A: IR spectrum for compound **88w**

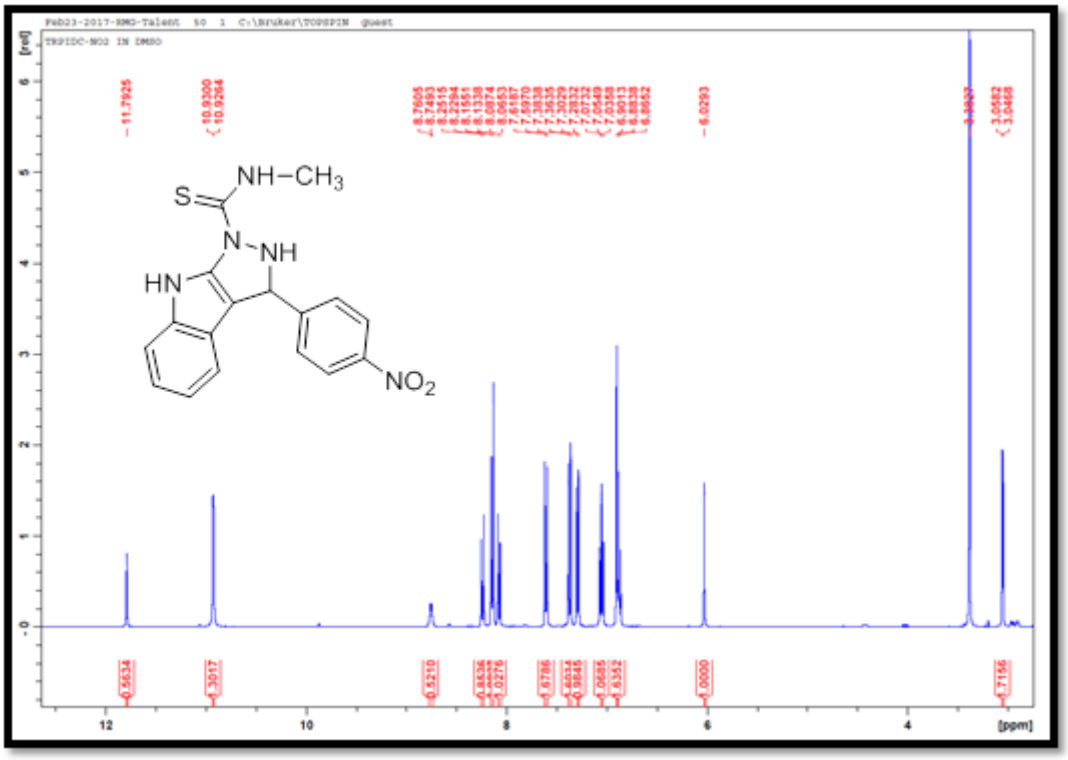

Appendix 5.115A: ^{1}H NMR spectrum for compound **88w**

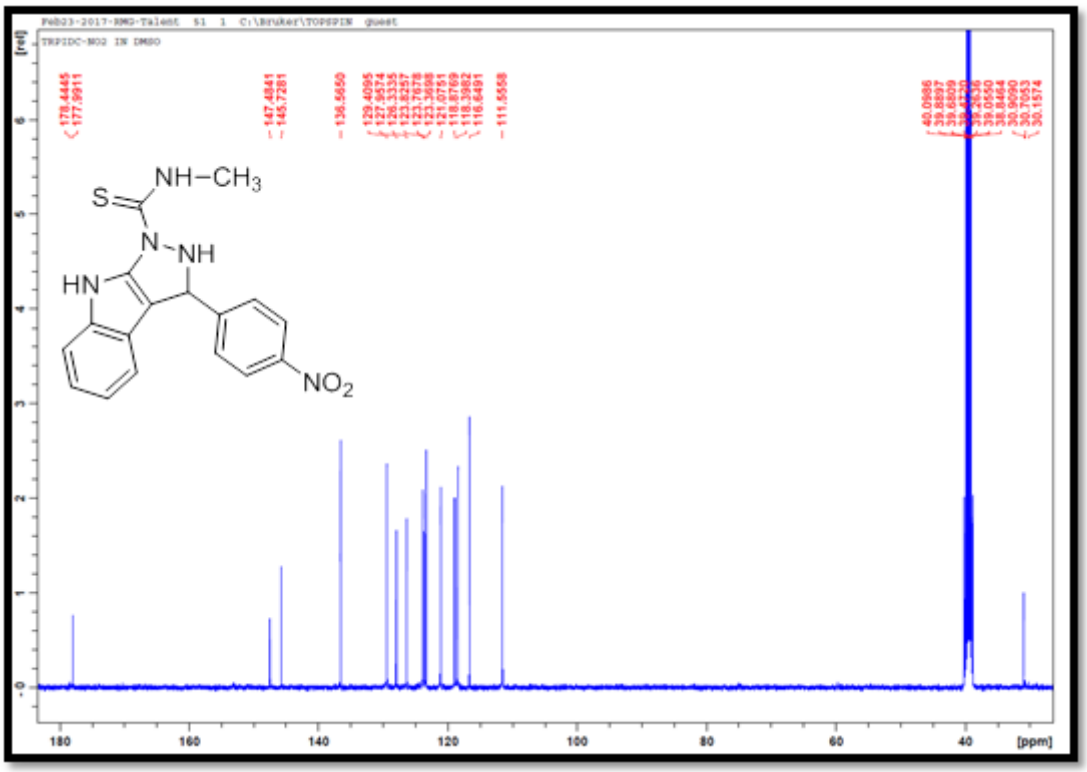

Appendix 5.116A: ^{13}C NMR spectrum for compound **88w**

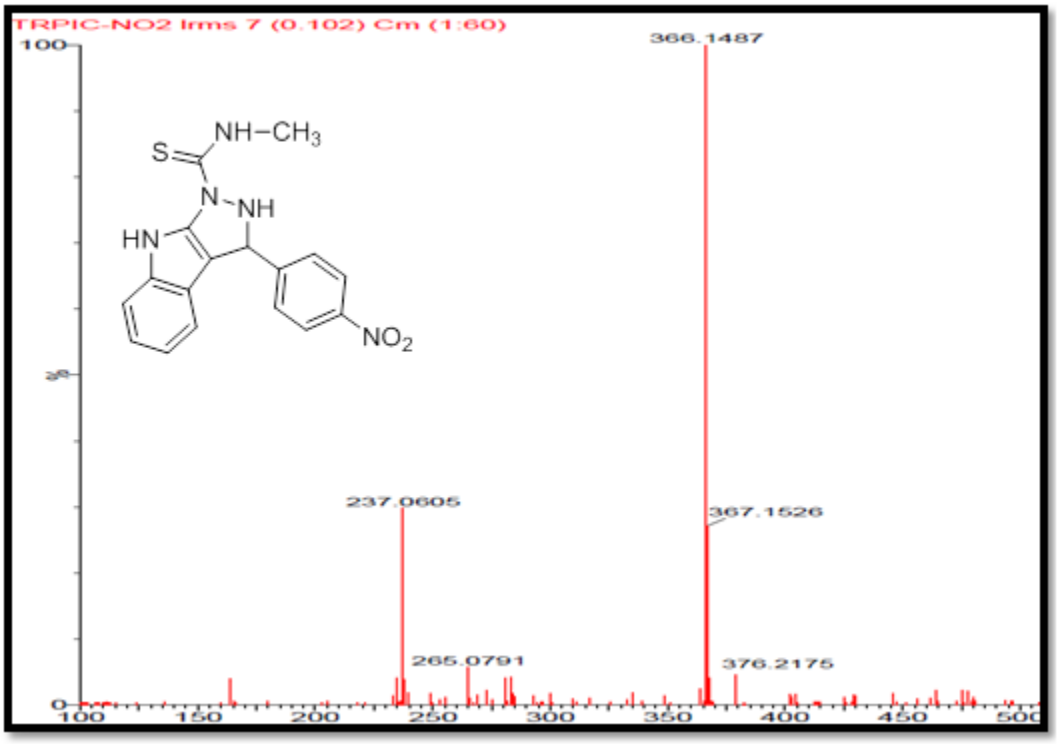

Appendix 5.117A: TOF-MS spectrum for compound **88w**

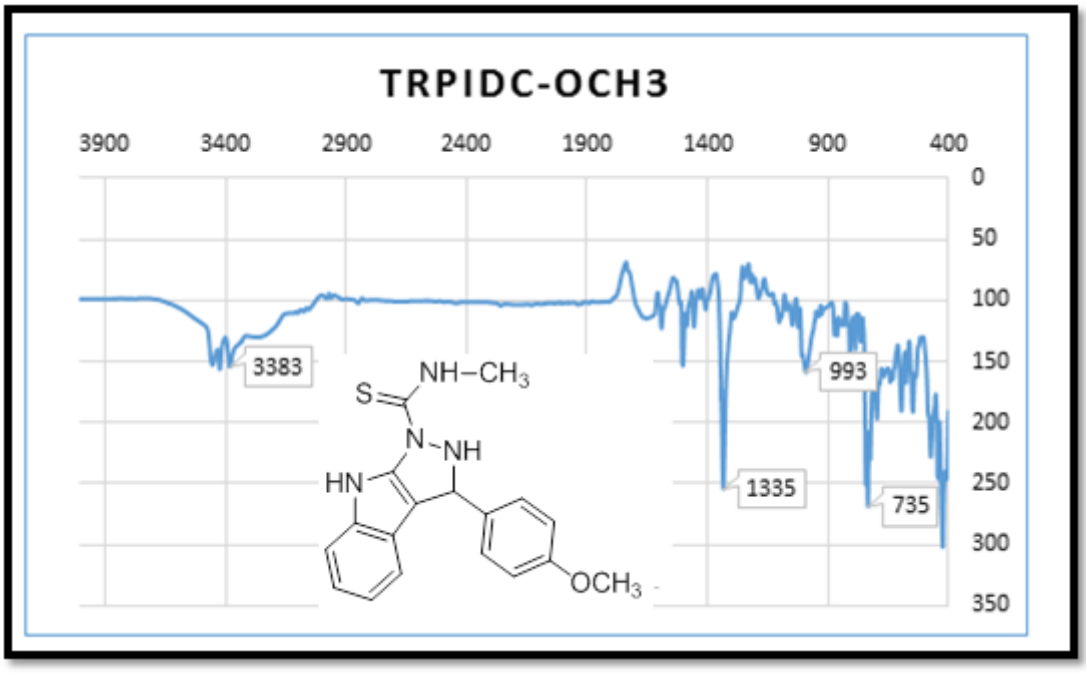

Appendix 5.118A: IR spectrum for compound **88x**

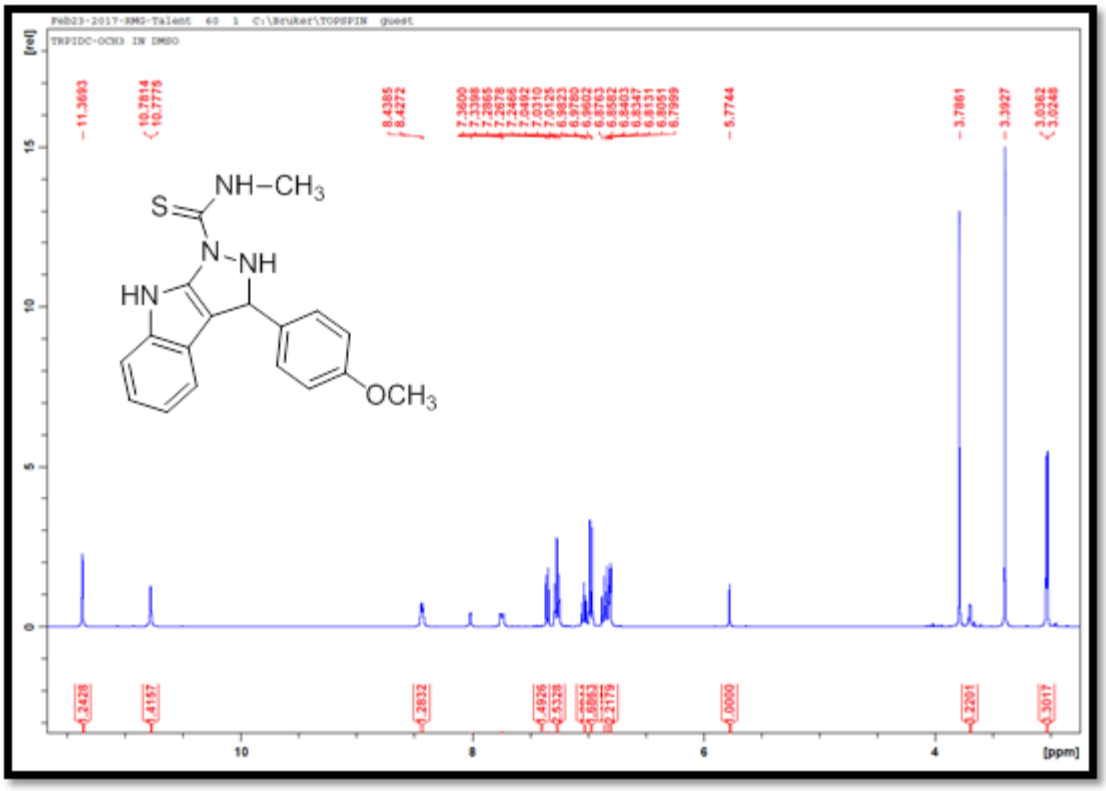

Appendix 5.119A: ^{1}H NMR spectrum for compound **88x**

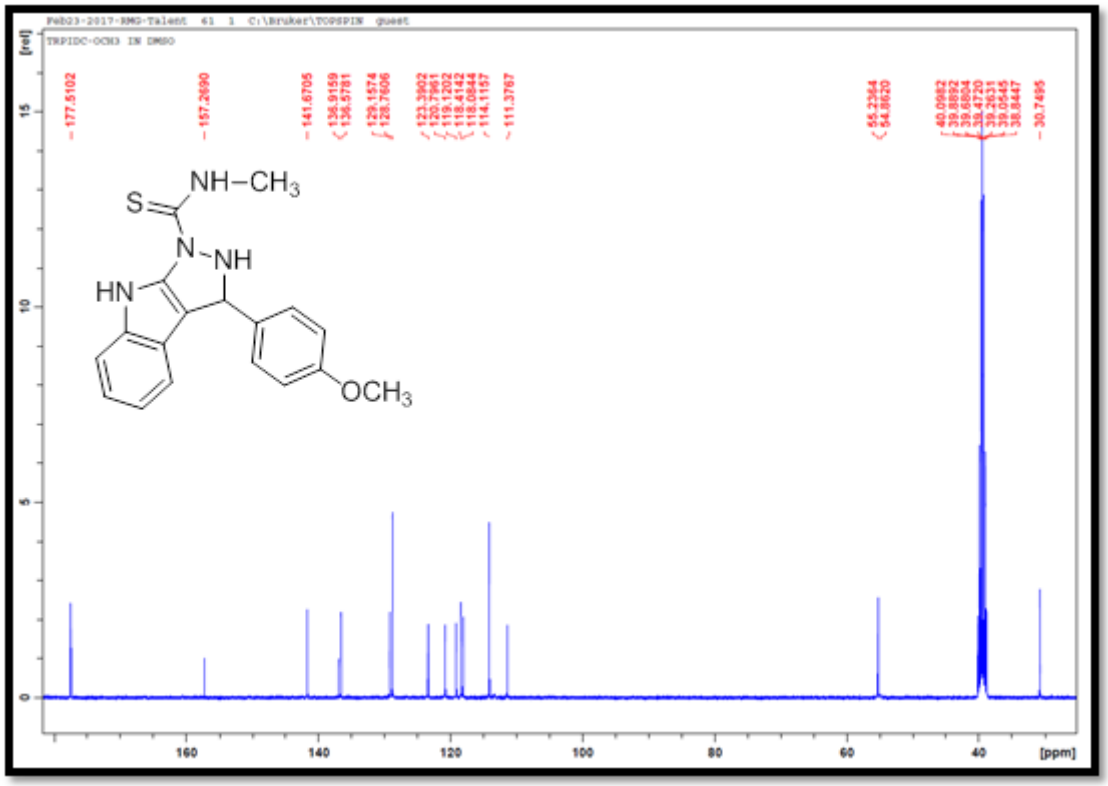

Appendix 5.120A: ^{13}C NMR spectrum for compound **88x**

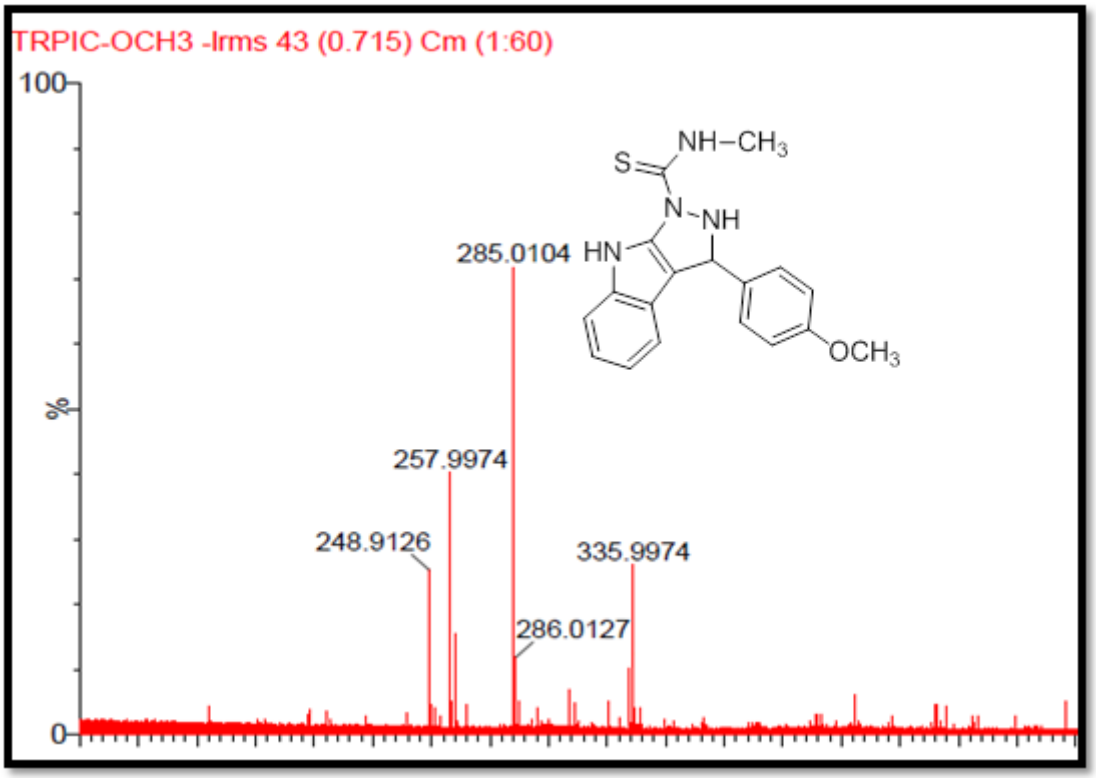

Appendix 5.121A: TOF-MS spectrum for compound **88x**

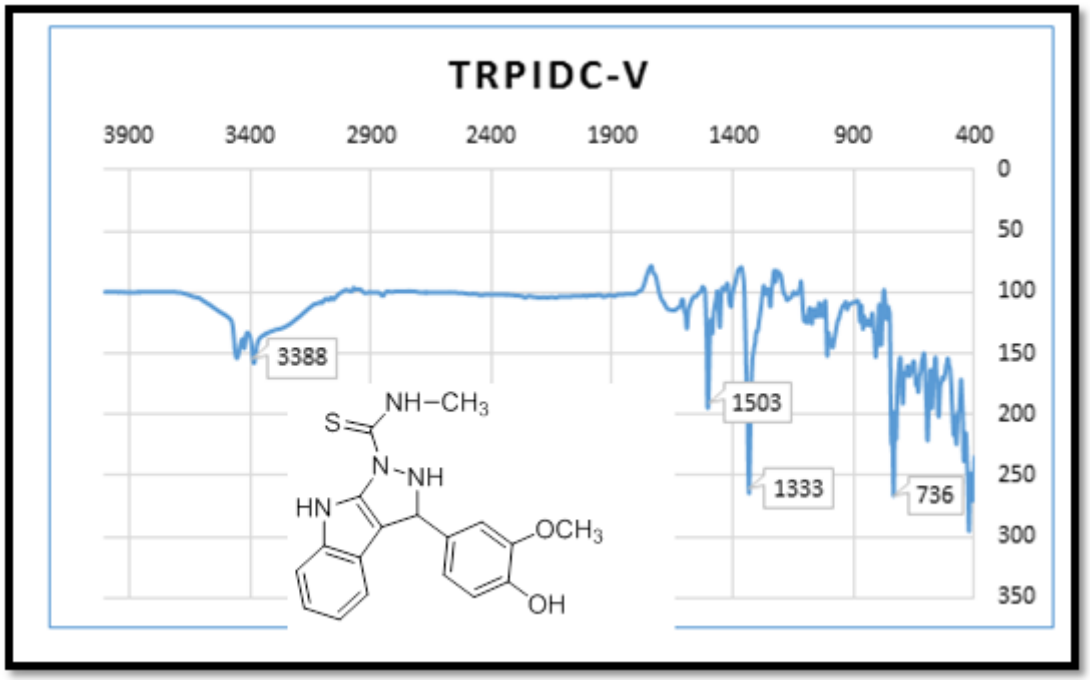

Appendix 5.122A: IR spectrum for compound **88y**

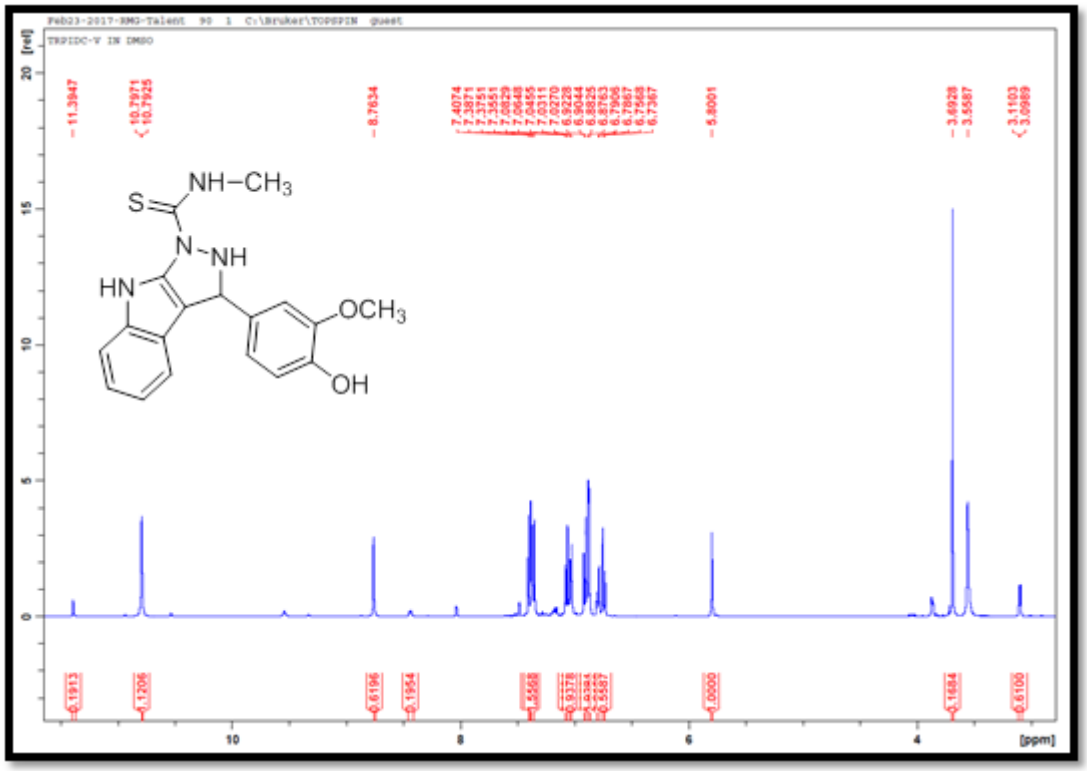

Appendix 5.123A: ^{1}H NMR spectrum for compound **88y**

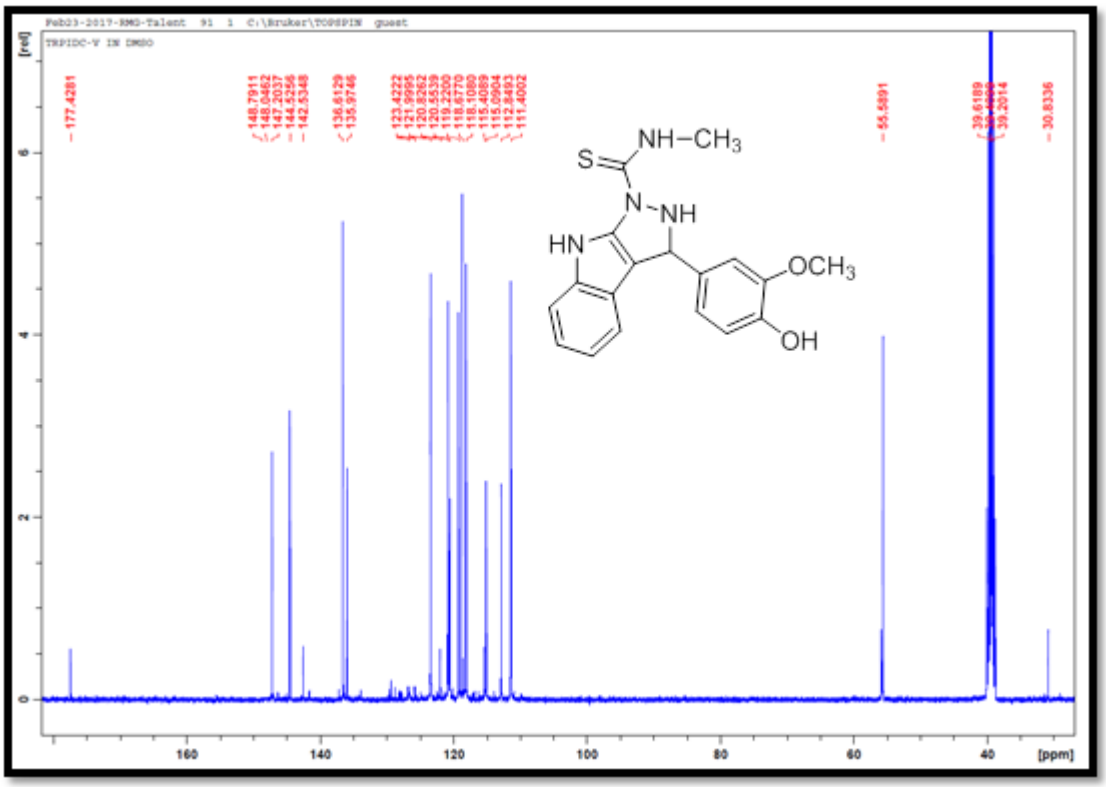

Appendix 5.124A: ^{13}C NMR spectrum for compound **88y**

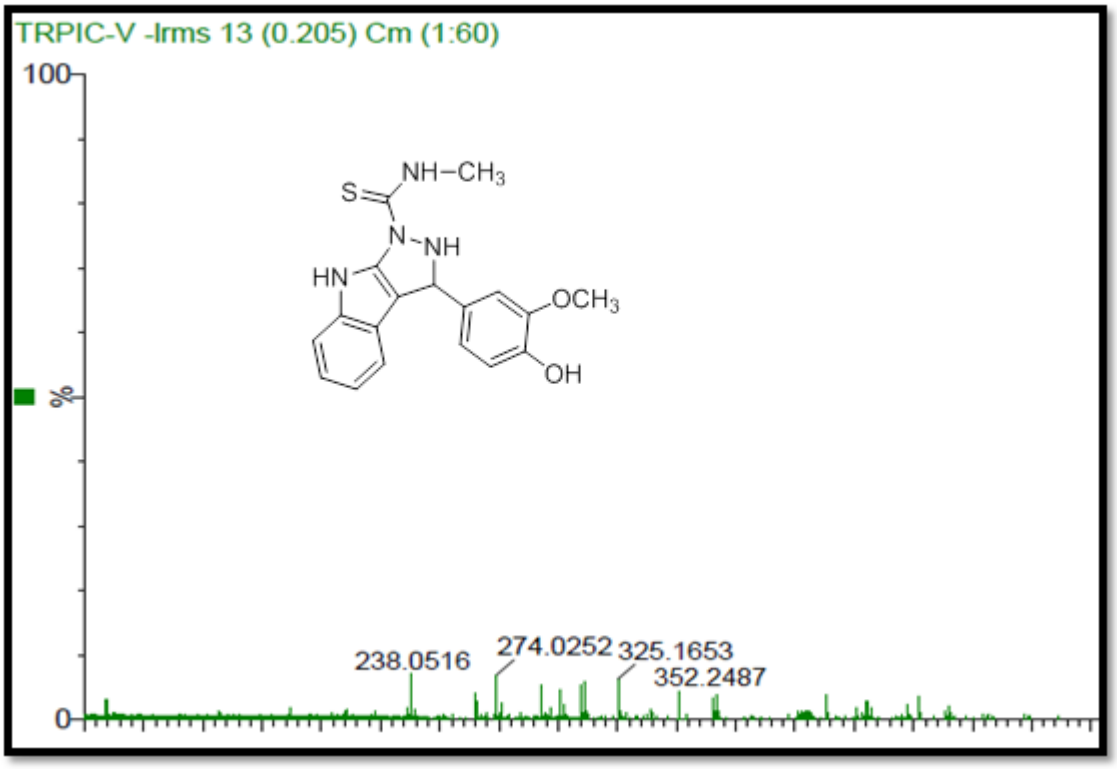

Appendix 5.125A: TOF-MS spectrum for compound **88y**

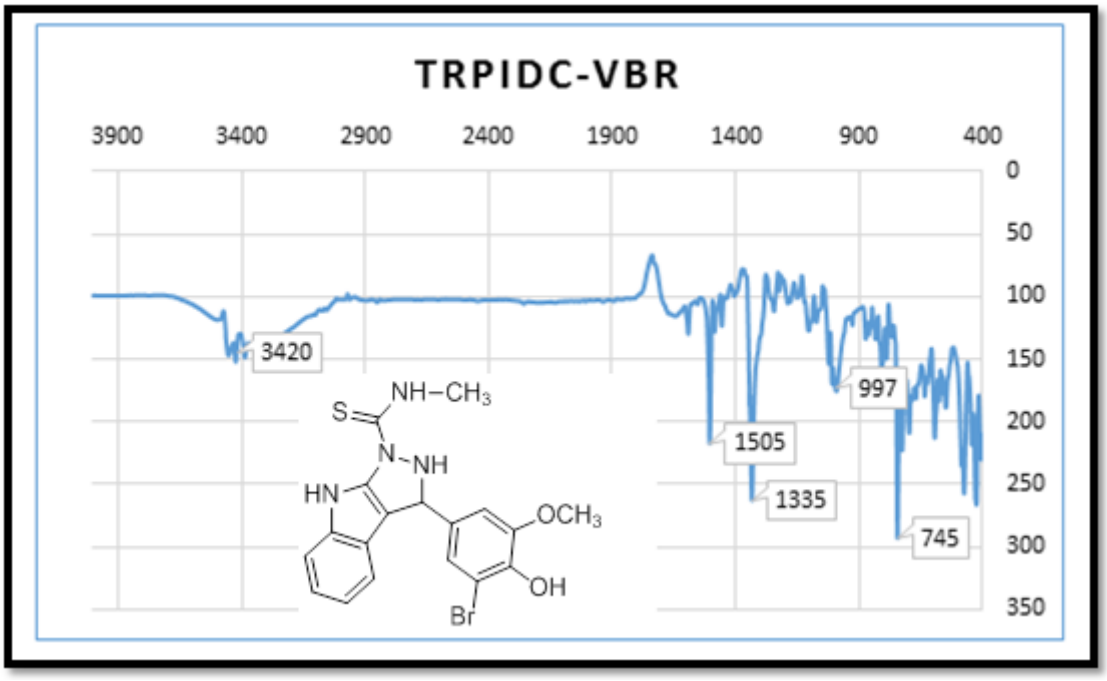

Appendix 5.126A: IR spectrum for compound **88z**

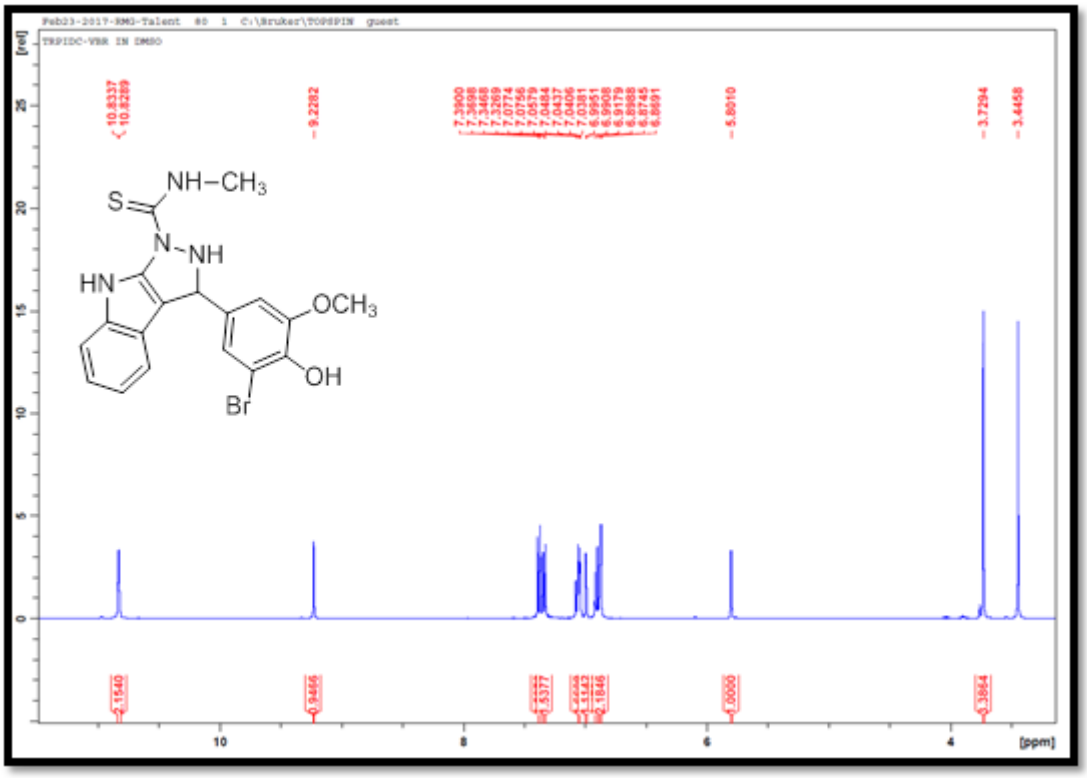

Appendix 5.127A: ^{1}H NMR spectrum for compound **88z**

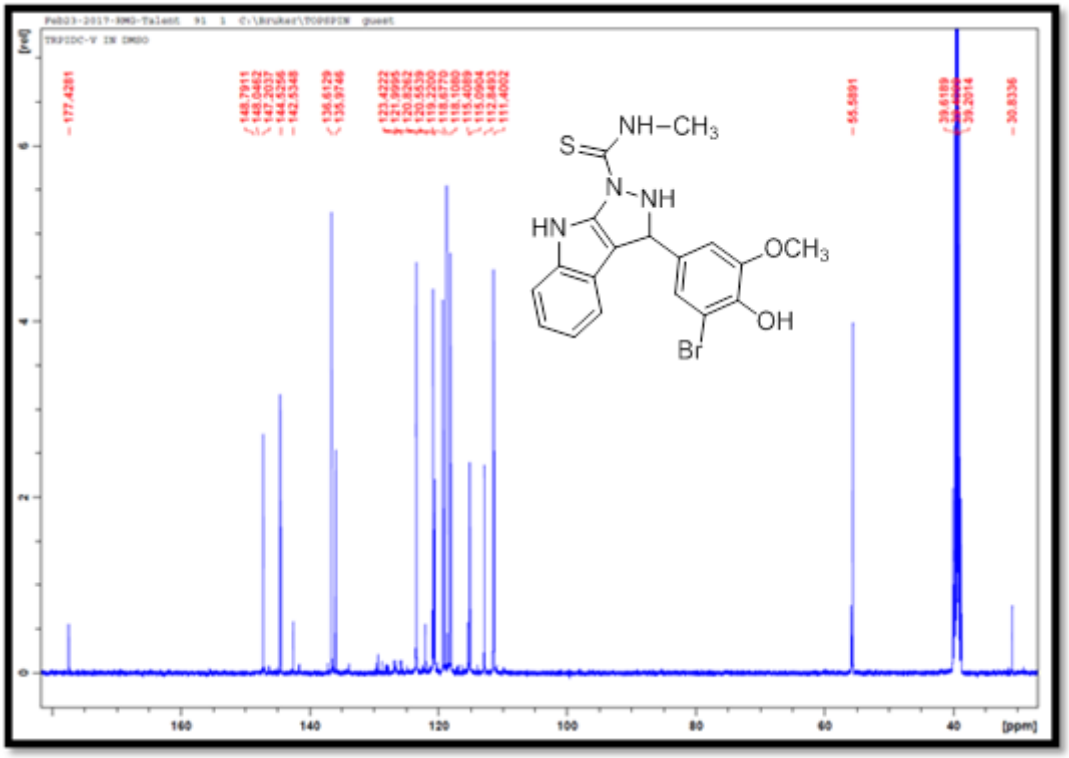

Appendix 5.128A: ^{13}C NMR spectrum for compound **88z**

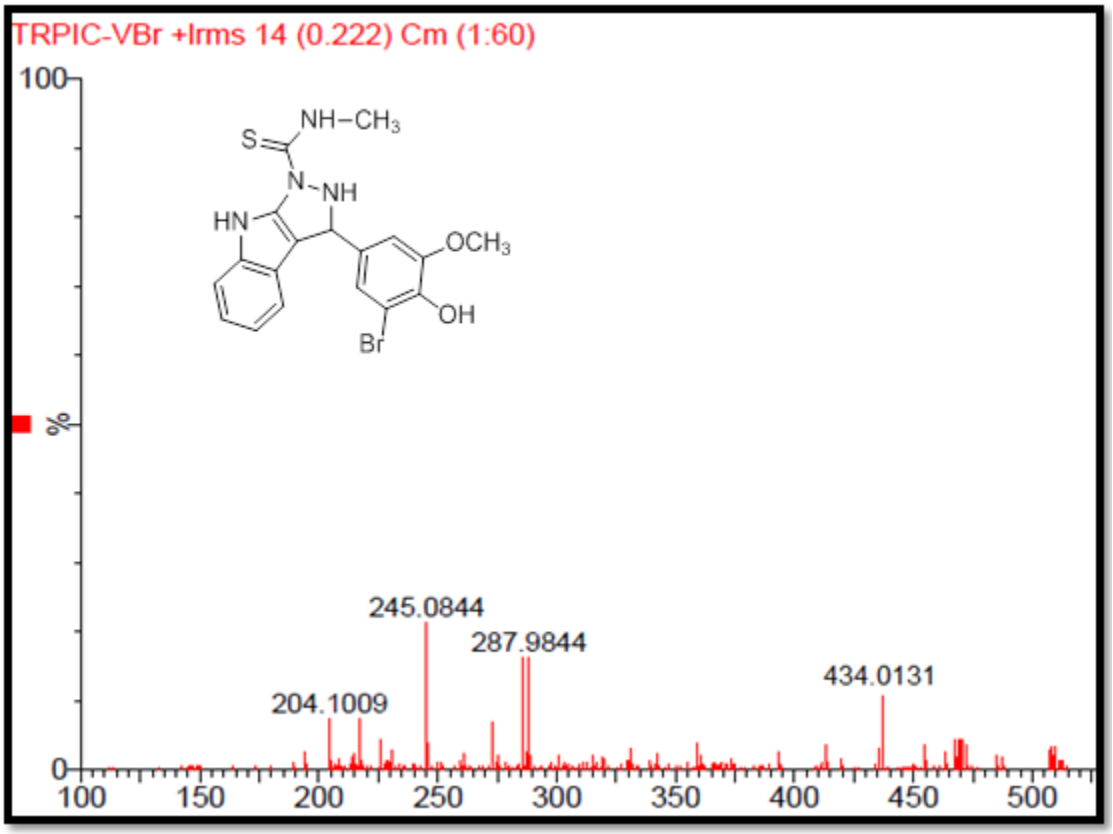

Appendix 5.129A: TOF-MS spectrum for compound **88z**

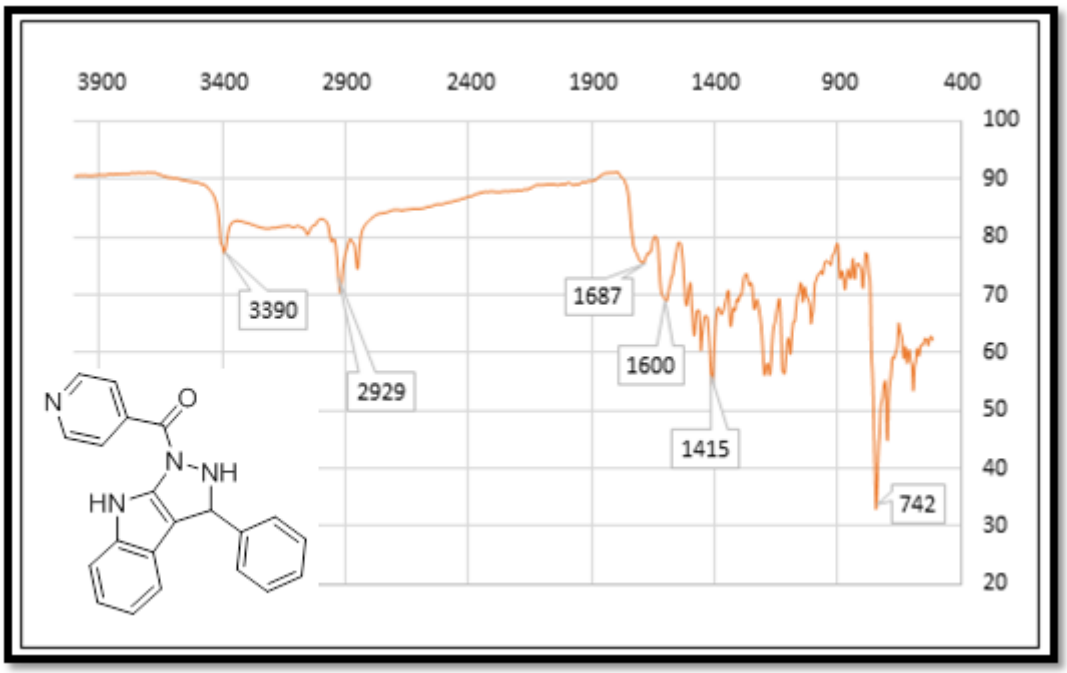

Appendix 5.1B: IR spectrum of compound **94a**

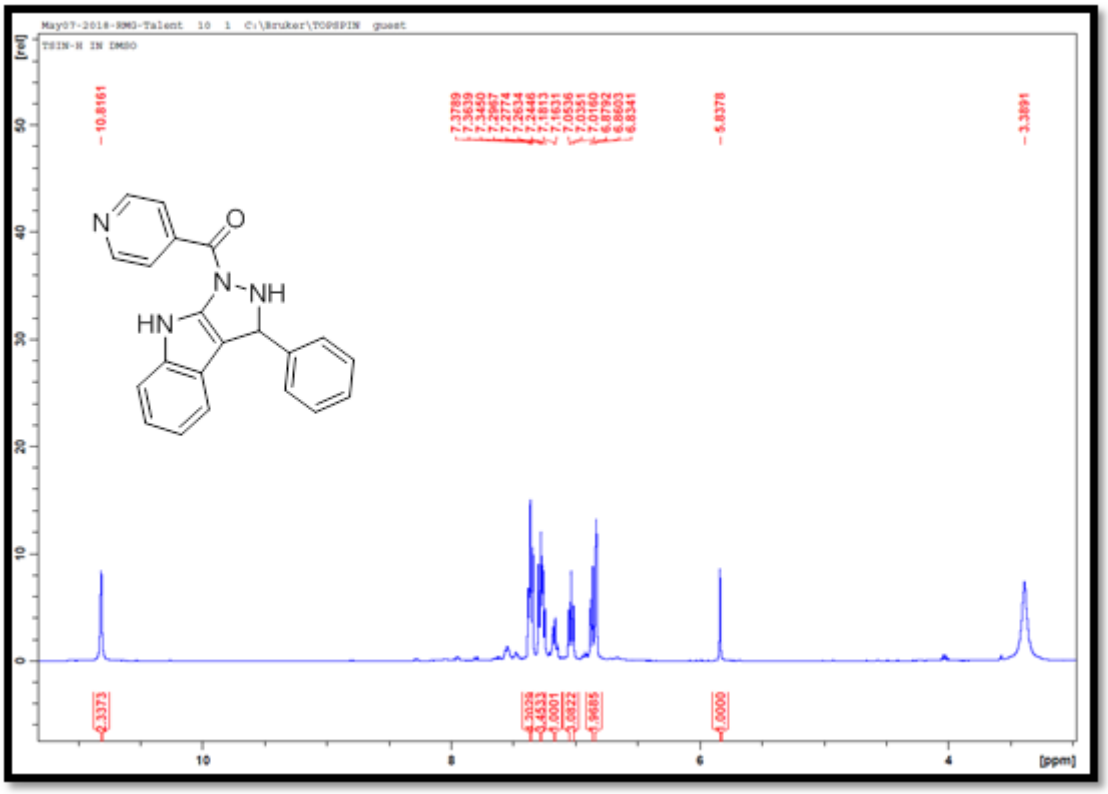

Appendix 5.2B: ^{1}H NMR spectrum of compound **94a**

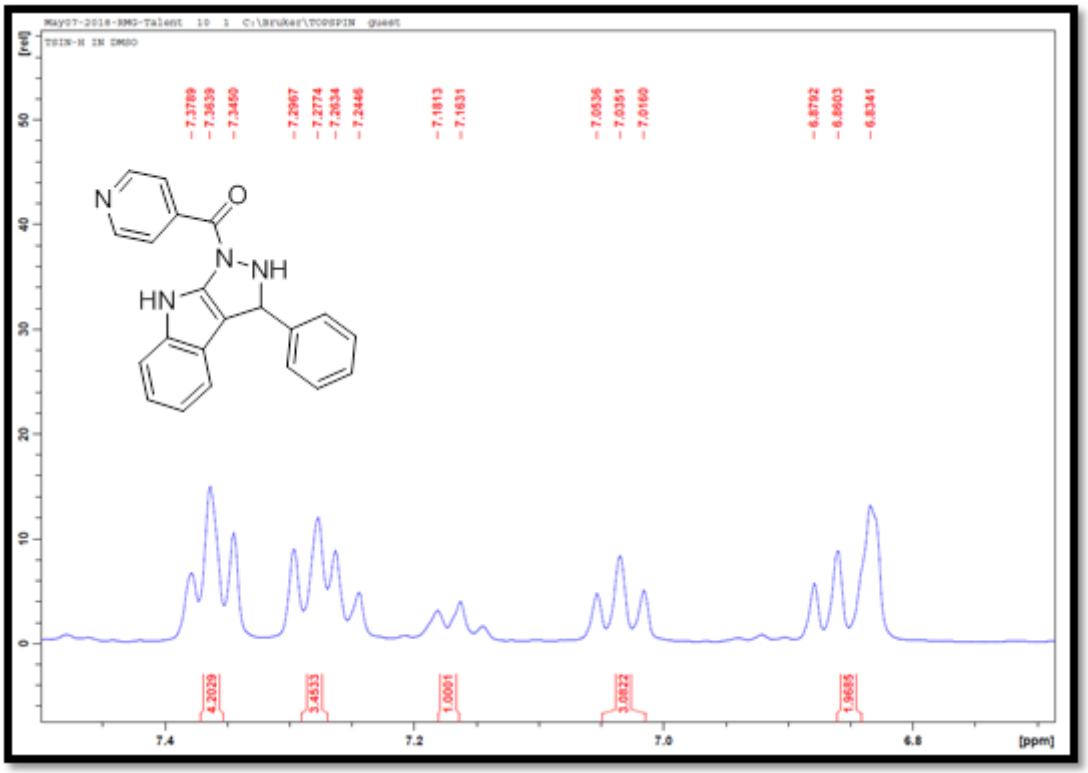

Appendix 5.3B: Expanded ^{1}H NMR spectrum of compound **94a**

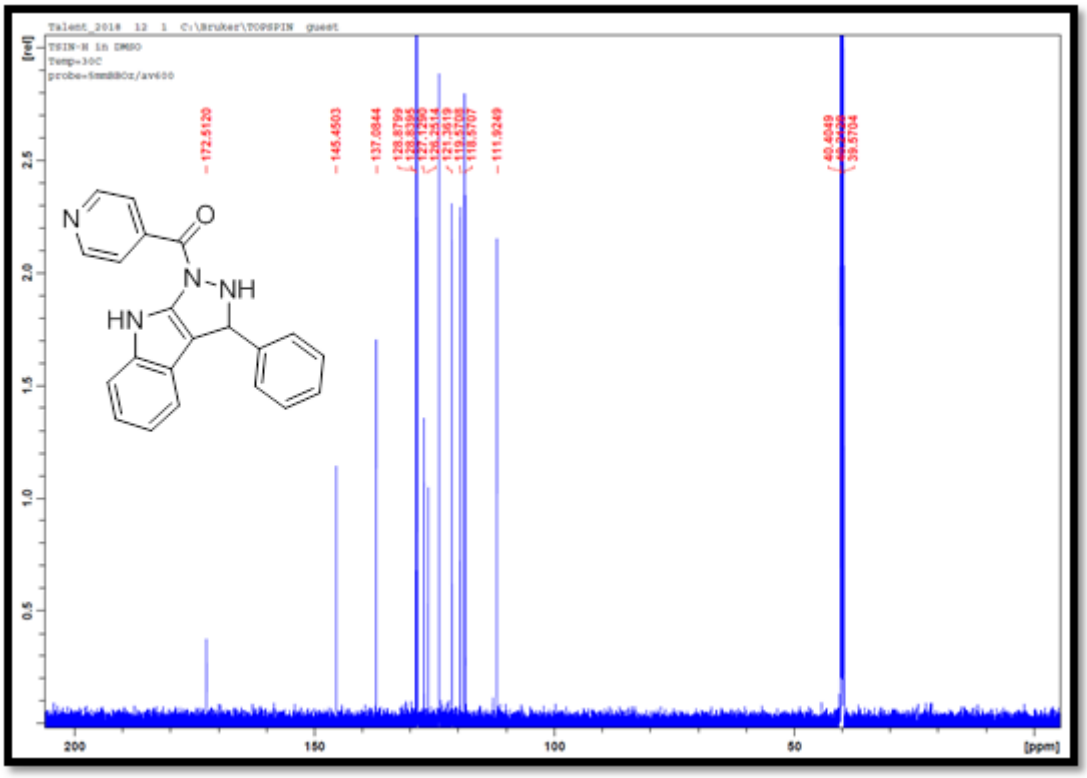

Appendix 5.4B: ^{13}C NMR spectrum of compound **94a**

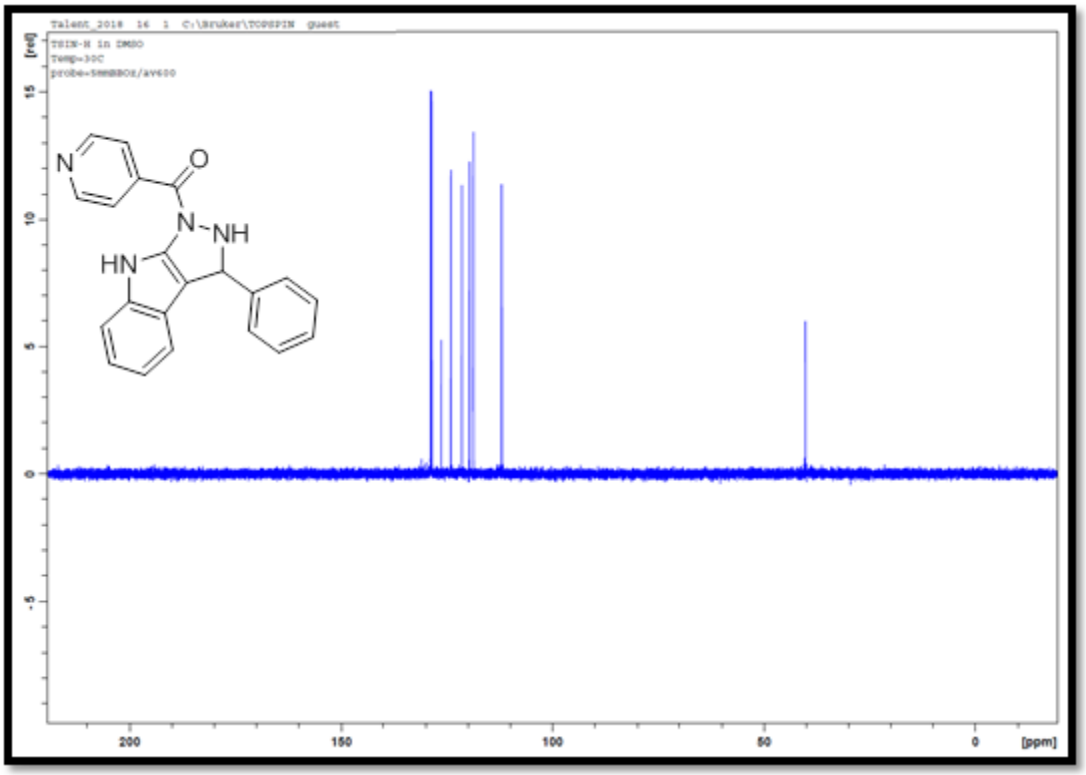

Appendix 5.5B: 135^0 DEPT NMR spectrum of compound **94a**

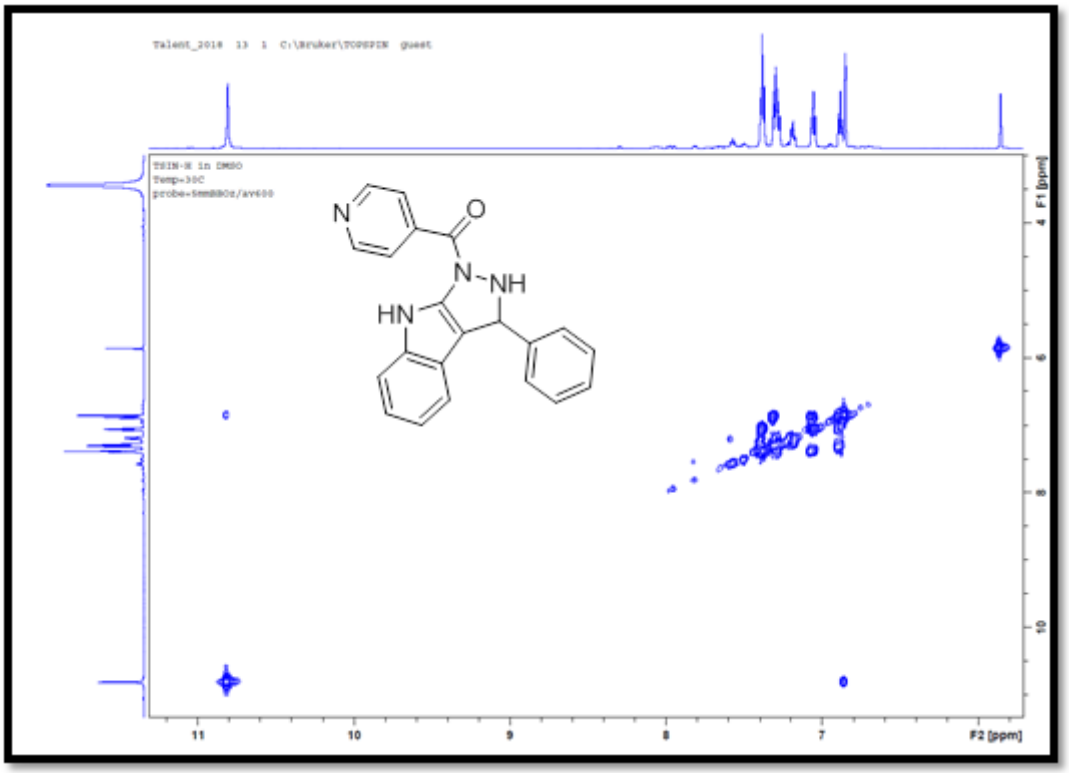

Appendix 5.6B: COSY NMR spectrum of compound **94a**

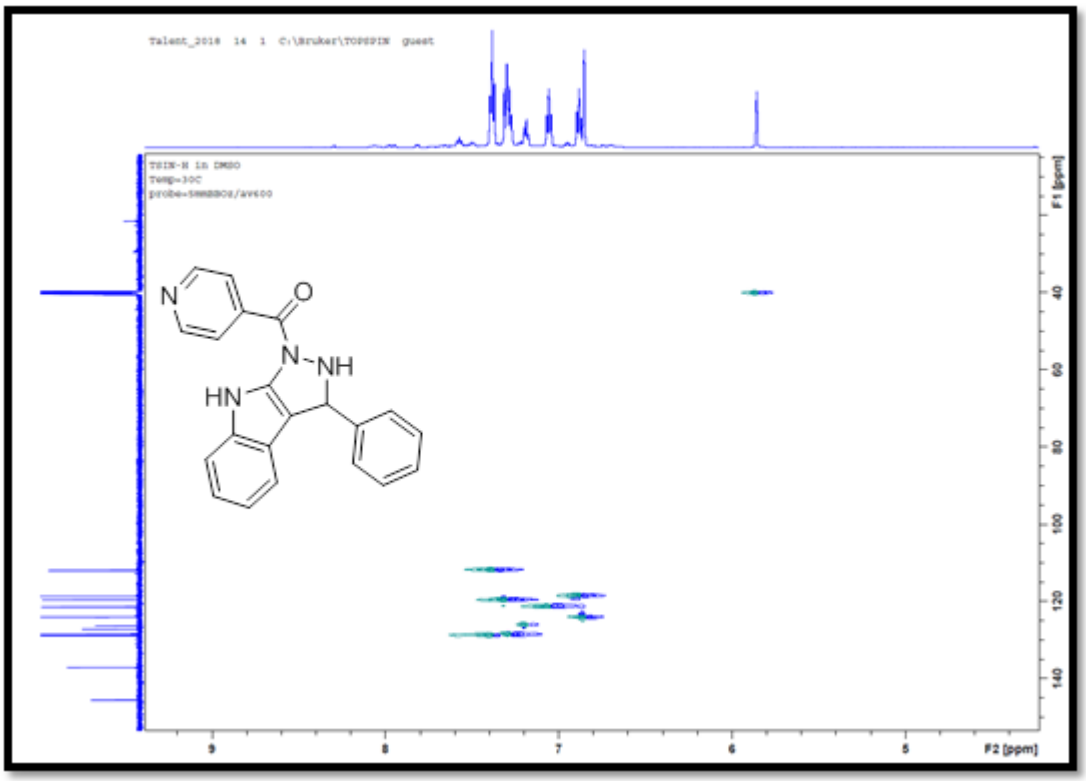

Appendix 5.7B: HSQC NMR spectrum of compound **94a**

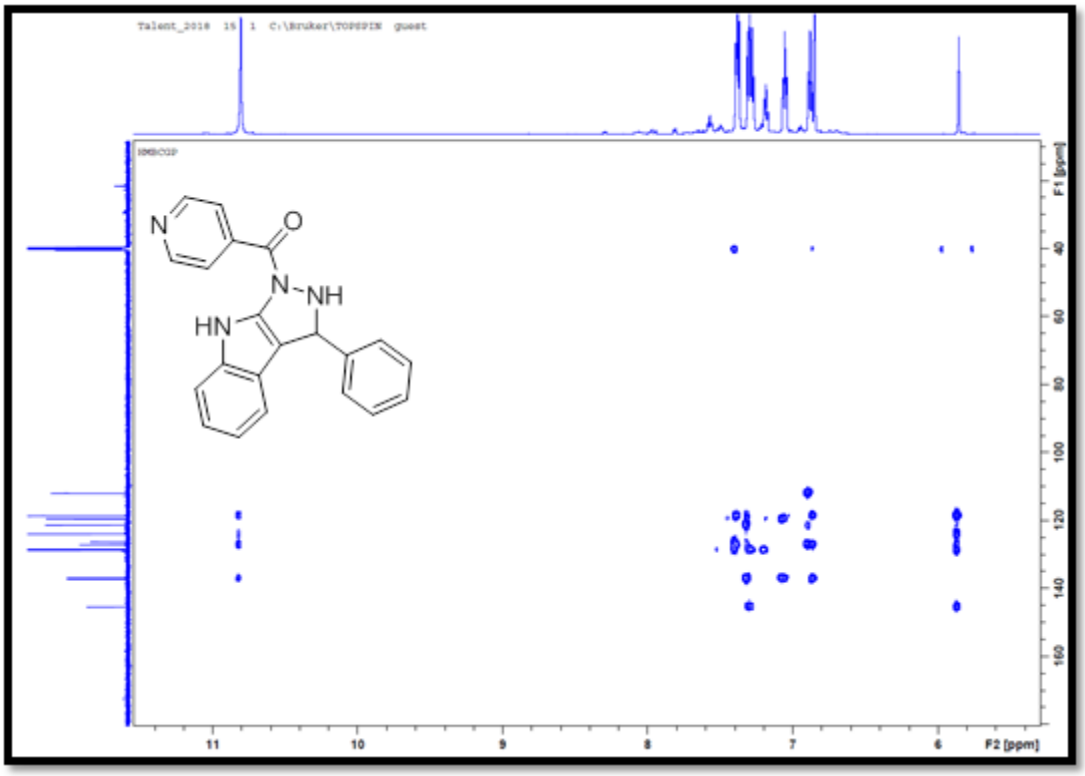

Appendix 5.8B: HMBC NMR spectrum of compound **94a**

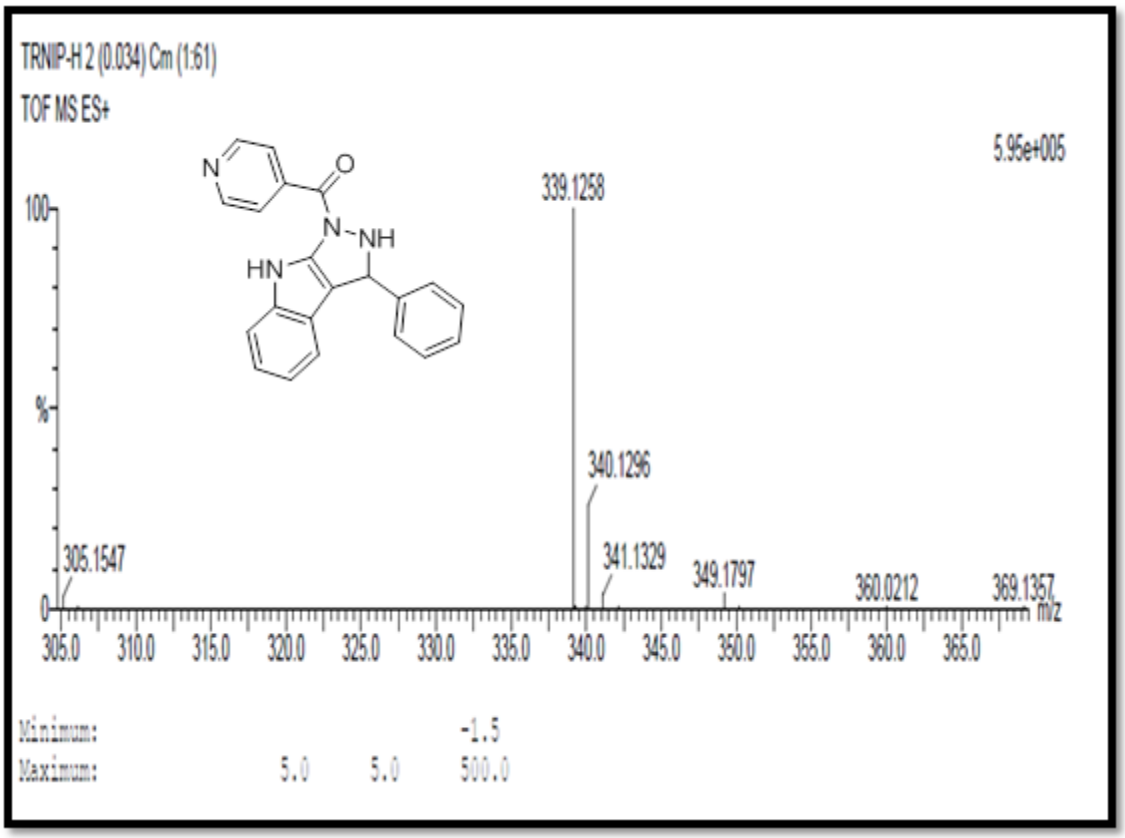

Appendix 5.9B: TOF-MS spectrum of compound **94a**

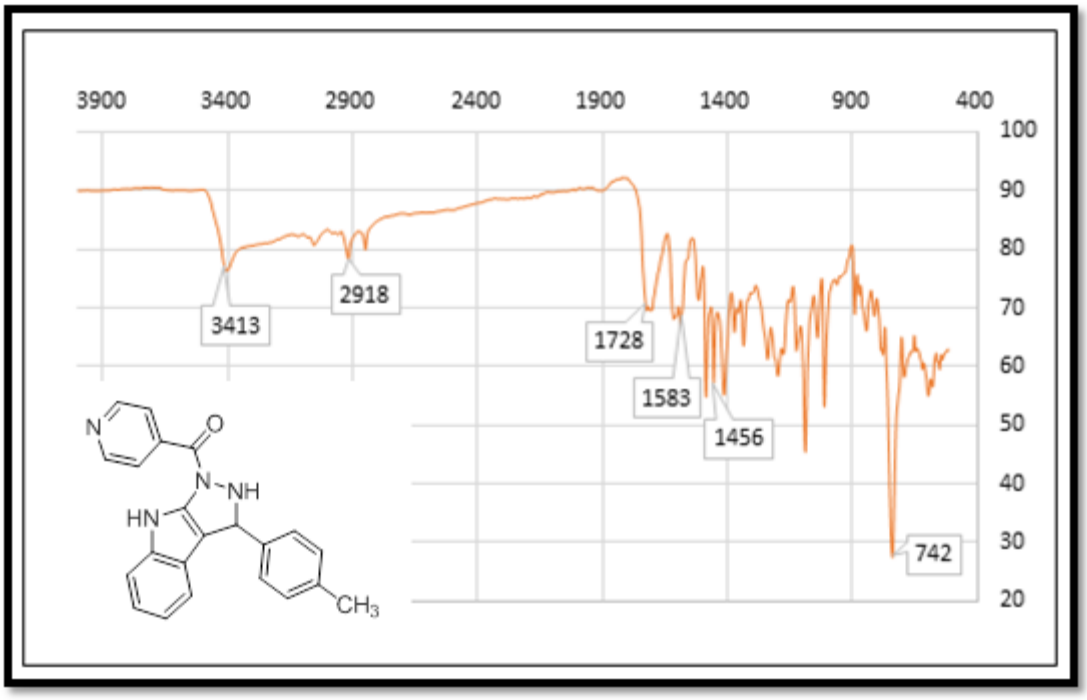

Appendix 5.10B: IR spectrum of compound 94**b**

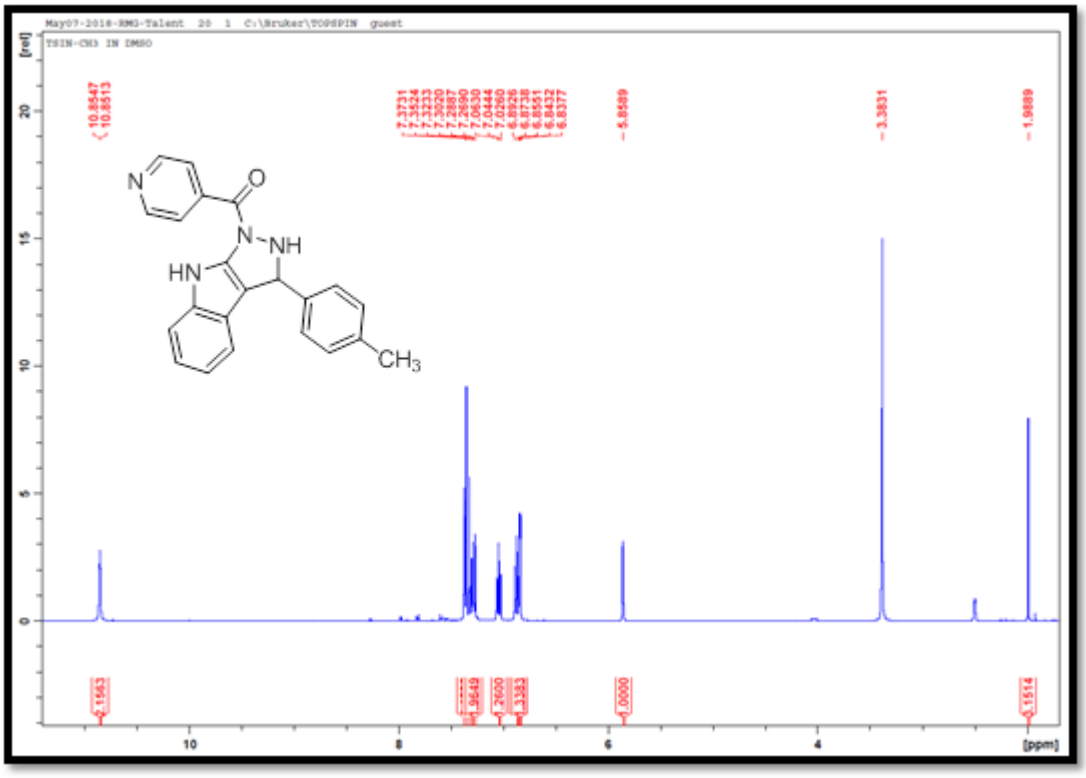

Appendix 5.11B: ^{1}H NMR spectrum of compound **94b**

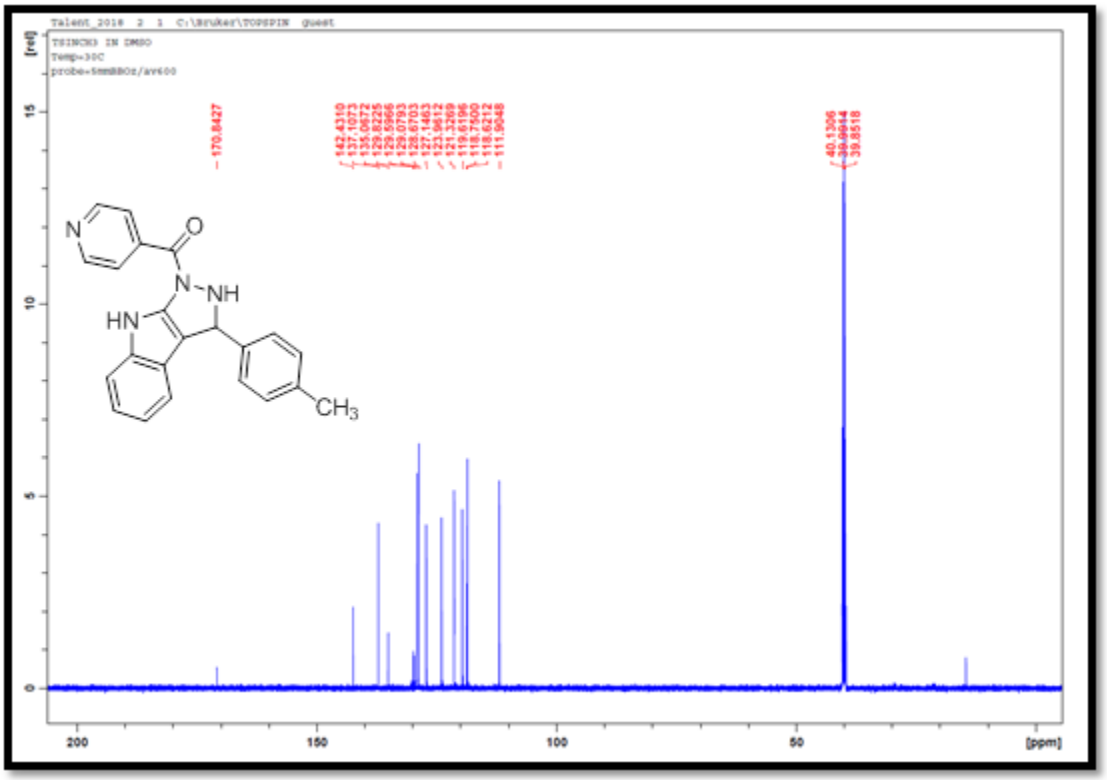

Appendix 5.12B: ^{13}C NMR spectrum of compound **94b**

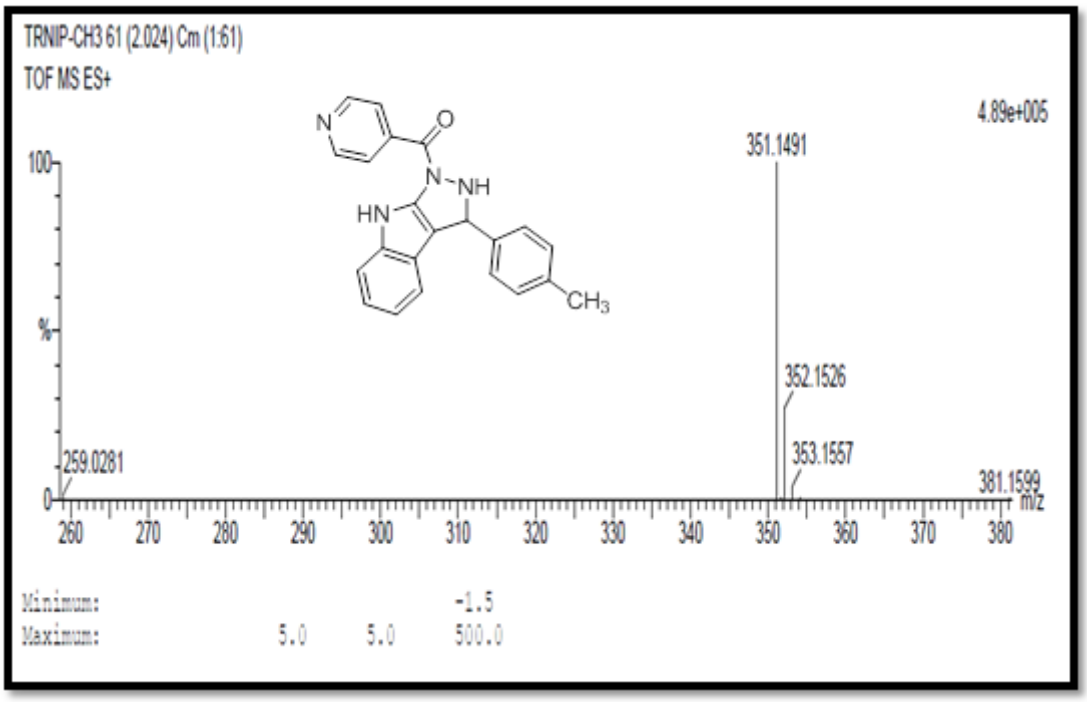

Appendix 5.13B: TOF-MS spectrum of compound **94b**

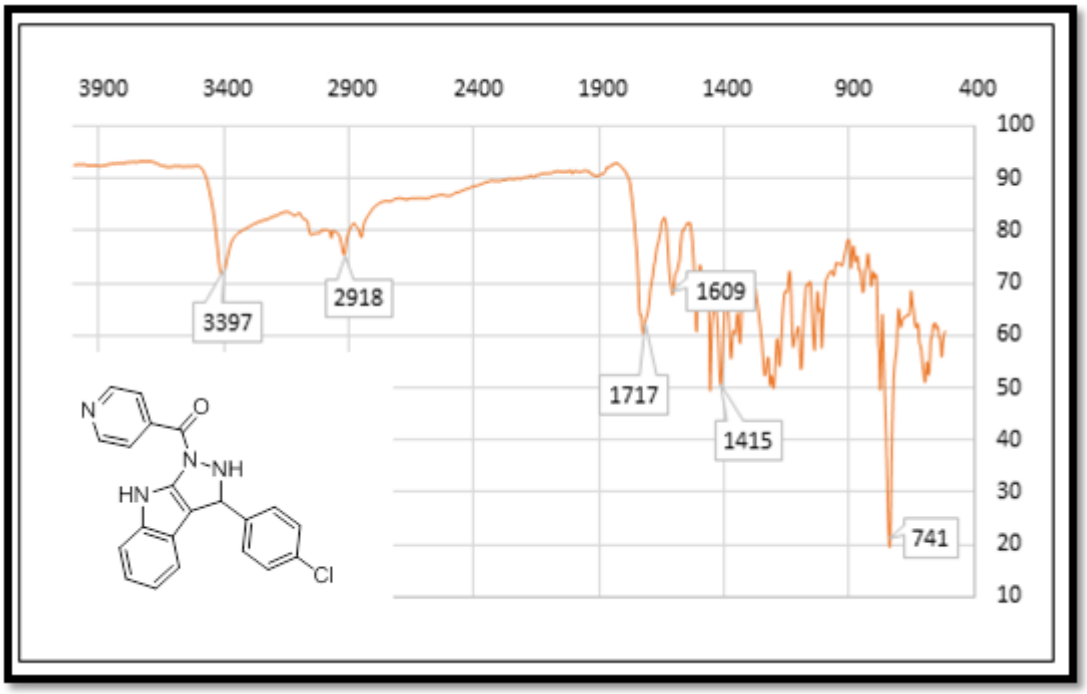

Appendix 5.14B: IR spectrum of compound **94c**

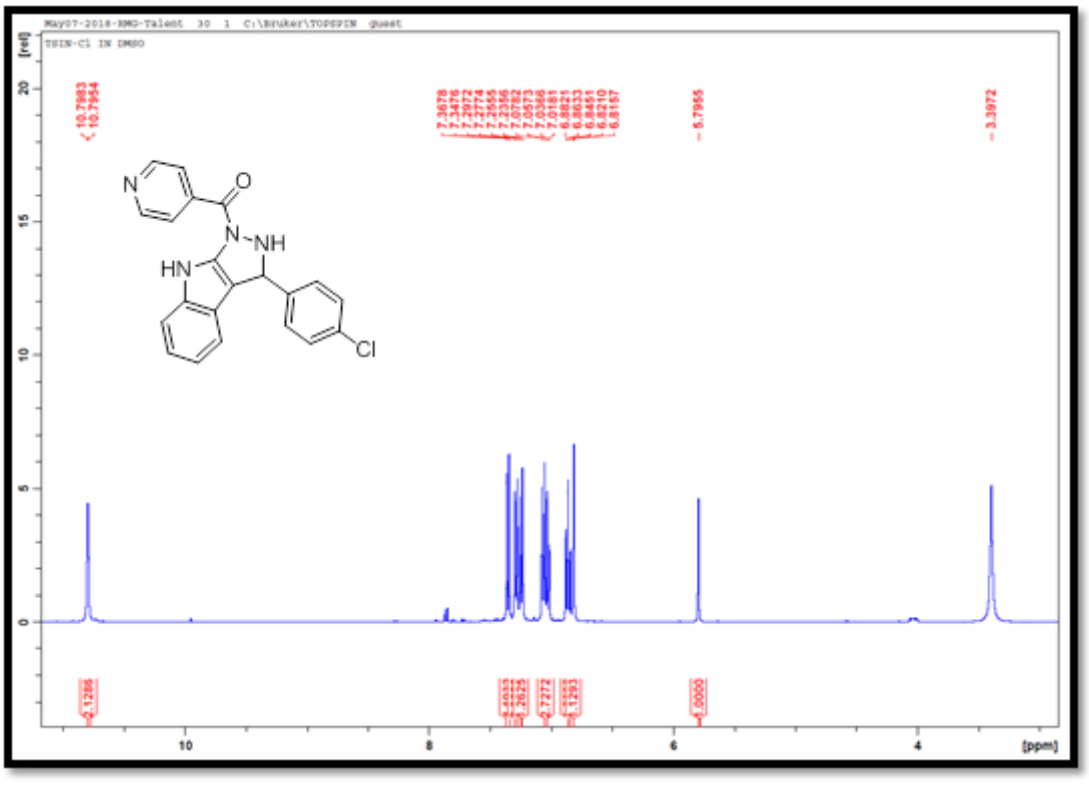

Appendix 5.15B: ^{1}H NMR spectrum of compound **94c**

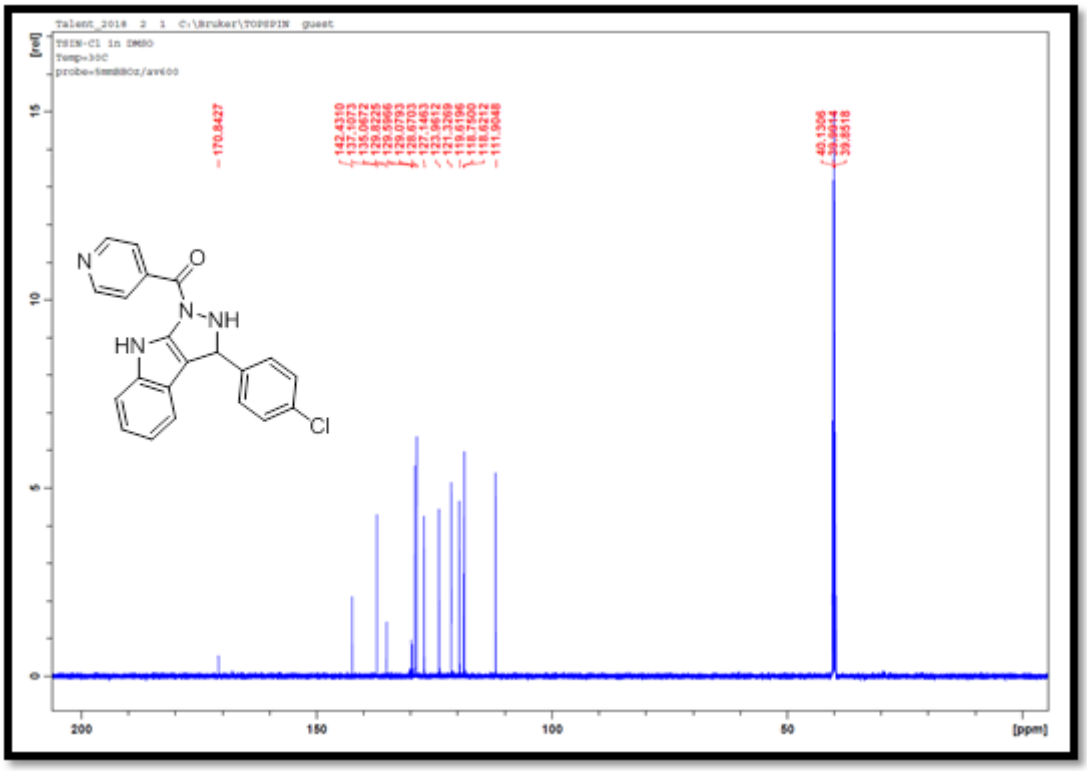

Appendix **5.16B:** ^{1}H NMR spectrum of compound **94c**

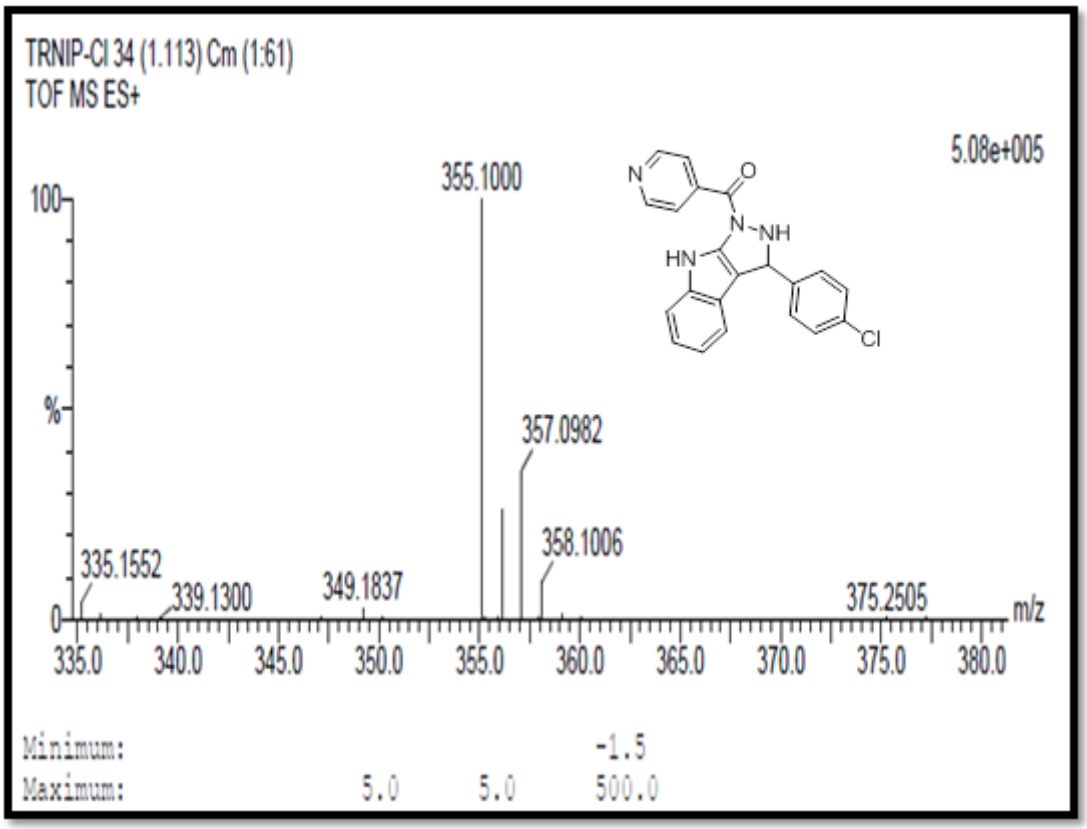

Appendix 5.17B: TOF-MS spectrum of compound **94c**

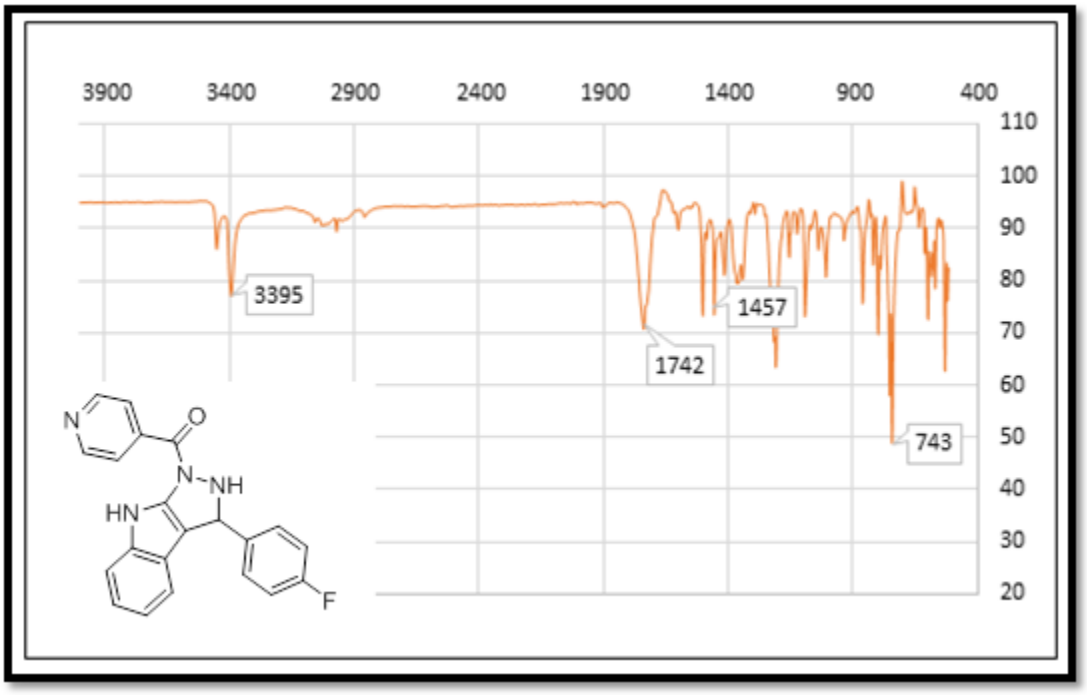

Appendix 5.18B: IR spectrum of compound **94d**

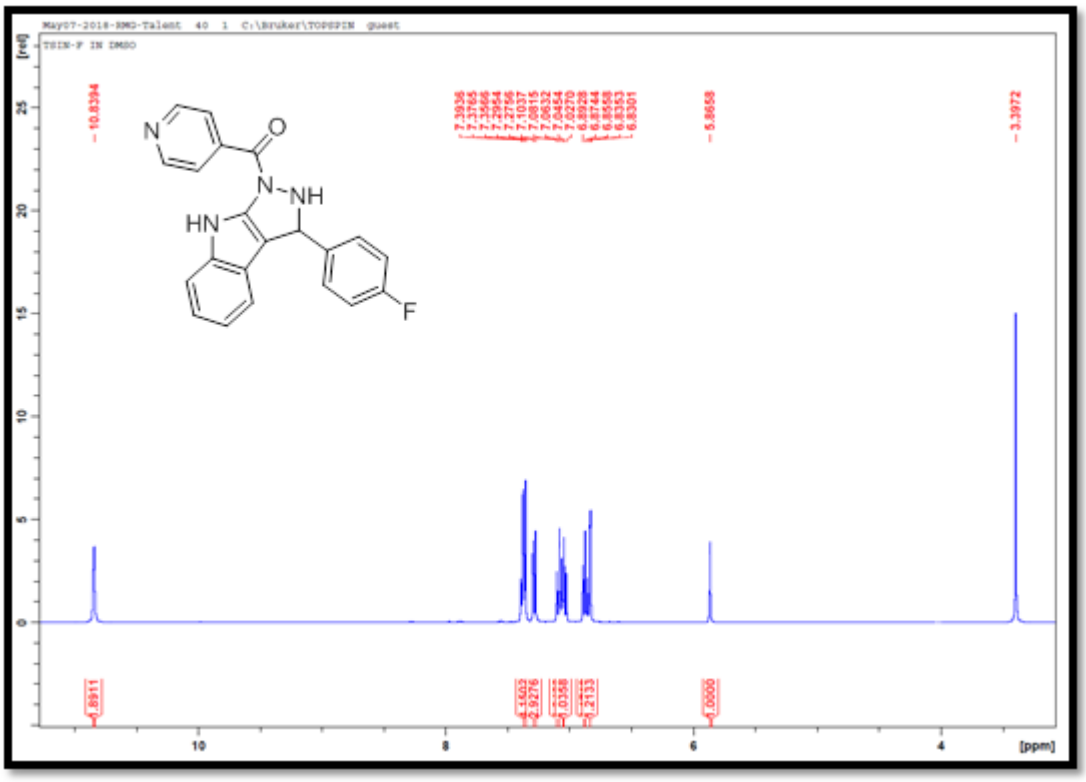

Appendix 5.19B: ^{1}H NMR spectrum of compound **94d**

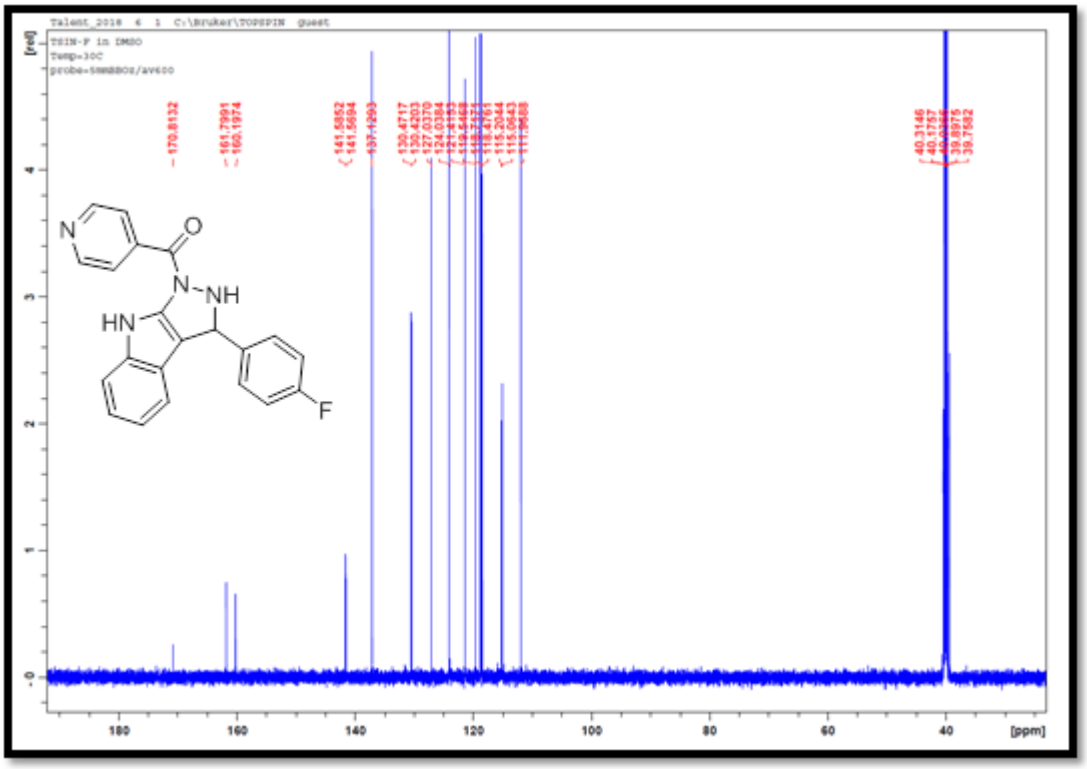

Appendix 5.20B: ^{13}C NMR spectrum of compound **94d**

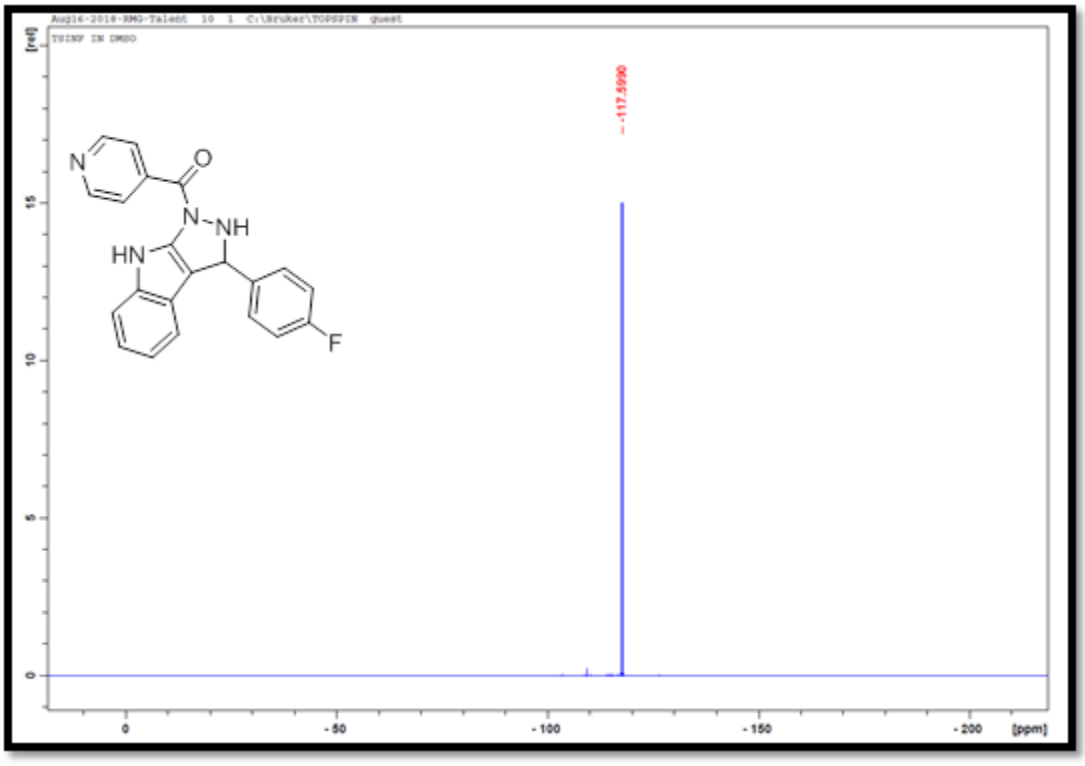

Appendix 5.21B: ^{19}F NMR spectrum of compound **94d**

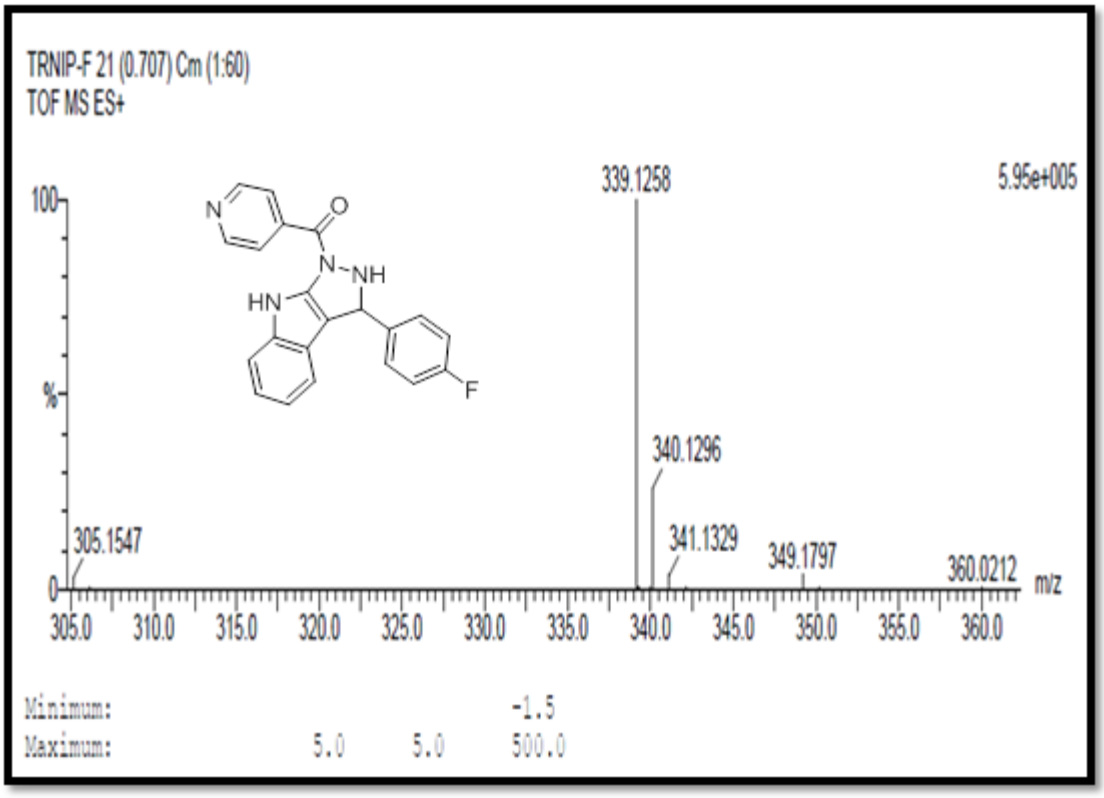

Appendix 5.22B: TOF-MS spectrum of compound **94d**

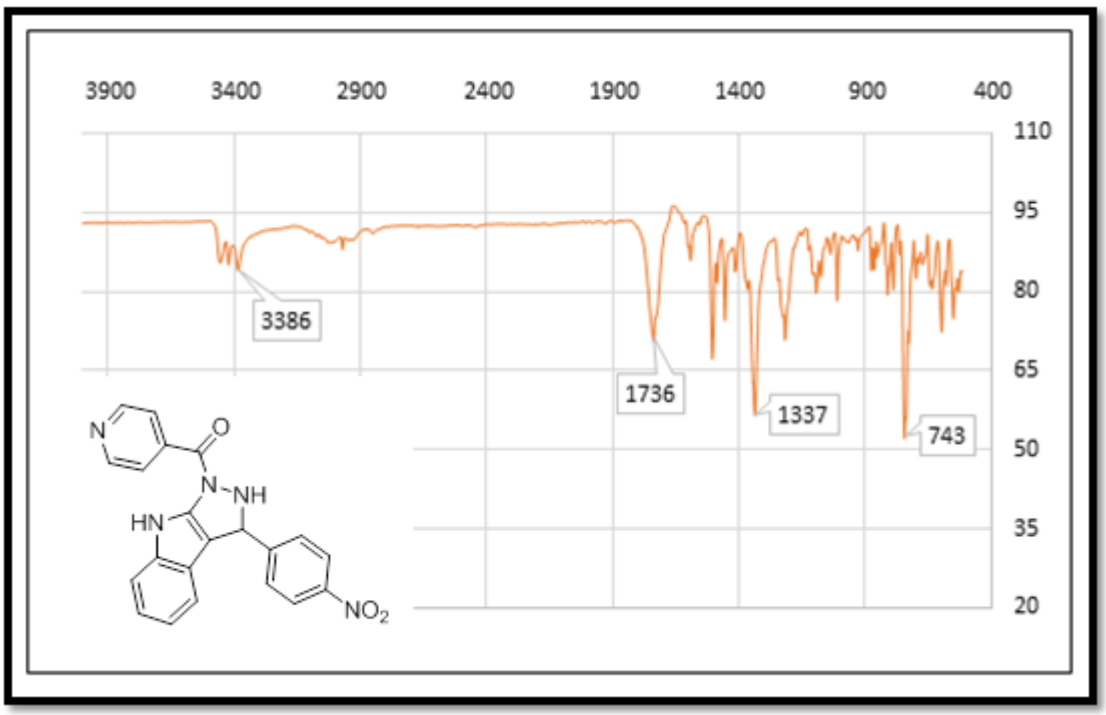

Appendix 5.23B: IR spectrum of compound **94e**

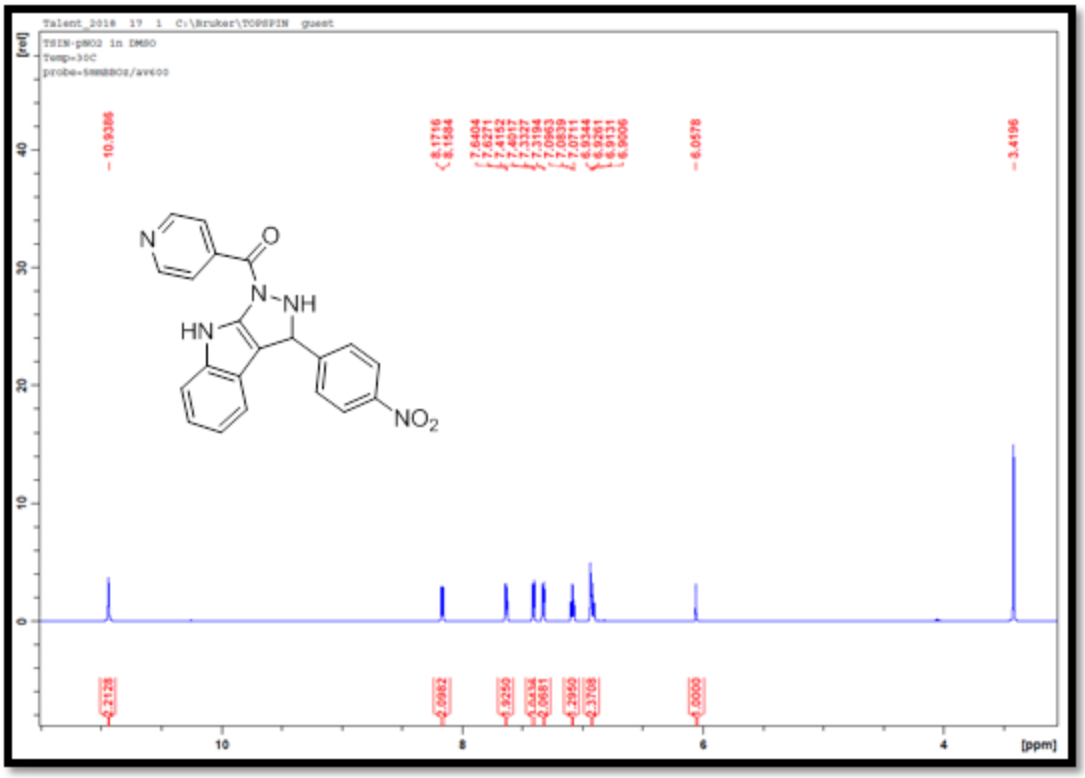

Appendix 5.24B: ^{1}H NMR spectrum of compound **94e**

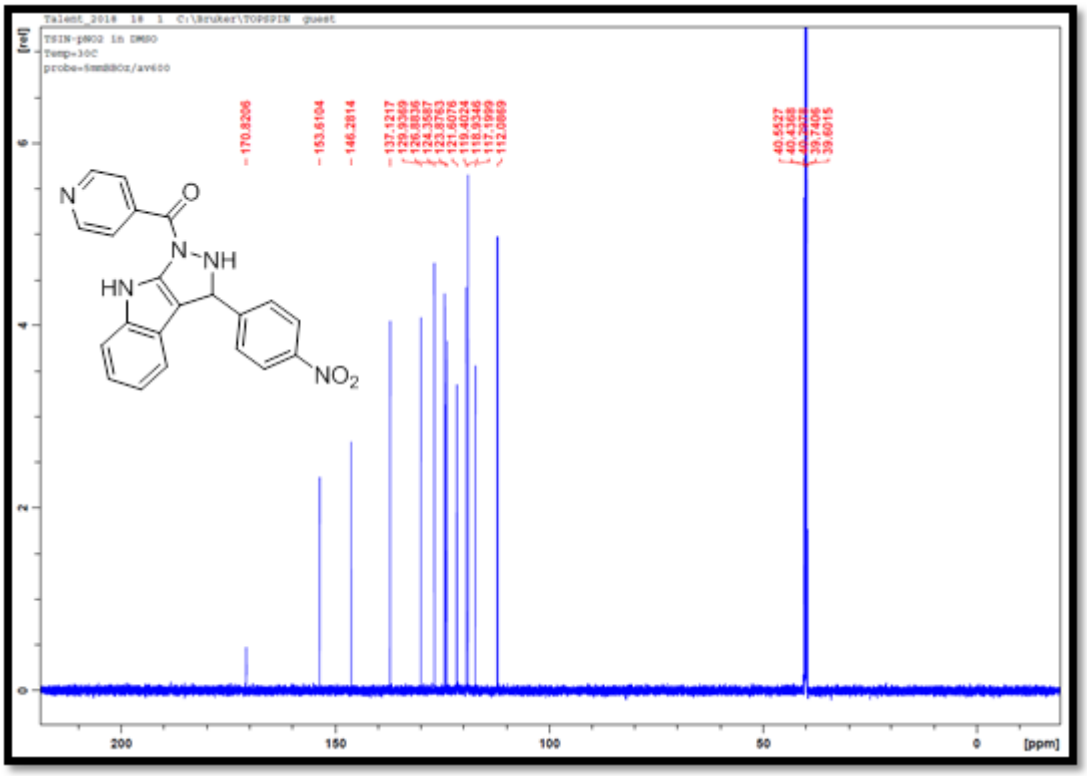

Appendix 5.25B: ^{13}C NMR spectrum of compound **94e**

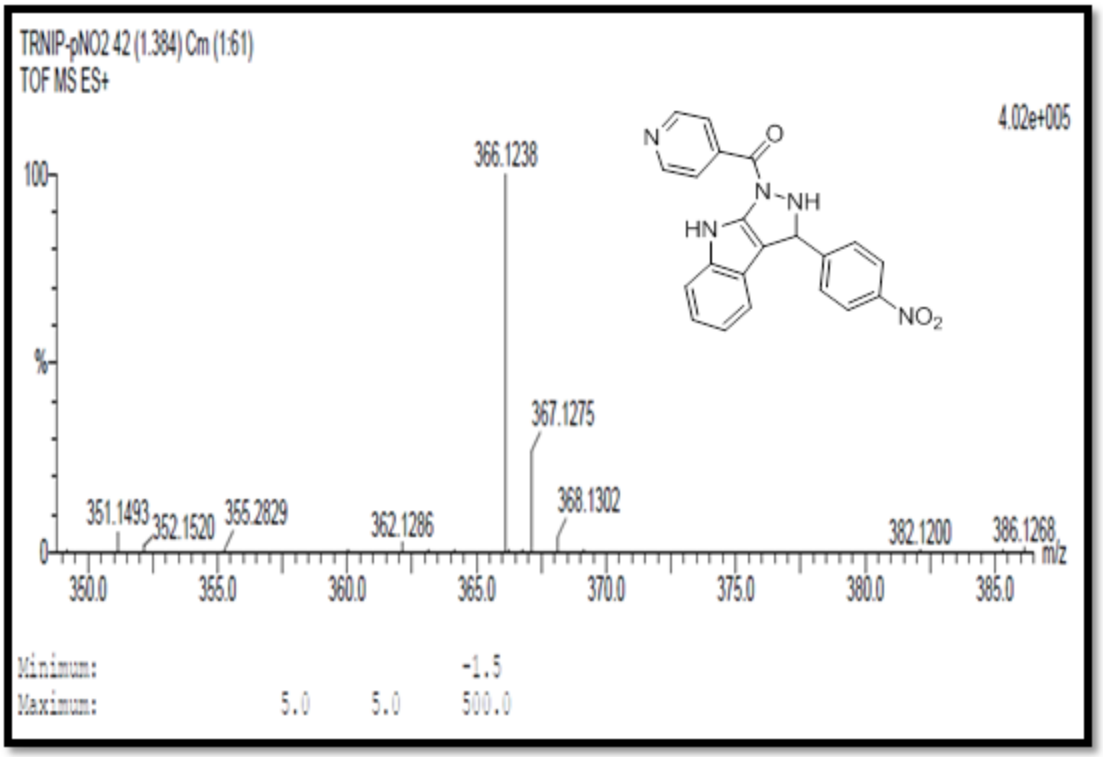

Appendix 5.26B: TOF-MS spectrum of compound **94e**

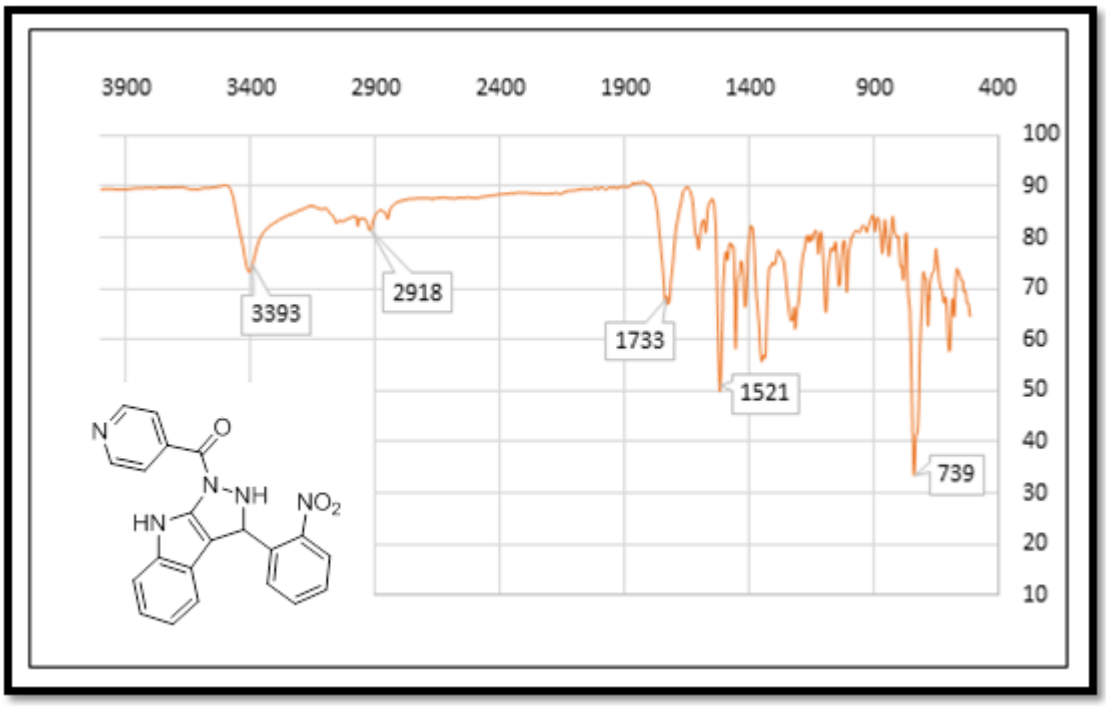

Appendix 5.27B: IR spectrum of compound **94f**

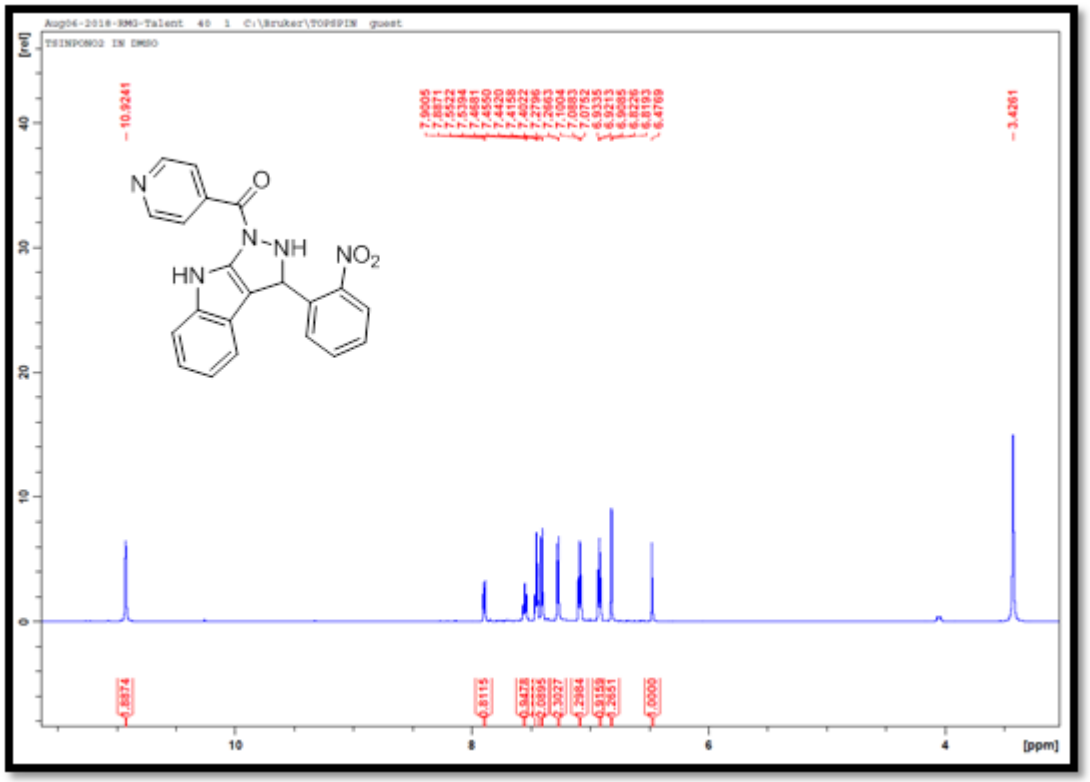

Appendix 5.28B: ^{1}H NMR spectrum of compound **94f**

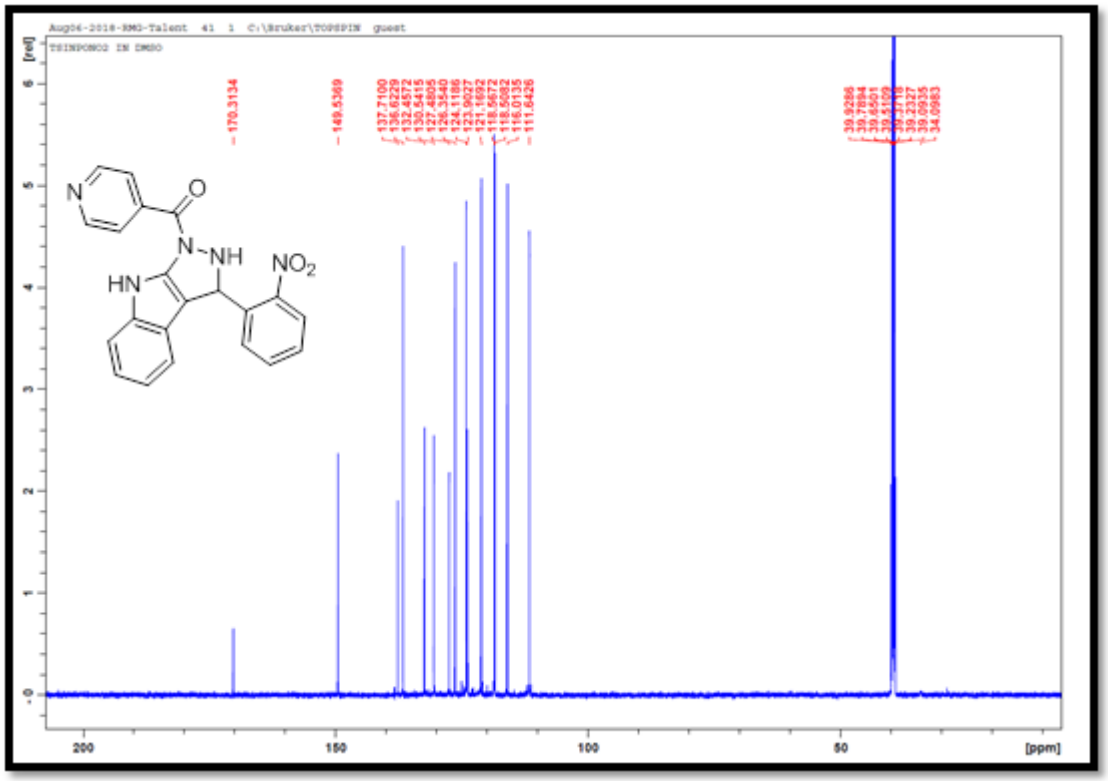

Appendix 5.29B: ^{13}C NMR spectrum of compound **94f**

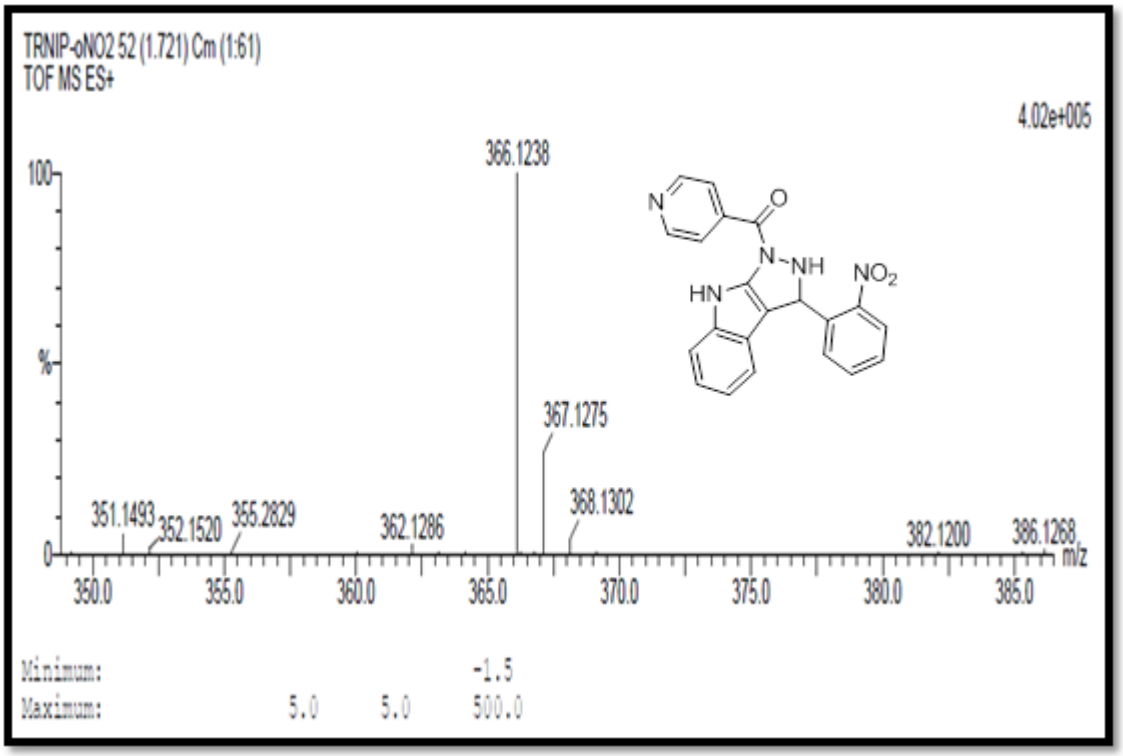

Appendix 5.30B: TOF-MS spectrum of compound **94f**

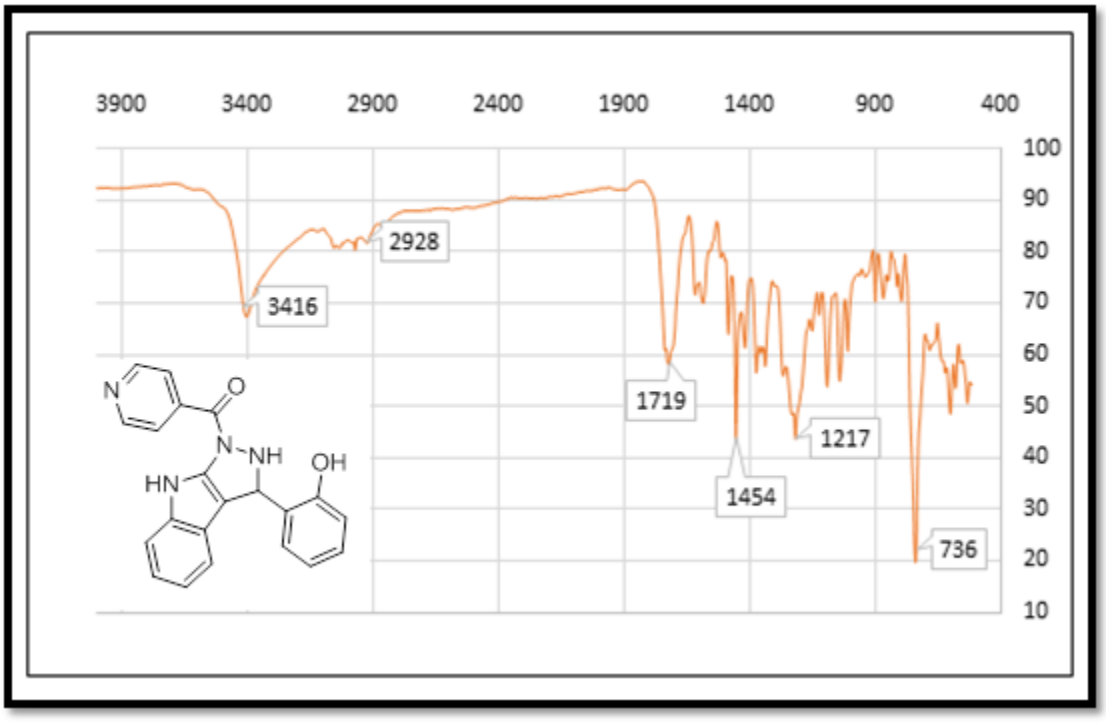

Appendix 5.31B: IR spectrum of compound **94g**

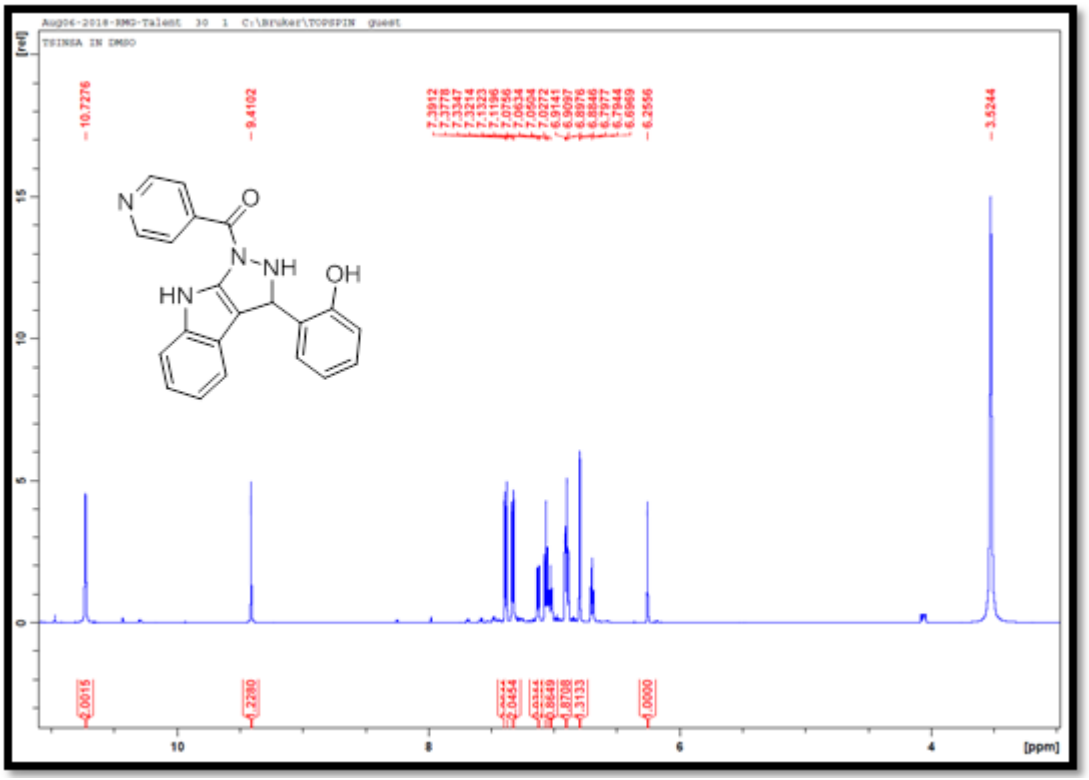

Appendix 5.32B: ^{1}H NMR spectrum of compound **94g**

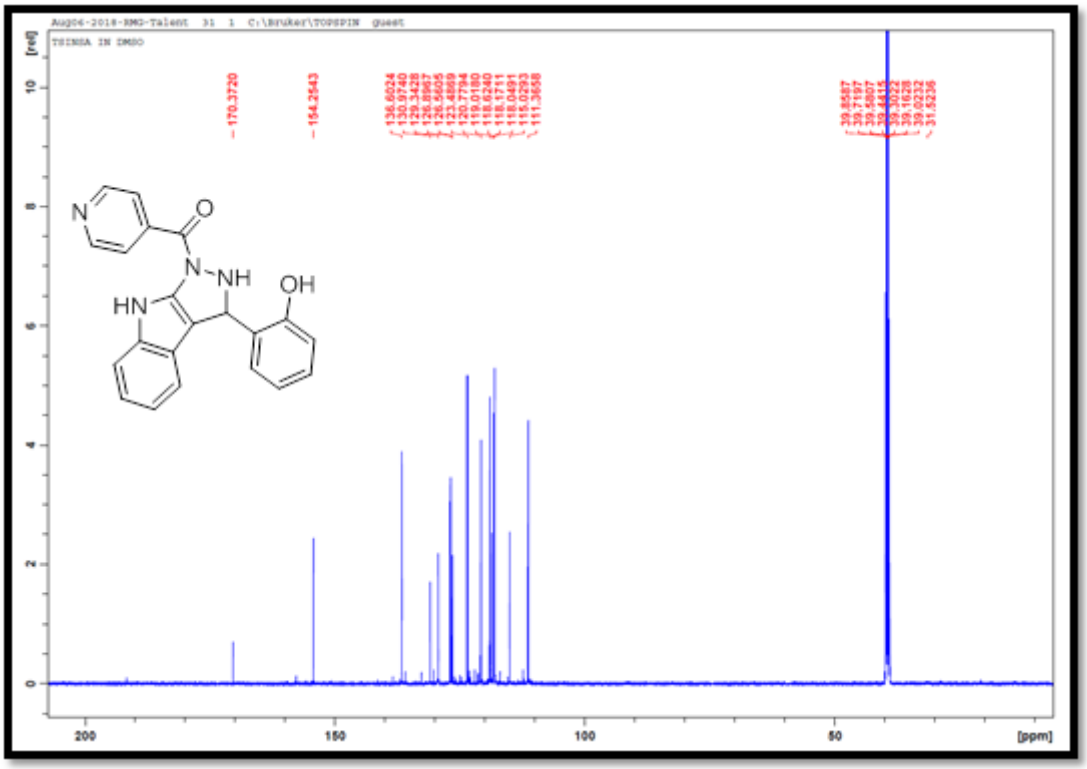

Appendix 5.33B: ^{13}C NMR spectrum of compound **94g**

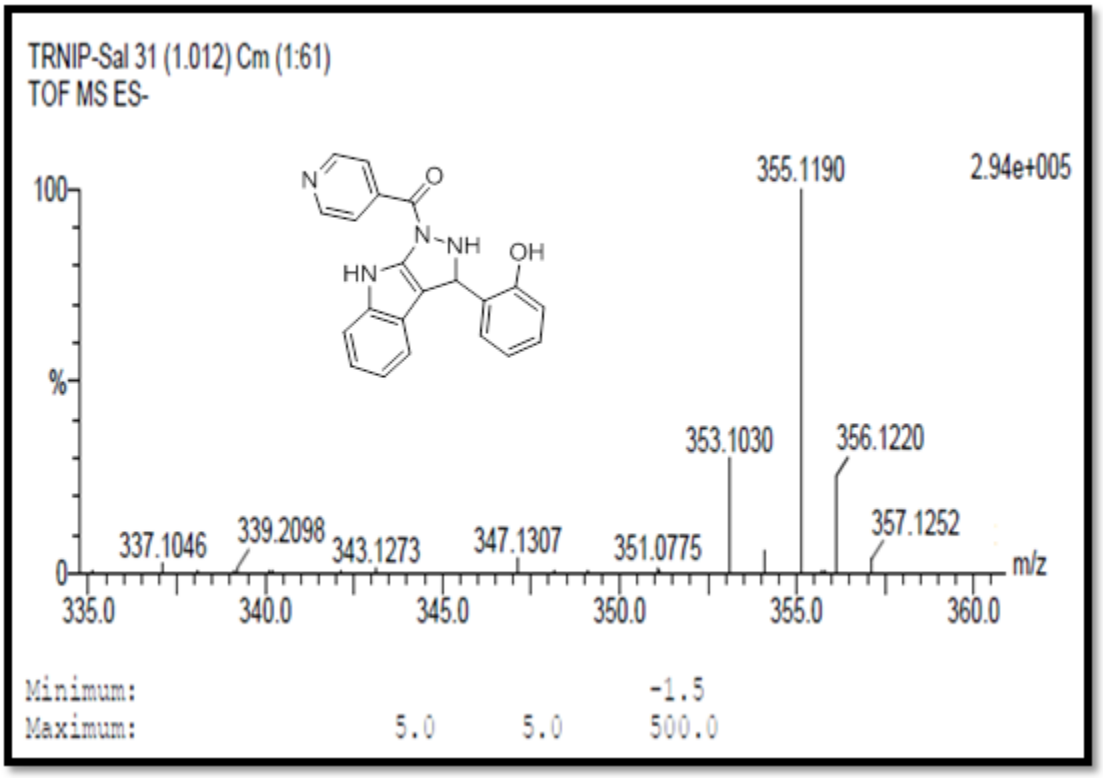

Appendix 5.34B: TOF-MS spectrum of compound **94g**

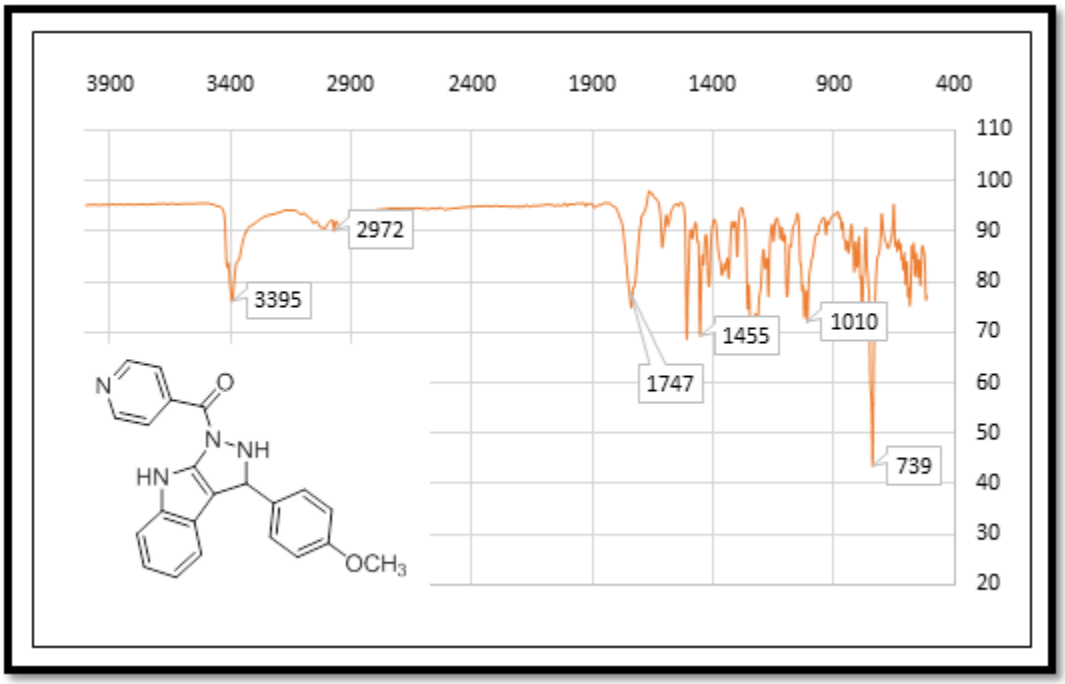

Appendix 5.35B: IR spectrum of compound **94h**

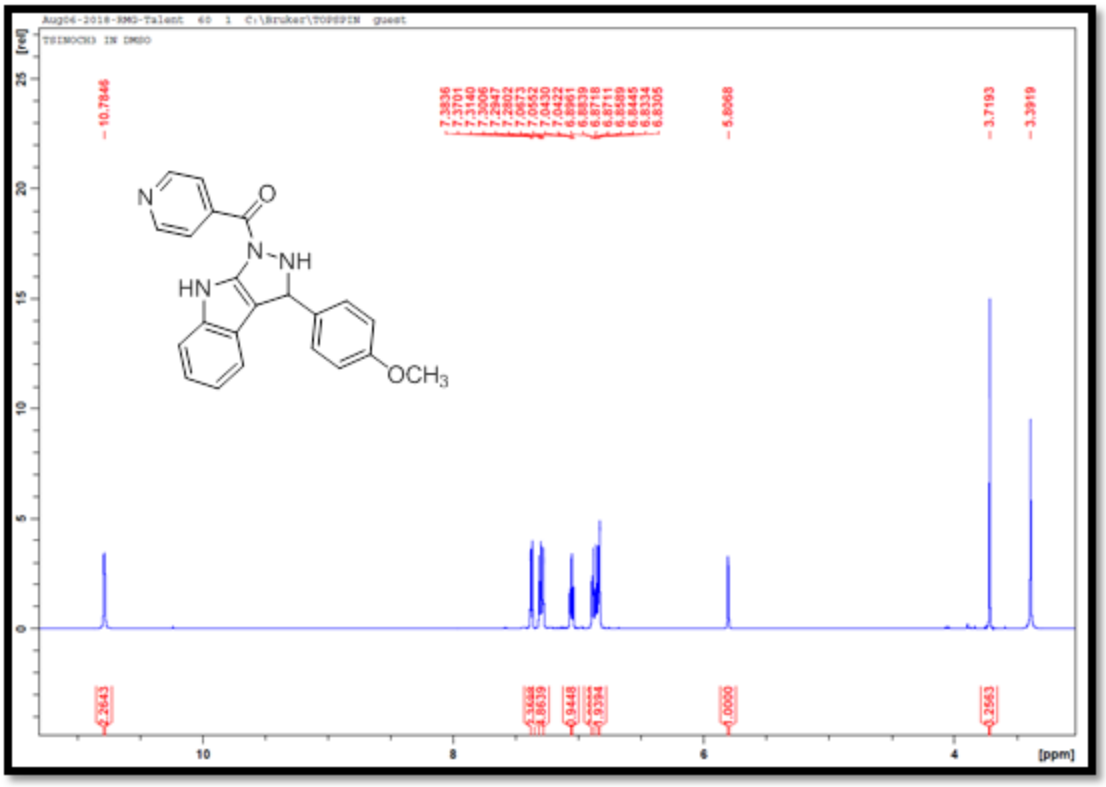

Appendix 5.36B: ^{1}H NMR spectrum of compound **94h**

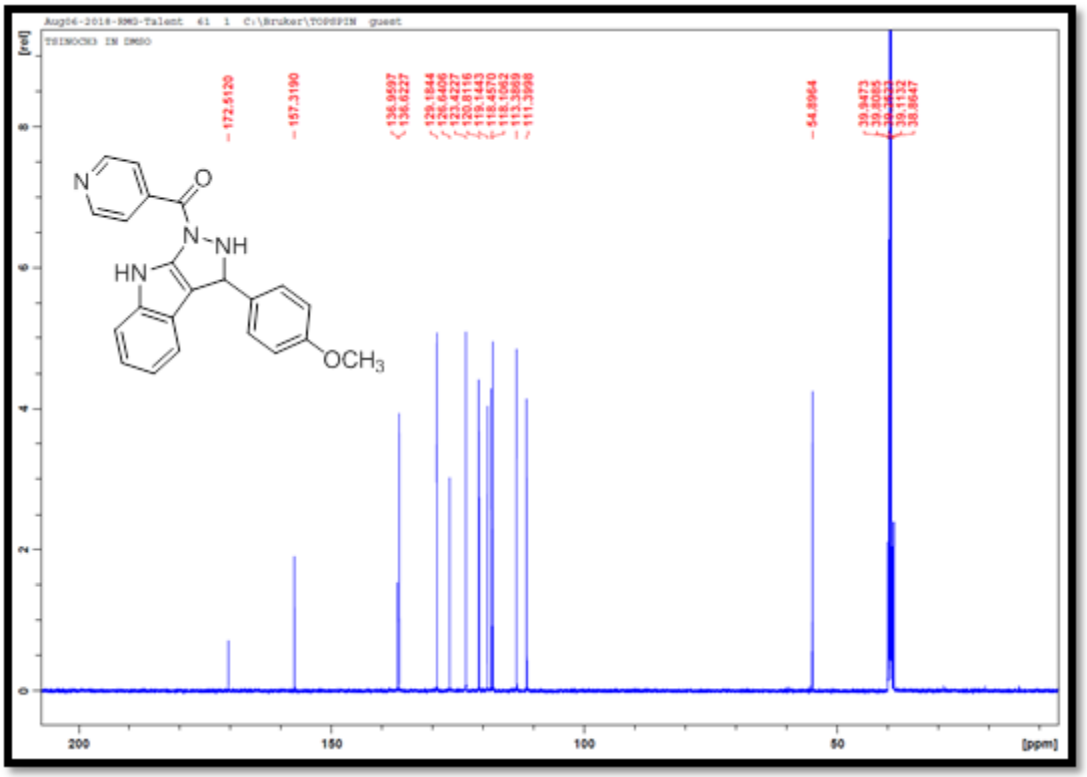

Appendix 5.37B: ^{13}C NMR spectrum of compound **94h**

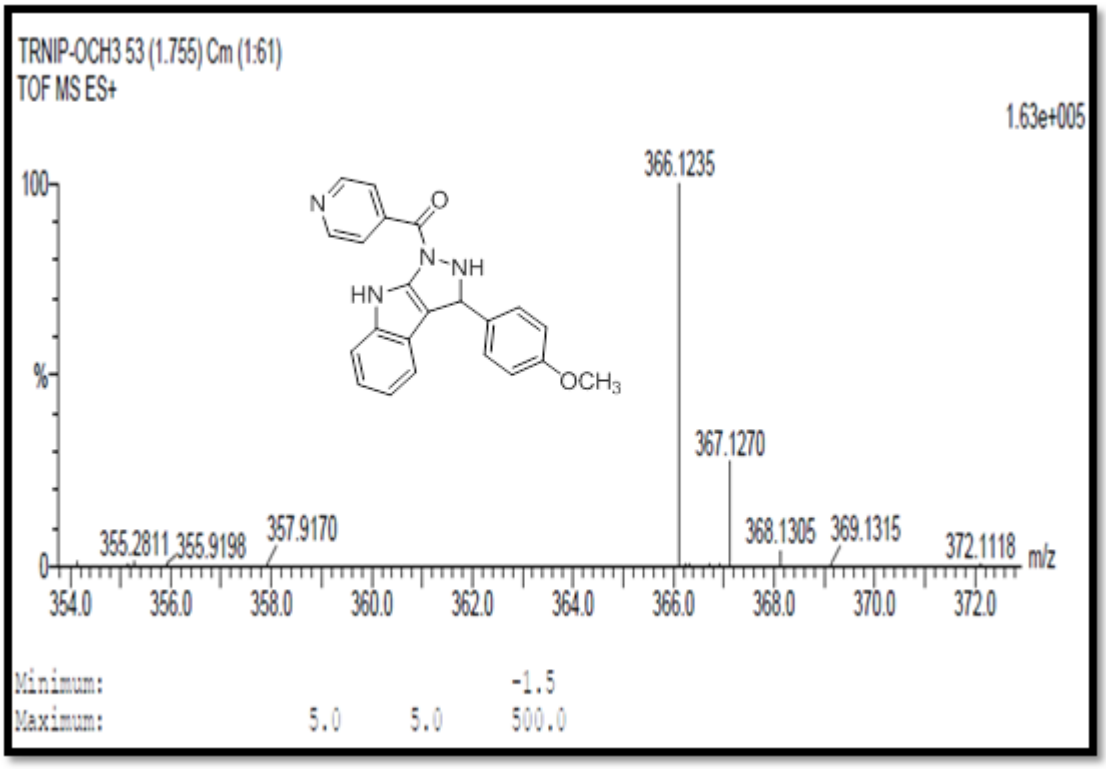

Appendix 5.38B: TOF-MS spectraum of compound **94h**

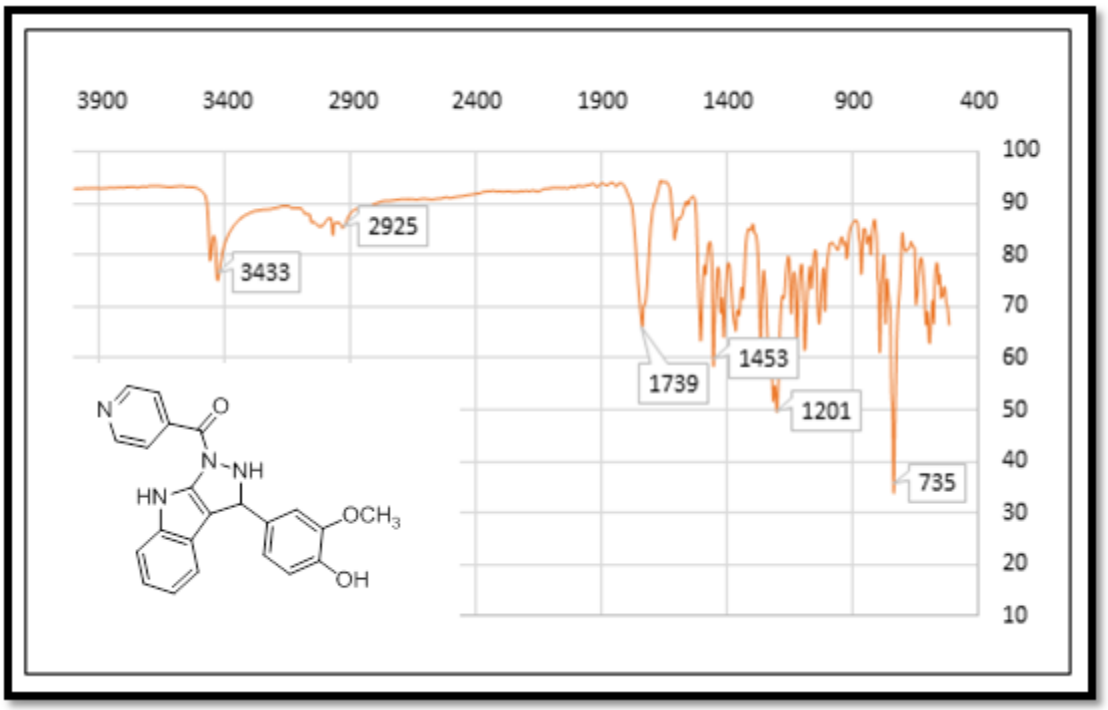

Appendix 5.39B: IR spectrum of compound **94i**

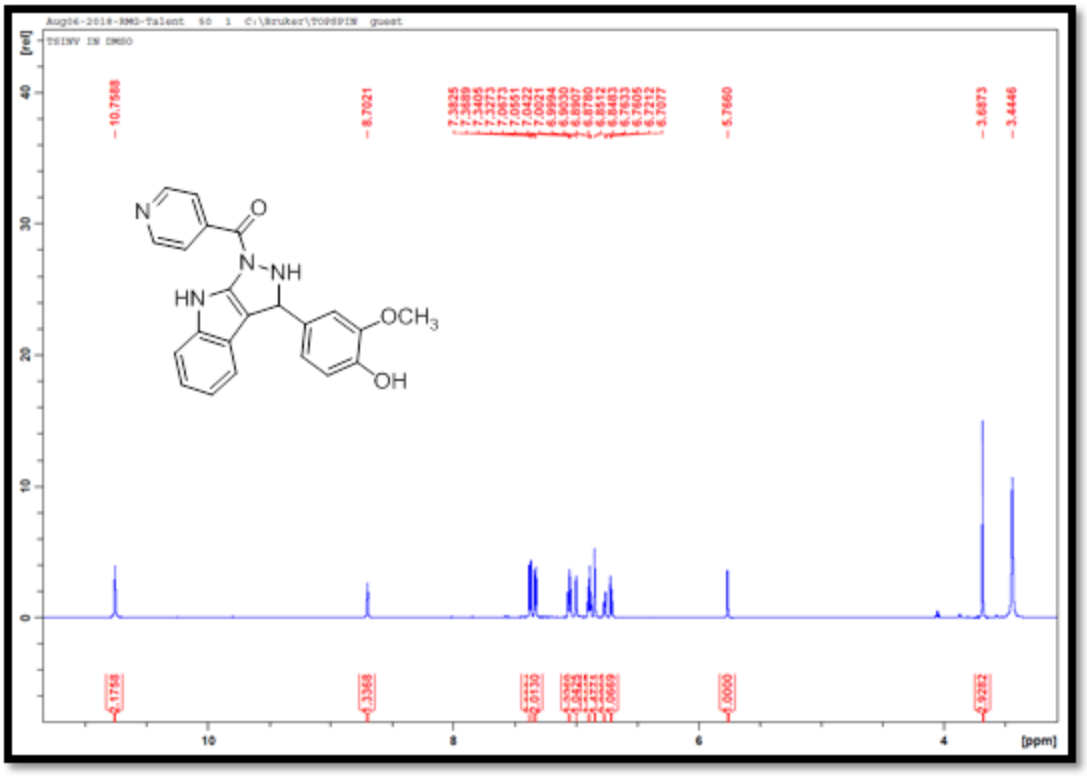

Appendix 5.40B: ^{1}H NMR spectrum of compound **94i**

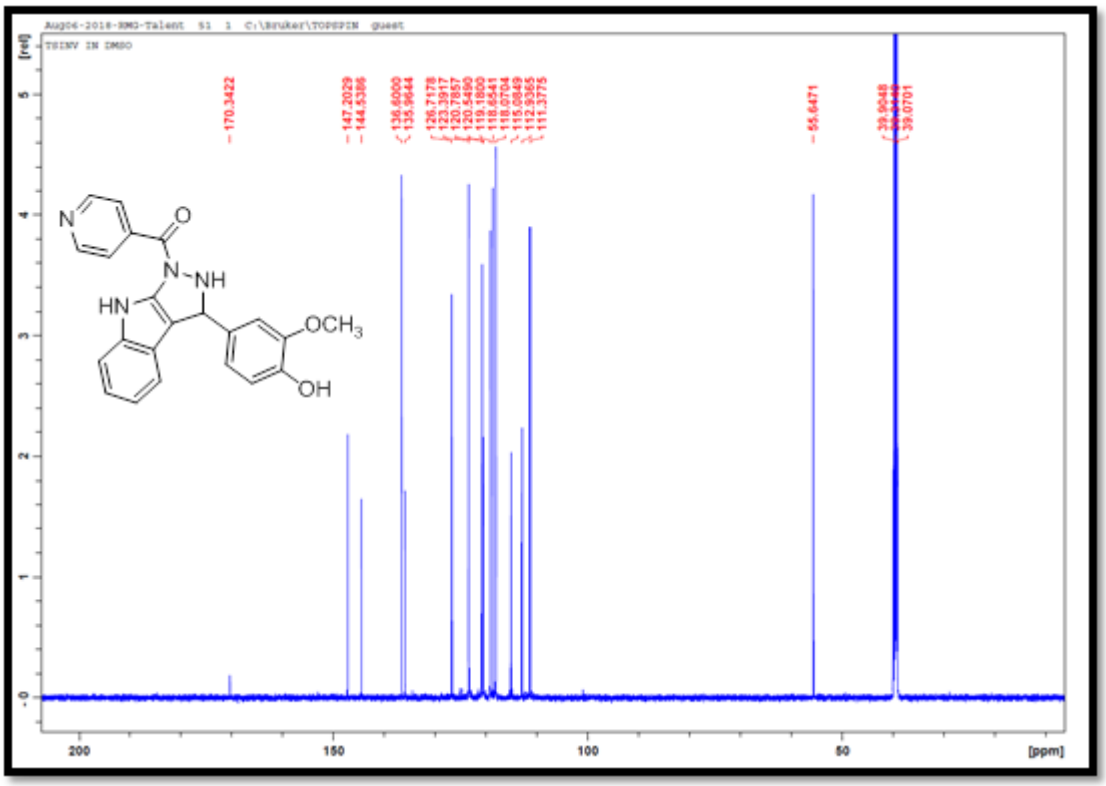

Appendix 5.41B: ^{13}C NMR spectrum of compound **94i**

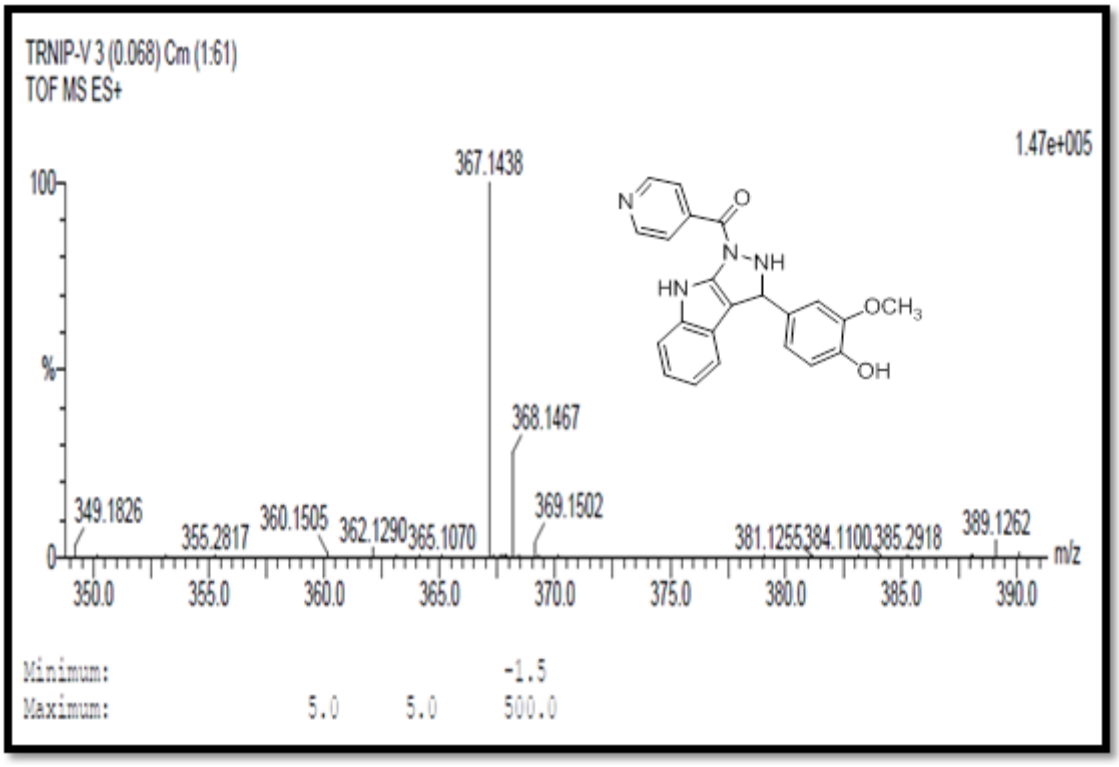

Appendix 5.42B: TOF-MS spectrum of compound **94i**

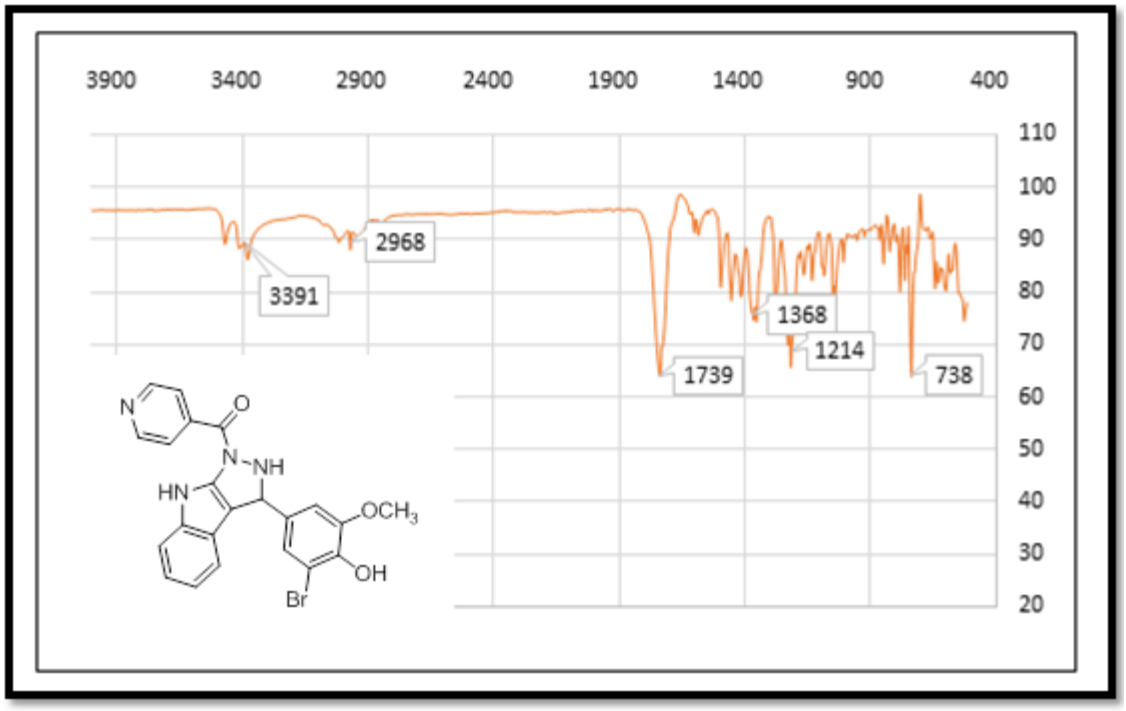

Appendix 5.43B: IR spectrum of compound **94j**

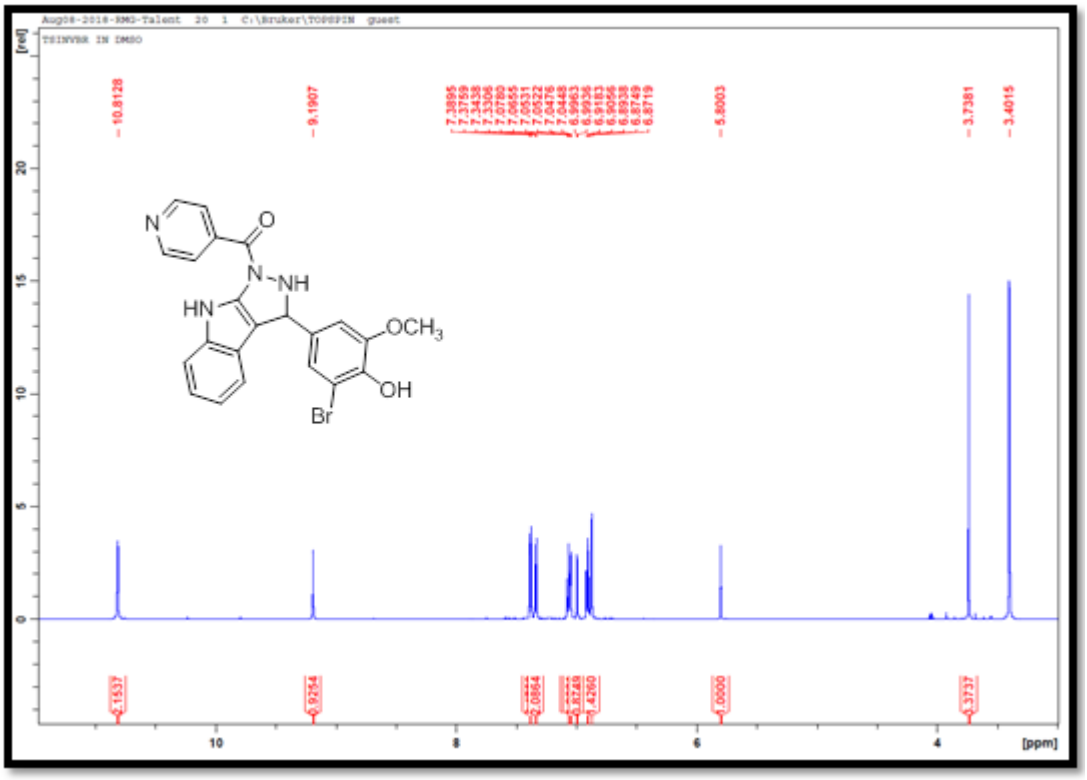

Appendix 5.44B: ^{1}H NMR spectrum of compound **94j**

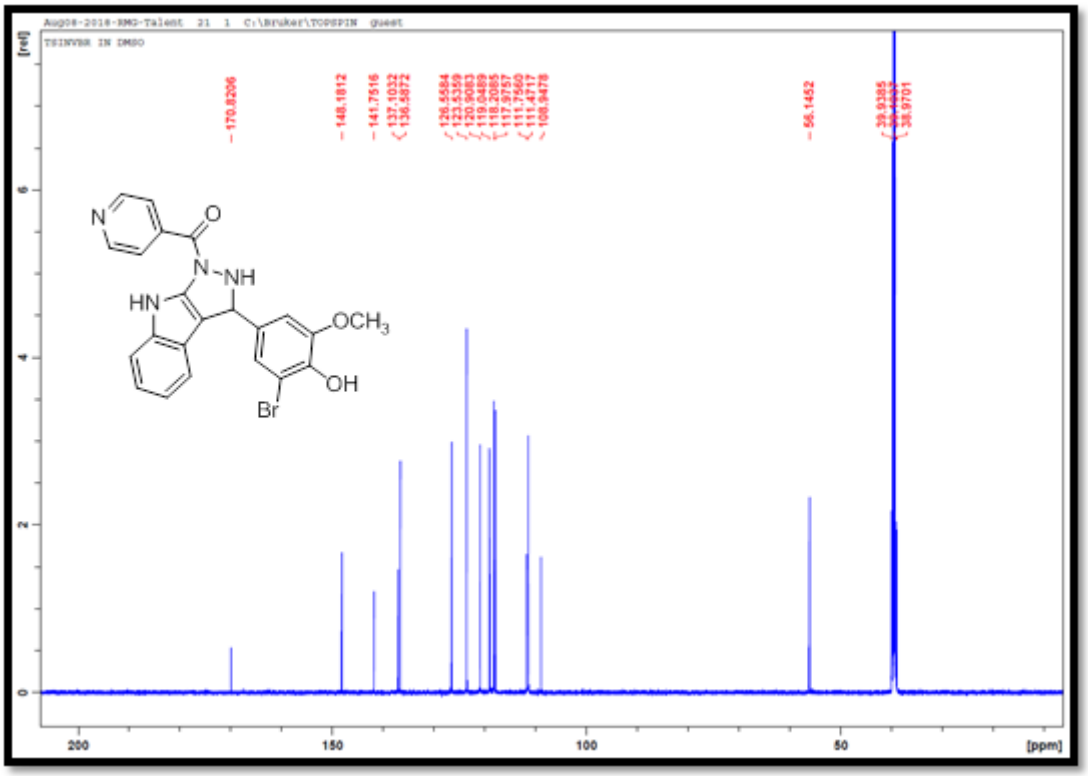

Appendix 5.45B: ^{13}C NMR spectrum of compound **94j**

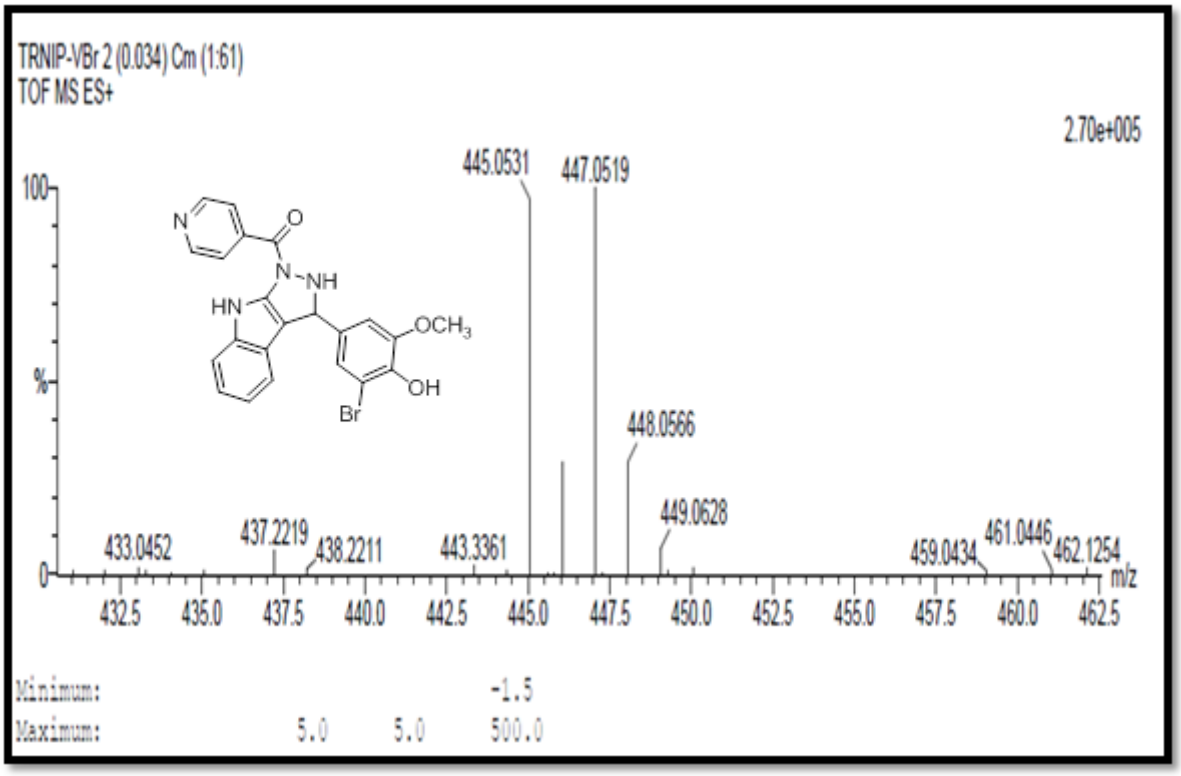

Appendix 5.46B: TOF-MS spectrum of compound **94j**

Chapter Six

Recommendation for Future Studies

An effiecient synthesis of novel biologically active nitrogen based heterocyclic compounds were successfully reported. A total of 53 compounds were prepared using multi-componet reactions and [1, 8] naphthyridinones were evaluated against Lung Cancer Cells whilst the indolo based naphthyridines and pyrazoles were investigated for antimicrobial activity.

1. The structural activity relationship studies will be investigated for the synthesized compound to determine the active sites of the molecule.
2. All synthesized compounds will be studied using molecular docking to determine their activity against cancer. Thereafter, invivo assay will be performed using synthesized compounds on the following cancer cell lines: MCF-7, MDA-MB-231, $SKBr_3$, A549 and T47D.
3. Further biological investigation will be conducted for anti-inflammatory, anti-malaria and anti-TB activities.
4. Developed Povarov protocols [4+2] and [3+2] cycloaddition reactions using indole will be further investigated using novel synthesized heterogenous catalyst to prepare novel nitrogen based heterocyclic compounds.
5. Propiolate ester will be utilized as a substrate in the synthesis of ester based pyrazoles via Povarov [3+2] cycloaddition reaction.

PUBLICATIONS

1. **TR Makhanya,** RM Gengan, P Pitchai, AA Chuturgoon, C Tiloke, A Atar**.** Phosphotungstic acid catalysed one pot synthesis of 4,8,8-trimethyl-5-phenyl-5,5a,8, 9-tetrahydrobenzo[b] [1, 8] naphthyridin-6(7H)-one derivatives and their biological evaluation against A549 lung cancer cells. ***Journal of Heterocyclic Chemistry***, **2018**, 55, 1193 - 1204.
2. **TR Makhanya**, RM Gengan and A Atar**.** Synthesis and biological evaluation of novel fused indolo [2, 3-c] [1, 8] naphthyridine derivatives as potential antibacterial agents. ***Synthetic communications***, **2019**, 49, 823-835.
3. **TR Makhanya**, RM Gengan and A Atar. Synthesis and biological evaluation of novel fused indolo pyrazole derivatives as potential antifungal agents. (To be communicated)
4. **TR Makhanya**, RM Gengan and A Atar. One pot synthesis of novel nicotinyl fused indolo pyrazole derivatives and their antimicrobial activity. (To be communicated)